

ACS SYMPOSIUM SERIES **639**

# Biomedical Frontiers of Fluorine Chemistry

**Iwao Ojima**, EDITOR

*State University of New York at Stony Brook*

**James R. McCarthy**, EDITOR

*Neurocrine Biosciences, Inc.*

**John T. Welch**, EDITOR

*State University of New York at Albany*

Developed from symposia sponsored  
by the Division of Fluorine Chemistry and  
the Division of Medicinal Chemistry



American Chemical Society, Washington, DC

In Biomedical Frontiers of Fluorine Chemistry; Ojima, I., et al.;  
ACS Symposium Series; American Chemical Society: Washington, DC, 1996.



## Biomedical frontiers of fluorine chemistry

### Library of Congress Cataloging-in-Publication Data

Biomedical frontiers of fluorine chemistry / Iwao Ojima, James R. McCarthy, John T. Welch, editors.

p. cm.—(ACS symposium series; 639)

“Developed from a symposium sponsored by the Division of Fluorine Chemistry and the Division of Medicinal Chemistry.”

Includes bibliographical references and indexes.

ISBN 0-8412-3442-6

1. Organofluorine compounds—Synthesis—Congresses.
2. Organofluorine compounds—Physiological effect—Congresses.
3. Organofluorine compounds—Therapeutic use—Congresses.

I. Ojima, Iwao, 1945— . II. McCarthy, James R., 1943—  
III. Welch, John T. IV. American Chemical Society. Division of  
Fluorine Chemistry. V. American Chemical Society. Division of  
Medicinal Chemistry. VI. Series.

RS431.073B55 1996  
615'.312—dc20

96-24784  
CIP

This book is printed on acid-free, recycled paper.



Copyright © 1996

American Chemical Society

All Rights Reserved. The appearance of the code at the bottom of the first page of each chapter in this volume indicates the copyright owner's consent that reprographic copies of the chapter may be made for personal or internal use or for the personal or internal use of specific clients. This consent is given on the condition, however, that the copier pay the stated per-copy fee through the Copyright Clearance Center, Inc., 222 Rosewood Drive, Danvers, MA 01923, for copying beyond that permitted by Sections 107 or 108 of the U.S. Copyright Law. This consent does not extend to copying or transmission by any means—graphic or electronic—for any other purpose, such as for general distribution, for advertising or promotional purposes, for creating a new collective work, for resale, or for information storage and retrieval systems. The copying fee for each chapter is indicated in the code at the bottom of the first page of the chapter.

The citation of trade names and/or names of manufacturers in this publication is not to be construed as an endorsement or as approval by ACS of the commercial products or services referenced herein; nor should the mere reference herein to any drawing, specification, chemical process, or other data be regarded as a license or as a conveyance of any right or permission to the holder, reader, or any other person or corporation, to manufacture, reproduce, use, or sell any patented invention or copyrighted work that may in any way be related thereto. Registered names, trademarks, etc., used in this publication, even without specific indication thereof, are not to be considered unprotected by law.

PRINTED IN THE UNITED STATES OF AMERICA  
**American Chemical Society**  
**Library**  
**1155 16th St., N.W.**  
**Washington, D.C. 20036**

In Biomedical Fluorine Chemistry; Ojima, I., et al.;  
ACS Symposium Series; American Chemical Society: Washington, DC, 1996.

# Advisory Board

## ACS Symposium Series

**Robert J. Alaimo**  
Procter & Gamble Pharmaceuticals

**Mark Arnold**  
University of Iowa

**David Baker**  
University of Tennessee

**Arindam Bose**  
Pfizer Central Research

**Robert F. Brady, Jr.**  
Naval Research Laboratory

**Mary E. Castellion**  
ChemEdit Company

**Margaret A. Cavanaugh**  
National Science Foundation

**Arthur B. Ellis**  
University of Wisconsin at Madison

**Gunda I. Georg**  
University of Kansas

**Madeleine M. Joullie**  
University of Pennsylvania

**Lawrence P. Klemann**  
Nabisco Foods Group

**Douglas R. Lloyd**  
The University of Texas at Austin

**Cynthia A. Maryanoff**  
R. W. Johnson Pharmaceutical  
Research Institute

**Roger A. Minear**  
University of Illinois  
at Urbana–Champaign

**Omkaram Nalamasu**  
AT&T Bell Laboratories

**Vincent Pecoraro**  
University of Michigan

**George W. Roberts**  
North Carolina State University

**John R. Shapley**  
University of Illinois  
at Urbana–Champaign

**Douglas A. Smith**  
Concurrent Technologies Corporation

**L. Somasundaram**  
DuPont

**Michael D. Taylor**  
Parke-Davis Pharmaceutical Research

**William C. Walker**  
DuPont

**Peter Willett**  
University of Sheffield (England)

# Foreword

**T**HE ACS SYMPOSIUM SERIES was first published in 1974 to provide a mechanism for publishing symposia quickly in book form. The purpose of this series is to publish comprehensive books developed from symposia, which are usually “snapshots in time” of the current research being done on a topic, plus some review material on the topic. For this reason, it is necessary that the papers be published as quickly as possible.

Before a symposium-based book is put under contract, the proposed table of contents is reviewed for appropriateness to the topic and for comprehensiveness of the collection. Some papers are excluded at this point, and others are added to round out the scope of the volume. In addition, a draft of each paper is peer-reviewed prior to final acceptance or rejection. This anonymous review process is supervised by the organizer(s) of the symposium, who become the editor(s) of the book. The authors then revise their papers according to the recommendations of both the reviewers and the editors, prepare camera-ready copy, and submit the final papers to the editors, who check that all necessary revisions have been made.

As a rule, only original research papers and original review papers are included in the volumes. Verbatim reproductions of previously published papers are not accepted.

**ACS BOOKS DEPARTMENT**

# Preface

THE EXTRAORDINARY POTENTIAL OF FLUORINE-CONTAINING biologically relevant molecules in biology, medicinal chemistry, and medical applications has recently been recognized by researchers who are not in the traditional fluorine chemistry arena. This emerging new wave of fluorine chemistry at the biomedical interface is rapidly expanding its frontiers. Consequently, it is the right time for us to review the recent advances in this field and envision the exciting future developments.

Bioactive organofluorine compounds showing promise in medicinal–medical research in the last five years include (a) enzyme inhibitors for human immunodeficiency virus protease, renin, thymidylate synthase, DC–MTase, elastases, PLP-dependent enzymes, etc.; (b) fluoroprostacyclins and thromboxanes as antithrombotics; (c) anticancer agents, e.g., gemcitabine (a gem-difluorinated analog of deoxycytidine), MDL 101731 (a mechanism-based inhibitor of ribonucleotide diphosphate reductase), bicalutamide (a nonsteroidal antiandrogenic agent), RU58668 (a steroid showing a similar activity as tamoxifen), DD–003 (a vitamin D<sub>3</sub> analog), and fluorodocetaxels (fluoro analogs of Taxol); (d) antiviral agents, e.g., fluorodideoxythiacytidine, L–FMAU, WIN–63843, and fluorodeoxyguanosine; (e) antibacterials, e.g., sparfloxacin, tosufloxacin, levofloxacin, and a fluoro-2-pyridone antimicrobial agent, A–86719.1; (f) antimalarial agents, e.g., mefloquine, artemether, and arteflene; (g) antifungal agents, e.g., fluconazole, ICI–D0870, and flutrimazole; (h) central nervous system agents, e.g., fluoxetine hydrochloride, paroxetine (an antidepressant), dexfenfluramine (an anorectic agent), tacrine, zifrosilone cerebrocrast (a cognition enhancer for Alzheimer’s disease), fluvastatin sodium (an HMG–CoA reductase inhibitor, i.e., a hypolipidemic drug), tolrestat, zopolrestat (an aldose reductase inhibitor, i.e., an antidiabetic agent); and many others.

Fluorine-containing amino acids and other biomolecules are extremely useful as probes for investigating biomedical problems. For example, the recent development of <sup>19</sup>F NMR techniques combined with genetic engineering allow us to use fluorine-labeled amino acids as structural and dynamic probes for the study of membrane-associated proteins.

neurotransmission have been substantially advanced by the use of fluoroamine neurotransmitters and their precursors. Remarkable developments have been made in the use of tracers labeled with fluorine-18 ( $^{18}\text{F}$ ) for positron emission tomography (PET) studies in the neurosciences, especially of the brain and the heart in living systems. This powerful diagnostic method finds many critical medical applications.

Because of the increasing interest and excitement about the fluorine-containing compounds relevant to biomedical research, three divisions of the American Chemical Society (ACS) held three symposia in 1995. The ACS Division of Fluorine Chemistry asked Iwao Ojima to organize its symposium entitled "Fluoro-Amino Acids and Peptides in Medicinal Chemistry" in conjunction with the Division of Medicinal Chemistry at the 210th ACS national meeting in Chicago. I. Ojima is grateful for the support of this symposium from Great Lakes Chemical Corporation; F-TECH, Inc.; Asahi Glass Company; Central Glass Company; Merck and Company, Inc.; and Yuki Gosei Kogyo Company. For the ACS Division of Medicinal Chemistry, James R. McCarthy organized the symposium entitled "Fluorine in Drug Design" in conjunction with the ACS Division of Fluorine Chemistry at the 210th ACS national meeting. J. R. McCarthy gratefully acknowledges the financial contributions from Air Products and Chemicals, Inc.; Allied-Signal, Inc.; and Hoechst Marion Roussel, Inc. John T. Welch organized the symposium "Fluorine in Biological Chemistry" for the ACS at the Fourth International Chemical Congress of Pacific Basin Societies in Honolulu in conjunction with the Chemical Society of Japan (Tomoya Kitazume, co-organizer) and the Canadian Chemical Society (Stephen G. Withers, co-organizer).

This book is designed to be useful to researchers who want to take advantage of the unique properties of fluorine in biomedical research including rational drug design and syntheses, the use of fluorine probes for metabolic studies, the determination of protein structures, and the development of clinical diagnostic agents. The 23 chapters discuss a wide range of topics such as synthetic methods, fluoro-peptides and peptide mimetics, enzyme inhibitors, fluorosteroids and taxoids, fluorosugars and nucleosides, fluorine probes for biochemical problems using  $^{19}\text{F}$  NMR, and fluorine-containing biomolecules in neuroscience including  $^{18}\text{F}$  labels for PET studies. Most of the authors in this book were invited speakers in the three symposia upon which this book is based; the remaining chapters were contributed by leading chemists in their fields. This publication maps out the newest developments in this growing research field for synthetic chemists, medicinal chemists, biochemists, biologists, and other biomedical scientists worldwide.

The editors and authors sincerely hope that this book stimulates this growing and exciting field of research at the interface of fluorine chemistry, biology, and medicine.

IWAO OJIMA  
Department of Chemistry  
State University of New York at Stony Brook  
Stony Brook, NY 11794-3400

JAMES R. MCCARTHY  
Department of Medicinal Chemistry  
Neurocrine Biosciences, Inc.  
3050 Science Park Road  
San Diego, CA 92121-1102

JOHN T. WELCH  
Department of Chemistry  
State University of New York at Albany  
Albany, NY 12222

April 4, 1996

# Chapter 1

## Recent Advances in the Biomedical Chemistry of Fluorine-Containing Compounds

Kenneth L. Kirk<sup>1</sup> and Robert Filler<sup>2</sup>

<sup>1</sup>Laboratory of Bioorganic Chemistry, National Institute of Diabetes and Digestive and Kidney Diseases, National Institutes of Health, Building 8A, Room B1A-02, Bethesda, MD 20892

<sup>2</sup>Department of Biological, Chemical, and Physical Sciences, Illinois Institute of Technology, Chicago, IL 60616-3793

Recent developments in biomedical applications of fluorine-containing compounds are reviewed. Biochemical and mechanistic aspects of this field are discussed first. The development of enzyme inhibitors and other pharmacological tools and medicinal agents is considered from the point of view of how the special properties of fluorine can be exploited in analogue design. In the second part of this review, an array of recent medicinal candidates is described, encompassing drugs that show promise for the treatment of a variety of diseases. In both sections, the emphasis has been on material published within the past five years.

Substitution of fluorine into a molecule introduces minimal steric alterations, a fact that can facilitate interactions of a fluorinated biomolecule with enzyme active sites, receptor recognition sites, transport mechanisms, and other biological systems. In contrast, the introduction of fluorine as a highly electronegative center can alter significantly the physico-chemical properties of the molecule, often in a predictable way. This modification, in turn, can produce altered biological responses. Strategies based on these special properties of fluorine continue to result in the production of new and effective biochemical tools, and pharmacological and medicinal agents. The development of new fluorinating agents, and new procedures that modify the reactivities of fluorinating agents, have contributed greatly to the present rapid pace of advancement in this field.

An understanding of the underlying biochemical mechanisms involved, coupled with knowledge of the physico-chemical properties accompanying fluorine substitution, have aided in the rational design of many pharmacological agents and drugs. Fluorinated analogues also can be excellent probes for biochemical mechanisms. Applications include the use of chiral and prochiral fluorinated substrates to probe reaction stereochemistry and examination of effects of electronegative centers on reaction rates. Many <sup>19</sup>F-NMR studies have demonstrated the utility of fluorine labelled proteins as mechanistic tools.

0097-6156/96/0639-0001\$16.00/0  
© 1996 American Chemical Society



In the first part of our review, biochemical aspects of the biomedical chemistry of fluorinated compounds will be covered. Medicinal aspects of this field are then discussed, with emphasis on drugs that have been recently marketed, or are in the final phases of testing.

### Fluorine-Containing Enzyme Inhibitors.

The dual advantages of fluorine substitution in analogue design -- small steric changes coupled with large electronic changes -- has been very advantageous in the design of enzyme inhibitors. Selected examples of these strategies will be given in this section.

**Fluorine as a Deceptor ( $H^+$  vs.  $F^+$ ).** Loss of a proton is a frequent event in enzyme-catalyzed reactions. The functioning of fluorine as a "deceptor" in the prototypical anticancer drug, 5-fluorouracil, takes advantage of the fact that a similar loss of positive fluorine cannot occur.

**Thymidylate Synthase Inhibition.** In the thymidylate synthase-catalyzed synthesis of thymidine monophosphate from deoxyuridine monophosphate, the substrate, enzyme and tetrahydrofolic acid ( $CH_2FAH_4$ ) form a ternary complex. Dissociation of this complex and elimination of  $FAH_4$  to form product requires loss of the C-5 proton. If this proton is replaced by fluorine, the dissociation would require loss of  $F^+$ , an energetically impossible event (equation 1). 5-Fluorouracil ( $fl^5ura$ ), synthesized by Heidelberger and coworkers almost 40 years ago (1), is converted in vivo to 5-fluorodeoxyuridine monophosphate ( $fl^5dUMP$ ), fluorine fulfills its role as a "deceptor" molecule, and DNA-directed cytotoxicity results (2).  $Fl^5ura$  also is converted to the riboside and incorporated into several types of RNA, producing RNA-directed toxicity (3). Not only does  $fl^5ura$  remain an important anticancer drug, but the success of this lead compound, and results of research on the mechanisms of action of  $fl^5ura$ , have had broad influence on the development of other pyrimidine- and purine-based anticancer drugs.

**2'-Deoxycytidine-(5-methyl) (DC-MTase) Transferase Inhibition.** DC-MTase-catalyzed formation of 5-methyl-2'-deoxycytidine, the sole methylated nucleoside found in eukaryotes, is important in cell differentiation and regulation of gene expression. In a process mechanistically similar to the inhibition of thymidylate by  $fl^5dUMP$ , 5-fluoro-2'-deoxycytidine ( $fl^5dC$ ) irreversibly inhibits DC-MTase-catalyzed methylation of 2'-deoxycytidine (dC). In the catalytic cycle, addition of a catalytic SH group on the enzyme to the 6-position of the pyrimidine ring is followed by transfer of a methyl group from *S*-adenosyl methionine (AdoMet) to the 5-position of dC. C-5 proton loss and elimination of enzyme-SH produces the methylated product. However, in the case of the inhibitor, the presence of fluorine in  $fl^5dC$  blocks the final elimination of enzyme-SH and an irreversible enzyme-inhibitor complex is formed (equation 2) (4-6).

**Fluorine-Containing Protease Inhibitors.** Proteases not only play important roles in normal physiologic functioning of mammalian cells and tissues, they also are involved in a host of pathological processes as well. The development of specific, orally active protease inhibitor has become an important strategy for potential treatment of such

diverse illnesses as metastatic cancer, malaria, arthritis, sleeping sickness, AIDS, and others (7). In this work, incorporation of fluorine has been key to the development of several clinical candidates.

**Fluoroketone-Containing Reversible Inhibitors of Elastases.** Trifluoromethyl ketones are potent reversible inhibitors of proteases. The highly electrophilic ketone associates with the enzyme as a hydrate, a tetrahedral structure that mimics the transition state of normal bond cleavage. Alternatively, in a slower process, reaction of the free ketone with an enzyme-associated nucleophile may occur.

Particularly impressive results using trifluoromethyl ketones have been seen in the development of inhibitors of human leukocyte elastase (HLE). This very destructive serine protease, produced by neutrophils, is critical to the body's inflammatory defense mechanism. However, imbalances of extracellular elastase levels are associated with the pathogenesis of several diseases. Examples include rheumatoid arthritis, smoking-induced emphysema, and cystic fibrosis. For this reason, over the past decade there has been intense interest in the development of clinically effective elastase inhibitors (8).

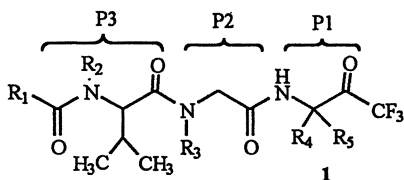
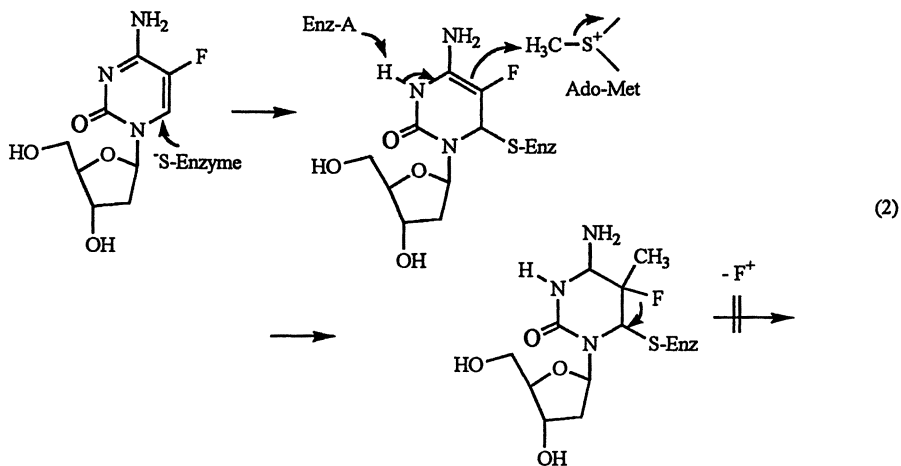
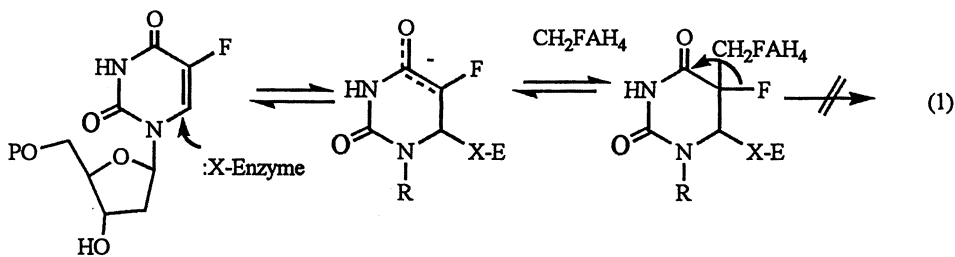
Several compounds in a series of tripeptide trifluoromethyl ketones **1** were potent and selective HLE inhibitors. This series features nonnaturally occurring *N*-substituted glycine residues at the P<sub>2</sub> position in place of Pro, present in many HLE inhibitors. The most active compounds, for example **1a**, had val-CF<sub>3</sub> at P<sub>1</sub> (9).

The Marion Merrell Dow group has incorporated tetra- and tripeptide recognition sequences into elastase inhibitors, using  $\alpha$ -diketone,  $\alpha$ -ketoesters, trifluoromethylketones, and pentafluoroethyl ketones as electrophilic centers at the carbonyl scissile bond site (10, 11). A major advantage of the pentafluoroethyl ketone series comes from the discovery that, in combination with certain *N*-protecting groups, this moiety confers oral bioavailability to the inhibitors.

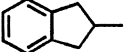
Research at ZENECA Pharmaceuticals also has produced trifluoromethyl ketone containing inhibitors that show high selectivity, and, in certain cases, oral bioavailability. The inhibitor ICI-200,355 (**2**) shows potent and sustained inhibition of elastase activity after intratracheal administration animal models, and has undergone clinical evaluation (12,13). This analogue, and other similar compounds, however, did not have oral activity. In recognition of the fact that peptidic compounds often suffer poor oral bioavailability, research was undertaken to replace the peptide portions of these inhibitors with mimetics. Modeling studies together with X-Ray data available from complexes of reversibly and irreversibly bound inhibitors and elastase were used to design non-peptide inhibitors, including a series of pyridone- (14) and  $\beta$ -carboline-containing trifluoromethyl ketones (15) (**3** and **4**, respectively).

In related research, increased affinity for the enzyme was realized by appropriate design of residues on both sides of the site corresponding to the scissile bond of the natural substrate. As with other protease inhibitors, the "difluorostatone" strategy was used. Structure **5** is a potent member of a series of inhibitors resulting from this work (16).

**Renin Inhibitors (the "Statine Strategy").** Renin is a highly specific aspartyl protease, secreted into the circulation by the kidneys, that cleaves the Leu-Val bond of angiotensinogen to produce angiotensin I, the precursor of the vasoconstricting peptide angiotensin II. Over the past 25 years an enormous amount of research has been directed



1a  $R_1 = p\text{-}[p\text{-Cl}(C_6H_4)SO_2NHCO](C_6H_4)\text{-}$ ,  $R_2 = H$ ,

$R_3 =$  ,  $R_4 = H$ ,  $R_5 = CH(CH_3)_3$

towards the development of specific inhibitors of renin as a strategy for treatment of hypertension (17). The vast amount of knowledge that has accumulated from these studies has assisted in the development of inhibitors of other aspartyl proteases, including HIV protease (see below).

Many transition state analogues have been prepared based on the structure of statine, a novel amino acid present in pepstatin, a naturally occurring pepsin inhibitor. A strategy introduced by Abeles in 1985 is based on the incorporation of difluorostatone in a peptide inhibitor at a site corresponding to the scissile bond of the natural substrate. Rapid onset of inactivation is among evidence that supports the hydrated form of the difluoro ketone as the inhibitory species.

Despite impressive progress in the development of potent and selective inhibitors based on difluoroketone and other transition state analogues, poor bioavailability has complicated clinical applications. Introduction of polar groups such as free amines to increase solubility often gave disappointing results, especially with lower molecular weight inhibitors. This has been attributed to the high solvation energy of the ammonium ion, energy that must be overcome in binding to the enzyme (17). Shirlin and coworkers recently have developed potent and selective inhibitors (for example, 6) based on the novel  $\beta$ -amino- $\alpha,\alpha$ -difluoroketone moiety. In this case, the difluoromethylene group serves to induce hydration of the ketone and in weakening the basicity of the amine function, the latter factor reducing the energy requirements for desolvation (18).

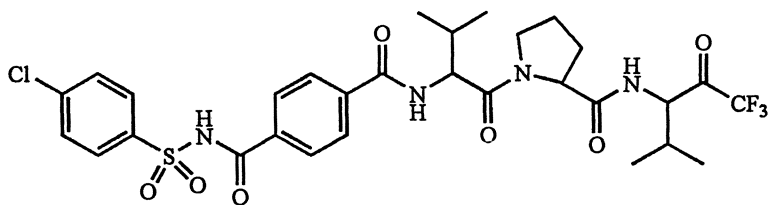
Doherty and coworkers found a series of fluoroketone inhibitors to have good oral activity. The difluoroketone 7, for example, was a potent member of this series (19).

**Fluorine-Containing HIV Protease Inhibitors.** The HIV-encoded protease, required for post-translational processing of polyprotein *gag* and *gag/pol* gene products, has attracted enormous attention as a potential chemotherapeutic target for treatment of HIV infection. The enzyme is an aspartyl protease that exists as a  $C_2$ -symmetric homodimer, with each monomer contributing a catalytic Asp to the active site. An important feature that must be addressed in the design of HIV protease inhibitors is that cellular penetration is a requirement for efficacy. Thus, small, lipophilic molecules become more attractive (20).

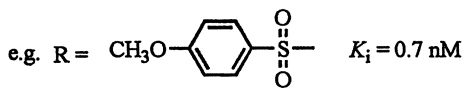
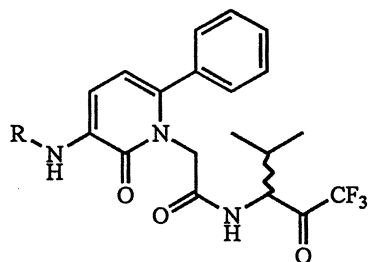
Difluoroketone inhibitors, included in a series of hepta- and hexapeptide substrate analogues reported by Dreyer and coworkers, were found to be potent competitive inhibitors of HIV protease (21), clearly demonstrating the validity of the difluorostatone approach. New inhibitors based on the difluorostatone type transition state mimic have been reported recently by the Marion Merrell Dow group. Small and potent dipeptide inhibitors were based on the lead structure 8 (22). Refinements in structure, including addition of a *p*-benzyloxy group and introduction of an unnatural *R*-valinol ether, resulted in the inhibitor 9 having high potency and low toxicity in HIV-infected cells (23).

Examples of potent low molecular weight fluoroketone inhibitors have been reported by Sham and coworkers. In most cases, these inhibitors, exemplified by structure 10, contained only a single amino acid. These inhibitors blocked the cytopathic effect of HIV *in vitro* (24).

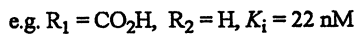
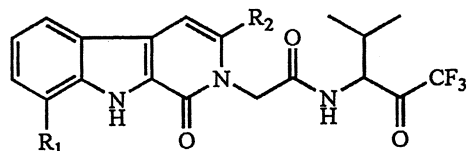
To exploit the  $C_2$ -symmetry resident in the homodimeric HIV-protease, Sham and coworkers prepared the pseudo  $C_2$ -symmetric difluoroalcohol and difluoroketone mimics 11 and 12 of the Phe-Pro cleavage site. Both were potent HIV protease inhibitors (1.0 and 0.1 nM, respectively) (25).



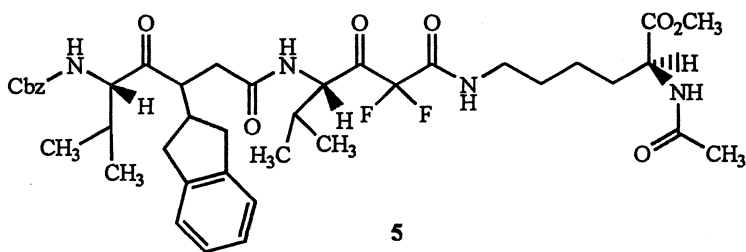
2



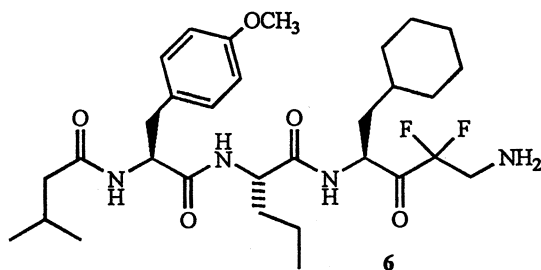
3



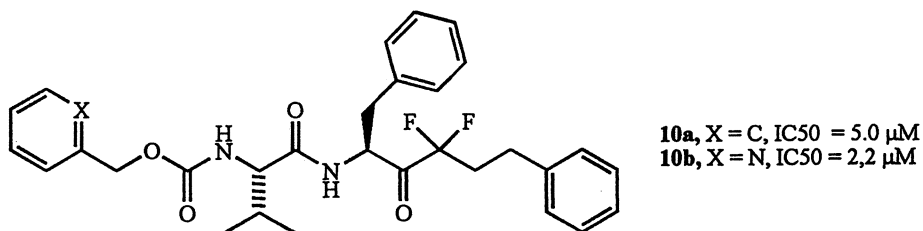
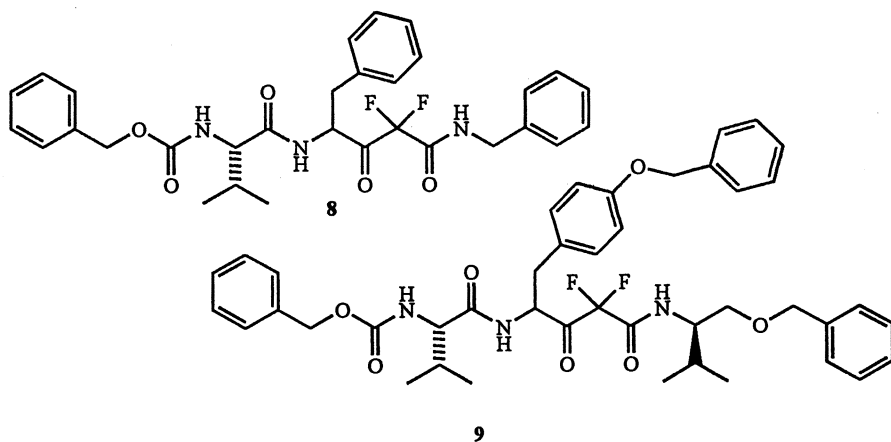
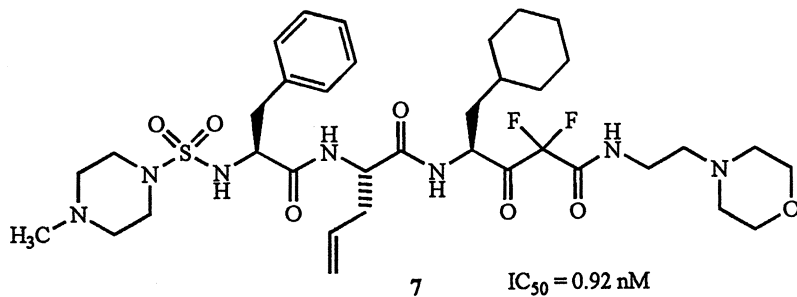
4



5



6



**Peptidylfluoroketones as Irreversible Inhibitors of Proteases.** Unlike the trifluoromethyl- or difluoromethylene ketones described above, fluoromethyl ketones often function as irreversible protease inhibitors as a result of displacement of fluoride by an enzyme-associated nucleophile. New synthetic strategies developed over the past 10 years were important in the development of fluoromethyl ketones as irreversible inhibitors of several proteolytic enzymes, including renin, chymotrypsin, elastase, and cathepsin (6). As with the reversible inhibitors described above, recognition sites are designed into the peptide portion of the molecule.

Biological evaluation of fluoromethyl ketone inhibitors have been extended to animal studies that suggest clinical applications may be realized, especially as targeted to cysteine proteases. Advantages noted with the new fluoromethyl ketone-derived inhibitors include the fact that they are highly specific, show little toxicity to mammalian cells or to animals, no mutagenicity, and can be given orally. Selected examples of applications will be given.

Cathepsin B is a cysteine protease capable of degrading collagen and proteoglycan. This enzyme also is present in the synovial fluid and synovial lining of patients with rheumatoid arthritis, suggesting that cathepsin B may contribute to destruction of extracellular matrix of cartilage and bone symptomatic of this disease. Oral administration of the peptidyl fluoromethylketone, (Z)-L-phenylalanine-L-alanine-CH<sub>2</sub>F (MDL 201,117), a potent inhibitor of human cathepsin, significantly reduced the clinical severity of symptoms of adjuvant-induced arthritis in rats (26).

The murine malaria parasite *Plasmodium vinckei* produces a cysteine protease that is thought to be responsible for the degradation of hemoglobin, the principal source of amino acids for parasite growth. A potent member in a series of inhibitors of this protease, morpholine urea (Mu)-Phe-Homophenylalanine-CH<sub>2</sub>F, gave 80% long term cures when administered for four days to *P. vinckei* infected mice. This has added significance in the fact that a similar cysteine protease appears to have an analogous role with *Plasmodium falciparum*, the parasite in humans (27).

Proteolytic activity of *Trypanosoma cruzi* also has been associated with a cathepsin-like cysteine protease. Peptidyl fluoromethyl ketones (Z-Phe-Ala-CH<sub>2</sub>F and Z-Phe-Arg-CH<sub>2</sub>F) also disrupt the life cycle of this parasite in cultured human cells (28).

**Pyridoxal Phosphate (PLP)-Dependent Enzymes.** Exemplified by the seminal work of Kollonitsch and coworkers, a host of fluorinated irreversible inhibitors of PLP-dependent enzymes have been developed. Mechanism-based inhibition is initiated by extrusion of fluorine situated adjacent to the site of negative charge formation required in these reactions (29). From this work have come clinically promising drugs, for example, DFMO, 13, and related analogues that are inhibitors of polyamine biosynthesis and have activity against microorganisms (30).

**Inhibitors of SAH Hydrolase.** S-Adenosylmethionine (AdoMet) serves as the methyl donor in many critical biological methylations. Loss of the methyl group from AdoMet produces S-adenosylhomocysteine (SAH), a feedback inhibitor of many methyl transferase enzymes. Inhibition is relieved by the action of SAH hydrolase, which converts SAH to

homocysteine and adenosine by the mechanism shown in equation 3. Inhibitors of SAH hydrolase have been shown to have antiviral activity through accumulation of SAH, the presence of which represses viral mRNA methylation necessary for viral replication. The Merrell Dow group has prepared a mechanism-based inhibitor **14** based on the proposal that oxidation of **14** would produce the intermediate  $\beta$ -fluoro- $\alpha,\beta$ -unsaturated ketone. Addition of enzyme nucleophile and elimination of fluoride would result in irreversible inhibition of the enzyme (equation 4) (31). Studies by Borchardt and coworkers have shown the actual mechanism to involve hydrolysis of the vinyl fluoride to the 5'-carboxaldehydes (32).

### Increased Hydrolytic Stability of Fluorinated Analogues.

Certain functional groups that are found in biomolecules are quite susceptible to hydrolysis, some at neutral, physiological pH, and even more so at the pH of stomach acid. Examples include such moieties as enol ethers, ketals, and glycosidic bonds. In efforts to increase biological half-life or to provide analogues of drugs that are suitable for oral delivery, introduction of fluorine proximal to a site where protonation initiates acid hydrolysis has proven to be quite successful.

**Fluorinated Prostacyclins and Thromboxane.** Fluorine substitution has been used effectively to increase the hydrolytic stability of prostacyclin (PGI<sub>2</sub>) and thromboxane (TXA<sub>2</sub>). PGI<sub>2</sub>, a potent inhibitor of platelet aggregation, has a  $t_{1/2}$  of two-three min while TXA<sub>2</sub>, which contracts the aorta and induces platelet aggregation, has a  $t_{1/2} = 30$  s at 37°. In contrast, 7-fluoro-PGI<sub>2</sub> (**15**) for example, has a half-life of one month in pH 7.4 buffer (33). Matsumura and coworkers have reported that fluoro-PGI<sub>2</sub> analogues (for example, **16**) having modified side chains are highly potent and orally active anti-anginal agents (34). The hydrolytically stable 10,10-difluoro-TXA<sub>2</sub> (**17**) was four to five times more potent than TXA<sub>2</sub> with respect to stimulation of platelet aggregation (35). Moreover, using difluoro-TXA<sub>2</sub>, differential effects on platelet aggregation and aorta were observed (36).

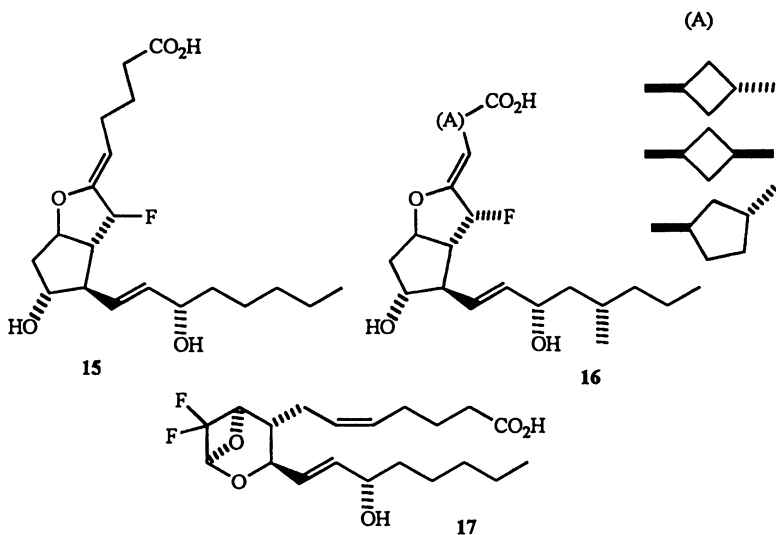
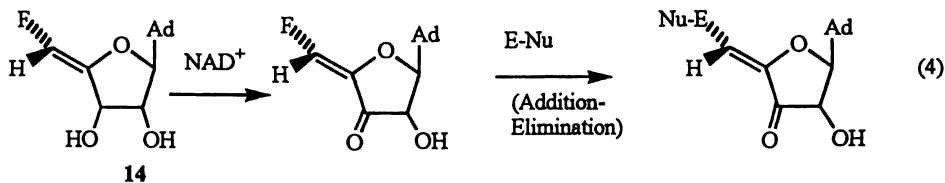
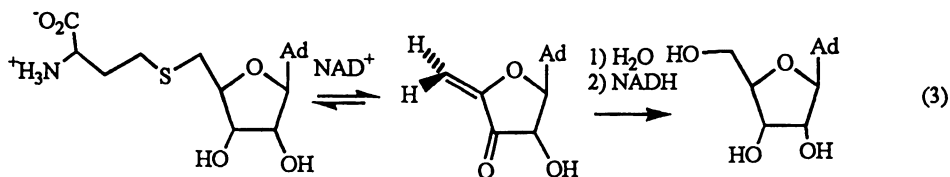
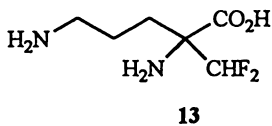
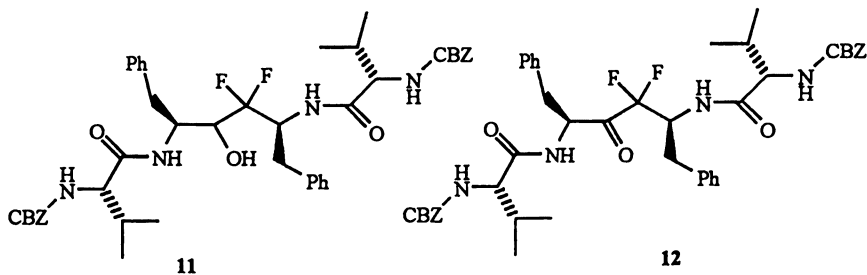
**2'-Deoxy-2-fluoronucleosides.** 2',3'-Dideoxynucleosides, including dideoxyadenosine (ddA), have shown promise as anti-HIV agents. There has been recent attention given to 2'- $\beta$ -fluorodideoxynucleosides, in part because of the much greater acid stability of these analogues. For example, 2'- $\beta$ -fluoro-dideoxyadenosine (**18**), equipotent with ddA, is acid stable, its rate of deamination relative to that of ddA is much slower, and has lower cellular toxicity (37,38). This, and related work, is covered in another chapter in this monograph.

### Fluorinated Analogues as Mechanistic Probes.

The ability of a fluorine substituent to inhibit incipient positive charge formation has been used very effectively to determine mechanistic details of enzyme-catalyzed reactions.

**Terpene Biosynthesis.** Fluorinated analogues have been used skillfully by Poulter and coworkers in their classic studies on the mechanism of terpene biosynthesis (39). Similar





strategies are being used to probe mechanistic details of other steps in the isoprenoid biosynthetic pathway.

**Peptidoglycan Biosynthesis.** UDP-GlcNAc enolpyruvyl transferase (MurZ) catalyzes the condensation of phosphoenolpyruvate and UDP-GlcNAc to form enol-pyruvyl-UDP-GlcNAc in the first committed step in the synthesis of the peptidoglycan layer of bacterial cell wall. A second enzyme (MurB) reduces the product to UDP muramic acid. Walsh and coworkers recently have studied several details of the MurZ-catalyzed reaction using *Z*- and *E*-3-fluorophospho-enolpyruvate (F-PEP). Using *E*-FPEP, two covalent products were isolated, including the intermediate fluoromethyl phosphate ester **19**. The inability of this intermediate to eliminate phosphate reflects a high energy barrier to proton abstraction in a stepwise E<sub>1</sub> mechanism. The authors attribute this barrier to "insurmountable destabilisation" of a carbonium ion centered on the carbon adjacent to the fluoromethyl group (equation 5) (40,41). In related research, advantage was taken of the chirality imposed by fluorine substitution to determine the stereochemistry of the addition of UDP-GlcNAc to phosphoenolpyruvate (42)

### CF and CF<sub>2</sub> as Replacements for O.

Phosphate esters are ubiquitous and important biological structures. Replacement of oxygen with CF<sub>2</sub> or CHF give hydrolytically stable analogues which, moreover, have electronic characteristics comparable to the parent phosphate. Recent highlights of work in this area include research dealing with the very important process of protein phosphorylation, a process that plays an important role in intracellular signal transduction. For example, binding of phosphotyrosine-containing proteins to the SH moiety in certain cytoplasmic proteins is crucial for signaling pathways of tyrosine kinase growth factor receptor. Two groups have reported the synthesis of the difluoromethylene phosphonate isostere **20** of phosphotyrosine (43,44). Likewise, the difluorophosphonate analogue **21** of phosphoserine has recently been synthesized. This is a potential inhibitor of phosphatase activity involved in signal transduction events (45,46). The difluoromethylene phosphonate analogue **22** of the ubiquitous phosphoenolpyruvate has been reported. This compound can function as a Michael acceptor, and has been found to inhibit EPSP synthase in a time dependent manner (47).

### Medicinal Aspects

The use of fluorine-containing compounds in medicine is now commonplace. The arsenal of such chemotherapeutic agents has expanded steadily over a forty year period and at a phenomenal rate during the past decade. It is known that factors, such as the relatively small size of fluorine, its electronegativity, its participation as a hydrogen acceptor, and enhanced lipophilicities of F- and CF<sub>3</sub>-substituted aryl compounds often contribute to improved therapeutic efficacy. While the basis for the routine introduction of fluorine at various molecular sites has been largely empirical, it is now feasible to understand the role of fluorine by a more rational approach, using mechanistic and physicochemical principles. We recommend an excellent contribution to this approach which was published recently (48). In our review, however, we continue to focus on developments in which

organofluorine compounds are significant players in the treatment of specific diseases and medical conditions. Since the most recent publications on this subject (49,50) include material through the early 1990's, this review will emphasize important advances since 1992, including newly marketed drugs, those in human trials, and other promising leads.

**Anticancer Agents.** Gemcitabine (Gemzar, Lilly) (23), a gem-difluorinated analogue of deoxycytidine, was initially prepared as a promising antiviral compound, but exhibited a narrow therapeutic index. It is now emerging as a leading drug in the treatment of human solid tumors, especially non-small cell lung and pancreatic cancer (51). The drug has been approved for use against lung cancer in Europe and South Africa. It is now available in the United States to patients with advanced pancreatic cancer who are not candidates for surgery. Full FDA approval is expected in early 1996.

Another drug candidate, MDL 101731 [(E)-2'-deoxy-2'-(fluoromethylene)cytidine] (24) (52,53), is a precursor of a mechanism-based inhibitor of ribonucleotide diphosphate reductase, an enzyme that catalyzes the rate-determining step in DNA biosynthesis. While still in early stages of human clinical trials, this compound appears to be promising for the treatment of solid tumors: breast, prostate, lung, and colon. The (Z)-isomer also exhibits activity.

The non-steroidal antiandrogenic agent bicalutamide (Casodex, Zeneca) (25) is in phase III trials for the treatment of advanced prostate cancer, especially in combination with luteinizing hormone-releasing hormone (LHRH) analogues or surgical castration. Application for FDA approval has been made (54,55).

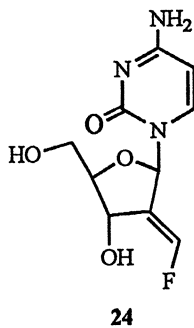
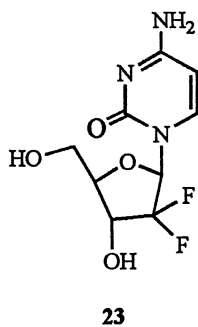
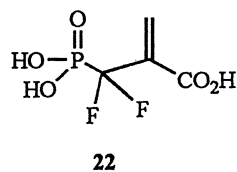
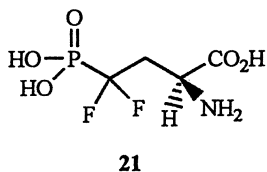
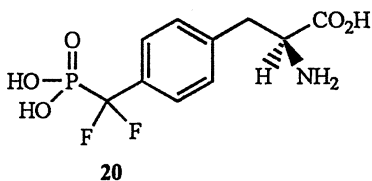
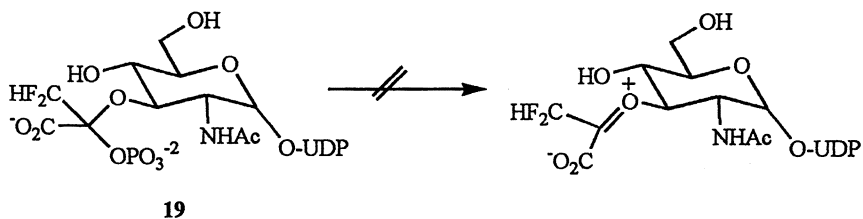
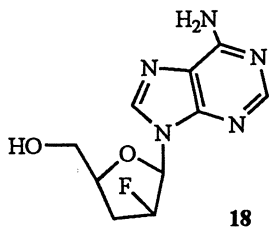
While tamoxifen is now the leading agent in the treatment of estrogen-dependent breast cancer, there is considerable interest in the highly substituted steroid RU58668 (26), which exhibits potent antitumor activity in vivo on estrogen-dependent human breast tumors implanted in mice (56).

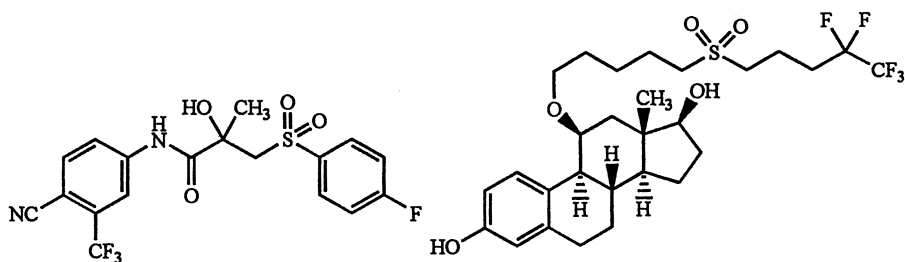
In early studies, a hexafluoro analogue of 1,25-dihydroxyvitamin D<sub>3</sub>, DD-003 (27) suppressed the growth of human colon cancer (adenocarcinoma) implanted in mice (57). As a spin-off of the successful fluoroquinolone antibacterials (vide infra), several related quinobenoxazines have demonstrated significant antitumor activity in vitro and in vivo. One of this series, A-84441 (28), a norvaline prodrug of 29 has shown promising preliminary activity and is being evaluated intensively (58,59).

**Antiviral Agents.** The evaluation of fluoro-substituted pyrimidine and purine nucleosides as antiviral agents continues at a brisk pace. Efforts to identify potentially effective inhibitors of human immunosuppressive virus-1 (HIV-1), the putative cause of acquired immune deficiency syndrome (AIDS), are being pursued aggressively. Although further studies of 2',3'-dideoxy-3'-fluorothymidine (Alovudine, Lederle) (30) are encouraging (60), progress remains slow. Another potential therapeutic agent against HIV is (-)-2',3'-dideoxy-5-fluoro-3'-thiacytidine (FTC) (31), which has been shown to be an extremely potent and selective inhibitor of HIV replication in vitro and in vivo (61).

Unusual structural features of 31 are the oxathiolane ring and the 1-β-L-configuration, rather than the 1-β-D- found in natural nucleosides. Phase I clinical trials have recently been completed in the United States.

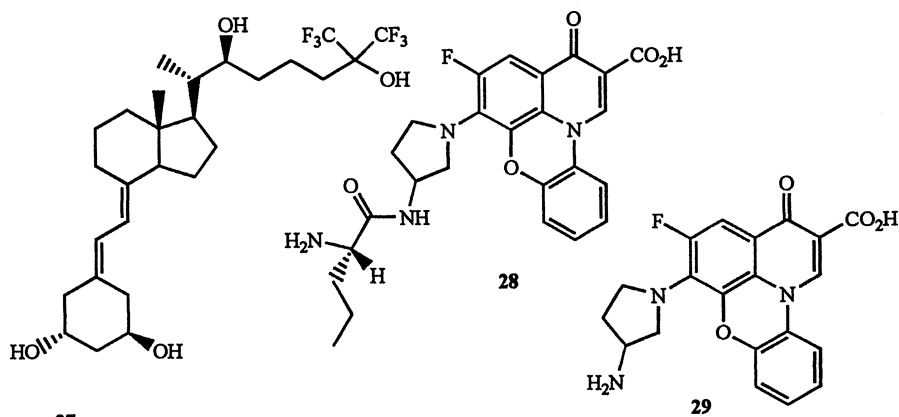
Hepatitis B virus (HBV) is a worldwide health threat. Although several nucleosides have been reported to be anti-hepatitis B virus (anti-HBV) agents, none have





25

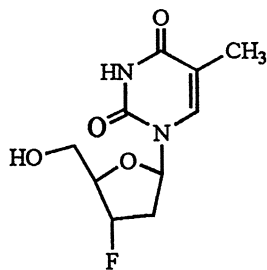
26



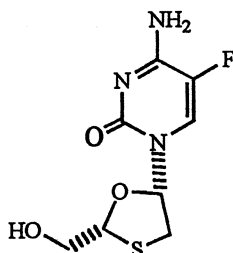
27

28

29



30



31

yet been shown to be clinically useful. Recently, there have been a couple of promising leads, including compound **31**, which, after phase I clinical trials, shows strong and selective inhibition of replication of HBV, as well as HIV (61). Another compound with the unnatural L-configuration, 2'-fluoro-5-methyl- $\beta$ -L-arabinofuranosyluracil (L-FMAU) (**32**) has been found to be a potent anti-HBV and anti-Epstein-Barr virus agent (62).

As part of extensive studies directed at the treatment of the common cold, a fluorine-containing antiviral agent, WIN-63843 (**33**), exhibits significant activity against picornaviruses, especially human rhinoviruses. The most distinctive feature of this compound is the unprecedented and not yet fully understood "global" protective metabolic effect of the trifluoromethyl group on the oxadiazole ring (63). The improved metabolic stability results in a substantial increase in oral bioavailability.

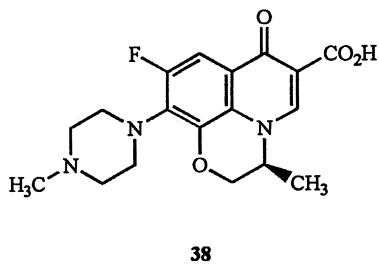
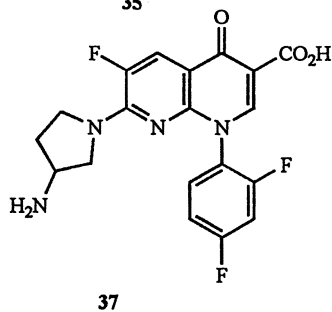
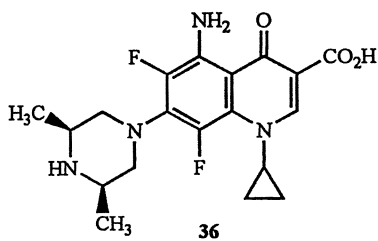
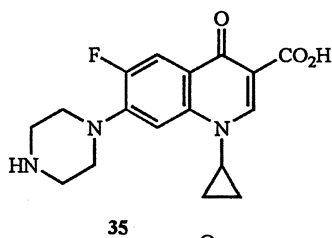
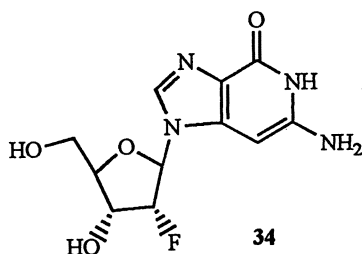
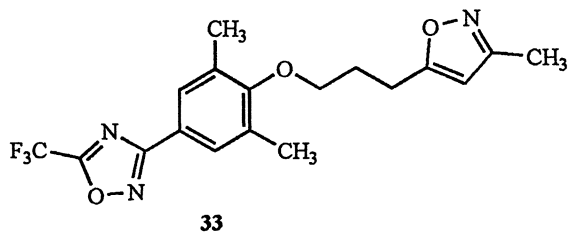
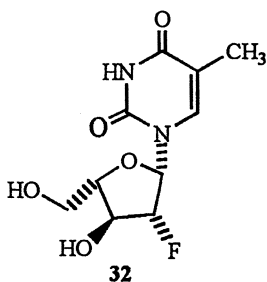
2'-Deoxy-2'-fluoroguanosine (**34**) is very active in inhibiting influenza viruses, particularly in human respiratory epithelial cells (64).

**Antibiotics.** The discussion will cover antibacterials, a new antimalarial drug, and antifungal agents.

**Antibacterials.** The fluoroquinolone and naphthyridine carboxylic acids, inhibitors of the DNA gyrase bacterial enzyme, continue to be major players in combating bacterial infections. They exhibit broad spectrum activity against various aerobic and anaerobic gram-positive and gram-negative organisms. There is a steady flow of new entries in the marketplace, with many others at various stages of clinical trials. Ciprofloxacin [Bayer] (**35**), the market leader in late 1995, is useful in upper respiratory and urinary tract infections. Sparfloxacin (**36**), used for community acquired and surgical infections and Tosufloxacin (**37**) are representative examples. The soon to be introduced Levofloxacin [Daiichi] (**38**), the S-isomer of Ofloxacin, is especially effective in lower respiratory, urinary tract, and prostate infections and in treating sexually transmitted diseases (65). The classification and structure-activity relationships of fluoroquinolones have been reviewed (66).

A novel class of 2-pyridone antimicrobial agents, which like the fluoroquinolones, inhibits bacterial DNA gyrase, has been described recently (67). At this early stage, the most effective member of this class, A-86719.1 (**39**), possesses potent antibacterial activity *in vitro*, but is also sensitive to bacteria resistant to ciprofloxacin, such as *Staph. aureus* and enterococci. Since the basic ring structure of **39** differs from those of the quinolones and naphthyridines, it may bind differently at the enzymatic site.

**Antimalarial Drugs.** Malaria is caused by parasitic protozoa, primarily *Plasmodium falciparum*. The treatment of malaria has become more difficult because of increasing resistance in *Plasmodium* against almost all existing antimalarial drugs. While mefloquine (**40**) is still the leading drug, when used singly or in combination with chloroquine, resistance is growing, prompting the search for alternatives. In studies of Chinese herbs used for treatment of malaria, two endoperoxide compounds were identified. A derivative of one, artemether (**41**) was introduced in China in 1992 (68). Arteflene [Hoffmann-La Roche] (**42**), a synthetic derivative of the other natural compound, has been tested *in vitro* and *in vivo* and is under further development, due to its promising biological pharmacokinetics and toxicological profile (68).



**Antifungal Agents.** Fluoroaryl-substituted triazoles have emerged in recent years as the dominant group of stable, orally-active and topical antifungal agents. The bis-triazole fluconazole [Diflucan] (**43**), which inhibits fungal ergosterol synthesis, has been very effective in dermal, vaginal, and other infections (*69*). Though first introduced in 1988, resistance to this drug is slowly increasing. A new antifungal, ICI-D0870 (**44**) shows significant activity and is receiving much attention when used singly or in combination with fluconazole or flucytosine, which has been used since the early 1980s (*70,71*). Flutrimazole (**45**) is an effective topical agent. Other promising agents are under investigation and a review of the subject has been published in 1995 (*72*).

**Central Nervous System (CNS) Agents.** While the pace of new developments of fluorine-containing CNS agents has slowed after the great successes of the past few decades, several recent advances are noteworthy.

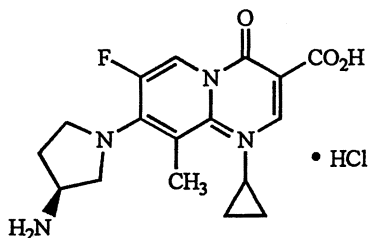
**Antidepressants.** Fluoxetine hydrochloride [Prozac, Lilly] (**46**) continues to be widely used for treatment of major depression. It has now received FDA approval for the treatment of obsessive-compulsive disorder (*73*). Paroxetine (**47**), introduced in 1991, also a highly selective serotonin reuptake inhibitor, exhibits activity similar to fluoxetine, but with a shorter duration of action.

**Anorectic Agents.** An FDA advisory committee has voted for approval of fluoxetine in the treatment of bulimia (*73*). Fenfluramine has been available for many years as an anti-obesity drug. Dexfenfluramine (**48**), the S enantiomer, has found wide favor in Europe and is awaiting final approval in the United States. The use of a combination of phentermine (an analogue of amphetamine) and fenfluramine ("phen/fen") is also increasing.

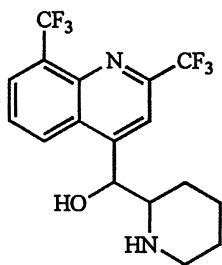
**Cognition Enhancers.** Studies are accelerating to identify drugs which counter cognitive dysfunction, especially in chronic neurodegenerative conditions, such as Alzheimer's and other dementia. Tacrine (**49**), a reversible inhibitor of acetylcholinesterase was the first drug launched (1993) specifically for treatment of Alzheimer's. A number of other inhibitors are now being evaluated. Zifosilone (MDL-73745) (**50**), one of a series of trimethylsilyl trifluoromethyl ketones, reacts very rapidly with the active site of acetylcholinesterase, while providing a highly lipophilic residue which increases brain penetration. Compound **50** is under development as a potential drug for treatment of Alzheimer's (*74*). Preliminary studies indicate that Cerebrocrast (**51**), a difluoromethoxy-1,4-dihydropyridine derivative is a highly active and long-lasting brain function enhancer (*75*). The underlying cause of the dementing process is not altered by use of these drugs.

**Hypolipidemic Drugs.** A new class of synthetic HMG-CoA reductase inhibitors, many of which contain p-fluorophenyl groups, are being designed as dietary adjuncts for lowering total and low-density lipoprotein (LDL) cholesterol and serum triglyceride levels (*76*). Fluvastatin sodium (**52**), brought to market in 1994, has more potent effects than lovastatin, one of the leading drugs prescribed for this purpose (*77*).

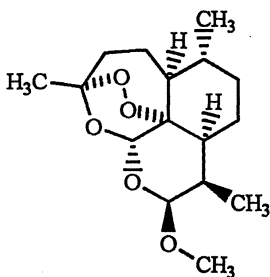




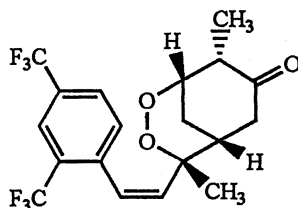
39



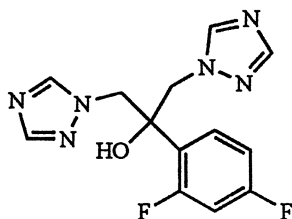
40



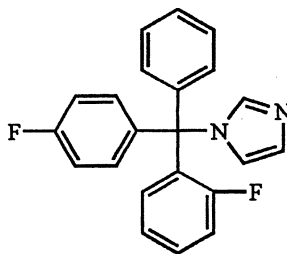
41



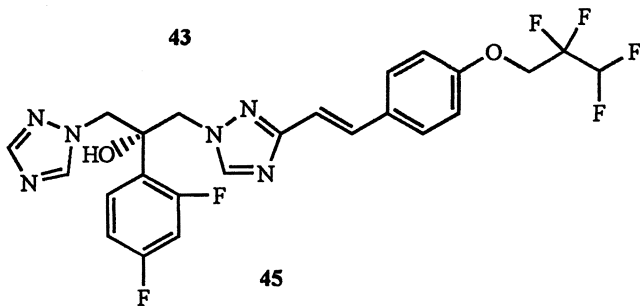
42



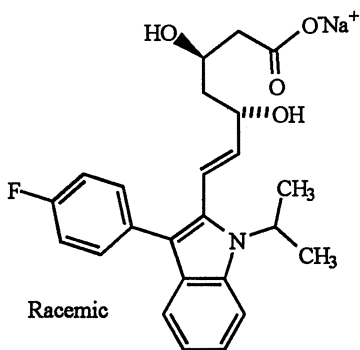
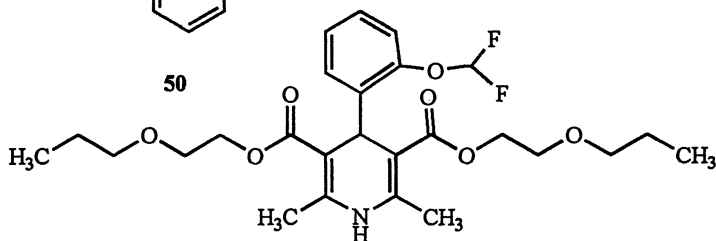
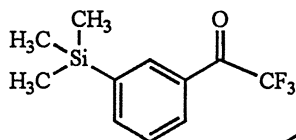
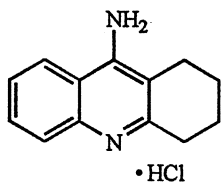
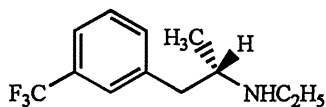
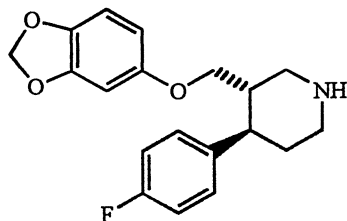
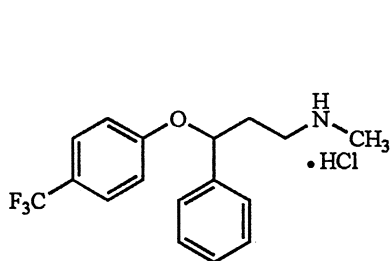
43



44



45



**Antidiabetics.** The first long-acting aldose reductase inhibitor (ARI), tolrestat (53), available since 1989, is useful for the management of diabetic complications: neuropathy, retinopathy and cataracts. In this active area of research, a number of other fluoroaryl ARIs are currently in clinical trials. Especially promising is zopolrestat (54), which is in phase III trials for the prevention of serious complications of both insulin dependent diabetes mellitus (IDDM) and non-insulin dependent diabetes (NIDDM) (78).

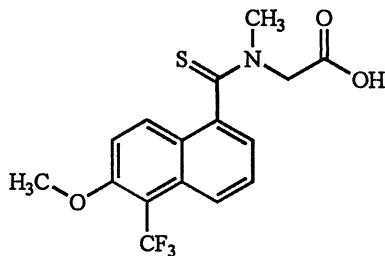
**Fluorinated Liposomal Membranes.** The vast research efforts by Riess and coworkers during the past twelve years has led to fluorinated ( $C_nF_{2n+1}$ ) amphiphiles for use as components of liposomal membranes and vesicles. Fluorinated moieties are much more hydrophobic than their hydrocarbon counterparts, have a larger cross section, are more rigid, and are also lipophobic. Fluorinated amphiphiles tend to self-assemble, with increased membrane ordering. Stacking creates a teflon-like repellent film within the liposomal membrane, which increases drug encapsulation stability. An excellent review, published in 1995, is highly recommended (79).

### Other Applications of Fluoroorganics in Medicine

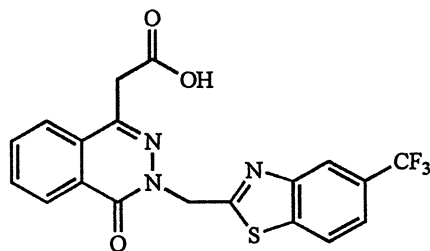
A wide array of fluorine-substituted compounds, beyond those already discussed, are used in medical applications. Several examples of new drugs or applications are listed in Table 1.

Table 1. Selected Fluorine-Containing Drugs

Compound	Application
Halobetasol propionate	potent topical antiinflammatory steroid
Fluticasone propionate (Flonase)	glucocorticosteroid for treatment of rhinitis and asthma
Riluzole (Rilutek)	glutamate release inhibitor for treating amyotrophic lateral sclerosis (ALS)
Desflurane	inhalation general anesthetic
Flosequinan (Manoplax)	cardiostimulant
Pantoprazole sodium (Pantozol)	irreversible proton pump inhibitor, antiulcer agent
Fluoxymesterone	steroidal androgen used to increase stature of short boys
Mofegiline.HCl(MDL-72974A)	treatment of Parkinson's disease (Phase III trials)



53



54

### Literature cited

1. Heidelberg, C.; Chaudhuri, N. K.; Danneberg, P.; Mooren D.; Griesbach, L.; Duschinsky, R.; Schnitzer, R. J.; Plevin, E.; Schneiner, J. *Nature* **1957**, *179*, 663-666.
2. Santi, D. V.; McHenry, C. S. *Proc. Natl. Acad. Sci. USA* **1972**, *69*, 1855-1857.
3. For a review, see Kirk, K. L. *Biochemistry of Halogenated Organic Compounds*, *Biochemistry of the Elements*, Vol. 9B; Plenum, New York, NY, 1991, pp 127-150.
4. Chen, L.; MacMillan, A. M.; Verdine, G. L. *J. Am. Chem. Soc.*, **1993**, *115*, 5318-5319.
5. Chen, L.; MacMillan, A. M.; Chang, W.; Ezaz-Nikpay, K.; Lane, W. S.; Verdine, G. L. *Biochemistry* **1991**, *30*, 11018-11025.
6. Osterman, D. G.; DePillis, G. D.; Wu, J. C.; Matsude, A.; Santi, D. V. *Biochemistry* **1988**, *27*, 5204-5210.
7. For a concise review, see Roose, J. P.; Van Noorden, J. F. *J. Lab. Clin. Med.* **1995**, *125*, 433-441.
8. For a review, see Edwards, P. D.; Berstein, P. R. *Med. Res. Rev.* **1994**, *14*, 127-194.
9. Skiles, J. W.; Fuchs, V.; Miao, C.; Sorcek, R.; Grozinger, K. G.; Mauldin, S. C.; Vitous, J.; Mui, P. W.; Jacober, S.; Chow, G.; Matteo, M.; Skoog, M.; Weldon, S. M.; Posanza, G.; Keirns, J.; Letts, G.; Rosenthal, A. S. *J. Med. Chem.* **1992**, *35*, 641-662.
10. Burkhart, J. P.; Koehl, J. R.; Mehdi, S.; Durham, S. L.; Janusz, M. J.; Huber, E. W.; Angelastro, M. R.; Sunder, S.; Metz, W. A.; Shum, P. W.; Chen, T.-M.; Bey, P.; Cregger, R. J.; Peet, N. P. *J. Med. Chem.* **1995**, *38*, 223-233.
11. Angelastro, M. R.; Baugh, L. E.; Bey, P.; Burkhart, J. P.; Chen, T.-M.; Durham, S.; Hare, D. M.; Huber, E. W.; Janusz, M. J.; Koehl, J. R.; Marquart, A. L. *J. Med. Chem.* **1994**, *37*, 4538-4554.
12. Sommerhoff, C. P.; Krell, R. D.; Williams, J. C.; Gomes, B. C.; Strimpler, A. M.; Nadel, J. A. *Eur. J. Pharmacol.* **1991**, *193*, 153-158.
13. Auger, W. R.; Moser, K. M.; Comito, R. M.; Kerr, K. M.; Bernardi, J. L.; Spragg, R. G. *Am. Respir. Crit. Care Med.* **1944**, *149*, 1032.
14. Bernstein, P. R.; Andisik, D.; Bradley, P. K.; Bryant, C. B.; Ceccarelli, C.; Damewood, J. R., Jr.; Earley, R.; Edwards, P. D.; Fenney, S.; Gomes, B. C.;

- Kosmider, B. J.; Steelman, G. B.; Thomas, R. M.; Vacek, E. P.; Veale, C. A.; Williams, J. C.; Wolanin, D. J.; Woolson, S. A. *J. Med. Chem.* **1994**, *37*, 3313-3326.
15. Veale, C. A.; Damewood, J. R., Jr.; Steelman, G. B.; Bryant, C.; Gomes, B.; Williams, J. *J. Med. Chem.* **1995**, *38*, 86-97.
16. Skiles, J. W.; Miao, C.; Sorek, R.; Jacober, S.; Mui, P. W.; Chow, G.; Weldon, S. M.; Possanza, G.; Skoog, M.; Keirns, J.; Letts, G.; Rosenthal, A. S. *J. Med. Chem.* **1992**, *35*, 4795-4808.
17. For a review, see Greenlee, W. *J. Med. Res. Rev.* **1990**, *10*, 173-236.
18. Shirlin, D.; Tarnus, C.; Baltzer, S.; Rémy, J. M. *Bioorg. Med. Chem. Lett.* **1992**, *2*, 651-654.
19. Doherty, A. M.; Sircar, I.; Kornberg, B. E.; Quinn, J., III; Winters, R. T.; Kaltenbronn, J. S.; Taylor, M. D.; Batley, B. L.; Rapundalo, S. R.; Ryan, M. J.; Painchaud, C. A. *J. Med. Chem.* **1992**, *35*, 2-14.
20. For a review, see Drake, P. L.; Huff, J. R. *Adv. Pharmacol.* **1994**, *25*, 399-454.
21. Dreyer, G. B.; Metcalf, B. W.; Tomaszek, T. A., Jr.; Carr, T. J.; Chandler, A. C., III; Hyland, L.; Fakhoury, S. A.; Magaard, V. M.; Moorek M. L.; Strickler, J. E.; Debouck, C.; Meek, T. D. *Proc. Natl. Acad. Sci. USA* **1989**, *86*, 9752-9756.
22. Schirlin, D.; Baltzer, S.; Van Dorsselaer, V.; Weber, F.; Weill, C.; Altenburger, J. M.; Neises, B.; Flynn, G.; Rémy, J. M.; Tarnus, C. *Bioorg. Med. Chem. Lett.* **1993**, *3*, 253-258.
23. Shirlin, D.; Van Dorsselaar, V.; Tarnus, C.; Taylor, D. L.; Tyms, A. S.; Baltzer, S.; Weber, F.; Remy, J. M.; Brennan, T.; Farr, R.; Janowick, D. *Bioorg. Med. Chem. Lett.* **1994**, *4*, 241-246.
24. Sham, H. L.; Betebenner, D. A.; Wideburg, N. E.; Saldivar, A. C.; Kohlbrenner, W. E.; Vasavanonda, S.; Kempf, D. J.; Norbeck, D. W.; Zhao, C.; Clement, J. J.; Erickson, J. E.; Plattner, J. J. *Biochem. Biophys. Res. Commun.* **1991**, *175*, 914-919.
25. Sham, H. L.; Wideburg, N. E.; Spanton, S. G.; Kohlbrenner, W. E.; Betebenner, D. A.; Kempf, D. J.; Norbeck, D. W.; Plattner, J. J.; Erickson, J. W. *J. Chem. Soc., Chem. Commun.* **1991**, 110-112.
26. Esser, R. E.; Watts, L. M.; Angelo, R. A.; Thornburg, L. P.; Prior, J. J.; Palmer, J. T. *J. Rheumatol.* **1993**, *20*, 1176-1183.
27. Rosenthal, P. J.; Lee, G. K.; Smith, R. E. *J. Clin. Invest.* **1993**, *91*, 1052-1056.
28. Harth, G.; Andrews, N.; Mills, A. A.; Engel, J. C.; Smith, R.; McKerrow, J. H. *Mol. Biochem. Parasitol.* **1993**, *58*, 17-24.
29. For a review, see ref. 3, pp 274-295.
30. Reguera, R. M.; Balafía Fouce, R.; Cubría, J. C.; Alvarez Bujidos, M. L.; Orduñz, D. *Life Sciences* **1995**, *56*, 223-230, and references contained therein.
31. Jarvi, E. T.; McCarthy, J. R.; Mehdi, S.; Matthews, D. P.; Edwards, M. L.; Prakash, N. J.; Bowlin, T. L.; Sunkarak P. S.; Bey, P. *J. Med. Chem.* **1991**, *34*, 647-656.
32. Yuan, C.-S.; Liu, S.; Wnuk, S. F.; Robins, M. J.; Borchardt, R. T. *Biochemistry* **1994**, *33*, 3758-3765.
33. Miauno, Y.; Ichikawa, A.; Tomita, K. *Prostaglandins* **1983**, *26*, 785-795.

34. Matsumura, Y.; Asai, T.; Shimada, T.; Nakayama, T.; Urushihara, M.; Morizawa, Y.; Yasuda, A.; Yamamoto, T.; Fujitani, B.; Hosoki, K. *Chem. Pharm. Bull.* **1995**, *32*, 353-355.
35. Morinelli, T. A.; Okwu, A. K.; Mais, D. E.; Halushka, P. V.; John, V.; Chen, C.-K.; Fried, J. *Proc. Natl. Acad. Sci. USA* **1989**, *86*, 5600-5604.
36. Witkowski, S.; Rao, Y. K.; Premchandran, R. H.; Haluska, P. V.; Fried, J. *J. Am. Chem. Soc.* **1992**, *114*, 8464-8472.
37. Tsai, C.-H.; Doong, S.-L.; Johns, D. G.; Driscoll, J. S.; Cheng, Y.-C. *Biochem. Pharmacol.* **1994**, *48*, 1477-1481.
38. Gao, W.-Y.; Mitsuya, H.; Driscoll, J. S.; Johns, D. G. *Biochem. Pharmacol.* **1995**, *50*, 274-276.
39. Poulter, C. D.; Rilling, H. *Acc. Chem. Res.* **1979**, *11*, 307-313.
40. Kim, D. H.; Lees, W. J.; Walsh, C. T. *J. Am. Chem. Soc.* **1994**, *116*, 6478-6479.
41. Kim, D. H.; Lees, W. J.; Haley, T. M.; Walsh, C. T. *J. Am. Chem. Soc.* **1995**, *117*, 1494-1502.
42. Kim, D. H.; Lees, W. J.; Walsh, C. T. *J. Am. Chem. Soc.* **1995**, *117*, 6380-6381.
43. Smyth, M. S.; Burke, T. R., Jr. *Tetrahedron Lett.* **1994**, *35*, 551-554.
44. Gordeev, M. F.; Patel, D. V.; Barker, P. L.; Gordon, E. M. *Tetrahedron Lett.* **1994**, *35*, 7585-7588.
45. Berkowitz, D. B.; Shen, Q.; Maeng, J.-H. *Tetrahedron Lett.*, **1994**, *35*, 6445-6448.
46. Otake, A.; Miyoshi, K.; Burker, T. R., Jr.; Roller, P. P.; Kubota, H.; Tamamura, H.; Fujii, N. *Tetrahedron Lett.* **1995**, *36*, 927-930.
47. Phillion, D. P.; Cleary, D. G. *J. Org. Chem.* **1992**, *57*, 2763-2764.
48. Edwards, P. N. In *Organofluorine Chemistry. Principles and Commercial Applications*; Banks, R. E.; Smart, B. E.; Tatlow, J. C., Eds.; Topics in Applied Chemistry; Plenum: New York, N.Y., **1994**, pp. 501-541.
49. *Organofluorine Compounds in Medicinal Chemistry and Biomedical Applications*; Filler, R.; Kobayashi, Y.; Yagupolskii, L. M., Eds.; Studies in Organic Chemistry 48; Elsevier: Amsterdam, **1993**.
50. Elliott, A. J. In *Chemistry of Organic Fluorine Compounds II*, Hudlicky, M.; Pavlath, A. E. Eds.; ACS Monograph 187; American Chemical Society: Washington, D.C., **1995**, pp. 1119-1125.
51. Prous, J. R. *Drugs Fut.* **1995**, *20*, 827-831.
52. McCarthy, J. R.; Matthews, D.P.; Stemerick, D. M.; Huber, E. W.; Bey, P.; Lippert, B. J. Snyder, R. D.; Sunkara, P. S. *J. Am. Chem. Soc.* **1991**, *113*, 7439-7440.
53. McCarthy, J. R. *Abstracts, Division of Medicinal Chem.*, 210th ACS National Meeting, Chicago, IL, August 20-24, **1995**, Papers 111 and 112.
54. Prous, J. R. *Annu. Drug Data Rep.* **1995**, *17*, 669.
55. Prous, J. R. *Drugs Fut.* **1995**, *20*, 297-298.
56. Prous, J. R. *Drugs Fut.* **1995**, *20*, 362-366.
57. Tanaka, Y.; Wu, A.-Y.S.; Ikekawa, N.; Iseki, K.; Kawai, M.; Kobayashi, Y. *Cancer Research* **1994**, *54*, 5148-5153.
58. Chu, D. T. W.; Hallas, R.; Tanaka, S. K.; Alder, J.; Balli, D.; Plattner, J. J. *Drugs Exptl. Clin. Res.* **1994**, *XX*, 177-183.
59. Clement, J. J.; Burren, N.; Jarvis, K.; Chu, D. T. W.; Swiniarski, J.; Alder, J. *Cancer*

60. Prous, J. R. *Drugs Fut.* **1994**, *19*, 221-224.
61. Prous, J. R. *Drugs Fut.* **1995**, *20*, 761-765.
62. Chu, C. K.; Ma, T.; Shanmuganathan, K.; Wang, C.; Xiang, Y.; Pai, S. B.; Yao, G. Q.; Sommadossi, J-P.; Cheng, Y-C. *Antimicrob. Agents Chemother.* **1995**, *39*, 979-981.
63. Diana, G. D.; Rudewicz, P.; Pevear, D. C.; Nitz, T. J.; Aldous, S. C.; Aldous, D. J.; Ribinson, D. T.; Draper, T.; Dutko, F. J.; Aldi, C.; Gendron, G.; Oglesby, R. C.; Volkots, D. L.; Reuman, M.; Bailey, T. R.; Czerniak, R.; Block, T.; Roland, R.; Oppermann, J. *J.Med. Chem.* **1995**, *38*, 1355-1371.
64. Boehme, R. E.; Borthwick, A. D.; Wyatt, P. G. in *Annual Reports in Medicinal Chemistry*, Bristol, J. A., Ed., Vol. 29, Academic: San Diego, **1994**, 150.
65. *Annual Reports in Medicinal Chemistry*, Bristol, J. A., Ed. Vol. 29, Academic: San Diego, **1994**, 340.
66. Bryskier, A.; Chantot, J-F. *Drugs* **1995**, *49*, Supplement 2, 16-28.
67. Eliopoulos, G. M.; Wennersten, C. B.; Cole, G.; Chu, D.; Pizzuti, D.; Moellering, R. C., Jr. *Antimicrob. Agents Chemother.* **1995**, *39*, 850-853.
68. Prous, J. R. *Drugs Fut.* **1995**, *20*, 341-343.
69. Goa, K. L.; Barradell, L. B., *Drugs* **1995**, *50*, 658-690.
70. Prous, J. R. *Drugs Fut.* **1993**, *18*, 424-427.
71. Graybill, J. R.; Najvar, L. K.; Holmberg, J. D.; Luther, M. F. *Antimicrob. Agents Chemother.* **1995**, *39*, 924-929.
72. van den Anker, J. N.; van Popele, N. M. L.; Sauer, P. J. J. *Antimicrob. Agents Chemother.* **1995**, *39*, 1391-1397.
73. Prous, J. R. *Drugs Fut.* **1995**, *20*, 83.
74. Prous, J. R. *Drugs Fut.* **1994**, *19*, 854-855.
75. Prous, J. R. *Drugs Fut.* **1995**, *20*, 135-138.
76. Jahng, Y. *Drugs Fut.* **1995**, *20*, 387-404.
77. *Annual Reports in Medicinal Chemistry*, Bristol, J. A., Ed., Vol. 30, Academic: San Diego, **1995**, 300.
78. Prous, J. R. *Drugs Fut.* **1995**, *20*, 33-36.
79. Riess, J. G. *J. Liposome Research* **1995**, *5*, 413-430.

## Chapter 2

# Practical Synthesis of Enantiopure Fluoroamino Acids of Biological Interest by Asymmetric Aldol Reactions

V. A. Soloshonok<sup>1</sup>

Institute of Bioorganic Chemistry and Petrochemistry, Ukrainian Academy of Sciences, 253660, Kiev-94, Murmanskaya 1, Ukraine

Presented herein is a short review of stoichiometric (Belokon') and catalytic (Hayashi) asymmetric aldol reactions involving fluorinated aldehydes and ketones. Synthetic opportunities and limitations of these methods for preparation of stereochemically defined fluoro-amino acids of biological interest is discussed. Apart from synthetic results, puzzling stereocontrolling features of fluorine-containing groups, discovered in these reactions, are highlighted.

Since rationalization of the basic principles for modification of biological activity of organic compounds *via* fluorine substitution for hydrogen (1), synthesis of fluorine-containing analogs of natural products has been an expanding area of research. Fluorinated derivatives of all key classes of naturally occurring compounds have been synthesized and investigation of their biological properties has proved the viability of "fluorine approach" in the rational design of drugs with maximal *in vivo* specificity (2-8). One of the most significant achievements of this field has been a creation of a new generation of fluorine-containing, mechanism-based enzyme inactivators (suicide substrates) of certain enzymes responsible for the metabolism of amino acids, steroids, and nucleosides (8, 9). However, most of the biomedical potential of fluoroorganic compounds remains unrealized and its future development is greatly dependent on an understanding of the molecular basis of biochemical transformations and the state of the art of fluoroorganic synthesis.

With the growing awareness of the relevance of chirality to *in vivo* molecular recognition and thus biological properties of a chiral compound, in recent years fluoroorganic synthesis has undergone profound methodological changes aimed at preparation of individual stereoisomers of selectively fluorinated compounds of biological importance (10-13). Efficient asymmetric approaches, achieving levels of stereoselectivity that rival enzymatic systems, have been developed for many classes of organic compounds. By contrast, fluoro-organic compounds turned out to be difficult targets for enantiocontrolled synthesis (11, 13). It has finally been recognized, that fluorine can dramatically alter both the course and stereochemical outcome of the established reactions of hydrocarbons, providing a challenge for the asymmetric

<sup>1</sup>Current address: National Industrial Research Institute of Nagoya, Hirate-cho 1-1, Kita-ku, Nagoya City, Aichi 462, Japan



synthesis of fluorinated compounds. We are engaged in the development of convenient synthetic routes to stereochemically defined fluoro-amino acids (8) by means of asymmetric synthesis (14) and biocatalysis (15). Our particular interest in asymmetric aldol reactions, discussed here, is two pronged. Recent evolution of aldol methodology into a general and highly stereoselective method for carbon-carbon bond formation renders the aldol reaction as the most potent and reliable tool for natural product synthesis (16, 17). Thus, it is very exciting to explore feasibility of asymmetric aldol methodology for the enantiocontrolled preparation of challenging fluorine-containing compounds; and, on the other hand, to study the stereochemical behavior of fluorine, and its influence on the outcome of enantioselective aldol reactions.

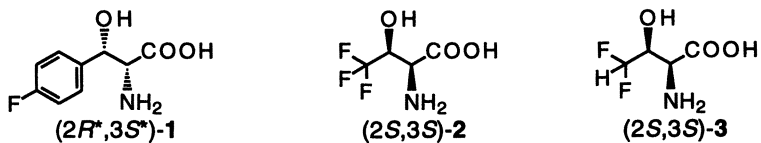
Here we present our results on the asymmetric Belokon' and Hayashi aldol reactions between nucleophilic glycine equivalents and fluorinated aldehydes and ketones. These reactions provide generalized and stereochemically flexible entry to the family of fluorine-containing  $\alpha$ -amino- $\beta$ -hydroxy carboxylic acids with proved or potential biological activity. In all cases, the reactivity pattern and stereochemical outcome from the use of fluorinated carbonyl compounds in asymmetric aldol condensations is compared with that of hydrocarbon aldehyde and ketones.

### Biomedical Interest in Fluorine-containing Analogs of $\alpha$ -Amino- $\beta$ -Hydroxy Carboxylic Acids

$\alpha$ -Amino- $\beta$ -hydroxy carboxylic acids are an important class of naturally occurring compounds. The most noted members of this family of amino acids, serine, and threonine, are essential constituents of human proteins and they exhibit diverse biological functions (18, 19). Other naturally occurring  $\beta$ -hydroxy amino acids, produced mostly by microorganisms, apart from their own normally high biological activity, are key structural components of complex bioactive molecules such as cyclic polypeptides and glycopeptides (e.g. edeine, vancomycin, cyclosporine, bouvardin, bleomycins) (20-22). Additionally,  $\beta$ -hydroxy amino acids, possessing the hydroxyethyleneamino pharmacophore moiety with proven therapeutic value, are valuable starting material for syntheses of other biologically active compounds, as, for example, neuroactive amines, peptidomimetics and  $\beta$ -lactams (23-25). Aside from the general advantageous characteristics imparted to all types of amino acids by fluorine substitution for hydrogen (3-8), selective incorporation of fluorine into the molecules of  $\alpha$ -amino- $\beta$ -hydroxy carboxylic acids would offer some specific opportunities. Due to the strong electron-withdrawing effect of polyfluoroalkyl and aryl groups, their presence geminal to a hydroxy group dramatically influences its acid-base properties while those of remote amino and carboxy groups are almost unaffected. For instance, the  $pK_a$  value of the  $\beta$ -hydroxy group in 4,4,4-trifluorothreonine is 12.7, a reduction of three  $pK_a$  units compared with that of fluorine-free threonine (26). Accordingly, the fundamentally important ability of the hydroxy group to hydrogen bond and chelate metals can be rationally modified in a series of fluorinated  $\alpha$ -amino- $\beta$ -hydroxy carboxylic acids to achieve desirable biochemical consequences. Furthermore, fluorine-containing  $\beta$ , $\beta$ -disubstituted- $\beta$ -hydroxy acids, which exert defined conformational constraints, could be of interest in the *de novo* design of peptides and proteins with specific conformational properties and biological functions (27). In view of the critical involvement of  $\beta$ -hydroxy amino acids in the biological activities of naturally occurring peptide and glycopeptide antibiotics mentioned above, application of fluorinated  $\beta$ -hydroxy amino acids as structural units for modification of these biological macromolecules might be promising.

Finally, there is some literature data on the proven biological activity of fluorine-containing analogs of  $\alpha$ -amino- $\beta$ -hydroxy carboxylic acids. Thus, racemic *syn*- $\beta$ -(4-fluorophenyl)serine (1) (Figure 1) was shown to prolong the life of rats transplanted with *Erhlich Ascites* (28, 29) and inhibit the growth of *E. coli* (30). (2*S*,3*S*)-4,4,4-trifluorothreonine (2) and (2*S*,3*S*)-4,4-difluorothreonine (3) [(2*S*,3*S*)-configuration of

**Figure 1. Some Fluorinated  $\beta$ -Hydroxy Amino Acids with Proven Biological Activity.**



amino acids **2** and **3** is a consequence of the Cahn-Ingold-Prelog priority and is stereochemically equivalent to the (2*S*,3*R*)-configuration in the hydrocarbon analogs] (**31**) were found to possess promising antitumour and antifungal activity (**32**, **33**).

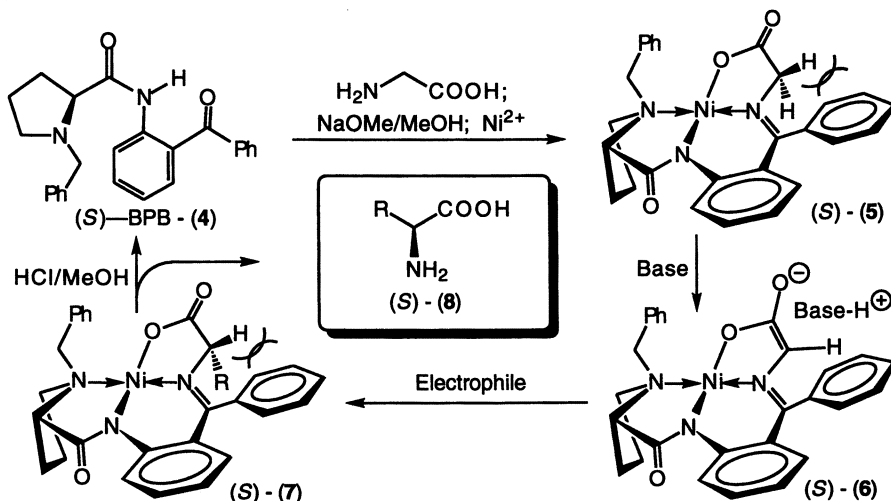
As it follows from this short overview, fluorine-containing analogs of  $\alpha$ -amino- $\beta$ -hydroxy carboxylic acids are of high biological interest both as individual compounds and as constituents of complex natural macromolecules. The biological data reported in the literature to date has been limited, in part, as a consequence of the challenge associated with the synthesis of these amino acids (**34**). Thus, before our project was started, no convenient preparatively valuable approaches to this type of fluoro-amino acids had been developed (**8**). In particular, only (2*S*,3*S*)-4,4,4-trifluorothreonine (**2**), (2*S*,3*R*)-3-(2-fluorophenyl)- and (2*S*,3*R*)-3-[4-(trifluoromethyl)phenyl]serines had been prepared *via* asymmetric synthesis by Seebach's group (**35**, **36**). We hope, our results presented herein, make some types of fluorinated  $\alpha$ -amino- $\beta$ -hydroxy carboxylic acids readily available in the structural and conformational variety needed to realize their biomedical potential.

## Belokon' Aldol Reaction

### General Characteristics and Reactivity of Chiral Glycine Ni(II) Complex **5**.

Among the synthetically valuable stoichiometric chiral glycine anion synthons (Evans, Oppolzer, Seebach, Schollkopf, Williams) (**37**, **38**), the Ni(II)-complex (Figure 2) of the chiral, non-racemic Schiff base of glycine with (*R*)- or (*S*)-*o*-[*N*-(*N'*-benzylpropyl)amino]-benzophenone (BPB) (**5**), introduced by Belokon' (**39**), possesses unique structural and stereochemical characteristics. Synthesis of Ni(II)-complex **5** in over 80% yield, is carried out *via* a one-pot procedure starting with the commercially available chiral auxiliary (*S*)-BPB **4**, glycine, and a source of Ni<sup>2+</sup> ions, usually Ni(NO<sub>3</sub>)<sub>2</sub> × 6H<sub>2</sub>O or NiCl<sub>2</sub> × 6H<sub>2</sub>O. Glycine Ni(II)-complex **5** is neutral, diamagnetic and readily soluble in organic solvents. The glycine methylene group in complex **5** has a significant CH acidity, allowing the use of a wide range of bases to generate corresponding enolate **6** under a variety of reaction conditions. Thus, the pK<sub>a</sub> value of (*S*)-**5** in DMSO is 18.8 (**40**), greater than that of acetophenone (pK<sub>a</sub> = 24.7) and fluorene

**Figure 2. Synthesis of the Chiral Ni(II) Complex of Glycine (*S*)-**5**, Its Reactions with Electrophiles, and Recycling of Chiral Auxiliary (*S*)-BPB.**

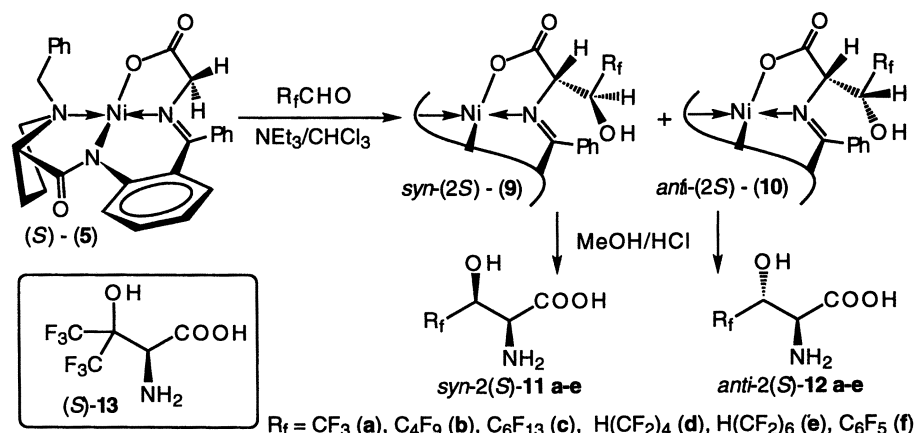


( $pK_a = 22.6$ ), and comparable with that of mononitro compounds ( $pK_a \approx 17$ ) (41). The presence of the proline stereogenic center imparts an asymmetric distortion to the rigid polycyclic system of complex **5** that, in turn, causes steric shielding of the enolate **6** re-face by ketimine phenyl. Thus, preferential electrophilic attack occurs on the *si*-face to form complex **7** with a pseudoaxial orientation of substituent R. Upon treatment with hydrochloric acid, diastereomerically pure complex **7** releases targeted amino acid **8** along with the initial chiral auxiliary (*S*)-BPB **4**. Ready recovery of the chiral auxiliary, without any loss of its optical purity, and its use in many synthetic cycles, makes this method particularly attractive since, with respect to consumption of asymmetric agent, the whole process has a catalytic character. Finally, positive and negative Cotton effects in the CD spectra or ORD curves of the Ni(II) complexes allows for unambiguous assignment of the pseudoaxial or pseudoequatorial orientation of the new amino acid side chain in **7** and thus the absolute configuration at the  $\alpha$ -position of the new amino acid.

Aldol condensations of Ni-complex **5** with carbonyl compounds have been much less investigated than alkyl halide alkylation and Michael addition reactions (39). Only formaldehyde, acetaldehyde, 3,4-(methylenedioxy)benzaldehyde, benzaldehyde and acetone condensations with complex **5** have been studied and a dramatic dependence of the stereochemical outcome of these reactions on the pH of the reaction medium has been revealed (42, 43). A systematic study conducted by our group in collaboration with Prof. Belokon', into the asymmetric aldol reactions of Ni(II) complex **5** with hydrocarbon and fluorocarbon carbonyl compounds has demonstrated the unique synthetic value of template **5** for the general preparation of stereochemically defined  $\beta$ -hydroxy amino acids. Our results can be classified into four main groups with regard to the nature of the stereoselectivity observed.

**Kinetic Control of Stereoselectivity. Aldol Reactions of Ni(II) Complex (S)-5 with Fluoro-Aldehydes and Ketones in a Solution at Low pH.** Hydrocarbon aldehydes and ketones do not react with complex **5** in chloroform solution in the presence of weak bases such as triethylamine (TEA) or DABCO. However, the highly electrophilic fluoroalkyl aldehydes and pentafluoro-benzaldehyde easily undergo aldol condensation with complex **5** under these reaction conditions, giving rise to a mixture (1/1) of diastereomeric complexes **9**, **10** (Figure 3) in excellent chemical yield (44, 45). Since under these conditions aldol condensations are irreversible, the stereochemistry of the products might reflect the kinetic effects influencing stereogenesis

**Figure 3. Aldol Reactions of Ni(II)-Complex (S)-5 with Per(poly)-fluoroalkyl Aldehydes, Pentafluorobenzaldehyde and Hexafluoroacetone.**

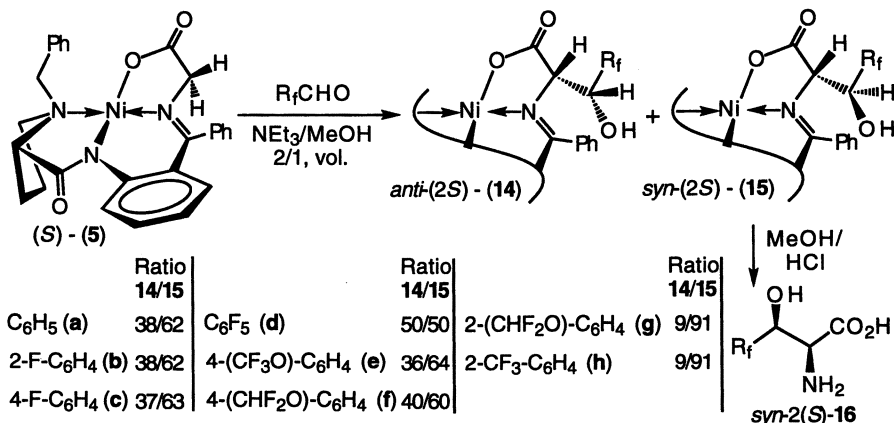


of these reactions. As it follows from the ratio of *syn*-(2*S*)-**9** and *anti*-(2*S*)-**10** (1 to 1) and their absolute configurations, kinetic recognition of the two enantiotopic faces of complex **5** is nearly complete [no complexes with  $\alpha$ -(*R*)-configured amino acid were isolated], while no recognition of enantiotopic faces of the aldehydes is observed in these aldol condensations. Complexes **9** and **10** can be easily isolated by column chromatography in a diastereo- and enantiomerically pure state and then decomposed to give the optically pure amino acids *syn*-(2*S*)-**11** and *anti*-(2*S*)-**12**, respectively, along with chiral auxiliary BPB (87-93% yield). The high level of kinetically controlled stereoselectivity at the  $\alpha$ -stereogenic center observed in these reactions is synthetically useful for preparation of symmetrically  $\beta,\beta$ -disubstituted  $\beta$ -hydroxy amino acids. This opportunity is demonstrated with an efficient asymmetric synthesis of (*S*)-hexafluorovaline **13**, isolated in an enantiopure state in 63% overall yield, *via* aldol reaction between (*S*)-**5** and hexafluoroacetone. Preliminary results show that this method might be easily generalized for the preparation of  $\beta,\beta$ -disubstituted fluoroalkyl, chloroalkyl or chlorofluoroalkyl  $\beta$ -hydroxy amino acids.

### Mixed Case of Kinetic and Thermodynamic Control of Stereoselectivity. Aldol Reactions of Ni(II) Complex (*S*)-**5** with Fluoro-Benzaldehydes.

Use of methanol as solvent, instead of chloroform, allows for aldol reaction of complex **5** with a wider range of aldehydes. It was shown that in methanol solution, with TEA as a base, formaldehyde and acetaldehyde undergo reversible aldol condensations with complex **5** and a large excess of the carbonyl compound is required to shift the equilibrium toward the desired aldol products. Under these reaction conditions, formaldehyde reacts with **5** to produce the (*S*)-serine containing complex with up to 96% de, while prochiral acetaldehyde condensation is less stereoselective giving rise to a mixture (32% yield) of Ni(II) complexes of (*S*)-threonine (78% de) and (*S*)-*allo*-threonine (76% de) in a ratio of 2/1, respectively (42, 43). We have found that under similar reaction conditions, benzaldehyde and its monofluoro-substituted derivatives also react reversibly with **5** forming a mixture of complexes **14** and **15** in high chemical yield and in a ratio of 1/1.7, respectively (Figure 4). Formation of  $\alpha$ -(*S*)-stereogenic center of amino acid residue in aldol products is kinetically controlled and thermodynamically favorable, therefore the corresponding amino acid complexes with an  $\alpha$ -(*R*)-configuration are contained in the reaction mixture in amounts not greater than 5-10%. In contrast, exothermic pentafluorobenzaldehyde condensation with **5** gives only the *anti*-(2*S*) and *syn*-(2*S*)-diastereomers **14** and **15** in 1/1 ratio. This result can be easily rationalized by assuming that, due to the strong electron-withdrawing effect of

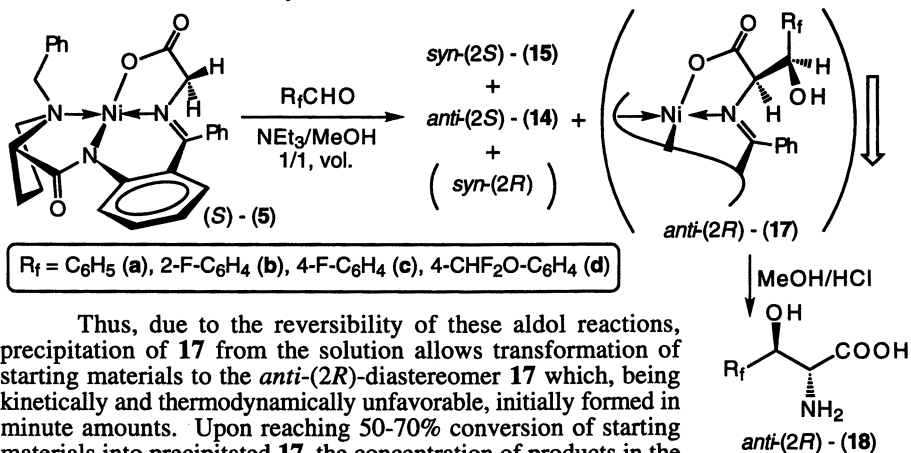
**Figure 4. Aldol Reactions of Complex (*S*)-**5** with Fluoro-Benzaldehydes.**



pentafluorophenyl ring, the rate of retroaldol condensation is too slow to effectively achieve thermodynamic equilibration of resultant complexes **14 d** and **15 d** and thus, the stereochemical outcome of the reaction is kinetically controlled, similar to that of the corresponding condensations in chloroform solution. The presence of a fluoroalkyl or fluoroalkoxy group in the *ortho*-position of starting aldehyde alters thermodynamic ratio of *anti*-(2*S*) and *syn*-(2*S*)-diastereomers **14** and **15**, strongly favoring the latter. Thus in the aldol reactions of *o*-difluoromethoxy and *o*-trifluoromethyl benzaldehydes with complex **5**, after equilibration, an excess of *syn*-(2*S*)-diastereomers **15 g,h** reaches a synthetically valuable level, over 80% de. The reasons behind greater thermodynamic stability of **15 g,h** is difficult to rationalize. It could be assumed that a weak attractive interaction of the Ni(II) ion with fluorine-containing *ortho*-substituent, allowed by the structure of **15 g,h**, renders these complexes more thermodynamically favorable than diastereomeric **14 g,h**. Complexes **15 g,h** can be easily purified by a single recrystallization and upon decomposition with aq. HCl in methanol release fluorinated *syn*-(2*S*)-phenylserines **16 g,h** in an enantiopure state (44 - 46).

**Second-Order Asymmetric Transformations of Products in the Aldol Reactions of Complex (S)-5 with Fluoro-Benzaldehydes.** Variation in the ratio of TEA/MeOH used as the reaction medium does not influence the relative ratio of diastereomeric products in the reactions discussed above. However, an increase in the concentration of TEA to a 1/1 volume ratio with MeOH affects the relative solubility of the products. As a result, under these reaction conditions, a second-order asymmetric transformation takes place *via* slow precipitation of the sparingly soluble complex **17** containing the *anti*-(2*R*)-configured amino acid from the solution (Figure 5).

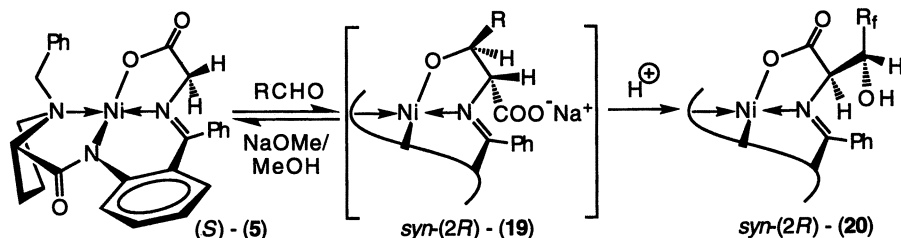
**Figure 5. Synthesis of Fluorinated *anti*-(2*R*)- $\beta$ -Phenylserines *via* Second-Order Asymmetric Transformation of Aldol Products.**



Thus, due to the reversibility of these aldol reactions, precipitation of **17** from the solution allows transformation of starting materials to the *anti*-(2*R*)-diastereomer **17** which, being kinetically and thermodynamically unfavorable, initially formed in minute amounts. Upon reaching 50-70% conversion of starting materials into precipitated **17**, the concentration of products in the reaction solution is changed, slowing precipitation of complex **17** significantly. However, this method is appealing from a preparative point of view, since the desired diastereomer **17** can be readily isolated in diastereo and enantiomerically pure state simply by filtration of the reaction solution. Decomposition of **17** gives pure *anti*-(2*R*)-amino acids **18** along with recovery of chiral auxiliary BPB (44, 46).

**Reactions of Complex (S)-5 with Fluoro-Aldehydes and Ketones in a High pH Solution. Thermodynamic Control of Products Stereochemistry.** Use of NaOMe as a base, instead of TEA, in methanol solution alters significantly the reactivity of carbonyl compounds toward complex **5** and stereogenesis of their aldol

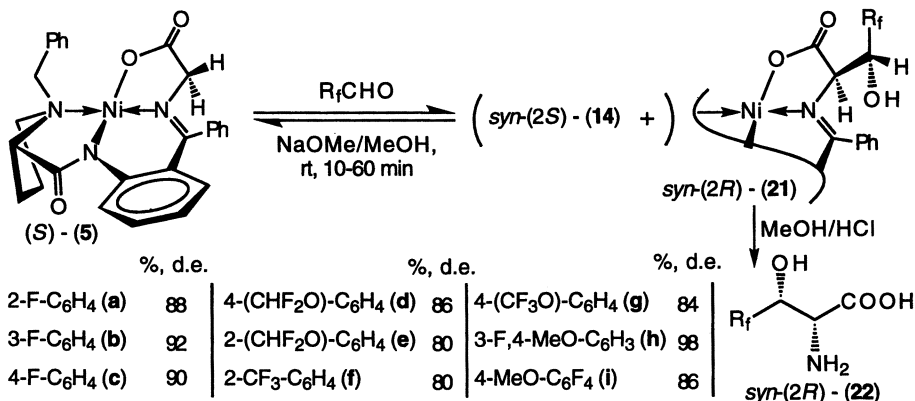
Figure 6. Rearrangements of Ni(II) Complexes.



reactions as well. In the presence of NaOMe rates of reactions, and consequently the thermodynamic equilibration of products are greatly increased. In a high pH reaction medium ( $> 0.1\text{M}$  NaOMe in MeOH) that provides ionization of the  $\beta$ -hydroxy group of the amino acid side chain of the aldol products, the sense of diastereoselection is changed. Substitution of an ionized carboxy group by an ionized hydroxy in the coordination sphere of Ni(II) is a thermodynamically advantageous process, giving rise to rearranged complex **19** (Figure 6). Owing to chelation of the amino acid moiety in a rigid five-membered ring, the stereochemistry within it, at both the  $\alpha$ - and  $\beta$ -positions, is effectively controlled. Pseudoaxial orientation of the ionized carboxy group [ $\alpha$ -(*R*)-configuration of the amino acid], like in the complex **19**, is energetically more favorable than its pseudoequatorial disposition [ $\alpha$ -(*S*)-configuration of amino acid], due to a strong repulsive interaction of the carboxylate with the ketimine phenyl, which can not be minimized within the rigid system of the polycyclic Ni(II) chelate. Relative stereochemistry within the amino acid moiety in the hydroxy-coordinated complex **19** is determined by the energetic advantage of having a *trans*-disposition of the substituents on the five-membered chelate ring. Accordingly, hydroxy-coordinated **19** is the most thermodynamically stable structure under the reaction condition discussed. Neutralization of reaction mixture causes rearrangement of complex **19** into the usual carboxy-coordinated **20** (39, 42).

**Aldol Reactions of Fluoro-Benzaldehydes with Complex 5. Synthesis of *syn*-(2*R*)- $\beta$ -(Fluorophenyl)serines.** It was shown (42) that benzaldehyde and 3,4-(methylenedioxy)benzaldehyde react with **5** to give a mixture of complexes containing *syn*-(2*S*) and *syn*-(2*R*) amino acids with up to 88% de of the *syn*-(2*R*)-diastereomer. Introduction of one fluorine atom or fluoroalkyl and fluoroalkoxy groups into any position of the phenyl ring of benzaldehyde does not influence significantly the pattern of reactivity and stereoselectivity, providing dominant formation (80-98% de) of *syn*-(2*R*)-diastereomers **21a-h** in high chemical yield (Figure 7). Complexes **21a-h** can be easily purified to an enantiopure state and then decomposed to give free amino acids *syn*-(2*R*)-**22a-h** (44, 47). The simplicity of the experimental procedure and the high chemical and stereochemical yields make this method synthetically useful for large scale preparation of fluorinated and enantiopure phenylserines **22**. However, due to the basic reaction conditions used, this method might be of limited application for the synthesis of polyfluoro-substituted amino acids, as for instance, (pentafluorophenyl)serine. Thus, aldol reaction of pentafluorobenzaldehyde with **5** is accompanied by substitution of a fluorine atom in the *para*-position of the perfluorophenyl ring, giving rise to *syn*-(2*R*)-**21i** containing (4-methoxy-2,3,5,6-tetrafluorophenyl)serine in high chemical yield and 86% de (46). On the other hand, this result could be a synthetic opportunity, because of the unavailability of the starting *p*-methoxy-tetrafluorobenzaldehyde for the preparation of amino acid **22i** by other methods (48).

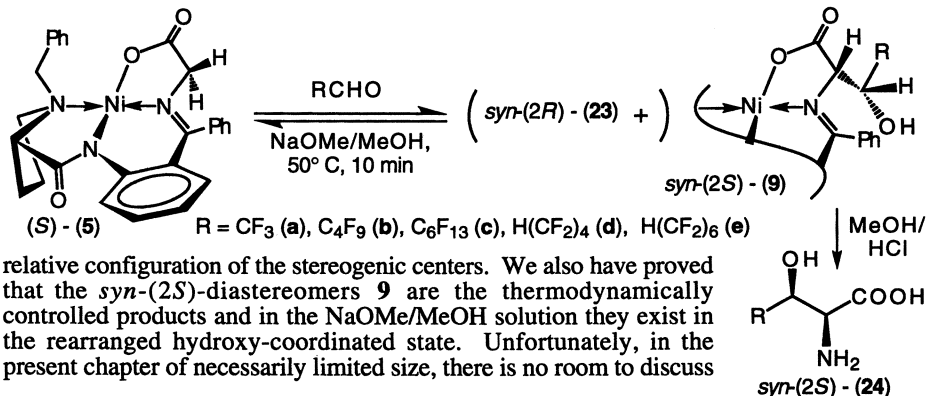
Figure 7. Aldol Reactions of Fluoro-Benzaldehydes with 5 at High pH.



**Aldol Reactions of Fluoroalkyl Aldehydes with Complex 5. Synthesis of *syn*-(2*S*)-β-(Fluoroalkyl)serines.**

As mentioned above, acetaldehyde aldol condensation with 5 at rt in NaOMe/MeOH, leads to a mixture of the (*R*)- and (*S*)-threonine containing complexes with sizable (84% de) domination of the (*R*)-diastereomer (42). Fluoral does not react with complex 5 at ambient temperature, probably due to formation of an unreactive hemiacetal in methanol solution (49). However, brief heating of the reaction mixture gives two new complexes with excellent (96/4 ratio) diastereoselectivity. Investigation of absolute configuration of the products (ORD curves and X-ray analysis) has revealed a totally unexpected result, *syn*-(2*S*)-configuration for the dominant diastereomer 9 and *syn*-(2*R*)-stereochemistry for the minor 23 (Figure 8). It follows that, in the aldol condensations of acetaldehyde and trifluoroacetaldehyde with 5, a similar pattern of reactivity but opposite stereochemical preferences are observed. High *syn*-(2*S*)-diastereoselectivity is not influenced by the length of fluoroalkyl group, allowing efficient (90-92% de) preparation of *syn*-(2*S*)-9, and thus amino acids 24, containing medium-to-long fluoroalkyl chains (44, 50). The reasons behind this surprising stereoselectivity, brought about by fluorine, is not yet clear. Both steric and electronic factors fail to rationalize the phenomenon (51). One explanation, supported by molecular mechanics calculations, assumes an electrostatic attraction between the partially positively charged Ni(II) and the perfluoroalkyl group, determining the β-(*S*)-absolute configuration of the amino acid moiety and, on the other hand, electrostatic repulsion between perfluoroalkyl and carboxy groups, fixing a *syn*-

Figure 8. Aldol Reactions of Fluoroalkyl Aldehydes with 5 at High pH.

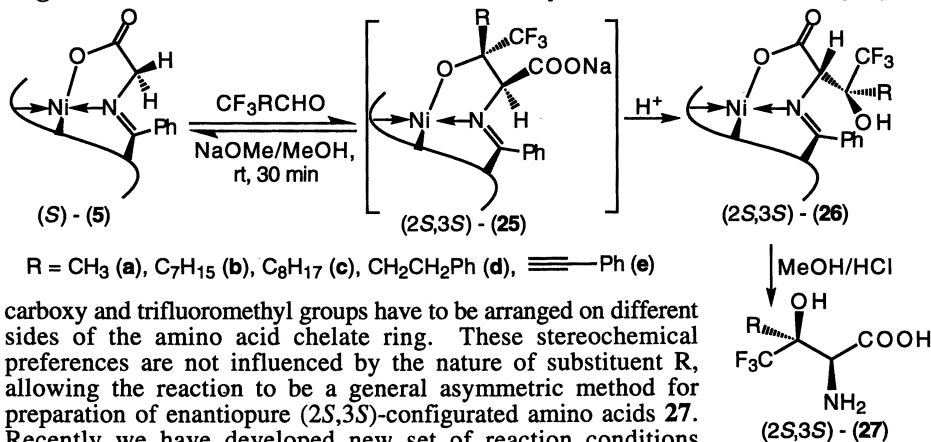




all aspects of this interesting case of stereoselectivity directed by fluorine.

**Aldol Reactions of Trifluoromethyl Ketones with Complex 5.** **Synthesis of (2*S*,3*S*)- $\beta$ -(Fluoroalkyl)- $\beta$ -Alkylserines.** Enantioselective formation of stereogenic quaternary carbon centers is one of the most challenging targets for asymmetric synthesis (52). Aldol reactions of prochiral ketones with complex 5 have not been previously studied. However, as it was shown for acetone condensation with complex 5, the presence of a second alkyl group in the  $\beta$ -position of the amino residue of the resultant complex partially destabilizes its rearranged hydroxy-coordinated structure of type 19 (Figure 6), decreasing the diastereoselectivity of the reaction. Thus, aldol condensation of acetone taken in great excess (1/100), with 5 in NaOMe/MeOH gives the corresponding Ni(II)-complex of (*R*)- $\beta$ -hydroxyvaline in low chemical yield and not higher than 72% de (42). In sharp contrast to this, trifluoroacetone easily reacts with 5 giving rise to a single reaction product 26a (Figure 9) with the (2*S*,3*S*)-absolute configuration, according to X-ray analysis (44). Thus, once again substitution of fluorine for hydrogen reverses the stereochemical preferences established for reactions of hydrocarbon analogs. Like Ni(II)-complexes of  $\beta$ -perfluoroalkylserines *syn*-(2*S*)-9 (Figure 8), complex 26 is the product of thermodynamic control and under the reaction conditions (NaOMe/MeOH) undergoes rearrangement to the hydroxy-coordinated structure 25. Obviously, of paramount importance for thermodynamic stability of 25 is that the trifluoromethyl group be situated in the pseudoaxial position, providing the shortest distance (2.83 Å) between the Ni(II) and fluorine atoms, and second, the

**Figure 9.** Aldol Reactions of Trifluoromethyl Ketones with 5 at High pH.



carboxy and trifluoromethyl groups have to be arranged on different sides of the amino acid chelate ring. These stereochemical preferences are not influenced by the nature of substituent R, allowing the reaction to be a general asymmetric method for preparation of enantiopure (2*S*,3*S*)-configured amino acids 27. Recently we have developed new set of reaction conditions providing an efficient preparation of complexes (2*S*,3*S*)-26a-e with up to 90% of chemical yield and over 95% of diastereomeric purity.

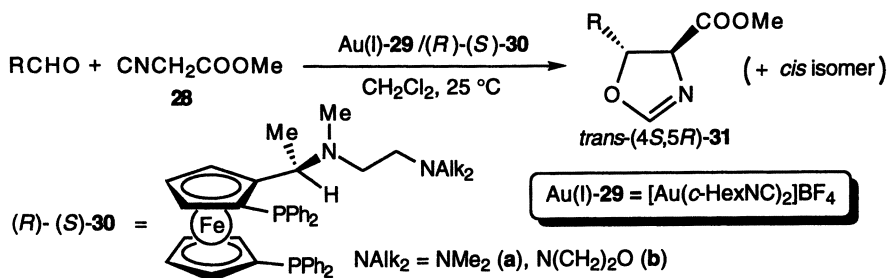
Systematic study of the asymmetric aldol reactions of chiral nickel-glycine complex 5 with fluorinated carbonyl compounds, briefly presented here, reveals that the stereochemical outcome of these reactions greatly depends on the reaction conditions and the nature of the carbonyl compound used and, in most cases, is different to that of analogous hydrocarbon reactions. Established reactivity and stereoselectivity under the definite reaction conditions allows preparation of various enantiopure fluorinated  $\beta$ -hydroxy amino acids such as symmetrically substituted hydroxy valines (irreversible, kinetically controlled aldol reactions at low pH, Figure 3), *syn*-(2*S*)- $\beta$ -phenylserines (reversible reactions at low pH in MeOH/TEA, Figure 4), *anti*-(2*R*)- $\beta$ -phenyl serines (second-order asymmetric transformation of aldol products, Figure 5), *syn*-(2*R*)- $\beta$ -phenylserines, *syn*-(2*S*)- $\beta$ -fluoroalkylserines and particularly challenging (2*S*,3*S*)- $\beta$ -

fluoroalkyl- $\beta$ -alkylserines (thermodynamically controlled aldol reactions at high pH in NaOMe/MeOH, Figures 7, 8 and 9, respectively).

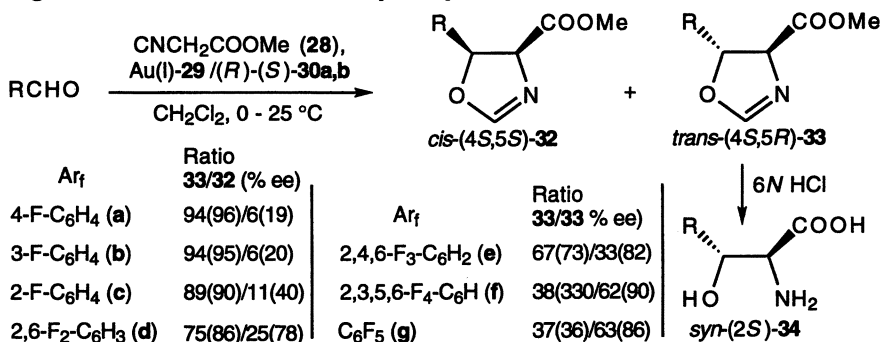
### Hayashi Aldol Reaction

Methods, wherein a catalytic amount of an asymmetric agent is required, represent the most desirable solutions to the preparation of stereochemically defined chiral compounds (53). The first synthetically useful, truly catalytic, asymmetric aldol methodology was developed by Hayashi *et al.* (54). This method consists in the reaction of between an aldehyde and an isocyanoacetic acid derivative (in particular the methyl ester, Figure 10) catalyzed by 1-2 mol % of a gold(I) complex coordinated with a chiral *N,N,N',N'*-tetraalkylethylenediamino-substituted bis(diphenylphosphino)ferrocene ligand, leading to optically active *trans*-oxazolines **31** with high enantio- and diastereoselectivity. Previous studies on the gold(I)-catalyzed asymmetric aldol reaction have demonstrated its generality for the asymmetric synthesis of various  $\beta$ -(substituted)serines. However, the stereochemical outcome of this reaction is not always unambiguous, varying from the excellent (100% de, 97% ee, R = *tert*-Bu) to poor (50% de, 6% ee, R = 2-C<sub>5</sub>H<sub>4</sub>N) depending on the nature of aldehyde used (54, 55). Behavior of fluoroaryl aldehydes in the gold(I)-catalyzed asymmetric aldol reaction was not previously studied.

Figure 10. Gold(I)-Catalyzed Asymmetric Aldol Reaction.

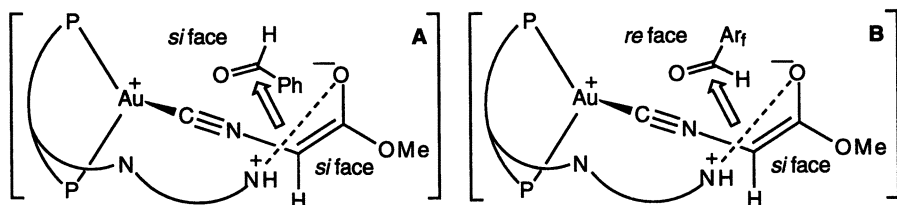


**Aldol Reactions with Methyl Isocyanoacetate.** As was found for aldol reaction of benzaldehyde with methyl  $\alpha$ -isocyanoacetate (**28**), the complex of bis(*cyclo*-hexyl isocyanide)-gold(I) tetrafluoroborate (**29**) with (*R*)-*N*-methyl-*N*-[2-(piperidino)ethyl]-1-[(*S*)-1',2-bis(diphenylphosphino)ferrocenyl]ethylamine (**30a**) is a superior catalyst for this condensation, forming the *trans*-oxazoline in 88% de and 95% ee (54). Under the same reaction conditions, *p*-fluoro- and *m*-fluorobenzaldehydes give the *trans*-oxazolines **33a,b** in excellent chemical yields, diastereo- and enantioselectivities (56, 57). A little lower selectivity is observed in the reaction of *o*-fluorobenzaldehyde with **28**. The absolute configuration of the *trans*-oxazolines were determined to be (4*S*,5*R*), by hydrolysis to the known *syn*-(2*S*)-(fluorophenyl)serines **34a-c**. The next experiments with di-, tri-, tetra- and pentafluorosubstituted benzaldehydes, which were carried out under similar (lower temperature, 0-1 °C) reaction conditions, revealed a surprising influence of the number of fluorine atoms in the phenyl ring of starting benzaldehyde on the stereochemical outcome of aldol reactions. Thus, an increase of fluorine substitution for hydrogen is accompanied by a gradual increase in the proportion of *cis*-oxazolines **32** and their enantiomeric purity as well. On the other hand, the ee values of the corresponding *trans*-oxazolines **33** are gradually decreased. The extremes of this trend are observed in the tetrafluoro- and pentafluorobenzaldehyde reactions with isocyanoacetate **28**, catalyzed by 2 mol % of gold(I)-complex **29** with morpholino derived ferrocenyl ligand **30b**, where *cis*-(4*S*,5*S*)-oxazolines **32f,g** are formed as the dominant diastereomers with 90 and 86% ee, respectively. (See Figure 11.)

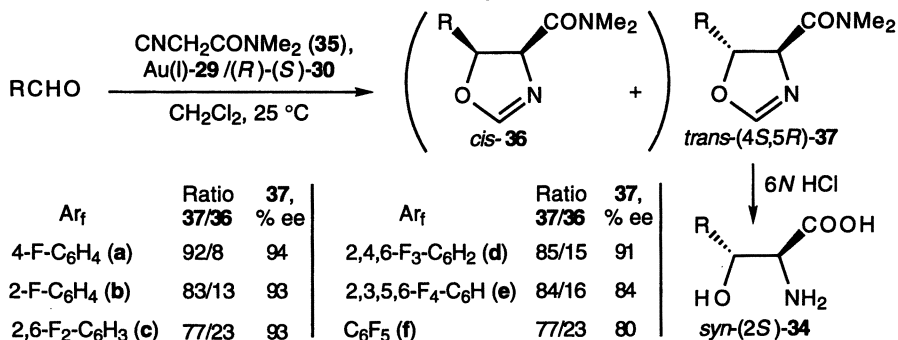
**Figure 11. Aldol Reactions of Methyl Isocyanoacetate with Fluoro-Benzaldehydes.**

Gold(I)-catalyzed asymmetric aldol reactions of methyl  $\alpha$ -isocyanoacetate (**28**) with tetrafluoro- and pentafluoro-benzaldehydes, in sharp contrast to that of benzaldehyde or monofluoro-substituted benzaldehyde, give *cis*-oxazolines **32f,g** as the main reaction products with high % ee. The reasons behind the gradual inversion of stereochemistry brought about by the presence of fluorine atoms, could be reasonably ascribed to the increasing electrophilicity (electron-deficiency) of the phenyl ring in the series from mono- to pentafluorosubstituted benzaldehydes. The working model for the transition-state of the stereoselective step of the gold(I)-catalyzed aldol reaction postulates the following features (Figure 12, transition-state **A**) (54, 55): a) the gold(I) cation is coordinated to the two phosphorus atoms of the ferrocenyl-phosphine ligand, and the carbon of methyl isocyanoacetate; b) the enolate anion of the isocyanoacetate is formed by the abstraction of one of the active methylene protons by the terminal dialkylamino group of the ligand's pendant side chain, that determines electrophilic attack by the *si*-face of an aldehyde on the *si*-face of the enolate. This mode of interactions, through transition state **A**, provides the normally *trans*-oxazoline. The absolute configuration of oxazolines **32f,g** suggests that electrophilic attack of pentafluorobenzaldehyde occurs on the same enolate  $\pi$ -face while the carbonyl  $\pi$ -face selectivity is different to that of the benzaldehyde reaction. Sterically unfavorable transition-state **B**, which leads to the formation of *cis*-(4*S*,5*S*)-oxazolines, could be stabilized by  $\pi$ - $\pi$  attractive interaction between the electron-deficient pentafluorophenyl ring and the negatively charged enolate anion. This assumption is supported by the close analogy between our observations and the results reported by Ojima and Kwon on the unique stereodifferentiation disclosed for reactions of pentafluorophenyl-containing chiral iron acyl complex [(C<sub>6</sub>F<sub>5</sub>)Ph<sub>2</sub>P](CO)CpFeCO<sub>2</sub>Me (Cp =  $\eta^5$ -cyclopentadienyl) (PFCHIRAC). They had proven that this very case of electron donor-acceptor type attractive interaction between the enolate oxygen and pentafluorophenyl moiety reverses the opposite stereochemical outcome in the aldol reactions of PFCHIRAC and fluorine-free CHIRAC (58).

Based on this reasoning, we envisioned that the use of *N,N*-dimethyl- $\alpha$ -isocyanoacetamide (**35**) instead of methyl ester **28**, based on both electronic and steric

**Figure 12. Transition-States Model for the Gold-Catalyzed Aldol Reaction.**

**Figure 13. Aldol Reactions of Isocyanoacetamide with Fluoro-Benzaldehydes.**

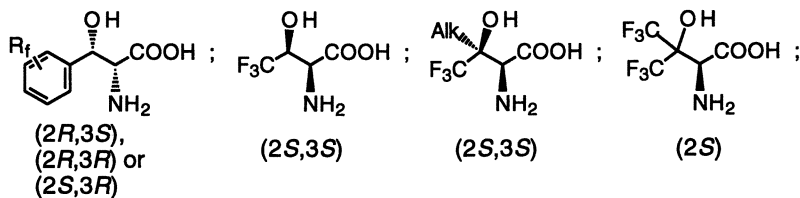


factors, might disturb transition-state **B** (Figure 12) and thereby enhance the *trans*-diastereoselectivity of the polyfluorobenzaldehydes aldol reactions. Indeed, the reaction of pentafluorobenzaldehyde with isocyanoacetamide **35**, catalyzed by 2 mol % of **29/30a**, gives a mixture of *cis/trans*-oxazolines **36f** and **37f** with remarkable domination of the latter, formed with 80% ee (Figure 13). Similar reactivity and stereochemical outcome is observed in the aldol reaction of 2,3,5,6-tetrafluorobenzaldehyde with isocyanoacetamide **35**. In the aldol reactions of trifluoro- and difluoro-benzaldehydes with **35**, the desirable *trans*-oxazolines **37d,c** are obtained with both higher diastereo- and enantioselectivity than the corresponding *trans*-oxazolines **33e,d** (Figure 11) from reaction of the fluoro-aldehydes with isocyanoacetate **28**. Finally, the aldol reactions of isocyanoacetamide **35** with monofluoro-substituted benzaldehydes give the *trans*-oxazolines **37a,b** with the expected high diastereo- and enantioselectivities. However, the use of isocyanoacetamide **35** for the synthesis of *syn*-(2*S*)- $\beta$ -(monofluorophenyl)serines **34**, through oxazolines **37a,b**, seems to have no advantages over the application of isocyanoacetate **28**, which provides a better stereochemical result, giving oxazolines **33a,c**.

The present results have revealed that the stereochemical outcome of the gold(I)-catalyzed asymmetric aldol reactions dramatically depends on the nature of both the fluorobenzaldehyde and the isocyanoacetic acid derivative being used. The results with methyl  $\alpha$ -isocyanoacetate (**28**) reactions and fluorinated benzaldehydes was shown to be controlled by the number of fluorine atoms in the aryl moiety of fluorobenzaldehyde used. Thus, aldol condensations of **28** with monofluorobenzaldehydes furnished *trans*-oxazolines with more than 90% of both *trans*-diastereoselectivity and ee, while in the case of the reactions with polyfluorobenzaldehydes, *cis*-oxazolines were formed as the dominant isomer with high ee (up to 90% ee). In marked contrast to this, reactions of isocyanoacetamide **35** with fluorobenzaldehydes provided preferential formation of *trans*-oxazolines with high % ee, regardless of the fluorosubstituted benzaldehyde used.

## Conclusion

In conclusion, we have demonstrated that various biologically interesting fluorine-containing  $\beta$ -hydroxy amino acids (Figure 14) are easily accessible in high diastereo and enantiomeric purity by means of the asymmetric aldol reactions of nickel-glycine complex or gold-catalyzed reactions of isocyanoacetic acid derivatives with fluorinated aldehydes or ketones. Apart from the synthetic results, this study highlights the surprising capability of polyfluoroalkyl and aryl groups, *albeit* for different reasons, to play the role of stereodirecting factors in the asymmetric aldol reactions explored. The origins of this unusual stereocontrolling effects provided by fluorine is not yet clear and we are currently studying this aspect in detail.

**Figure 14. Some Fluorinated  $\beta$ -Hydroxy Amino Acids Readily Available via Asymmetric Aldol Reactions.**

### Acknowledgments

Financial support of this work by the International Science Foundation (U6M000, U6M200), INTAS (Network 93-799), JSPS Foundation (Japan), Ministry of Education, Japan, for a Grant-in-Aid for Scientific Research, and Uehara Memorial Foundation, is gratefully acknowledged. The author's deepest gratitude goes to The Science and Technology Agency (STA) for the award of Fellowship Program, which is managed by the Research Development Corporation of Japan (JRDC) in cooperation with the Japan International Science and Technology Exchange Center (JISTEC), allowing continuation of active research in the field of enantiocontrolled fluoro-organic synthesis.

### Literature Cited

1. Filler, R. *Chemtech* **1974**, 752.
2. *Biochemistry Involving Carbon-Fluorine Bonds*; Filler, R., Ed.; ACS Symp. Ser. 28; American Chemical Society: Washington, D.C., 1976.
3. *Biomedical Aspects of Fluorine Chemistry*; Filler, R.; Kobayashi, Y., Eds.; Elsevier Biomedical Press: New York and Kodansha Ltd: Tokyo, 1982.
4. *Fluorinated Carbohydrates*, Taylor, N. F., Ed., ACS Symp. Ser. 374; American Chemical Society: Washington, D.C., 1988.
5. *Selective Fluorination in Organic and Bioorganic Chemistry*, Welch, J. T. Ed.; ACS Symp. Ser. 456; American Chemical Society: Washington, D.C., 1991.
6. Welch, J. T.; Eswarakrishnan, S. *Fluorine in Bioorganic Chemistry*; John Wiley & Sons: New York, 1991.
7. *Organofluorine Compounds in Medicinal Chemistry and Biomedical Applications*; Filler, R.; Kobayashi, Y.; Yagupolskii, L. M., Eds.; Elsevier: Amsterdam, 1993.
8. *Fluorine-containing Amino Acids. Synthesis and Properties*; Kukhar, V. P.; Soloshonok, V. A., Eds.; John Wiley & Sons: Chichester, 1994.
9. Walsh, C. *Tetrahedron* **1982**, 38, 871.
10. Resnati, G. *Tetrahedron* **1993**, 42, 9385.
11. *Enantiocontrolled Synthesis of Fluoro-Organic Compounds*; Hayashi, T.; Soloshonok, V. A., Eds.; Tetrahedron: Asymmetry. Special Issue; *Tetrahedron: Asymmetry* **1994**, 5, issue N 6.
12. Iseki, K.; Kobayashi, Y. In *Reviews on Heteroatom Chemistry*; Oae, S., Ed.; MYU: Tokyo, 1995.
13. *Fluoroorganic Chemistry: Synthetic Challenges and Biomedical Rewards*; Resnati, G.; Soloshonok, V. A., Eds.; Tetrahedron Symposium in Print, **58**; *Tetrahedron* **1996**, 52, issue N 1.
14. Kukhar, V. P.; Resnati, G.; Soloshonok, V. A. in *Fluorine-containing Amino Acids. Synthesis and Properties*; Kukhar, V. P.; Soloshonok, V. A., Eds.; John Wiley & Sons: Chichester, 1994.
15. Soloshonok, V. A. In *Enantioselective Synthesis of  $\beta$ -Amino Acids*; Juaristi, E. Ed., VCH: New York, scheduled to appear in 1996.

16. Heathcock, C. H. In *Asymmetric Synthesis*; Morrison, J. D., Ed.; Academic Press: New York, 1984; Vol. 3.
17. Seebach, D. *Angew. Chem. Int. Ed. Engl.* **1990**, *29*, 1320.
18. *Chemistry and Biochemistry of the Amino Acids*; Barrett, G. C., Ed.; Chapman and Hall: London, 1985.
19. Greenstein, J. P.; Winitz, M. *Chemistry of the Amino Acids*; Robert E. Krieger: FL, 1984; Vols. 1-3.
20. Williams, D. H. *Acc. Chem. Res.* **1984**, *17*, 364.
21. Jolad, S. D.; Hoffmann, J. J.; Torance, S. J.; Wiedhopf, R. M.; Cole, J. R.; Arora, S. K.; Bates, R. B.; Garguilo, R. L.; Kriek, G. R. *J. Amer. Chem. Soc.* **1977**, *99*, 8040.
22. Owa, T.; Haupt, A.; Otsuka, M.; Kobayashi, S.; Tomioka, N.; Itai, A.; Ohno, M. *Tetrahedron* **1992**, *48*, 1193.
23. Kirk, K. L. In *Selective Fluorination in Organic and Bioorganic Chemistry*, Welch, J. T. Ed.; ACS Symp. Ser. 456; American Chemical Society: Washington, D.C., 1991.
24. Giannis, A.; Kolter, T. *Angew. Chem. Int. Ed. Engl.* **1993**, *32*, 1244.
25. Miller, M. J. *Acc. Chem. Res.* **1986**, *19*, 49.
26. Walborsky, H. M.; Lang, J. H. *J. Amer. Chem. Soc.* **1956**, *78*, 4314.
27. *Peptide Chemistry: Design and Synthesis of Peptides, Conformational Analysis and Biological Functions*; Hruby V. J.; Schwyzer, R., Eds.; Tetrahedron-Symposia-in-Print, **31**; *Tetrahedron* **1988**, *44*, 661.
28. Yun, C.-Y.; Chang, C.-N.; Yeh, I.-F. *Yao Hsueh Hsueh Pao*, **1959**, *7*, 237; *Chem. Abstr.* **1960**, *54*, 12097c.
29. Blazevic, N.; Zymalkowsky, F. *Arch. Pharm. (Weinheim, Ger.)* **1975**, *305*, 541; *Chem. Abstr.* **1975**, *83*, 179533q.
30. Edmonds, E. J.; Volkman, C. M.; Beerstecher, E. J. *Chem. Zbl.* **1957**, 5315.
31. Cahn, R.S.; Ingold, C.; Prelog, V. *Angew. Chem. Int. Ed. Engl.*, **1966**, *5*, 385.
32. Kitazume, T.; Lin, J. T.; Yamazaki, T. *Tetrahedron: Asymmetry* **1991**, *2*, 235.
33. Yamazaki, T.; Haga, J.; Kitazume, T. *Bioorg. Med. Chem. Lett.* **1991**, *1*, 271.
34. Sting, A. R.; Seebach, D. *Tetrahedron* **1996**, *52*, 279.
35. Seebach, D.; Juaristi, E.; Miller, D. D.; Schickli, C.; Weber, T. *Helv. Chim. Acta* **1987**, *70*, 237.
36. Blaser, D.; Seebach, D. *Liebigs Ann. Chem.* **1991**, 1067.
37. Williams, R. M. *Synthesis of Optically Active  $\alpha$ -Amino Acids*; Vol.7 of Organic Chemistry Series; Baldwin, J. E.; Magnus, P. D., Eds.; Pergamon Press: Oxford, 1989.
38. Duthaler, R. O. *Tetrahedron* **1994**, *50*, 1539.
39. Belokon', Yu. N. *Pure Appl. Chem.* **1992**, *64*, 1917.
40. Belokon', Yu. N.; Maleev, V. I.; Vitt, S. V.; Ryzhov, M. G.; Kondrashov, Y. D.; Golubev, S. N.; Vauchskii, Y. P.; Novikova, M. I.; Krasutskii, P. A.; Yurchenko, A. G.; Dubchak, I. L.; Shklover, V. E.; Struchkov, Y. T.; Bakhmutov, V. I.; Belikov, V. M. *J. Chem. Soc., Dalton Trans.* **1985**, 17.
41. Matthews, W. S.; Baras, J. E.; Bartmess, J. E.; Bordwell, F. G.; Cornoforth, F. J.; Drucker, G. E.; Margolin, Z.; McCallum, R. S.; McCallum, G. J.; Vanier, N. R. *J. Am. Chem. Soc.*, **1975**, *97*, 7006.
42. Belokon', Yu. N.; Bulychev, A. G.; Vitt, S. V.; Struchkov, Yu. T.; Batsanov, A. S.; Timofeeva, T. V.; Tsyryapkin, V. A.; Ryzhov, M. G.; Lysova, L. A.; Bakhmutov, V. I.; Belikov, V. M. *J. Am. Chem. Soc.* **1985**, *107*, 4252.
43. Belokon', Yu. N.; Sagyan, A. S.; Djamgaryan, S. A.; Bakhmutov, V. I.; Vitt, S. V.; Batsanov, A. S.; Struchkov, Yu. T.; Belikov, V. M. *J. Chem. Soc. Perkin Trans. 1*, **1990**, 2301.

44. Soloshonok, V. A.; Kukhar, V. P.; Galushko, S. V.; Svistunova, N. Y.; Avilov, D. V.; Kuzmina, N. A.; Raevski, N. I.; Struchkov, Y. T.; Pisarevsky, A. P.; Belokon, Y. N. *J. Chem. Soc. Perkin Trans 1* **1993**, 3143.
45. Soloshonok, V. A.; Svistunova, N. Y.; Kukhar, V. P.; Kuzmina, N. A.; Belokon, Y. N. *Izv. Akad. Nauk SSSR, Ser. Khim.* **1992**, 687; *Chem. Abstr.* **117**: 212905h.
46. Soloshonok, V. A.; Kukhar, V. P.; Galushko, S. V.; Rozhenko, A. B.; Kuzmina, N. A.; Kolycheva, M. T.; Belokon, Y. N. *Izv. Akad. Nauk SSSR, Ser. Khim.* **1991**, 1906; *Chem. Abstr.* **116**: 21426x.
47. Soloshonok, V. A.; Kukhar, V. P.; Galushko, S. V.; Kolycheva, M. T.; Rozhenko, A. B.; Belokon, Y. N. *Izv. Akad. Nauk SSSR, Ser. Khim.* **1991**, 1166; *Chem. Abstr.* **115**: 136682z.
48. Gerasimova, T. N.; Fokin, E. P. *Usp. Khim.* **1980**, *49*, 1057; *Russ. Chem. Rev. Transl.* **1980**, *49*, 558.
49. Filler, R.; Schure, R. M. *J. Org. Chem.* **1967**, *32*, 1217.
50. Soloshonok, V. A.; Avilov, D. V.; Kukhar, V. P.; Tararov, V. I.; Saveleva, T. F.; Churkina, T. D.; Ikonnikov, N. S.; Kochetkov, K. A.; Orlova, S. A.; Pysarevsky, A. P.; Struchkov, Y. T.; Raevsky, N. I.; Belokon, Y. N. *Tetrahedron : Asymmetry* **1995**, *6*, 1741.
51. Soloshonok, V. A.; Kukhar, V. P.; Batsanov, A. S.; Galakhov, M. A.; Belokon, Y. N.; Struchkov, Y. T. *Izv. Akad. Nauk SSSR, Ser. Khim.* **1991**, 1548; *Chem. Abstr.* **115**: 256590q.
52. Weber, B.; Seebach, D. *Tetrahedron* **1994**, *50*, 6117.
53. *Catalytic Asymmetric Synthesis*, Ojima, I. Ed.; VCH Publishers, New York, **1993**.
54. Hayashi, T. *Pure Appl. Chem.* **1988**, *60*, 7.
55. Togni, A.; Pastor, S. D. *J. Org. Chem.* **1990**, *55*, 1649.
56. Soloshonok, V. A.; Hayashi, T. *Tetrahedron Lett.* **1994**, *35*, 2713.
57. Soloshonok, V. A.; Kacharov, A. D.; Hayashi, T. *Tetrahedron* **1996**, *52*, 245.
58. Ojima, I.; Kwon, H. B. *J. Am. Chem. Soc.* **1988**, *110*, 5617.
59. Soloshonok, V. A.; Hayashi, T. *Tetrahedron: Asymmetry* **1994**, *5*, 1091.

## Chapter 3

# Synthesis and Incorporation of $\alpha$ -Trifluoromethyl-Substituted Amino Acids into Peptides

Beate Kokschi<sup>1</sup>, Norbert Sewald<sup>2</sup>, Hans-Dieter Jakubke<sup>1</sup>,  
and Klaus Burger<sup>2</sup>

<sup>1</sup>Department of Biochemistry, University of Leipzig, Talstrasse 33,  
D-04103 Leipzig, Germany

<sup>2</sup>Department of Organic Chemistry, University of Leipzig, Talstrasse 35,  
D-04103 Leipzig, Germany

Methodology for synthesis and incorporation of  $\alpha$ -trifluoromethyl substituted amino acids into N- and C-terminal position of peptides is described. The incorporation of  $\alpha$ -trifluoromethyl substituted amino acids into peptides retards proteolytic degradation, enhances lipophilicity, and induces secondary structures. The influence of the trifluoromethyl group on the structure and the receptor affinity of different biologically active peptides (TRH, GnRH, SP) has been studied.

A major drawback of peptide drugs is their rapid degradation by proteases, their low lipophilicity and the lack of transport systems to direct peptides into cells. Therefore, cell membranes generally resist passage of most peptides. Peptides are rapidly excreted via liver and kidney. The high conformational flexibility of peptides creates another problem: bioactive peptides often bind to different receptor sites causing undesired side effects (1).

The incorporation of  $\alpha,\alpha$ -disubstituted amino acids into key positions of peptides is an efficient strategy to retard proteolytic degradation and to stabilize secondary structures (2,3). Due to the unique properties of the trifluoromethyl group (high electronegativity, high lipophilicity and high steric demand),  $\alpha$ -trifluoromethyl amino acids ( $\alpha$ -TFM amino acids) are a special class of  $\alpha,\alpha$ -disubstituted amino acids which can profoundly improve the above mentioned characteristics of peptides.

The structural alteration influences hydrolytic stability of peptides containing  $\alpha$ -TFM amino acids resulting in retarded degradation by peptidases (4) and consequently in prolonged intrinsic activity. The high lipophilicity (5) enhances *in vivo* absorption and improves permeability through certain body barriers. However, the lipophilic effect of a trifluoromethyl group depends very much on its position in a molecule (6). The steric bulk of a trifluoromethyl group is still a

0097-6156/96/0639-0042\$15.00/0  
© 1996 American Chemical Society

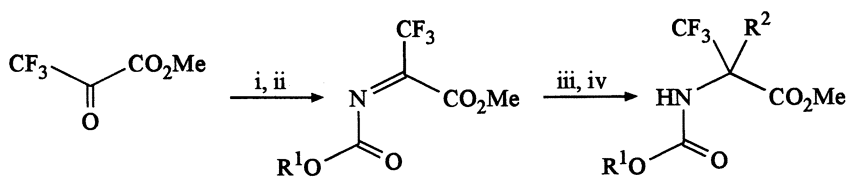


controversial issue (7); it should be close to that of an isopropyl group. Doubtlessly, it exerts severe conformational restrictions on the peptide chain inducing secondary structures (8).

Furthermore, because of the high electron density, trifluoromethyl groups are capable of participating in hydrogen bonding and of acting as coordinative sites in metal complexes. Another attractive feature of the trifluoromethyl group is its relatively low toxicity and high stability compared to monofluoromethyl and difluoromethyl groups (9). Finally,  $^{19}\text{F}$  NMR spectroscopy provides a very efficient method for conformational studies of fluorine containing peptides and glycopeptides as well as for the elucidation of metabolic processes.

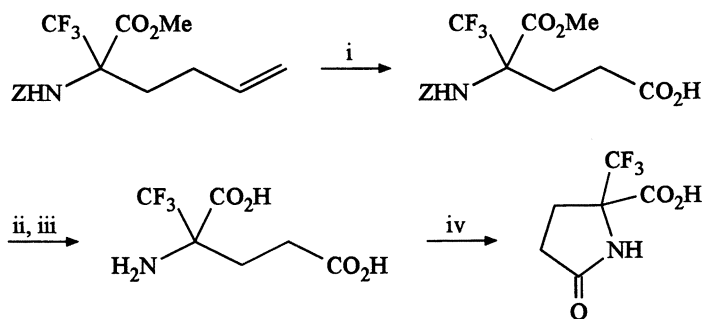
### Synthesis of $\alpha$ -Trifluoromethyl Amino Acids

Several routes towards  $\alpha$ -trifluoromethyl amino acids ( $\alpha$ -TFM amino acids) have been developed. The most general approach is the amidoalkylation of carbon nucleophiles with alkyl 2-(alkoxycarbonylimino)-3,3,3-trifluoropropionates (10).



i)  $\text{R}^1\text{OCONH}_2$ ; ii)  $(\text{CF}_3\text{CO})_2\text{O}$ /pyridine; iii)  $\text{R}^2\text{MgX}$ ; iv)  $\text{H}_3\text{O}^+$

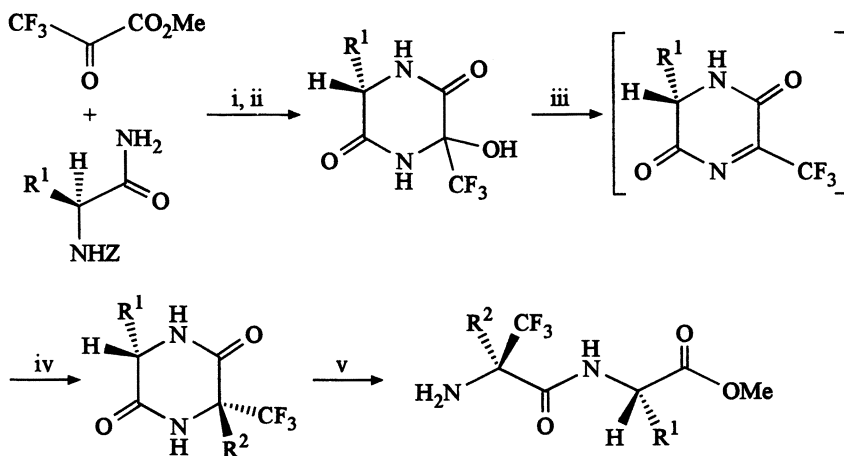
Multifunctional  $\alpha$ -TFM amino acids can be synthesized via the above mentioned route from carbon nucleophiles. Appropriately protected additional functionalities may be present in the nucleophile or can be introduced by transformation of CC double and triple bond systems which can be introduced into the side chain without protection (11).



i)  $\text{KMnO}_4/\text{dil. H}_2\text{SO}_4$ ; ii)  $\text{NaOH}$  (5%); iii)  $\text{H}_2$ ,  $\text{Pd/C}$ ,  $\text{MeOH}/\text{H}_2\text{O}$  (2:1), r.t.;  
iv) r.t.

Most synthetic routes to optically pure  $\alpha$ -TFM amino acids rely on chemical (12,13) and enzymatic resolution (14). A promising strategy for a diastereoselective

synthesis of  $\alpha$ -TFM amino acids proceeds via amidoalkylation of carbon nucleophiles with *in situ* formed homochiral cyclic acyl imines. The dioxopiperazines (DOP) obtained with good stereoselectivity can be transformed into homochiral dipeptide esters on regioselective acidolysis in methanol (15).



i)  $\text{CH}_2\text{Cl}_2$ , r.t.; ii)  $\text{H}_2$ , Pd/C, MeOH, r.t.; iii)  $(\text{CF}_3\text{CO})_2\text{O}$ , THF,  $0^\circ\text{C}$ ; iv)  $\text{R}^2\text{M}$ , THF, then buffer, pH 7; v) HCl, MeOH,  $\Delta\text{T}$ , then propylene oxide

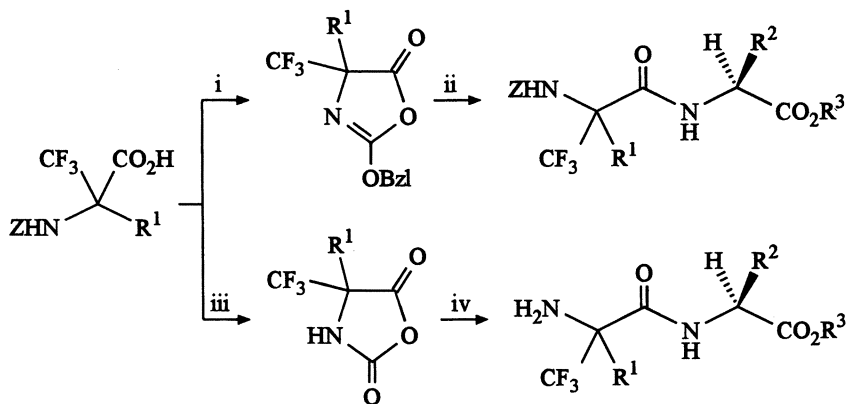
### Peptide Synthesis with $\alpha$ -TFM Amino Acids Protective Group Strategy

$\alpha$ -TFM amino acids with orthogonal protective groups (BOC, Z and OMe, OEt) are readily obtained from alkyl 2-(alkoxycarbonylimino)-3,3,3-trifluoropropionates via amidoalkylation of carbon nucleophiles (16). Alkaline hydrolysis with 1N KOH/methanol 1:1 (v/v), followed by acidic work-up provides the free carboxylic acids BOC-( $\alpha$ -TFM)Xaa-OH and Z-( $\alpha$ -TFM)Xaa-OH, respectively. Cleavage of the BOC and the Z group can be accomplished using standard procedures (4). The presence of the electron-withdrawing trifluoromethyl group in the  $\alpha$ -position exerts considerable electronic and steric effects on the reactivity of both the carboxylic and the amino group [pK<sub>a</sub> values: H-Ala-OH: 2.34; H-( $\alpha$ -TFM)Ala-OH: 1.98; H-Ala-NH<sub>2</sub>: 9.87; H-( $\alpha$ -TFM)Ala-NH<sub>2</sub>: 5.91 (17)]. The low nucleophilicity of the amino group of  $\alpha$ -TFM amino acid esters prevents dioxopiperazine formation. Esters of  $\alpha$ -TFM amino acids can be distilled *in vacuo* without appreciable oligomerization or decomposition (16,18).

### $\alpha$ -TFM Amino Acids as Acyl Donors in Peptide Synthesis

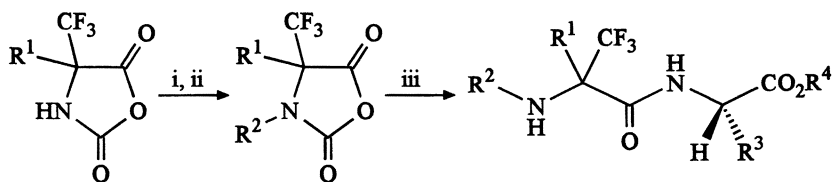
Carboxylic group activation of  $\alpha$ -TFM amino acids can be achieved by standard activation methods, e.g. DCCI, diphenylchlorophosphate, mixed anhydrides, Leuchs anhydrides (N-carboxy anhydrides, NCA) and azides (19,20), respectively.

The mixed anhydrides cyclize spontaneously to give trifluoromethyl substituted 5(4H)-oxazolones which also are formed on reaction of *Z*-( $\alpha$ -TFM)Xaa-OH with DCCI (even in the presence of HOBT) or with diphenylchlorophosphate in the presence of a base. Epimerization of the 5(4H)-oxazolone is only a problem in the case of ( $\alpha$ -TFM)Gly; all other oxazolones derived from  $\alpha,\alpha$ -disubstituted amino acids do not possess a proton at C(4). Trifluoromethyl substituted 5(4H)-oxazolones readily react with amino acid derivatives to give dipeptides (4). However, 2-*tert*-butoxy-4-trifluoromethyl-5(4H)-oxazolones decompose at room temperature to give Leuchs anhydrides via retro-ene reaction. Therefore, the BOC group is of limited value for peptide synthesis with  $\alpha$ -TFM amino acids (21).



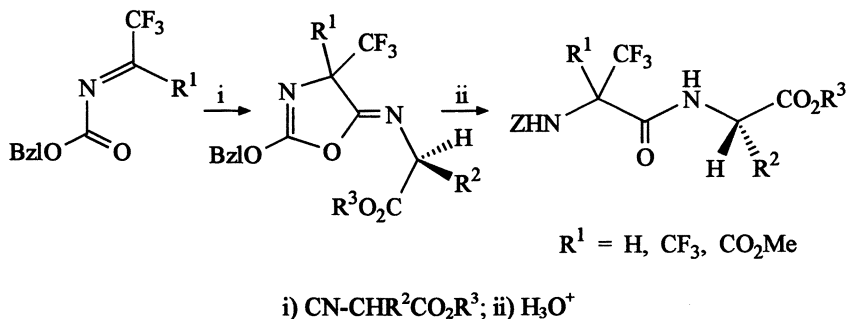
- i) DCCI or EtOCOC1, base; ii)  $\text{H}_2\text{N-CHR}^2\text{CO}_2\text{R}^3$ ; iii)  $\text{SOCl}_2$  or  $\text{Cl}_3\text{COCOC1}$ ;  
iv)  $\text{H}_2\text{N-CHR}^2\text{CO}_2\text{R}^3$

N-Carboxy anhydrides derived from  $\alpha$ -TFM amino acids can be prepared in very good yields on heating *Z*-( $\alpha$ -TFM)Xaa-OH with phosphorus trichloride, diposgene, triphosgene, or thionyl chloride. The major drawback of the NCA method in classical peptide chemistry is their pronounced tendency to oligomerize, because the amino group of the newly formed peptide competes with the amino acid ester as a nucleophile. This problem does not arise on ring opening of a NCA derived from an  $\alpha$ -TFM amino acid due to the low nucleophilicity of the amino function (22). Furthermore, this type of NCA can be easily deprotonated at the nitrogen atom and subsequently N-alkylated, providing N-alkyl  $\alpha$ -TFM amino acid precursors (23). As a consequence of the highly crowded stereochemistry, the reactivity of an N-alkylated NCA towards nucleophiles is considerably lower than that of the N-unsubstituted derivative.



- i) NaH, DMF; ii)  $\text{R}^2\text{I}$ ; iii)  $\text{H}_2\text{N-CHR}^3\text{-CO}_2\text{R}^4$ ,  $\text{CHCl}_3$ ,  $20^\circ\text{C}$

Amides of ( $\alpha$ -TFM)Gly, hexafluoroaminoisobutyric acid, and ( $\alpha$ -TFM) amino malonate, respectively, are obtained on [4+1] cycloaddition of isocyanides to trifluoromethyl or bis(trifluoromethyl) substituted acyl imines and subsequent cleavage of the resulting 5-imino-4-trifluoromethyl-2-oxazoline with dilute acid. When isonitriles derived from N-formyl amino acid esters are used as dienophiles, hydrolysis of the [4+1] cycloadducts provides dipeptides with ( $\alpha$ -TFM)Gly, hexafluoroaminoisobutyrate and TFM amino malonate in the N-terminal position (19,24).



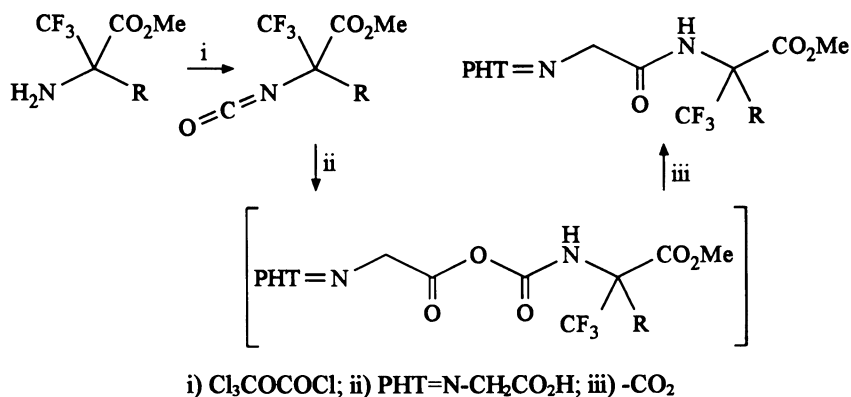
### $\alpha$ -TFM Amino Acids as Nucleophiles in Dipeptide Synthesis Amino Group "Activation"

The low nucleophilicity of the amino group and the steric bulk of the trifluoromethyl group requires modification of standard procedures for peptide synthesis. Only the least bulky amino acid esters H-( $\alpha$ -TFM)Gly-OMe and H-( $\alpha$ -TFM)Ala-OMe can be coupled using classical methodology (4). For  $\alpha$ -TFM amino acids with bulkier side chains, all classical activation methods examined remain unsuccessful or result in substantial epimerization of the non-fluorinated amino acid. Peptide bond formation under quite drastic reaction conditions is only reasonable in substrates when epimerization is not possible (19,20).

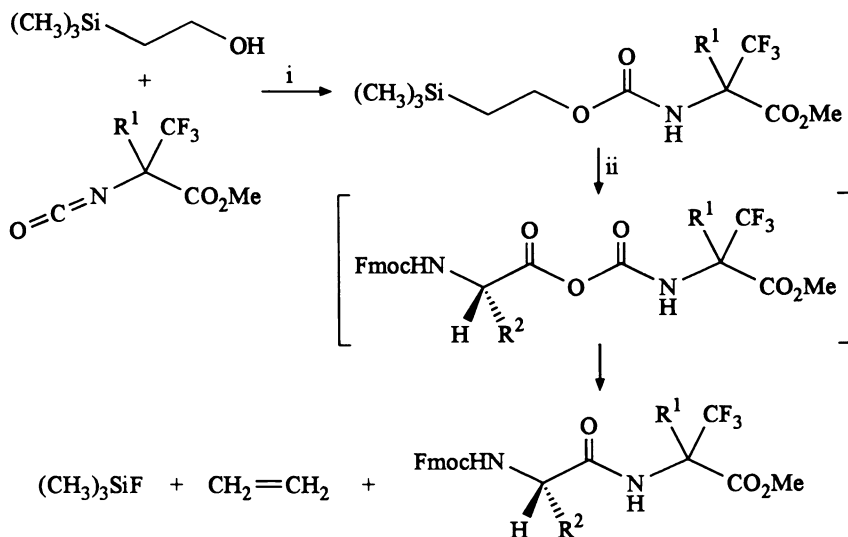
Amino group activation via trimethylsilylation is described in the case of  $\alpha,\alpha$ -disubstituted amino acids (25). However, the usual trimethylsilylation reagents (trimethylsilyl chloride / triethylamine, trimethylsilyl acetamide, and N,O-bis(trimethylsilyl) acetamide) fail to react with  $\alpha$ -TFM amino acids (20).

Peptide couplings involving the amino group of ( $\alpha$ -TFM) amino acid esters can be achieved by conversion to the corresponding isocyanates by treatment with trichloromethyl chloroformate (26). The isocyanates can be coupled directly with N-protected amino acids, e.g. PHT=Yaa-OH via a mixed anhydride of the corresponding carbamic acid (20).

The same mixed anhydride presumably is involved in an *in situ* deprotection/coupling procedure of Teoc (2-trimethylsilylethoxycarbonyl) protected  $\alpha$ -TFM amino acids. The introduction of the Teoc group can be achieved on reaction of



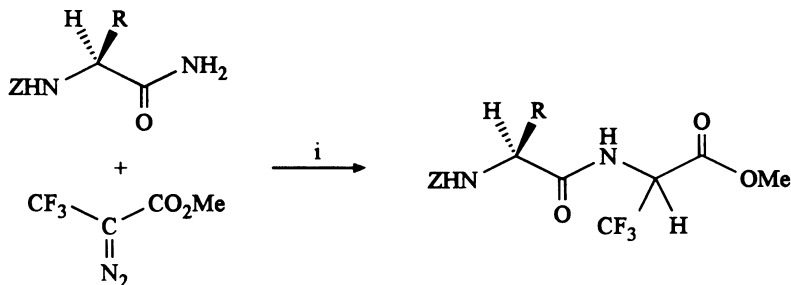
$\alpha$ -TFM amino acid derived isocyanates with 2-trimethylsilyl ethanol. In the presence of catalytic amounts of fluoride ions, Teoc protected  $\alpha$ -TFM amino acids react with Fmoc amino acid fluorides to give Fmoc protected dipeptide esters with an  $\alpha$ -TFM amino acid in the C-terminal position in reasonable to good yields (20,27).



$\alpha$ -TFM amino acids can be transformed into the N-formyl derivatives on treatment with formic acid /acetic anhydride and subsequent dehydration to give the corresponding isonitriles, which have been introduced successfully into Ugi's four component condensation (4CC) (28). Tripeptides with N-terminal and C-terminal

$\alpha$ -TFM amino acids result from this reaction, but the stereoselectivity is only moderate (19).

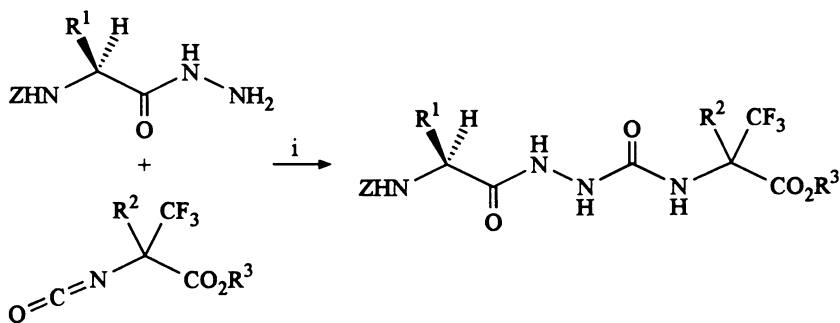
( $\alpha$ -TFM)Gly can be introduced into the C-terminal position of peptides on reaction of N-protected amino acid and peptide amides in a one step process at room temperature with methyl 3,3,3-trifluoro-2-diazopropionate in the presence of catalysts like Cu(0) and Rh<sub>2</sub>(OAc)<sub>4</sub> (29).



i) Cu(0) or Rh<sub>2</sub>(OAc)<sub>4</sub>, CH<sub>2</sub>Cl<sub>2</sub>, r.t.

A promising strategy for the general synthesis of dipeptide esters with optically pure  $\alpha$ -TFM amino acids in the C-terminal position is the regioselective cleavage of the dioxopiperazines (*vide supra*). Further N-terminal chain elongation can be achieved by chemical as well as enzymatic methods without problems (15).

Isocyanates derived from amino acids are valuable precursors for the synthesis of azapeptides, which are obtained in good yields on reaction of the corresponding isocyanates with amino acid hydrazides (30). Azapeptides with  $\alpha$ -TFM amino acids in the N-terminal [H-( $\alpha$ -TFM)Xaa-Agly-Yaa-OR], C-terminal [Z-Xaa-Agly-( $\alpha$ -TFM)Yaa-OR] and in both positions [H-( $\alpha$ -TFM)Xaa-Agly-( $\alpha$ -TFM)Yaa-OR] are readily available by this strategy. Because of the low nucleophilicity of the amino group in  $\alpha$ -TFM amino acid hydrazides, N-protection is not necessary on reaction with isocyanates (31).



i) CHCl<sub>3</sub>, 0°C

### Hydrolytic and Proteolytic Stability of Z-protected $\alpha$ -TFM Amino Acid Derivatives Protease catalyzed Peptide Synthesis with $\alpha$ -TFM Amino Acids

Z-( $\alpha$ -TFM)Gly-OMe is unstable at pH 7 and is converted into Z-amino malonate via a sequential base-catalyzed HF elimination / H<sub>2</sub>O addition process. All other  $\alpha$ -TFM amino acids lacking the  $\alpha$ -proton are stable towards base. The presence of a trifluoromethyl group in the  $\alpha$ -position decreases the rate of alkaline hydrolysis considerably. At pH 9, for example, only 4% of Z-( $\alpha$ -TFM)Phe-OMe is hydrolyzed after 20 min, whereas Z-Phe-OMe is hydrolyzed completely after 5 min under the same reaction conditions. These results demonstrate that a trifluoromethyl group in the  $\alpha$ -position slows down hydrolysis by a factor of approximately 12 (4).

Proteases like subtilisin,  $\alpha$ -chymotrypsin or papain accept  $\alpha$ -TFM amino acid esters only to a very limited extent. Both the hydrolysis rate and the turnover decrease in the order Z-( $\alpha$ -TFM)Gly-OMe > Z-( $\alpha$ -TFM)Ala-OMe > Z-( $\alpha$ -TFM)Leu-OMe. Z-( $\alpha$ -TFM)Phe-OMe is not turned over at all. These data exclude the application of proteases in the resolution of enantiomeric  $\alpha$ -TFM amino acid derivatives except in the case of Z-( $\alpha$ -TFM)Gly-OMe.

However, dipeptide esters with N-terminal TFM amino acid are accepted as substrates by proteolytic enzymes. H-( $\alpha$ -TFM)Phg-Phe-OMe is hydrolyzed by  $\alpha$ -chymotrypsin or subtilisin within short reaction times to give the unprotected dipeptide. H-( $\alpha$ -TFM)Phg-Phe-OMe and H-( $\alpha$ -TFM)Phe-Phe-OMe are converted by  $\alpha$ -chymotrypsin in the presence of H-Leu-NH<sub>2</sub> to give the tripeptides H-( $\alpha$ -TFM)Phg-Phe-Leu-NH<sub>2</sub> and H-( $\alpha$ -TFM)Phe-Phe-Leu-NH<sub>2</sub>, respectively (4,32). Stereoselective aminolysis of R,S-H-( $\alpha$ -TFM)Phe-Tyr-OMe by peptide amides can be achieved using cryoenzymatic reaction conditions (33,34). Consequently, several tachykinin analogs containing  $\alpha$ -TFM amino acids have been synthesized by enzymatic fragment condensation (*vide infra*).

### Proteolytic Stability of $\alpha$ -TFM Amino Acid Substituted Peptides

$\alpha$ -TFM amino acid substitutions influence the interaction between substrate and enzyme, depending on both the enzyme used and the position relative to the cleavage site. The catalytic mechanism and the substrate specificity of the pancreatic protease  $\alpha$ -chymotrypsin is well understood. Therefore, it represents an ideal model protease for the investigation of proteolytic stability conferred to peptides modified chemically by incorporation of non-natural amino acids, e.g.  $\alpha$ -TFM amino acids. The model peptides synthesized by solution methods contain a well-defined cleavage site, namely an aromatic amino acid at P<sub>1</sub> position [P-nomenclature according to Schechter and Berger, (35)] (36) and an  $\alpha$ -TFM amino acid. Variation of the position of the latter relative to the cleavage site (in the range P<sub>3</sub>-P'<sub>2</sub>) and qualitative determination of the hydrolysis rates directly reveals the influence of an  $\alpha$ -TFM amino acid in a specific position of the peptide on its proteolytic stability. Comparison with peptides containing the fluorine-free disubstituted amino acid Aib ( $\alpha$ -aminoisobutyric acid) allows to separate electronic from steric effects (37).

Model Peptides:

cleavage site					
↓					
P <sub>3</sub>	P <sub>2</sub>	P <sub>1</sub>	P <sub>1</sub> '	P <sub>2</sub> '	
	Z	(α-TFM)Phe	Leu	NH <sub>2</sub>	
	Z	(α-CH <sub>3</sub> )Phe	Leu	NH <sub>2</sub>	
	Z	(α-TFM)Ala	Leu	NH <sub>2</sub>	
	Z	Aib	Leu	NH <sub>2</sub>	
Z	(α-TFM)Ala	Phe	Leu	NH <sub>2</sub>	
Z	Aib	Phe	Leu	NH <sub>2</sub>	
	Z	Phe	(α-TFM)Ala	Ala	NH <sub>2</sub>
	Z	Phe	Aib	Ala	NH <sub>2</sub>
	Z	Phe	Leu	(α-TFM)Ala	NH <sub>2</sub>
	Z	Phe	Leu	Aib	NH <sub>2</sub>

Figures 1 and 2 summarize the results of the proteolysis studies. Substitutions at P<sub>1</sub>-position result in an absolute proteolytic stability towards enzymatic hydrolysis whereas substitutions at P<sub>2</sub> significantly increase the proteolytic stability compared to the unsubstituted model peptide. Even for peptides substituted at P<sub>3</sub> a diminished rate of degradation is observed. Comparison of the proteolysis data for the α-TFM substituted peptides shows that not only the position of the substitution but also the absolute configuration of the α-TFM amino acid significantly influences the proteolytic stability of peptides.

Similar effects are observed in the case of α-TFM substitution in P<sub>1</sub>' and P<sub>2</sub>'. There is a significant difference between α-methyl and α-TFM substituted peptides in the sense that the former show a stronger retardation of proteolysis at all positions.

The strongest influence of the configuration is detected for the diastereomeric model peptides containing an α-TFM amino acid in P<sub>1</sub>'-position. While the (SRS)-diastereomer is hydrolyzed rapidly, the (SSS)-diastereomer shows an extraordinary proteolytic stability which is similar to that of the Aib substituted peptide. This surprising effect can not be explained by the steric constraints of the TFM group. The steric bulk of a TFM group seems to be close to that of an isopropyl group. Moreover, the hydrolysis rate of the (SRS) configured TFM substituted diastereomer compares to that of the unsubstituted model peptide. The different proteolytic stability of the diastereomers results from a specific interaction between the substrate and the enzyme induced by the high electron density of the TFM group.



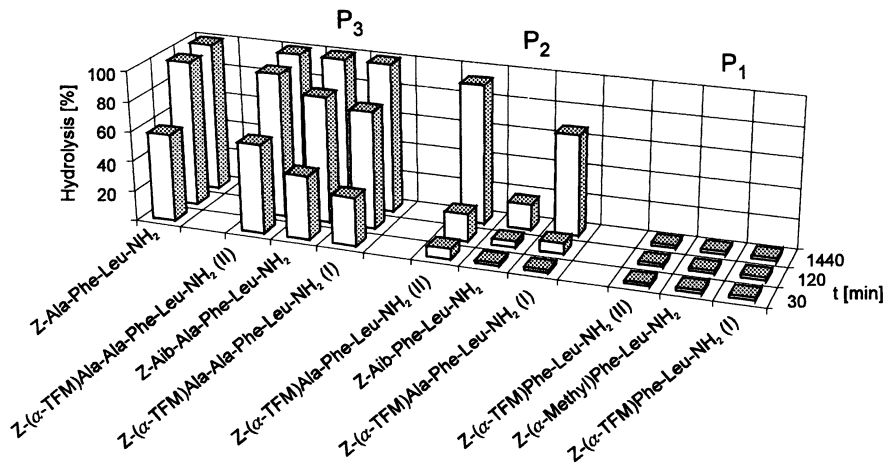


Figure 1: Results of the proteolysis studies of the model peptides with  $\alpha$ -TFM amino acids in P position

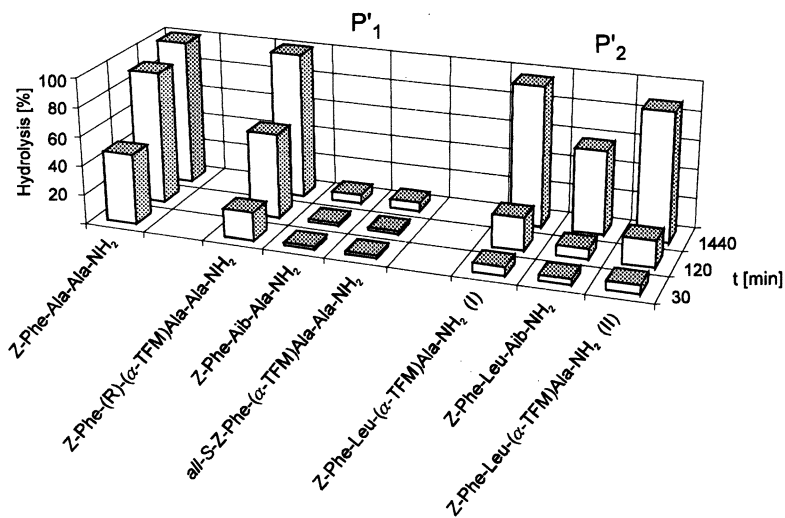


Figure 2: Results of the proteolysis studies of the model peptides with  $\alpha$ -TFM amino acids in P' position

The catalytic triad of  $\alpha$ -chymotrypsin consists of serine 195, histidine 57 and asparagine 102. In the first step of  $\alpha$ -chymotrypsin-catalyzed hydrolysis, a nucleophilic attack takes place by the serine 195 oxygen on the carbonyl function of the substrate. A tetrahedral transition state stabilized by two additional hydrogen bonds between substrate and enzyme is formed. The nucleophilic attack by the serine 195 oxygen on the substrate carbonyl is accompanied by a proton transfer from the serine 195 oxygen to the histidine 57 nitrogen (38).

A qualitative explanation of the observed phenomena is derived from force field calculations. The structure of  $\alpha$ -chymotrypsin is available from the Brookhaven Protein Data Bank (39). Before energy minimization (CHARMm 22 force field, Quanta) the substrates Z-Phe-Ala-Ala-NH<sub>2</sub>, (SRS)-Z-Phe-( $\alpha$ -TFM)Ala-Ala-NH<sub>2</sub>, (SSS)-Z-Phe-( $\alpha$ -TFM)Ala-Ala-NH<sub>2</sub> and Z-Phe-Aib-Ala-NH<sub>2</sub> are pasted into the active site of  $\alpha$ -chymotrypsin so that the phenylalanine residue occupies the hydrophobic pocket and the peptide bond to be cleaved is close to the serine 195.

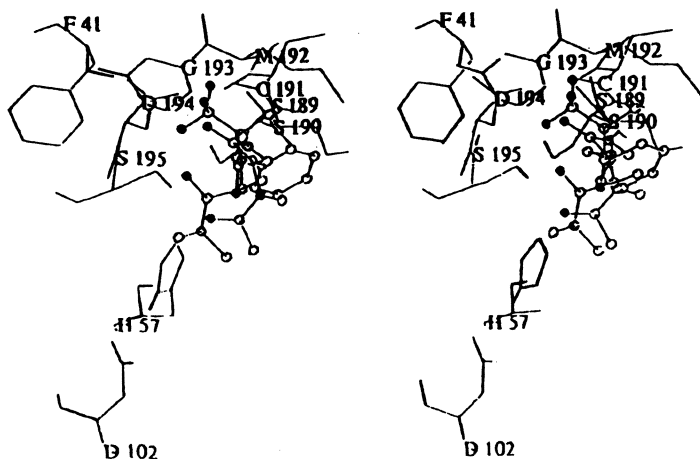


Figure 3: *Stereoview of the energy minimized complex between  $\alpha$ -chymotrypsin and the Z-(S)-Phe-(R)-( $\alpha$ -TFM)Ala-(S)-Ala-NH<sub>2</sub>*

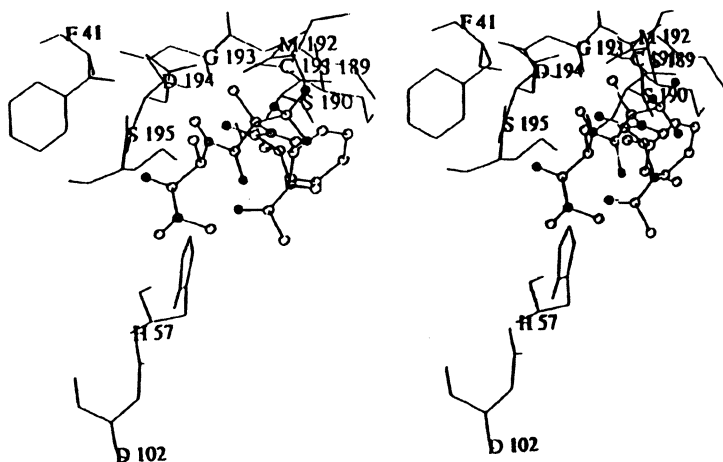


Figure 4: *Stereoview of the energy minimized complex between  $\alpha$ -chymotrypsin and the Z-(S)-Phe-(S)-( $\alpha$ -TFM)Ala-(S)-Ala-NH<sub>2</sub>*

Figure 3 shows a stereoview of the complex between  $\alpha$ -chymotrypsin and the (SRS)-diastereomer. In this case the steric constraints exhibited by the  $\alpha,\alpha$ -disubstituted amino acid are outweighed by an advantageous interaction of the TFM group with the serine side chain of the enzyme. The fluorine substituents can presumably act as electron pair donors in hydrogen bonding, thereby enhancing the nucleophilicity of the serine oxygen. For the (SSS)-diastereomer a favourable interaction between substrate and enzyme is impossible because the TFM group points at the opposite direction. The large distance between the serine oxygen and the fluorine atoms of the TFM group prevents the formation of a hydrogen bond (Figure 4).

### Incorporation of $\alpha$ -TFM Amino Acids into Biologically Active Peptides TRH Modification

A structurally simple peptide like TRH (thyrotropin releasing hormone: pGlu-His-Pro-NH<sub>2</sub>) having high biological activity and pronounced specificity represents a model of choice for the synthesis of analogs in order to study structure-activity-relationships. TRH is the central stimulator of TSH (thyroid stimulating hormone) secretion by anterior pituitary cells and is regulated by peripheral and pituitary hormone levels. It is used for the treatment of various neurologic and neuropsychiatric disorders (40,41). The degradation of TRH *in vivo* is initiated by pyroglutamyl aminopeptidase II which selectively cleaves the pGlu-His bond (42).

The substitution of pGlu by ( $\alpha$ -TFM)pGlu at position 1 of TRH is assumed to protect this hormone against hydrolysis by pyroglutamyl aminopeptidase II. The introduction of the strongly electron withdrawing trifluoromethyl group should influence charge distribution, three dimensional conformation and, therefore, profoundly affect the interaction between substrate and receptor. ( $\alpha$ -TFM)pGlu can be introduced into the TRH sequence by solid phase peptide synthesis (SPPS) (43).

The metabolic stability of [( $\alpha$ -TFM)pGlu<sup>1</sup>]-TRH towards cleavage by membrane bound TRH degrading ectoenzyme from Wistar rat anterior pituitary cells can be monitored in an assay detecting the decrease of the pGlu<sup>[3H]</sup>TRH degradation rate (44). As expected, the degradation of pGlu<sup>[3H]</sup>TRH is not effectively influenced by [( $\alpha$ -TFM)pGlu<sup>1</sup>]-TRH. Thus, trifluoromethyl substitution at position 1 results in complete resistance to proteolysis (45).

The receptor binding affinity of ( $\alpha$ -TFM)pGlu substituted TRH is measured in terms of its potency to decrease the [<sup>3H</sup>]CH<sub>3</sub>-TRH receptor binding. The receptor affinity of the trifluoromethyl substituted analog is two to three orders of magnitude less than the native compound.

Comparison of the NMR shift values of the native sequence and of the  $\alpha$ -TFM substituted analog implies a significant change in the chemical environment of the pGlu-His region. In particular, the NH groups of pGlu and His and the C <sub>$\alpha$</sub>  atoms are deshielded. The introduction of the trifluoromethyl group as well as the stereochemistry at C <sub>$\alpha$</sub>  of ( $\alpha$ -TFM)pGlu seem to influence the ability of the pGlu residue to participate in hydrogen bonding. The polarization effect of the  $\alpha$ -TFM group obviously decreases the capacity of the pGlu residue to form a hydrogen bond between the pGlu carboxy function and the amino function of the Pro moiety (46). Together with the steric constraints of the TFM group, this might prevent formation of a stable hairpin turn required for an optimal interaction with the receptor.

## GnRH Modification

Gonadotropin-releasing hormone (GnRH) is a decapeptide (pGlu<sup>1</sup>-His<sup>2</sup>-Trp<sup>3</sup>-Ser<sup>4</sup>-Tyr<sup>5</sup>-Gly<sup>6</sup>-Leu<sup>7</sup>-Arg<sup>8</sup>-Pro<sup>9</sup>-Gly<sup>10</sup>-NH<sub>2</sub>) synthesized in the cell bodies of hypothalamic neurons and secreted at their terminals directly into the hypophyseal-portal blood supply (47). GnRH selectively stimulates the gonadotrope cells to release the gonadotropines, luteinizing hormone (LH) and follicle stimulating hormone (FSH). In turn, LH and FSH stimulate gonadal production of sex steroids and gametogenesis. GnRH is resistant to exopeptidase cleavage because of the blocked N- and C-termini but is rapidly degraded *in vivo* by endopeptidases. The major enzymes which are responsible for the degradation of GnRH are pyroglutamate aminopeptidase, GnRH degrading endopeptidase, and post proline cleaving enzyme (48). Proteolytic cleavage predominantly takes place at the pGlu-His, Trp-Ser, Tyr-Gly, and Pro-Gly bonds. D-amino acid substitution at position 6 blocks proteolysis by the GnRH cleaving endopeptidase. In addition, substitutions at position 6 by hydrophobic residues give analogs with still higher binding affinity.

The replacement of pGlu by ( $\alpha$ -TFM)pGlu at position 1 of GnRH is assumed to protect this hormone against cleavage by pyroglutamyl aminopeptidase while the substitution of Gly in position 6 by the lipophilic ( $\alpha$ -TFM)Ala should result in a high receptor affinity, improved resistance to proteolysis and thus, in a higher *in vivo* potency. These building blocks can be introduced into the GnRH sequence by SPPS. Due to the low amino group reactivity of the  $\alpha$ -TFM amino acid the introduction of ( $\alpha$ -TFM)Ala into position 6 of the GnRH molecule requires a combination of solid phase strategy and solution methods. Only a tripeptide building block e.g. consisting of Fmoc-Tyr(tBu)-( $\alpha$ -TFM)Ala-Leu-OH can be incorporated into the GnRH sequence using SPPS fragment condensation (32,45).

The receptor binding affinity of ( $\alpha$ -TFM)pGlu substituted GnRH is related to its potency towards decreasing [<sup>3</sup>H]CH<sub>3</sub>-GnRH receptor binding. The receptor affinity of the trifluoromethyl substituted analog is two to three orders of magnitude less than the native compound (Fig. 5).

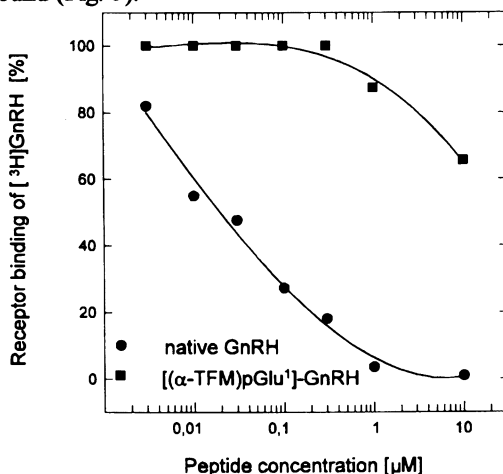


Figure 5: Receptor binding affinity of [( $\alpha$ -TFM)pGlu<sup>1</sup>]-GnRH compared to the native sequence

Comparison of the NMR shift values of the native sequence and of the  $\alpha$ -TFM substituted analog shows no significant changes in the chemical environment except for the pGlu-His-Trp region. The signals of the NH groups of His and Trp in particular are downfield shifted. The native molecule is folded, bringing both the N-terminal and the C-terminal residues into close proximity whilst the side chains of Trp and Arg are in an orientation such that a possible receptor binding site may be defined (49). The polarization effect of the  $\alpha$ -TFM group together with the steric constraints seem to prevent the folded conformation of the GnRH which is necessary for its affinity to the receptor. Further studies concerning the influence of the ( $\alpha$ -TFM)Ala-substitution on the biological activity of GnRH are in progress (50).

### Substance P Modification

Tachykinins are peptides with relatively low molecular weight and characteristic chemical and pharmacological properties, such as contracting activity on various smooth muscles, hypotensive and sialogogic effects (51). Moreover, substance P (SP) acts as a neurotransmitter (52). All members of this family share a common substructure, *i.e.* a C-terminal sequence -Gly-Leu-Met-NH<sub>2</sub> and a Phe residue in position five from the C-terminus. The mammalian tachykinins include SP, neurokinin A and B (NKA, NKB), and forms of NKA extended at the N-terminus. In addition, several other structurally related peptides have been isolated from octopods and amphibians, which show similiar activity compared to mammalian tachykinins (53). The minimal sequence required to exhibit significant biological activity consists of the C-terminal hexapeptide (54).

SP (Arg<sup>1</sup>-Pro<sup>2</sup>-Lys<sup>3</sup>-Pro<sup>4</sup>-Gln<sup>5</sup>-Gln<sup>6</sup>-Phe<sup>7</sup>-Phe<sup>8</sup>-Gly<sup>9</sup>-Leu<sup>10</sup>-Met<sup>11</sup>-NH<sub>2</sub>) is degraded *in vivo* by SP endopeptidase catalyzing predominantly the hydrolysis of the Phe<sup>7</sup>-Phe<sup>8</sup> and to a minor extent of the Phe<sup>8</sup>-Gly<sup>9</sup> peptide bond (55).

To date, four diastereomeric C-terminal pentapeptide analogs of SP with replacement of Phe<sup>7</sup> by ( $\alpha$ -TFM)Phe and ( $\alpha$ -TFM)Phg, respectively, synthesized by combination of solution methods and enzymatic fragment condensation using  $\alpha$ -chymotrypsin have been examined (Figure 6). Resolution of the diastereomers can be achieved using HPLC (27,32).

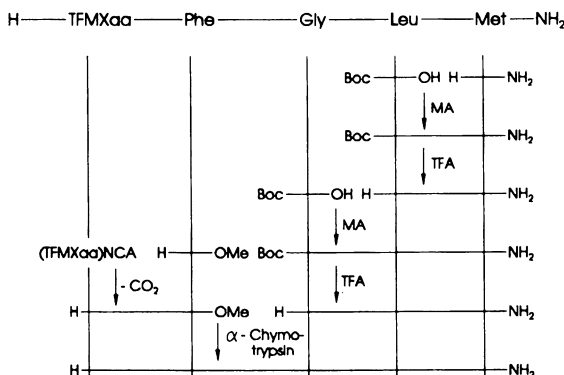


Figure 6: *Synthesis of  $\alpha$ -TFM amino acid substituted SP pentapeptide analogs; Xaa: Phe, Phg*

The biological activity of SP analogs can be tested in the guinea pig ileum contraction assay [GPI assay (56)]. As shown in figure 7 one diastereomer of the  $[(\alpha\text{-TFM})\text{Phe}^7]$  substituted pentapeptide analog (denominated Diastereomer I in Figure 8) inhibits GPI contraction in a small concentration range of  $10^{-7}$ - $10^{-8}$  M. At higher concentrations a contracting activity of this analog is observed. A 300-400 fold concentration of the analog is necessary to induce the same contracting activity as the native peptide (Figure 8). Similar results are detected for the other diastereomer. Both  $[(\alpha\text{-TFM})\text{Phg}^7]$  substituted SP pentapeptide analogs show neither agonistic nor antagonistic effects. Thus, substitution of the Phe residue by Phg exhibits a stronger influence on the biological activity than the incorporation of the TFM group (57).

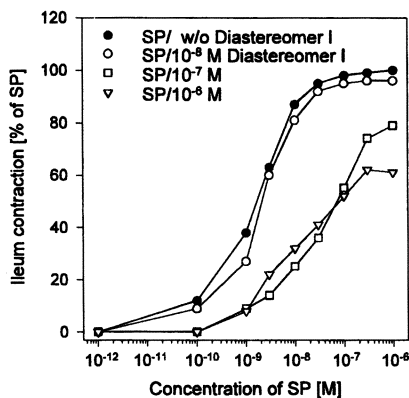


Figure 7: Inhibitory activity of the  $[(\alpha\text{-TFM})\text{Phe}^7]$ -SP pentapeptide (7-11)

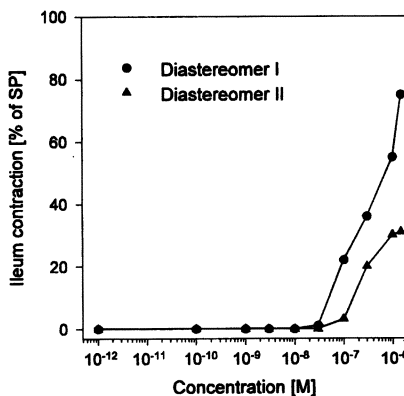


Figure 8: Contracting activity of the  $[(\alpha\text{-TFM})\text{Phe}^7]$ -SP pentapeptide (7-11) diastereomers

## Acknowledgements

This work was funded by Deutsche Forschungsgemeinschaft ( $\alpha$ -TFM amino acids) and Deutscher Akademischer Austauschdienst (stereoselective synthesis). Support with chemicals came from HOECHST AG, ASTA Medica, and Degussa AG. The biological tests were performed by Prof. Dr. Karl Bauer, Max-Planck-Institute of Experimental Endocrinology, Hannover, Germany (TRH), Dr. Bernd Kutscher and Dr. Michael Bernd, ASTA Medica, Frankfurt (GnRH), and Prof. Eisuke Munekata, Tsukuba University, Japan (SP). The force field calculations were carried out by Prof. Dr. Hans-Jörg Hofmann, University of Leipzig.

## References

1. Giannis, A.; Kolter, T. *Angew. Chem.* **1993**, *105*, 1303; *Angew. Chem., Int. Ed. Engl.* **1993**, *32*, 1244, and references cited therein.
2. Toniolo, C.; Benedetti, E. *Macromolecules* **1991**, *24*, 4004.

3. Marshal, G.R.; Clarc, J.D.; Dunbar, J.B., jr.; Smith, G.D.; Zabrocki, J.; Redlinski, A.S.; Leplawy, M.T. *Int J. Pept. Protein Res.* **1988**, *32*, 544.
4. Burger, K.; Mütze, K.; Hollweck, W.; Koksche, B.; Kuhl, P.; Jakubke, H.-D.; Riede, J.; Schier, A. *J. prakt. Chem.* **1993**, *335*, 321.
5. Fujita, T. *Prog. Phys. Org. Chem.* **1983**, *14*, 75.
6. Muller, N. *J. Pharm. Sci.* **1986**, *75*, 987.
7. Nagai, T.; Nishioka, G.; Koyama, M.; Ando, A.; Miki, T.; Kumadaki, I. *J. Fluorine Chem.* **1992**, *57*, 320.
8. Koksche, B.; Gußmann, M.; Sewald, N.; Heckel, M.; Hiller, W.; Pink, M.; Burger, K.; Jakubke, H.-D.; Hofmann, H.-J., manuscript in preparation.
9. Welch, J.T., in: *Selective Fluorination in Organic and Bioorganic Chemistry*, Welch, J.T. (Ed.), ACS Symposium Series, No. 456, ACS Washington DC, **1991**, 1, and references cited therein.
10. Sewald, N.; Burger, K. in: *Synthesis of  $\beta$ -Fluorine-containing Amino Acids, Synthesis and Properties*, Kukhar` V.P., Soloshonok, V.A. (Eds.), Wiley & Sons, **1995**, 139, and references cited therein.
11. Sewald, N.; Hollweck, W.; Mütze, K.; Schierlinger, C.; Seymour, L.C.; Gaa, K.; Burger, K.; Koksche, B.; Jakubke, H.-D. *Amino Acids*, **1995**, *8*, 187, and references cited therein.
12. Galushko, S.V.; Shiskina, I.P.; Kobzev, S.P.; Soloshonok, V.A.; Yagupol'skii, Yu.L.; Kukhar`, V.P. *Zh. Anal. Khim.* **1988**, *43*, 2067; *C.A.* **1989**, *110*, 111035z.
13. Keller, J.W.; Dick, K.O. *J. Chromatogr.* **1986**, *367*, 187.
14. Keller, J.W.; Hamilton, B.J. *Tetrahedron Lett.* **1986**, 1249.
15. Sewald, N.; Seymour, L.C.; Burger, K.; Osipov, S.N.; Kolomiets, A.F.; Fokin, A.V. *Tetrahedron: Asymmetry* **1994**, *5*, 1051.
16. Burger, K.; Gaa, K. *Chem.-Ztg.* **1990**, *114*, 101.
17. Kobzev, S.P.; Soloshonok, V.A.; Galushko, S.V.; Yagupol'skii, Yu.L.; Kukhar`, V.P. *Zh. Obshch. Khim.* **1989**, *59*, 909; *J. Gen. Chem. USSR*, **1989**, *59*, 801.
18. a) Burger, K.; Höss, E.; Gaa, K.; Sewald, N.; Schierlinger, C. *Z. Naturforsch.* **1991**, *46b*, 361.  
b) Schierlinger, C. *PhD Thesis, Technical University Munich*, **1991**.
19. Mütze, K. *PhD Thesis, Technical University Munich*, **1993**.
20. Hollweck, W. *PhD Thesis, Technical University Munich*, **1994**.
21. Hollweck, W.; Burger, K. *J. prakt. Chem.* **1995**, *337*, 391.
22. Schierlinger, C.; Burger, K. *Tetrahedron Lett.* **1992**, 193.
23. Burger, K.; Hollweck, W. *Synlett* **1994**, 751.
24. Weygand, F.; Steglich, W.; Oettmeier, W.; Maierhofer, A.; Loy, R.S. *Angew. Chem.* **1966**, *78*, 640; *Angew. Chem., Int. Ed. Engl.* **1966**, *5*, 600.
25. a) Bambino, F.; Brownlee, R.T.C.; Chiu, F.C.K. *Tetrahedron Lett.* **1991**, *32*, 3407.  
b) Altmann, K.-H.; Altmann, E.; Mutter, M. *Helv. Chim. Acta* **1992**, *75*, 1198.
26. Burger, K.; Schierlinger, C.; Hollweck, W.; Mütze, K. *Liebigs Ann. Chem.* **1994**, 399.
27. Sewald, N.; Hollweck, W.; Mütze, K.; Seymour, L.C. Osipov, S.N.; Schierlinger, C.; Burger, K.; Koksche, B.; Jakubke, H.-D. in: *Peptides: Proceedings of the Twenty-Third European Peptide Symposium, Maia, H.L.S.* (Ed.), Escom **1995**, 327.

28. Ugi, I.; *Angew. Chem.* **1982**, *94*, 826; *Angew. Chem., Int. Ed. Engl.* **1982**, *21*, 810.
29. Osipov, S.N.; Sewald, N.; Kolomiets, A.F.; Fokin, A.V., Burger, K. *Tetrahedron Lett.* **1996**, 615.
30. Gante, J. *Synthesis* **1989**, 405, and references cited therein.
31. Burger, K.; Schierlinger, C.; Mütze, K.; Hollweck, W. *Liebigs Ann. Chem.* **1994**, 407.
32. Koksich, B. *PhD Thesis, University Leipzig*, **1995**.
33. Gerisch, S. *PhD Thesis, University Leipzig*, in preparation.
34. Jakubke, H.-D., *J. Chin. Chem. Soc.* **1994**, *41*, 355.
35. Schechter, I.; Berger, A., *Biochem. Biophys. Res. Commun.* **1968**, *32*, 888.
36. Schellenberger, V.; Schellenberger, U.; Mitin, Y. V.; Jakubke, H.-D. *FEBS Lett.* **1990**, *187*, 163.
37. Koksich, B.; Sewald, N., manuscript in preparation.
38. Duttler, H.; Bizzozero, S., *Acc. Chem. Res.* **1989**, *22*, 322.
39. Tulinsky, A.; Blevins, R.A. *J. Biol. Chem.* **1987**, *262*, 7737; BH, PDB file: 6cha.pdb
40. Ladram, A.; Bulant, M.; Delfour, A.; Montagne, J. J.; Vaudry, H.; Nicolas, P. *Biochimie* **1994**, *76*, 320.
41. Metcalf, G.; Jackson, I. M. D. *Ann. NY Acad. Sci.*, **1989**, *553*, 1.
42. Bauer, K.; Nowak, P.; Kleinkauf, H. *Eur. J. Biochem.*, **1981**, *118*, 173.
43. Koksich, B.; Ullmann, D.; Jakubke, H.-D.; Burger, K. *J. Fluorine Chem.*, submitted.
44. Bauer, K.; Carmelit, P.; Schulz, M.; Baes, M.; Deneff, C. *Endocrinology*, **1990**, *127*, 1224.
45. Koksich, B.; Ullmann, D.; Jakubke, H.-D.; Sewald, N.; Burger, K. in: *Peptides: Proceedings of the Twenty-Third European Peptide Symposium* Maia, H.L.S. (Ed.) Escom **1995**, 323.
46. Grant, G.; Ling, N.; Rivier, J.; Vale, W. *Biochemistry* **1972**, *11*, 3070.
47. Conn, P. M.; Crowley, W. F. *New Engl. J. Med.* **1991**, 324, 93.
48. Vickery, B. H.; Nestor I. I. Jr.; Hafez, E. S. E. in: "LHRH and its Analogs" *Contraceptive and Therapeutic Applications*, MTP Press Limited, **1984**.
49. Gupta, H. M.; Talwar, G. P.; Salunke, D. M. *Proteins: Structure, Function, and Genetics* **1993**, *16*, 48.
50. Koksich, B.; Ullmann, D.; Sewald, N.; Burger, K.; H.-D. Jakubke, manuscript in preparation.
51. Munekata, E. *Comp. Biochem. Physiol.* **1991**, *98C*, 1, 171.
52. Nicoll, R. A., *Ann. Rev. Neurosci.* **1980**, *3*, 227.
53. Maggi, C. A.; Patacchini, R.; Rovero, P.; Giachetti, A. *J. Auton. Pharmacol.* **1993**, *13*, 23.
54. Bergmann, J.; Bienert, M.; Niedrich, H.; Mehliß, B.; Oehme, P. *Experientia* **1974**, *30*, 401.
55. Jenmalm, A.; Luthman, K.; Lindeberg, G.; Nyberg, F.; Terenius, L.; Hacksell, U. *Bioorg. Med. Chem. Lett.* **1992**, *2*, 12, 1693.
56. Couture, R.; Fournier, A.; Magnan, J.; St-Pierre, S.; Regoli, D. *Can. J. Physiol. Pharmacol.* **1979**, *57*, 1427.
57. Koksich, B.; Sewald, N.; Burger, K.; H.-D. Jakubke, manuscript in preparation.



## Chapter 4

# Trifluoromethylated Amino Alcohols: New Synthetic Approaches and Medicinal Targets

Jean-Pierre Bégué and Danièle Bonnet-Delpon

Faculté de Pharmacie, BIOCIS—Centre National de la Recherche Scientifique, Université Paris-Sud, 5 rue Jean Baptiste Clément, 92296 Châtenay-Malabry, France

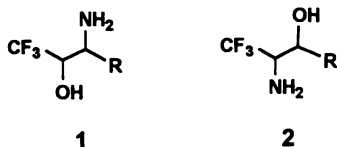
Due to its high electronegativity, a trifluoromethyl substituent can enhance the biological activity of inhibitors of enzymes. In this regard fluorinated aminoalcohol unit **1** can be considered as a peptidomimetic moiety of importance in the design of proteases inhibitors. A review of the published synthetic methods leading to trifluoromethylated aminoalcohols is presented as well as a new stereoselective approach for the synthesis of *syn*- and *anti*- aminoalcohols **1** with particular focus on examples relevant to enzyme inhibition. Investigations on the preparation of the amino alcohols **2** will be also presented.

$\beta$ -Amino alcohols are important targets since they present at least three interests: they are used in the treatment of a wide variety of human disorders (1), they are peptidomimetic units and they are chiral auxiliaries in organic synthesis (2). For the same reasons, fluoroalkyl  $\beta$ -amino alcohols **1** aroused increasing interest. Moreover fluoroalkyl  $\beta$ -amino alcohols are precursors of the corresponding fluoroalkyl peptidyl ketones which have been shown to be effective inhibitors of proteolytic enzymes (3) such as serine proteases (4) (chymotrypsin (5), elastases (6,7), trypsin (8), thrombin (9)), aspartyl proteases (renine) (10,11) or cysteine proteases (papain, cathepsin B) (12). In some cases fluoroalkyl  $\beta$ -amino alcohols are themselves inhibitors of the same enzymes (6,11).

Despite this large interest in fluoroalkyl  $\beta$ -amino alcohols, only few methods are available for the synthesis of these compounds. Furthermore, properties of trifluoromethyl  $\beta$ -hydroxy amines **2**, regioisomers of **1**, have been unexplored because of the lack of methods for their preparation.

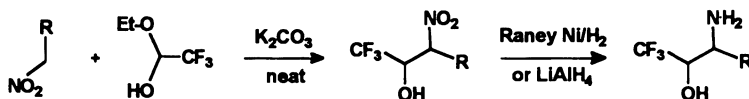
0097-6156/96/0639-0059\$15.00/0  
© 1996 American Chemical Society

After a short survey of the previously reported routes to trifluoromethyl  $\beta$ -amino and  $\beta$ -peptidyl alcohols, we describe in this chapter our investigations on new methodologies for synthesis of compounds **1** and **2**. These units are incorporated into appropriate systems and the activity of resulting molecules towards specific biological targets is evaluated.



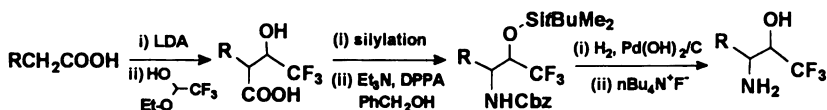
### Synthesis of Trifluoromethyl $\beta$ -Amino Alcohols **1** and $\beta$ -Peptidyl Alcohols.

The earlier route was based on the reactivity of trifluoroacetaldehyde. This compound, available as ethyl hemiketal, was used as an electrophile in the condensation with a carbanion. Abeles used the anion of a nitroalkane (Henry condensation) and the resulting trifluoromethyl  $\alpha$ -nitro carbinol was then reduced into the amino alcohol (**13**) (Scheme 1).



Scheme 1

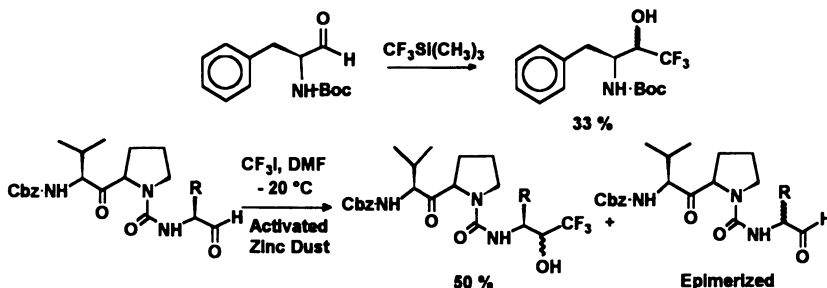
Squibb's researchers reported condensation reaction of the trifluoroacetaldehyde with the lithium dianion of a carboxylic acid (**11**). After protection of the hydroxyl group, the protected amino alcohol was obtained through the Curtius rearrangement (Scheme 2). By these two methods, amino alcohols **1** were isolated as a racemic mixture of diastereoisomers.



Scheme 2

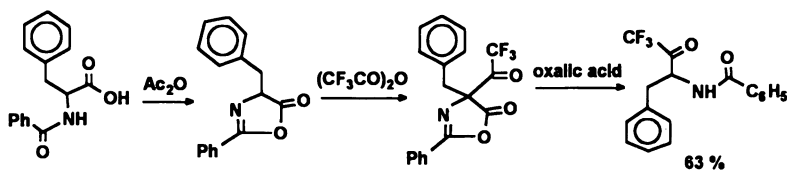
Another attractive approach based on direct trifluoromethylation (**14**) is the addition of a trifluoromethyl anion equivalent on protected  $\alpha$ -amino aldehydes which can be prepared from natural amino acids (**7b**, **15**). However, these reactions using the

Ruppert's reagent ( $\text{CF}_3\text{TMS}$ ) (16) or  $\text{CF}_3\text{I}/\text{Zn}$  (17) have been described only in moderate yield with a lack of selectivity and part of racemisation (7b,15).



Scheme 3

A direct route to trifluoromethyl  $\alpha$ -amino ketones is the Dakin-West reaction, largely developed by the Merrell-Dow group (Scheme 4) (7a,18). This route is of great interest for the preparation of fluoro amino ketones, and hence corresponding alcohols, where the R chain bears a functionality.



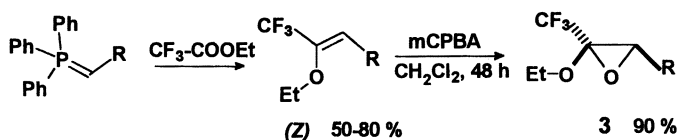
Scheme 4

These different routes have been largely used for the preparation of fluoro amino alcohols despite their lack of stereoselectivity, since the authors were generally interested in the corresponding amino ketones, obtained through the oxidation of the protected  $\beta$ -amino or the  $\beta$ -peptidyl alcohols.

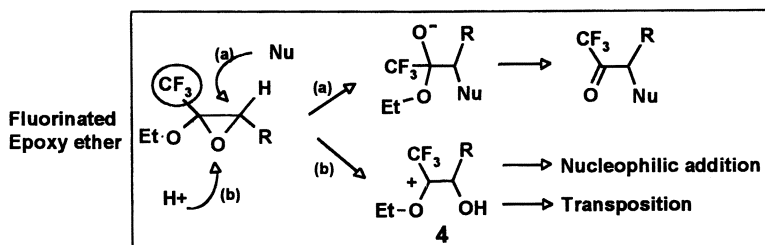
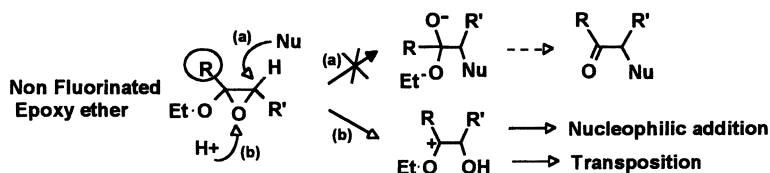
**Enzyme inhibitory properties of Fluoroalkyl ketones and Alcohols.** The enhanced electrophilicity of the fluorinated ketonic functionality facilitates the enzyme-catalyzed addition of a nucleophile of the active site to form a metastable hemiketal, which resembles the tetrahedral intermediate occurring in the enzyme hydrolysis. In a general way the replacement of the scissile amide bond by peptidomimetics such as hydroxyethylene dipeptide analogues and amino alcohols can also provide transition-state analogue protease inhibitors (19). The interaction does not occur through a covalent bond but through hydrogen bonds. The replacement of an alkyl group by a trifluoromethyl group in an peptidyl alcohol increases the acidity of the adjacent hydroxyl group by about 4 pKa units, making it a better hydrogen atom donor (11). Thereby, racemic mixtures of trifluoromethyl peptidyl alcohols have been reported to act

as reversible inhibitors towards proteolytic enzymes. They are 10-fold less active than corresponding ketones towards human renin (*10a,11*) and only 2-fold less active towards cathepsin B (*12b*). Against serine proteases, the difference of inhibitory potency between peptidyl ketones and alcohols are greater (*4b,6b*). However these reported investigations generally concern a mixture of diastereoisomers and the influence of relative and absolute configurations on activity has not been explored. We thus searched for diastereoselective and enantioselective routes to trifluoromethyl  $\beta$ -amino alcohols **1**, which could avoid the use of expensive or troublesome reagents such as trifluoroacetaldehyde,  $\text{CF}_3\text{I}$  or  $\alpha$ -amino aldehyde.

**Diastereoselective synthesis of trifluoromethyl  $\beta$ -amino alcohols **1**.** Our synthetic approach is based on the nucleophilic ring opening of 1-trifluoromethyl epoxy ethers **3**. We have prepared these new synthons in two steps from the cheap ethyl trifluoroacetate through the mCPBA epoxidation of the (*Z*) vinyl ethers (**20**) resulting from the Wittig reaction of the fluorinated ester with an alkylidene phosphorane generated under lithium salt-free conditions (Scheme 5) (*21*).



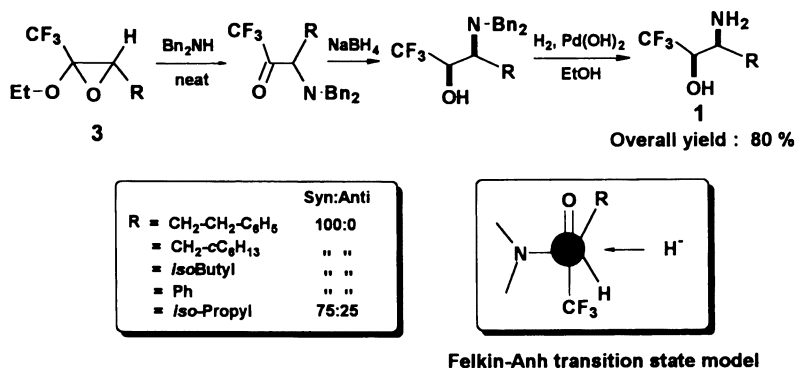
Scheme 5



Scheme 6

Unlike non-fluorinated parent epoxy ethers, epoxy ethers **3** are stable in protic medium, even in the presence of a trace of acid, since the alkoxy carbenium ions **4**, resulting from an acid-catalyzed opening of the oxiran ring, are strongly destabilized by the fluorinated moiety (22). Consequently the acid-catalysed ring opening process is so disfavored that a nucleophilic ring opening process leading to  $\alpha$ -substituted trifluoromethyl ketones can compete (Scheme 6).  $\alpha$ -Thioalkyl ketones (**23**) and  $\alpha$ -bromo trifluoromethylketones (**20**) were successfully prepared from epoxy ethers **3** by reactions with sodium thiolates and with magnesium bromide, respectively.

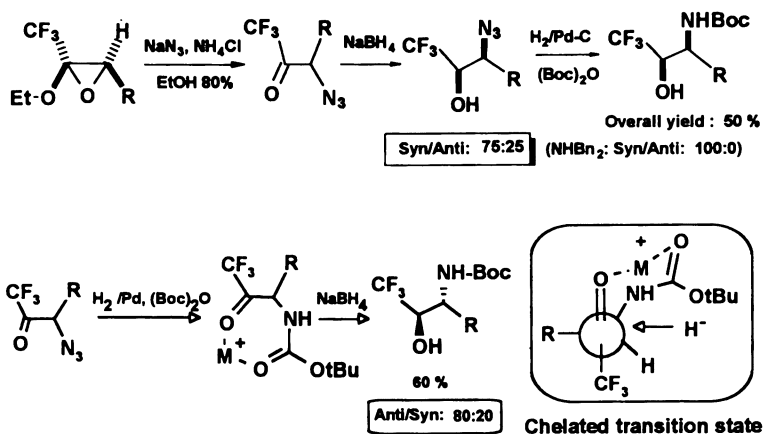
In view to prepare fluoroalkyl  $\beta$ -amino alcohols, the reactions with nitrogen nucleophiles were investigated. Unfortunately, the reaction with a primary amine leads to an unidentified mixture, possibly due to the rapid degradation of the unstable *N*-monosubstituted amino ketone produced by the nucleophilic ring opening of epoxy ethers **3** (7a,24). On the contrary, secondary amines, such as dibenzylamine, easily react with epoxy ethers **3** providing stable *N,N*-disubstituted amino fluorinated ketones in good yields (25). Reduction of the carbonyl group leads stereoselectively to the *syn* amino alcohols. The *syn/anti* ratio is generally 100:0. However the degree of selectivity decreases when R is a very bulky group (*iso*-Propyl: *syn/anti* = 75:25) (25). The stereocontrol of the reduction follows the Felkin-Anh model, where the amino group is the bulkier group, as usually observed in the reduction of trifluoromethyl  $\alpha$ -functionalized ketones (26). After hydrogenolysis, the *syn* amino alcohols **1** are obtained in about 80 % overall yield from epoxy ethers **3** (Scheme 7). The *syn* configuration has been determined by NMR data of the corresponding isoxazolidinones (27), and confirmed by X-ray diffraction in one case.



Scheme 7

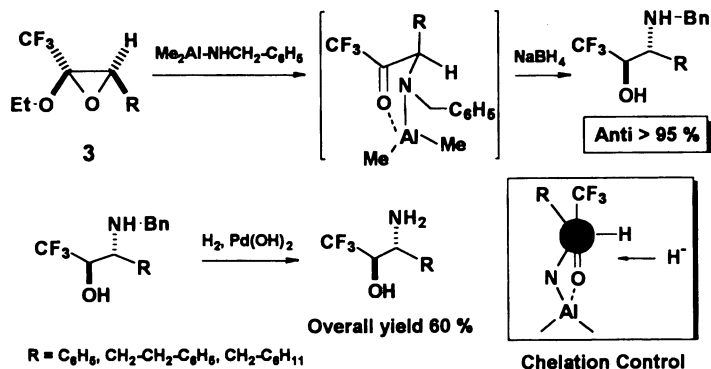
In order to prepare the *anti* diastereoisomer, we first envisaged a nucleophilic ring opening with a small nitrogen nucleophile, such as an azide anion, since in this case the R group could take the place of the bulky group in the Felkin-Anh model. Epoxy ethers

**3** are less reactive towards azides than towards secondary amines, but finally with sodium azide in ethanol the  $\alpha$ -azido ketones are obtained in moderate yields (27). Reduction of the ketonic group with sodium borohydride or with other hydrides affords the *syn*  $\beta$ -azido alcohols with a moderate stereoselectivity (75:25). This suggests that steric hindrance is not the dominant factor in the Felkin-Anh transition state model: the azido group acts as a repulsive substituent by electronic effects and the major diastereoisomer is still the *syn*. Catalytic hydrogenation of the azido group provides the *syn*  $\beta$ -amino alcohols **1**. However, the *anti* diastereoisomer can be also prepared if the order of the two reduction steps are reversed. When catalytic hydrogenation and *N*-Boc protection are performed before the reduction of the ketonic group ( $\text{NaBH}_4$ ), the *anti* *N*-Boc amino alcohol is obtained as the major product (*anti/syn* 80:20). The latter reduction is controlled by the chelation of the two carbonyl groups with the metallic cation of the hydride (Scheme 8).



Scheme 8

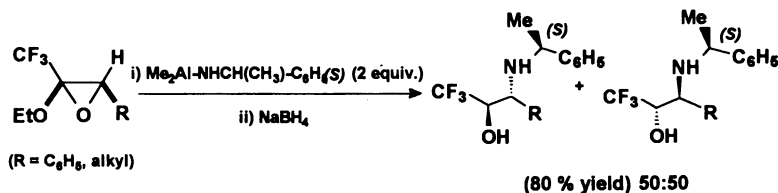
Taking advantage of this chelation control we investigated the reaction of epoxy ethers **3** with a dimethylaluminum amide, generated from  $\text{Me}_2\text{Al}$  and benzylamine. The use of such a reagent could present three advantages (i) a facilitated reaction by the Lewis acid; (ii) an increased stability of the produced  $\alpha$ -amino ketones, (iii) the control of the further reduction step by chelation of the oxygen and the nitrogen with aluminum, providing the *anti* diastereoisomer. The epoxy ethers **3** react at  $-20^\circ\text{C}$  with two equivalents of the dimethylaluminum benzylamide leading to the aluminum-amino ketone complex. The further *in situ* reduction of the ketonic functionality with sodium borohydride leads exclusively to the *anti* *N*-monosubstituted amino alcohols which are then debenzylated by hydrogenation (Scheme 9) (28).



Scheme 9

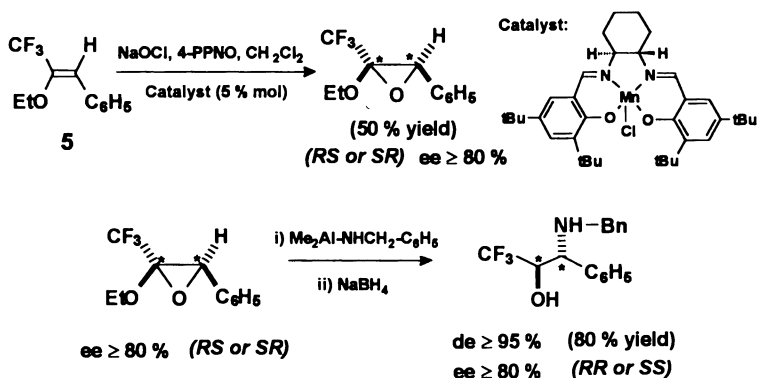
So, a good and concise synthesis of any of each diastereoisomer of amino alcohols **1** in only four steps from ethyl trifluoroacetate is now available. It is noteworthy that these strategies can be extended to other fluoroalkyl amino alcohols ( $\text{R}_F = \text{C}_2\text{F}_5, \text{C}_3\text{F}_7, \text{CF}_2\text{Cl}$ ) using the corresponding starting epoxy ethers being also prepared in two steps from  $\text{R}_F\text{-COOEt}$  (*20, 22b, 29*).

**Synthesis of Homochiral Trifluoromethyl  $\beta$ -Amino Alcohols.** Two approaches have been investigated for the access to homochiral *anti* isomers of amino alcohols **1**. The first one takes advantage of the high stereoselectivity of the reaction of epoxy ethers **3** with a dimethylaluminum amide. When the Lewis acid is generated from  $\text{Me}_3\text{Al}$  and a chiral amine, its reaction with the epoxy ethers **3** provides two stereoisomers which were easily separated by crystallisation of mandelate salts. The conventional debenzylation process leads to the homochiral *anti* amino alcohols **1**.



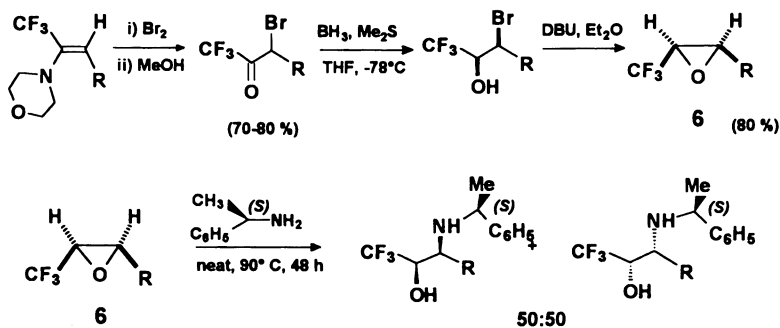
Scheme 10

The second approach is based on the asymmetric epoxidation of enol ether **5** which is performed according to the Jacobsen's procedure (*30*) giving rise to the epoxy ether of 80 % ee. Enantiomeric excess has been determined by  $^1\text{H}$  NMR in the presence of a chiral shift reagent ( $\text{Eu}(\text{hfc})_3$ ). Ring opening by the aluminum benzylamide occurs without racemization (80 % ee), leading to the chiral *anti* aminoalcohol (d.e. > 95 %) after reduction. The determination of the absolute configuration is under investigation.



Scheme 11

In order to prepare homochiral *syn* isomers an approach based on the reactivity of racemic *cis* CF<sub>3</sub>-epoxides **6** towards chiral amines was investigated. *Cis* 1-CF<sub>3</sub>-epoxides **6** are now easily available for example through the bromination of 1-CF<sub>3</sub>-enamines, followed by methanolysis (21,31). The resulting  $\alpha$ -bromo ketones are reduced with the BH<sub>3</sub>-dimethyl sulfide complex into pure *syn* bromohydrins, which are then cyclised into racemic *cis* epoxides in the presence of base (32) (Scheme 12). Chiral approach to these *cis* epoxides is under investigation (33). However, the ring opening by (*S*)  $\alpha$ -methylbenzyl amine provides the mixture of the two diastereoisomers which can be separated as for the *anti* series.



Scheme 12

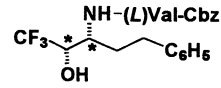
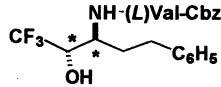
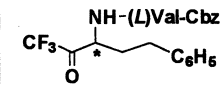
**Inhibition of Serine Proteases.** In order to evaluate the influence of relative and absolute configurations of trifluoromethyl peptidyl alcohols on inhibitory activities, we have chosen three serine proteases: Human leukocyte elastase (HLE) which is involved in chronic inflammatory diseases (34), cathepsin G which is thought to act in synergy with HLE (35) and porcine pancreatic elastase (PPE) which is structurally close to HLE.



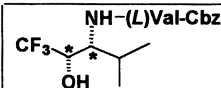
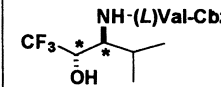
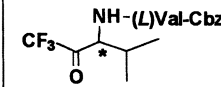
In recent years, considerable efforts have been made to design synthetic inhibitors of HLE as drug against the elastase-induced diseases (36) while cathepsin G has been much less studied.

Taking in account that, in  $S_1$ , HLE usually accommodates residues of medium size such as valine, and that cathepsin G prefers bulkier aliphatic or aromatic residues, two series of amino alcohols ( $R = isoPropyl$  and  $R = CH_2-CH_2-C_6H_5$ ) were synthesized. For preliminary tests, only  $L(Val)$  has been coupled to each stereoisomers of these two series leading to homochiral trifluoromethyl  $\beta$ -peptidyl alcohols (**7a,b**, **8a,b**) and (**10a,b**, **11a,b**). For the series ( $R = CH_2-CH_2-C_6H_5$ ) only two alcohols **7a** and **8a** show inhibitory activity towards HLE and cathepsin G, but not towards PPE (Table 1). It is surprising that these two enzymes have not only the same preference among the stereoisomers but also with similar affinities. Unexpectedly the corresponding ketones **9a** et **9b** have no inhibitory potency towards any of the three enzymes even at concentration of 400  $\mu$ M.

**Table 1:**  $K_i$  (M) inhibition constants towards HLE, PPE and cathepsin G (25 °C, pH 8), standard deviation < 20 %. NI : No Inhibition.

		HLE	PPE	Cathepsin G
	<b>7a</b> (SRS or RSS)	$1.26 \times 10^{-4}$	NI	$1.98 \times 10^{-4}$
	<b>7b</b> (RSS or SRS)	NI	NI	NI
	<b>8a</b> (SSS or RRS)	$9.45 \times 10^{-4}$	NI	$6.08 \times 10^{-4}$
	<b>8b</b> (RRS or SSS)	NI	NI	NI
	<b>9a</b> (RS or SS) (from <b>7a</b> )	NI	NI	NI
	<b>9b</b> (SS or RS) (from <b>7b</b> )	NI	NI	NI

**Table 2:**  $K_i$  (M) inhibition constants towards HLE, PPE and cathepsin G (25 °C, pH 8), standard deviation < 15 %. NI : No Inhibition.

		HLE	PPE	Cathepsin G
	<b>10a</b> (SRS or RSS)	$5.65 \times 10^{-4}$	NI	NI
	<b>10b</b> (RSS or SRS)	NI	NI	NI
	<b>11a</b> (SSS or RRS)	NI	NI	NI
	<b>11b</b> (RRS or SSS)	NI	NI	NI
	<b>12a</b> (RS or SS) (from <b>10a</b> )	$2.37 \times 10^{-6}$	$4.39 \times 10^{-5}$	NI
	<b>12b</b> (SS or RS) (from <b>10b</b> )	$8.30 \times 10^{-6}$	$7.69 \times 10^{-5}$	NI

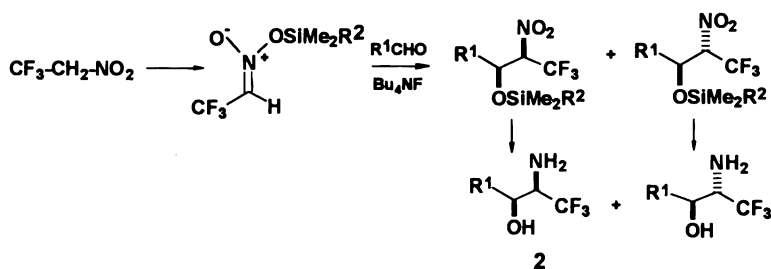
In the second series ( $R = isoPropyl$  group) only one stereoisomer **10a** shows competitive inhibition of HLE, with no inhibitor activity for PPE or cathepsin G. In

contrast both ketones **12a** and **12b** inhibit HLE and, to a less extent PPE, behaving as rapidly competitive inhibitors (37).

From this study, some informations can be drawn on the influence of configurations of peptidyl alcohols on inhibitory activity. The inhibitory activity of peptidyl alcohols is due only to one enantiomer even when both diastereoisomers are active (**7a** and **8a**). Despite of a lower inhibition constant than that of corresponding ketone **12a**, the homochiral peptidyl alcohol **10a** exhibits a selectivity for HLE. Another interesting result is the inhibition activity of the peptidyl alcohols **7a** and **8a** while the two corresponding ketones were unable to inhibit HLE.

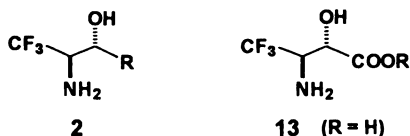
### Fluorinated Aminoalcohols 2: Synthesis of the *syn*-3-trifluoromethyl isoserine.

Conversely to fluoroalkyl  $\beta$ -amino alcohols **1**, properties of  $\beta$ -fluoroalkyl amino alcohols **2** have not been explored probably because until now, there was no described preparation. The only paper devoted to their synthesis appeared during the preparation of this chapter and is based on the chemistry of the non easily available trifluoronitroethane (38) (Scheme 13).



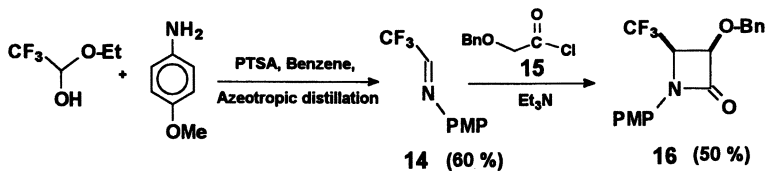
Scheme 13

However, like their regioisomers **1**, compounds of type **2** could act as chiral auxiliaries and could exhibit specific properties as peptidomimetic units since first, the basicity of amine is strongly decreased and second, the fluorinated moiety can bring a protecting effect towards proteases (39).



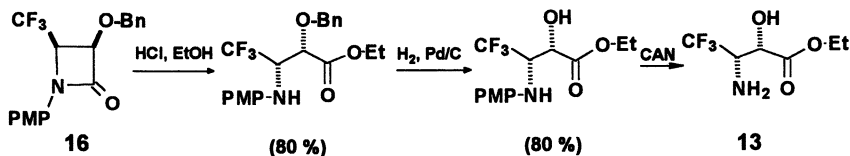
In our aim to synthesize one particular type of compounds **2**, the 3-trifluoromethyl isoserine **13**, we investigated the [2+2] addition between the trifluoromethyl imine **14**,

derived from ethyl fluoral hemiketal, and the functionalized ketene prepared from the acid chloride **15**, which led stereoselectively to the *syn*  $\beta$ -lactam **16** (Scheme 14).



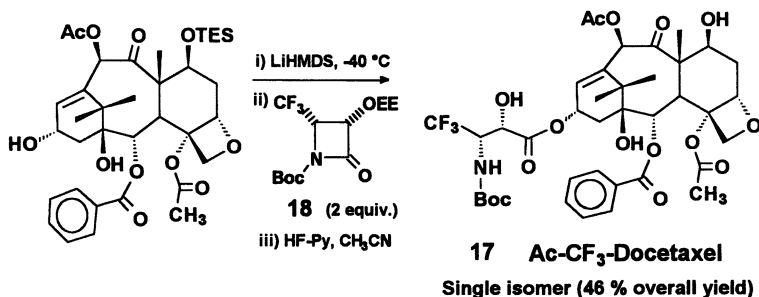
Scheme 14

This synthon is the precursor of the new trifluoromethylisoserine **13** converted by acidic hydrolysis, protection and deprotection (Scheme 15) (40).



Scheme 15

Interestingly, the fluoro taxoid **17** can be prepared from the racemic  $\beta$ -lactam **18**, obtained from **16** by several steps of protection-deprotection. Coupling with acetyl baccatin III occurs with kinetic resolution of the  $\beta$ -lactam leading to a single isomer, the homochiral (*2R,3S*) fluoro taxoid **17**. This compound presents an antitumoral activity against human cancer cell lines, stronger than that of taxol and taxotere (Scheme 16) (41).



Scheme 16

**Acknowledgements:** We thank the contribution of our coworkers Drs H. Sdassi, N. Fischer-Durand, A. Kornilov, M.H. Rock and D. Bouvet, M. Le Gall, S. Guenais, C. Richard, M. Ourevitch and in particular the essential part due to Dr A. Abouabdellah. We are grateful to Dr Reboud-Ravaux and A. Amour for the enzymology and Dr I. Ojima and J.C. Slater for the collaboration on fluoro taxoids. This research was supported by grants from the CNRS, Paris-Sud University, Foundation for Medical Research (Sidaction) and European Union (CHM Network "Synthesis and Molecular Recognition of Fluorinated Bioactive Compounds").

### References:

1. Grayson, M. Ed. *Kirk-Othmer Encycl. Chem. Techno.* **1982**, *17*, 311-345.
2. Tomioka, K. *Synthesis* **1990**, 541; Noyori, R.; Kitamura, M. *Angew. Chem. Int. Ed. Engl.* **1991**, *30*, 49-68.
3. Imperiali, B. *Synthetic Peptides in Biotechnology*, A. R. Liss, Inc. **1988**, 97-129.
4. Imperiali, B.; Abeles, R.B. *Biochemistry* **1985**, *24*, 1813-1817; Imperiali, B.; Abeles, R.B. *Biochemistry* **1986**, *25*, 3760-3767.
5. Brady, K.; Liang, T.C.; Abeles, R.H. *Biochemistry* **1989**, *28*, 9066-9070; Liang, T.C.; Abeles, R.H. *Biochemistry* **1987**, *26*, 7603-7608; Brady, K.; Wei, A.; Ringe, D.; Abeles, R.H. *Biochemistry* **1990**, *29*, 7600-7607; Brady, K.; Abeles, R.H. *Biochemistry* **1990**, *29*, 7608-7617.
6. (a) Dunlap, R.P.; Stone, P.J.; Abeles, R.H. *Biochem. Biophys. Res. Comm.* **1987**, *145*, 509-513; (b) Stein, R.L.; Strimpler, A.M.; Edwards, P.D.; Lewis, J.J.; Mauger, R.C.; Schwartz, J.A.; Stein, M.M.; Trainor, D.A.; Wildonger, R.A.; Zottola, M.A. *Biochemistry* **1987**, *26*, 2682-2689; (c) Govardhan, C.P.; Abeles, R.H. *Arch. Biochem. Biophys.* **1990**, *280*, 137-146; (d) Warner, P.; Green, R.C.; Gomes, B.; Strimpler, A.M. *J. Med. Chem.* **1994**, *37*, 3090-3099; (e) Berstein, P.R.; Gomes, B.C.; Kosmider, B.J.; Vacek, E.P.; Williams, J.C. *J. Med. Chem.* **1995**, *38*, 212-215; (f) Veale, C.A.; Damewood, J.R.; Steelman, G.B.; Bryant, C.; Gomes, B.; Williams, J.C.; Thomas, R.M.; Vacek, E.P.; Veale, C.A.; Tuthill, P.A.; Warner, P.; Williams, J.C.; Wolanin, D.J.; Woolson, S.A. *J. Med. Chem.* **1994**, *37*, 1259-1261.
7. (a) Peet, N.P.; Burkhart, J.P.; Angelastro, M.R.; Giroux, E.L.; Mehdi, S.; Bey, P.; Kolb, M.; Neises, B.; Schirlin, D. *J. Med. Chem.* **1990**, *33*, 394-407; (b) Skiles, J.W.; Fuchs, V.; Miao, C.; Sorcek, R.; Grozinger, K.G.; Mauldin, S.C.; Vitous, J.; Mui, P.W.; Jacober, S.; Chow, G.; Matteo, M.; Skoog, M.; Weldon, S.M.; Possanza, G.; Keirns, J.; Letts, G.; Rosenthal, A.S. *J. Med. Chem.* **1992**, *35*, 641-662; (c) Angelastro, M.R.; Baugh, L.E.; Bey, P.; Burkhart, J.P.; Chen, T.M.; Durham, S.L.; Hare, C.M.; Huber, E.W.; Janusz, M.J.; Koehl, J.R.; Marquart, A.L.; Mehdi, S.; Peet, N.P. *J. Med. Chem.* **1994**, *37*, 4538-4554.
8. Ueda, T.; Kam, C.M.; Powers, J.C. *Biochem. J.* **1990**, *265*, 539-545.

9. Neises, B.; Ganzhorn, A. Eur. Pat. Appl. EP 503,203, 1992; *Chem. Abstract* 1993, 118, 148063y.
10. (a) Sham, H.L.; Stein, H.; Rempel, C.A.; Cohen, J.; Plattner, J.J. *FEBS Lett.* 1987, 220, 299-301; (b) Tarnus, C.; Jung, M.J.; Rémy, J.M.; Baltzer, S.; Schirlin, D. *FEBS Lett.* 1989, 249, 47-50; (c) Thaisrivongs, S.; Pals, D.T.; Turner, S.R. in *Selective Fluorination in Organic and Bioorganic Chemistry*, J. T. Welch Ed., ACS Symposium Series 456, Washington D.C. 1991, pp 164-173.
11. Patel, D.V.; Rielly-Gauvin, K.; Ryono, D.E. *Tetrahedron Lett.* 1988, 29, 4665-4668; Patel, D.V.; Rielly-Gauvin, K.; Ryono, D.E.; Free, C.A.; Smith, S.A.; Petrillo Jr, E.W. *J. Med. Chem.* 1993, 36, 2431-2447.
12. (a) Giordano, C.; Gallina, C.; Consalvi, V.; Scandurra, R. *Eur. J. Med. Chem.* 1989, 24, 357-362; (b) Smith, R.A.; Copp, L.J.; Donnelly, S.L.; Spencer, R.W.; Krantz, A. *Biochemistry* 1988, 27, 6568-6573.
13. Imperiali, B.; Abeles, R.H. *Tetrahedron Lett.* 1986, 27, 135-138; Bergeson, S.H.; Schwartz, J.A.; Stein, M.M.; Wildonger, R.A.; Edwards, P.D.; Shaw, A; Trainor, D.A.; Wolanin, D.J. U.S. Pat. 4,910,190; 1990; *Chem. Abstr.* 1991, 114, 120085m.
14. Mc Clinton, M.A.; McClinton, D.A. *Tetrahedron*, 1992, 48, 6555-6666. Burton, D.J.; Yang, Z.Y. *Tetrahedron* 1992, 48, 189-275.
15. Edwards, P.D. *Tetrahedron Lett.* 1992, 33, 4279-4282.
16. Ruppert, I.; Schlich, K.; Volbach, W. *Tetrahedron Lett.* 1984, 25, 2195-2198; Prakash, G.K.S.; Krishnamurti, R. Olah, G.A. *J. Am. Chem. Soc.* 1989, 111, 393-395. Krishnamurti, R.; Bellew, D.R.; Prakash, G.K.S.; R. Olah, G.A. *J. Org. Chem.* 1991, 56, 984-989.
17. Kitazume, T.; Ishikawa, N. *J. Org. Chem.* 1988, 107, 53, 2349-2350. Kitazume, T.; Ishikawa, N. *J. Am. Chem. Soc.* 1985, 107, 5186-5191. O'Reilly, N.; Maruta, M. Ishikawa, N. *Chem. Lett.* 1984, 517-520.
18. Kolb, M.; Neises, B. *Tetrahedron Lett.* 1986, 27, 4437-4440; Kolb, M.; Barth, J.; Neises, B. *Tetrahedron Lett.* 1986, 27, 1579-1582; Kolb, M.; Neises, B.; Gerhart, F. *Liebigs Ann. Chem.* 1990, 1-6.
19. Rich, D.H. *J. Med. Chem.* 1985, 28, 263-273; Rich, D.H., Salituro, F.G.; Holladay, M.W.; Schmidt, P.G. In *Conformationally Directed Drug Design*; Vida, J.A., Gordon, M., Eds; ACS Symposium Series 251; ACS: Washington, DC, 1984; pp 211-237; Harbeson, S.L.; Rich, D.H. *J. Med. Chem.* 1989, 32, 1378-1392. Rosenberg, S.H.; Kleinert, H.L.D.; Stein, H.H.; Martin, D.L.; Chekal, M.A.; Cohen, J.; Egan, D.A.; Tricarico, K.A.; Baker, W.R. *J. Med.* 1991, 34, 469-471. Rich, D.H.; Green, J.; Toth, M.V.; Marshall, G.R.; Kent, S.B.H. *J. Med. Chem.* 1990, 33, 1288-1295.
20. Bégué, J.P.; Benayoud, F.; Bonnet-Delpon, D.; Fischer-Durand, N.; Sdassi, H. *Synthesis*, 1083-1085.
21. Bégué, J.P.; Mesureur, D. *J. Fluorine Chem.* 1988, 39, 271; Bégué, J.P.; Bonnet-Delpon, D.; Née, G.; Wu, S.W. *J. Org. Chem.* 1992, 57, 3807; Bégué, J.P.; Bonnet-Delpon, D.; Kornilov, A. *Organic Synthesis* in press.

- 22 (a) Bégué, J.P.; Bonnet-Delpon, D.; Benayoud, F.; Tidwell, T.T.; Cox, R.A.; Allen, A. *Gazz. Chim. Ital.* **1995**, *125*, 399-402; (b) Bégué, J.P.; Bonnet-Delpon, D.; Benayoud, F. *J. Org. Chem.* **1995**, *60*, 5029-5036.
- 23 Bégué, J.P.; Bonnet-Delpon, D.; Kornilov, A. *Synthesis* in press.
- 24 Angelastro, M.R.; Burkhart, J.P.; Bey, P.; Peet, N.P. *Tetrahedron Lett.* **1992**, *33*, 3265-3268.
- 25 Bégué, J.P.; Bonnet-Delpon, D.; Sdassi, H. *Tetrahedron Lett.* **1992**, *33*, 1879-1882.
- 26 The reduction of  $\alpha$ -bromo and  $\alpha$ -thioalkyl trifluoromethyl ketones leads respectively to the *syn*-bromohydrins and *syn*-thioalkyl alcohols. Bégué, J.P.; Bonnet-Delpon, D.; Bouvet, D.; Kornilov, A.; Rock, M. H. *unpublished results*.
- 27 Bégué, J.P.; Bonnet-Delpon, D.; Fischer-Durand N.; Reboud-Raveaux, M.; Amour, A. *Tetrahedron: Asymmetry* **1994**, *5*, 1099-1110.
- 28 Abouabdellah, A.; Bégué, J.P.; Bonnet-Delpon, D.; Le Gall, M.; Richards, C. *unpublished results*.
- 29 Bégué, J.P.; Bonnet-Delpon, D.; Rock, M.H. *Tetrahedron Lett.* **1994**, *35*, 2907-2910.
- 30 Jacobsen, E.N.; Zhang, W.; Muci, A.R.; Ecker, J.R.; Deng, L. *J. Am. Chem. Soc.* **1991**, *113*, 7063-7064. Brandes, B.D.; Jacobsen, E.N. *J. Org. Chem.* **1994**, *59*, 4378-4380.
- 31 Bégué, J.P.; Bonnet-Delpon, D.; Bouvet, D.; Rock, M. H. *J. Fluorine Chem.* in press.
- 32 Bégué, J.P.; Bonnet-Delpon, D.; Bouvet, D.; Rock, M. H. *unpublished results*.
- 33 Bégué, J.P.; Bonnet-Delpon, D.; Kornilov, A.; Resnati, G. *unpublished results*.
- 34 Janoff, A. *Am. Rev. Respir. Dis.* **1985**, *132*, 417-433; Ekerot, L.; Ohlsson, K. *Adv. Exp. Med. Biol.* **1984**, *167*, 335-344; Stockley, R.A.; Hill, S.L.; Burnett, D. *Ann. N.Y. Acad. Sci.* **1991**, *624*, 257-266; Merritt, T.A.; Cochrane, C.G.; Holcomb, K.; Bohl, B.; Hallman, M.; Strayer, D.; Edwards, D.; Gluck, L. *J. Clin. Invest.* **1983**, *72*, 656-666.
- 35 Boudier, C.; Holle, C.; Bieth, P.R. *J. Biol. Chem.* **1981**, *256*, 10256-10258.
- 36 Edwards, P.D.; Berstein, P.R. *Med. Res. Rev.* **1994**, *14*, 127-194; Berstein, P.R.; Edwards, P.D.; Williams, J.C. *Progress Med. Chem.* **1994**, *31*, 59-120.
- 37 Abouabdellah, A.; Bégué, J.P.; Bonnet-Delpon, D.; Le Gall, M. Reboud-Raveaux, M.; Amour, A. *Eur. J. Med. Chem.* submitted.
- 38 Marti, R.E.; Heinzer, J.; Seebach, D. *Liebigs Ann.* **1995**, 1193-1215.
- 39 Ojima, I.; Kato, K.; Jameison, F.A.; Conway, J. *Bioorganic Med. Chem. Lett.* **1992**, *2*, 219-222.
- 40 Abouabdellah, A.; Bégué, J.P.; Bonnet-Delpon, D. *Synlett* in press.
- 41 Ojima, I.; Slater, J.C.; Abouabdellah, A.; Bégué, J.P.; Bonnet-Delpon, D. *unpublished results*.

## Chapter 5

# Asymmetric Synthesis of Functionalized Fluorinated Cyclopropanes and Its Application to Fluoromethano Amino Acids

Takeo Taguchi, Akira Shibuya, and Tsutomu Morikawa

Tokyo College of Pharmacy, 1432-1 Horinouchi, Hachioji,  
Tokyo 192-03, Japan

Asymmetric syntheses of functionalized fluorinated cyclopropanes developed in our group are described. These are 1) the Simmons-Smith reaction of fluoroallyl alcohol derivatives, 2) difluorocarbene addition to chiral olefins, and 3) utilization of 4-bromo-4,4-difluoro crotonate as a building block. As an application, synthesis of 2-fluoro-2,3-methano-GABA and 3,4-(difluoromethano)glutamic acid is also described.

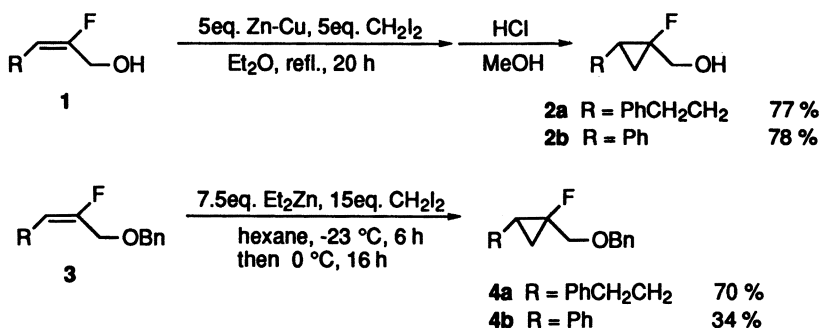
The cyclopropane subunit can be found in a number of natural and unnatural substrates, and some of these have attracted attention due to their interesting biological effects (1). Introduction of the cyclopropane moiety into biologically active substances has been recognized as one of the important chemical modifications owing to conformational rigidity and potential chemical reactivity brought about by this modification (1-4). For example, conformationally restricted analogs of glutamic acid having the cyclopropane moiety were studied so as to elucidate the conformational requirements (extended and folded forms) for the receptor subtype specificity (5, 6). For such chemically modified substances, the introduction of fluorine atom(s) onto the cyclopropane ring would lead to interesting results in consideration of characteristic features of fluorinated compounds based on both steric and electronic effects (7). In general, chirality at the asymmetric center in the molecule is quite important with respect to its biological response. For this, it should be needed to develop an efficient method for the preparation of suitably functionalized fluorinated cyclopropanes in a stereo- and enantioselective manner. In this review, some asymmetric syntheses of monofluoro- and difluorocyclopropanes mainly developed in our group are described.

### Simmons-Smith Reaction of Fluoroallyl Alcohol Derivative.

The Simmons-Smith reaction is extensively used in the synthesis of cyclopropanes from olefins (8). Functional groups on the double bond influence the reactivity of cyclopropanation of alkenes; electron-donating groups activate and electron-with-

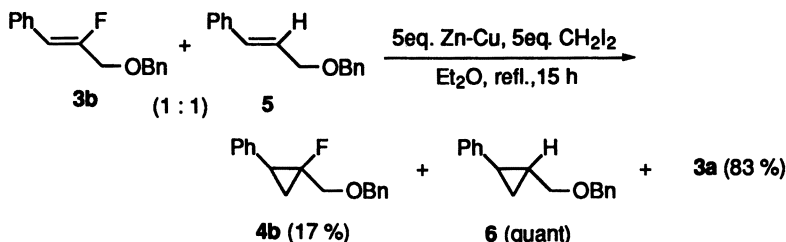
0097-6156/96/0639-0073\$15.00/0  
© 1996 American Chemical Society

drawing groups deactivate the methylene-transfer reaction from the zinc reagent to alkenes. A fluorine-substituted double bond is regarded as a deactivated substrate for the Simmons-Smith reaction due to the electron-withdrawing nature of the fluorine substituent. Since in the Simmons-Smith reaction, allylic oxygen functionality accelerates the reaction rate (8, 9), a fluorinated double bond having an allylic oxygen functionality would be expected to show enhanced reactivity toward the zinc reagent. Typical examples using fluoroallyl alcohol **1** and its benzyl ether **3** are summarized in Scheme 1 (10). To obtain the cyclopropane in reasonable yield, excess amount of the zinc reagent (5-15 eq) is required. Since with hydroxyl free substrate **1**, scrambling at the hydroxyl group of cyclopropane by the formation of the mixture of acetal derivatives (*e.g.* formaldehyde acetal derivatives) occurs extensively, acidic hydrolysis of the crude reaction mixture is needed to obtain the cyclopropane compound **2**. The complete stereospecificity (*cis* addition) is also confirmed with both (*E*)- and (*Z*)-fluoroallyl alcohol derivatives.



Scheme 1

A competitive cyclopropanation reaction with fluorinated and non-fluorinated substrates (**3b** and **5**, respectively) shows a considerable decrease in reactivity by the fluorine substituent (Scheme 2).

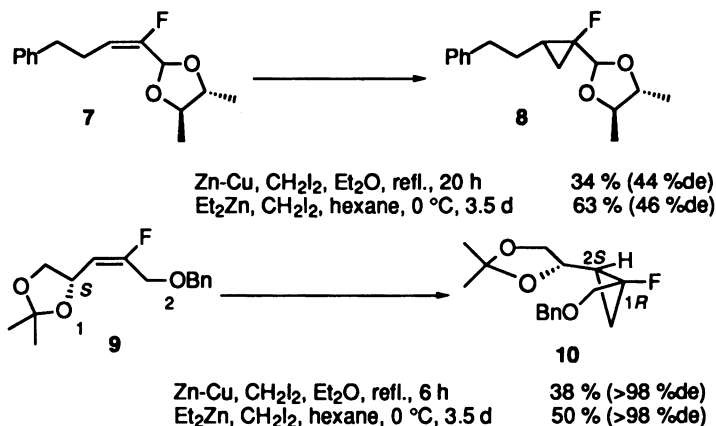


Scheme 2

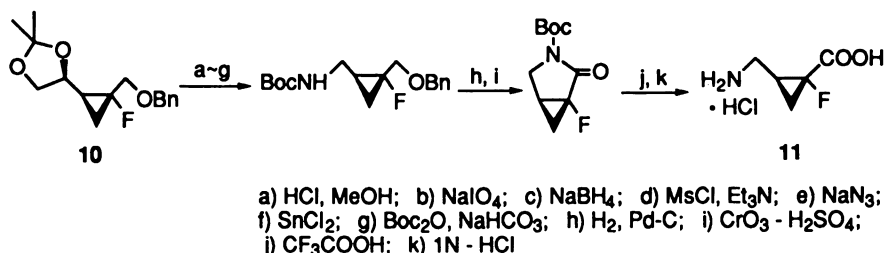
A diastereoselective Simmons-Smith reaction was conducted using a *C*<sub>2</sub>-symmetric acetal **7** and the benzyl ether **9** derived from (*R*)-2,3-*O*-isopropylidene-glyceraldehyde (Scheme 3) (11). While moderate diastereoselectivity was observed in the cycloropanation reaction of **7**, extremely high chiral induction was realized



with the enantio pure allylic alcohol derivative **9** under both Zn-Cu/CH<sub>2</sub>I<sub>2</sub> and Et<sub>2</sub>Zn/CH<sub>2</sub>I<sub>2</sub> conditions. The absolute stereochemistry of the cyclopropane **10** was confirmed to be (1*R*, 2*S*, 1'*S*). Highly diastereoselective cyclopropanations of non-fluorinated chiral allyl alcohol derivatives structurally similar to **9** were also demonstrated and it was proposed that the specific coordination of the zinc reagent to the allylic oxygen (O-1) of the dioxolane ring would be crucial for the stereocontrol (*12*). The cyclopropane **10** may be a versatile synthetic intermediate due to its functionality. Preparation of fluoromethano-GABA **11** is illustrated (Scheme 4).



Scheme 3

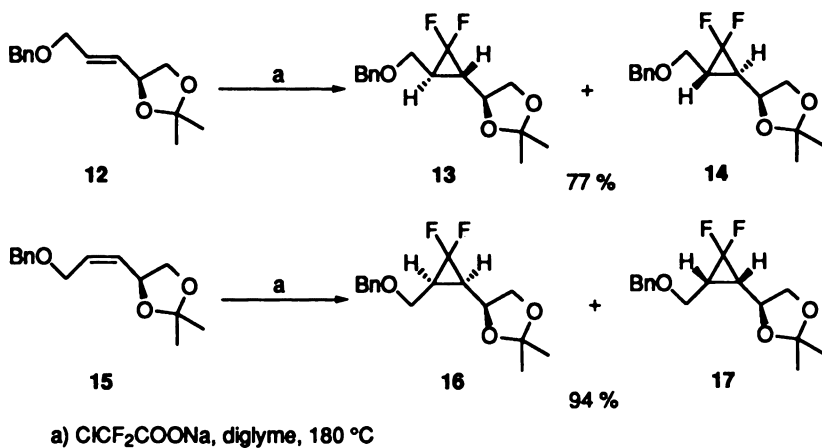


Scheme 4

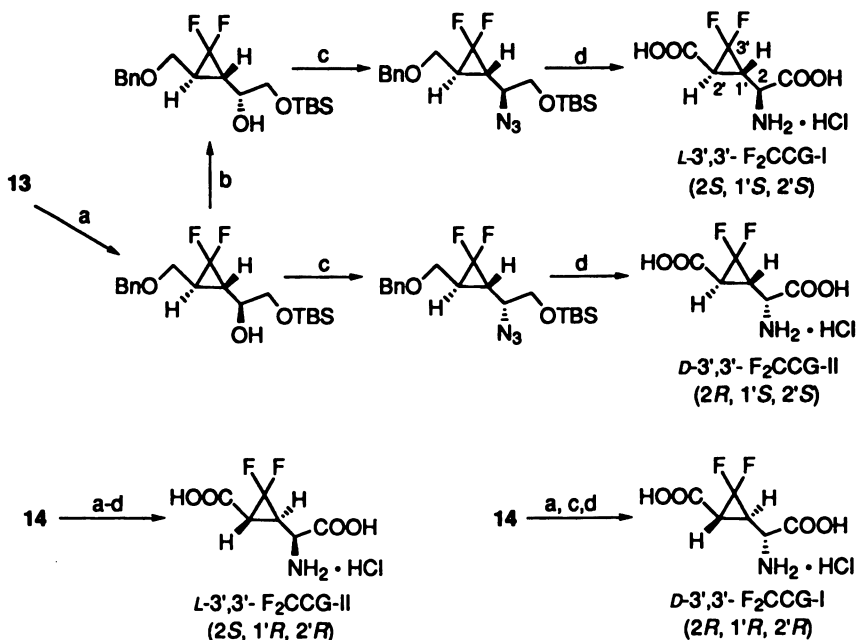
### Difluorocarbene Addition to a Chiral Olefin.

Difluorocarbene addition to an olefin is a fundamental reaction for the preparation of difluorocyclopropane derivatives (*13*). Reaction of the allylic alcohol derivatives, *E*-isomer **12** and *Z*-isomer **15**, derived from (*R*)-2,3-*O*-isopropylidenglyceraldehyde with difluorocarbene generated by thermal decarboxylation of sodium chlorodifluoroacetate, proceeds in stereospecific manner to give the difluorocyclopropanes; **13**, **14** from **12** and **16**, **17** from **15**, respectively (*14*, *15*). In both cases, diastereoselectivities are low; 2.6:1 for *E*-isomer **12** and 1.4:1 for *Z*-isomer **15** (Scheme 5).

The *trans*-difluorocyclopropanes **13** and **14**, were easily separable by column chromatography, and can serve as precursors for the preparation of 3',3'-difluoro-2'-carboxycyclopropylglycines (3',3'-F<sub>2</sub>C<sub>2</sub>CGs) as shown in Scheme 6 (*16*). From the



Scheme 5



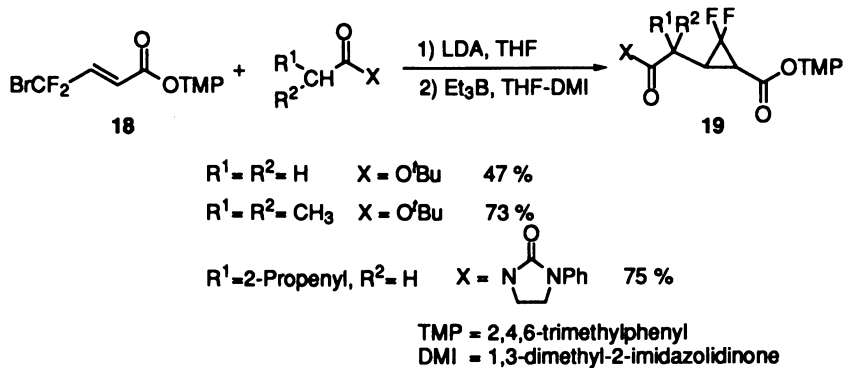
- a) i) HCl / MeOH, ii) TBDMS-Cl, Imidazole; b) i) PhCOOH, DEAD, Ph<sub>3</sub>P, ii) <sup>-</sup>OH; c) (PhO)<sub>2</sub>P(O)N<sub>3</sub>, DEAD, Ph<sub>3</sub>P; d) i) H<sub>2</sub>, Pd-C, ii) Boc<sub>2</sub>O, NaHCO<sub>3</sub>, iii) HCl / MeOH, iv) RuCl<sub>3</sub>, NaIO<sub>4</sub> then CH<sub>2</sub>N<sub>2</sub>, v) H<sub>2</sub>, Pd-C, vi) RuCl<sub>3</sub>, NaIO<sub>4</sub> then CH<sub>2</sub>N<sub>2</sub>, vii) Ti(OBn)<sub>4</sub>, BnOH, viii) H<sub>2</sub>, Pd-C, ix) HCl / H<sub>2</sub>O

Scheme 6

study of conformational requirement of L-glutamic acid to receptor subtype-specificity using CCGs, it was proposed that the extended form of L-glutamic acid, which corresponds to *trans*-isomers of 3,4-methano analogs (CCG-I and CCG-II), is possibly an active conformation to the metabotropic glutamate receptors. In particular, L-CCG-I was reported to be a highly potent and specific agonist to the metabotropic receptors (17). As a preliminary result of pharmacological activity of these fluorinated CCGs, it would be noteworthy that L-3',3'-F<sub>2</sub>CCG-I was found to be a more potent agonist than L-CCG-I.

### Regio- and Stereoselective Synthesis of Functionalized Difluorocyclopropane Using Bromodifluorocrotonate.

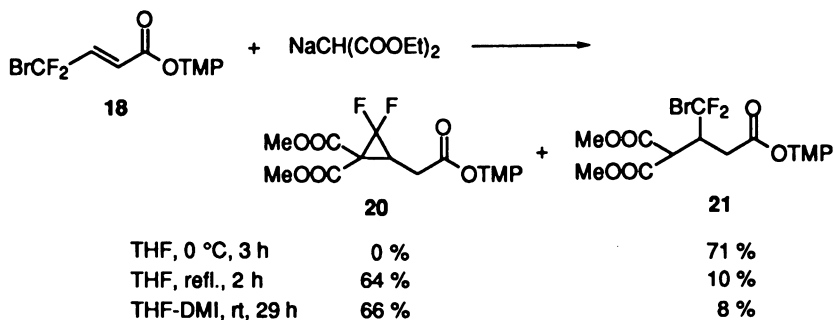
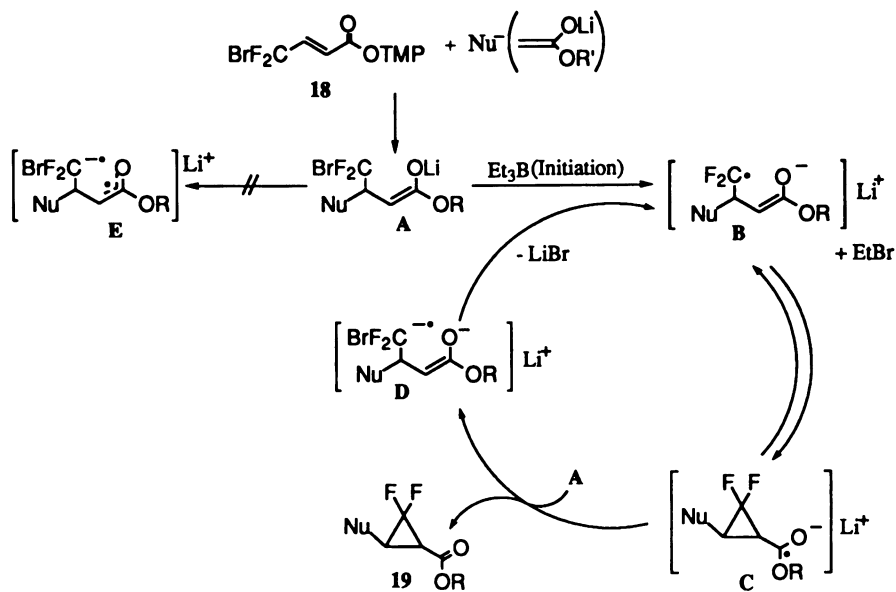
4-Bromo-4,4-difluorocrotonate **18** was shown to be an efficient building block for the preparation of functionalized difluorocyclopropane **19** (18). Thus, reaction of **18** with lithium enolate of ester or amide in the presence of triethylborane (Et<sub>3</sub>B) provides the *trans*-difluorocyclopropane **19** in regio- and stereoselective manner (Scheme 7). The reaction pathway involves the sequential Michael addition of enolate to **18** and the intramolecular substitution, in which Et<sub>3</sub>B acts as a radical initiator (19) to cleave the CF<sub>2</sub>-Br bond as shown in Scheme 8.



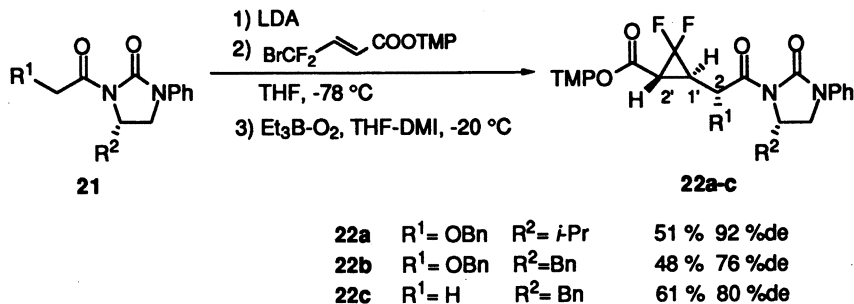
Scheme 7

Bromodifluorocrotonate **18** shows a high reactivity as a Michael acceptor against active methylene compounds. Reaction of **18** with sodium salt of malonate provides the Michael adduct **21** and/or the difluorocyclopropane **20** depending on the reaction conditions (Scheme 9). In the case of non-fluorinated crotonate, ethyl 4-bromocrotonate, only direct S<sub>N</sub>2 displacement occurred with malonate anion (20).

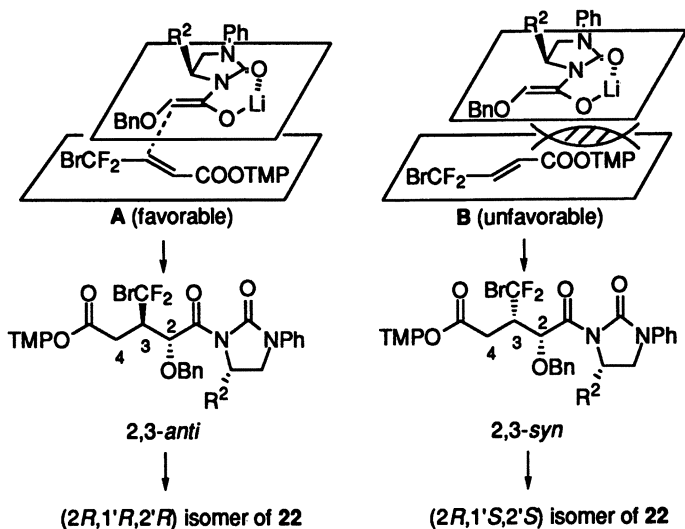
Asymmetric synthesis of difluorocyclopropanes was studied as an extension of the above mentioned methodology using a chiral Michael donor (14) or acceptor (15). According to the reaction pathway (Scheme 8), the enantiomeric purity of the difluorocyclopropane would depend on the degree of chiral induction of the Michael addition step. As a chiral Michael donor, *N*-acylimidazolidinone **21** provided a good result (Scheme 10). When the chiral auxiliary has *S*-configuration, the major *trans*-difluorocyclopropane **22a** or **22b**, obtained by the sequential Michael addition and Et<sub>3</sub>B-mediated substitution reaction, has (2*R*,1'*R*,2'*R*)-configuration (Scheme 10). The observed diastereoselectivity may be explained by considering the transition state model A, in which the reaction at the *re*-face of the (*Z*)-enolate of **21** (R<sup>1</sup>=OBn) with the crotonate **18** proceeds preferentially when **18** approaches in a way to minimize steric interaction between TMP ester part and the imidazolidinone part as illustrated in Scheme 11.



Scheme 9

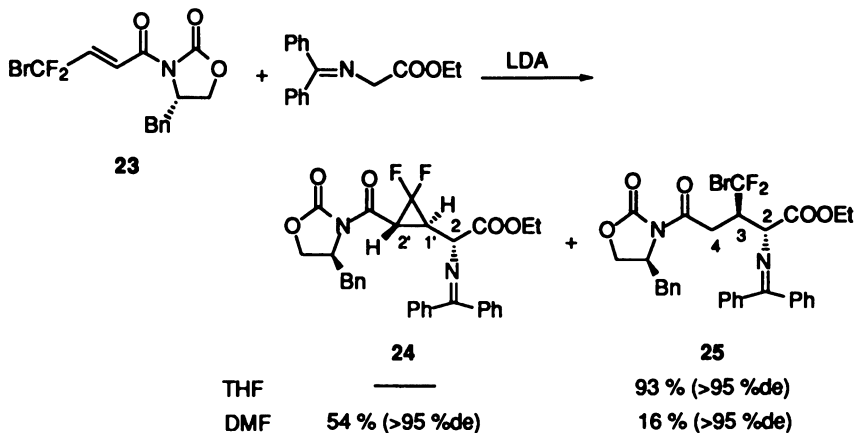


Scheme 10

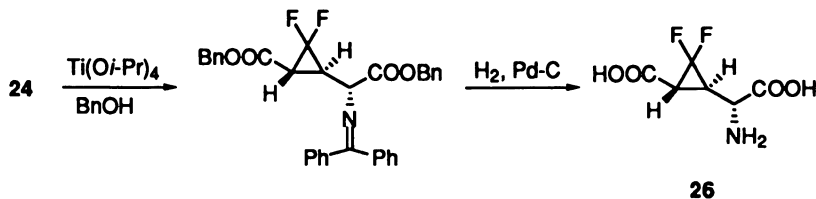


Scheme 11

As an alternative method, in particular for the preparation of 3,4-(difluoromethano) glutamic acid **26**, the use of the chiral Michael acceptor, *N*-(4'-bromo-4',4'-difluoro crotonyl)oxazolidinone **23**, provided excellent diastereoselectivity (15). Thus, the reaction of (*S*)-imide **23** with lithium enolate of *N*-(diphenylmethylidene)glycinate in DMF gave (2*R*,1'*R*,2'*R*)-**24** as an almost single isomer (Scheme 12). Conversion of **24** to 3,4-(difluoromethano)glutamic acid **26** is readily achieved by titanium isopropoxide-catalyzed ester exchange reaction with benzyl alcohol followed by hydrogenolysis (Scheme 13).



Scheme 12



Scheme 13

## Acknowledgements

We thank the contribution of our coworkers whose names are shown as co-authors in published papers, in particular the essential part due to Mr. H. Sasaki. We are grateful to Dr. M. Shiro of Rigaku Corporation for X-ray analyses, and to Dr. H. Shinozaki of the Tokyo Metropolitan Institute of Medical Science for pharmacological study of F<sub>2</sub>CCGs.

## References

- (a) Lin, H. W.; Walsh, C. T. *Biochemistry of the Cyclopropyl Group*; In "The

- Chemistry of the Cyclopropyl Group'; Patai, S.; Rappoport, Z., Eds.; Wiley, New York, 1987; Chapter 16. (b) Suckling, C. J. *Angew. Chem. Int. Ed. Engl.* 1988, 27, 537-552. (c) Wong, H. N. C.; Hon, M.-Y.; Tse, C.-W.; Yip, Y.-C.; Takano, J. *Chem. Rev.* 1989, 89, 165-198. (d) Salaun, J. *Chem. Rev.* 1989, 89, 1247-1270.
- (a) Stammer, C. H. *Tetrahedron* 1990, 46, 2231-2254. (b) Shimohigashi, Y.; Costa, T.; Pfeiffer, A.; Herz, A.; Kimura, H.; Stammer, C. H. *FEBS Lett.* 1987, 222, 71-74. (c) Pirrug, M. C.; Dunlup, S. E.; Trinks, U. P. *Helv. Chim. Acta* 1989, 1301-1310. (d) Burgess, K.; Ho, K.-K. *J. Org. Chem.* 1992, 57, 5931-5936. (e) Burgess, K.; Ho, K.-K.; Pettitt, B. M. *J. Am. Chem. Soc.* 1994, 116, 799-800. (f) Kodama, H.; Shimohigashi, Y. *J. Syn. Org. Chem. Jpn.* 1994, 52, 180-191.
  - Tamura, O.; Hashimoto, M.; Kobayashi, Y.; Katoh, T.; Nakatani, K.; Hayata, I.; Akiba, T.; Terashima, S. *Tetrahedron Lett.* 1992, 33, 3483-3486 and 3487-3490.
  - (a) Paech, C.; Salach, J. L.; Singer, T. P.; *J. Biol. Chem.* 1980, 255, 2700-1704. (b) Silvermann, R. B.; Hoffmann, S. J.; Catus, II, W. B. *J. Am. Chem. Soc.* 1980, 102, 7120-7128. (c) MacDonald, T. L.; Zirvi, K.; Burka, L. T.; Peyman, P.; Guengrich, F. P. *J. Am. Chem. Soc.* 1982, 104, 2050-2052.
  - (a) Yamanoi, K.; Ohfuné, Y.; Watanabe, K.; Li, P.-N.; Takeuchi, H. *Tetrahedron Lett.* 1988, 29, 1181-1184. (b) Shimamoto, K.; Ishida, M.; Shinozaki, H.; Ohfuné, Y. *J. Org. Chem.* 1991, 56, 4167-4176. (c) Raghavan, S.; Ishida, M.; Shinozaki, H.; Nakanishi, K.; Ohfuné, Y. *Tetrahedron Lett.* 1993, 34, 5765-5768. (d) Pellicciari, R.; Natalini, B.; Marinizzi, M.; Monahan, J. B.; Snyder, J. P. *Tetrahedron Lett.* 1990, 31, 139-142.
  - (a) Shinozaki, H.; Ishida, M.; Shimamoto, K.; Ohfuné, Y. *Brain Res.* 1989, 480, 355-359. (b) Shinozaki, H.; Ishida, M.; Shimamoto, K.; Ohfuné, Y. *Br. J. Pharmacol.* 1989, 98, 1213-1224. (c) Kawai, M.; Horikawa, Y.; Ishihara, T.; Shimamoto, K.; Ohfuné, Y. *Eur. J. Pharmacol.* 1992, 211, 195-202.
  - (a) Welch, J. T. *Tetrahedron* 1987, 43, 3123-3197. (b) Kirk, K. L. "Fluorine-Substituted Neuroactive Amines". In 'Selective Fluorination in Organic and Bioorganic Chemistry'; Welch, J. T. Ed.; ACS Symposium Series 456, Washington DC, 1991; pp136-155.
  - (a) Simmons, H. E.; Cairns, T. L.; Vladuchick, S. A.; Hoiness, C. M. *Org. React.* 1973, 20, 1-131. (b) Furukawa, J.; Kawabata, N.; Nishimura, J. *Tetrahedron* 1968, 24, 53-58.
  - (a) Poulter, C. D.; Friedrich, E. C.; Winstein, S. *J. Am. Chem. Soc.* 1969, 91, 6892-6894. (b) Molander, G. A.; Haring, L. S. *J. Org. Chem.* 1989, 54, 3525-3532. (c) Denmark, S. E.; Edwards, J. P.; Wilson, S. R. *J. Am. Chem. Soc.* 1991, 113, 723-725.
  - Morikawa, T.; Sasaki, H.; Mori, K.; Shiro, M.; Taguchi, T. *Chem. Pharm. Bull.* 1992, 40, 3189-3193.
  - For recent examples of asymmetric Simmons-Smith reactions: (a) Mori, A.; Arai, I.; Yamamoto, H. *Tetrahedron* 1986, 42, 6447-6458. (b) Mash, E. A.; Torok, D. S. *J. Org. Chem.* 1989, 54, 250-253. (c) Frutos, M. P.; Fernandez, M. D.; Alvarez, E. F.; Bernarbe, M. *Tetrahedron Lett.* 1991, 32, 541-542. (d) Charette, A. B.; Cote, B.; Marcoux, J.-F. *J. Am. Chem. Soc.* 1991, 113, 8166-8167. (e) Ukaji, Y.; Nishimura, M.; Fujisawa, T. *Chem. Lett.* 1992, 61-64. (g) Takahashi, H.; Yoshioka, M.; Ohno, M.; Kobayashi, S. *Tetrahedron Lett.* 1992, 33, 2575-2578.
  - Morikawa, T.; Sasaki, H.; Hanai, R.; Shibuya, A.; Taguchi, T. *J. Org. Chem.* 1994, 59, 97-103.
  - (a) Burton, D. J.; Hahnfeld, J. C. *Fluorine Chemistry Reviews*; Tarant, P., Ed.; Marcell Dekker Inc.; New York, 1977, Vol 8, pp 153-179. (b) Dolbier, Jr., W. R.; Wojtowicz, H.; Burkholder, C. R. *J. Org. Chem.* 1990, 55, 5420-5422.
  - Taguchi, T.; Shibuya, A.; Sasaki, H.; Endo, J.; Morikawa, T.; Shiro, M. *Tetrahedron: Asymmetry* 1994, 5, 1423-1426.
  - Shibuya, A.; Kurishita, M.; Ago, C.; Taguchi, T. *Tetrahedron* 1996, 52, 271-278.

16. Taguchi, T.; Shibuya, A.; Kurishita, M. 1995 International Chemical Congress of Pacific Basin Societies; Honolulu, HI, USA, Dec. 1995. Abstract No. 666.
17. (a) Ishida, M.; Akagi, H.; Shimamoto, K.; Ohfune, Y.; Shinozaki, H. *Brain Res.* **1990**, *537*, 311-314. (b) Nakagawa, Y.; Saito, K.; Ishihara, T.; Shinozaki, H.; *Eur. J. Pharmac.* **1990**, *184*, 205-206. (c) Hayashi, Y.; Tanaka, Y.; Aramori, I.; Masu, M.; Shimamoto, K.; Ohfune, Y.; Nakanishi, S. *Br. J. Pharmacol.* **1992**, *107*, 539-543. (d) Lombardi, G.; Alesiami, M.; Leonardi, P.; Cherizzi, G.; Pellicciari, R.; Moroni, F. *Br. J. Pharmacol.* **1993**, *110*, 1407-1412. (e) Costantino, G.; Natalini, B.; Pellicciari, R.; Moroni, F.; Lombardi, G. *Bioorg. Med. Chem.* **1993**, *1*, 259-265.
18. Taguchi, T.; Sasaki, H.; Shibuya, A.; Morikawa, T. *Tetrahedron Lett.* **1994**, *35*, 913-916.
19. (a) Takeyama, Y.; Ichinose, Y.; Oshima, K.; Utimoto, K. *Tetrahedron Lett.* **1989**, *30*, 3159-3162. (b) Iseki, K.; Nagai, T.; Kobayashi, Y. *Tetrahedron Lett.* **1993**, *34*, 2169-2170.
20. (a) Prempee, P.; Radviroongit, S.; Thebtaranonth, Y. *J. Org. Chem.* **1983**, *48*, 3553-3556. (b) Yamaguchi, M.; Tsukamoto, M.; Hirano, I. *Tetrahedron Lett.* **1985**, *26*, 1723-1726.



## Chapter 6

# Synthesis and Properties of Novel Fluoroprostacyclins Potent and Stable Prostacyclin Agonists

Yasushi Matsumura, Takashi Nakano, Tomoyuki Asai,  
and Yoshitomi Morizawa

Research Center, Asahi Glass Company, Ltd., 1150 Hazawa,  
Kanagawa-ku, Yokohama 221, Japan

Synthesis and structure-activity relationship of novel 7-fluoroprostacyclin derivatives stabilized by one or two fluorine atoms adjacent to the acid labile enol ether has been studied. A variety of  $\alpha$ -chain modified 7-fluoroprostacyclin derivatives bearing cycloalkylene groups were synthesized by three-component coupling approach or utilization of methylenecyclopentanone (the Stork's intermediate) and pharmacologically evaluated. 7-Fluoro-2,4-methylene-17,20-dimethylprostacyclin (**1**) exerted potent and long-lasting anti-anginal activity *in vivo* in oral administration. Novel 7,7-difluoroprostacyclin derivatives were also synthesized and found to be more stable analogs with very potent inhibitory activities for platelet aggregation. 7,7-Difluoro-18,19-didehydro-16,20-dimethylprostacyclin (AFP-07, **2**) was shown to be a highly selective and potent agonist for prostacyclin receptor.

Since the discovery of prostacyclin (PGI<sub>2</sub>) by Vane *et al.* in 1976 (**1**), manufactured as a unstable metabolite of arachidonic acid in the vascular cell wall, the research related to prostacyclin has been extensively developed (**2**). Prostacyclin, one of the members of prostaglandin (PG) family has powerful actions opposite to those of thromboxane (TX) A<sub>2</sub> to maintain homeostasis in circulation as an antiplatelet agent preventing and even reversing existing platelet clumping, and also as a vasodilator causing increase of blood flow and hypotension. The therapeutical application of natural prostacyclin is very limited due to its inherent chemical and metabolic instability. A large number of its stabilized new analogs have been synthesized (Figure 1), and some of those have been applied to clinical trials or marketed as powerful agents for ischaemic peripheral vascular disease, Raynaud's disease, primary pulmonary hypertension, and myocardial infarction (**3**).

According to the recent dramatic progress of the study on the cloning and classification of prostanoid receptors, their sequences and main functions are well characterized (**4**). Natural prostacyclin itself has only a low selectivity for IP receptor (prostacyclin receptor), because it has agonist activity at EP1 receptor (one of four kinds of PGE receptor (EP) subtype) and TP receptor (TXA<sub>2</sub> receptor) (**5**). EP receptors mediate an broad range of biological activities, including contraction

0097-6156/96/0639-0083\$15.00/0  
© 1996 American Chemical Society

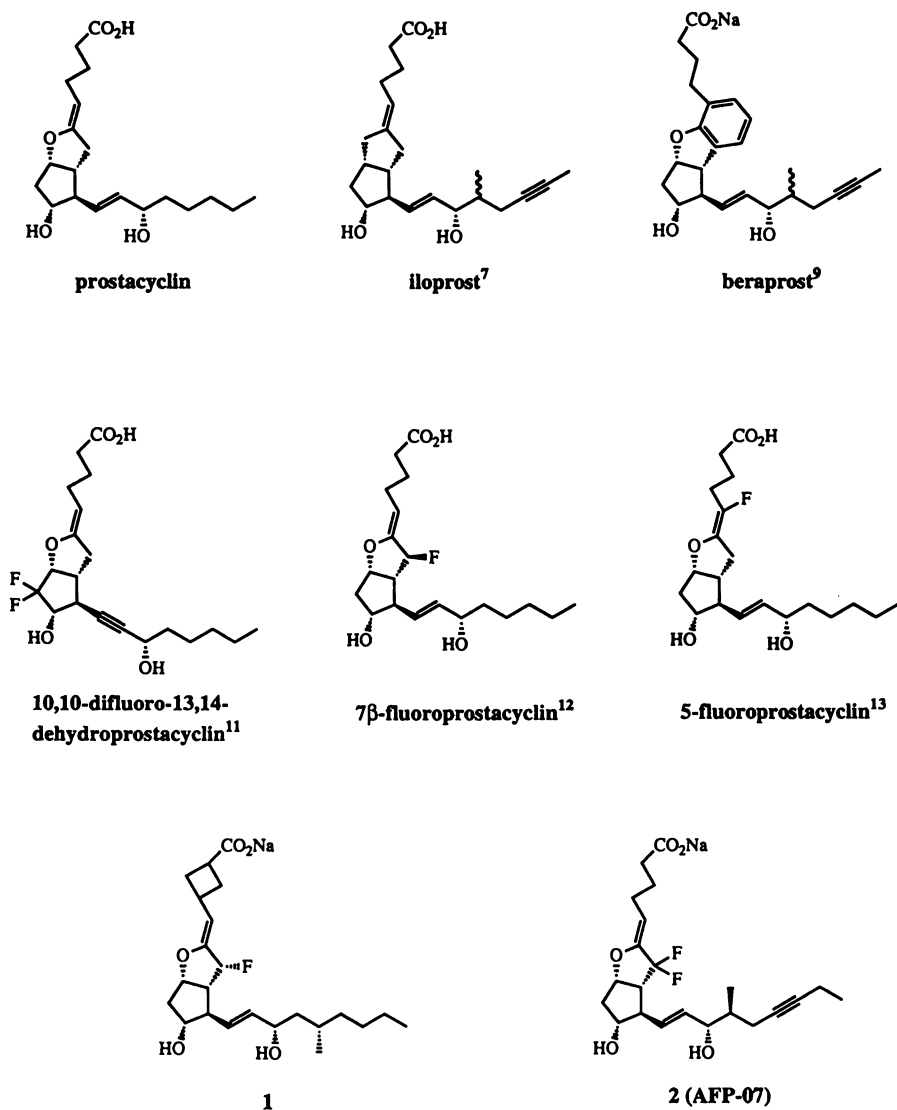


Figure 1. Prostacyclin and its stable analogs.

and relaxation of smooth muscle, inhibition of lipolysis, inhibition of gastric secretion, inhibition of inflammatory mediator release, immunoregulation, etc. TP receptor mediates activation of platelet, contraction of vascular and respiratory smooth muscle, etc. Chemically stabilized prostacyclin agonists such as carbacyclin (6), iloprost (7) or isocarbacyclin (8) have agonist activity at IP receptor as well as strong affinity with EP1 receptor (5). Further explorative research for more selective prostacyclin agonists is needed in order to elucidate diverse functions of the receptors and overall mechanism of signal transduction in molecular level and also to develop as potentially valuable medicines without undesirable side effects.

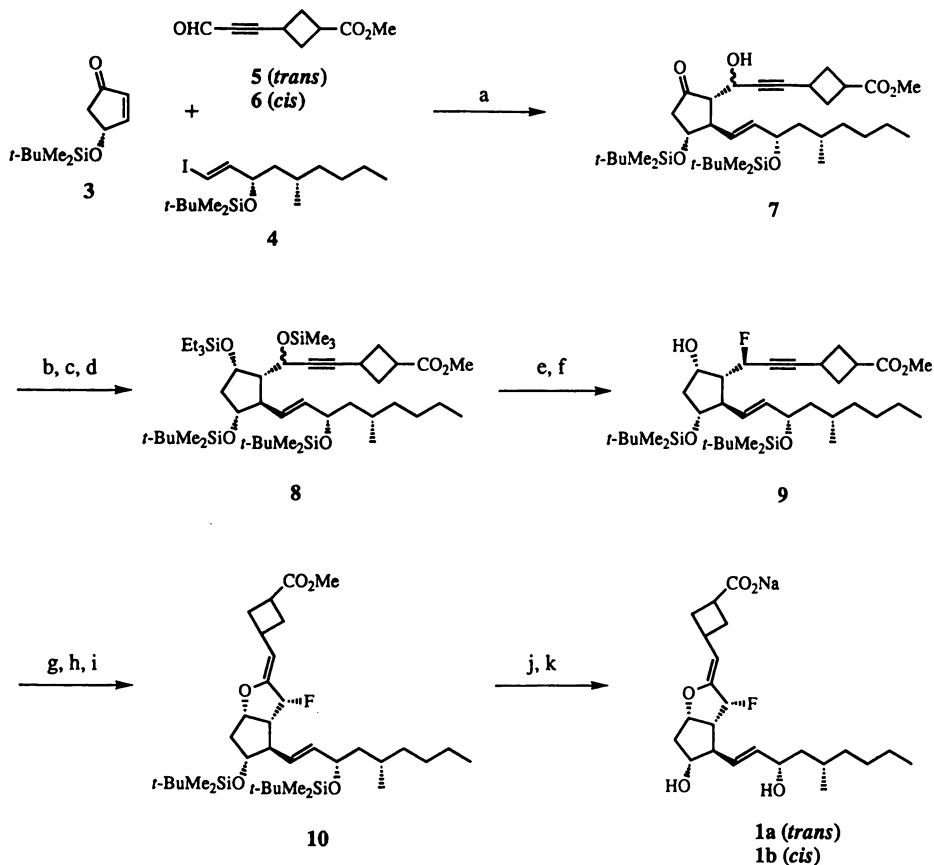
Fluorine-containing prostacyclin derivatives have been studied to modify the physical and physiological properties utilizing unique characters of fluorine atoms such as strong electron negativity, high carbon-fluorine bond energy and a small van der Waals radius (10). Especially, introduction of fluorine atoms adjacent to the acid sensitive enol ether moiety is proved to be very effective to protect it against hydrolysis. Fried *et al.* (11) first synthesized 10,10-difluoro-13,14-dehydroprostacyclin as a stable fluorine-containing analog with remarkable biological activity. Bannai *et al.* (12) and Djuric *et al.* (13) reported later 7 $\beta$ -fluoroprostacyclin and 5-fluoroprostacyclin respectively as PGI<sub>2</sub> mimetics.

We have focused on the study of novel designs of 7-fluoroprostacyclin derivatives. First, we present here the synthesis of monofluoroprostacyclin derivatives modified at the upper side chain (14), and the biological data of the representative compounds (15). Secondly, we introduce novel difluoroprostacyclin derivatives with very high stability and potent platelet anti-aggregatory activity (16). The study on the binding affinity for prostacyclin receptor is also described (17).

### Monofluoroprostacyclin Derivatives.

Introduction of a fluorine atom on the 7-position of prostacyclin could help to stabilize chemically the enol ether function due to its high electron withdrawing ability. Our modifications have been mainly targeted toward the upper side chain to prevent it from being metabolized by  $\beta$ -oxidation (18). The modifications of the chain of prostacyclin analogs have been limited to a few reports (19), probably due to the subtlety of their activities and the difficulty of the synthesis. We designed the synthesis of the derivatives bearing a variety of cycloalkylene groups as a substituent of linear side chain. It is optimistically supposed that regulation of the flexibility of the chain could be one of the chemical approaches to discriminate the multiple actions as the prostacyclin agonist. We describe here the synthesis of the representative derivative, 7-fluoro-2,4-methylene-17,20-dimethylprostacyclins 1 by different approaches (14, 20), and its biological results.

**Three-component Coupling Approach.** Our strategy for generating the prostaglandin skeleton employed Noyori's three-component coupling process (21) (Scheme 1). The cyclobutylene  $\alpha$ -side chain subunits 5 and 6 were prepared from 3-chlorocyclobutanecarboxylic acid in 8 steps and separated by chromatography. Michael addition of the copper reagent derived from iodide 4 to cyclopentenone 3 and successive trapping with the *trans*-cyclobutylene aldehyde 5 efficiently constructed the desired 7-hydroxyprostaglandin 7 in 65% yield as an approximately 1 : 1 mixture of the diastereomers at 7-position. After treatment of 7 with chlorotrimethylsilane and pyridine, stereoselective reduction of the resulting cyclopentanone with sodium borohydride in methanol followed by protection of the hydroxyl group with triethylsilyl group furnished the silyl ether 8.



(a) i. 4, *t*-BuLi (2.2 eq), ether, then  $C_3H_7C\equiv CCu$ ,  $(Me_2N)_3P$ ,  $-78^\circ C$  ii. 3,  $-78^\circ C$  iii. 5,  $-40^\circ C$  (b)  $Me_3SiCl$ , Py,  $0^\circ C$  (c)  $NaBH_4$ , MeOH,  $-20^\circ C$  (d)  $Et_3SiCl$ , Py,  $CH_2Cl_2$ ,  $0^\circ C$  (e) piperidinosulfur trifluoride,  $ClCF_2CFCl_2$ , r.t. (f) pyridinium *p*-toluenesulfonate, EtOH, r.t. (g) 1atm  $H_2$ , Pd-CaCO<sub>3</sub>-Pb,  $0^\circ C$  (h) NIS,  $CH_3CN$ ,  $40^\circ C$  (i) DBU, toluene,  $110^\circ C$  (j)  $Bu_4NF$ , THF, r.t. (k) NaOH, EtOH, r.t.

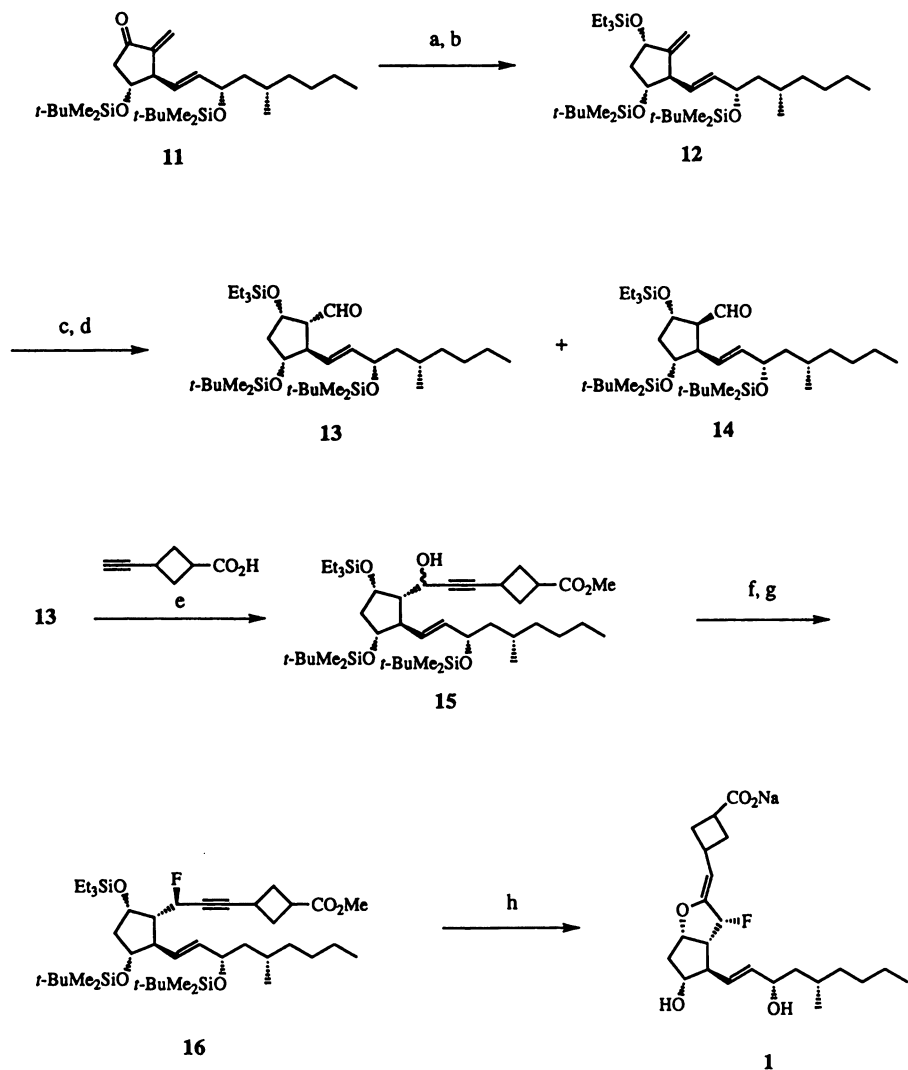
### Scheme 1

Our initial attempts to fluorinate the 7-hydroxyl group of the known prostaglandin derivatives with various fluorinating reagents resulted in the obtention of dehydrated compounds as major products. We examined a modified fluorination reaction using (*R*)-2-octanol as a model substrate. While fluorination of the alcohol with diethylaminosulfur trifluoride (DAST) in dichloromethane resulted in the poor selectivity (fluoride : olefins = 48 : 52), modified fluorination of the corresponding silyl ether was found to give the products with high selectivity (fluoride : olefins = 89 : 11) (14b). The modified fluorination of the trimethylsilyl ether suppressed the side products probably because the reaction formed inert trimethylsilyl fluoride *in situ*, instead of acidic hydrogen fluoride which usually causes undesirable dehydration reaction as well. Desilylative fluorination of compound **8** (a 1 : 1 mixture of *C*-7 diastereomers) with piperidinosulfur trifluoride in less-polar solvent, 1,1,2-trichloro-1,2,2-trifluoroethane at room temperature and subsequent deprotection with pyridinium *p*-toluenesulfonate gave the hydroxy fluoride (7*R*)-**9** in 51% yield, accompanied with a small amount of the dehydrated product (< 10%). It is supposed that the bulky triethylsiloxy group at the 9-position influenced the stereochemical outcome through the attack of fluoride anion to the propargylic carbonium ion. The fluoride anion would approach only from the  $\beta$ -side of *C*-7 position avoiding the steric hinderance of the  $\alpha$ -face to form exclusively the (7*R*)-diastereomer. After quantitative hydrogenation with Lindlar catalyst, cyclization of the resulted olefinic alcohol with *N*-iodosuccinimide (NIS) in acetonitrile and subsequently dehydroiodination of the resulting iodide with 1,8-diazabicyclo[5.4.0]-7-undecene (DBU) afforded the desired vinyl fluoride **10**. Deprotection of **10** and following saponification provided the prostacyclin derivative **1** containing *trans*-cyclobutylene moiety (14). The *cis*-isomer was synthesized in a similar synthetic pathway starting from the corresponding *cis*-aldehyde **6**.

**Utilization of Methylenecyclopentanone.** Recently, a new class of methodologies for prostaglandin synthesis featuring the Stork's intermediate (22) **11** has appeared (23). In addition to strong demand for a practical process suitable for large scale synthesis, the commercial availability of a chiral methylenecyclopentanone **11** was a strong appeal to us to examine its applicability in our prostaglandin synthesis. We set out an alternative approach to synthesize 7-hydroxyprostaglandin framework **15**, a key intermediate obtained by simple reactions of an acetylenic acid with aldehydes **13**.

The synthesis of **1** was started from methylenecyclopentanone having 17,20-dimethyl  $\omega$ -side chain **11** (Scheme 2). Reduction of **11** with sodium borohydride in the presence of cerium trichloride and the following protection with chlorotriethylsilane in pyridine gave **12** in 90% yield with 10 : 1 stereoselectivity. Hydroboration of **12** with 9-borabicyclo[3.3.1]nonane (9-BBN) in tetrahydrofuran and subsequent oxidation with pyridinium chlorochromate in dichloromethane in the presence of molecular sieves 4A afforded a 6 : 1 mixture of the desired triethylsiloxy aldehyde **13** and the isomer **14**. The coupling reaction of **13** with 3-ethynylcyclobutanecarboxylic acid after treatment with *n*-butyllithium followed by esterification provided **15** in 52% yield. After the stereospecific fluorination of the corresponding trimethylsilyl ether of **15** as described above, the fluoride **16** was transformed easily to the 7-fluoroprostacyclin **1** (20).

**Synthesis of Various  $\alpha$ -Chain Modified Analogs.** A variety of analogs modified at the upper side chain were conveniently synthesized by the same methodology (**15**) (Figure 2). The cycloalkylene analogs bearing three- to six-membered ring **17** - **22** were prepared in order to understand structure-activity relationship. The



a)  $\text{NaBH}_4$ ,  $\text{CeCl}_3 \cdot 7\text{H}_2\text{O}$ ,  $\text{MeOH}$ ,  $0^\circ\text{C}$  b)  $\text{Et}_3\text{SiCl}$ , pyridine,  $0^\circ\text{C}$  (2 steps, 90%) c) 9-BBN, THF,  $0^\circ\text{C}$  ~ r.t. then  $\text{NaOH} \cdot \text{H}_2\text{O}_2$ , d) PCC, molecular sieves 4A,  $\text{CH}_2\text{Cl}_2$  r.t. (2 steps, 61%) e)  $n\text{-BuLi}$ , HMPA, THF,  $-20^\circ\text{C}$ , then  $\text{CH}_2\text{N}_2$ , r.t. (52%) f)  $\text{Me}_3\text{SiCl}$ , pyridine,  $0^\circ\text{C}$  g) piperidinosulfur trifluoride,  $\text{ClCF}_2\text{CFCl}_2$ , r.t. (2 steps, 65%) h) 6 steps

**Scheme 2**

interphenylene analog **23**, the branched methyl analog at 4-position **24**, and methylene-elongated analog **25** were also synthesized to compare their biological effects with those of the cycloalkylene modified analogs (**24**).

**Biological Studies.** The pharmacological results on antiplatelet activity of **1a**, **1b** and **17-25** are summarized in Table I (**25**). Among the cycloalkylene compounds, the cyclobutylene compounds **1a**, **1b** and *trans*-cyclopentylene derivative **17** indicated strong inhibition of ADP-induced platelet aggregation *in vitro*, which was comparable to iloprost. In contrast, *cis*-cyclopentylene analog **18** and the cyclobutylene derivative **21** one-carbon elongated between the cyclobutylene group and the carboxyl terminal exerted considerably weaker action. The derivatives having smaller or larger cyclic side chain, **19**, **20**, and **22** also revealed weak potency, especially the effect of the 1,4-substituted cyclohexylene analog **22** was very faint. Despite the successful example of interphenylene moiety in Taprostene (**19b**), the compound **23** showed considerably weak inhibitory activity on platelet aggregation, which was 4 - 16 times less potent than **1a**, **1b** or **17**. On the one-carbon elongated compounds, both branched analog **24** and the linear derivative **25** exerted the faint inhibitory effect.

From these observations not only the distance but also the angle between the carboxyl group and the vinyl ether should significantly affect the affinity of the agonists to the platelet prostacyclin receptor. Conformational rigidity of the side chains in the cycloalkylene derivatives seems to magnify the sensitive nature of the receptor to distinguish the chemical structure.

Anti-anginal potency of **1a**, **1b** and **17** given intravenously (*i.v.*) and orally (*p.o.*) were evaluated by preventive effect on vassopressin-induced ST depression of rat electrocardiogram (**26**) as demonstrated in Table II. Minimum effective doses (MED) in intravenous and oral administration of **1a** indicated 10 - 100 fold more potency compared to iloprost. The effect of **1a** lasted 3 h after the oral administration, whereas iloprost was only effective within 0.5 h. The long duration should be attributed to the chemical and metabolic stability of **1a**. The isomer **1b** and the cyclopentylene analog **17** showed weaker effects than **1a**. Compounds **1a**, **1b** and **17** showed similar hypotensive effect to iloprost for a short period, however the decrease of blood pressure at the effective doses on ST-depression were very slight. It suggests that compounds **1a**, **1b** and **17** have remarkable potency as anti-anginal agents with good separation from hypotensive effects.

### Difluoroprostacyclin Derivatives.

We next targeted our research to novel 7,7-difluoroprostacyclin derivatives (Figure 3). The stabilizing effect of fluorine atoms at 7-position for the enol ether functionality was proved through the study described so far without a significant loss of inhibitory activity on platelet aggregation. We therefore turned our attention to evaluation of the contribution of the second fluorine atom at this position to stability and the inhibitory activity. According to our expectation, the 7,7-difluoroprostacyclin derivatives showed much higher chemical stability and potent activities.

**Synthesis and Properties.** We synthesized novel 7,7-difluoroprostacyclin derivatives, 7,7-difluoro-18,19-didehydro-16,20-dimethylprostacyclin (AFP-07) **2** and 7,7-difluoro-17,20-dimethylprostacyclin **26** by manganese salt catalyzed novel electrophilic fluorination of Corey lactone and subsequent stereoselective Wittig reaction of the difluorolactone (**16**). The stability of **2** in aqueous solution was examined in pH 6.5 buffer at 25 °C. Compound **2** did not decompose even after 30 days, which was in a sharp contrast with natural prostacyclin (half life: 76.2 sec

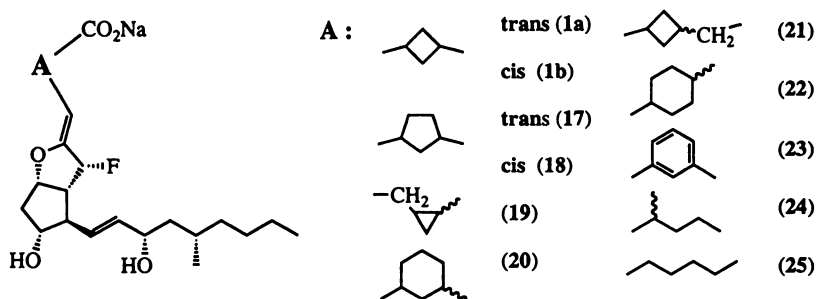


Figure 2. 7-Fluoroprostacyclin derivatives modified at  $\alpha$ -chain.

**Table I.** Inhibitory effects of **1a,b, 17-25** and iloprost on ADP-induced guinea pig platelet aggregation *in vitro* (ADP=1  $\mu$ M)

Substance	<b>1a</b>	<b>1b</b>	<b>17</b>	<b>18</b>	<b>19</b>	<b>20</b>
Inhibition of platelet aggregation (PGE <sub>1</sub> =1) <sup>a)</sup>	3.4	13.3	7.0	0.85	0.34	0.6
Substance	<b>21</b>	<b>22</b>	<b>23</b>	<b>24</b>	<b>25</b>	iloprost
Inhibition of platelet aggregation (PGE <sub>1</sub> =1) <sup>a)</sup>	1.27	0.05	0.80	0.13	0.25	10.8

a) Relative potency to PGE<sub>1</sub>.

(Reprinted with permission from ref. 15. Copyright 1995 The Pharmaceutical Society of Japan.)



**Table II.** Preventive effects on ST depression and hypotensive effects of **1a,b, 17** and iloprost

Substance	Preventive effect on vassopressin-induced ST depression in rats <sup>a)</sup>		Effect on mean blood pressure in rats <sup>b)</sup>	
	<i>i.v.</i> (MED, $\mu\text{g}/\text{kg}$ )	<i>p.o.</i> (MED, $\text{mg}/\text{kg}$ )	<i>i.v.</i> ( $\mu\text{g}/\text{kg}$ , $\Delta\text{mmHg}$ )	<i>p.o.</i> ( $\text{mg}/\text{kg}$ , $\Delta\text{mmHg}$ )
<b>1a</b>	0.1	0.01	0.1, -19 0.01, -5	0.1, -19 0.01, 0
<b>1b</b>	0.1	0.1	0.1, -19 0.01, -5	1.0, -27 0.1, -9
<b>17</b>	1.0	0.1	1.0, -10 0.1, 0	1.0, -29 0.1, 0
iloprost	1.0	1.0	1.0, -34 0.1, 0	1.0, -3

a) Substances were intravenously or orally administered before vassopressin injection.

b) Changes in mean blood pressure in anesthetized rats (*i.v.*) and conscious rats (*p.o.*).

(Reprinted with permission from ref. 15. Copyright (1995) The Pharmaceutical Society of Japan)

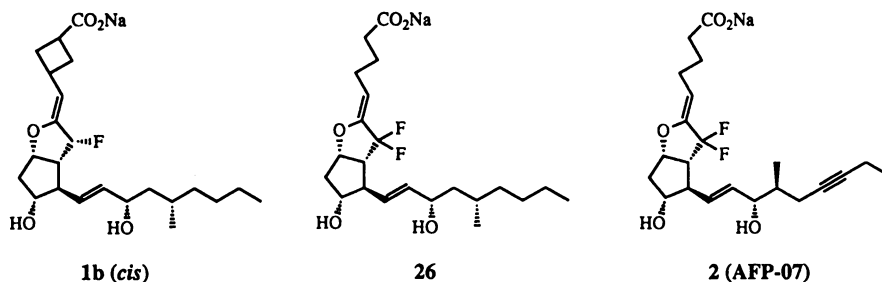


Figure 3. Chemical structures of three fluoroprostacyclin derivatives.

(27)), and it was even much more stable than the monofluoroprostacyclin derivatives. Protonation on the carbon in the vinyl ether of **2**, probably the rate limiting step in the hydrolysis, should be strongly retarded by destabilizing effect of the adjacent difluoromethylene group on carbocation formation (28). It is consistent with a previous report on acid-catalyzed hydration of  $\alpha$ -trifluoromethyl vinyl ether in aqueous acid (29). Inhibitory activity of **2** on ADP-induced human platelet aggregation *in vitro* was > 200 times more potent than prostaglandin E<sub>1</sub>.

**Receptor Binding Study.** The binding affinities of the difluoroprostacyclin derivatives **2** and **26**, the monofluoroprostacyclin **1b**, and iloprost on specific [<sup>3</sup>H]iloprost binding to the membrane of Chinese hamster ovary (CHO) cells expressing the IP receptor (30) were examined (17). The specific binding to the IP receptor was inhibited by these ligands in the order of **2** > **26** > iloprost > **1b**. The agonist activity for the IP receptor was coupled to the stimulation of adenylate cyclase. These agonists stimulated the increase in the cAMP level of the IP receptor expressing cells in the same order as the IP receptor binding affinities. Among them, **2** is the most potent IP agonist, its potency being one order magnitude stronger than that of iloprost.

The effects of **2** and iloprost on specific [<sup>3</sup>H]PGE<sub>2</sub> binding to CHO cell membranes expressing the four PGE receptor subtypes, EP1 (31), EP2 (32), EP3 (33), and EP4 (34) were studied in comparison with PGE<sub>2</sub> in order to evaluate the selectivity of **2** and iloprost for IP receptor. The specific binding to the EP1 receptor subtype was weakly inhibited by **2**. In contrast, iloprost showed the same strong affinity as PGE<sub>2</sub> as reported previously (5). The affinities for **2** in all four PGE receptor subtypes were weaker than PGE<sub>2</sub> which showed that **2** was a highly selective IP agonist (17).

IP receptors are distributed and expressed in platelets, vascular smooth muscle, etc. The four subtypes of EP receptors are more widely distributed in various tissues such as kidney, ileum, uterus, spleen, lung, heart, brain, etc. These receptors should play an important physiological role to control multiple functions in each tissues. For instance, EP1 receptor in gastrointestinal tissue is mediated the contraction of smooth muscle (5b, 35). The selective IP agonist should alleviate the complex adverse effects in gastrointestinal system such as diarrhea or nausea caused often with the prostacyclin mimetics.

## Conclusions.

We describe here the synthesis and evaluation of novel fluoroprostacyclin derivatives. Introduction of one or two fluorine atoms adjacent to the enol ether efficiently stabilized the parent prostacyclin structure. Further pharmacological study of the potent and orally active difluoroprostacyclin **2** is in progress.

In addition, the approaches from molecular biology such as the assay system using established cell lines expressing each receptors will aid the discovery of selective receptor agonists or even antagonists as valuable medicines. It is not certain whether subtypes of IP receptor exist, or whether the arginine residue in the seventh transmembrane domain serve as the binding site for prostanoid (36). The important structural information of the receptors will clearly accelerate the studies from chemical approaches on structure-activity relationship.

## Acknowledgments

The authors are grateful to Prof. A. Ichikawa, Prof. M. Negishi, and Mr. C-S. Chang of Faculty of Pharmaceutical Sciences, Kyoto University, for receptor binding assay of fluoroprostacyclin derivatives and fruitful discussions. The authors

thank Dr. K. Hosoki, Dr. B. Fujitani, and Mr. T. Yamamoto of Department of Pharmacology, Dainippon Pharmaceutical Co., Ltd., for pharmacological evaluation of monofluoroprostacyclin derivatives. The authors also thank to Mr. T. Shimada, Mr. T. Nakayama, Mr. M. Urushihara, Dr. S-Z. Wang, Ms. M. Makino and Dr. A. Yasuda of Asahi Glass Co., Ltd., for their contributions and helpful discussions.

### Literature Cited

1. Moncada, S.; Gryglewski, R. J.; Bunting, S.; Vane, J. R.; *Nature* **1976**, *263*, 663.
2. Collins, P. W.; Djuric, S. W. *Chem. Rev.* **1993**, *93*, 1533.
3. *Therapeutic Applications of Prostaglandins*; Vane, J.; O'Grady, J., Eds.; Edward Arnold: London, 1993.
4. a) Coleman, R. A.; Kennedy, I.; Humphrey, P. P. A.; Bunce, K.; Lumley, P. In *Comprehensive Medicinal Chemistry*, Emmett, J. C., Ed.; Pergamon: Oxford, 1990, Vol. 3; pp 643-714; b) Coleman, R. A.; Smith, W. L.; Narumiya, S. *Pharmacol. Rev.* **1994**, *46*, 205; c) Namba, T.; Oida, H.; Sugimoto, Y.; Kakizuka, A.; Negishi, M.; Ichikawa, A.; Narumiya, S. *J. Biol. Chem.* **1994**, *269*, 9986; d) Boie, Y.; Rushmore, T. H.; Darmon-Goodwin, A.; Grygorczyk, R.; Slipetz, D. M.; Metters, K. M.; Abramovitz, M. *J. Biol. Chem.* **1994**, *269*, 12173.
5. a) Dong, Y. J.; Jones, R. L.; Wilson, N. H. *Br. J. Pharmacol.* **1986**, *87*, 97; b) Armstrong, R. A.; Lawrence, R. A.; Jones, R. L.; Wilson, N. H.; Collier, A. *Br. J. Pharmacol.* **1989**, *97*, 657.
6. a) Nicolaou, K. C.; Sipiro, W. J.; Magolda, R. L.; Seitz, S.; Barnette, W. E. *J. Chem. Chem. Commun.* **1978**, 1067; b) Kojima, I.; Sakai, K.; *Tetrahedron Lett.* **1978**, *19*, 3743; c) Shibasaki, M.; Ueda, J.; Ikegami, S. *Tetrahedron Lett.* **1979**, *20*, 433.
7. a) Skuballa, W.; Vorbrüggen, H. *Angew. Chem. Int. Ed. Engl.* **1981**, *20*, 1046.
8. Shibasaki, M.; Torisawa, Y.; Ikegami, S. *Tetrahedron Lett.* **1983**, *24*, 3493.
9. Murata, T.; Sakaya, S.; Hoshino, T.; Umetsu, T.; Hirano, T.; Nishio, S. *Arzneim. Forsch.* **1989**, *39(II)*, 860.
10. a) Yasuda, A. In *Organofluorine Compounds in Medicinal Chemistry and Biomedical Applications*; Filler, R.; Kobayashi, Y.; Yagupolskii, L. M., Eds.; Elsevier: Amsterdam, 1993, p 275; b) *Fluorine in Bioorganic Chemistry*; Welch, J. T.; Eswarakrishnan, S., Eds.; John Wiley & Sons: New York, 1991.
11. Fried, J.; Mitra, D. K.; Nagarajan, M.; Mehrotra, M. M. *J. Med. Chem.* **1980**, *23*, 234.
12. Bannai, K.; Toru, T.; Oba, T.; Tanaka, T.; Okamura, N.; Watanabe, K.; Hazato, A.; Kurozumi, S. *Tetrahedron* **1983**, *39*, 3807.
13. Djuric, S. W.; Garland, R. B.; Nysted, L. N.; Pappo, R.; Plume, G.; Swenton, L. *J. Org. Chem.* **1987**, *52*, 978.
14. a) Asai, T.; Morizawa, Y.; Shimada, T.; Nakayama, T.; Urushihara, M.; Matsumura, Y.; Yasuda, A. *Tetrahedron Lett.* **1995**, *36*, 273; b) Matsumura, Y.; Shimada, T.; Nakayama, T.; Urushihara, M.; Asai, T.; Morizawa, Y.; Yasuda, A. *Tetrahedron* **1995**, *51*, 8771.
15. Matsumura, Y.; Asai, T.; Shimada, T.; Nakayama, T.; Urushihara, M.; Morizawa, Y.; Yasuda, A.; Yamamoto, T.; Fujitani, B.; Hosoki, K. *Chem. Pharm. Bull.* **1995**, *43*, 353.
16. a) A preliminary report of this work was presented at the AFMC International Medicinal Chemistry Symposium 95, Tokyo, September 1995; b) Nakano, T.; Makino, M.; Morizawa, Y.; Matsumura, Y. *Angew. Chem.* in press.
17. Submitted for publication.
18. Hamberg, M. *Eur. J. Biochem.* **1968**, *6*, 135.
19. a) Skuballa, W.; Schillinger, E.; Stuerzebechert, C. S.; Vorbrüggen, H. *J. Med. Chem.* **1986**, *29*, 313; b) Flohe, L.; Böhlke, H.; Frankus, E.; Kim, S. M. A.;

- Lintz, W.; Loschen, G.; Michel, G.; Müller, B.; Schneider, J.; Seipp, U.; Vollenberg, W.; Wilsmann, K. *Arzneim. Forsh.* **1983**, *33(II)*, 1240; c) Iseki, K.; Kanayama, T.; Hayasi, Y.; Shibasaki, M. *Chem. Pharm. Bull.* **1990**, *38*, 1769.
20. Matsumura, Y.; Wang, S. -Z.; Asai, T.; Shimada, T.; Morizawa, Y.; Yasuda, A. *Synlett*, **1995**, 260.
21. a) Suzuki, M.; Kawagishi, T.; Suzuki, T.; Noyori, R. *Tetrahedron Lett.* **1982**, *23*, 4057; b) Noyori, R.; Suzuki, M. *Angew. Chem. Int. Ed. Engl.* **1984**, *23*, 847; c) Noyori, R. *Asymmetric Catalysis in Organic Synthesis*; John Wiley & Sons: New York, 1994; pp 298-322.
22. a) Stork, G.; Kraus, G. *J. Am. Chem. Soc.*, **1975**, *97*, 4745; b) Stork, G.; Kraus, G. *J. Am. Chem. Soc.* **1976**, *98*, 6747.
23. a) Okamoto, S.; Kobayashi, Y.; Kato, H.; Hori, K.; Takahashi, T.; Tsuji, J.; Sato, F. *J. Org. Chem.* **1988**, *53*, 5590; b) Takahashi, T., Shimayama, T., Miyazawa, M.; Nakazawa, M.; Yamada, H.; Takatori, K.; Kajiwara, M. *Tetrahedron Lett.*, **1992**, *40*, 5973; c) Nakazawa, M.; Sakamoto, Y.; Takahashi, T.; Tomooka, K.; Ishikawa, K.; Nakai, T. *Tetrahedron Lett.* **1993**, *34*, 5923.
24. Unpublished results.
25. For the biological test method, see: Born, G. V. R. *Nature* **1962**, *194*, 927.
26. Yamamoto, T.; Nakatsuji, K.; Hosoki, K.; Karasawa, T. *Clin. Exp. Pharmacol. Physiol.*, **1993**, *20*, 673.
27. a) Cho, M. J.; Allen, M. A. *Prostaglandins* **1978**, *15*, 943; b) Chiang, Y.; Cho, M. J.; Euser, B. A.; Kresge, A. J. *J. Am. Chem. Soc.* **1986**, *108*, 4192.
28. a) Kirmse, W.; Wonner, A.; Allen, A. D.; Tidwell, T. T. *J. Am. Chem. Soc.* **1992**, *114*, 8828; b) Creary, X. *Chem. Rev.* **1991**, *91*, 1625; c) Gassman, P. G.; Tidwell, T. T. *Acc. Chem. Res.* **1983**, *16*, 279.
29. Allen, A. D.; Shahidi, F.; Tidwell, T. T. *J. Am. Chem. Soc.* **1982**, *104*, 2516.
30. Namba, T.; Oida, H.; Sugimoto, Y.; Kakizuka, A.; Negishi, M.; Ichikawa, A.; Narumiya, S. *J. Biol. Chem.* **1994**, *269*, 9986.
31. Watabe, A.; Sugimoto, Y.; Honda, A.; Irie, A.; Namba, T.; Negishi, M.; Ito, S.; Narumiya, S.; Ichikawa, A. *J. Biol. Chem.* **1993**, *268*, 20175.
32. Honda, A.; Sugimoto, Y.; Namba, T.; Watabe, A.; Irie, A.; Negishi, M.; Narumiya, S.; Ichikawa, A. *J. Biol. Chem.* **1993**, *268*, 7759.
33. a) Sugimoto, Y.; Namba, T.; Honda, A.; Hayashi, Y.; Negishi, M.; Ichikawa, A.; Narumiya, S. *J. Biol. Chem.* **1992**, *267*, 6463; b) Negishi, M.; Sugimoto, Y.; Irie, A.; Narumiya, S.; Ichikawa, A. *J. Biol. Chem.* **1993**, *268*, 9517.
34. Nishigaki, N.; Negishi, M.; Honda, A.; Ichikawa, A.; Narumiya, S. *FEBS Lett.* **1995**, *364*, 339.
35. Lanthorn, T. H.; Bianchi, R. G.; Perkins, W. E.; *Drug Develop. Res.* **1995**, *34*, 35.
36. a) Hirata, M.; Hayashi, Y.; Ushikubi, F.; Yokota, Y.; Kageyama, R.; Nakanishi, S.; Narumiya, S. *Nature*, **1991**, *349*, 617; b) Narumiya, S.; Hirata, M.; Namba, T.; Hayashi, Y.; Ushikubi, F.; Sugimoto, Y.; Negishi, M.; Ichikawa, A. *J. Lipid Mediators*, **1993**, *6*, 155.

## Chapter 7

# Preparation of Fluorinated Amino Acids with Tyrosine Phenol Lyase

## Effects of Fluorination on Reaction Kinetics and Mechanism of Tyrosine Phenol Lyase and Tyrosine Protein Kinase Csk

R. L. VonTersch<sup>1</sup>, F. Secundo<sup>2</sup>, R. S. Phillips<sup>3,4</sup>, and M. G. Newton<sup>3</sup>

<sup>1</sup>Department of Chemistry, U.S. Naval Academy, Annapolis, MD 21402

<sup>2</sup>Instituto di Chimica degli Ormoni, CNR, via Mario Bianco 9,  
20131 Milan, Italy

<sup>3</sup>Department of Chemistry and <sup>4</sup>Department of Biochemistry and  
Molecular Biology, University of Georgia, Athens, GA 30602-2556

Fluorinated analogues of L-tyrosine were synthesized enzymatically from the corresponding fluorinated phenols and ammonium pyruvate using tyrosine phenol-lyase. The isolated yields ranged from 0.5 -2.8 g per liter (10-42% based on phenol added). The structure of 2,3,6-trifluoro-L-tyrosine hydrochloride hydrate was determined by x-ray crystallography. The fluorinated tyrosines are good substrates for the  $\beta$ -elimination reaction catalysed by tyrosine phenol-lyase, except for 3,5-difluoro and the trifluorotyrosines. Fluorine at the 3-position increases the steady-state concentration of quinonoid intermediate absorbing at 500 nm compared to L-tyrosine, while fluorine at the 2-position dramatically decreases the intensity of the 500 nm absorbance peak. Reaction of tyrosine phenol-lyase with  $\beta,\beta,\beta$ -trifluoroalanine and fluorophenols generates transient ring-fluorinated  $\beta,\beta$ -difluorotyrosines. 2,3,5-Trifluoro-L-tyrosine synthesized using tyrosine phenol-lyase was incorporated into a peptide substrate for tyrosine protein kinase Csk, and the resultant fluorinated peptide was found to be a good substrate for phosphorylation, suggesting that general base catalysis with early deprotonation is not involved in the reaction mechanism.

Tyrosine is an abundant amino acid in cellular metabolism and in proteins. There has been a continuing interest in the biological and biochemical properties of fluorinated analogues of L-tyrosine. 3-Fluorotyrosine has been incorporated into proteins in place of tyrosine for mechanistic studies (1). The monofluoro analogs, 2-fluoro- and 3-fluorotyrosine, as well as 3,5-difluoro and 2,6-difluorotyrosine, have been prepared by synthetic methods (2,3). In addition, the enzymatic preparation of 2-fluoro-L-tyrosine

0097-6156/96/0639-0095\$15.00/0  
© 1996 American Chemical Society

and 3-fluoro-L-tyrosine from the corresponding fluorophenols and ammonium pyruvate or serine using tyrosine phenol-lyase has been reported (4,5). The enzymatic synthesis is highly stereoselective, resulting in only the biologically active L-isomer even when achiral ammonium pyruvate is used as the source of the amino acid side chain. However, 2,3-difluoro-, 2,5-difluoro-, 2,3,5-trifluoro- and 2,3,6-trifluorotyrosine have not been previously prepared, either synthetically or enzymatically. We have now used tyrosine phenol-lyase to prepare all of the mono-, di-, and trifluoro-L-tyrosines, and we have evaluated the effects of fluorination on the kinetic parameters of the tyrosine phenol-lyase reaction. We have also found that phenol and fluorinated phenols react with  $\beta,\beta,\beta$ -trifluoroalanine in the presence of tyrosine phenol-lyase to form transient  $\beta,\beta$ -difluorotyrosines. In addition, we have prepared a fluorinated peptide analog of a tyrosine protein kinase Csk substrate and determined the effect of fluorination on the phosphorylation reaction. The results of these studies are reported herein.

### Experimental Methods

**Materials.** Tyrosine phenol-lyase (TPL) was purified from *Citrobacter freundii* (ATCC 29063) (6) grown in a tyrosine rich medium, or from *Escherichia coli* SVS370 cells containing pTZTPL, with the *tpl* gene from *C. freundii* (7), as described previously (8). The pyruvic acid and pyridoxal-5'-phosphate were purchased from United States Biochemical Co., 2-mercaptoethanol from Sigma, ammonium acetate from Fisher Scientific Company. 2-Fluorophenol was obtained from Chemical Dynamics Corporation, 2,5-difluorophenol from PCR Incorporated, and all the other fluorinated phenols used were purchased from Aldrich, as was  $\beta,\beta,\beta$ -trifluoro-DL-alanine.

**Synthesis.** All the reactions were performed using 0.1 M ammonium acetate, 50  $\mu$ M pyridoxal-5'-phosphate, 5 mM 2-mercaptoethanol, and 63 mM pyruvic acid (except for the reaction with 2-fluorophenol where the concentration was 50 mM). In order to avoid rapid denaturation of the enzyme due to the phenol, the fluorophenol was added in several portions, starting with an initial concentration of 10 mM. Then, increments of about 5 mM each were added periodically (every time that the reaction appeared to reach equilibrium as determined by HPLC analysis) until the following total concentrations were obtained: 3-fluorophenol, 36 mM; 2-fluorophenol, 40 mM; 2,3-difluorophenol, 35 mM; 2,5-difluorophenol, 33 mM; 3,5-difluorophenol, 27 mM; 2,6-difluorophenol, 34 mM; 2,3,5-trifluorophenol, 24 mM; 2,3,6-trifluorophenol, 24 mM. The amount of pyruvic acid also was added in two portions; the initial concentration was 50 mM, and after all the fluorophenol had been added, an additional 13 mM of pyruvic acid was added. The reaction volumes were: 0.25 L for 2,6-difluorotyrosine, 2,3,5-trifluorotyrosine and 2,3,6-trifluorotyrosine, and 1 L in all other cases. Since the enzyme lost all activity in 4-5 days, and the time of reaction was up to 2 weeks, TPL also was added in several portions, using 25 units/L as the initial concentration, and

adding 5 or 10 units/L after each increment of fluorophenol was added. The total amounts of enzyme used were: 45 units for 2-fluorotyrosine; 60 units for 3-fluorotyrosine; 100 units for 2,3-difluorotyrosine; 125 units for 2,5-difluorotyrosine; 40 units for 2,6-difluorotyrosine; 60 units for 3,5-difluorotyrosine; 40 units for 2,3,5-trifluorotyrosine; and, 30 units for 2,3,6-trifluorotyrosine. The pH of the reaction was maintained between 8 and 8.3, and it always was checked before adding the enzyme. In all cases the reactions were performed at room temperature, which was approximately 25 °C. The progress of the reactions was monitored by HPLC using an instrument from Rainin Instruments, with detection by UV (LDC Spectromonitor 3000) at 220 nm. The components of the reaction mixture were resolved using a 5 micron Econosphere C18 analytical column (Alltech/Applied Science), and using as eluent 25 mM potassium phosphate buffer, pH 5.6. The progress of the reaction was estimated assuming equal values of  $\epsilon$  at 220 nm for the fluorophenol and corresponding fluorotyrosine.

**Purification of fluorotyrosine.** At the end of the reaction, each reaction mixture was loaded onto a Dowex 50W-X8 cation exchange column (2.6 cm x 45 cm for the 1 L reactions, and 2.6 cm x 25 cm for the 0.25 L reactions). Then, 1.5-2 L of water were used to wash the unreacted phenol and the pyruvic acid completely off the column. The fluorotyrosine product was then eluted using 1.5 M aqueous ammonia. The tyrosine containing fractions were identified by reaction with ninhydrin, the solvent was evaporated *in vacuo*, and the resulting solid was crystallized once from a minimum volume of hot H<sub>2</sub>O. Yields calculated on the basis of limiting phenol are reported in Table I. The <sup>1</sup>H and <sup>19</sup>F NMR (300 MHz and 282.2 MHz, respectively, obtained on a Bruker AC-300 spectrometer) spectra of the products were consistent with the expected structures.

**Kinetic studies of fluorotyrosines with tyrosine phenol-lyase.** The assays were performed at 25 °C in a Gilford Response spectrophotometer with a thermoelectric cell holder using a coupled assay with lactate dehydrogenase and NADH, as described previously (7). The concentrations of the fluorotyrosines were varied from approximately 1/2 K<sub>m</sub> to 4 K<sub>m</sub> in the reactions. Kinetic parameters ( $k_{cat}$ ,  $k_{cat}/K_m$ ) were determined by nonlinear fitting using the program, ENZFITTER (Elsevier). Pre-steady state kinetic measurements were performed using a single-wavelength stopped-flow instrument, as described previously (8) or with a rapid-scanning stopped-flow instrument (RSM) from OLIS, Incorporated.

**Structure determination of 2,3,6-trifluoro-L-tyrosine hydrochloride hydrate.** Crystal data: C<sub>9</sub>H<sub>8</sub>N<sub>03</sub>F<sub>3</sub>·HCl·H<sub>2</sub>O, M = 289.64, monoclinic, space group P2<sub>1</sub>, a 6.551(1)Å, b 6.701(2)Å, c 13.795(4)Å,  $\beta$  103.14(2)°, V 589.8(2) Å<sup>3</sup>, Z=2, D<sub>c</sub> = 1.63 g cm<sup>-3</sup>. Of the 1349 unique reflections measured on an Enraf-Nonius CAD4 diffractometer using CuK $\alpha$  radiation, 1274 had I > 3 $\sigma$ (I) and were used for all calculations in the teXsan X-ray analysis package. Most H atomic positions were located from a difference map; others H atomic positions were calculated. Anisotropic refinement of all non-hydrogen atoms gave final R = 0.034, R<sub>w</sub> = 0.045.

## Results and Discussion

**Synthesis of Fluorinated Tyrosines.** Tyrosine phenol-lyase has been used previously to prepare L-tyrosine and L-dopa from ammonium pyruvate and phenol or catechol, respectively, in a single step (10). In addition, 3-fluoro and 2-fluoro-L-tyrosine have been prepared from 2-fluorophenol or 3-fluorophenol, respectively, and ammonium pyruvate using tyrosine phenol-lyase (4,5). However, the preparation of multiply fluorinated tyrosine derivatives using tyrosine phenol-lyase has not been previously reported. In the present study, we found that all of the isomers of difluoro- and trifluoro-L-tyrosine can be prepared from ammonium pyruvate and the difluoro- and trifluorophenols, respectively.

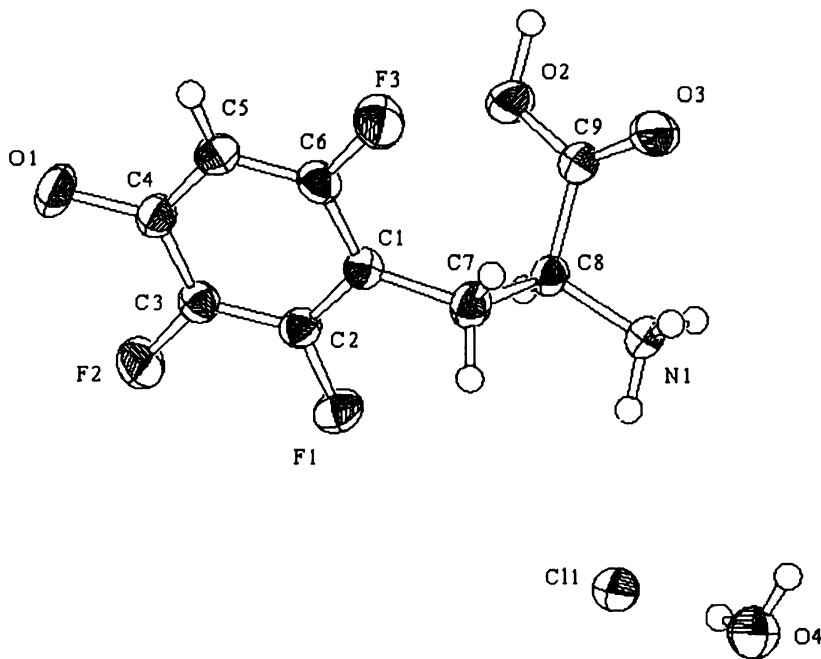
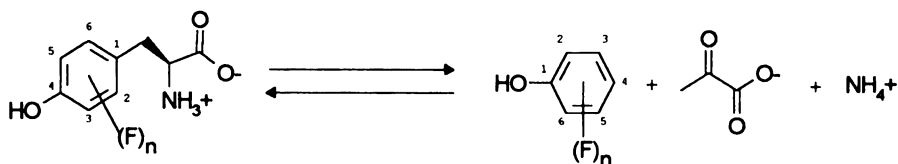


Figure 1. Structure of 2,3,6-trifluoro-L-tyrosine hydrochloride hydrate.



Isolated yields after recrystallization ranged from 0.5 to 2.8 g/L (10–42% based on phenol added (Table I)). In contrast, reaction of 2,3,5,6-tetrafluorophenol under these conditions did not provide more than a trace of 2,3,5,6-tetrafluoro-L-tyrosine, even with greater amounts of enzyme and with extended incubation. It is not clear why there is such a dramatic effect of a fourth fluorine on the synthetic reaction, as both 2,3,5 and 2,3,6-trifluorophenol react readily, though slowly. The electronic effect of a fourth fluorine should be incremental, and would be expected to be no greater than the effect on going from two to three fluorines. Hence, it seems more likely that the low reactivity of 2,3,5,6-tetrafluorophenol is due to steric restriction in the active site. The structure of the hydrochloride salt of 2,3,6-trifluoro-L-tyrosine was determined by x-ray crystallography (Figure 1). The structure clearly shows the presence of the expected fluorine substituents, and there are intermolecular hydrogen bonds between a water molecule and the carboxylic acid, and also with the phenolic hydroxyl of an adjacent tyrosine. The chloride ion is involved in five H-bonding interactions: Cl $\cdots$ O(2) 3.119(3), Cl $\cdots$ O(1) 3.128(3), Cl $\cdots$ O(4) 3.146(3), Cl $\cdots$ O(4') 3.211(3), Cl $\cdots$ N(1) 3.293(3). The ammonium group is H-bonded to three groups other than the chloride ion: N(1) $\cdots$ O(3) 2.826(4), N(1) $\cdots$ O(4'') 2.865(4), N(1) $\cdots$ O(4''') 2.922(4).

Table I

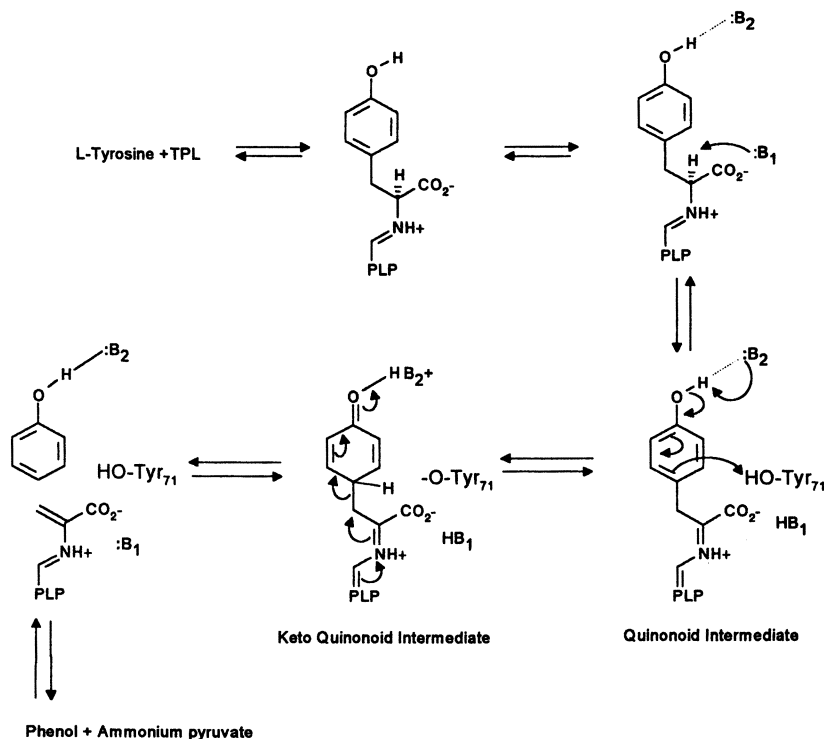
Synthesis and Steady-state Kinetic Parameters of Fluorinated Tyrosines with *C. freundii* Tyrosine Phenol-lyase

Compound	$k_{\text{cat}}$ , s $^{-1}$	$k_{\text{cat}}/K_m$ , M $^{-1}$ s $^{-1}$	Isolated Yield/L, g (%)
Tyrosine	3.5	1.80E+04	-
2-F-Tyrosine	0.4	1.80E+04	2.6 (36)
3-F-Tyrosine	1.4	1.30E+04	2.8 (34)
2,3-diF-Tyrosine	1	1.90E+04	2.5 (33)
2,5-diF-Tyrosine	0.1	6.90E+03	1.3 (18)
3,5-diF-Tyrosine	0.08	7.20E+02	2.0 (27)
2,6-diF-Tyrosine	0.6	2.30E+04	2.5 (42)
2,3,5-triF-Tyrosine	0.05	1.10E+03	0.5 (10)
2,3,6-triF-Tyrosine	0.1	5.10E+02	1.8 (32)

**Reactivity of Fluorinated Tyrosines with Tyrosine Phenol-lyase.** We determined the steady-state kinetic parameters,  $k_{\text{cat}}$  and  $k_{\text{cat}}/K_m$ , for the reactions of all of the fluorinated tyrosines with tyrosine phenol-lyase. These values were determined spectrophotometrically at 340 nm by measurement of the elimination of the fluorinated phenols from the fluorinated tyrosines to form ammonium pyruvate, using a coupled reaction with lactate dehydrogenase and NADH. In contrast, there is no convenient continuous spectrophotometric assay to follow the formation of fluorotyrosines from fluorophenols. As expected, all of the mono-, di- and trifluorinated tyrosines showed activity for  $\beta$ -elimination by tyrosine phenol-lyase. 2-Fluoro, 3-fluoro, 2,3-difluoro and 2,6-difluoro-L-tyrosine exhibit values of the specificity constant,  $k_{\text{cat}}/K_m$  (the apparent second-order rate constant for reaction of enzyme and substrate), comparable to that

for L-tyrosine (Table I). In contrast, 3,5-difluoro and 2,5-difluoro-L-tyrosine and both isomers of trifluorotyrosine exhibited values of  $k_{cat}/K_m$  that are reduced 5-20 fold (Table I). However, there is not a direct correlation between the  $k_{cat}/K_m$  values and the yields obtained in preparative reactions, since the preparative reactions are performed under thermodynamic control. It is interesting that the slowest values of  $k_{cat}$  (apparent first order rate constant for conversion of substrate to product) are seen for 3,5-difluoro and 2,3,5-trifluorotyrosine, which have fluorine substituents in both *ortho* positions flanking the phenol (Table I).

The interaction of these fluorinated tyrosines with tyrosine phenol-lyase was also examined by rapid-scanning stopped-flow spectrophotometry. The mechanism of the  $\beta$ -elimination catalysed by tyrosine phenol-lyase has been proposed by ourselves and others (5,11,12) to involve the formation of a Schiff's base (external aldimine) with the substrate, followed by  $\alpha$ -proton abstraction to form a carbanionic quinonoid intermediate (Scheme I). Subsequent tautomerization and elimination of the phenol gives an  $\alpha$ -aminoacrylate, which undergoes hydrolysis to give ammonium pyruvate. Recently, we demonstrated that Tyrosine-71 is a general acid catalyst for the



Scheme I. Mechanism of tyrosine phenol-lyase.

tautomerization of the phenol of the substrate to give the activated 1,4-cyclohexadienone intermediate (Scheme I). The mutation of Tyr-71 to phenylalanine

resulted in an enzyme with no detectable activity for  $\beta$ -elimination of L-tyrosine, although it retained significant activity with S-alkyl- and S-aryl-L-cysteines and  $\beta$ -chloroalanine (13). Furthermore, the structure of the complex of tyrosine phenol-lyase with 3-(4'-hydroxyphenyl)propionic acid shows that the phenolic OH of Tyr-71 is located 3.1 Å from C1' of the aromatic ring, ideally situated for the proton transfer shown in Scheme II (14). Proton transfer between Tyr-71 and B1, the base which removes the  $\alpha$ -proton, is suggested by the isotope labeling experiments of Faleev et al. (15), who demonstrated that 10% of the deuterium label of  $\alpha$ -[ $^2\text{H}$ ]-L-tyrosine was transferred to C-4 of the phenol product.

The reaction of L-tyrosine with wild-type tyrosine phenol-lyase shows rapid formation (within 100 msec) of a quinonoid intermediate with  $\lambda_{\text{max}}$  at 501 nm and relatively low absorbance (Figure 2). The complexes of 3-fluoro-L-tyrosine and 3,5-difluoro-L-tyrosine with tyrosine phenol-lyase also exhibit absorbance peaks at 501 nm, with significantly higher absorbance than L-tyrosine, indicating greater steady state concentrations of quinonoid intermediates (Phillips, R. S., VonTersch, R. L., and Secundo, F., unpublished observations). The first-order rate constant for quinonoid intermediate formation from 3-fluoro-L-tyrosine is comparable to that of tyrosine ( $k=70 \text{ s}^{-1}$  at 2 mM) (compare progress curves in Figure 2). In contrast, 2-fluoro-L-

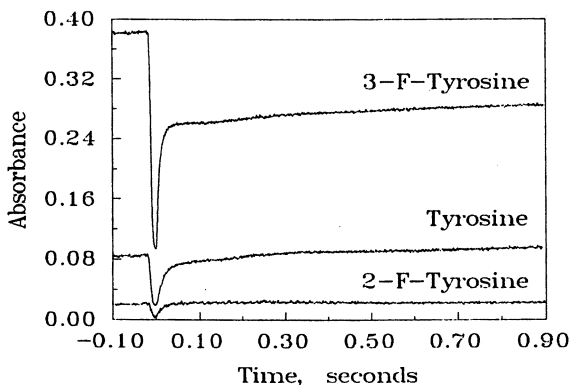
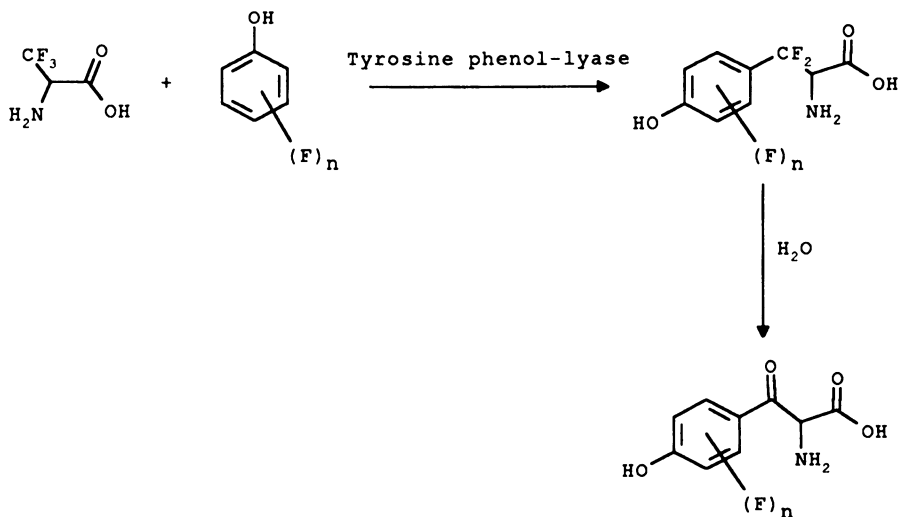


Figure 2. Time courses for the pre-steady state reaction of tyrosine phenol-lyase with tyrosine and fluorinated tyrosines. The absorbance changes at 500 nm were then monitored, and the reaction was started about 100 msec after the start of data acquisition. The concentration of tyrosine phenol-lyase was 20  $\mu\text{M}$ , and the concentrations of substrates were 2 mM for L-tyrosine and 10 mM for the fluorinated tyrosines.

tyrosine, and di- and tri-fluoro-L-tyrosines with fluorine at the 2-position, exhibit complexes with tyrosine phenol-lyase with very weak absorbance peaks at 501 nm (Figure 2), even though the rates of intermediate formation are increased ( $k=120 \text{ s}^{-1}$  for 2,3-difluoro-L-tyrosine at 2 mM). In addition, the complexes of tyrosine phenol-lyase with 2-fluorinated tyrosines exhibit distinct peaks at about 350 nm. Thus, the presence of ring fluorine substituents remote from the site of the chemical transformation has significant effects on the rates and equilibria of intermediate formation in the reaction of tyrosine phenol-lyase. As there is no direct electronic communication between the ring fluorines, which are at least 5  $\sigma$  bonds away, and the  $\alpha$ -CH bond during deprotonation, any effects on this step must be due to steric constraints in the active site. Thus, although it is commonly thought that fluorine substitution will not result in any significant steric effects in analogues, our results suggest that steric effects of fluorine substitution are significant in the reaction of fluorinated tyrosines with tyrosine phenol-lyase.

**Reaction of tyrosine phenol-lyase with  $\beta,\beta,\beta$ -trifluoroalanine and phenols: Formation of  $\beta,\beta$ -difluorotyrosines.**  $\beta,\beta,\beta$ -Trifluoroalanine has been reported to be an irreversible inactivator of several pyridoxal phosphate dependent enzymes, including tryptophan synthase, tryptophan indole-lyase, and  $\gamma$ -cystathionase (16). We have found that indole could protect *E. coli* tryptophan indole-lyase, but not tryptophan synthase, from the inactivating effects of  $\beta,\beta,\beta$ -trifluoroalanine (17). Based on the stimulation of fluoride ion formation in the presence of indole, we suggested that indole reacted with the  $\beta,\beta$ -difluoroacrylate intermediate to form  $\beta,\beta$ -difluorotryptophan, which hydrolysed under the reaction conditions to give  $\beta$ -ketotryptophan and fluoride ion. However, we were not able to obtain direct evidence for the formation of  $\beta,\beta$ -difluorotryptophan.

In the present work, we examined the reaction of tyrosine phenol-lyase with  $\beta,\beta,\beta$ -trifluoroalanine in the absence and in the presence of phenol and fluorinated phenols. As we had observed with *E. coli* tryptophan indole-lyase, a highly homologous enzyme (44% identical residues) (7),  $\beta,\beta,\beta$ -trifluoroalanine is an irreversible inactivator of tyrosine phenol-lyase. In contrast to tryptophan indole-lyase, an absorbance peak at 496 nm forms concomitant with inactivation. Addition of phenol during incubation with  $\beta,\beta,\beta$ -trifluoroalanine not only prevents formation of this 496 nm peak and inactivation of tyrosine phenol-lyase, but also results in the formation of an intense UV absorption band at 310 nm, very similar to that of *p*-hydroxyacetophenone in pH 8 buffer.  $^{19}\text{F}$  NMR spectra of reaction mixtures containing phenol and  $\beta,\beta,\beta$ -trifluoroalanine showed only the formation of fluoride ion in these reactions. However, when fluorinated phenols were incubated with  $\beta,\beta,\beta$ -trifluoroalanine and tyrosine phenol-lyase, new  $^{19}\text{F}$  resonances at about -70 ppm were observed that could be assigned to  $\beta,\beta$ -difluorotyrosines (Scheme II) based on the similarity of the  $^{19}\text{F}$  chemical shift to 1',1'-difluoroethylbenzene, and long range H-F and F-F couplings. Thus, the electron-withdrawing effect of the ring fluorines appears to exert a stabilizing effect on the  $\beta,\beta$ -difluorotyrosines toward hydrolysis, allowing their accumulation and detection.



Scheme II. Reaction of tyrosine phenol-lyase with  $\beta,\beta,\beta$ -trifluoroalanine and fluorinated phenols.

**2,3,5-Trifluorotyrosine as a mechanistic probe in tyrosine protein kinase substrates.** 2,3,5-Trifluoro-L-tyrosine was synthesized enzymatically as described above and used to prepare a peptide substrate analog, EDNE(F3Y)TA, for the tyrosine protein kinase Csk (18). Because of the low  $pK_a$  (6.5) of the phenol of 2,3,5-trifluoro-L-tyrosine in the peptide, this fluorinated peptide was used to probe the role of general base catalysis in the tyrosine kinase reaction. Surprisingly, the fluorinated peptide is a good substrate for tyrosine kinase Csk, with  $k_{cat}$  and  $K_m$  values of  $18 \text{ min}^{-1}$  and  $12 \text{ mM}$ , respectively, not unlike those of the corresponding peptide containing tyrosine,  $14 \text{ min}^{-1}$  and  $6.1 \text{ mM}$ . These results are not consistent with mechanisms involving general base catalysis with early deprotonation, since the trifluorotyrosinate anion would be expected to be as much as  $10^4$ -fold less nucleophilic than the tyrosinate anion. However, the decrease in nucleophilicity could be compensated by the increased concentration of the trifluorophenolate anion if deprotonation of tyrosine occurs late, concomitant with or subsequent to P-O bond formation. Analysis of the effects of viscosity and thionucleotide substitution on the reaction of wild-type and D314E mutant enzymes are consistent with this interpretation.

## Conclusions

Tyrosine phenol-lyase can be used to prepare mono-, di-, and trifluorinated analogs of L-tyrosine in a single step from the corresponding fluorinated phenols and ammonium pyruvate in moderate yield. These fluorinated tyrosines are useful mechanistic probes of the reactions of enzymes which react with tyrosine, including tyrosine phenol-lyase

and tyrosine protein kinase Csk. Reaction of tyrosine phenol-lyase with phenols and  $\beta,\beta,\beta$ -trifluoroalanine produced  $\beta,\beta$ -difluorotyrosines as transient intermediates.

### Acknowledgements

This work was partially supported by a grant from the National Institutes of Health (GM42588) to RSP.

### References

1. Brooks, B.; Benisek, W. F. *Biochemistry* **1994**, *33*, 2682.
2. Kirk, K. L. *J. Org. Chem.* **1980**, *45*, 2015..
3. Pascal, R. A., Jr.; Chen, Y.-C. J. *J. Org. Chem.* **1985**, *50*, 408.
4. Phillips, R. S.; Fletcher, J. G.; Von Tersch, R. L.; Kirk, K. L. *Arch. Biochem. Biophys.* **1990**, *276*, 65.
5. Nagasawa, T.; Utagawa, T.; Goto, J.; Kim, C.-J.; Tani, Y.; Kumagai, H.; Yamada, H. *Eur. J. Biochem.* **1981**, *117*, 33.
6. Carman, G. M.; Levin, R. E. *Appl. Envir. Microbiol.* **1977**, *33*, 192.
7. Antson, A. A.; Demidkina, T. V.; Gollnick, P.; Dauter, Z.; Von Tersch, R. L.; Long, J.; Berezhnoy, S. N.; Phillips, R. S.; Harutyunyan, E. H.; Wilson, K. S. *Biochemistry* **1993**, *32*, 4195.
8. Chen, H.; Gollnick, P.; Phillips, R. S. *Eur. J. Biochem.* **1995**, *229*, 540.
9. Phillips, R. S. *Biochemistry* **1991**, *30*, 5927.
10. Enei, H.; Nakazawa, H.; Okumura, S.; Yamada, H. *Agr. Biol. Chem.* **1973**, *37*, 725.
11. Faleev, N. G.; Ruvinov, S. B.; Demidkina, T. V.; Myagkikh, I. V.; Gololobov, M. Y.; Bakhmutov, V. I.; Belikov, V. M. *Eur. J. Biochem.* **1988**, *177*, 395.
12. Chen, H.; Phillips, R. S. *Biochemistry* **1993**, *32*, 11591.
13. Chen, H. Y.; Demidkina, T. V.; Phillips, R. S. *Biochemistry* **1995**, *34*, 12276.
14. Antson, A. A.; Dodson, G. G.; Wilson, K. S.; Pletnev, S. V.; Harutyunyan, E. G., and Demidkina, T. V., In *Biochemistry of Vitamin B6 and PQQ*; Marino, G., Sannia, G., and Bossa, F., Eds.; Birkhauser Verlag Basel/Switzerland, 1994; pp 187-191.
15. Faleev, N. G.; Lyubarev, A. E.; Martinkova, N. S.; Belikov, V. M. *Enzyme Microb. Technol.* **1983**, *5*, 219-224.
16. Silverman, R. B.; Abeles, R. H. *Biochemistry*, **1976**, *15*, 4718.
17. Phillips, R. S.; Dua, R. K. *Arch. Biochem. Biophys.* **1992**, *296*, 489.
18. Cole, P. A.; Grace, M. R.; Phillips, R. S.; Burn, P.; Walsh, C. T. *J. Biol. Chem.* **1995**, *270*, 22105.

## Chapter 8

# Efficient Synthetic Routes to Chiral 6-Deoxy-6,6,6-trifluorosugars via Intramolecular 1,2-*O,O*-Silyl Migration

Takashi Yamazaki, Kenji Mizutani, and Tomoya Kitazume<sup>1</sup>

Department of Bioengineering, Tokyo Institute of Technology,  
4259 Nagatsuta-cho, Midori-ku, Yokohama 226, Japan

Novel and efficient routes to access a variety of chiral 6-deoxy-6,6,6-trifluorosugars by way of enzymatic optical resolution as well as 1,2-*O,O*-silyl migration as key steps are described in detail. MOPAC AM1 calculation of the latter process suggests the ready migration so as to furnish the thermodynamically more stable alkoxide close to a trifluoromethyl group.

It is well documented that, in sharp contrast to readily accessible mono- or difluorinated compounds by the conventional fluorination pathways towards the corresponding alcohols (1-3) or carbonyls (4), respectively, trifluoromethyl (CF<sub>3</sub>)-containing molecules are much more difficult to obtain, especially in optically active forms, by way of similar processes (5-9). Moreover, although a variety of procedures have been developed for the introduction of this group (12-18), there still remain such problems to be solved as the handling and availability of reagents, or selectivity (stereo-, regio-, and/or chemo-) of products. As an alternative route for obtaining trifluoromethylated compounds, we have been studying the preparation of chiral building units possessing this moiety as well as readily distinguishable plural functionalities (19-23), which permitted us to construct the desired CF<sub>3</sub>-containing units with a high degree of stereoselectivity.

Building blocks thus prepared are usually employed as the key units of fluorinated analogs of appropriate natural products or synthetic biologically active materials (24-26). Among such useful compounds, fluorinated carbohydrates constitute one of the most interesting fields where intensive study has been still going on (27,28). Various types of mono- or difluorinated sugars have been synthesized thus far via the above discussed fluorination technique, but the corresponding trifluorinated analogs are very rare (29-32). As briefly mentioned above, this might be mainly due to the requirement for harmful reagents (like SF<sub>4</sub> or HF) under vigorous reaction conditions or the use of special and/or expensive substances sometimes not easily available. These problems as well as the interest in the 6-deoxysugars as the relatively common components of naturally occurring antibiotics

<sup>1</sup>Corresponding author

0097-6156/96/0639-0105\$15.00/0  
© 1996 American Chemical Society

led us to start this study on the preparation of a variety of 6-deoxy-6,6,6-trifluoro-sugars using enzymatically resolved building blocks (33-38). In this article is described our recent progress on this subject in detail.

### 1,2-*O*,*O*-Silyl Migration

The authors first selected 6,6,6-trifluorinated rhodnose and amicitose as target compounds because their simple structures made them suitable to start with (Figure 1). Our synthetic plan to access these sugars was to employ silylated furanols with a

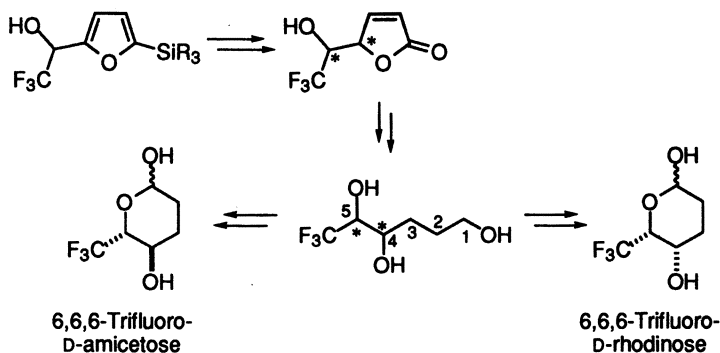
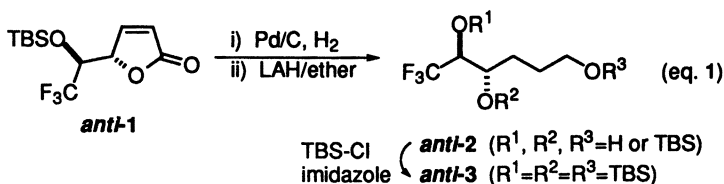


Figure 1. Possible Reaction Schemes

trifluoromethyl moiety, which, after optical resolution by lipase, would be converted into the corresponding butenolide by the previously reported oxidation pathway (39). Ring opening of this butenolide might lead to the formation of the triol, and, considering that the terminal primary hydroxyl group can be selectively protected with such protective groups as *tert*-butyl-dimethylsilyl (TBS) or trityl groups, discrimination of the other two hydroxyl functionalities at 4 and 5 positions was the problem to be solved.

During the course of determination of the stereochemistry of *anti*-1, when this compound was hydrogenated and reduced to the corresponding diol at 0 °C, we noticed that the product obtained was unexpectedly an inseparable mixture instead of pure *anti*-2a ( $R^1$ =TBS,  $R^2$ = $R^3$ =H). However, trisilylated ether was eventually isolated as the only product (84% total yield) after the routine silylation procedure (eq. 1). Thus, the above mixture was concluded to be a mixture of several forms of *anti*-2. This phenomenon was interpreted as the migration of a TBS group (at least in part) from the original 5 position to either the 1 or 4 positions during the LAH reduction step, which might be reasonably explained as the result of the





formation of thermodynamically more favorable alkoxide stabilized by an *inductively* electron-withdrawing CF<sub>3</sub> group. If this was really the case, control of the reduction step after hydrogenation of *anti-1* would be considered the crucial step for the completion of the syntheses of our targets. Thus, partial reduction of the butyrolactone from *anti-1* would yield the lactol *anti-4*, which, on treatment with an appropriate base, would be transformed into the corresponding alkoxide form. The resultant anionic species would be in equilibrium with the corresponding acyclic alkoxide by analogy with well-established sugar chemistry, and if the above migration reaction was operative at this step, construction of pyranose *anti-5* would be completed after recyclization and quenching processes (Figure 2).

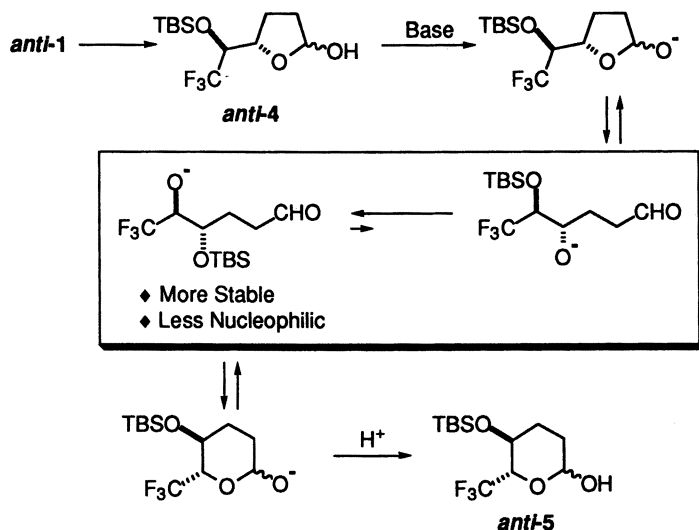


Figure 2. Transformation of Furanose into Pyranose

Prior to starting our project, MOPAC AM1 semiempirical calculations (40,41) were carried out to obtain quantum chemical information on two acyclic model alkoxides derived from 1,1,1-trifluoro-2,3-butanediol possessing both *anti* and *syn* relative stereochemistries (Figure 3). This type of silyl group migration was already reported by a couple of research groups (42-45). However their previous examples proceeded to yield the more substituted alkoxide: in other words, a silyl group migrates to a less hindered site and liberation from the steric congestion is considered to be the important driving force of this reaction. On the other hand, to the best of our knowledge, no example has appeared in the literature of the molecules containing an atom or a group with a strong electronic effect (46).

The result unambiguously demonstrated the energetic preference of the alkoxide close to a CF<sub>3</sub> group to the other by 10.6 kcal/mol for the *anti* isomer and 12.9 kcal/mol for the *syn* isomer, respectively (the Gibbs' free energy values at -78 °C were used). In both cases, the most stable conformers were computationally proved to be the 5-membered intermediates with the pentavalent silicon atom, *anti*- and *syn*-b, and both of them showed the tendency for the O<sup>b</sup>-Si bond to be stronger than the O<sup>a</sup>-Si bond (Figure 3). It was apparent that this difference did not stem from their inherent bond characteristics because the O-Si bond properties of a and c of

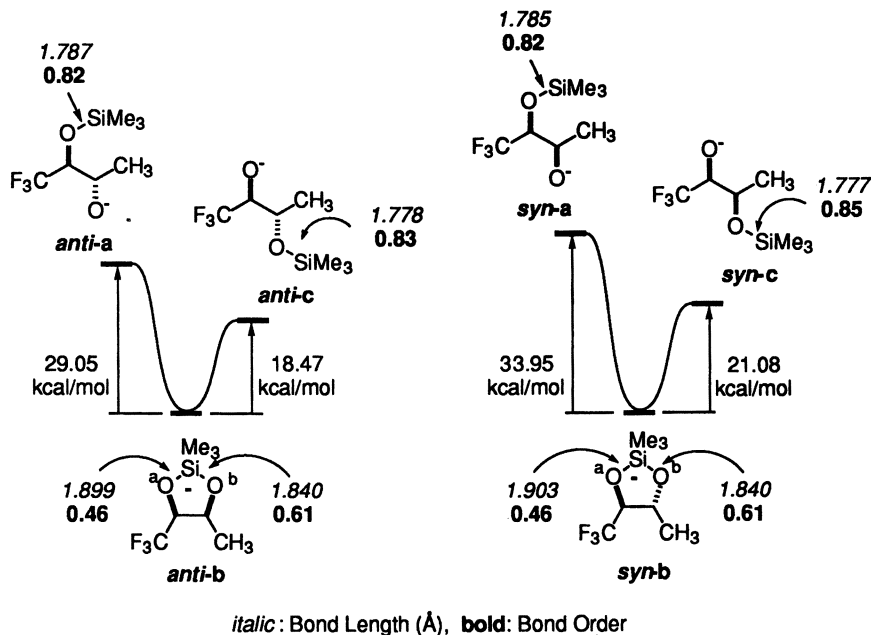


Figure 3. Energy Profile for the 1,2-O,O-Silyl Migration

both diastereomers were much closer than the one of the **b** series. Thus, from the standpoint of the energetic preference as well as the bond strengths, conformers **c** with both *anti* and *syn* stereochemical relationship would be expected to be preferred to the corresponding regioisomers **a**. These calculation results, clearly supporting our hypothesis, prompted us to start the experiments.

### Preparation of 6-Deoxy-6,6,6-trifluorosugars via *Syn*- and *Anti*-1

The key materials, chiral butenolides *anti*- and *syn*-1, were conveniently prepared as shown in Figure 4 via the peracid oxidation (39) of the lipase-resolved optically active furanol (*S*)-6 (38). Although this procedure furnished only a diastereorandom mixture of 1, it was demonstrated that epimerization at the 4 position was possible by treatment with LDA, followed by quenching with AcOH at -78 °C to change the isomeric composition to 3:1 in favor of the *anti* isomer (Figure 4). The butenolides obtained, after separation by simple silica gel column chromatography, were subjected to hydrogenation, followed by DIBALH reduction to afford lactols *anti*- and *syn*-4. Independent treatment of both diastereomeric furanoses with a stoichiometric amount of KOBu<sup>*t*</sup> in THF at -78 °C brought about the smooth conversion into the desired pyranoses in almost quantitative yields (38). As described in eq. 1, usage of LAH instead of DIBALH at this stage led to partial 1,2-O,O-silyl migration, which proved the importance of the choice of reducing reagent (47). Mulzer and coworker (42) have also observed the reagent dependence of the silyl migration as shown in eq. 2, which described two examples affording the completely opposite results (TBSPS: *tert*-butyldiphenylsilyl).

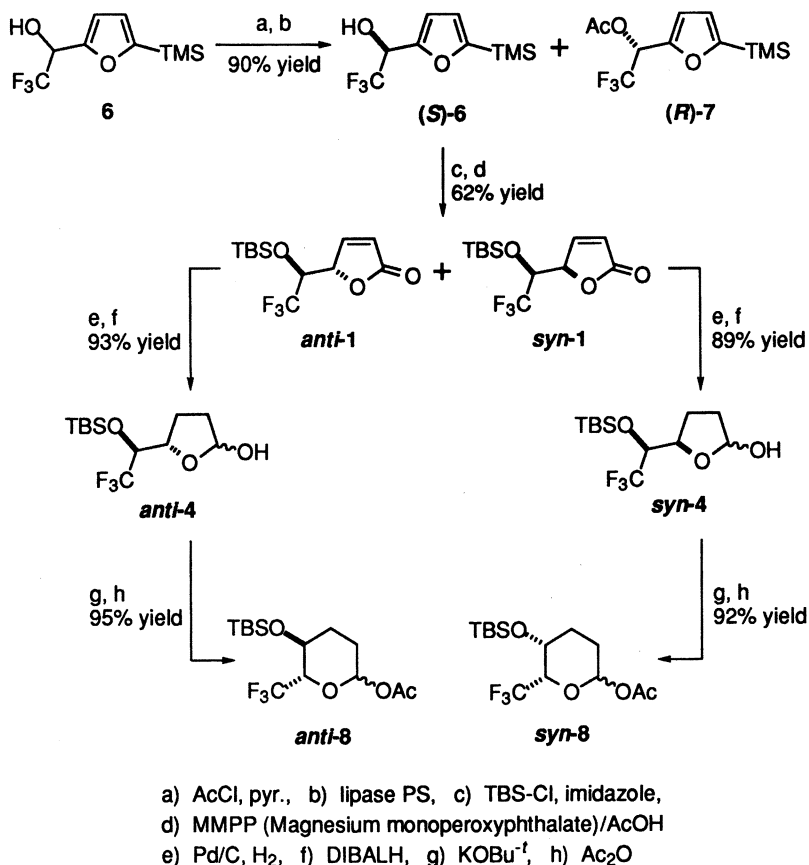
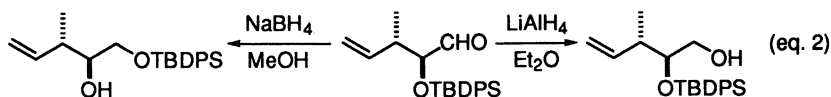


Figure 4. Preparation of 6,6,6-Trifluoro Analogs of *D*-Amictose and *D*-Rhodinose

Application of the present 1,2-*O,O*-silyl migration strategy has led to great success in decreasing the number of the reaction steps by avoiding the troublesome protection-deprotection processes. The authors further utilized this pathway for the synthesis of the similar 6-deoxy-6,6,6-trifluorosugars.

Silylated butenolide, *anti*-1, was diastereoselectively converted to the vicinal diol with potassium permanganate in the presence of a catalytic amount of 18-crown-6 (48), which, after protection of the resultant two hydroxyl moieties as an acetonide, was further treated with DIBALH and KOBu<sup>t</sup> to furnish the pyranose *anti*-10



(Figure 5). On the other hand, the opposite order of 1,2-*O*-silyl migration and oxidation enabled the formation of the epimeric sugars both at the 2 and 3 positions (37). Although we were able to synthesize the desired sugars in a highly diastereoselective fashion as above, these examples have unfortunately led to lower isolated yields (46% recovery of *anti*-9 at the oxidation step; for the synthesis of *anti*-11, 33% recovery of the 5-membered lactol from *anti*-1 at the silyl migration step), which might be understood by such additional structural constraints as the 1,3-dioxolane ring (for *anti*-9) or the *Z*-olefinic bond (for *anti*-11). In the cases of the corresponding *syn* series, the situation became less favorable. The formation of *syn*-10 was not observed possibly due to the congested stereostructure of the product with *syn* alignment of the all substituents, and *syn*-11 was obtained only in 23% yield after *in situ* acetylation without recovery of the starting substrate *syn*-4 because this compound, also acetylated during the reaction, underwent the elimination of AcOH at the purification step (36). Although cyclic structures are sometimes very convenient and effective for controlling the stereoselectivity as shown in the oxidation in Figure 5, it might work in an opposite sense during our key steps, the ring opening  $\rightarrow$  1,2-*O*,*O*-silyl migration  $\rightarrow$  ring closure process. Therefore, it was decided to investigate different systems, especially those possessing the more flexible acyclic structures.

#### Preparation of 6-Deoxy-6,6,6-trifluorosugars via (*S*)-14

The next route we developed was that via the terminally-trifluoromethylated propargylic alcohol (*S*)-14. The ready preparation of this key compound was

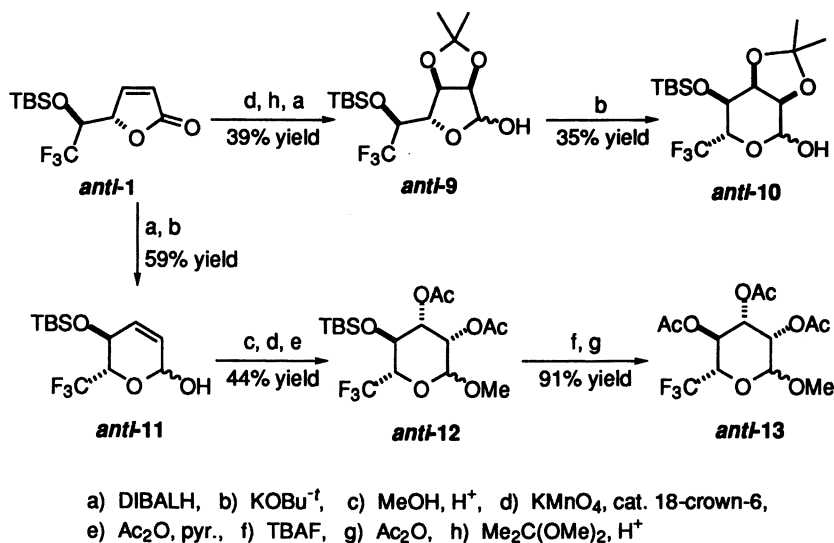
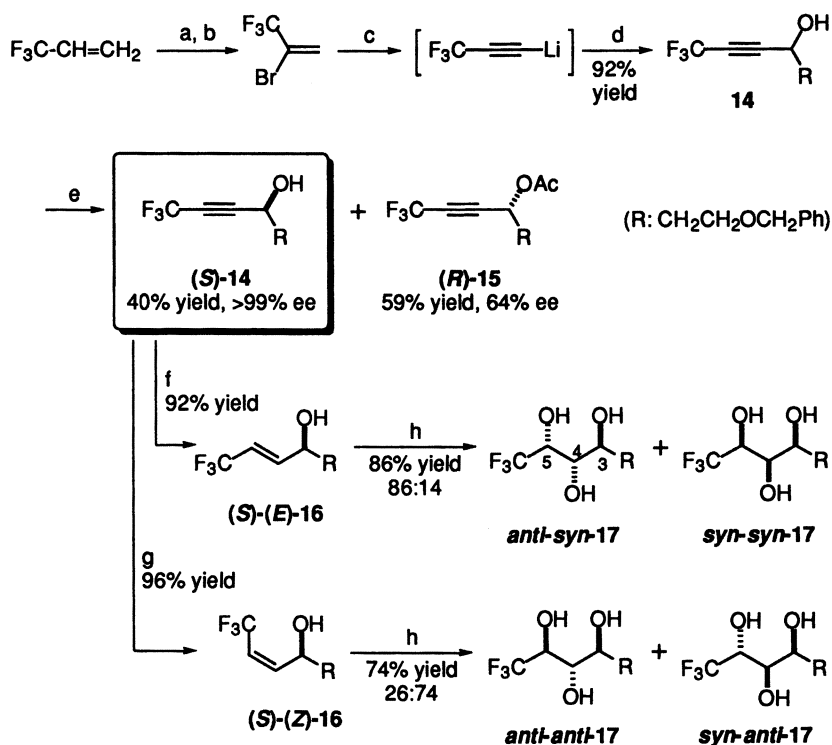


Figure 5. Preparation of 6,6,6-Trifluoro Analogs of D-Rhamnose and 6-Deoxy-D-allose

anticipated by condensation of *in situ* generated 3,3,3-trifluoropropynyllithium with 3-benzyloxypropionaldehyde by our recently reported method (33). This might be further converted to the triols **17** in a diastereoselective fashion by the osmium-catalyzed oxidation of **16**, whose stereoisomers, in turn, are easily accessible by well-established methods with a high degree of stereoselectivity, would lead to the preferential formation of diastereomeric **17**.

As expected, propargylic alcohol **14** was found to be very smoothly prepared even at  $-78\text{ }^{\circ}\text{C}$  and was obtained in high isolated yield (Figure 6). The value of this procedure was apparent when compared with the traditional method utilizing commercially available but very expensive and gaseous 3,3,3-trifluoro-propyne (49). Our starting material, oily 2-bromo-3,3,3-trifluoropropene, could be purchased and even readily prepared in high yield from the industrial raw material, 3,3,3-trifluoropropene (50). The propargylic alcohol **14** obtained was transformed into the corresponding *E*- and *Z*-allylic alcohols after successful enzymatic optical resolution (34).  $\text{OsO}_4$ -catalyzed oxidation (51-57) eventually led to the formation of the desired triols **17** in a diastereoselective manner. Kishi and his coworkers have previously



- a)  $\text{Br}_2$ , b)  $\text{NaOH/EtOH}$ , c)  $\text{LDA}$  (2 equiv), d)  $\text{RCHO}$ ,  
 e) Lipase QL, vinyl acetate/hexane, f) Red-Al, g) Lindlar cat.,  $\text{H}_2$  h) cat.  $\text{OsO}_4$ , NMO

Figure 6. Stereoselective Synthesis of Trifluorinated Triols

pointed out (54) the general *anti* selective oxidation course between the preexisting hydroxyl moiety at the allylic position and the introduced OH group (thus, between 3 and 4 positions of *anti-syn-17* in Figure 6 (58)), irrespective of the *E, Z* stereochemistries of the starting allylic alcohol derivatives. To the best of our knowledge, there have been reported very few examples affording the unexpected *syn* selectivity (59-64), whose substrates usually possessed the same structural feature,  $\alpha, \beta$ -unsaturated carbonyl with *Z* stereochemistry (65-69). Our  $\text{OsO}_4$ -catalyzed oxidation from *Z* substrate added the new exceptional entry to lead to the *syn* selective diol formation.

At this stage, **17** contained three hydroxyl groups at the 3, 4, and 5 positions with one benzyl group ( $X=\text{Bn}$ ) at the terminus (see the drawing on the right), and the above discussion allowed us to expect the OH functionality at the 5 position to be the least nucleophilic and the most stable of the three as its anionic form. These electrostatic properties would allow the regioselective protection of hydroxyl moieties at 3 and 4 positions while leaving the other unprotected. Furthermore, the subsequent deprotection at the terminal would afford a 1,5-diol and the same idea might lead to the conclusion that the hydroxyl group at 1 position would be much more readily oxidized than the one at the 5 position. If this was the case, the syntheses of our final products would be possible via a very short reaction course by eliminating the tedious protection-deprotection processes.

As shown in Figure 7, when *anti-syn-17* was subjected to the usual acetonide formation condition, the corresponding 5- and 6-membered acetonides,

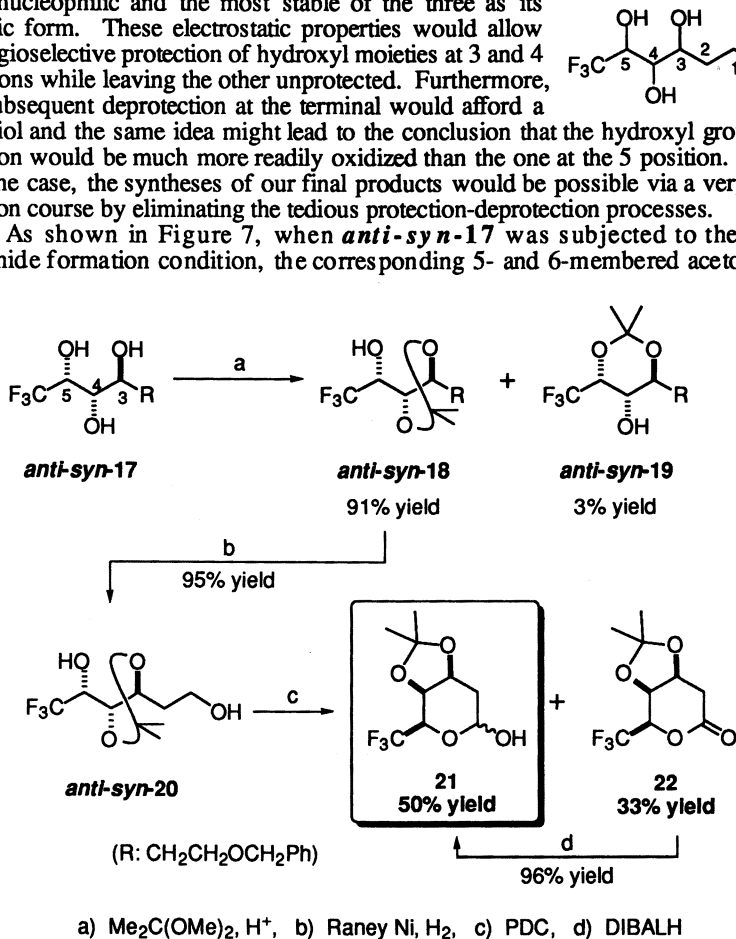


Figure 7. Preparation of 6,6,6-Trifluoro-L-oliiose

*anti-syn-18* and *anti-syn-19*, respectively, were obtained in a ratio of 91:3 in spite of the steric congestion in the major product by the *syn* relationship of the two substituents, which would be a clear reflection of the above hypothesis (Figure 7). *Anti-syn-18*, after separation by column chromatography, was deprotected and oxidized with an excess amount of PDC to be converted into a mixture of **21** and **22** and the latter was readily transformed into the corresponding lactol **21** in high yield (34). At this stage, it was noteworthy that no isomeric product based on the oxidation of an OH group at 5 position was formed. On the other hand, the authors were confronted with the difficulty which called for the alternative route to access the targets because of the failure to utilize the same strategy for the diastereomeric *syn-syn-17* due to the *anti* relationship of the substituents required for pyranose ring formation (Figure 8). Then, taking the electrostatic consideration and the above

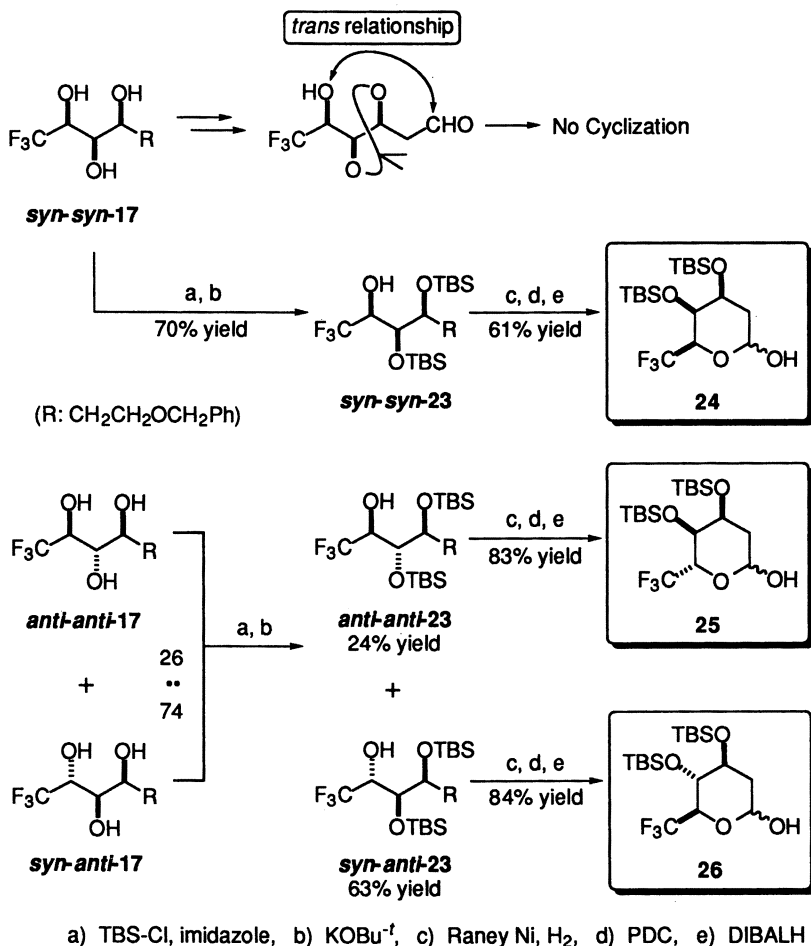


Figure 8. Preparation of Other 6,6,6-Trifluorinated Analogs

experience into account, the protective group was changed to a TBS group. In contrast to our expectation, reaction of *syn-syn-17* with 3 equiv of TBS chloride did not lead to complete conversion (22% of monosilylethers was produced at the same time) nor regioselection for the synthesis of bisilylethers, while the latter problem was solved by the subjection of this mixture to the previous 1,2-*O,O*-silyl migration condition, affecting the smooth and perfect conversion to the thermodynamically more favorable *syn-syn-23*. Transformation of this product to the 6,6,6-trifluoro-D-boivnose was successfully carried out in a similar way (13% recovery of *syn-syn-23* at the deprotection step) and the target material was obtained in 61% yield for these three steps. In spite of the inseparable nature of *anti-anti*- and *syn-anti-17*, ready separation after the silylation-silyl migration procedure to the corresponding bisilylethers *anti-anti*- and *syn-anti-23* realized the construction of 6,6,6-trifluoro-D-digitoxose and L-olivose, respectively.

## Conclusion

As described above, the authors have succeeded in developing two novel path-ways to access 6-deoxy-6,6,6-trifluorosugars in a highly efficient manner via enzymatic kinetic resolution and 1,2-*O,O*-silyl migration as key steps. Employment of enzymes opens an easy route to obtain the both stereoisomers, which is of course highly important from the pharmaceutical point of view. Noteworthy is the silyl migration process (70), which allowed us to take an effective shortcut to the targets. In particular the final product discussed in the latter section was furnished within only 10 steps from the very first starting material in more than 20% total yield. In the former example via the chiral butenolides, although the pathways became longer, the interesting application of the obtained sugar derivatives as the chiral part of the ferroelectric liquid crystals with very high potency has already been disclosed (71-73).

## Acknowledgment

The authors gratefully acknowledge F-TECH, INC., Japan, for their generous gift of 2-bromo-3,3,3-trifluoropropene.

## Literature Cited

- 1) Wilkinson, J. A. *Chem. Rev.* **1992**, *92*, 505.
- 2) Boswell, Jr., G. A.; Ripka, W. C.; Scribner, R. M.; Tullock, C. W. *Org. React.* **1974**, *21*, 1.
- 3) Sharts, C. M.; Sheppard, W. A. *Org. React.* **1974**, *21*, 125.
- 4) Hudlicky, M. *Org. React.* **1988**, *35*, 513.
- 5) Wang, C.-L. J. *Org. React.* **1985**, *34*, 319.
- 6) Kuroboshi, M.; Hiyama, T. *Chem. Lett.* **1992**, 827.
- 7) Matthews, D. P.; Whitten, J. P.; McCarthy, J. R. *Tetrahedron Lett.* **1986**, *27*, 4861.
- 8) Zupan, M.; Bregar, Z. *Tetrahedron Lett.* **1990**, *31*, 3357.
- 9) There have been reported very few examples for the conversion of carboxylic acids into the corresponding CF<sub>3</sub> derivatives with almost complete retention of configuration as well as high chemoselectivity. See, the references 10 and 11.
- 10) Shustov, G. V.; Denisenko, S. N.; Chervin, I. I.; Kostyanovskii, R. G. *Bull. Acad. Sci. USSR Div. Chem. Sci.* **1988**, *37*, 1422.



- 11) Peters, H. M.; Feigl, D. M.; Mosher, H. S. *J. Org. Chem.* **1968**, *33*, 4245.
- 12) Iseki, K.; Nagai, T.; Kobayashi, Y. *Tetrahedron Lett.* **1994**, *35*, 3137.
- 13) Iseki, K.; Nagai, T.; Kobayashi, Y. *Tetrahedron Lett.* **1993**, *34*, 2169.
- 14) Urata, H.; Fuchikami, T. *Tetrahedron Lett.* **1991**, *32*, 91.
- 15) Krishnamurti, R.; Bellew, D. R.; Prakash, G. S. K. *J. Org. Chem.* **1991**, *56*, 984.
- 16) Umemoto, T.; Fukami, S.; Tomizawa, G.; Harasawa, K.; Kawada, K.; Tomita, K. *J. Am. Chem. Soc.* **1990**, *112*, 8563.
- 17) Kitazume, T.; Ishikawa, N. *J. Am. Chem. Soc.* **1985**, *109*, 5186.
- 18) Kobayashi, Y.; Yamamoto, K.; Kumadaki, I. *Tetrahedron Lett.* **1979**, *20*, 4071.
- 19) Shinohara, N.; Haga, J.; Yamazaki, T.; Kitazume, T.; Nakamura, S. *J. Org. Chem.* **1995**, *60*, 4363.
- 20) Yamazaki, T.; Hiraoka, S.; Kitazume, T. *J. Org. Chem.* **1994**, *59*, 5100.
- 21) Yamazaki, T.; Iwatsubo, H.; Kitazume, T. *Tetrahedron: Asym.* **1994**, *5*, 1823.
- 22) Yamazaki, T.; Haga, J.; Kitazume, T. *BioMed. Chem. Lett.* **1991**, *1*, 271.
- 23) Yamazaki, T.; Haga, J.; Kitazume, T. *Chem. Lett.* **1991**, 2175.
- 24) Resnati, G. *Tetrahedron*, **1993**, *42*, 9385.
- 25) Welch, J. T.; Eswarakrishnan, S. *Fluorine in Bioorganic Chemistry*, John Wiley & Sons: New York, 1991.
- 26) Welch, J. T. *Tetrahedron* **1987**, *43*, 3123.
- 27) Tsuchiya, T. *Adv. Carbohydr. Chem. Biochem.* **1990**, *48*, 91.
- 28) *Fluorinated Carbohydrates. Chemical and Biochemical Aspects*, Taylor, N. F., Ed.; ACS symposium Series No. 374; ACS: Washington, D. C., 1988.
- 29) Munier, P.; Krusinski, A.; Picq, D.; Anker, D. *Tetrahedron* **1995**, *51*, 1229.
- 30) Bansal, R. C.; Dean, B.; Hakomori, S.; Toyokuni, T. *J. Chem. Soc., Chem. Commun.* **1991**, 796.
- 31) Hanzawa, Y.; Uda, J.; Kobayashi, Y.; Ishido, Y.; Taguchi, T.; Shiro, M. *Chem. Pharm. Bull.* **1991**, *39*, 2459.
- 32) Differding, E.; Frick, W.; Lang, R. W.; Martin, P.; Schmit, C.; Veenstra, S.; Greuter, H. *Bull. Soc. Chim. Belg.* **1990**, *99*, 647.
- 33) Yamazaki, T.; Mizutani, K.; Kitazume, T. *J. Org. Chem.* **1995**, *60*, 6046.
- 34) Mizutani, K.; Yamazaki, T.; Kitazume, T. *J. Chem. Soc., Chem. Commun.* **1995**, 51.
- 35) Yamazaki, T.; Mizutani, K.; Kitazume, T. *J. Synth. Org. Chem. Jpn.* **1994**, *52*, 734.
- 36) Yamazaki, T.; Mizutani, K.; Kitazume, T. *J. Org. Chem.* **1993**, *58*, 4346.
- 37) Yamazaki, T.; Mizutani, K.; Kitazume, T. *Tetrahedron: Asym.* **1993**, *4*, 1059.
- 38) Yamazaki, T.; Mizutani, K.; Takeda, M.; Kitazume, T. *J. Chem. Soc., Chem. Commun.* **1992**, 55.
- 39) Kuwajima, I.; Urabe, H. *Tetrahedron Lett.* **1981**, *22*, 5191.
- 40) Calculations were performed by MOPAC v 6.10 (AM1) implemented in CAChe Worksystem (SONY/Tektronix Corporation) for the conformers obtained from the rigid search method followed by the optimization by the eigenvector following minimization (EF) method with the extra keyword "PRECISE", final gradient norm being less than 0.01 kcal/Å.
- 41) AM1 was selected because this Hamiltonian furnished the closest carbon-carbon bond length of 2,2,2-trifluoroethoxide, CF<sub>3</sub>CH<sub>2</sub>O<sup>-</sup> (MNDO: 1.735 Å, AM1: 1.654 Å, PM3: 1.918 Å), to the one obtained by *ab initio* calculations (HF/3-21G: 1.523 Å, HF/6-31G\*: 1.529 Å, MP2/6-31G\*: 1.529 Å). MOPAC, in the calculation of this alkoxide, tends to give longer and shorter

- bond lengths for C-C and C-O with the difference of 0.13~0.39 Å and 0.04~0.06 Å, respectively.
- 42) Mulzer, J.; Schölnhorn, B. *Angew. Chem. Int. Ed. Engl.* **1990**, *29*, 431.
  - 43) Peters, U.; Bankova, W.; Welzel, P. *Tetrahedron* **1987**, *43*, 3803.
  - 44) Jurczak, J.; Pikul, S.; Ankner, K. *Pol. J. Chem.* **1987**, *61*, 767.
  - 45) Jones, S. S.; Reese, C. B. *J. Chem. Soc. PerkinTrans. 1* **1979**, 2762.
  - 46) Very recently, Percy and his coworkers have reported the similar type of 1,2-migration of a carbamoyl group. Howarth, J. A.; Owton, W. M.; Percy, J. *M. J. Chem. Soc., Chem. Commun.* **1995**, 757.
  - 47) Reaction temperature would also be the important factor because, as shown in the text, LAH reduction was conducted at 0 °C, while the mixture was cooled to -78 °C for DIBALH reduction.
  - 48) Mukaiyama, T.; Tabusa, F.; Suzuki, K. *Chem. Lett.* **1983**, 173.
  - 49) Previously, the similar type of compounds were synthesized in a isolated yield range of 70 to 80%. See, Hanzawa, Y.; Kawagoe, K.; Tanahashi, N.; Kobayashi, Y. *Tetrahedron Lett.* **1984**, *25*, 4749.
  - 50) Henne, A. L.; Nager, M. *J. Am. Chem. Soc.* **1952**, *74*, 650.
  - 51) Cha, J. K.; Kim, N.-S. *Chem. Rev.* **1995**, *95*, 1761.
  - 52) Houk, K. N.; Duh, H.-Y.; Wu, Y.-D.; Moses, S. R. *J. Am. Chem. Soc.* **1986**, *108*, 2754.
  - 53) Vedejs, E.; McClure, C. K. *J. Am. Chem. Soc.* **1986**, *108*, 1094.
  - 54) Cha, J. K.; Christ, W. J.; Kishi, Y. *Tetrahedron* **1984**, *40*, 2247.
  - 55) Schröder, M. *Chem. Rev.* **1980**, *80*, 187.
  - 56) Ray, R.; Matteson, D. S. *Tetrahedron Lett.* **1980**, *21*, 449.
  - 57) VanRheenen, V.; Kelley, R. C.; Cha, D. Y. *Tetrahedron Lett.* **1976**, 1973.
  - 58) Sugar numbering system was used.
  - 59) DeNinno, M. P.; Danishefsky, S. J.; Schulte, G. *J. Am. Chem. Soc.* **1988**, *110*, 3925.
  - 60) Brimacombe, J. S.; Kabir, A. K. M. S. *Carbohydr. Res.* **1986**, *150*, 35.
  - 61) Brimacombe, J. S.; Hanna, R.; Kabir, A. K. M. S.; Bennett, F.; Taylor, I. D. *J. Chem. Soc. PerkinTrans. 1* **1986**, 815.
  - 62) Brimacombe, J. S.; Hanna, R.; Bennett, F. *Carbohydr. Res.* **1985**, *135*, c17.
  - 63) Stork, G.; Kahn, M. *Tetrahedron Lett.* **1983**, *24*, 3951.
  - 64) Fujioka, H.; Christ, W. J.; Cha, J. K.; Leder, J.; Kishi, Y.; Uemura, D.; Hirata, Y. *J. Am. Chem. Soc.* **1982**, *104*, 7367.
  - 65) OLeary, D. J.; Kishi, Y. *J. Org. Chem.* **1993**, *58*, 304.
  - 66) Garner, P.; Park, J. M. *J. Org. Chem.* **1990**, *55*, 3772.
  - 67) Barnes, J. C.; Brimacombe, J. S.; McDonald, G. *J. Chem. Soc. Perkin Trans. 1* **1989**, 1483.
  - 68) Bernardi, A.; Cardani, S.; Scolastico, C.; Villa, R. *Tetrahedron* **1988**, *44*, 491.
  - 69) Danishefsky, S. J.; DeNinno, M. P.; Phillips, G. B.; Zelle, R. E.; Lartey, P. A. *Tetrahedron* **1986**, *42*, 2809.
  - 70) Yamazaki, T.; Oniki, T.; Kitazume, T. unpublished data. The details will be published elsewhere.
  - 71) Itoh, K.; Takeda, M.; Namekawa, M.; Nayuki, S.; Murayama, Y.; Yamazaki, T.; Kitazume, T. *Chem. Lett.* **1995**, 641.
  - 72) Koden, M.; Kaneko, T.; Tamai, K.; Takeda, H.; Miyoshi, S.; Wada, T.; Takeda, M.; Itoh, K.; Yamazaki, T.; Kitazume, T. *Jpn. J. Appl. Chem.* **1994**, *33*, 1096.
  - 73) Itoh, K.; Takeda, M.; Namekawa, M.; Nayuki, S.; Murayama, Y.; Yamazaki, T.; Kitazume, T. *Chem. Lett.* **1994**, 839.

## Chapter 9

# Fluoroamino Acid Containing Analogues of Folic Acid and Methotrexate

Takashi Tsukamoto<sup>1</sup>, James K. Coward<sup>1</sup>, and John J. McGuire<sup>2</sup>

<sup>1</sup>Departments of Chemistry and Medicinal Chemistry, University of Michigan, Ann Arbor, MI 48109-1055

<sup>2</sup>Department of Experimental Therapeutics, Grace Cancer Drug Center, Roswell Park Cancer Institute, Buffalo, NY 14263

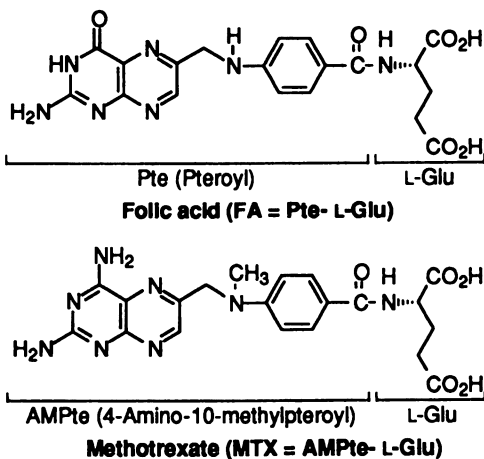
Various fluorinated analogues of folic acid and methotrexate have been synthesized from fluorine-containing glutamic acids, ornithine, and dipeptides. These analogues were evaluated as substrates or inhibitors of three folate-dependent enzymes, folylpoly- $\gamma$ -glutamate synthetase (FPGS),  $\gamma$ -glutamyl hydrolase ( $\gamma$ -GH) and dihydrofolate reductase (DHFR), and also for their effects on intact mammalian cells; e.g., transport and cytotoxicity. The most marked effects of fluorine substitution were observed with FPGS and  $\gamma$ -GH which catalyze the ligation or hydrolysis of glutamyl moieties, respectively.

In the biosynthesis of amino acids and nucleotides in mammalian cells and tissues, several derivatives of tetrahydrofolic acid (THF, H<sub>4</sub>PteGlu), the metabolically significant forms of the vitamin folic acid (FA, PteGlu), act as carriers of one-carbon units. Several antifolate drugs have as their primary target dihydrofolate reductase (DHFR). For example, methotrexate (MTX, AMPteGlu), one of the most potent inhibitors of DHFR, is extremely cytotoxic and is used extensively as a chemotherapeutic anticancer agent. Dihydrofolic acid (DHF, H<sub>2</sub>PteGlu) is the oxidation product arising from reductive methylation of deoxyuridylate to thymidylate. DHFR catalyzes the reduction of H<sub>2</sub>PteGlu to H<sub>4</sub>PteGlu, a reaction that is required to maintain thymidylate biosynthesis. Thus, the inhibition of the enzyme causes a deficiency in thymidylate, ultimately leading to cell death.

The reduced folates are present in cells as poly- $\gamma$ -glutamate conjugates. These polyglutamates, the physiological substrates for folate-dependent enzymes (1,2), are polyanionic and do not readily cross the cell membrane, and thus are also involved in cellular retention of folates. Folylpoly- $\gamma$ -glutamate synthetase (FPGS) is responsible for the biosynthesis of poly- $\gamma$ -glutamyl conjugates of folates (Scheme I). In contrast,  $\gamma$ -glutamyl hydrolase ( $\gamma$ -GH) catalyzes the hydrolysis of poly- $\gamma$ -glutamates, resulting in regeneration of a pteroylmonoglutamate. Cells are believed to maintain a balance of the poly- $\gamma$ -glutamates through the activities of these two enzymes. Interestingly both enzymes utilize not only naturally occurring folates but also antifolates such as MTX (3).

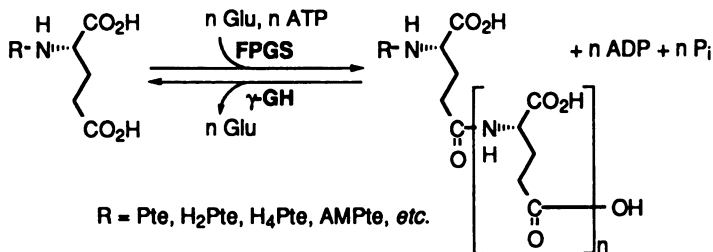
In order to distinguish the two glutamate species involved in the FPGS reaction, the terminal glutamate residue of the folate substrate is referred to as the 'accepting' glutamate. Similarly, the glutamate to be incorporated in the growing folate polyglutamate is defined as the 'incoming' glutamate. In our studies of FPGS and  $\gamma$ -GH, fluorine-containing glutamic acids have been essential materials from two perspectives. The fluorinated amino acids can be evaluated as incoming substrates

0097-6156/96/0639-0118\$15.00/0  
© 1996 American Chemical Society



for FPGS-catalyzed polyglutamylation. In addition, effects of fluorine substitution on the accepting glutamate can be investigated by incorporation of these fluoroglutamates in folic acid or MTX analogues. In this regard, we have synthesized several folic acid and MTX analogues in which the accepting L-glutamate moiety is replaced by a fluorinated glutamic acid (4). This research has been extended to the use of fluorinated peptides or ornithine as glutamate replacements. This Chapter describes our recent studies on the synthesis and biological evaluation of fluorine-containing analogues of folic acid and MTX. In the text and tables, the simple abbreviation L-Glu-L-Glu is used when referring to a  $\gamma$ -glutamyl peptide. For example, the peptide product of the FPGS-catalyzed reaction (Scheme I) where  $n = 1$  is R-L-Glu-L-Glu.

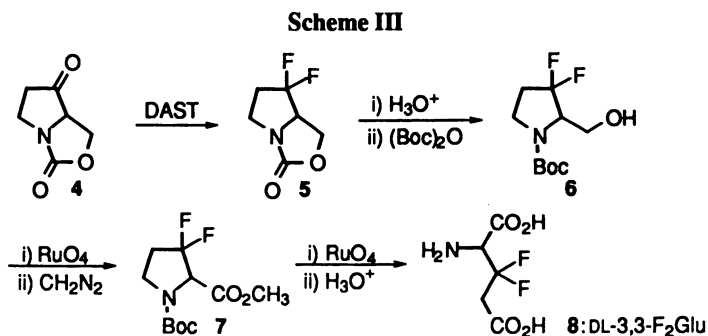
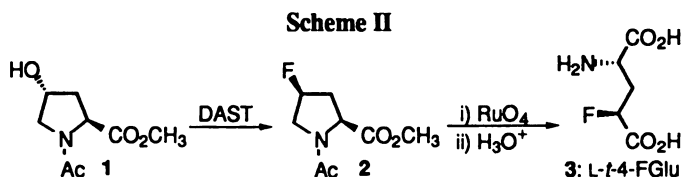
Scheme I



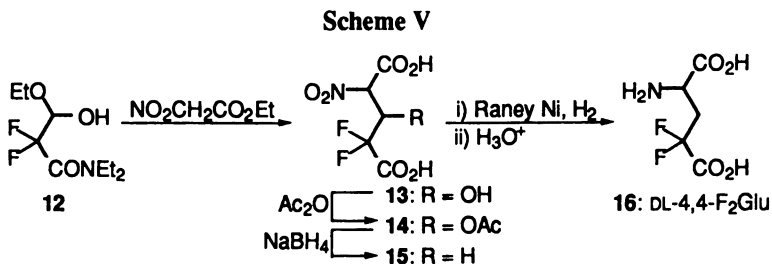
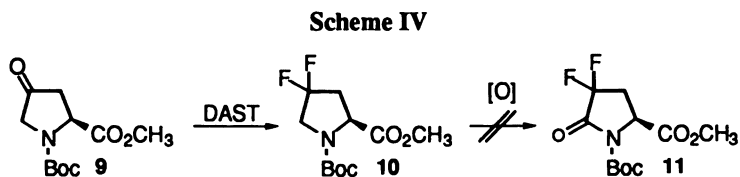
## Chemistry

**Fluorinated glutamic acids.** Syntheses of several fluorinated glutamic acids have been reported previously by us and others (5-14). Despite possessing the same underlying carbon backbone, fluorinated glutamic acids must be synthesized by different methods depending on the number and position of the fluorine atom(s).

4-Fluoroglutamic acid (4-FGlu) was synthesized initially as a mixture of four stereoisomers. More recently, the stereoselective synthesis of all four isomers was reported by Hudlicky's group (7,13). Scheme II depicts the synthesis of *L-threo*-4-fluoroglutamic acid, *L-t*-4-FGlu **3** which involves the fluorination of an optically active proline derivative **1**. A similar approach was applied to the synthesis of DL-3,3-difluoroglutamic acid, DL-3,3-F<sub>2</sub>Glu **8** (Scheme III), in which a racemic 3-oxoprolinol derivative **4** was employed as the starting material (10,11). Both

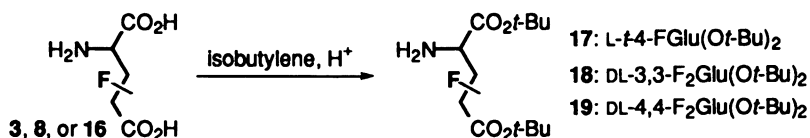


syntheses involve an oxidation of the  $\delta$ -carbon late in the synthesis, a reaction which is very sensitive to the position and/or number of fluorine atoms incorporated into the proline rings (15). Indeed, our attempt to synthesize L-4,4-difluoroglutamic acid (L-4,4-F<sub>2</sub>Glu) through 4,4-difluoroproline derivative 10 was unsuccessful due to its extremely poor oxidative reactivity (Scheme IV). Synthesis of DL-4,4-F<sub>2</sub>Glu 16 (Scheme V) was accomplished through a completely different approach involving the nitroaldol reaction of ethyl nitroacetate with a difluorinated aldehyde ethyl hemiacetal 12 as the key step (12).



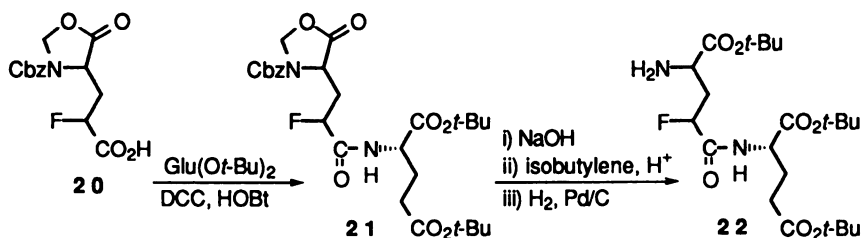
Fluorinated amino acids 3, 8, and 16 were evaluated as incoming FPGS substrates and were also converted into the corresponding di-*tert*-butyl esters 17, 18, and 19, (Scheme VI) which are essential precursors for the synthesis of fluorine-containing folic acid and MTX analogues as described later in this Chapter (Scheme X).

## Scheme VI

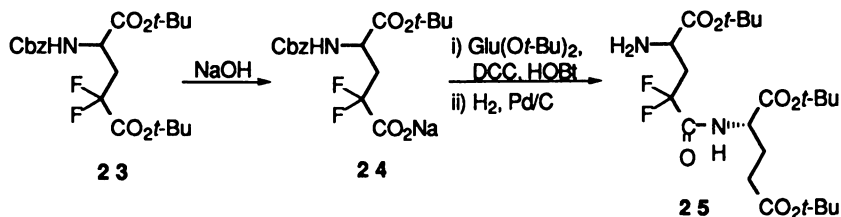


**Fluorinated dipeptides.** Although  $\gamma$ -glutamyl-glutamate is inactive as an incoming FPGS substrate (1), fluorinated analogues of this dipeptide are of importance for the synthesis of fluorine-containing MTX- $\gamma$ -oligoglutamates. To this end two fluorinated dipeptides have been synthesized in protected forms. Synthesis of  $\gamma$ -(4-fluoroglutamyl)glutamate, tri-*tert*-butyl ester **22** has been carried out by using 5-oxo-4-oxazolidinone **20**, derived from 4-fluoroglutamic acid, as a key intermediate (**16**) (Scheme VII). On the other hand,  $\gamma$ -(4,4-difluoroglutamyl)glutamate, tri-*tert*-butyl ester **25** has been synthesized through the half ester **24** that was obtained by the regiospecific hydrolysis of **23** (**17**) (Scheme VIII). These dipeptides were successfully converted to MTX analogues as described later in this Chapter.

## Scheme VII

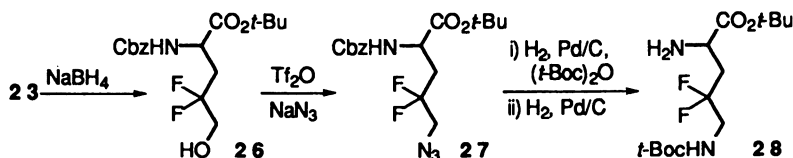


## Scheme VIII



**Fluorinated ornithine.** In addition to fluorinated glutamic acids and dipeptides, a protected derivative of 4,4-difluoroornithine **28** has also been synthesized as a suitably protected side chain precursor of a desired MTX analogue (**18**) (Scheme IX). The synthesis of **28** involves regiospecific reduction of **23** to **26** followed by the

## Scheme IX



transformation of the terminal hydroxy function of **26** to the *t*-Boc protected amine of **28**. Compound **28** was employed for the synthesis of fluoroornithine-containing MTX analogue as described below.

**Methotrexate Analogues.** Two major methods have been used for the synthesis of MTX analogues (Scheme X) by the coupling of the fluorinated precursors **17-19** to: 1) *N*-Cbz-protected *N*-methyl-*p*-aminobenzoic acid **29** followed by the removal of the Cbz group and *N*-alkylation with 6-(bromomethyl)-2,4-pteridinediamine hydrobromide **31** (Method A) (*19*); or 2) 4-amino-10-methyl-ptericoic acid (AMPteOH) (Method B) (*20*). The coupling reactions were followed by hydrolysis of *tert*-butyl esters to complete the syntheses. Various fluorinated MTX analogues were successfully synthesized by either Method A or B as summarized in Table I.

**Folic Acid Analogues.** The synthesis of folic acid analogues (Scheme X) involves coupling of fluorinated precursors to *N*<sup>10</sup>-TFA ptericoic acid (*N*<sup>10</sup>-TFA-PteOH) followed by cleavage of the *tert*-butyl ester and removal of the *N*<sup>10</sup>-trifluoroacetyl group (Method C) (*11,21*). Two fluorinated analogues, Pte-*L-t*-4-FGlu and Pte-DL-3,3-F<sub>2</sub>Glu (Table I) have been synthesized by this method from **17** and **18**, respectively (*11*).

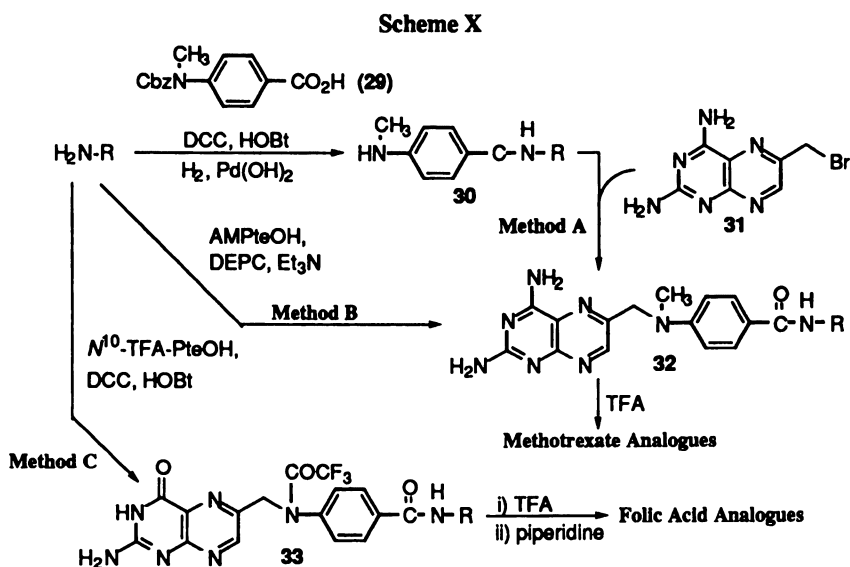


**Table I. Synthesis of Fluorinated Methotrexate and Folic Acid Analogues**

H <sub>2</sub> N-R	Method	Products	Ref.
<b>17</b>	A	AMPte- <i>L-t</i> -4-FGlu (L- <i>t</i> -γ-FMTX)	(11)
<b>18</b>	A	AMPte-DL-3,3-F <sub>2</sub> Glu (DL-β,β-F <sub>2</sub> MTX)	(11)
<b>19</b>	A	AMPte-DL-4,4-F <sub>2</sub> Glu (DL-γ,γ-F <sub>2</sub> MTX)	(12)
<b>22</b>	A	AMPte-DL- <i>er</i> -4-FGlu-L-Glu (DL- <i>er</i> -γ-FMTX-L-Glu)	(16)
<b>25</b>	B	AMPte-DL-4,4-F <sub>2</sub> Glu-L-Glu (DL-γ,γ-F <sub>2</sub> MTX-L-Glu)	<sup>a</sup>
<b>28</b>	A	AMPte-DL-4,4-F <sub>2</sub> Orn	(18)
<b>17</b>	C	Pte- <i>L-t</i> -4-FGlu (L- <i>t</i> -γ-FFA)	(11)
<b>18</b>	C	Pte-DL-3,3-F <sub>2</sub> Glu (DL-β,β-F <sub>2</sub> FA)	(11)

<sup>a</sup> T. Tsukamoto and J.K. Coward, unpublished results.

## Biochemistry and Pharmacology

**Fluorinated Glutamic Acids.** A simple competition assay can be carried out to evaluate fluorinated glutamates as possible incoming FPGS substrates. The assay employs a fluorinated glutamate as a competitor of L-[<sup>3</sup>H]glutamic acid (L-[<sup>3</sup>H]Glu) ligation to MTX. If L-[<sup>3</sup>H]Glu incorporation into MTX in the presence of an analogue is less than a control in which only L-[<sup>3</sup>H]Glu is present, the analogue must interact with the enzyme either as substrate or inhibitor. As shown in Figure I, the effect of fluorinated glutamates on the ligation of L-[<sup>3</sup>H]Glu to MTX was compared directly to that of simple isotopic dilution by non-radioactive L-Glu (12). DL-4,4-F<sub>2</sub>Glu shows only slight inhibition of this FPGS-catalyzed reaction. Although L-*t*-4-FGlu is a better inhibitor, it is less effective than non-radioactive glutamate. However, DL-3,3-F<sub>2</sub>Glu inhibits ligation of L-[<sup>3</sup>H]Glu to MTX more effectively than is observed with non-radioactive glutamate.

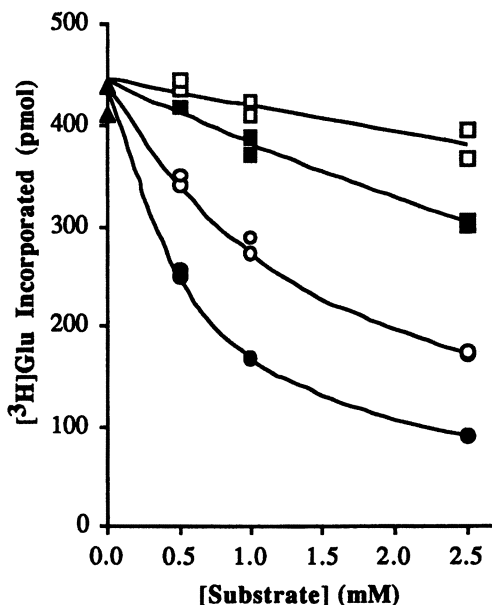


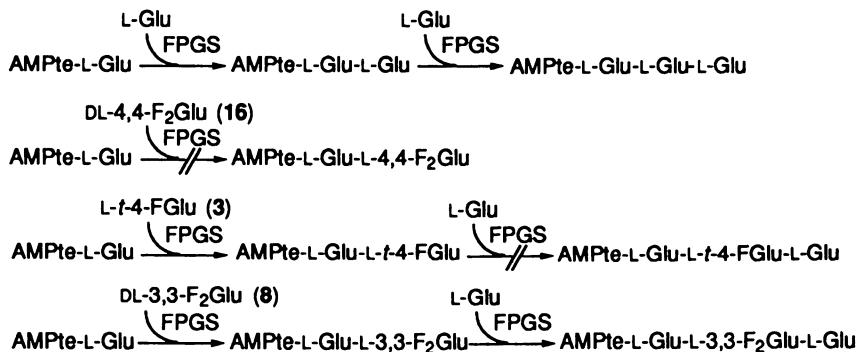
**Figure I.** Effects of fluorinated glutamates on the incorporation of L-[<sup>3</sup>H]Glu into MTX by human FPGS. CCRF-CEM FPGS was incubated with 0.5 mM L-[<sup>3</sup>H]Glu in the absence (▲) or presence of unlabeled DL-4,4-F<sub>2</sub>Glu (□), L-*t*-4-FGlu (■), L-Glu (○), or DL-3,3-F<sub>2</sub>Glu (●) at the indicated concentration for 3 h. For racemic substrates, only the concentrations of L-isomers are indicated.

To determine whether an analogue inhibited [<sup>3</sup>H]Glu binding or was an alternate substrate, each was assayed by HPLC analysis for FPGS-mediated ligation to [<sup>3</sup>H]MTX (Scheme XI). DL-4,4-F<sub>2</sub>Glu is a very poor FPGS substrate. 4-FGlu is a better FPGS substrate than DL-4,4-F<sub>2</sub>Glu but is less active than L-Glu. Further studies using separated 4-FGlu isomers revealed that the racemic *threo* isomer (2*S*, 4*S* and 2*R*, 4*R*) is slightly better than the racemic *erythro* form (2*S*, 4*R* and 2*R*, 4*S*). More interestingly, AMPte-L-Glu-L-*t*-4-FGlu, the product derived by ligation of L-*t*-4-FGlu to MTX is an extremely poor substrate for further polyglutamylation, i.e., chain-termination (22).



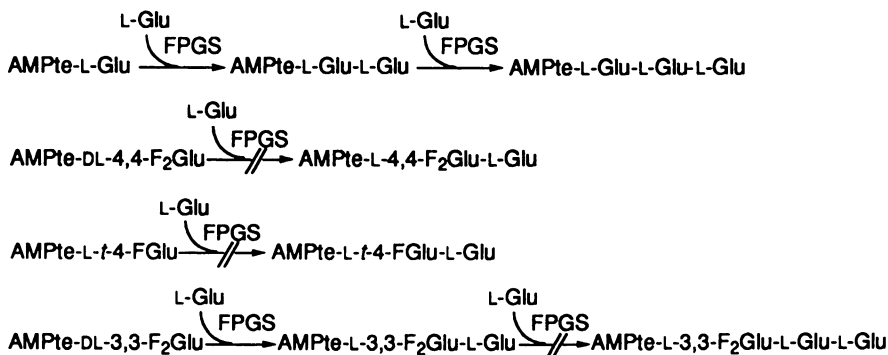
The activity of DL-3,3-F<sub>2</sub>Glu is completely different from the other analogues described above. This fluorinated analogue is a better FPGS substrate than L-Glu (23). Furthermore, AMPte-L-Glu-L-3,3-F<sub>2</sub>Glu, the product derived by ligation of L-3,3-F<sub>2</sub>Glu to MTX, undergoes further glutamylation at a higher rate than the corresponding protio compound, AMPte-L-Glu-L-Glu, i.e., enhanced elongation.

### Scheme XI



**Fluorinated Glutamate-containing Methotrexate Analogues.** Evaluation of the fluorinated MTX analogues as FPGS substrates or inhibitors was carried out and the results are summarized in Scheme XII. AMPte-DL-4,4-F<sub>2</sub>Glu is an extremely poor FPGS substrate and does not form any detectable polyglutamate product(s) (12). Earlier work with either a mixture of four stereoisomers of AMPte-4-FGlu or the separated diastereomers showed that this fluoroanalogue is a very poor FPGS substrate (24,25). As expected from those results, AMPte-L-t-4-FGlu is not an FPGS substrate (11). Further studies revealed that AMPte-DL-4,4-F<sub>2</sub>Glu and isomers of AMPte-4-FGlu are weak inhibitors of FPGS, indicating that these non-substrate analogues bind very poorly to the enzyme. In contrast, AMPte-DL-3,3-F<sub>2</sub>Glu is a good substrate ( $K_m = 5.4 \mu\text{M}$ , rel  $V_{\text{max}} = 0.84$  based on the assumption that only the L-isomer is a substrate) and is ligated more efficiently than L-MTX ( $K_m = 47 \mu\text{M}$ , rel  $V_{\text{max}} = 1$ ) (26). These results are consistent with data obtained with AMPte-L-Glu-L-t-4-FGlu (poor substrate) and AMPte-L-Glu-L-3,3-F<sub>2</sub>Glu (better substrate than AMPte-L-Glu-L-Glu) described above (Scheme XI) and indicate that the accepting glutamate residue has a dramatic effect on FPGS substrate activity of MTX analogues. However, it was also found that while addition of the first glutamate to

### Scheme XII



AMPte-DL-3,3-F<sub>2</sub>Glu is highly efficient, subsequent addition of L-Glu to AMPte-L-3,3-F<sub>2</sub>Glu-L-Glu occurs at a negligible rate (26). The results indicate that glutamate analogues in positions distal to the acceptor site can still affect ligation.

In contrast to the sharply divergent effects observed with different fluorinated MTX analogues as FPGS substrates, more comparable activities were observed when these fluorinated MTX analogues were evaluated as inhibitors of DHFR, cell growth (continuous exposure), and [<sup>3</sup>H]MTX uptake (11,12). Assuming that only L-isomers act as DHFR inhibitors, the fluorinated MTX analogues are nearly equivalent to MTX in inhibitory potency (Table II). Although AMPte-L-*t*-4-FGlu is less effective, the other fluorinated analogues are potent inhibitors of CCRF-CEM human leukemia cell growth with potency similar to MTX (Table III), indicating that these analogues are transported into cells as effectively as MTX. Indeed, further studies on the inhibition of [<sup>3</sup>H]MTX uptake by CCRF-CEM cells (Table IV) indicate that these analogues use the reduced folate/MTX carrier system for uptake with as high an affinity as does MTX. In addition, an MTX-resistant subline, defective in MTX uptake, is cross-resistant to these fluorinated compounds (12,25,26) confirming that these analogues utilize the reduced folate/MTX carrier system as their primary means of uptake.

**Table II. Inhibition of CCRF-CEM Human Leukemia Cell DHFR by Fluorinated Glutamate-containing Analogues of MTX**

Inhibitor	IC <sub>50</sub> (nM)		
	Expt 1	Expt 2	Expt 3
AMPte-L-Glu	0.72 ± 0.07	0.60 ± 0.03	0.72 ± 0.04
AMPte-DL-Glu	1.18 ± 0.08	1.40 ± 0.06	-
AMPte-L- <i>t</i> -4-FGlu	0.84 ± 0.10	-	-
AMPte-DL- <i>t</i> -4-FGlu	1.35 ± 0.05	-	-
AMPte-DL-3,3-F <sub>2</sub> Glu	-	1.34 ± 0.03	-
AMPte-DL-4,4-F <sub>2</sub> Glu	-	-	1.53 ± 0.03

**Table III. Inhibition of CCRF-CEM Cell Growth by Fluorinated Glutamate Analogues of MTX During Continuous (120 h) Exposure**

Inhibitor	EC <sub>50</sub> (nM)		
	Expt 1 <sup>a</sup>	Expt 2	Expt 3
AMPte-L-Glu	14.0 ± 0	14.6 ± 1.3	13.7 ± 0.5
AMPte-DL-Glu	30.0 ± 0	30.8 ± 1.5	-
AMPte-L- <i>t</i> -4-FGlu	102 ± 23	-	-
AMPte-DL- <i>t</i> -4-FGlu	133 ± 12	-	-
AMPte-DL-3,3-F <sub>2</sub> Glu	-	16.3 ± 1.8	-
AMPte-DL-4,4-F <sub>2</sub> Glu	-	-	29.0 ± 3.4

<sup>a</sup> J.J. McGuire, unpublished results

**Table IV. Inhibition of [<sup>3</sup>H]MTX Uptake in CCRF-CEM Human Leukemia Cells by Fluorinated Glutamate Analogues of MTX**

Inhibitor	IC <sub>50</sub> (μM)		
	Expt 1	Expt 2	Expt 3
AMPte-L-Glu	8 (IC <sub>48</sub> )	10.6 ± 1.1	14.5 ± 1.5
AMPte-DL-Glu	-	18.3 ± 3.3	-
AMPte-L- <i>t</i> -4-FGlu	-	-	-
AMPte-DL- <i>t</i> -4-FGlu	16 (IC <sub>27</sub> )	-	-
AMPte-DL-3,3-F <sub>2</sub> Glu	-	9.3 ± 0.9	-
AMPte-DL-4,4-F <sub>2</sub> Glu	-	-	8.72 ± 0.5

**Fluorinated Dipeptide-containing Methotrexate Analogues.** Unlike AMPte-L-3,3-F<sub>2</sub>Glu-L-Glu, an inactive substrate for rat liver FPGS (see Scheme XII), FPGS activity (rel  $V_{\max}/K_m$  = ca. 20% that of the corresponding protio compound) was observed with AMPte-DL-*et*-4-FGlu-L-Glu (16). AMPte-DL-*et*-4-FGlu-L-Glu was found to be a poor substrate for  $\gamma$ -GH from hog kidney when compared to the protio dipeptide, AMPte-L-Glu-L-Glu. The results are surprising because one would think that the incorporation of fluorine would accelerate the hydrolysis reaction due to the enhanced electrophilicity of the carbonyl carbon of the amide bond. Since the compound consists of four stereoisomers, the identification of the active isomer(s) must await the stereospecific synthesis of the analogue. The unique properties of AMPte-DL-*et*-4-FGlu-L-Glu prompted our interest in another fluorinated dipeptide analogue, AMPte-DL-4,4-F<sub>2</sub>Glu-L-Glu in which two fluorine atoms are incorporated adjacent to the scissile peptide bond. Evaluation of this newly synthesized analogue is currently in progress in our laboratory.

**Fluorinated Ornithine-containing Methotrexate Analogue.**  $N^{\alpha}$ -(4-Amino-4-deoxy-10-methylpteroyl)-L-ornithine (AMPte-L-Orn) has been found to be a potent inhibitor of both FPGS and DHFR (27,28). This compound, however, is a weak inhibitor of cell growth. This low cytotoxicity has been attributed to poor transport of the inhibitor across the cell membrane caused by the positively charged  $\delta$ -amino group ( $pK_a$  = 10.8) of ornithine. In attempt to overcome this poor transport, we have evaluated the biological activity of  $N^{\alpha}$ -(4-amino-4-deoxy-10-methylpteroyl)-DL-4,4-difluoroornithine (AMPte-DL-4,4-F<sub>2</sub>Orn), in which the  $\delta$ -amino group is mostly uncharged at physiological pH due to the electron-withdrawing effect of the two adjacent fluorine atoms. Although the  $pK_a$  of the  $\delta$ -amino group in AMPte-DL-4,4-F<sub>2</sub>Orn has not been determined, a  $pK_a$  of 6.88 has been reported for the terminal amino group of the closely related free amino acid, 5,5-difluorolysine.(29)

The biological activity of AMPte-DL-4,4-F<sub>2</sub>Orn has been compared to the corresponding protio compound, AMPte-L-Orn as shown in Table V (18). Although the fluorinated analogue is a potent inhibitor of DHFR, it is a poor inhibitor of FPGS. However, the compound is efficiently transported across the cell membrane and inhibits cell growth probably due to the inhibition of DHFR. The data obtained with the fluorinated analogue are in contrast to those of the corresponding protio compound, AMPte-L-Orn, which is a potent inhibitor of both FPGS and DHFR but shows very low cytotoxicity due to poor transport.

**Table V. Inhibitory activities of AMPte-L-Orn and AMPte-DL-4,4-F<sub>2</sub>Orn**

Inhibitor	FPGS <sup>a</sup>	DHFR <sup>a</sup>	Cell Growth <sup>b</sup>
	IC <sub>50</sub> ( $\mu$ M)	IC <sub>50</sub> (nM)	IC <sub>50</sub> (nM)
AMPte-L-Orn	33 $\pm$ 2	2.5 <sup>c</sup>	740 <sup>c</sup>
AMPte-DL-4,4-F <sub>2</sub> Orn	>300	1.3 $\pm$ 0	93 $\pm$ 17
AMPte-L-Glu	-	0.82 $\pm$ 0.04	14.5 $\pm$ 0.5

<sup>a</sup> Isolated from CCRF-CEM human leukemia cells.

<sup>b</sup> 120 hours continuous exposure of CCRF-CEM human leukemia cells.

<sup>c</sup> Literature data (28).

**Fluorinated Glutamate-containing Folic Acid Analogues.** Most of our biological studies on FPGS and  $\gamma$ -GH have been carried out using MTX analogues because of their limited intracellular metabolism. In addition, compared to naturally occurring folates (e.g., PteGlu, H<sub>2</sub>PteGlu, and H<sub>4</sub>PteGlu) MTX analogues are more stable during synthetic manipulation. The natural folates, however, have higher FPGS activities than MTX and the corresponding fluoroanalogues could be interesting alternate probes for studying FPGS.

Two analogues of folic acid, Pte-L-*t*-4-FGlu and Pte-DL-3,3-F<sub>2</sub>Glu have been investigated as FPGS substrates (11,26). As described earlier, AMPte-L-*t*-4-FGlu is an extremely poor FPGS substrate while AMPte-DL-3,3-F<sub>2</sub>Glu is a better substrate

than MTX. We were interested to determine if these properties would be mirrored in the folic acid analogues. As clearly shown in Figure II, Pte-L-*t*-4-FGlu is again a poor FPGS substrate and Pte-DL-3,3-F<sub>2</sub>Glu is polyglutamylated at a higher maximum rate and with higher efficiency ( $K_m = 25 \mu\text{M}$ ,  $\text{rel } V_{\text{max}} = 1$  based on the assumption that only L-isomer acts as a substrate) than Pte-L-Glu ( $K_m = 132 \mu\text{M}$ ,  $\text{rel } V_{\text{max}} = 0.52$ ). Further studies with Pte-DL-3,3-F<sub>2</sub>Glu also revealed that polyglutamylation is terminated after the ligation of a single glutamate as is observed with AMPte-DL-3,3-F<sub>2</sub>Glu. In summary, FPGS substrate activity of the fluorinated folate analogues is analogous to that observed with fluorinated MTX analogues (Scheme XII).

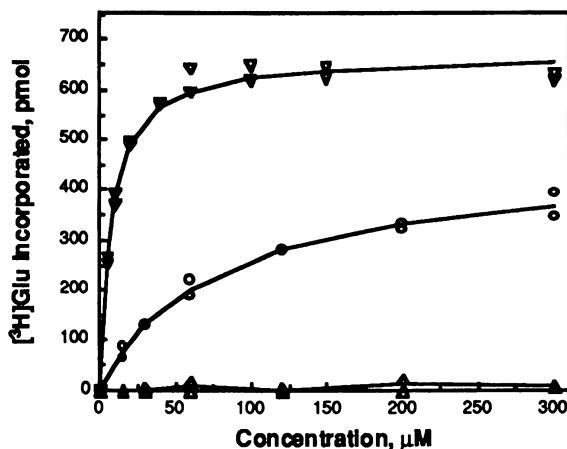


**Figure II.** Substrate activity of Pte-L-Glu (○), Pte-L-*t*-4-FGlu (△), and Pte-L-3,3-F<sub>2</sub>Glu (▽) with CCRF-CEM human leukemia cell FPGS.

## Summary

Modification of the glutamyl moiety of folates and antifolates is a straightforward approach to the design of powerful and specific probes for studying FPGS and  $\gamma$ -GH. In our research, fluorine-containing amino acids and peptides have been utilized as replacements of the glutamyl moiety. The resulting folate and MTX analogues were found to have diverse FPGS activities depending on the structure of the fluorinated amino acid replacement. All of the MTX analogues, however, were found to retain other biochemical properties (DHFR inhibition, cell growth inhibition, cell uptake) almost identical to those of MTX. These compounds will be useful tools in further dissecting the role of FPGS and  $\gamma$ -GH in folate biochemistry and antifolate cytotoxicity.

## Acknowledgments

This research was supported by grants from the National Cancer Institute, CA28097 (J.K.C.), CA43500 (J.J.M.), and CA16056 (J.J.M.). We thank Dr. Barry P. Hart and William Haile for their important contributions to this research.

## Literature Cited

1. McGuire, J. J.; Coward, J. K. In *Folates and Pterins*; R. L. Blakley and S. J. Benkovic, Eds.; Wiley: New York, 1984; Vol. 1; pp 135-190.
2. Shane, B. *Vitam. Horm.* **1989**, *45*, 263-335.
3. Matherly, L. H.; Seither, R. L.; Goldman, I. D. *Pharmacol. Ther.* **1987**, *35*, 27-56.
4. Coward, J. K.; McGuire, J. J.; Galivan, J. In *Selective Fluorination in Organic and Bioorganic Chemistry*; J. T. Welch, Eds.; American Chemical Society: Washington, D.C., 1991; pp 196-204.
5. *Fluorine-containing Amino Acids, Synthesis and Properties*; Kukhar', V. P.; Soloshonok, V. A., Ed.; Wiley: Chichester, West Sussex, England, 1995, p 411.
6. Vidal-Cros, A.; Gaudry, M.; Marquet, A. *J. Org. Chem.* **1989**, *54*, 498-500.
7. Hudlicky, M. *J. Fluorine Chem.* **1993**, *60*, 193-210.
8. Kitagawa, O.; Hashimoto, A.; Kobayashi, Y.; Taguchi, T. *Chem. Lett.* **1990**, 1307-1310.
9. Hudlicky, M. *Tetrahedron Lett.* **1960**, 21.
10. Hart, B. P.; Coward, J. K. *Tetrahedron Lett.* **1993**, *34*, 4917-4920.
11. Hart, B. P.; Licato, N. J.; Bolanowska, W. E.; McGuire, J. J.; Coward, J. K. *J. Med. Chem.* **1996**, *39*, 56-65.
12. Tsukamoto, T.; Kitazume, T.; McGuire, J. J.; Coward, J. K. *J. Med. Chem.* **1996**, *39*, 66-72.
13. Hudlicky, M.; Merola, J. S. *Tetrahedron Lett.* **1990**, *31*, 7403-7406.
14. Shi, G.-q.; Cai, W.-l. *J. Org. Chem.* **1995**, *60*, 6289-6295.
15. Hart, B. P. Ph.D. Thesis, The University of Michigan, Ann Arbor, May, 1995.
16. Licato, N. J.; Coward, J. K.; Nimec, Z.; Galivan, J.; Bolanowska, W. E.; McGuire, J. J. *J. Med. Chem.* **1990**, *33*, 1022-1027.
17. Tsukamoto, T.; Coward, J. K. *J. Org. Chem.*, **1996**, in press.
18. Tsukamoto, T.; Haile, W. H.; McGuire, J. J.; Coward, J. K. *J. Med. Chem.*, submitted.
19. Piper, J. R.; Montgomery, J. A. *J. Org. Chem.* **1977**, *42*, 208-211.
20. Rosowsky, A.; Freisheim, J. H.; Bader, H.; Forsch, R. A.; Susten, S. S.; Cucchi, C. A.; Frei, E., III *J. Med. Chem.* **1985**, *28*, 660-667.
21. Godwin, H. A.; Rosenberg, I. H.; Ferenz, C. R.; Jacobs, P. M.; Meienhofer, J. J. *Biol. Chem.* **1972**, *247*, 2266-2271.
22. McGuire, J. J.; Coward, J. K. *J. Biol. Chem.* **1985**, *260*, 6747-6754.
23. McGuire, J. J.; Haile, W. H.; Bey, P.; Coward, J. K. *J. Biol. Chem.* **1990**, *265*, 14073-14079.
24. Galivan, J.; Inglese, J.; McGuire, J. J.; Nimec, Z.; Coward, J. K. *Proc. Natl. Acad. Sci., U.S.A.* **1985**, *82*, 2598-2602.
25. McGuire, J. J.; Graber, M.; Licato, N.; Vincenz, C.; Coward, J. K.; Nimec, Z.; Galivan, J. *Cancer Res.* **1989**, *49*, 4517-4525.
26. McGuire, J. J.; Hart, B. P.; Haile, W. H.; Rhee, M.; Galivan, J.; Coward, J. K. *Arch. Biochem. Biophys.* **1995**, *321*, 319-328.
27. Rosowsky, A.; Freisheim, J. H.; Moran, R. G.; Solan, V. C.; Bader, H.; Wright, J. E.; Radike-Smith, M. *J. Med. Chem.* **1986**, *29*, 655-660.
28. McGuire, J. J.; Hsieh, P.; Franco, C. T.; Piper, J. R. *Biochem. Pharmacol.* **1986**, *35*, 2607-2613.
29. Shirota, F. N.; Nagasawa, H. T.; Elberling, J. A. *J. Med. Chem.* **1977**, *20*, 1623-1627.

## Chapter 10

# Fluoro-olefin Isosteres as Peptidomimetics

J. T. Welch, J. Lin, L. G. Boros<sup>1</sup>, B. DeCorte<sup>2</sup>, K. Bergmann<sup>3</sup>,  
and R. Gimi<sup>4</sup>

Department of Chemistry, State University of New York at Albany,  
Albany, NY 12222

Fluoroolefin dipeptide isosteres were synthesized applying the Peterson reaction as a novel method for fluoroolefination. Gly- $\psi$ [CF=C]-Pro dipeptide isosteres were elaborated to provide conformationally constrained analogs of the Suc-Ala-Gly-Pro-Phe-pNA tetrapeptide substrate for cyclophilin. Ala- $\psi$ [CF=C]-Pro containing *N,O*-diacylhydroxamic acid type protease inhibitors were synthesized for the study of the influence of prolylamide bond geometry on the inhibition of dipeptidyl peptidase IV(CD26).

Peptides have been modified to improve their activity, stability or bioavailability in a variety of ways, but altering the backbone structure by replacing the amide bond itself can be especially effective. The use of amide bond surrogates can not only impart peptidase resistance but can facilitate conformational control of the target peptide. Amide isosteric replacements are commonly indicated using the symbol  $\psi$ [], where the  $\psi$  indicates the absence of an amide bond and the structure that is replacing the amide is indicated in the brackets(1). The alkene  $\psi$ [C=C] isostere is an accurate mimic of the steric demand, bond lengths and bond angles of the amide bond(2-6). When the  $\psi$ [C=C] isostere is employed both (*E*) and (*Z*) (*cis*- and *trans*-) isomers are possible and unlike the amide bond which has some degree of flexibility the  $\psi$ [C=C] isostere is conformationally fixed(7-8). The  $\psi$ [CF=C] isostere retains these attributes but also much more effectively mimics the electronic features of the amide bond (9-11), including dipole moment, charge distribution and electrostatic potential.(See Figure 1)

<sup>1</sup>Current address: Albany Molecular Research, 21 Corporate Circle, Albany, NY 12203

<sup>2</sup>Current address: Janssen Research Foundation, Welsh and McKean Roads,  
Spring House, PA 19477

<sup>3</sup>Current address: Syracuse Research Corporation, 1745 Jefferson Davis Highway, Suite 504,  
Arlington, VA 22202

<sup>4</sup>Current address: Brookhaven National Laboratory, Upton, NY 11973

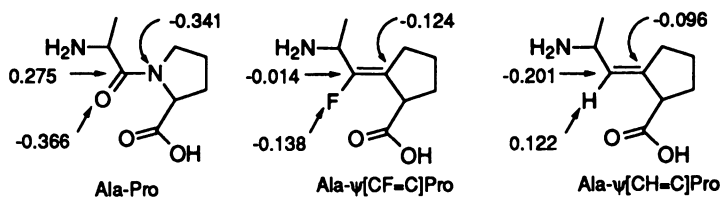


Figure 1. Charges Calculated using AM1 for the dipeptide Ala-Pro and two dipeptide alkene isosteres.

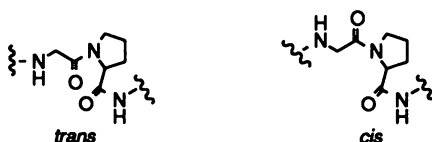
The  $\psi$ [CF=C] isostere has recently been employed in the preparation of a number of peptidomimetics whose preparation and utility will be discussed in this article. (See Table 1.)

**Table 1.  $\psi$ [CF=C] Isostere Containing Peptides**

Peptide	Fluoroolefin Construction Methods	Ref.
Phe- $\psi$ [(Z)-CF=CH]-Gly	CHCl <sub>2</sub> F, NaOH	10
Phe- $\psi$ [(E)-CF=CH]-Gly	(EtO) <sub>2</sub> POCHFCO <sub>2</sub> Et, LDA	10
Arg-Pro-Lys-Pro-Gln-Gln-Phe-Phe- $\psi$ [(Z)-CF=CH]-Gly-Leu-Met	CHCl <sub>2</sub> F, NaOH	12
Phe- $\psi$ [(Z)-CF=C]-Pro	(EtO) <sub>2</sub> POCHFCO <sub>2</sub> Et, LDA	12
Gly- $\psi$ [(Z)-CF=CH]-Gly	CHCl <sub>2</sub> F, NaOH	10
Phe- $\psi$ [(Z)-CF=C]-Phe	(EtO) <sub>2</sub> POCHFCO <sub>2</sub> Et, LDA	12
Ala- $\psi$ [(Z)-CF=CH]-Gly	3,3-sigmatropic rearrangement	13
Gly- $\psi$ [(Z)-CF=CH]-Leu	EtO <sub>2</sub> CCHFCOCO <sub>2</sub> Et	14
Gly- $\psi$ [(Z)-CF=CH]-Leu-Gly	EtO <sub>2</sub> CCHFCOCO <sub>2</sub> Et	14
Gly- $\psi$ [(Z)-CF=CH]-Leu-Ala	EtO <sub>2</sub> CCHFCOCO <sub>2</sub> Et	14
Gly- $\psi$ [(Z)-CF=CH]-Leu-Leu	EtO <sub>2</sub> CCHFCOCO <sub>2</sub> Et	14
Gly- $\psi$ [(Z)-CF=CH]-Leu-Phe	EtO <sub>2</sub> CCHFCOCO <sub>2</sub> Et	14

### Prolylamides

Prolylamides differ from the other amide bonds linking amino acids in peptides in the relative stability of the *cis* and *trans* amide bond conformations; both the *cis* and *trans* conformations have very similar energies with a rotation activation barrier of approximately 20 kcal/mol(15).



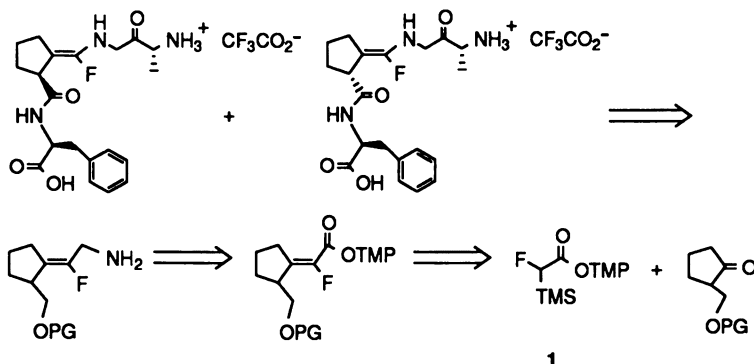
In peptides not containing prolylamide bonds the linkages are normally *trans*, with the *cis* conformation approximately 5 kcal per mole less stable(16). Prolylamide bond conformations can be crucial to the folding of proteins, therefore the *cis-trans* conformations of prolylamides are very important in the establishment of the secondary structure of peptides(17,18). Recently it has been found that the *cis/trans* isomerization of a peptidyl-prolyl amide bond (Xaa-Pro bond) is catalyzed by a family of ubiquitous enzymes called prolyl isomerases, PPIases(19, 20). In addition to their postulated role in facilitating peptide folding, PPIases may have several additional functions one of which, isomerization of Xaa-Pro bonds to regulate enzyme activity(21), is of interest in the second section of this chapter. Although a great deal is known about the mechanism by which the amide bond is isomerized by these enzymes, the structure-function relationship of these enzymes might be profitably be examined by the use of conformationally constrained peptide analogs(8). Our strategy was to prepare both Gly- $\psi$ [CF=C]-Pro and Gly- $\psi$ [CH=C]-Pro containing tetrapeptides and to compare the relative binding affinities of these materials with cyclophilin A. In light of the proposal that the  $\psi$ [CF=C] and the



$\psi$ [CH=C] isosteres should show a difference in binding affinity to the enzyme as a result of differences in electrostatic interactions(22), a comparison of the result of the binding of these two isostere types might lead to some insight on the nature of the interactions that were important to the differential binding of the *cis* and *trans* amides.

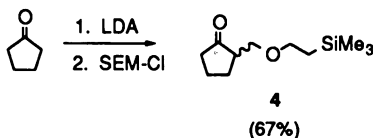
### Gly- $\psi$ [CF=C]-Pro Preparation via Peterson Fluoroolefination

A brief retrosynthetic analysis of our approach to the synthesis of the Gly- $\psi$ [CF=C]-Pro dipeptide isostere as incorporated into the tetrapeptides required for binding studies with cyclophilin A is outlined below.

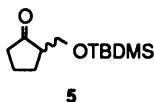


The key step was the stereoselective construction of the fluoroolefin, which was effected by a Peterson olefination reaction of 2,4,6-trimethylphenyl  $\alpha$ -fluoro- $\alpha$ -(trimethylsilyl)acetate, **1**, with a protected 2-(hydroxymethyl)cyclopentanone, **3**. Consecutive transformation of the ester into the primary amine, and oxidation of the protected primary alcohol to the acid resulted in formation of the desired isosteres.

**2-(Hydroxymethyl)cyclopentanone Construction.** To expedite our synthesis we have developed a procedure for the preparation of protected 2-(hydroxymethyl)cyclopentanone in one step. Treatment of the lithium enolate of cyclopentanone with 2-(trimethylsilyl)ethoxymethyl chloride yielded the necessary derivative **4** in 67% yield(23).

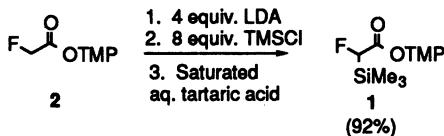


Subsequently due to the expense of 2-(trimethylsilyl)ethoxymethyl chloride we employed both the less efficient route of treatment of cyclopentanone with aqueous formaldehyde in the presence of calcium hydroxide (15% yield for two steps)(24) and the lengthy Dieckmann condensation strategy (45% yield for four steps) (25) to prepare the unprotected hydroxymethylcyclopentanone. In both cases protection was effected with *tert*-butyldimethylsilyl chloride to yield **5**.

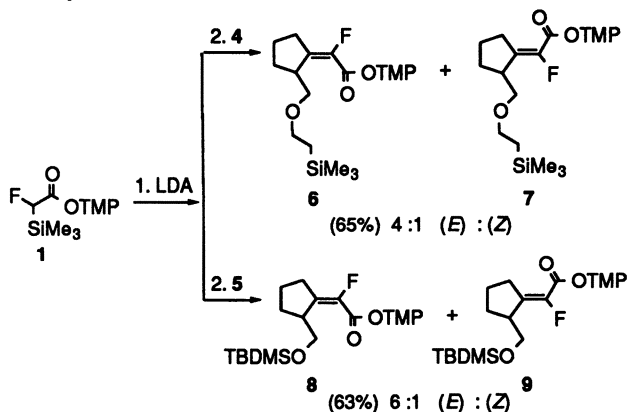


Both **4** and **5** were employed in further synthetic transformations as identified.

**2,4,6-Trimethylphenyl  $\alpha$ -fluoro- $\alpha$ -(trimethylsilyl)acetate.** Peterson olefination of **4** required the preparation of  $\alpha$ -fluoro- $\alpha$ -silylacetate **1**, from the  $\alpha$ -fluoroacetate **2**. Bissilylation was effected by treatment of **2** with 4 equiv. of LDA and 8 equiv. of chlorotrimethylsilane. Hydrolysis of the bissilylated product with a saturated tartaric acid solution resulted in selective formation of **1** in 86% yield.



**Olefination.** Reaction of the **4** with the enolate of **1** generated with LDA at  $-90^\circ\text{C}$  formed the olefins **6** and **7** in 65% yield and with moderate selectivity favoring the (*Z*)-isomer (*Z* : *E* ratio 4 : 1)(23). Attempts to change the selectivity of the olefination reaction by changing the counterion were not successful. Olefination of **5** under the same conditions yielded a 6 : 1 mixture of the (*E*)- and (*Z*)-isomers **8** and **9** in 63% combined yield(24).



The stereochemistry of the major product was confirmed by single crystal X-ray diffraction study of the phthalimide protected alcohol **16**, the product of a later step in the synthesis. (See Figure 2.)

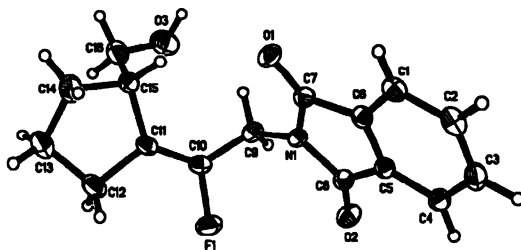
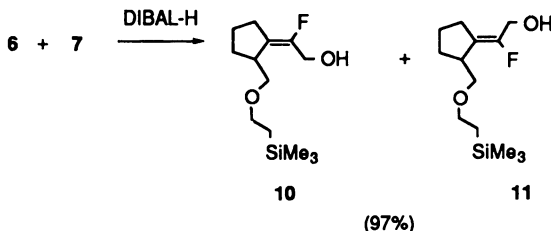
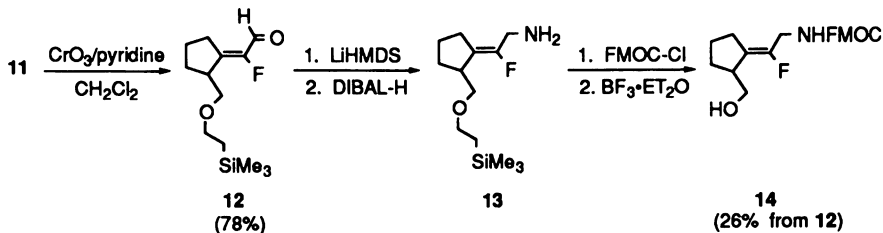


Figure 2. ORTEP of phthalimide protected alcohol **16**.

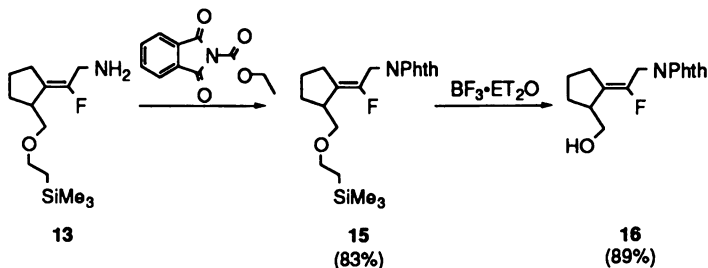
**Elaboration of the Dipeptide Isostere Functionality.** Reduction of the esters **6** and **7** diisobutylaluminum hydride (DIBAL-H) resulted in the formation of the corresponding alcohols **10** and **11** in quantitative yield. The isomeric alcohols were separated by column chromatography, also facilitating removal of 2,4,6-trimethylphenol.



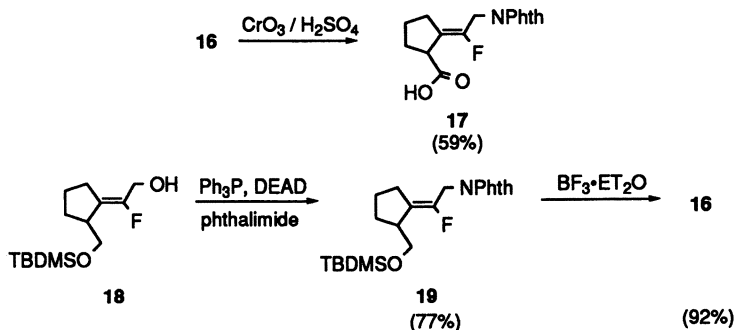
Oxidation of the alcohol **11** to the aldehyde **12** proceeded in 78% yield using a modified Collins procedure. The aldehyde was converted into the primary amine **13** on treatment of **12** with lithium hexamethyldisilazide followed by DIBAL-H (26).



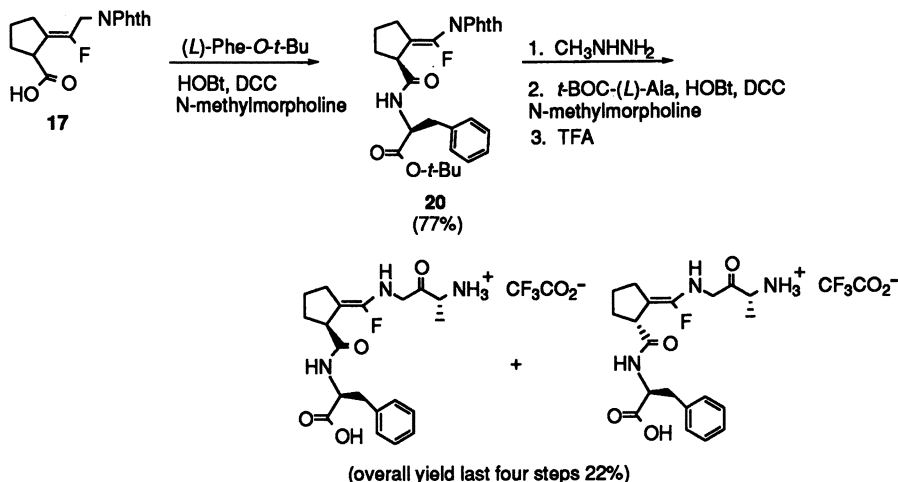
In our initial experiments **12** was protected as the FMOC derivative **14** and the 2-(trimethylsilylethyl) group was removed with boron trifluoride etherate. Surprisingly all attempts to oxidize the alcohol **14** to the corresponding acid with chromium trioxide/sulfuric acid in acetone or pyridinium dichromate in dimethylformamide proved unsuccessful. Substitution of FMOC-protecting group by *t*-butoxycarbonyl (*t*-BOC) or benzyloxycarbonyl (*Z*) lead to the same side reactions on attempted oxidation. Deblocking of the ether **15**, robustly protected as the phthalimide (Phth) **15** with no remaining protons on the allylic nitrogen, formed alcohol **16** which was easily oxidized with chromium trioxide/sulfuric acid in acetone to form the desired dipeptide isostere **17**.



Once the utility of the Phth protected material was recognized, the synthesis was shortened by treatment of **12** with triphenylphosphine, diethyl azodicarboxylate (DEAD) and phthalimide to form the Phth protected fluoroolefin **15** in excellent yield (99%). Similarly **18** could be converted to **19**.



**Peptide Synthesis.** As the exchange of Phth group for Fmoc that was required to facilitate solid phase peptide synthesis proceeded in poor yield, we decided to block the C-terminus of the dipeptide by coupling to the required phenylalanine residue. Coupling the acid 17 with (*L*)-phenylalanine-*tert*-butyl ester using dicyclohexylcarbodiimide, in the presence of 1-hydroxy-benzotriazole and *N*-methylmorpholine led to the bisprotected tripeptide mimic 20 in 77% yield(24). The phthaloyl group was removed by stirring 20 in excess methylhydrazine at room temperature for 48 hours. The free amine of was then coupled with *t*-BOC-(*L*)-alanine to obtain a diastereomeric mixture of the protected tetrapeptide isosteres. After separating the two diastereomers by column chromatography, deprotection of the *t*-BOC and *t*-butyl group with trifluoroacetic acid of each diastereomer provided the optically active tetrapeptide isosteres.



**Cyclophilin A Inhibition Studies.** Both diastereomers of the (*E*) and (*Z*) dipeptide isosteres were inhibitors of Cyclophilin A (See Table 2) in the standard assay.(27) As ground state analog inhibitors these materials show surprisingly good inhibition of the enzyme. The greatest utility of these compounds may lie in a comparison of these findings with those obtained with the non-fluorinated analogs. In preliminary studies we have found significant differences between the tetrapeptides containing the  $\Psi[\text{CF}=\text{C}]$  and  $\Psi[\text{CH}=\text{C}]$  isosteres.(28) Since the two isosteres possess insignificant

differences in steric demand it is proposed that the differences in binding between the  $\Psi[\text{CF}=\text{C}]$  and  $\Psi[\text{CH}=\text{C}]$  isosteres reflect the importance of electrostatic or solvation differences on binding of the *cis* and *trans* form of the natural tetrapeptide substrate Suc-Ala-Ala-Pro-Phe-pNA.

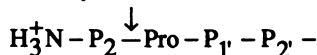
**Table 2. Cyclophilin Inhibition Results**

Isostere <sup>b</sup>	Inhibitor Concentration <sup>a</sup>		
	1.0 mM	0.5 mM	0.25 mM
(Z')	41% <sup>c</sup>	30±2% (2) <sup>d</sup>	0 (2)
(Z'')	40%	30±13 (2)	7±2 (2)
(E')	13%	34±6 (3)	24±4 (2)
(E'')	50%	43 (1)	26 (1)

a. Substrate Suc-Ala-Ala-Pro-Phe-pNA (0.07mM), cyclophilin (0.5 $\mu$ m). Percent inhibition =  $(K_{\text{inh}} - K_{\text{ctl}})/K_{\text{Cyp}} - K_{\text{ctl}}$ . b. Separated diastereomers of (E)- and (Z)-Ala Gly- $\Psi[\text{CF}=\text{C}]$ -Pro-Phe.

### Dipeptidyl Peptidase IV (CD26)

It has previously been postulated that dipeptidyl peptidase IV (EC 3.4.14.5, DPP IV, CD26) possessed a high conformational specificity for a *trans* P<sub>2</sub>-Pro bond, a requirement exhibited by other enzymes as mentioned earlier in this article(29-31).



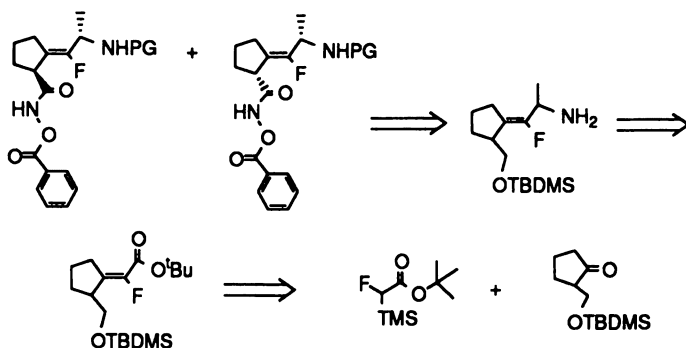
DPP IV discovered in 1966(32), is a transmembrane serine peptidase found in a variety of human tissues and organs(33-35). In particular DPP IV, when expressed on the surface of CD4+ T-cells is identical with the CD26 antigen and is considered to be a lymphocyte activation marker(36,37). Although the involvement of DPP IV in the immune response and regulation of lymphocyte activation has been implicated, the mechanism of the involvement is not clear.

Relatively few effective inhibitors of DPP IV have been reported(38-45). Given the requirement for a DPP IV substrate to have a free *N*-terminal amino group, it is not surprising that the inhibitors which have been reported generally suffer from instability. The cyclization reaction of the free *N*-terminal amino group with the reactive site of the inhibitor does however require the molecule to assume the *cis* conformation, the conformation that was previously proposed to be unreactive with the DPP IV(29-31). In order to obviate this mode of inactivation and to rigorously examine the *cis-trans* selectivity of DPP IV we prepared a series of conformationally constrained acyl hydroxamic acid type inhibitors(40,46,47) containing the fluoroolefin dipeptide isostere(48).

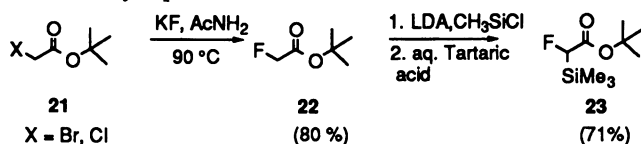
### Ala- $\Psi[(Z)\text{-CF}=\text{C}]$ -Pro Isostere for the Study of Dipeptidyl Peptidase IV

To study DPP IV the synthetic strategy described above for the preparation of the Gly- $\Psi[\text{CF}=\text{C}]$ -Pro isosteres had to be extended to include isosteres where the *N*-terminus would bear a secondary amine such as the Ala- $\Psi[(Z)\text{-CF}=\text{C}]$ -Pro dipeptide isostere. An alternative route using a new, simple and convenient to prepare  $\alpha$ -fluoro- $\alpha$ -trialkylsilyl acetate was developed(49) to facilitate this synthesis. Additionally it was necessary to select an amine protecting group compatible with

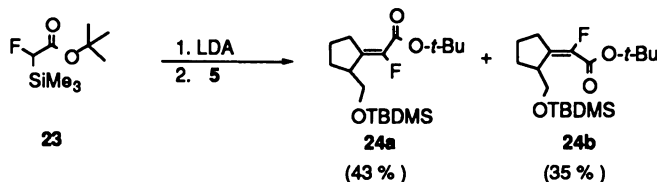
both conventional *N*-terminal peptide synthesis protocols and that possessed sufficient lability to be removed without affecting the hydroxamate functionality. The *t*-BOC group satisfies these requirements but necessitated some additional changes in the synthesis as outlined below.



***tert*-Butyl  $\alpha$ -Fluoro- $\alpha$ -trimethylsilylacetate.** Treatment of commercially available *tert*-butyl  $\alpha$ -chloroacetate or *tert*-butyl  $\alpha$ -bromoacetate **21** with potassium fluoride easily yielded *tert*-butyl  $\alpha$ -fluoroacetate **22** in 80% yield. The outcome of the direct *C*-silylation of **22** is highly dependent on the molar ratio of the reagents employed, as well as the reaction temperature and time. It was found that *C,O*-bissilylation and Claisen condensation always accompanied the desired *C*-silylation reaction. After careful optimization, **23** was formed in 71% yield by treatment of **22** with 4 equivalents of LDA and 6 equivalents of chlorotrimethylsilane at  $-78^\circ\text{C}$ . The purification of **23** was achieved by fractional distillation where higher boiling point by-products were easily separated.

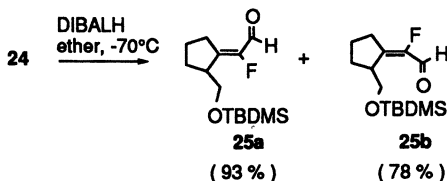


**Olefination and Functional Group Elaboration.** Peterson olefination of the TBDMS-protected 2-(hydroxymethyl)cyclopentanone(**50**). **5** under our modified conditions employing *tert*-butyl  $\alpha$ -fluoro- $\alpha$ -trimethylsilylacetate **23**. The fluoroolefin product **24** was obtained as a 1.2 : 1 ratio of (*Z*): (*E*) isomers (as determined by  $^{19}\text{F}$  NMR) in 78 % yield.

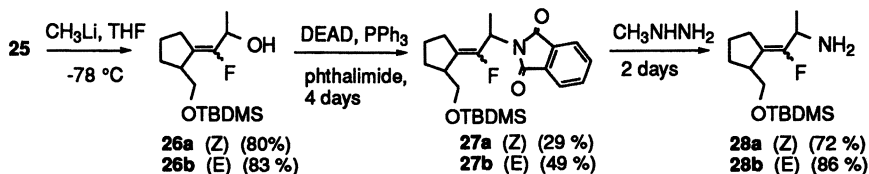


Following separation of the double bond isomers by column chromatography, treatment of **24a** or **24b** was treated with a slight excess of DIBALH (1.2 to 1.5 molar equivalents) in diethyl ether at  $-78^\circ\text{C}$  for 1 h, formed the aldehyde **25** in excellent yield. The success of these reaction conditions was in contrast with our

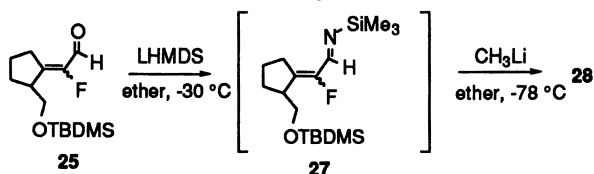
earlier reported results where reduction of **6** or **7** led only to formation of the alcohol on treatment with DIBALH.



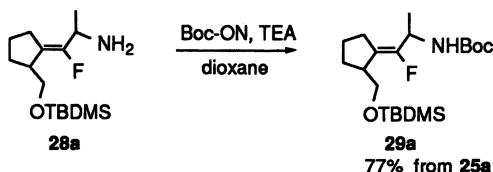
The selective 1,2-addition of methyl lithium to aldehyde **25** was easily accomplished. After purification by chromatography according to Still, the combined yield of the separated diastereomers of the secondary alcohol **26** was 80%. Transformation of **26** to the protected amine **27** was carried out under standard Mitsunobu conditions over four days. As could be anticipated, low yields resulted in both the (*E*) and (*Z*) cases (29% and 49%) probably as a result of the steric effect of secondary alcohol on the displacement reaction. Unfortunately, the phthalimide protecting group was not suitable in these cases because of the forcing conditions required for its removal; the phthalimide group could only be liberated by treatment of **27** with excess methylhydrazine at room temperature for two days. The long reaction times and low yields of the Mitsunobu reaction when combined with the difficult deprotection resulted in depressingly low overall yields of amine **28**.



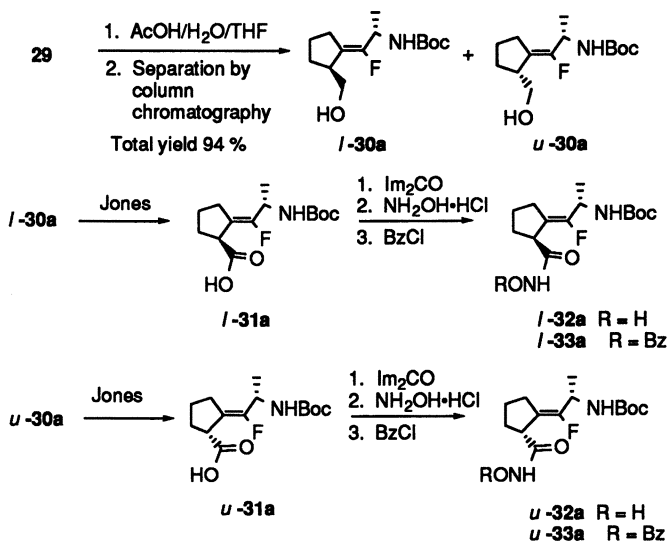
Although there was literature precedent for the direct alkylative amination of aldehydes, repeated attempts to form the desired amine **28** from aldehydes **25a** or **25b** under these conditions (10, 26, 51, 52) failed. Treatment of aldehyde **25a** with LHMDS (1.2 equiv.) in diethyl ether at  $-30^\circ\text{C}$  for 1 h, then subsequent addition of methyl lithium (2.0 equiv.) in ether at  $-78^\circ\text{C}$  followed by stirring for an additional hour afforded the desired amine **28a** in 93% yield as a 1.3:1 ratio of diastereomers.



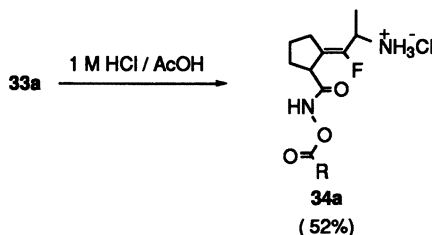
The mixture of diastereomers was protected using 2-(Boc-oxyimino)-2-phenylacetoneitrile (Boc-ON) according to the standard procedure (53) in good yield (77%, overall from aldehyde **25a**).



Selective cleavage of the silyl ether **29a**, in the presence of the Boc-group, was accomplished by treatment with acetic acid-water-THF liberating the primary alcohol **30a** in 94% yield as a 1.2 : 1 ratio of diastereomers (**54**). Following separation of the diastereomers by column chromatography, Jones oxidation of the alcohols *l*-**30a** and *u*-**30a**, respectively, yielded the corresponding crystalline carboxylic acids, *l*-**31a** and *u*-**31a**, without loss of the acid-sensitive Boc-group.



**Hydroxamic Acid Introduction.** Diastereomer **31a** was hydroxylated via addition of 1,1'-carbonyldiimidazole to form the reactive acylimidazole, which was subsequently condensed with hydroxylamine hydrochloride (**55**, **56**) in the same manner to form the hydroxamic acid **32a** in 20% yield. Acylation of the **32a** with benzoyl chloride by addition of equimolar amount of benzoyl chloride and pyridine formed the **33a** in 51% yield. Deblocking of the Boc-groups was accomplished by using 1 M HCl in AcOH to give compound **34a**.



### DPP IV Inhibition.

In comparison with other inhibitors described in the literature one of the diastereomers of **34a**, **34a'**, showed superior inhibitory properties for DPP IV (See Tables 3 and 4). Both the *u* and *l*, diastereomers were tested but the structures have not yet been assigned. Both **34a''** and **34a'** were stable in aqueous solution at neutral pH for a period of 25 days. In contrast to Ala-Pro-NHO-Bz(4-NO<sub>2</sub>) which had a



half-life under the assay conditions of 9 hr,(40) **34a''** and **34a'** had a half-life of 103 hr.

**Table 3. Inhibition of DPP IV by Fluoroolefin Containing *N*-peptidyl-*O*-hydroxylamines**

	Inhibitors	[I] mM	% Inhibition <sup>a</sup>	
			2 min	30 min
<b>34a'</b>	Ala-ψ[(Z)CF=C]-Pro-NHO-Bz	0.01	4	1
		0.05	17	25
<b>34a''</b>	Ala-ψ[(Z)CF=C]-Pro-NHO-Bz	0.01	42	39
		0.25	100	100
		1.10	29 <sup>b</sup>	60

a. Percentage inhibition was measured after 2 or 30 min incubation in 45 mM phosphate buffer, pH 7.7 at 30 °C. Gly-Pro-*p*-nitroanilide was used as substrate.

b. Incubation time 10 min.

**Table 4. Inhibition constants of inhibitors of DPP IV, **34a'** and **34a''****

	Inhibitors	K <sub>i</sub> (nM)
<b>34a'</b>	Ala-ψ[(Z)CF=C]-Pro-NHO-Bz	14,400
<b>34a''</b>	Ala-ψ[(Z)CF=C]-Pro-NHO-Bz	188

**Acknowledgments.** It is a pleasure to acknowledge Prof. Paul Toscano of the University at Albany for his help with the single crystal X-ray diffraction studies of **16**. We would also like to thank Prof. R. E. Handschumacher of Yale University not only for his generosity and assistance with the binding studies of cyclophilin but also for his enthusiastic encouragement for us to continue this work. Lastly we gratefully acknowledge the financial support of the National Science Foundation of this work.

#### Literature Cited.

1. Fok, Y.F. Yankeelow, J.A., Jr. *Biochem. Biophys. Res. Commun.* **1977**, *74*, 273.
2. Hann, M.M.; Sammes, P.G. *J. Chem. Soc., Chem. Commun* **1980**,234
3. Cox, M.T.; Heaton, D.W.; Horbury, J. *J. Chem. Soc., Chem. Commun.* **1980**, 799
4. Cox, M.T.; Gormley, J.J.; Hayward, C.F.; Pettern, N.N. *J. Chem. Soc., Chem. Commun* **1980**, 800
5. Hann, M.M.; Sammes, P.G.; Kennewell, P.D.; Taylor, J.B. *J. Chem. Soc., Perkin Trans. I* **1982**, 307.
6. Miles, N.J.; Sammes, P.F. Kennewell, P.D.; Westwood, R. *J. Chem. Soc., Perkin Trans. I* **1985**, 2299.
7. Kaltenbronn, J.S.; Hudspeth, J.P.; Lunney, E.A.; Michniewicz, B.M.; Nicolaides, E.D.; Repine, J.T.; Roark, W.H.; Stier, M.A.; Tinney, F.J.; Woo, P.K.W.; Essenberg, A. D. *J. Med. Chem.* **1990**, *33*, 838.
8. Andres, C.J.; Macdonald.T.L.; Ocain, T.D.; Longhi, D. *J. Org. Chem.* **1993**, *58*, 6609-6613.

9. Abraham, R. J.; Ellison, S. L. R.; Schonholzer, P.; Thomas, W. A. *Tetrahedron* **1986**, *42*, 2101-2110.
10. Allmendinger, T.; Furet, P.; Hungerbühler, E. *Tetrahedron Lett.* **1990**, *31*, 7297-7300.
11. Cieplak, P.; Kollman, P. A. *J. Comp. Aided. Mole. Design* **1993**, *7*, 291-304.
12. Allmendinger, T.; Felder, E.; Hungerbühler, E. in *Selective Fluorination in Organic and Bioorganic Chemistry*, Welch, J. T. Ed. ACS Books: Washington, D.C., 1991, pp 186-195.
13. Allmendinger, T.; Angst, C.; Karfunkel, H. *Proc. Intl. Conf. Fluor. Chem.*, 155th Committee on Fluorine Chemistry 1994, Jap Soc. Prom. Science **1994**, 149-162.
14. Bartlett, P. A.; Otake, A. *J. Org. Chem.* **1995**, *60*, 3107-3111.
15. Stein, R. L. and Schmid, F. X. et al. In: *Advances in Protein Chemistry*, Anfinsen, C. B.; Edsall, J. T.; Richards, F. M. and Eisenberg, D. S., Eds.; Academic Press: New York; 1993, Vol 44, pp. 1-66.
16. Deber, C.M.; Madison, V.; Blout, E.R. *Acc. Chem. Res.* **1976**, *9*, 106.
17. Creighton, T. E. *Proteins: Structures and Molecular Principles*, W.H. Freeman and Co.: New York, 1984.
18. Schmid, F.X.; Mayr, L.M.; Mücke, M. Schönbrunner, E.R. In *Accessory Folding Proteins*; Lorimer, G., Ed.; Adv. Protein Chem.; Academic Press: San Diego, Ca 1993, Vol. 44; pp 25-66.
19. Fischer, G.; Wittmann-Liebold, B.; Lang, K.; Kiefhaber, T.; Schmid, F. X. *Nature* **1989**, *337*, 476.
20. Takahashi, N.; Hayano, T.; Suzuki, M. *Nature* **1989**, *337*, 473.
21. Stein, R.L. In *Accessory Folding Proteins*; Lorimer, G., Ed.; Adv. Protein Chem.; Academic Press: San Diego, Ca 1993, Vol. 44; pp 1-24.
22. Cieplak, P.; Kollman, P. A. *J. Comp. Aided. Mole. Design* **1993**, *7*, 291-304.
23. DeCorte, B. Ph. D. Dissertation, University at Albany, Albany, NY, 1992.
24. Boros-Gregor, L.; DeCorte, B.; Gimi, R.; Welch, J. T.; Wu, Y.; Handschumacher, R. *Tetrahedron Letters* **1994**, *33*, 6033-6036.
25. Eschenmoser, A.; Frey, A. *Helv. Chim. Acta* **1952**, *35*, 1660.
26. Cainelli, G.; Giacomini, D.; Panunzio, M.; Martelli, G.; Spunta, G. *Tetrahedron Lett.* **1987**, *28*, 5639.
27. Kofron, J. L.; Kuzmic, P.; Kishore, V.; Gemmecker, G.; Fesik, S. W.; Rich, D. *H. J. Am. Chem. Soc.* **1992**, *114*, 2670.
28. Unpublished results, Bergmann, K.; Boros, L.G.; Welch, J.T. 1996.
29. *Dipeptidyl IV-General and Applied Aspects*; Barth, A.; Schowen, R. L. Eds.; Institut für Pharmakologische Forschung: Berlin, 1990; Vol. 38.
30. Yaron, A.; Naider, R. *Crit. Rev. Biochem. Mol. Biol.* **1993**, *28*, 31-81.
31. McDonald, J. K.; Barrett, A. J. *Mammalian Proteases: A Glossary and Bibliography*, Academic Press, London, 1986, Vol.2, pp 132-144.
32. Hopsu-Havu, V. K.; Sarimo, S. R. *Hoppe-Seyler's Z. Physiol. Chem.* **1967**, *348*, 1540-1550.
33. Mentlein, R.; Heymann, E.; Scholz, W.; Feller, A. C.; Flad, H. -D. *Cell. Immunol.* **1984**, *89*, 11-19.
34. Feller, A. C.; Heijnen, C. J.; Ballieux, R. E.; Parwaresc, M. R. *Br. J. Haematol.* **1982**, *51*, 227-234.
35. Schön, E.; Demuth, H. U.; Barth, A.; Ansorge, S. *Biochem. J.* **1984**, *223*, 255-258.
36. Matern, T.; Flad, H. D.; Feller, A. C.; Heymann, E. and Ulmer, A. J. In: *Leukocyte Typing IV*, Knapp, E. Ed., New York: Oxford University Press, 1989, p. 417-418.
37. Barton, R. W.; Prendergast, J.; Kennedy, C. A. *J. Leukoc. Biol.* **1990**, *48*, 291-296.

38. Flentke, G. R.; Munoz, E.; Huber, B. T.; Plaut, A. G.; Kettner, C. A.; Bachovchin, W. W. *Proc. Natl. Acad. Sci. U. S. A.* **1991**, *88*, 1556-1559.
39. Snow, R. J.; Bachovchin, W. W.; Barton, R. W.; Campbell, S. J.; Coutts, S. J.; Freeman, D. M.; Gutheil, W. G.; Kelly, T. A.; Kennedy, C. A.; Krolikowski, D. A.; Leonard, S. F.; Pargellic, S. A.; Tong, L. Adams, J. *J. Am. Chem. Soc.* **1994**, *116*, 10860-10869.
40. Demuth, H. U.; Baumgrass, R.; Schaper, C.; Fischer, G.; Barth, A. *J. Enzyme Inhib.* **1988**, *2*, 129-142.
41. Demuth, H. U.; Neumann, U.; Barth, A. *J. Enzyme Inhib.* **1989**, *2*, 239-248.
42. Neumann, U.; Steinmetzer, T.; Barth, A.; Demuth, H.-U. *J. Enzyme Inhib.* **1991**, *4*, 213-226.
43. Kelly, T. A.; Adams, J.; Bachovchin, W. W.; Barton, R. W.; Campbell, S. J.; Coutts, S. J.; Kennedy, C. A.; Snow, R. J. *J. Am. Chem. Soc.* **1993**, *115*, 12637-12638.
44. Powers, J. C. *Methods Enzymol.* **1977**, *46*, 197-208.
45. Boduszek, B.; Oleksyszyn, J.; Kam, C. -M.; Selzler, J.; Smith, R. E.; Powers, J. C. *J. Med. Chem.* **1994**, *37*, 3969-3976.
46. Demuth, H. -U. *J. Enzyme Inhibition* **1990**, *3*, 249-278.
47. Demuth, H.-U.; Schlenzig, D.; Schierhorn, A.; Groasche, G.; Chapot-Chartier, M.-P.; Gripon, J.-C. *FEBS Lett.* **1993**, *320*, 23-27
48. Welch, J.T.; Lin, J. *Tetrahedron*, **1996**, *52*, 291-304.
49. Lin, J.; Welch, J. T. *Abstracts of Papers*, 208th National Meeting of the American Chemical Society, Washington, D.C.; American Chemical Society: Washington, D.C., 1994; ORGN 277.
50. Fischer, G.; Demuth, H. U.; Barth, A. *Pharmazie* **1983**, *38*, 249-250
51. Hart, D. J.; Kanai, K.; Thomas, D. G.; Yang, T. -K. *J. Org. Chem.* **1983**, *48*, 289-298.
52. Hirao, A.; Hattori, I.; Yamaguchi, K.; Nakahama, S. *Synthesis* **1982**, 461-462.
53. Itoh, M.; Hagiwara, D. Kamiya, T. *Bull. Chem. Soc. Jpn.* **1977**, *50*, 718-721.
54. Kawai, A.; Hara, O.; Hamada, Y.; Shioiri, T. *Tetrahedron Lett.* **1988**, *29*, 6331-6334
55. Staab, H. A.; Luking, M.; Durr, F. H. *Chem. Ber.* **1962**, *95*, 1275-1283.
56. Brown, D. A.; Geraty, R. A.; Glennon, J. D.; Choileain, N. *Synth. Commun.* **1985**, *15*, 1159

## Chapter 11

# Molecular Design of Fluorine-Containing Peptide Mimetics

Piotr Cieplak<sup>1</sup>, Peter A. Kollman<sup>2</sup>, and Jan P. Radomski<sup>3</sup>

<sup>1</sup>Quantum Chemistry Laboratory, Department of Chemistry, University of Warsaw, Pasteura 1, Warsaw 02–093, Poland

<sup>2</sup>Department of Pharmaceutical Chemistry, University of California, San Francisco, CA 94143

<sup>3</sup>Interdisciplinary Center for Modeling, University of Warsaw, Banacha 2, Warsaw 02–097, Poland

The free energy perturbation (FEP) and free energy derivatives (FED) methodology with molecular dynamics simulations has been applied to study possible improvement of the inhibition properties of the JG-365 inhibitor toward HIV aspartic protease. Our study concerns the assessment of the effect of replacement of some peptide bonds in JG-365 by trans-ethyleneic or fluoroethyleneic units. According to our free energy perturbation simulations such replacement could be beneficial for two of those peptide bonds but not for the others. The results of application of the free energy derivative technique confirms the FEP results and also suggest other possible modification of the JG-365 inhibitor which could lead to increased potency. Our results are only predictive in nature, since the proposed pseudopeptidic inhibitors have not yet been synthesized.

Finding therapeutics against diseases like AIDS, malaria, cancer and many others, is an important but very difficult task. Theoretical methods and the use of computational techniques can be very helpful in the process of developing new drugs. The main effort in this area is focused on designing new enzyme inhibitors. Theoretical methods are used for predicting binding trends in enzyme - inhibitor complexes. Although not all the effects accompanying such a binding could be taken into account in computer simulations, some insights could be gained if the free energy differences could be calculated. Free energy is the main quantity used to describe the general trends in any chemical processes and since it is a state function, only the knowledge of the initial and the final states is needed. In this article we present the results of applying free energy perturbation (FEP) (1,2) and free energy derivative (FED) (3,4) methodologies to designing peptide mimetic inhibitors of the HIV protease enzyme. The first method provides appropriate free energy differences of binding and the latter one point out at the places in the inhibitor where the chemical modifications could be performed in order to increase binding properties.

In recent years significant work has been directed toward the inhibition of the HIV reverse transcriptase and the HIV aspartic protease as a most accessible target for chemotherapeutic intervention in fighting the AIDS disease (5,6). In our study we have been focused on inhibition of the HIV aspartic protease. The HIV protease is responsible for cleaving a polypeptide precursor into the functional proteins, which are essential for virial replication (6). It is estimated that more than 160 structures of different inhibitors with HIV protease

0097–6156/96/0639–0143\$15.00/0  
© 1996 American Chemical Society

complexes have been determined by X-ray crystallography. These structures could be used as a starting point in any further molecular modelling. A summary of a variety of molecular dynamics and free energy calculations for some of those structures are presented in Ref. (7).

Our calculations, partially described in Ref. (8), have been performed for one of such structure, solved by Wlodawer et al (9-11), containing the potent JG-365 inhibitor (0.24nM inhibition constant). This is hydroxyethylamine (HEA) analog of the ACE-Ser-Leu-Asn-Phe-Pro-Ile-Val-OMe peptide (Fig.1). The hydroxyethylamine (HEA) analog of the Phe-Pro peptide bond resembles the tetrahedral intermediate for the peptide bond hydrolysis reaction. It is well established that among the most effective protease inhibitors are modified peptides that act as transition state analogues (12). The JG-365 is an example of such inhibitor and has been used as our lead compound in molecular dynamics simulations. The purpose of those calculations was to suggest chemical changes within the inhibitor which could possibly improve its binding. We propose that this goal could be achieved by replacing some of the peptide bonds with either ethylene or fluoroethylene units. JG-365 has seven peptide bonds and each of them could be replaced by its nonpeptidic isostere (see Fig.1). In the following discussion we will use the standard notation (13) for the inhibitor amino acids, i.e. P4 for SER, P3 - LEU, P2 - ASN, P1 - PHE, P1' - PRO, P2' - ILE, P3' - VAL.

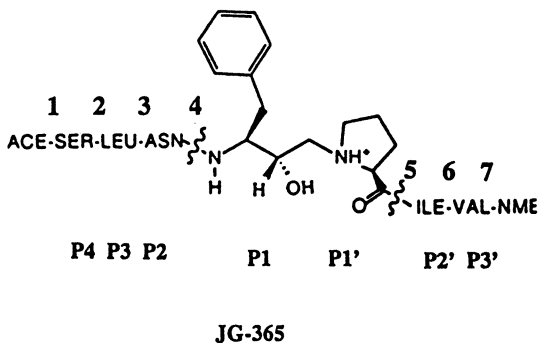


Figure 1. Amino acid sequence in the inhibitor

### Why were peptidomimetics chosen as a target?

The usefulness of peptide mimetics, (e.g. ethylenic or fluoroethylenic derivatives) have already been demonstrated (14-16). Why could peptidomimetics be a good choice for possible modification of the original inhibitor?

One of the important arguments is that replacing the peptide bond by its isosteric ethylenic or fluoroethylenic unit does not change the already appropriate conformation of the inhibitor needed in the active site, and thus it fulfills conformational constraints.

The fluoroolefin unit, as an excellent steric and electronic mimic for the peptide bond, was recently used in organic synthesis as a tool for controlling peptide conformations (17,18). The synthesized peptide mimetics exhibited inhibitory effects on the cyclophilin enzyme. In another case, the ethylene unit was incorporated into the met-enkephalines and the resulting derivative exhibited biological activity (19-22)]. It was found that such a modification prevented premature degradation of pseudo-peptide bonds by amino-peptidase

and it was assumed that the increased lipophilicity of the peptide should facilitate its passage through the blood-brain barrier and membranes. Incorporation of the olefinic bond into substance P also increased its biological potency compared to the unmodified compound (21).

The dipole moment of the trans ethylene (~0.1D) and trans fluoro-ethylene units (~1.5D) have different values, and orientation than the peptide bond itself (~4.5D), (see Fig.2). Thus, one might observe a totally different pattern of intermolecular interactions with the enzyme. Replacing the strongly interacting peptide bond for another chemical unit which does not form strong hydrogen bonds could be advantageous in some cases. This is especially important when one must compare the two states of the inhibitor, one in the enzymatic site and the other in aqueous solution.

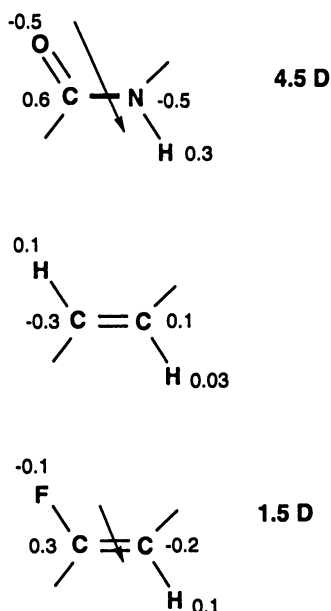


Figure 2 Charge distribution and dipole moments for peptide bond and for ethylenic and fluoroethylenic units.

Olefin and fluoro containing molecules were also used in studies devoted to inhibiting HIV protease. For example difluoroketones HIV-1 protease inhibitors exhibit nanomolar activity (23). Keenan *et al* (24) attempted to synthesize the olefin-hydroxyethylene peptide mimetics. They showed that replacing the peptide bond by an ethylene unit in the P2-P1 sites decreases the association of the inhibitor from  $K_i=37$  nM to 3.6  $\mu$ M. This was expected, since that peptide bond is engaged in holding the inhibitor in the active site. That also means that replacing the peptide bond between P2-P1 into a weaker interacting unit should be unfavorable. This example shows using a more weakly interacting peptide mimetic unit to replace the peptide bond could serve as a probe for testing the importance of the hydrogen bond pattern in the active site.

Peptidomimetics have attained a prominent position in rational drug design (16). Olson *et al* (16) proposed some general criteria which should be fulfilled in designing peptide mimetics. These can be summarized as follows: a) replace as much of the peptide backbone

as possible by a nonpeptide framework, b) maintain the peptide side chain pharmacophoric groups as in the peptide, since they are most likely to be recognized by a receptor, c) do not change or restrict conformational flexibility too much in the first iteration step of generating mimetics, d) select appropriate targets based on availability of a pharmacophore hypothesis.

In our studies we propose to modify the very potent JG-365 inhibitor by replacing peptide bonds by ethylene or fluoro-ethylene units. Such modifications satisfy all requirements for peptide mimetics mentioned above. We expect that such modified inhibitors could have many desired properties, for example, the increased resistance to enzymic degradation by amino-peptidases and thus longer duration of their inhibition action.

### The Free Energy Perturbation Method

To study the JG-365 inhibitor and the HIV-aspartic protease complex as well as the inhibitor itself in water solution we used the molecular dynamics method (25), the AMBER program (26) and the empirical potential function (27,28) for energy calculation:

(1)

$$E_{total} = \sum_{bonds} K_r (r - r_{eq})^2 + \sum_{angles} K_\theta (\theta - \theta_{eq})^2 + \sum_{dihedrals} \frac{V_n}{2} [1 + \cos(n\phi - \lambda)] + \sum_{i < j} \left[ \frac{A_{ij}}{R_{ij}^{12}} - \frac{B_{ij}}{R_{ij}^6} + \frac{q_i q_j}{\epsilon R_{ij}} \right] + \sum_{H-bonds} \left[ \frac{C_{ij}}{R_{ij}^{12}} - \frac{D_{ij}}{R_{ij}^{10}} \right]$$

Molecular dynamics (MD) is a deterministic method for simulating complex molecular systems. An MD simulation is performed by integrating Newton's equations of motion over time for the molecular system:

(2)

$$F_i = m_i \frac{d^2 r_i}{dt^2}$$

where,  $F_i$  is the force on atom  $i$  calculated at time  $t$ ,  $r_i$  - position of atom  $i$  at time  $t$ ,  $m_i$  - mass of that atom. Forces are calculated by differentiating appropriate expression (Eq.1) for potential energy.

In order to estimate the free energies associated with replacing the peptide bond into its isostere mimetics we applied the free energy perturbation (FEP) method with molecular dynamics simulations and used the appropriate thermodynamic cycle (1,2). In the free energy perturbation method, the free energy differences between two states **a** and **b** is calculated according to the following formula, provided by statistical mechanics:

(3)

$$\Delta G = -RT \ln \langle \exp(-\Delta H/RT) \rangle_a$$

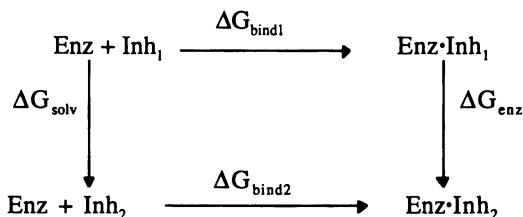
where:

$$\Delta H = H_b - H_a,$$

where  $H_a$  and  $H_b$  are the Hamiltonians for given states, which can be represented by our empirical force field given in Eq. 1. Averages are calculated during molecular dynamics simulations over the state  $\mathbf{a}$ . If  $\Delta G$  is large then one can introduce a parameter  $\lambda$  and make  $H$  dependent on  $\lambda$ , e.g.  $H = H(\lambda)$ . A given state can be associated with the value of the  $\lambda$  parameter, with the value of  $\lambda=0$  defined as the  $\mathbf{a}$  state and the  $\lambda=1$  the  $\mathbf{b}$  state. During the molecular dynamics simulation, the parameter  $\lambda$  is changed gradually by  $\delta\lambda$ , which means that the system is perturbed from the initial state into the final one, through many nonphysical, intermediate states, and then the total free energy is summed up over those states:

$$(5) \quad \Delta G = \sum_{\lambda} \Delta G(\lambda_i)$$

The difference in free energy of binding between normal and modified (peptide mimetic) inhibitor is calculated according to the following thermodynamic cycle:



The appropriate binding free energy difference is calculated from:

$$\Delta\Delta G_{\text{bind}} = \Delta G_{\text{bind2}} - \Delta G_{\text{bind1}} = \Delta G_{\text{enz}} - \Delta G_{\text{solv}}$$

Molecular dynamics simulation for the horizontal processes can not be easily performed. Instead, one simulates the two vertical processes which involve perturbation of the inhibitor in water solution, yielding  $\Delta G_{\text{solv}}$  and in the enzyme environment ( $\Delta G_{\text{enz}}$ ). Based on those two simulations one can calculate  $\Delta\Delta G_{\text{bind}}$ . The main idea behind this approach is that when the ligand/inhibitor binds to the active site there is a competition between solvation and binding interactions. Free energy calculation can show which effect is dominant when comparing two ligands.

Free energy perturbation technique have become a powerful method, which allows for the direct comparison between experimental and calculated free energies (29) In drug design, the FEP method could be effectively used as an aid in the selection process of new compounds with better binding affinities, and could possibly save significant laboratory time and materials. This approach has been used to obtain the results cited in this paper.

### Results of the Free Energy Perturbation Simulations for the JG-365 Inhibitor

A thorough description of the molecular dynamics protocol used in our simulations is in Ref (8). The initial structure of the HIV-1 protease with the JG-365 inhibitor bound to it was taken from crystallographic data of Ref (11). Because the protons are not located in



such structure the protonation state of the two important enzymatic aspartic acids residues is not clear. According to theoretical free energy calculations of Tropsha *et al* (30) the protonation of Asp-125 should be favorable. Here, we report the results from the calculations performed for both protonation states of the enzyme.

A more difficult problem is how to choose the initial conformational state of the inhibitor in water solution. The reliability of the results depend on the convergence of the free energy calculations and a knowledge of the proper or most representative conformations of the flexible inhibitor in water. The main uncertainty of the results stems from the total lack of the information about the conformational states of the inhibitor in water. JG-365 inhibitor is a relatively large and flexible molecule, containing about 30 dihedral angles around which bond rotations could take place. In order to find the most abundant conformation in water we performed long, 10nsec molecular dynamics simulation of the inhibitor in water solution and analyzed its trajectory using a neural network clustering approach (31,32). The conformation taken as a starting point for the free energy perturbation calculations was chosen as a representative from the largest cluster obtained from such analysis. The free energy perturbation results in water, reported here are obtained from 52 psec or in two, the most promising cases, 306 psec of molecular dynamics simulations.

All free energy perturbations results are collected in Tables I and II. The data shows that the most promising peptide bonds for ethylene or fluoroethylene units replacements are the 3rd between Leu-Asn (P3-P2) and the 5th between Pro-Ile (P1'-P2').

The results obtained here are consistent with the work of Keenan *et al* (24) and the theoretical results of Rao and Murcko (33). According to Keenan *et al* (24) replacing the peptide bond by an ethylene unit in the P2-P1 site decreases the inhibition of their hydroxyethylene HIV-1 aspartic protease inhibitor. They argued that this peptide bond is engaged in important interactions with the rest of the enzyme holding the inhibitor in the active site. That means also that in our JG-365 inhibitor the replacement of the fourth peptide bond by units not capable of forming strong enough hydrogen bonds with the enzyme should not be attempted. As noted in Table I, our calculations find the  $\Delta\Delta G_{\text{bind}} = +6.2$  kcal/mole, in qualitative agreement with the experimental value of  $\sim 4$  kcal/mole. In other theoretical work, B.G.Rao, and M.A.Murcko (33) presented calculations for an inhibitor aspartic protease, Ro-31-8959. It was shown that the conformation adopted by the carbonyl of the P1' group when bound to the active site is considerably higher in energy compared to its global minimum energy. If the inhibitor is modified to minimize these conformational energies without disrupting of the strong enzyme-inhibitor intermolecular interactions, then its potency can be improved considerably. Thus, this suggests that the P1'-P2' peptide bond (5th bond in JG-365) replacement into a less interacting group might lead to better binding.

Since the values of the  $\Delta G_{\text{soln}}$  in Tables I and II vary significantly for the different peptide bonds, we were also interested in finding the limiting values of the hydration free energy differences between peptide bond and its ethylene or fluoroethylene mimetics. The knowledge of those quantities could be helpful in assessing the effect of screening of a given peptide bond from water solution by the rest of the inhibitor molecule. In order to get such information, we calculated the hydration free energy differences between the N-methyl-acetamide (NMA) and trans-butene as well as between N-methyl-acetamide and trans-2-fluoro-butene (Fig.3). Calculations were performed using our new force field (28) and the new RESP charges (34,35). Free energies were obtained from 104 psec molecular dynamics simulations.

**Table I.** The best estimates of the free energies for the -CO-NH- substitution by -CH=CH- unit. (ASP25 protonated).  $\Delta G_{\text{solv}}$  results are the averages from forward and reverse, 52psec each, simulations or from 306psec if stated otherwise.

bond no.	between	$\Delta G_{\text{enz}}$	$\Delta G_{\text{solv}}$	$\Delta\Delta G_{\text{bind}} = \Delta G_{\text{enz}} - \Delta G_{\text{solv}}$
1	ACE-SER	4.0	-0.9	4.9±0.2
2	SER-LEU	4.5	-0.5	5.0±0.2
3	LEU-ASN	-0.8	1.1 1.3 (306ps)	-1.9±0.2 -2.1±0.3
4	ASN-PHE	7.9	1.7	6.2±0.3
5	PRO-ILE	6.9	11.4 9.7 (306ps)	-4.5±0.4 -2.8±0.5
6	ILE-VAL	4.2	5.0 5.5 (306ps)	-0.8±0.2 -1.3±1.3
7	VAL-NME	5.8	-2.3	8.1±2.1

**The best estimates of the free energies for the -CO-NH- substitution by -CH=CH- unit. (ASP125 protonated)**

bond no.	between	$\Delta G_{\text{enz}}$	$\Delta G_{\text{solv}}$	$\Delta\Delta G_{\text{bind}} = \Delta G_{\text{enz}} - \Delta G_{\text{solv}}$
3	LEU-ASN	0.6	1.1 1.3 (306ps)	-0.5±0.2 -0.7±0.3
5	PRO-ILE	11.4	11.4 9.7 (306ps)	0.0±0.4 1.7±0.5

**Table II.a.** The best estimates of the free energies for the -CO-NH- substitution by -CF=CH- unit. (ASP25-protonated). All "new" results are from 52ps (or 306psec if stated otherwise) md simulations in each forward and backward perturbation.

bond no.	between	$\Delta G_{\text{enz}}$	$\Delta G_{\text{solv}}$	$\Delta\Delta G_{\text{bind}} = \Delta G_{\text{enz}} - \Delta G_{\text{solv}}$
1	ACE-SER	3.7	3.4	0.3±0.8
2	SER-LEU	4.7	1.1	3.6±1.0
3	LEU-ASN	2.3	2.5 2.0 (306ps)	-0.2±0.4 0.3±0.4
4	ASN-PHE	4.4	5.4	-1.0±1.0
5	PRO-ILE	4.8	3.0 2.6 (306ps)	1.8±0.6 2.2±0.2
6	ILE-VAL	4.2	5.0 5.4 (306ps)	-0.8±0.4 -1.2±0.4
7	VAL-NME	5.7	-0.1	5.8±1.4

**Table II.b.** The best estimates of the free energies for the -CO-NH- substitution by -CF=CH- unit. (ASP125-protonated). All  $\Delta G_{\text{solv}}$  results are from 52psec forward and backward perturbation (or 306ps if stated otherwise).

bond no.	between	$\Delta G_{\text{enz}}$	$\Delta G_{\text{solv}}$	$\Delta\Delta G_{\text{bind}} = \Delta G_{\text{enz}} - \Delta G_{\text{solv}}$
1	ACE-SER	3.8	3.4	0.4±0.9
2	SER-LEU	4.8	1.1	3.7±1.1
3	LEU-ASN	1.8	2.5 2.0 (306ps)	-0.7±0.4 -0.2±0.4
4	ASN-PHE	5.8	5.4	0.4±1.0
5	PRO-ILE	3.6	3.0 2.6 (306ps)	0.6±0.6 1.0±0.2
6	ILE-VAL	7.0	5.0 5.4 (306ps)	2.0±0.9 1.6±0.9
7	VAL-NME	5.2	-0.1	5.3±1.7

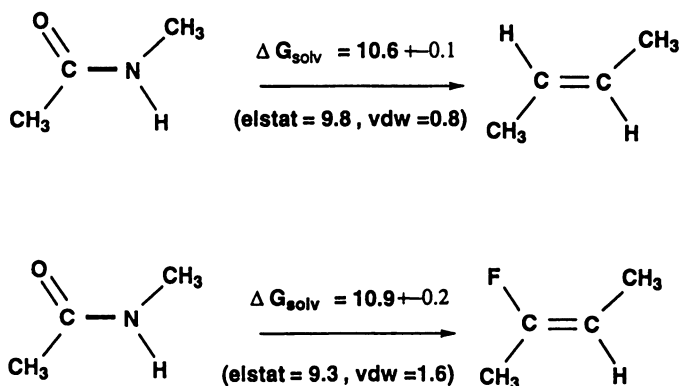


Figure 3. Hydration free energy differences for NMA - trans-butene and for NMA - trans-2-fluoro-butene systems.

For the first system NMA - trans-butene, the hydration free energy difference is  $10.6 \pm 0.1$  kcal/mol, dominated by the electrostatic contribution (9.8 kcal/mol). For the second system this value is  $10.9 \pm 0.2$  kcal/mol, also dominated by a slightly smaller electrostatic contribution (9.3 kcal/mol). The above results show that fluorine atom exhibit hydrophobic properties to almost the same extent as a hydrogen atom when placed in trans-ethylene units.

### Free energy derivatives approach

Another approach which is used for calculating free energy differences is known as the thermodynamic integration (TI) method (2). The free energy difference between two states associated with the limiting values of the  $\lambda$  parameter: 0 and 1 could be also calculated according to the Eq.6:

(6)

$$\Delta G = \int_0^1 \left\langle \frac{\partial H(x, \lambda)}{\partial \lambda} \right\rangle_{\lambda} d\lambda$$

Also in this case the parameter  $\lambda$  - is used to perturb the system from state **a** to state **b** during molecular dynamics simulation. One can also rewrite Eq. 6 into the differential form:

(7)

$$\frac{\partial G}{\partial \lambda} = \left\langle \frac{\partial H(x, \lambda)}{\partial \lambda} \right\rangle_{\lambda}$$

which has been shown to be potentially useful in drug design. (3,4), In Eq.7  $\lambda$  could be any arbitrary parameter describing the thermodynamical state or associated with intermolecular interaction potentials, for example: atomic van der Waals parameters  $R_{ij}^*$ ,  $\epsilon_i$  or partial atomic charge  $q_i$ . The appropriate free energy derivatives for the latter case are as follows:

(8)

$$\frac{\partial G}{\partial q_i} = \left\langle \sum_j \frac{q_j}{\epsilon_0 R_{ij}} \right\rangle = \frac{1}{\epsilon_0 q_i} \langle E_{Coul}(i) \rangle$$

(9)

$$\frac{\partial G}{\partial \epsilon_i} = \left\langle \sum_j \frac{1}{2\epsilon_i} \epsilon_{ij} \left[ \left( \frac{R_{ij}^*}{R_{ij}} \right)^{12} - 2 \left( \frac{R_{ij}^*}{R_{ij}} \right)^6 \right] \right\rangle = \frac{1}{2\epsilon_i} \langle E_{L-J}(i) \rangle$$

(10)

$$\frac{\partial G}{\partial R_i^*} = \left\langle \sum_j \epsilon_{ij} \left[ \frac{12}{R_{ij}^*} \left( \frac{R_{ij}^*}{R_{ij}} \right)^{12} - \frac{12}{R_{ij}^*} \left( \frac{R_{ij}^*}{R_{ij}} \right)^6 \right] \right\rangle$$

where:  $R_{ij}^* = R_i^* + R_j^*$ ,  $\epsilon_{ij} = (\epsilon_i \times \epsilon_j)^{1/2}$ ,  $\langle E_{Coul}(i) \rangle$  - mean coulombic interaction,  $\langle E_{L-J}(i) \rangle$  - mean Lennard-Jones interaction of  $i$ -th atom with the rest of the system. The mean values are easily calculated during molecular dynamics simulation.

The free energy derivatives can be obtained for only one (for example, initial or final) value of the  $\lambda$  parameter. The sign and magnitude of the derivatives show qualitatively whether given interaction parameters associated with a given atom should be decreased or increased in order to lower the free energy of binding. These changes of  $R_i^*$ ,  $\epsilon_i$  or the partial atomic charge  $q_i$  could then be translated into the appropriate chemical modifications of the inhibitor.

The predictive ability of the free energy derivative approach has been suggested by molecular dynamics simulations on simple systems of 18-crown-6 and ion complexes in water solution (4) and in antiparasitic drug design (36). Pang and Kollman (37) have pointed out that free energy derivatives with respect to the interaction parameters could be used more conservatively, for predicting those sites in the molecule which should not undergo any chemical modifications in the drug design process.

The net effect of binding and solvation forces on free energy derivatives has been calculated in the same way as on the free energy differences of binding, i.e. by subtracting the values obtained from "in enzyme" and "in water" simulations:

(11)

$$\Delta \left( \frac{\partial G}{\partial \lambda} \right) = \left( \frac{\partial G}{\partial \lambda} \right)_{enz} - \left( \frac{\partial G}{\partial \lambda} \right)_{solv}$$

If  $\Delta(\partial G/\partial \lambda) > 0$  then the  $\lambda$  parameter should be decreased in order to lower  $\Delta G$ , otherwise  $\lambda$  should be increased.

## Results of the free energy derivatives calculations for JG-365

The results reported here for the free energy derivatives for the inhibitor's atoms were obtained from two 200 psec molecular dynamics simulations of the inhibitor in the enzymatic pocket and in water solution. The initial conformation of the inhibitor in water simulation was the same as used in the free energy calculations and was obtained from long 10 nsec dynamics and using the neural network clustering technique (31). There is a great number of FED data obtained for 131 atoms of the inhibitor from these simulations, and only few general observations will be summarized below.

$\Delta(\partial G / \partial \epsilon)$  are negative for most of the atoms, which suggests that  $\epsilon$  should be increased in order to make the inhibitor interact stronger. The largest negative values are on the Phe and Pro residues. Positive values are observed on the end ACE and NME groups and some hydrogen atoms, mainly  $H_{\alpha}$ .

$\Delta(\partial G / \partial R^*)$  are usually small, negative values. They are positive on most  $H_{\alpha}$  atoms, which means that it would be favorable to have there smaller groups. The smallest values are observed on Leu, NME, and the largest are on Phe or Pro atoms.

$\Delta(\partial G / \partial q)$  are negative for all atoms, which means the need for more positive groups in the inhibitor to increase binding. The smallest values of this derivative are calculated to be on C=O group of the 3rd peptide bond and the largest on the N-H at the end NME group.

It is interesting to look closer at the derivatives for the atoms at peptide bonds number 3 (between P3-P2) and 5 (between P1'-P2'), which could be possibly the most promising for substituting them into ethylene or fluoroethylene units.

At the 3rd peptide bond the  $\Delta(\partial G / \partial \epsilon)$  for O atom is positive which means that smaller  $\epsilon$  value is required, or in other words, a less strongly interacting atom would be favorable at this place, e.g. H or F would be a good choice (Fig.4)). The same is true for the N atom, but for H atom  $\Delta(\partial G / \partial \epsilon)$  is negative pointing to the need for the atom with increased value of  $\epsilon$ , i.e. stronger interacting a hydrogen substituent. The  $\Delta(\partial G / \partial R^*)$  for O and N atoms is positive - atoms with decreased value of  $R^*$  would be more beneficial there, whereas the derivative on H atom indicate that no changes are required for this atom. The  $\Delta(\partial G / \partial q)$  values on all third peptide bond atoms, C,O,N,H are small and negative, which means that the whole group should be changed into a more positive unit.

Inspection of the derivatives on the 5th peptide bond atoms also point out to the need for more positive unit, and smaller and weaker interacting atom at the oxygen position. In contrast derivatives on the nitrogen atom shows that larger and positive atom could replace it (Fig.4).

As one example of different behavior we can cite only the results for the 6th peptide bond. Free energy derivatives point out to the need of larger and stronger interacting group in the place of the oxygen atom, and larger group instead of the nitrogen atom (Fig.4).

The results described above are consistent with those obtained by free energy perturbation calculations, pointing to the 3rd and the 5th peptide bonds as the best candidates for modifications into less interacting isosteric units. Free energy gradient shows also that above peptide bonds and all other could possibly be

## Conclusions

In summary, we think that changing normal peptide inhibitors into their isostere mimetics could possibly lead to new better inhibitors. In order to check this hypothesis we applied two computational techniques - free energy perturbation method (FEP) and free energy

**3rd peptide bond** $\Delta (\delta G/\delta \epsilon)$  O - positive  $\rightarrow$  decrease  $\epsilon$ N - positive  $\rightarrow$  decrease  $\epsilon$ H - negative  $\rightarrow$  increase  $\epsilon$  $\Delta (\delta G/\delta r^*)$  O - positive  $\rightarrow$  decrease  $r^*$ N - positive  $\rightarrow$  decrease  $r^*$ 

H - don't change

 $\Delta (\delta G/\delta q)$  C,O - small negative

N,H - small negative

make the whole group more positive

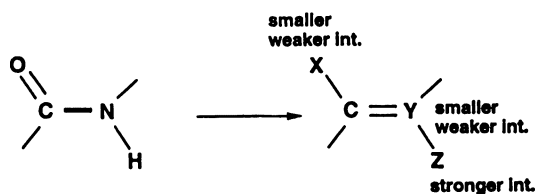
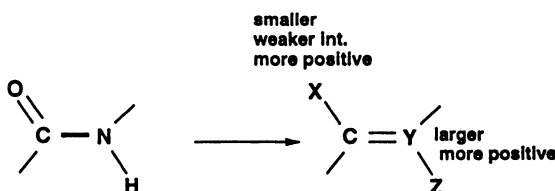
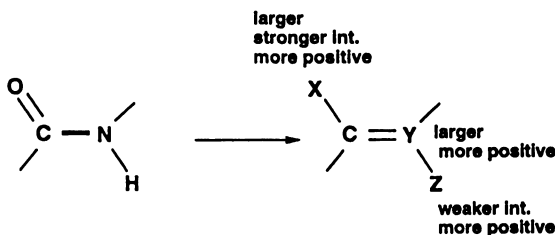
**5th peptide bond****6th peptide bond**

Figure 4 The chemical changes proposed based on the free energy derivatives required for the 3rd, 5th and 6th peptide bond in order to get better binding of the inhibitor.

derivatives (FED), which could be very useful in predicting new compounds in the drug design process. In the case studied here the results of FEP and FED calculations are consistent with each other. The methods suggest that the third (between P3-P2) and the fifth (between P1'-P2') peptide bonds could be replaced by its ethylene or fluoroethylene units leading to better inhibition effects. As a control, we predicted some time ago (8) and also found here that replacing the 4th peptide bond with ethylene should be very unfavorable, and this prediction was confirmed.(24) The effect of 3rd and 5th bond replacement should be additive in nature, because of their relatively large distance apart. Our hope is that such new compounds could be useful, or at least not ignored in the search of better inhibitors. Additionally, we have shown in our calculations that fluorine atom exhibit hydrophobic property, and it could be useful in design of inhibitors, where changing polarity is important.

We would like to stress that the results described here are predictive and qualitative in nature, since many of the proposed isosteric mimetic inhibitors have not been synthesized and tested experimentally yet.

### Acknowledgements

We are glad to acknowledge research support of the NIH (GM29072 to P.A.K.) and NSF (NSF-INT - 9115796). P.C. was partially supported by KBN funds through the Department of Chemistry, University of Warsaw, within the grant BW-1301/36/95. Some of these calculations were carried out at the Pittsburgh and San Diego Supercomputer Centers through supercomputer support provided to P.A.K. Calculations were also carried out at the Interdisciplinary Center for Modeling of the University of Warsaw. We also acknowledge the UCSF Computer Graphics Laboratory (supported by RR-1081 to T. Ferrin).

### Literature Cited

- (1) Bash, P. A.; Singh, U. C.; Langridge, R.; Kollman, P. A. *Science* **236**, 564, (1987).
- (2) Beveridge, D. L.; DiCapua, F. M. In *Computer Simulation of Biomolecular Systems, Theoretical and Experimental Applications*; van Gunsteren, W. F., Weiner, P. K. Eds.; ESCOM: Leiden, 1989; p.1.
- (3) Pearlman, D. A. *J. Comp. Chem.* **1994**, *15*, 105.
- (4) Cieplak, P.; Pearlman, D. A.; Kollman, P. A. *J. Chem. Phys.* **1994**, *101*, 627.
- (5) Johnson, M. I.; Hoth, D. F. *Science* **1993**, *260*, 1286.
- (6) Roberts, N. A.; Martin, J. A.; Kinchington, D.; Broadhurst, A. V.; Craig, J. C.; Duncan, I. B.; Galpin, S. A.; Handa, B. K.; Kay, J.; Krohn, A.; Lambert, R. W.; Merrett, J. H.; Mills, J. S.; Parkes, K. E. B.; Redshaw, S.; Ritchie, A. J.; Taylor, D. L.; Thomas, G. J.; Machin, P. J. *Science* **1990**, *248*, 358.
- (7) McCarrick, M. A.; Kollman, P. A. In *Methods in Enzymology* **1994**, *241*, 370.
- (8) Cieplak, P.; Kollman, P. A. *J. Comp.-Aided Mol. Design* **1993**, *7*, 291.
- (9) Swein, A. L.; Miller, M. M.; Green, J.; Rich, D. H.; Schneider, J.; Kent, S. B. H.; Wlodawer, A. *Proc. Natl. Acad. Sci. U.S.A.* **1990**, *87*, 8805.
- (10) Miller, M. M.; Schneider, J.; Sathyanarayanan, B. K.; Toth, M. V.; Marshall, G. R.; Clawson, L.; Selk, L.; Kent, S. B. H.; Wlodawer, A. *Science* **1989**, *246*, 1149.
- (11) Jaskolski, M.; Tomasselli, A. G.; Sawyer, T. K.; Staples, D. G.; Heinrichson, R. L.; Schneider, J.; Kent, S. B. H.; Wlodawer, A. *Biochemistry* **1991**, *30*, 1600.
- (12) Holloway, M. K.; Wai, J. M.; Halgren, T. A.; Fitzgerald, P. M. D.; Vacca, J. P.; Dorsey, B. D.; Levin, R. B.; Thompson, W. J.; Chen, L. J.; deSolms, S. J.; Gaffin, N.; Ghosh, A. K.; Giuliani, E. A.; Graham, S. L.; Guare, J. P.; Hungate,



- R. W.; Lyle, T. A.; Sanders, W. M.; Tucker, T. J.; Wiggins, M.; Wiscourt, C. M.; Woltersdorf, O. W.; Young, S. D.; Darke, P. L.; Zugay, J. A. *J. Med. Chem.* **1995**, *38*, 30.
- (13) Schechter, I.; Gerger, A. *Biochem. Biophys. Res. Commun.* **1967**, *27*, 157.
- (14) Farmer, P. S. In *Drug Design*; Ariens, E. J. Ed.; Academic Press: New York, 1980; Vol X, pp 119-143.
- (15) Moore, G. J. *TIPS*, **1994**, *15*, 124.
- (16) Olson, G. L.; D.R.Bolin, D. R.; Bonner, M. P.; Bös, M.; Cook, C. M.; Fry, D. C.; Graves, B. J.; Hatada, M.; Hill, D. E.; Kahn, M.; Madison, V. S.; Rusiecki, V. K.; Sarabu, R.; Sepinwall, J.; Vincent, G. P.; Voss, M. E. *J. Med. Chem.* **1993**, *36*, 3039.
- (17) Boros, L G.; DeCorte, B.; Gimi, R. H.; Welch, J. T.; Wu, Y.; Handschumacher, R. E. *Tetrahedron Lett.* **1994**, *35*, 6033.
- (18) Abraham, R. J.; Ellison, S. L. R.; Schonholzer, P.; Thomas, W. A. *Tetrahedron*, **1986**, *42*, 2101.
- (19) Hann, M. M.; Sammes, P. G. *J. Chem. Soc., Chem. Comm.* **1980**, 234.
- (20) Cox, M. T.; Heaton, D. W.; Horbury, J. *J. Chem. Soc., Chem. Comm.* **1980**, 799.
- (21) Cox, M. T.; Gormley, J. J.; Hayward, C. F.; Petter, N. N. *J. Chem. Soc., Chem. Comm.* **1980**, 800.
- (22) Hann, M. M.; Sammes, P. G.; Kennewell, P. D.; Taylor, J. B. *J. Chem. Soc., Perkin I*, **1982**, 307.
- (23) Sham, H. L.; Betebenner, D. A.; Wideburg, N. E.; Saldivar, A. C.; Kohlbrenner, W. E.; Craig-Kennard, A.; Vasavanonda, S.; Kempf, D. J.; Clement, J. J.; Erickson, J. E.; Plattner, J. J.; Norbeck, D. W. *FEBS Lett.* **1993**, *329*, 144.
- (24) Keenan, R. M.; Eppley, D. F.; Tomaszek, Jr., Th. A. *Tetrahedron Lett.* **1995**, *36*, 819.
- (25) Allen, M. P.; Tildesley, D. J. *Computer Simulation of Liquids*; Clarendon Press: Oxford, 1987.
- (26) AMBER version 4.0, (1991): Pearlman, D. A.; Case, D. A. Caldwell, J.; Seibel, G. L.; Singh, U. C.; Weiner, P.; Kollman, P. A. *Department of Pharmaceutical Chemistry, University of California, San Francisco*.
- (27) Weiner, S. J.; Kollman, P. A.; Nguyen, D. T.; Case, D. *J. Comput. Chem.* **1986**, *7*, 230.
- (28) Cornell, W.; Cieplak, P.; Bayly, C. I.; Gould, I.; Merz, Jr., K. M.; Ferguson, D.; Spellmeyer, D. C.; Fox, T.; Caldwell, J. W.; Kollman, P. A. *J. Am. Chem. Soc.* **1995**, *117*, 5179.
- (29) Kollman, P. A. *Chem. Rev.*, **1993**, *93*, 2395.
- (30) Chen, X.; Tropsha, A. *J. Med. Chem.* **1995**, *38*, 42048.
- (31) Radomski, J. P.; Cieplak, P. "Conformational states of JG-365 in water solution", in preparation.
- (32) Karpen, M. E.; Tobias, D. J.; Brooks, C. L. *Biochemistry*, **1993**, *32*, 412.
- (33) Murcko, M. A.; Rao, B. G. *J. Comp. Chem.* **1993**, *14*, 1446.
- (34) Bayly, C.; Cieplak, P.; Cornell, W.; Kollman, P. A. *J. Phys. Chem.* **1993**, *97*, 10269.
- (35) W.Cornell, P.Cieplak, C.Bayly, P.A.Kollman *J.Am.Chem.Soc.*, **115**, 9620, (1993).
- (36) Cieplak, P.; Kollman, P. A. *J. Mol. Recognition* **1995**, in press.
- (37) Y.-P.Pang, Y.-P.; P.A.Kollman, P. A. In *Perspectives in Drug Discovery and Design*; Muller, K.; Ed.; ESCOM: Leiden, 1995; Vol. 3, pp.106-122 .

## Chapter 12

# Mechanistic Studies of the Prenyl Transfer Reaction with Fluorinated Substrate Analogs

C. Dale Poulter

Department of Chemistry, University of Utah, Salt Lake City, UT 84112

Fluorinated analogs for allylic diphosphate substrates are important tools for studying the chemical mechanisms of enzyme catalyzed prenyl transfer reactions. Syntheses were developed for a series of mono-, di-, and trifluoromethyl geranyl and farnesyl derivatives. Comparisons of the effects of fluorine substitutions on the rates of prenyl transfer with those of model displacement reactions indicated that the enzymatic transformations proceeded through highly electrophilic transition states. Prenyl transfer to weakly nucleophilic carbon-carbon double bond acceptors are stepwise, while those to more nucleophilic sulfhydryl acceptors appear to be enforced.

Isoprenoid compounds constitute the most chemically diverse group of metabolites found in nature. Over 23,000 individual molecules are known, and the list expands substantially each year. They are widely distributed in nature and perform an amazing variety of essential roles for their host organisms. Some of the commonly encountered classes of isoprenoids are mono- and sesquiterpenes that function as attractants and defensive agents in plants, fungi, and insects. Sterols are important constituents of eukaryotic membranes and are essential reproductive hormones in animals. Carotenoids are photoprotective agents in plants and are essential for vision. Ubiquinones are universal redox couples in cells. The lipid components of archaeobacterial membranes are saturated C<sub>20</sub> isoprenoid chains. Eukaryotic prenylated proteins are the most recently discovered class of isoprenoid compounds. These molecules perform a variety of roles, including serving as structural components of nuclear membranes, as switches in signal transduction, and as agents to direct the traffic of vesicles within eukaryotic cells. Isoprenoid compounds are found in eukaryotic, bacterial, and archaeobacterial organisms, representing all three major life forms. The functions that the molecules perform are so universal and their occurrence so widespread that it is likely that metabolites from the isoprenoid pathway are essential for the viability of all organisms.

0097-6156/96/0639-0158\$15.00/0  
© 1996 American Chemical Society

## Prenyl Transfer Reactions

The major building reactions in the isoprenoid pathway are catalyzed by prenyltransferases. The prenyl transfer reaction attaches the hydrocarbon moiety of linear allylic isoprenoid diphosphates to an electron-rich group in an acceptor substrate with the concomitant expulsion of inorganic pyrophosphate (PP<sub>i</sub>) and a proton (1). Individual prenyltransfer reactions are catalyzed by enzymes that exhibit high selectivity for the chain length and double bond stereochemistry of the allylic substrate and for the acceptor (2). A variety of electron-rich groups are alkylated by prenyltransferases, including the carbon-carbon double bond in isopentenyl diphosphate (IPP) (1), the aromatic ring in 4-hydroxybenzoic acid (3), the hydroxyl groups in 1-phosphoglycerol (4), the amino moiety in adenosine residues (5), and the sulfhydryl group of cysteine residues in proteins (6) (see Scheme 1). In each instance, a specific prenyltransferase has evolved to catalyze each reaction. While phylogenetic relationships are not well established among prenyltransferases that require different acceptors, isoprenyl diphosphate synthases that catalyze chain elongation by alkylation of IPP form a sub-family that apparently evolved from a common ancestor (7).

Prenyl transfer reactions can be regarded as nucleophilic substitutions where the diphosphate moiety is replaced by an electron-rich acceptor as illustrated in Scheme 2. Within this framework are several possible mechanisms ranging from a stepwise process with carbocationic intermediates (steps a, b, and d) to a concerted displacement through an early transition state where there is no significant development of positive charge in the allylic moiety of the isoprenoid diphosphate with concomitant removal of the proton (step e). Which path is traversed depends on a variety of factors, including the nucleophilicity of the acceptor, the ability of the allylic moiety to stabilize developing positive charge, and the structure of the active site. For prenyl transfer reactions, the electronic properties of the isoprenoid substrates are similar. All are allylic diphosphate esters with two alkyl substituents on the distal carbon in the double bond. The combination of a strong leaving group and the powerful stabilizing effect of the alkyl substituents on the resulting allylic carbocation are favorable for an electrophilic mechanism for the alkylation. However, the nucleophilicity of the acceptor also has a major influence on the course of the reaction. For prenyl transfer reactions where the acceptor is a weak nucleophile, such as during chain elongation by alkylation of the carbon-carbon double bond in IPP, one might anticipate a late transition state with substantial development of positive charge in the allylic moiety, resulting in stepwise alkylation ( steps a, b, and d) or a concerted alkylation (steps c and d) through a late charge separated transition state. However, when the acceptor is a thiol or perhaps thiolate, its nucleophilicity might result in a much earlier transition state (also path c) with substantially less charge separation. If elimination of the proton is synchronous with alkylation, steps b and d in a stepwise alkylation would merge into f, while steps c and d in the concerted alkylation would merge into step e.

Pronounced biological effects are often seen when hydrogen atoms in a natural metabolite are replaced by fluorine. Although fluorine (van der Waals radius ~1.35 Å) is not isosteric with hydrogen (van der Waals radius ~1.2 Å), the difference in steric bulk does not normally preclude binding. However, fluorine is the most electronegative of the elements,

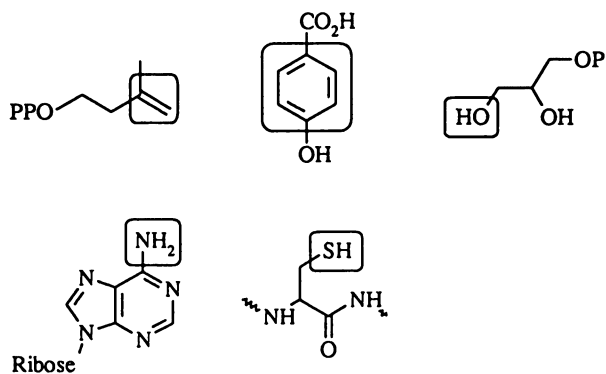
and the C-F bond is considerably more polar than its C-H counterpart. Substitution of a hydrogen atom by fluorine can lead to perturbations in binding that can either enhance or decrease the affinity of a prenyltransferase for its substrate. The effect of replacing a hydrogen near the putative developing allylic carbocation in an electrophilic alkylation by fluorine should have a profound influence on the reaction, especially if the substitutions are made on a carbon adjacent to the carbocationic center in order to maximize inductive effects and eliminate resonance interactions. The magnitude of the effect should parallel the extent to which positive charge develops in the allylic moiety at the transition state during alkylation of the acceptor. Fluorinated analogs of the isoprenoid substrates for prenyltransferases that meet these criteria have provided important insights about the mechanisms of the enzyme catalyzed reactions.

### Synthesis of Fluorinated Allylic Isoprenoid Substrates

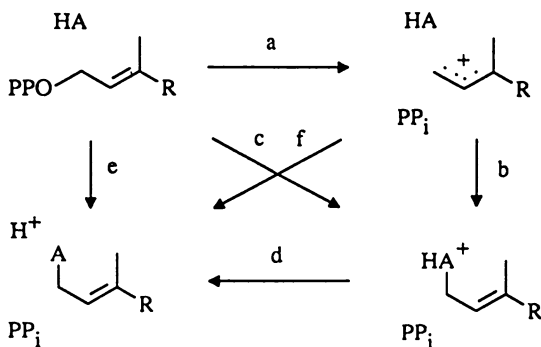
There are three hydrogen bearing carbons in allylic isoprenoid diphosphates such as dimethylallyl diphosphate (DMAPP), geranyl diphosphate (GPP), and farnesyl diphosphate (FPP) that meet the criteria of maximizing the inductive effects of a fluorine substituent on developing positive charge in the related allylic carbocations without accompanying complications from resonance stabilization. These are C(2), C(4), and the methyl group at C(3). Analogs with fluorine at C(2) are the easiest to prepare, but that position is particularly sensitive to substitution for some prenyltransferases. The least sensitive location is the C(3) methyl, where a wide variety of other alkyl substituents are tolerated (1). Several approaches are described for synthesis of DMAPP, GPP, and FPP analogs with one, two, and three fluorine atoms in the C(3) methyl.

**Dimethylallyl Analogs.** Analogs of DMAPP were prepared from the corresponding ketones as shown in Scheme 3. The Horner-Emmons modification of the Wittig reaction was used to convert 1-monofluoro, 1,1-difluoro, and 1,1,1-trifluoroacetone to a mixture of *E* and *Z* isomers of the corresponding  $\alpha,\beta$ -unsaturated esters (1: Y = CH<sub>2</sub>F, CHF<sub>2</sub>, CF<sub>3</sub>; Z = CH<sub>3</sub>) (8). The mixture of esters proved to be difficult to separate. However, after reduction with diisobutyl aluminum hydride (DIBAL), the mixture of alcohols was purified as individual isomers by chromatography on silica gel. The fluorinated dimethylallyl alcohols (2: Y = CH<sub>2</sub>F, CHF<sub>2</sub>, CF<sub>3</sub>; Z = CH<sub>3</sub>) were then converted into their respective diphosphate esters by the displacement procedure of Davisson *et al.* (9).

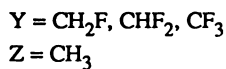
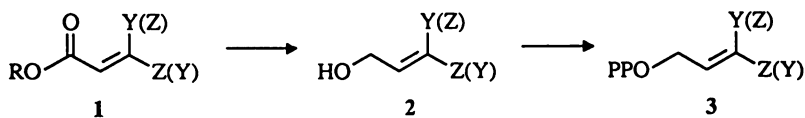
**Geranyl Analogs.** Poulter *et al.* (10) investigated routes for a stereoselective synthesis of the mono-, di-, and trifluoromethyl analogs of GPP. Their initial approach was based on the stereoselective syn addition of an organo-cuprate to the appropriately substituted  $\alpha,\beta$ -unsaturated propargylic ester (Scheme 4). The mono- and trifluoromethyl derivatives of 4 (R = C<sub>2</sub>H<sub>5</sub>; Y = CH<sub>2</sub>F, CF<sub>3</sub>) were successfully synthesized as shown in Scheme 5. However, attempts to prepare the difluoromethyl derivative (4: R = C<sub>2</sub>H<sub>5</sub>; Y = CHF<sub>2</sub>) by oxidation of alcohol 4 (R = C<sub>2</sub>H<sub>5</sub>; Y = CH<sub>2</sub>OH) followed by treatment with DAST or (diethylamino)(dimethylamino)sulfur difluoride were unsuccessful. The stereoselective alkylation of 4 (R = CH<sub>2</sub>Ph; Y = CF<sub>3</sub>) went smoothly. Ester 1 (R = CH<sub>2</sub>Ph; Y = CF<sub>3</sub>; Z = C<sub>6</sub>H<sub>11</sub>) was then converted to the corresponding diphosphate as illustrated in Scheme 3. In contrast, alkylation of monofluoro ester 4 (R = C<sub>2</sub>H<sub>5</sub>; Y = CH<sub>2</sub>F) was capricious, and new routes were sought to synthesize the mono- and difluoro analogs of GPP.



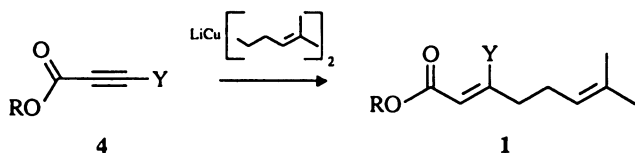
Scheme 1. Common Prenyl Acceptors.



Scheme 2. Mechanisms for the Prenyl Transfer Reaction.

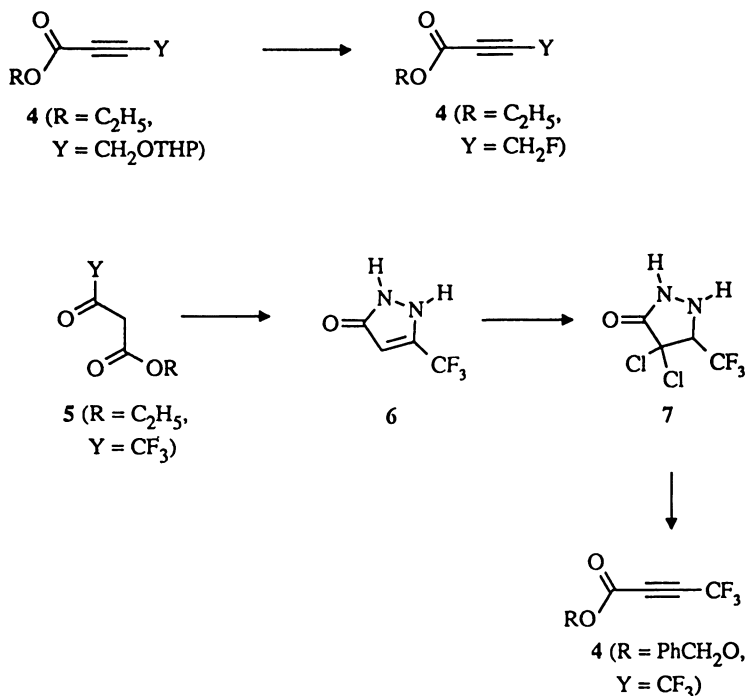


Scheme 3. Synthesis of Dimethylallyl Analogs.



**Scheme 4.** Stereoselective Synthesis of Geranyl Analogs by Addition of Cuprates to  $\alpha,\beta$ -Unsaturated Esters.

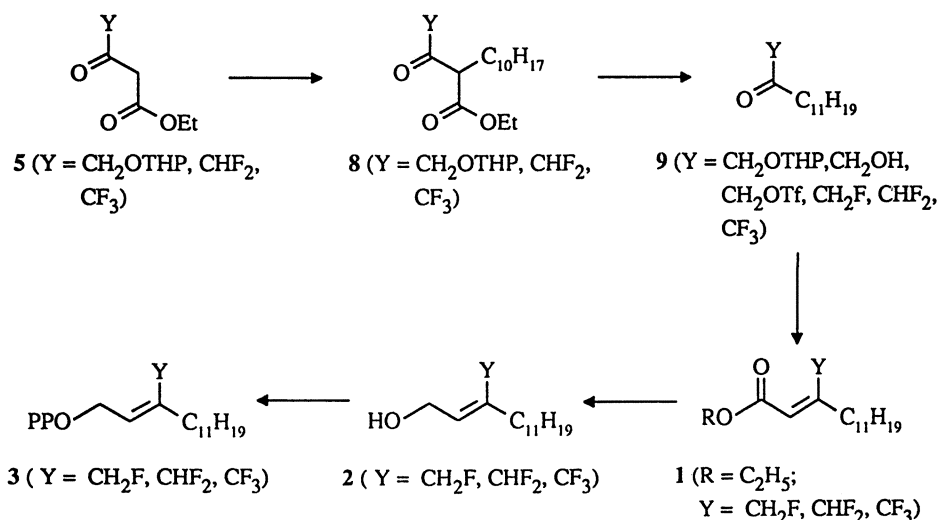
The monofluoro analog of GPP was prepared by addition of lithium di-(4-methyl-3-pentenyl)cuprate to the tetrahydropyranyl derivative of **4** ( $R = C_2H_5$ ;  $Y = CH_2OTHP$ ) to give a 95:5 *Z/E* mixture of **1** ( $R = C_2H_5$ ;  $Y = CH_2OTHP$ ). The isomers were separated by chromatography on silica gel. Attempts to remove the THP moiety in order to fluorinate the hydroxymethyl group before reduction of the ester gave the corresponding  $\gamma$ -lactone as the only product. As an alternative, **1** ( $R = C_2H_5$ ;  $Y = CH_2OTHP$ ;  $Z = C_6H_{11}$ ) was reduced with hydride, and the resulting allylic alcohol was acetylated before treatment with pyridinium *p*-toluenesulfonate to remove the blocking group. This reaction gave a mixture of acetate regioisomers, presumably from migration of the acetyl moiety, and the progress of the reaction had to be monitored carefully to obtain a good yield of the desired monoacetate. Treatment of the acetate with (diethylamino)(dimethylamino)sulfur difluoride followed by hydrolysis gave geraniol derivative *Z*-**2** ( $Y = CH_2F$ ;  $Z = C_6H_{11}$ ), which was then converted to the corresponding diphosphate.



**Scheme 5.** Synthesis of Fluorinated  $\alpha,\beta$ -Unsaturated Esters.

The difluoro analog of GPP was synthesized from difluoroacetic acid. Treatment of the lithium salt of the acid with (4-methyl-3-pentenyl)magnesium bromide gave 1,1-difluoro-6-methyl-5-hepten-2-one in modest (35%) yield. The ketone was then converted to ester **1** ( $R = C_2H_5$ ;  $Y = CHF_2$ ;  $Z = C_6H_{11}$ ) as described for the dimethylallyl derivative, to afford a 72:28 mixture of *Z* and *E* isomers. The esters were separated by chromatography on silica gel, and the *Z* isomer was converted to diphosphate **3** ( $Y = CHF_2$ ;  $Z = C_6H_{11}$ ) as outlined in Scheme 3.

**Farnesyl Analogs.** A general route to allylic isoprenoid diphosphate analogs of different chain lengths with a variety of replacements for the C(3) methyl group was developed for synthesis of the mono-, di-, and trifluoromethyl derivatives of FPP. The approach is outlined in Scheme 6. In each case, a  $\beta$ -ketoester (**5**) was alkylated with geranyl bromide and then converted to ketone **9** (**11**). In the fluoromethyl series, **5** ( $Y = CH_2OTHP$ ) was alkylated to yield **8** ( $Y = CH_2OTHP$ ), followed by decarboxylation to give ketone **9** ( $Y = CH_2OTHP$ ). The blocking group was removed, and the alcohol was treated with triflic anhydride to activate the hydroxymethyl moiety. Treatment of the triflate with *n*-tetrabutylammonium fluoride gave fluoroketone **9** ( $Y = CH_2F$ ). Fluorinated derivatives of **5** ( $Y = CHF_2, CF_3$ ) were used to synthesize the di- and trifluoromethyl analogs. Ethyl difluoroacetoacetate (**5**;  $Y = CHF_2, CF_3$ ) was synthesized by a Reformatsky condensation of ethyl bromoacetate with ethyl difluoroacetate. The trifluoromethyl analog was available commercially. Alkylation of the fluorinated acetoacetates with geranyl bromide was sluggish, presumably because of the reduced nucleophilicity of the fluorinated enolates. Both acetoacetates were decarboxylated with lithium chloride in aqueous dimethylformamide at reflux. The fluorinated ketones (**9**;  $Y = CH_2F, CHF_2, CF_3$ ) were first converted to esters **1** ( $R = C_2H_5$ ;  $Y = CH_2F, CHF_2, CF_3$ ;  $Z = C_{11}H_{19}$ ) and then to the mono-, di-, and trifluoromethyl analogs (**3**;  $Y = CH_2F, CHF_2, CF_3$ ;  $Z = C_{11}H_{19}$ ) as previously described for DMAPP and GPP analogs.



**Scheme 6.** Synthesis of Farnesyl Analogs.

## Mechanistic Studies of the Prenyl Transfer Reaction

Nucleophilic substitution reactions are among the most studied transformations in organic chemistry. Out of these studies have come many of the tools used to establish the mechanisms of organic reactions. There are, however, several important limitations that one encounters when attempting to elucidate the mechanism of a nucleophilic displacement that occurs within the catalytic site of an enzyme. For example, stereochemistry, which can sometimes distinguish between concerted and non-concerted displacements, may be dictated solely by the binding properties of the enzyme rather than chemical demands of the reaction. Many parameters such as solvent or ionic strength cannot be adjusted within the catalytic site of an enzyme to provide information about transition state structure, and changes in temperature are usually restricted to a rather narrow range. One approach that has proved useful is a comparison of the reactivities of substrate analogs used as replacements for the normal substrate in an enzyme catalyzed reaction with those of closely related model compounds whose mechanistic properties are well established through linear free energy correlations. In this regard, the ability of fluorine to destabilize positively charged transition states through its powerful electron withdrawing inductive effect relative to those of the corresponding hydrogen species has provided important insights about the chemical mechanisms of prenyl transfer reactions with olefinic and sulphydryl acceptors.

**Model Studies.** To calibrate the effects of substitution at C(3) on the reactivity of an allylic isoprenoid moiety, the first order rate constants,  $k_s$ , for solvolysis of substituted dimethylallylic 4-methoxybenzene sulfonate derivatives were measured in a mixture of dioxane and water (12). As illustrated in Table I, the substituent at C(3) exerted a

**Table I. Relative Rates for Solvolysis and Nucleophilic Capture by Azide**

Substituent	$k_s, s^{-1}$	$k_{Nu}, s^{-1}$
CH <sub>3</sub>	1	1
H	$1.5 \times 10^{-3}$	0.1
CH <sub>2</sub> F	$9.1 \times 10^{-4}$	$6.1 \times 10^{-2}$
CHF <sub>2</sub>	$7.4 \times 10^{-6}$	$1.2 \times 10^{-2}$
CF <sub>3</sub>	$6.7 \times 10^{-7}$	$6.5 \times 10^{-3}$

tremendous effect on the rate of the reaction. The least reactive derivative (R = CF<sub>3</sub>) was approximately a million times less reactive than the parental dimethylallyl 4-methoxybenzene sulfonate (R = CH<sub>3</sub>). The correlation between a decrease in reactivity with an increase in the electron-withdrawing power of substituent at C(3) is consistent with the formation of a positively charged transition state, as expected for generation of an allylic carbocation that subsequently reacts with water to form substitution products.

When sodium azide was added, the rates for the solvolysis of the 4-methoxybenzene sulfonates increased. The effect was small for the dimethylallyl moiety, but increased with the introduction of increasingly electron-withdrawing groups at C(3). The second order



rate constants for added azide as a nucleophile,  $k_{Nu}$ , were calculated from  $k_{obs}$  and  $k_s$ , as shown in Equation 1. As observed for solvolysis in the absence of azide, the rate for

$$k_{obs} = k_s + k_{Nu} \quad (1)$$

reaction with azide decreased as increasingly electron-withdrawing groups were substituted at C(3). However, the magnitude of the effect was compressed from a million-fold for solvolysis to a thousand-fold for reaction with azide. While this trend indicates a highly electrophilic transition state for the azide reaction, the compression suggests a shift in the mechanism from a stepwise process for solvolysis to an enforced reaction when azide is the nucleophile. A shift in mechanism is consistent with the much higher nucleophilicity of azide than water (13).

**Enzyme Catalyzed Reactions. Farnesyl Diphosphate Synthase.** Farnesyl diphosphate synthase (FPPSase) is an ubiquitous enzyme that catalyzes the chain elongation of DMAPP to FPP (7). The reaction occurs in two steps as shown in Scheme 7. The first is the synthesis of GPP by addition of IPP to DMAPP, followed by the addition of IPP to GPP to form FPP. The effect of substitution of C(3) on the rate of the 1'-4 condensation reaction for addition of IPP to GPP was studied for the reaction catalyzed by avian FPPSase. As shown in Table II, introduction of electron-withdrawing substituents at C(3)

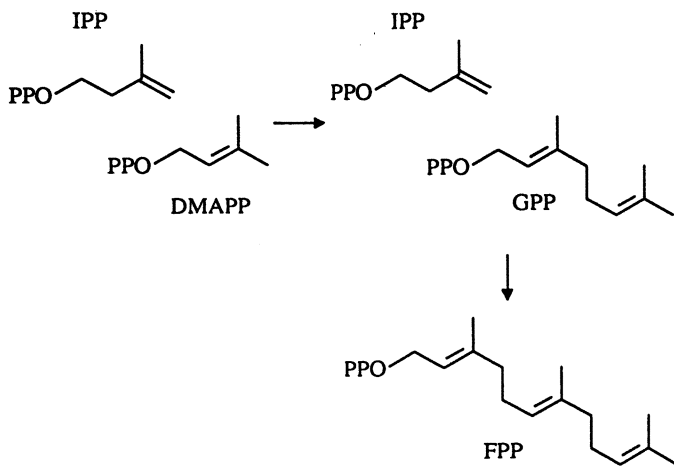
**Table II. Relative Catalytic Rate Constants for Prenyl Transfer**

Substituent	$k_{FPPSase}, s^{-1}$	$k_{PFTase}, s^{-1}$
CH <sub>3</sub>	1	1
H	$2.3 \times 10^{-4}$	$1.5 \times 10^{-2}$
CH <sub>2</sub> F	$3.7 \times 10^{-4}$	$1.5 \times 10^{-1}$
CHF <sub>2</sub>	$4.0 \times 10^{-8}$	$6.3 \times 10^{-3}$
CF <sub>3</sub>	$7.7 \times 10^{-9}$	$7.6 \times 10^{-4}$

reduced the rates for the prenyl transfer reaction catalyzed by FPPSase in a manner similar to that seen for solvolysis of the 4-methoxybenzene sulfonates (14). In particular, a Hammett plot of the logarithm of the solvolysis rate constants, normalized to the rate when R = CH<sub>3</sub>, versus the rates for the 1'-4 condensation reaction shown in Figure 1 gave an excellent correlation with a slope of 0.7. These results suggest that the development of positive charge in the allylic moieties is similar for both the model solvolysis reaction and 1'-4 condensation and that allylic carbocations are intermediates in both reactions. These results are also consistent with the carbocationic rearrangements seen for bisubstrate analogs of IPP and DMAPP when incubated with FPPSase. In this case, carbocationic intermediates are necessary for the rearrangements to proceed.

**Protein Farnesyltransferase.** Protein farnesyltransferase (PFTase) catalyzes the posttranslational modification of several eukaryotic proteins. In each case a cysteine located at the fourth position from the carboxyl terminus of the protein substrate is alkylated by FPP to form a farnesyl thioether. The enzyme prefers FPP over other

isoprenoid diphosphates but accepts a wide variety of proteins and small peptides as substrates. We studied the alkylation of cysteine in the pentapeptide dansyl-Gly-Cys-Val-Ile-Ala by FPP (see Scheme 8) and fluorinated farnesyl analogs in order to determine the mechanism of the alkylation reaction (15). A Hammett plot of solvolysis rate constants  $k_s$  versus  $k_{cat}$  for alkylation of cysteine by yeast protein farnesyltransferase was also linear, but the slope was only 0.3, indicative of substantially less developed positively charged



**Scheme 7.** Synthesis of FPP from DMAPP by FPPSase.

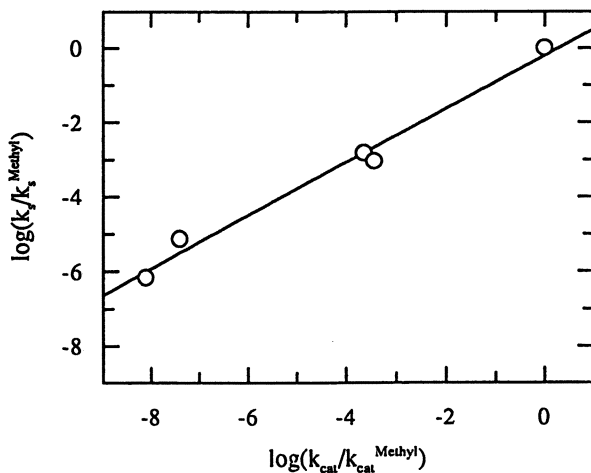
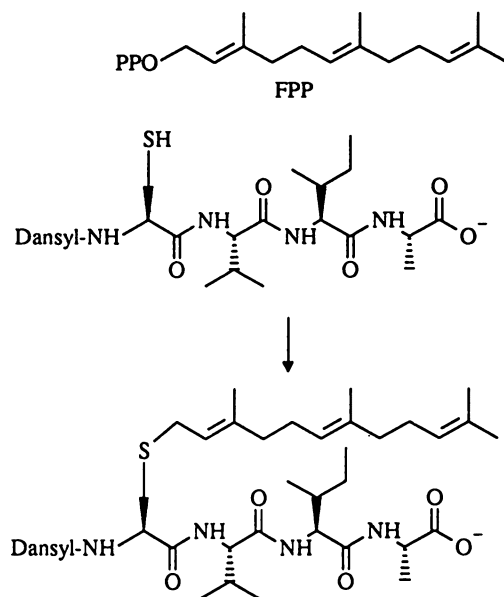


**Figure 1.** A Hammett Plot of the Relative Kinetic Constants for Solvolysis of Dimethylallyl 4-Methoxybenzene Sulfonates versus the Catalytic Constants for Addition of Geranyl Analogs to IPP.



**Scheme 8.** Modification of Cysteine by FPP.

transition state for prenyl transfer to a strongly nucleophilic acceptor. However, a similar plot of nucleophilic rate constants,  $k_{\text{Nu}}$  against  $k_{\text{cat}}$  for the farnesylation of cysteine was linear and gave a slope of 0.6, see Figure 2. Thus, the rate constants for a prenyl transfer reaction involving a highly nucleophilic acceptor such as thiol, or perhaps thiolate, correlated with an enforced reaction where the allylic moiety has considerable electrophilic character at the transition state and is stabilized by participation of the nucleophile.

## Conclusions

Fluorinated analogs of the allylic diphosphate substrates for prenyl transfer reactions, which form the backbone of the isoprenoid biosynthetic pathway, are powerful tools for elucidating the mechanisms of the reactions. A wide variety of fluorinated allylic diphosphates can be synthesized, and the compounds serve as alternate substrates for prenyltransferases. Linear free energy comparisons between model solvolysis reactions that proceed through allylic carbocationic species by established mechanisms and the enzymatic reactions indicate that the alkylation of carbon-carbon double bonds during 1'-4 chain elongation is a stepwise process, while alkylation of the sulfhydryl moiety in cysteine is an enforced reaction with substantial electrophilic character in the allylic moiety at the transition state.

**Acknowledgments.** The author wishes to thank the coworkers whose names appear in the cited literature for their essential contributions to this project. This research was supported by NIH grant GM 21328.

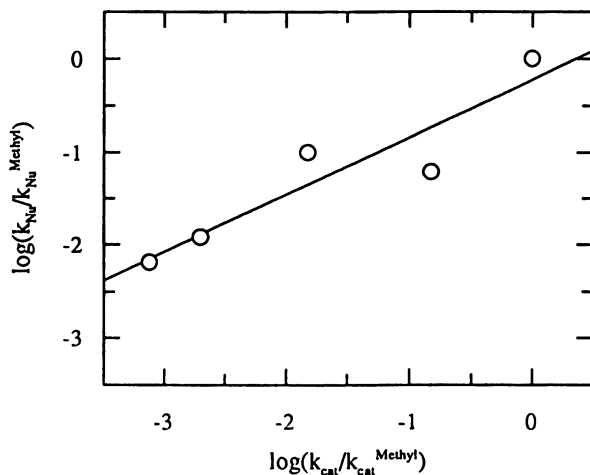


**Figure 2.** A Hammett Plot of the Relative Kinetic Constants for Azide Addition to Dimethylallyl 4-Methoxybenzene Sulfonates versus the Catalytic Constants for Alkylation of Cysteine by FPP Analogs.

### Literature.

- 1) Poulter, C. D.; Rilling, H. C. In *Biosynthesis of Isoprenoid Compounds*; Porter, J. W.; Spurgeon, S. L., Ed.; John Wiley and Sons: New York, 1981, pp 162-224.
- 2) Poulter, C. D.; Rilling, H. C. *Acc. Chem. Res.* **1978**, *11*, 307-313.
- 3) Ashby, M. N.; Edwards, P. A. *J. Biol. Chem.* **1990**, *265*, 13157-13164.
- 4) Chen, A.; Zhang, D.; Poulter, C. D. *J. Biol. Chem.* **1993**, *268*, 21701-21705.
- 5) Caillet, J.; Droogmans, L. *J. Bacteriol.* **1988**, *170*, 4147-4152.
- 6) Mayer, M. P.; Prestwich, G. D.; Dolence, J. M.; Bond, P. D.; Wu, H.; Poulter, C. D. *Gene* **1993**, *132*, 41-47.
- 7) Chen, A.; Kroon, P. A.; Poulter, C. D. *Prot. Sci.* **1994**, *3*, 600-607.
- 8) Gebler, J. C.; Woodside, A. B.; Poulter, C. D. *J. Am. Chem. Soc.* **1992**, *114*, 7354-7360.
- 9) Davisson, V. J.; Woodside, A. B.; Neal, T. R.; Stremler, K. E.; Muehlbacher, M.; Poulter, C. D. *J. Org. Chem.* **1986**, *51*, 4768-4779.
- 10) Poulter, C. D.; Wiggins, P. L.; Plummer, T. L. *J. Org. Chem.* **1981**, *46*, 1532-1538.
- 11) Dolence, J. M.; Poulter, C. D. *Tetrahedron* **1996**, *52*, 119-130.
- 12) Rodriguez, C. L. *PhD Dissertation* **1990**, University of Utah.
- 13) Mayer, H.; Patz, M. *Angew. Chem. Int. Ed. Engl.* **1994**, *33*, 938-957.
- 14) Poulter, C. D.; Wiggins, P. L.; Le, A. T. *J. Am. Chem. Soc.* **1981**, *103*, 3926-3927.
- 15) Dolence, J. M.; Poulter, C. D. *Proc. Natl. Acad. Sci., USA* **1995**, *92*, 5008-5011.

## Chapter 13

# Elucidation of the Mechanism of Inhibition of Human Immunodeficiency Virus 1 Protease by Difluorostatones

D. Schirlin<sup>1</sup>, J. M. Rondeau<sup>1</sup>, B. Podlogar<sup>2</sup>, C. Tardif<sup>1</sup>, C. Tarnus<sup>1</sup>,  
V. Van Dorsselaer<sup>1</sup>, and R. Farr<sup>3</sup>

<sup>1</sup>Strasbourg Center, Marion Merrell Dow Research Institute,  
16 rue d'Ankara, 67080 Strasbourg Cedex, France

<sup>2</sup>R. W. Johnson Pharmaceutical Research Institute, Route 202,  
P.O. Box 300, Raritan, NJ 08869

<sup>3</sup>Cincinnati Center, Marion Merrell Dow Research Institute,  
2110 East Galbraith Road, Cincinnati, OH 45200

Short carboxytermini difluorostatones are potent inhibitors of HIV-1 protease, a key enzyme of the Human Immunodeficiency Virus replication cycle. These inhibitors bind in an extended conformation and interact through a structural water molecule with the two enzyme's flap regions. The central hydrated difluoromethyleneketone moiety binds by positioning the geminal hydroxyl groups and the adjacent fluorine atoms within hydrogen bonding distance from the catalytic aspartyl residue carboxylates. These structures mimic a key intermediate formed during a rate limiting step of the normal hydrolysis of a substrate.

No therapeutic target ever stimulated the creativity of medicinal chemists to the extent that HIV-1 protease has over the past seven to eight years. HIV-1 protease, a member of the aspartic acid protease family, plays a key role in the replication of HIV-1 virus, the causative agent of AIDS (1).

### Catalytic Mechanism of HIV-1 Protease.

Numerous approaches to its inactivation have been described based either on the C-2 symmetrical nature of this homodimeric protein and/or on its catalytic mechanism of action (2). The classical mechanism for proteolytic cleavage of peptide bonds by an aspartic protease as originally proposed by Suguna et al. (3) and more recently by Veerapandian et al. (4) is shown in Figure 1. The scissile bond carbonyl is protonated by one of the aspartates with concomitant attack of the catalytic water molecule polarized into a nucleophilic state by the charged aspartate (step a, Figure 1); this leads to tetrahedral intermediate I (step b, Figure 1) which is stabilized by hydrogen bonds from the gem-diol unit to the negatively charged aspartate residue and from the second protonated aspartate to the statine-like hydroxyl oxygen of the intermediate. According to the principles of stereoelectronic control (5) the amide nitrogen will have been pyramidalized in

0097-6156/96/0639-0169\$15.00/0  
© 1996 American Chemical Society

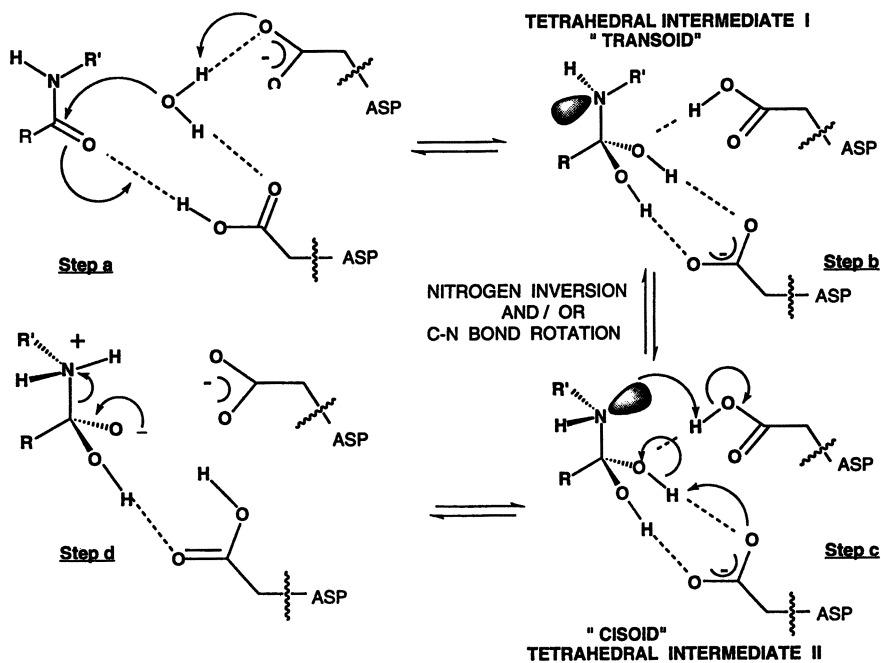


Figure 1. Mechanism of substrate hydrolysis by aspartic acid proteases.

this process with the lone pair disposed antiperiplanar to the newly formed carbon-oxygen bond ("transoid" conformation). Protonation of the secondary amine nitrogen by the uncharged aspartate makes nitrogen inversion and rotation around the C(OH)<sub>2</sub>-N bond possible leading to a staggered disposition of the substrate P<sub>1</sub> and P<sub>1</sub>' α carbons ("cisoid" conformation, intermediate II, step c, Figure 1). Tetrahedral intermediate II is destabilized by removal of the hydrogen bond to the statine-like hydroxyl. Formation of the products would be achieved by a concomitant deprotonation of the statine-like hydroxyl by the charged aspartate residue (step d, Figure 1).

For HIV-1 protease, the mechanism differs only slightly from the classical aspartyl protease catalytic mechanism (Figure 1), by involving not only one essential water molecule (the catalytic water) but probably two. Several groups have demonstrated by X-ray crystallography that competitive inhibitors of the HIV-1 protease, such as acetylpeptastatine (6) or 7 (MDL 73669, Table I) (Rondeau J.-M., *manuscript in preparation*) bind to the active site by forming stable complexes in which the flexible flap regions of the protein monomers interact with the inhibitor backbone through a "structural" water moiety resulting in a distorted tetrahedral network of hydrogen bonds (Figure 2). This water molecule has been found in every crystal structure of complexes with peptidomimetics reported so far.

On the basis of the structure of complexes of HIV-1 protease with a reduced amide (7) or a hydroxyethylene analogue (8) a mechanism of hydrolysis of substrate by HIV-1 protease was postulated by Gustchina and Weber(9). The normal enzymatic machinery of aspartyl protease would cleave the scissile amide bond by attack of the catalytic water molecule under general acid-base catalysis

**Table I. Binding affinities ( $K_i$  or  $IC_{50}^*$  /  $10^{-9}$  M)**

2 (160); Dreyer et al. (19)	1 (18); Dreyer et al. (19)
3 (600)	12 (60000)
4 (400) $R_1 = H; R_2 = n Pr; X_{1,2} = O$	15 (3000*) $R'_1 = H; R'_2 = COCH_3$
5 (750*) $R_1 = H; R_2 = i Bu; X_{1,2} = O$	16 (20*) $R'_1 = H; R'_2 = D\text{-ValCbz}$
6 (1) $R_1 = H; R_2 = i Pr; X_{1,2} = O$	17 (0.1) $R'_1 = CH_2C_6H_5; R'_2 = L\text{-ValCbz}; Sham et al. (25)$
7 (5) $R_1 = OCH_2C_6H_5; R_2 = i Pr; X_{1,2} = O$	
10 (5000*) $R_1 = H; R_2 = i Pr; X_{1,2} = H, OH$	

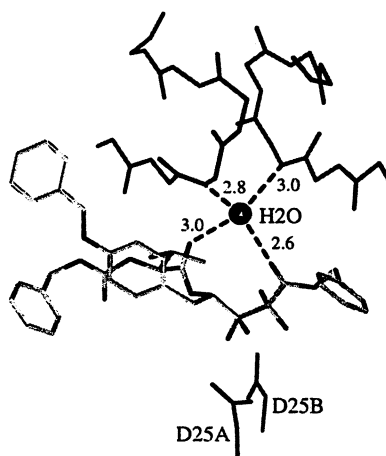
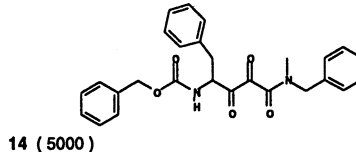
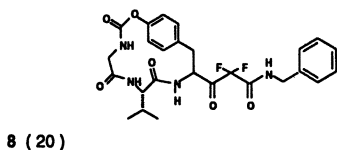
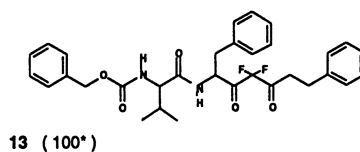
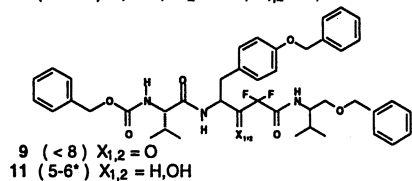


Figure 2. Interactions made by the structural water molecule with compound 7 and with the flaps of the HIV-1 protease (only main-chain atoms are shown). The water molecule accepts two hydrogen-bonds from the main-chain amide nitrogen of I50A and I50B, and donates two hydrogen-bonds to the inhibitor.

(Figure 1) while the enzyme, in order to optimally perform and facilitate this cleavage, binds to the substrate and/or some intermediate formed during catalysis (Figure 1) by forming a bridge with the two flexible flaps through the so-called "structural" water molecule (Figure 2).

### Drug Design Strategies: Difluoromethyleneketones

In our quest for potent inhibitors of this attractive antiviral target, two parallel strategies were followed: an approach based on rational design of peptidomimetic inactivators and one based on "rational" screening (the only rational being an analogy with the preferred P<sub>1</sub> or P'<sub>1</sub> subsite specificity). From a rational design point of view, several types of difluoromethyleneketones developed by us and others for various protease inhibition programmes have been incorporated into substrate sequences around known cleavage sites. Difluoromethyleneketones easily form hydrates and are therefore among the few structures that can mimic the two adjacent sp<sup>3</sup> atoms (geminal diol unit and pyramidalized amide nitrogen atom) of the putative transition-state or tetrahedral intermediate (Figure 1, steps b or c) formed during catalysis by aspartyl proteases. The strong electron-attracting and inductive effects of fluorine atoms play a crucial role in stabilizing the hydrate of the ketone functionality (Figure 3) (10).

However, in contrast to serine protease inhibition (e.g. elastase) (11), there is no evidence in the literature demonstrating that these fluorine atoms play an additional role in forming hydrogen bonds with the active site residues of their target protein. Of the different types of difluoromethyleneketones, difluorostatones V, difluoro-methyleneketone retroamides VI and difluoromethylene-1,3-diketones VII (Figure 4) were evaluated for their potential to inactivate HIV-1 protease. The difluorostatone mimetic, first described by Abeles and coll. in 1985 (12) and applied since to the inhibition of several mammalian (13) or other fungal (14) aspartyl proteases, is peculiar in that like statine itself (15), it is either one carbon atom too short to be a real dipeptide isostere, or two carbon atoms too long to resemble a normal amino-acid residue. Our experience with aspartyl proteases (human, primate and dog plasma renins (16) and pepsin) has shown that for a given backbone, the difluoromethyleneketone retroamide VI (17) and difluorostatone V transition-state mimics yield equipotent inhibitors. This was also true for HIV-1 protease when dealing with relatively large structures (tetrapeptide analogues and larger). However this trend did not hold true with shorter structures like difluorostatone 3 (Table I). Difluorostatone 3, identified by "rational" screening (18), is much more potent than corresponding difluoromethyleneketone retroamide 12 (Table I). This finding became even more intriguing in light of data reported by Dreyer and coworkers (19) where several known transition-state analogues for aspartyl proteases (statine I, reduced amide II, hydroxyethylene III, phosphinic acid IV as well as difluorostatone V, Figure 4) were also incorporated within a gag-like protein sequence and evaluated for their potential to inactivate purified HIV-1 protease.

Based on the sequence (Ser)AlaAlaPheValVal, the hydroxyethylene containing peptide 1 (Table I) exhibited the highest potency, being about 10 times more potent than the analogous difluorostatone containing peptide 2 (K<sub>i</sub> = 160 nM, Table I). Although this can be rationalized qualitatively it is surprising in view of our results showing that the one amino acid residue fluorinated statone 3 (K<sub>i</sub> = 600 nM) was only approximately 3.5 times less potent than a hexapeptide analogue 2 (Table I).



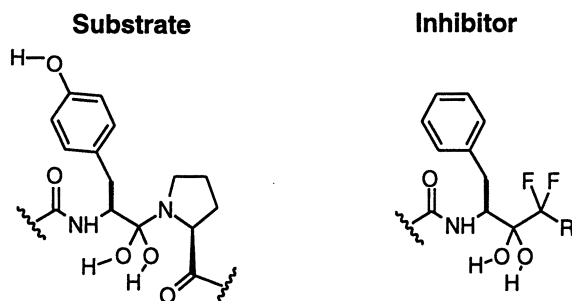


Figure 3. Putative tetrahedral intermediate and difluoromethyleneketone hydrate analog.

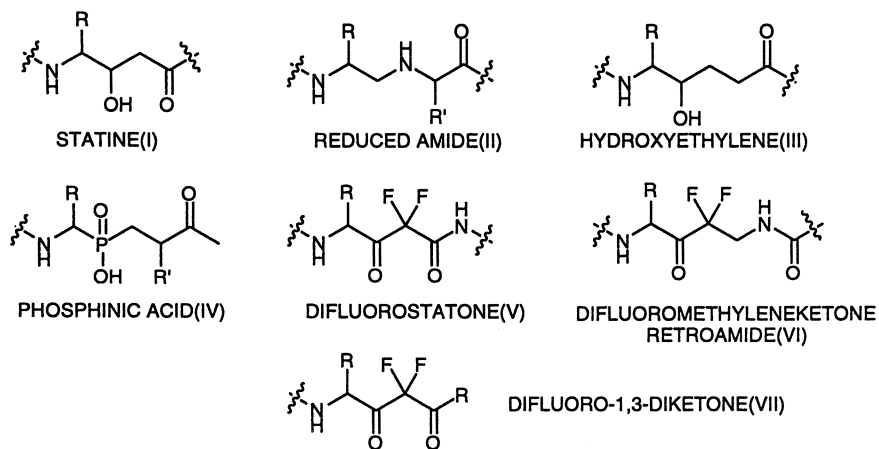


Figure 4. Various transition-state mimics of HIV-1 protease.

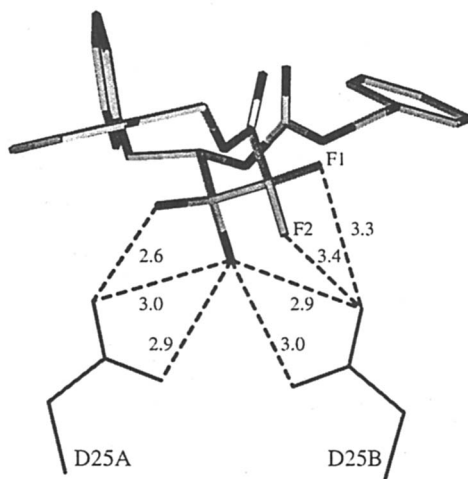


Figure 5. Interactions made by inhibitor **3** with the two catalytic aspartic acid residues.

In order to understand the reasons for the high potency of difluorostatone **3**, and to clarify the discrepancy between results observed for short statones when compared to their corresponding difluoromethyleneketone retroamides, we embarked upon a series of cocrystallisation experiments.

### Structural analysis of short C-termini difluorostatones

The results of our investigations are intriguing and suggest the following overall lesson : "bigger is not always better !". Analysis of our structures showed that inhibitor **3** binds to the active site of HIV-1 protease in an optimum fashion with respect to the widely accepted mechanism of substrate hydrolysis. The fluoroketone is hydrated as expected; the geminal hydroxyl substituents mimic the tetrahedral intermediate b or c of Figure 1 perfectly and form an optimum network of hydrogen bonds with both catalytic aspartic acid residues (Figure 5). One hydroxyl group (the pro-R, statine-like hydroxyl) is superimposable with the catalytic water molecule of the native enzyme (Figure 6) and is therefore at hydrogen bonding distance from both aspartic acid residues. The second hydroxyl group (the pro-S) binds to the site which is presumably that of the scissile amide bond carbonyl of a peptide substrate, and is at hydrogen bonding distance from only one of the aspartyl residues; the P<sub>1</sub> benzyl substituent sits in the S<sub>1</sub> recognition subsite mimicking the P<sub>1</sub> phenylalanyl residue preference of the protein (20) and the amino terminus carbobenzoxy protecting group fits in the S<sub>2</sub> recognition subsite (Figure 7) (this result might explain the fact that this small structure is equipotent to dipeptide analogues like **4** or **5**, Table I). Finally both the amide and carbobenzoxy carbonyls form a distorted tetrahedral network of hydrogen bonds with the structural water molecule and the flap regions of the protein monomers, stabilizing efficiently the overall architecture .

As shown in Figures 8 and 9, bound conformations of difluorostatones **3**, **6** and **7** are nearly superimposable. Despite the difference in the amino terminus sequence for compound **3** versus **6** and **7**, and despite differences in the P<sub>1</sub> side chain for compounds **6** versus **7** (21), the position of the atoms around the difluorostatone unit are virtually identical. The amino termini of inhibitors **6** and **7** are also superimposable. The binding affinities of structures **7** and **6**, when

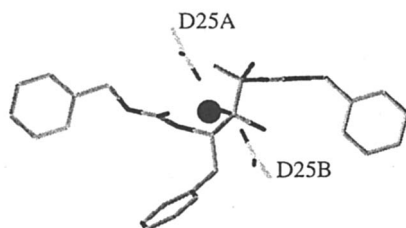


Figure 6. Positioning of inhibitor **3** with respect to the binding site of the catalytic water molecule found in the unliganded enzyme (shown as a solid sphere). The statine-like, pro-R hydroxyl of the gem-diol unit of the inhibitor occupies the site of the catalytic water.

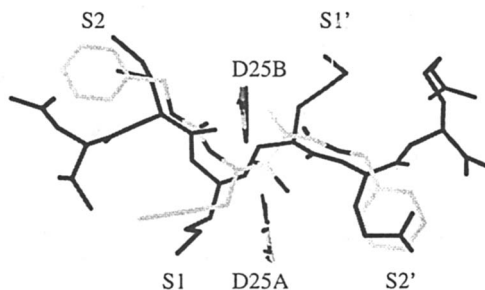


Figure 7. Overlay of the bound conformations of inhibitor **3** and MVT-101 (PDB entry 4HVP). All C $\alpha$  atoms of the HIV-1 protease were used in the superposition. The amino terminus carbobenzyloxy protecting group occupies the S2 enzyme subsite.

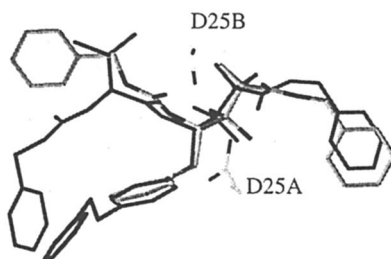


Figure 8. Overlay of the bound conformations of inhibitors **3** (shown in shades of grey) and **7** (shown in black).

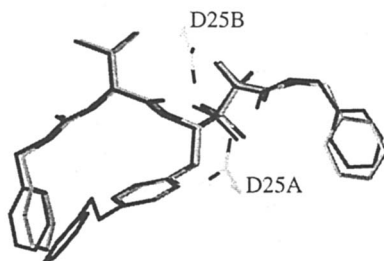


Figure 9. Overlay of the bound conformations of inhibitors **6** (shown in shades of grey) and **7** (shown in black).

compared to **3**, **4** and **5** are however respectively 100 to 600 times superior (Table I). The preference for beta disubstituted amino-acid residues in position  $P_2$  has been extensively demonstrated for substrates as well as for inhibitors of this enzyme (20) and is illustrated by the essential contribution of the  $P_2$  valine residue to the binding of **6** and **7** as compared to the carbobenzoxy amino terminal of **3** or the  $P_2$  norvaline or leucine of structures **4** and **5** respectively.

### Structure-assisted Design of a Macrocyclic Analog

As seen in the crystal structure of the complex formed between **7** and HIV-1 protease, the carbobenzoxy benzyl moiety and the tyrosine O-benzyl substituent are not engaged in major interactions with the enzyme, and as they project into the solvent medium, they probably create unfavorable surface/solvent interactions (Figure 10). The logical design modification was to eliminate these rings outright, or replace them with groups that could lessen the severity of the hydrophobic/solvent gradient. However, our studies had established the need for steric bulk in the region occupied in part by the O-benzyl ring (decreased cytotoxicity) (21). Furthermore, the dynamics of the ligand bound to the enzyme, as determined by molecular dynamics simulations, showed the formation of a well defined bound conformation for the  $P_1/P_3$  region, characterized by a close proximity of the  $P_1$  and  $P_3$  sidechains (22). This conformation, which is not strictly maintained in solution, was considered significant since the sidechain arms join into the inhibitor adjacent to the difluorostatone functionality, which in turn interacts directly with the enzyme active site. The  $P_1$  and  $P_3$  sidechains were thus covalently linked to form a macrocyclic analogue. Cyclization was performed by replacing the  $P_3$  protecting group by a latent nucleophile (a suitably protected amino acid) and the benzyl substituent of the tyrosyl residue by an ester leaving group, yielding inhibitor **8** (Table I) (22). This design resulted in an inhibitor of HIV-1 protease *in vitro* with a  $K_i$  of 20 nM as compared to 5 nM for the linear structure **7** (Table I).

Analysis of the three dimensional structure of compound **8** / HIV-1 protease complex illustrates once more the optimal binding of the difluorostatone unit to the essential amino acid residues of the active site (Figure 11).

### Alternate Binding Mode of Extended Difluorostatones

However, the bound conformations of structure **7** and of the homologous structure **9** (23) reveal a significant difference in their binding mode; the central difluorostatone unit of **9** is rotated with respect to the active site aspartyl residues

(Figure 12). As a consequence and in contrast to inhibitor **7** the pro-S hydroxyl of inhibitor **9** replaces the catalytic water molecule; the pro-R hydroxyl is located in a region opposite to the putative binding site of the scissile amide bond carbonyl of a substrate. Despite an additional R-valinol ether residue in position P<sub>1</sub>' , inhibitor **9** is equipotent or only slightly more active (slow binding) (Table I). This finding may be rationalized on the basis of a weakened interaction of the difluoroketone moiety with the important catalytic residues (D25A and D25B) caused by the binding of the additional carboxy terminus R-valinol residue to the S<sub>1</sub>' subsite.

The optimal binding of small hydrated difluorostatone structures has been confirmed by a number of additional experiments and suggest that the geminal hydroxyl groups must be surrounded by two amide or carbamate carbonyl units positioned at a given distance from each other.

### Difluorostatones versus Difluorostatines

The requirement for the geminal hydroxyl substituents is illustrated by the following data:

- structure activity relationship studies performed on the elongated difluorostatone **9** and difluorostatine **11** showed little or no difference in potency (Table I) (23). However, difluoroalcohol **10** is about 5000 times less active on purified enzyme than its corresponding ketone **6** (Table I) (18). This large difference in potency between a difluorostatine and its oxidized analogue (difluorostatone) is extremely unusual. The replacement of the difluorostatone unit by a difluorostatine one has so far been reported to give only marginal or moderate (10 - 100 fold) loss of binding affinity (see previous studies performed on pepsin (12) and renin (13)). These and our data can be reconciled if one considers the following points: i) the difluorostatone unit is a better transition-state analogue than its difluorostatine counterpart with respect to aspartic acid proteinases. ii) the relative contribution of the difluorostatone (-statine) unit to the total binding energy decreases when the size of the inhibitor increases. Therefore, the replacement of the difluorostatone unit by a difluorostatine one is expected to have a relatively smaller effect in longer peptidomimetics. Conversely, the most dramatic effect is observed with a compound such as **6**, which is among the smallest difluorostatone-bearing peptidomimetic with nanomolar potency described up to now. iii) the difluorostatone (-statine) unit is two carbon atoms too long to mimic a substrate amino-acid residue and one carbon atom too short to be a dipeptide isostere. Therefore, optimum binding of the difluorostatone unit will not be possible when it is incorporated in peptidomimetics filling both the S<sub>1</sub> and S'<sub>1</sub> enzyme subsites. Compound **9** provides a very nice illustration of this point. In cases like this, replacement of the difluorostatone by a difluorostatine moiety is not expected to impact inhibitor binding very much (compounds **9** and corresponding alcohol **11** being almost equipotent).

### Difluorostatones versus other Related Transition-state Mimics

**Difluoromethyleneketone retroamide 12** can also form a hydrated ketone and thus the network of hydrogen bonds around the active site aspartyl residues. Despite this, it is much less active on the purified enzyme than the corresponding difluorostatone **3** (Table I). Difluoromethyleneketone retroamide **15** is similarly less active when compared to difluorostatone **6** (Table I); it is 3000 times less potent. The large difference in binding between these pairs of compounds is rationalized by a weaker complexation of the structural water molecule by difluoromethyleneketone retroamides. This is supported by larger distances observed between chelating carbonyl units of difluoromethyleneketone

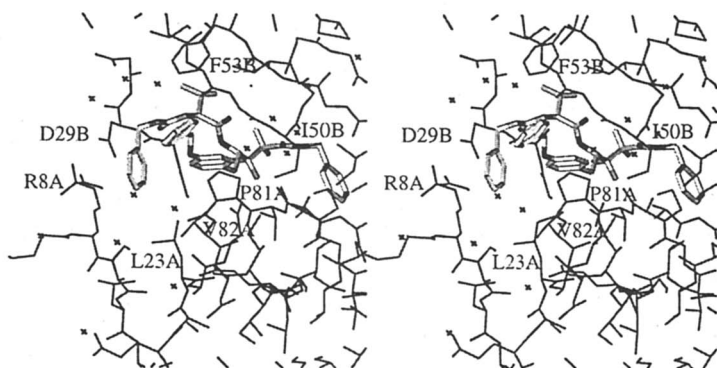


Figure 10. Stereo view of the HIV-1 protease complex with inhibitor **7**. The environment of the carbobenzoxy protecting group and of the tyrosine O-benzyl substituent is shown.

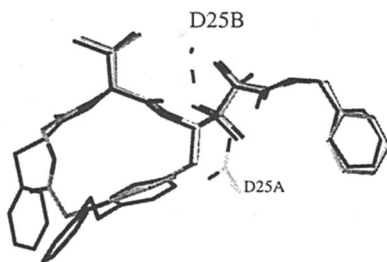


Figure 11. Overlay of the bound conformations of inhibitors **8** (shown in shades of grey) and **7** (shown in black).

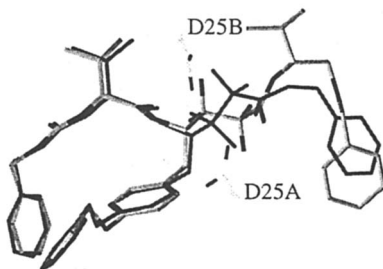


Figure 12. Overlay of the bound conformations of inhibitors **9** (shown in shades of grey) and **7** (shown in black).

retroamides **12** or **15** as compared to difluorostatones **3** or **6** respectively. However, difluoromethyleneketone retroamides, which are true dipeptide isosteres (**24**), can generate extremely potent inactivators of HIV-1 protease. For instance, difluoromethyleneketone retroamide **16** (Table I), which bears a protected valine residue on both the amino and carboxytermini, exhibits a much stronger potency against our target protein. Compound **16** is 150 times more potent than retroamide **15** (Table I). The beneficial effect of adding residues to the basic skeleton of difluoromethyleneketone retroamide culminates in the pseudo-symmetrical structure **17** described in 1991 by Sham and coworkers (25). A dramatic enhancement of the binding affinity was achieved for this inhibitor by stereoselective addition of a P<sub>1</sub>' benzyl residue. Inhibitor **17** is 200 times more potent than the corresponding P<sub>1</sub>' unsubstituted **16** and 10 times more potent than difluorostatone **6** (Table I).

**Difluoromethylene-1,3-diketone 13** (**18**) exhibits an inhibitory activity that is about 100 times less potent than difluorostatone **6** (Table I). All the essential binding features of difluorostatone **6** are present in diketone **13**: the tetrahedral intermediate can be mimicked by the hydrate of the central difluoromethyleneketone, residues P<sub>1</sub> and P<sub>2</sub> are identical to the ones present in difluorostatone **6**, and the distance between the two oxygens liganding the structural water molecule (the aminoterminal carbobenzyloxy carbonyl and the carboxyterminal ketone) is identical to the corresponding distance in **6**. The difference in binding affinity in this series may be attributed to a "dilution" of the "biologically active" species of product **13** as the compound exists in solution in an equilibrium between three potential hydrates (Piriou, F., *personal communication*): monohydrates **13a**, **13b** and bishydrate **13c** (Figure 13).

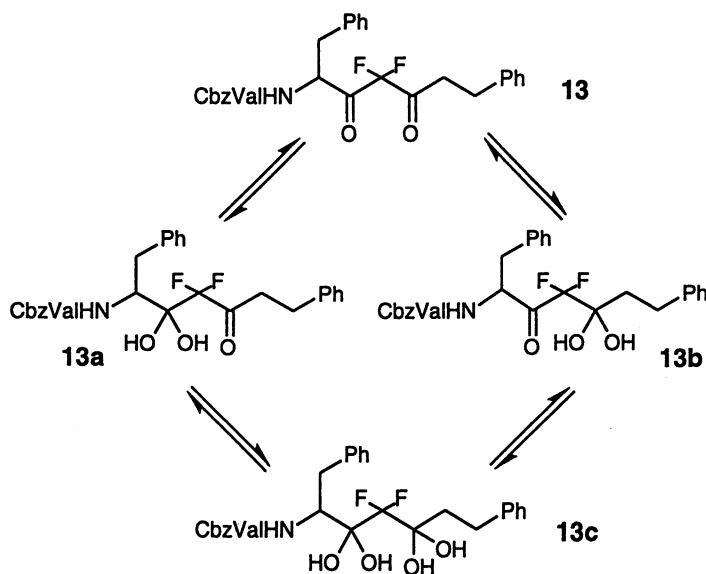


Figure 13. Proposed hydration scheme of difluoromethylene-1,3-diketone **13**.

While all three hydrated species probably have good affinity for the active site of HIV-1 protease, the monohydrate **13a** should demonstrate the highest affinity. This was based on two assumptions. Firstly, the hydrated form **13a** most closely mimics the hydrated form of difluorostatone **6**. Secondly, hydrated carbonyls are less efficient hydrogen-bond acceptors than non hydrated carbonyls (**26**) and the hydrated carbonyls at the carboxy termini of **13b** and **13c** will be less prone to efficiently chelate the structural water molecule in HIV-1 protease than the remaining non hydrated carbonyl in **13a**, resulting in less stable inhibitor / protease complexes.

**Diketoamide 14** (Table I) is a close analogue of difluorostatone **3**. Although this compound may exist in solution or in the enzyme active site as a bishydrated diketoamide (a possible mimic of the hydrated difluorostatone), it exhibits approximately one tenth of the potency of **3** on purified HIV-1 protease (Table I) (**18**).  $^1\text{H}$  NMR experiments have demonstrated that only the central carbonyl is hydrated in solution. Hence, the low potency of inhibitor **14** may be explained by the fact that the compound bears only one  $\text{sp}^3$  unit and is thus a poor mimic of the tetrahedral intermediate.

In addition to the aforementioned arguments, it should be noted that, in compounds **13** and **14** (Table I) the C-terminal amide NH is lacking and is replaced respectively by a methylene unit or a N-methylated amide nitrogen. In contrast, in compound **6**, this C-terminal amide NH is at hydrogen bonding distances from the main chain carbonyl of Glycine **27** and from a bound water molecule. These interactions are no longer possible for compounds **13** and **14**, which may also explain their weaker activities.

### Resemblance to a key reaction intermediate

X-ray analysis of the bound conformations of inhibitors **3,6,7** and **8** reveals that the essential hydrated fluorinated ketone is present as a staggered conformer (gauche arrangement corresponding to a "cisoid" conformation)(**5**) about the  $\text{C}(\text{OH})_2\text{-CF}_2$  linkage (Figure 14) (Rondeau, J.-M., *manuscript in preparation*). According to previously published accounts, both hydroxyl groups of the hydrated difluorostatones are protonated (**3,14,27**). Consequently and as proposed by these authors one of the catalytic aspartyl residue is charged while the other is protonated (Figure 14).

Unfortunately, protons are not seen at the resolution of protein crystallography, precluding direct experimental determination of the protonation state of the catalytic aspartic acids. However, the present structures with difluorostatones provide novel and interesting clues to address this problem. In all structures, the fluorine atoms are pointing towards the side-chain carboxylate of D25B, making short contacts (3.0-3.3 Å) with Oδ1. Although this distance could correspond to a very acceptable Van der Waals contact between a fluorine and an oxygen atom, it strongly suggests that D25B is not in the negatively charged carboxylate form. The observed distances between the fluorine atoms and Oδ1 of D25B would therefore be most consistent with the existence of an intermolecular hydrogen bond (**28**). Therefore, D25B would be in the uncharged acidic form, while D25A would be in the charged carboxylate form. This conclusion is also supported by the inferred hydrogen-bonding pattern between the gem-diol unit and the two catalytic aspartates. We would thus advocate that our difluorostatones with a short C-terminus (**3,6,7** and **8**, Table I) are close mimics of the reaction intermediate c of Figure 1. A closer look at related recent reports of three dimensional structures of fungal pepsin / difluorostatone complexes (**3,14, 27**) seems to indicate that our finding is NOT unique (Figure 15). Instead, the central



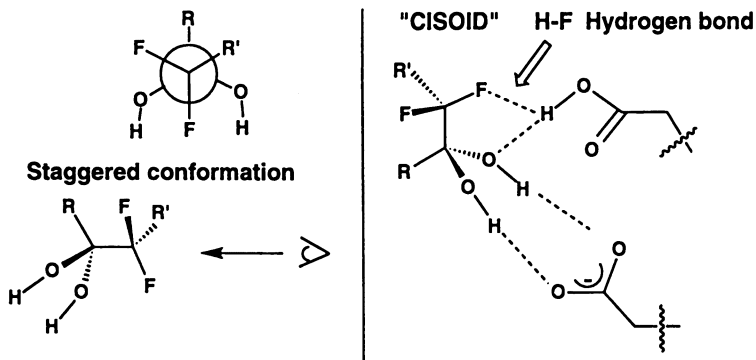


Figure 14. Bound conformation and hydrogen bond network of short C-termini difluorostatones (**3**, **6**, **7** or **8**) to HIV-1 protease.

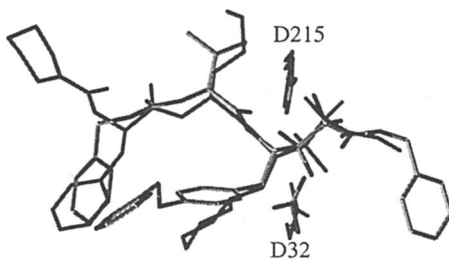


Figure 15. Overlay of the bound conformations of inhibitors **7** to HIV-1 protease (shown in shades of grey) and of CP-81,282 to endothiapepsin (PDB entry 1EPO) (shown in black). All side-chain atoms and the C $\alpha$  of the two catalytic aspartates were used in the superposition.

difluorostatone moiety of **7** and CP-81,282 superimposes remarkably well, as shown in Figure 15, despite the differences in inhibitor structure, in the target enzyme (endothiapepsin and HIV-1 protease are distantly related aspartic acid proteases), in the crystallization conditions and in the packing of the molecules in the crystals.

## Conclusion

In conclusion, HIV-1 protease can form optimal interactions with short difluorostatones in an extended conformation by building a network of hydrogen bonds with the inhibitor, the structural water molecule and the two flap regions. As a consequence the hydrated difluoroketone unit will bind to the catalytic aspartyl residues in a way that forces the gem-fluorine atoms to be at hydrogen bonding distance from one of the active site aspartic acid residue. The overall and extremely interesting consequence of such a binding mode is that inhibitors **3,6,7** and **8** (Table I), in their biologically active conformation, perfectly mimic tetrahedral intermediate II (Figure 1), in which transfer of a proton from one of the aspartic acid to the scissile amide bond nitrogen is close to occurring. In contrast to longer peptidomimetics such as **9** (Table I), the hydrated difluoroketone of our short peptidomimetics mimics the hydrated carbonyl of the scissile amide bond and the transfer of a proton to the pyramidalized nitrogen is mimicked by the H-F hydrogen bond interaction between the inhibitor and the protein (28). The resemblance of our short peptidomimetics to this rate limiting step of proteolysis would explain their surprisingly high affinity for HIV-1 protease (Figure 16).

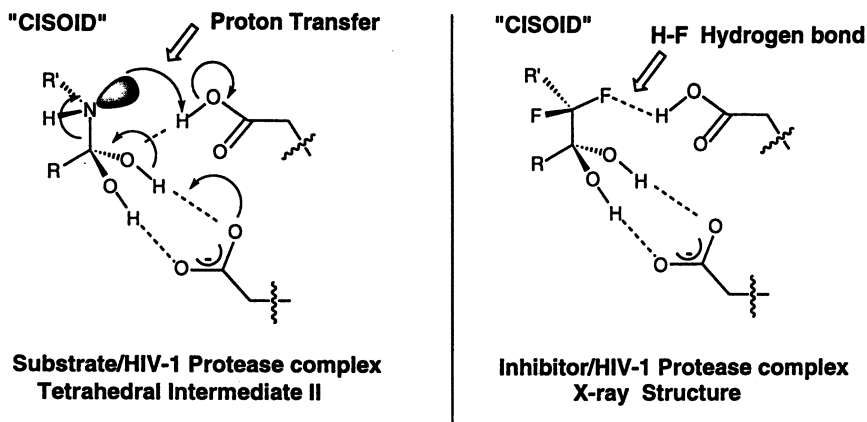


Figure 16. Comparison of a putative tetrahedral intermediate formed during enzyme catalysis with the bound conformations of short C-termini difluorostatones (**3, 6, 7** or **8**) to HIV-1 protease.

## Acknowledgements.

We express our thanks to S. Baltzer, J.M. Remy and F. Weber for their excellent technical assistance and C. Reeb for her valuable preparation of the manuscript.

**Literature cited**

1. Krausslich, H. G.; Wimmer, E. *Ann. Rev. Biochem.* **1988**, *57*, 701.
2. West, M. L.; Fairlie, D. P. *TIPS* **1995**, *16*, 67.
3. Suguna, K.; Padlan, E. A.; Smith, C. W.; Carlson, W. D.; Davies, D. *Proc. Natl. Acad. Sci. USA* **1987**, *84*, 7009.
4. Veerapandian, B.; Cooper, J. B.; Sali, A.; Blundell, T. L.; Rosati, R. L.; Dominy, B. W.; Damon, D.B.; Hoover, D.J. *Protein Science* **1992**, *1*, 322.
5. Deslongchamps, P. *Tetrahedron* **1975**, *31*, 2463.
6. Fitzgerald, P. M. O.; Mc Keever, B. M.; Van Middlesworth, J. F.; Springer, J. P.; Heimbach, J. C.; Leu, C. T.; Herber, W. K.; Dixon, R. A. F.; Darke, P. L. *J. Biol. Chem.* **1990**, *265*, 14209.
7. Miller, M.; Schneider, J.; Sathyanarayana, B. K.; Toth, M. V.; Marshall, G. R.; Clanson, L.; Selk, L.; Kent, S. B. H.; Wlodawer, A. *Science* **1989**, *246*, 1149.
8. Swain, A. L.; Miller, M. M.; Green, J.; Rich, D. H.; Kent, S. B. H.; Wlodawer, A. *Proc. Natl. Acad. Sci. USA*, **1990**, *87*, 8805.
9. Gustchina, A.; Weber, I. T. *FEBS Letters* **1990**, *269*, 269.
10. Abeles, R.H.; Alston, T.A. *J. Biol. Chem.* **1990**, *265*, 16705.
11. Takahashi, L. H.; Radhakrishnan, R.; Rosendield, R. E., Jr; Meyer, E. F., Jr; Trainor, D. A. *J. Am. Chem. Soc.* **1989**, *111*, 3368.
12. Gelb, M. H.; Svaren, J. P.; Abeles, R. H. *Biochemistry* **1985**, *24*, 1813.
13. Thaisrivongs, S.; Pals, D. T.; Kati, W. M.; Turner, S. R.; Thomasco, L. M.; Watt, W. *J. Med. Chem.* **1986**, *29*, 2080.
14. James, M. N. G.; Sielecki, A. R.; Hayakawa, K.; Gelb, M. H. *Biochemistry* **1992**, *31*, 3872.
15. Boger, J.; Lohr, N.S.; Ulm, E. H.; Poe, M.; Blaine, E. H.; Fanelli, G. M.; Lin, T. Y.; Payne, L. S.; Schorn, T. W.; Lamont, B. I.; Vassil, T. C.; Stabilito, I. I.; Veber, D. F.; Rich, D. H.; Bopari, A. S. *Nature* **1983**, *303*, 81.
16. Tarnus, C.; Jung, M. J.; Remy, J. M.; Baltzer, S.; Schirlin, D. G. *FEBS Letters* **1989**, *249*, 47.
17. Schirlin, D.; Baltzer, S.; Altenburger, J.M.; Tarnus, C.; Remy J.M. *Tetradedron Symp. in print*, **1995**, in press.
18. Schirlin, D.; Baltzer, S.; Van Dorsselaer, V.; Weber, F.; Weill, C.; Altenburger, J. M.; Neises, B.; Flynn, G.; Remy, J. M.; Tarnus, C. *Bioorg. and Med. Chem. Lett.* **1993**, *3*, 253.
19. Dreyer, G. B.; Metcalf, B. W.; Tomaszek, T. A., Jr; Carr, T. J.; Chandler, A. C. III; Hyland, L.; Fakhoury, S. A.; Magaard, V. W.; Moore, M. L.; Strickler, J. E.; Debouck, C.; Meek, T. D. *Proc. Natl. Acad. Sci. USA* **1989**, *86*, 9752.
20. Poorman, R.A.; Tomasselli, A. G.; Heinrikson, R. L.; Kezdy, F. J. *J. Biol. Chem.* **1991**, *266*, 14554.
21. Schirlin, D.; Van Dorsselaer, V.; Tarnus, C.; Taylor, D. L.; Tyms, A. S.; Baltzer, S.; Weber, F.; Remy, J. M.; Brennan, T.; Farr, R.; Janowick, D. *Bioorg. and Med. Chem. Lett.* **1994**, *4*, 241.
22. Podlogar, B. L.; Farr, R. A.; Friedrich, D.; Tarnus C.; Huber, E. W.; Cregge, R. J.; Schirlin, D. *J. Med. Chem.* **1994**, *37*, 3684.
23. Van Dorsselaer, V.; Schirlin, D.; Tarnus, C.; Taylor, D. L.; Tyms, A. S.; Weber, F.; Baltzer, S.; Remy, J.M.; Brennan, T.; Janowick, D. *Bioorg. and Med. Chem. Lett.* **1994**, *4*, 1213.
24. Schirlin, D.; Baltzer, S.; Altenburger, J.M. *Tetrahedron Lett.* **1988**, 3687.
25. Sham, H. L.; Wideburg, N. E.; Spanton, S. G.; Kohlbrenner, W. E.; Betebenner, D. A.; Kempf, D. J.; Norbeck, D. W.; Plattner, J. J.; Erickson, J. W. *J. Chem. Soc. Chem. Commun.* **1991**, 110.
26. Kamlet, M. J.; Abboud, J. L.; Abraham, M. H.; Taft, R. W. *J. Org. Chem.* **1983**, *48*, 2877.
27. Parris, K. D.; Hoover, D. J.; Damon, D. B.; Davies, D. R. *Biochemistry* **1992**, *31*, 8125.
28. Murray-Rust, P.; Stallings, W. C.; Monti, C. T.; Preston, R. K.; Glusker, J. P. *J. Am. Chem. Soc.* **1983**, *105*, 3206.

## Chapter 14

# Fluorine-Containing Peptidomimetics as Inhibitors of Aspartyl Proteases

Hing L. Sham

Anti-infective Research, Abbott Laboratories, Department 47D,  
Building AP9A, Abbott Park, IL 60064-3500

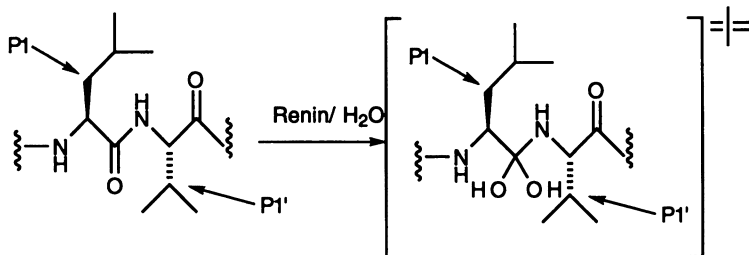
Due to its very strong electronegativity, fluorine has a strong effect on its neighboring functional groups in a molecule. Fluoroketones, for example, in which the carbonyl group is next to fluorine substituents, are usually fully hydrated and act as transition-state mimic of the  $sp^3$  hybridized-hydrated carbonyl at the cleavage site of substrate peptides. In many cases, the fluorine containing compounds are more lipophilic than their counterparts wherein the fluorine atom is replaced by hydrogen. As a result, the solubility and log P characteristics are also affected. Two therapeutically important target enzymes that belong to the aspartyl proteases family are 1. human renin and 2. HIV-protease. Fluorine containing peptidomimetic inhibitors of these two enzymes are described.

The renin-angiotensin system has been successfully manipulated to control hypertension. Many angiotensin-converting enzyme (ACE) inhibitors have been reported to be effective therapy for the control of high blood pressure. Renin is an aspartyl protease that catalyzes the first step in the angiotensinogen cascade to produce angiotensin II, a very potent vasoconstrictor. Renin is an enzyme of high substrate specificity and its inhibition has the potential of providing specific therapy for hypertension (1).

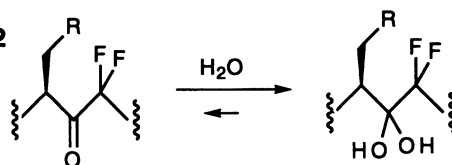
During the hydrolysis of the peptide bond of the substrate by an aspartyl protease such as renin, the amide carbonyl group is postulated to be hydrated to form a tetrahedral transition state intermediate as shown in Equation 1. The collapse of this high energy intermediate give rise to angiotensin I and the other fragments. Fluorine, because of its strong electronegativity, has an important effect on its neighboring functional groups in a molecule. Both fluoroalcohols and fluoroketones have been reported to be potent inhibitors of renin. Fluoroketones, in which the carbonyl group is next to fluoro-substituents, are usually fully hydrated (Equation 2). As a result of this hydration, fluoroketones are good transition-state mimics of the  $sp^3$  hybridized hydrated carbonyl at the cleavage site of substrate peptides (2). Renin inhibitors with fluorine containing peptidomimetics including fluoroketones are described below.

0097-6156/96/0639-0184\$15.00/0  
© 1996 American Chemical Society

Equation 1



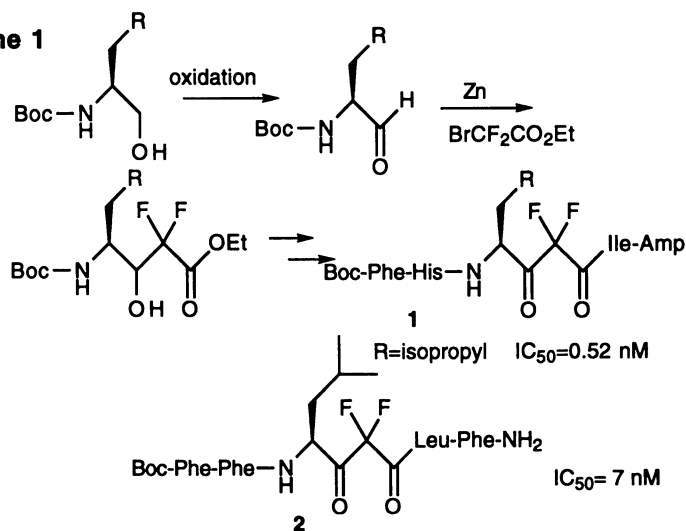
Equation 2



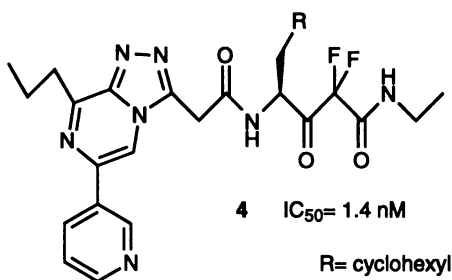
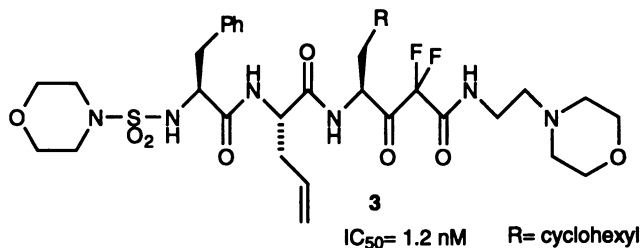
### Renin Inhibitors

Highly potent renin inhibitors containing a difluorostatine or difluorostatone (or their side-chain modified analogs) have been reported by Thaisrivongs, et al. (3). The key reaction is the Reformatsky-type addition of the organometallic species generated from zinc and bromodifluoroethyl acetate to a N-protected aminoaldehyde as shown in Scheme 1. Compound 1, which contains the difluorostatone unit, is a potent inhibitor of renin. A closely related compound 2 in which some of the amino acids were changed has been reported (4). Doherty, et al. (5) have reported on a range of difluoroketones-containing inhibitors of renin and their precursor difluorocarbinols, prepared in an attempt to design potent and selective and, most importantly, orally active renin inhibitors.

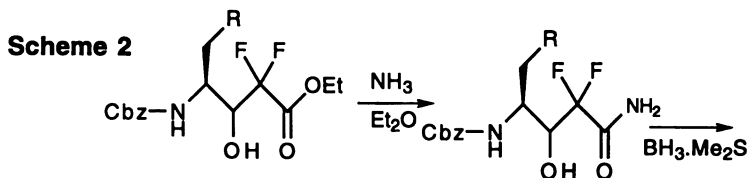
Scheme 1

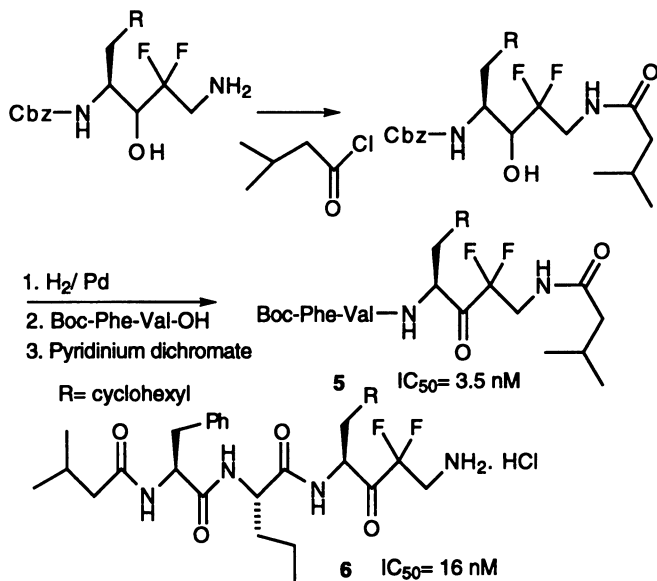


By modification of the substituents at the  $P_2$  and  $P_2'$  sites, it was possible for them to synthesize compounds with good aqueous solubility and a representative compound **3**, has shown good oral efficacy. Low molecular weight difluoroketones incorporating 2-(8-alkyl-6-aryl-1,2,4-triazolo[4,3-a]pyrazin-3-yl)-3-pyridin-3-ylpropionyl moiety as end group to increase aqueous solubility has been reported (6). A representative example is compound **4**, which has low molecular weight (<600) and retains good *in vitro* renin inhibitory potency.

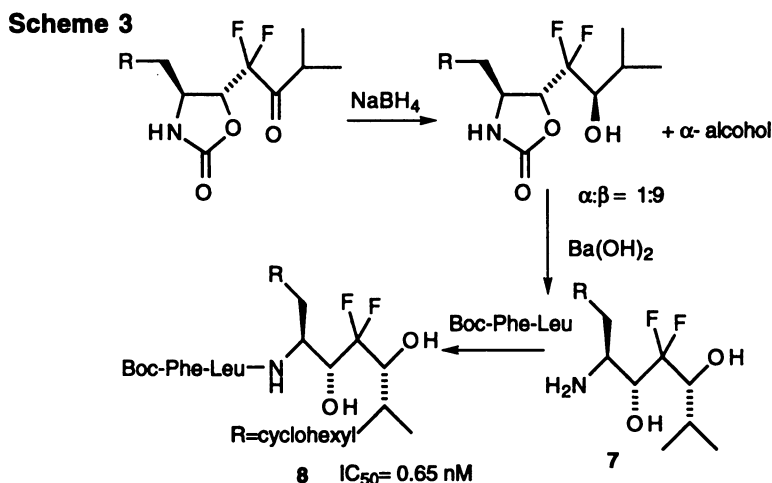


Fluoroketones containing the retroamide-type bond at the normally carboxyl terminus has been reported (7,8). The difluorostatine analog (with the leucine side chain changed to a cyclohexylalanine side chain) was prepared as reported by Thaisrivongs, et al. (3) and reaction with ammonia provided the primary amide. Reduction of the primary amide with borane-dimethyl sulfide provided the primary amine (Scheme 2). Further elaboration of this intermediate gave compound **5** which is a highly potent renin inhibitor. A related series of renin inhibitors which are less active, but highly selective and more water soluble were derived by leaving the primary amine group unacylated. This series of compounds is represented by the prototypical compound **6**. The basic amino alkyl group enhances the solubility of the compound in aqueous media.



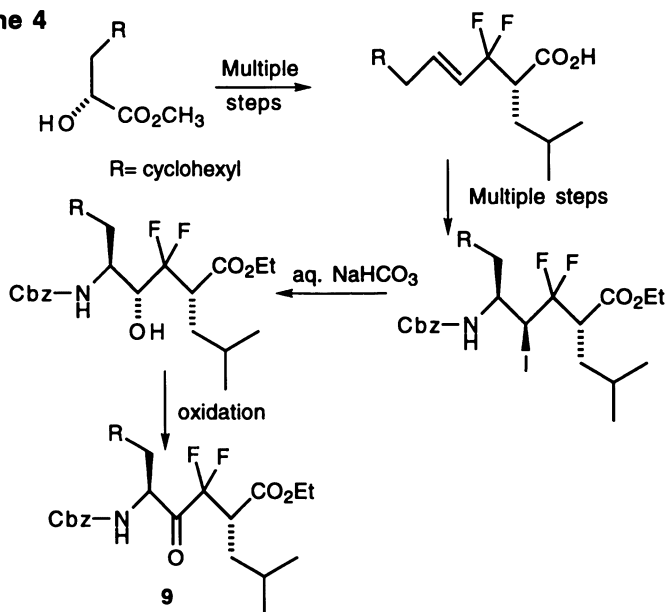


Potent renin inhibitors containing the novel fluorodipeptide mimic **7** has been described (9). As shown in Scheme 3, the reduction of the keto-oxazolidinone by sodium borohydride gave predominantly the  $\beta$ -OH isome ( $\beta$ : $\alpha$ :1). Opening of the oxazolidinone ring via basic hydrolysis followed by coupling with a protected dipeptide fragment provided the potent and selective renin inhibitor **8**.



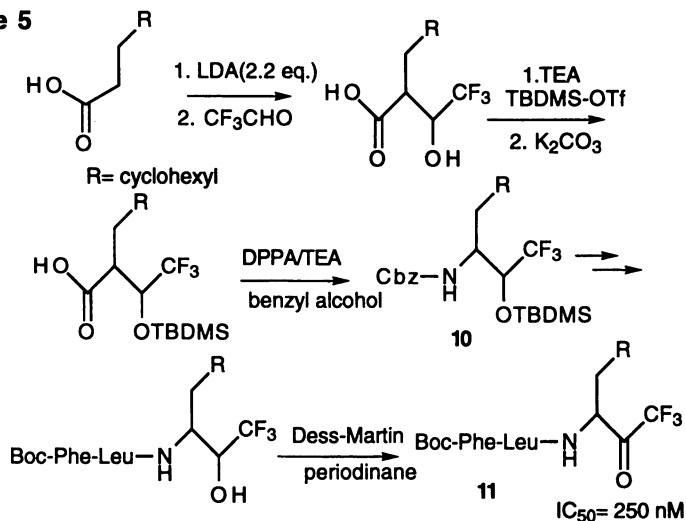
Yet another interesting difluoroketone-containing dipeptide isostere that maintains the normal sequence length of the substrate has been synthesized by a multi-step synthesis (10). When compared to the difluorostatone series, the dipeptide isostere **9** retains the  $\text{P}_1'$  side chain which is absent in the difluorostatone type compounds (Scheme 4).

Scheme 4



Several different syntheses of renin inhibitors incorporating trifluoromethyl alcohols and trifluoromethyl ketones at the C-terminus of peptide sequences has been reported. One of these syntheses (11) uses 3-cyclohexylpropionic acid as starting material (Scheme 5). Lithiation and aldol reaction with trifluoromethylacetaldehyde

Scheme 5

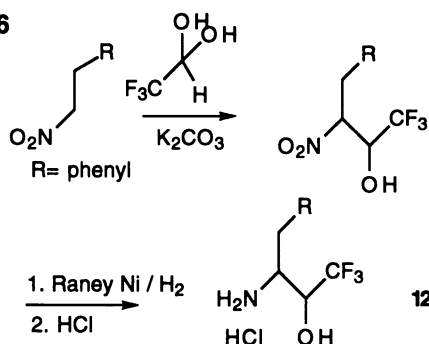




provided the corresponding trifluoromethyl alcohol. Protection of the hydroxy functional group as the silyl ether and Curtius rearrangement with diphenylphosphoryl azide in the presence of benzyl alcohol gave the key intermediate **10**. Coupling of this intermediate with an appropriate peptide sequence, followed by unmasking the hydroxy group and oxidation provided the trifluoromethyl ketone **11**. Compound **11** is a relatively weak inhibitor of human renin.

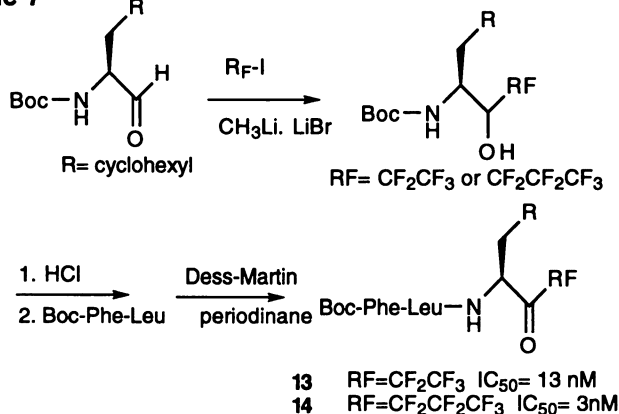
An alternate synthesis of trifluoromethyl alcohols and ketones using 2-phenyl-1-nitroethane has been reported (12). Aldol-type condensation of 2-phenyl-1-nitroethane with trifluoromethyl acetaldehyde provided the corresponding trifluoromethyl alcohol (Scheme 6). Reduction of the nitro group to the amino group is accomplished by hydrogenation with Raney nickel catalyst to give the corresponding amine **12**. Incorporation of this amine into the C-terminus of a peptide sequence followed by oxidation provided the trifluoromethyl ketone.

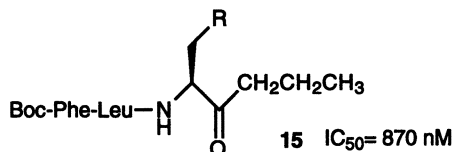
Scheme 6



An efficient synthesis of renin inhibitors containing perfluoroalkyl ketones at the C-terminus of a peptide sequence has been reported (13). Reaction of perfluoroalkyllithium (generated in situ from methyl lithium and perfluoroalkyl iodide) at low temperature with an aldehyde derived from an N-terminal protected amino acid produced the corresponding perfluoroalkyl alcohol (Scheme 7). Incorporation of the perfluoroalkyl alcohol at the C-terminus of a peptide sequence followed by oxidation provided perfluoroalkyl ketones such as **13** and **14**, both of which are potent inhibitors of human renin. It is interesting to compare the activity of compound **15**, in

Scheme 7

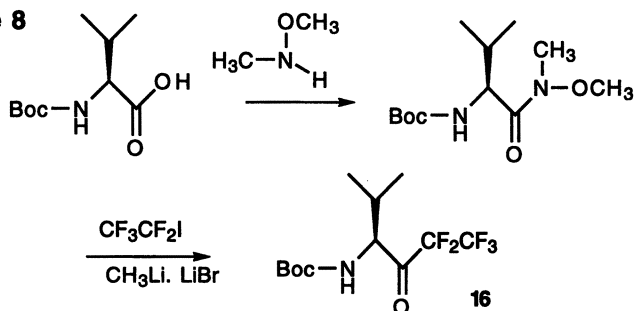




which all the fluorine atoms in compound **14** are replaced by hydrogens, with **14**. Compound **14** is 270 times more potent. The reason is probably that the carbonyl group in **14**, with the perfluoroalkyl group next to it, is fully hydrated, while the carbonyl group in **15** is not.

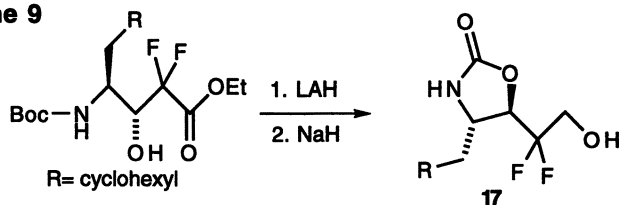
A closely related synthesis of perfluoroethyl ketones has been reported (*14*). Instead of starting with a *N*-terminal protected  $\alpha$ -aminoaldehyde, the synthesis started with *N*-terminal protected  $\alpha$ -amino acids (Scheme 8). Coupling of the amino acids with *N*-methyl-*N*-methoxyamine provided the Weinreb amide (*15*). Reaction of the resulting Weinreb amide with perfluoroethyl lithium generated in situ from perfluoroethyl iodide and methyl lithium gave the perfluoroethyl ketones such as **16**. Incorporation of **16** in an appropriate peptide sequence similar to those reported in (*13*) should provide inhibitors of human renin.

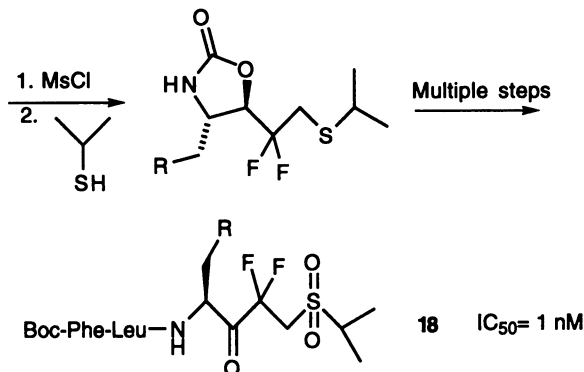
Scheme 8



Starting with a *N*-terminal protected difluorostatine analog, synthesis of difluoroketones incorporating a sulfone moiety at the *C*-terminus has been reported (*16*). Reduction of the ethyl ester to the corresponding alcohol (Scheme 9), followed by treatment with sodium hydride provided the oxazolidinone alcohol **17**. Mesylation of the primary alcohol in **17**, and displacement with isopropyl mercaptan provided the corresponding sulfide which was oxidized to the sulfone. Further elaboration of the sulfone provided the difluoroketone **18** with a sulfone moiety at the *C*-terminus. Compound **18** is a potent inhibitor of human renin.

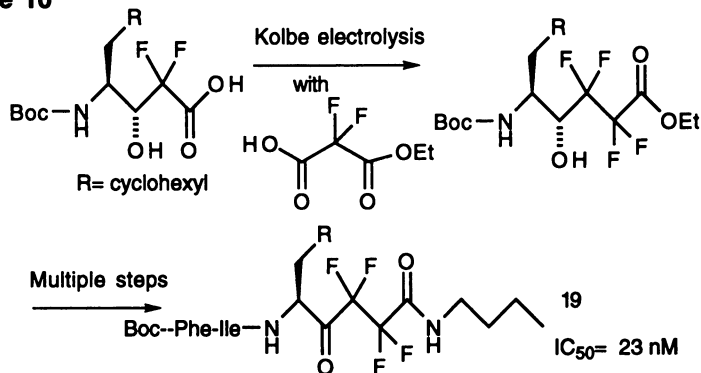
Scheme 9





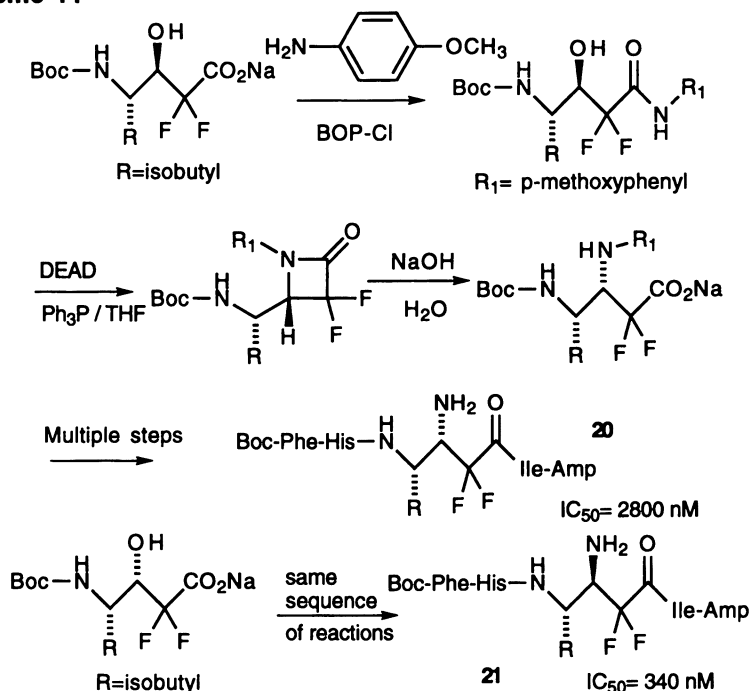
A synthesis of tetrafluoroketones via an electrochemical method has been reported (17). Electrochemical reaction of a difluorostatine analogue with monoethyl difluoromalonate provided the tetrafluoro alcohol intermediate (Scheme 10), which when coupled to a peptide sequence followed by oxidation provided the tetrafluoroketone 19. Compound 19 is a relatively potent inhibitor of human renin.

### Scheme 10



Renin inhibitors containing an  $\alpha,\alpha$ -difluoro- $\beta$ -aminodeoxystatine group was reported by Thaisrivongs, et al. (18). The starting material for the synthesis is *N*-protected difluorostatine. As shown in Scheme 11, the 4-methoxyphenyl-protected  $\alpha,\alpha$ -difluoro- $\beta$ -aminodeoxystatine was synthesized in three steps from the sodium salt of difluorostatine. Coupling of the protected  $\alpha,\alpha$ -difluoro- $\beta$ -aminodeoxystatine with an appropriate peptide sequence, followed by deprotection of the 4-methoxyphenyl group via oxidation with ceric ammonium nitrate provided 20, which is a relatively weak inhibitor of human plasma renin. Employing the same sequence of reactions, but starting with the  $\alpha$ -hydroxy isomer of difluorostatine provided compound 21, which is epimeric at the amino group as compared to 20. Compound 21 is a more potent inhibitor than 20.

## Scheme 11

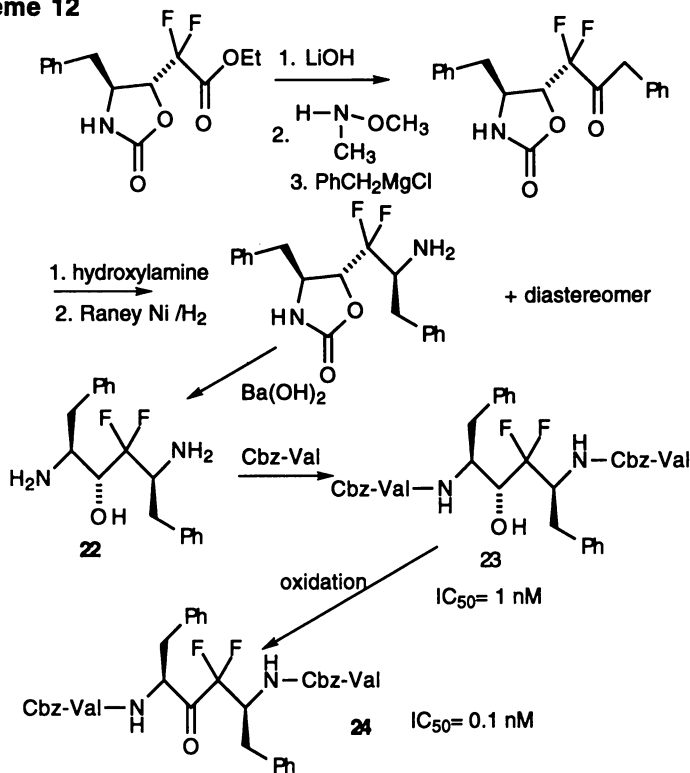


## HIV-1 Protease Inhibitors

Human immunodeficiency virus (HIV) is the causative agent of acquired immunodeficiency syndrome (AIDS). One of the key steps in the replication cycle of this virus is when HIV-1 protease, the proteolytic enzyme encoded by the retrovirus, cleaves specific amide bonds (e.g. between Phe-Pro) in precursor *gag* and *gag-pol* polyproteins to form the mature proteins needed for production of infectious viral particles (19). It is found that inactivation of this enzyme by site directed mutagenesis leads to the formation of non-infectious virions (20). X-ray crystal structures have established that the HIV-1 protease is a C-2 symmetric aspartyl protease consisting of two identical 99 amino acids subunits, with each subunit contributing one aspartic acid residue to the active site of the enzyme (21).

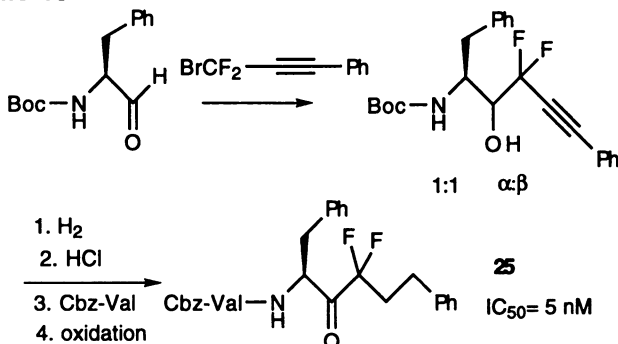
Diffluoroalcohols and difluoroketones, utilizing the pseudo-symmetric compound **22** as the key intermediate in the synthesis have been reported (22). Using the known oxazolidinone (**9**) as the starting material, hydrolysis of the ethyl ester, formation of the Weinreb amide followed by addition of benzyl magnesium chloride provided the corresponding ketone (Scheme 12). Oxime formation from the ketone followed by hydrogenation gave the diastereomeric amines. Opening of the oxazolidinone ring by basic hydrolysis provided the pseudo-symmetric diamine **22** and its diastereomer. Coupling to Cbz-valine gave difluoroalcohol **23**, which is a potent inhibitor of HIV-1 protease. Oxidation of the alcohol **23** provided the corresponding difluoroketone **24**, which is ~10x more potent. This series of difluoroketones also possess good antiviral activity in vitro in MT-4 cell culture assay (23).

Scheme 12



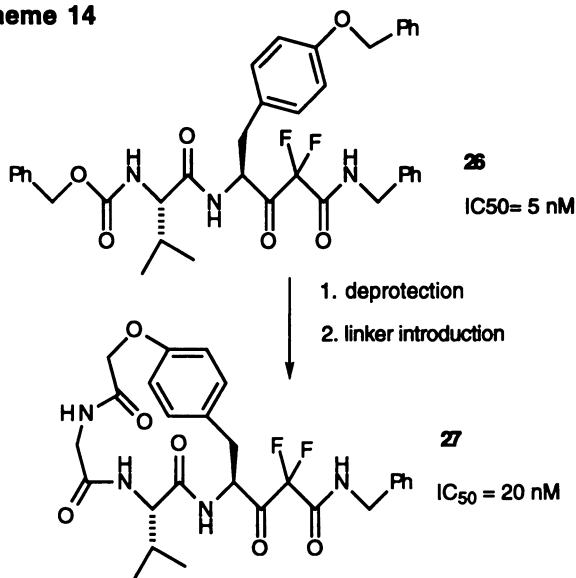
A related series of difluoroketones in which the C-terminus portion is truncated has been reported (24). The synthesis is highly efficient. Reformatsky reaction of bromodifluoromethylphenyl acetylene with N-Boc-phenylalaninal provided the acetylenic difluoroalcohol (Scheme 13). A sequence of reactions on this alcohol that include 1. hydrogenation, 2. Boc deprotection, 3. coupling to Cbz-Val-OH, 4. oxidation, provided the difluoroketone **25**. Compound **25** when compared to **24** still is a fairly potent HIV-1 protease inhibitor, though it is truncated in size.

Scheme 13



A short and unexpectedly potent difluorostatone type inhibitors of HIV-1 protease, compound **26**, has been described (25). An interesting extension of this work was also reported (26). By deprotecting both the Cbz- and benzyl ether groups in compound **26** and linking the free amino and hydroxy groups through a linker, a novel macrocyclic HIV protease inhibitor **27** was synthesized (Scheme 14).

Scheme 14



### Summary

A wide variety of fluorine containing peptidomimetics that are inhibitors of human renin and HIV-1 protease, both of which belong to the aspartyl protease family, are described. In general, most of the difluoroketones are more potent inhibitors than their fluoroalcohol counterparts. This lends support to the assumption that the tetrahedral hydrated carbonyl (due to the strong electronegativity of the adjacent fluorines) mimics well the tetrahedral hydrated carbonyl formed during the hydrolysis of peptide amide bonds catalyzed by the aspartyl proteases.

### Acknowledgments

I am grateful to Ms. Cynthia Mordhorst for the preparation of this manuscript.

### Literature Cited

- Greenlee, W. J. *Med. Res. Rev.*, **1990**, *10*, 173.
- Gelb, M. H.; Svaren, J. P.; Abeles, R. H. *Biochemistry* **1985**, *24*, 1813.
- Thaisrivongs, S.; Pal, D. T.; Kati, W. M.; Turner, S. R.; Thomasco, L. M.; Watt, W. *J. Med. Chem.* **1986**, *29*, 2080.
- Fearon, K.; Spaltenstein, A.; Hopkins, P. B.; Gelb, M. H. *J. Med. Chem.* **1987**, *30*, 1617.
- Doherty, A. M.; Sisear, I.; Kornberg, B. E.; Quin, J.; Winters, R. T.; Kaltebronn, J. S.; Taylor, M. D.; Batley, B. L.; Rapundalo, S. R.; Ryan, M. J.; Painchaud, C. A. *J. Med. Chem.* **1992**, *35*, 2.

- 6) Bradbury, R. H.; Rivett, J. E. *J. Med. Chem.* **1991**, *34*, 151.
- 7) Schirlin, D.; Baltzer, S.; Altenburger, J. M. *Tetrahedron Lett.* **1988**, *29*, 3687.
- 8) Tarnus, D.; Jung, M. J.; Remy, J. M.; Baltzer, S.; Schirlin, D. *FEBS Lett.* **1989**, *249*, 47.
- 9) Sham, H. L.; Rempel, C. A.; Stein, H.; Cohen, J. *J. Chem. Soc. Chem. Comm.* **1990**, 904.
- 10) Hoover, D. J.; Damon, D. B. *J. Am. Chem. Soc.* **1990**, *112*, 6439.
- 11) Patel, D. V.; Gauvin, K. R.; Ryono, D. E. *Tetrahedron Lett.* **1988**, *29*, 4665.
- 12) Imperiali, B.; Abeles, R. H. *Tetrahedron Lett.* **1986**, *27*, 135.
- 13) Sham, H. L.; Stein, H.; Rempel, C. A.; Cohen, J.; Plattner, J. J. *FEBS Lett.* **1987**, *220*, 299.
- 14) Angelastro, M. R.; Burkhart, J. P.; Bey, P.; Peet, N. P. *Tetrahedron Lett.* **1992**, *33*, 3265.
- 15) Nahm, S.; Weinreb, S. M. *Tetrahedron Lett.* **1981**, *22*, 3815.
- 16) Rosenberg, S. *U.S. Patent 4857507* **1989**.
- 17) Pfenninger, E.; Weidmann, A. *Br. Pat. Appl. 86-19182*, **1986**.
- 18) Thaisvivongs, S.; Schostarez, H. J.; Pal, D. J.; Turner, S. R. *J. Med. Chem.* **1987**, *30*, 1837.
- 19) Norbeck, D. W. *Ann. Rep. Med. Chem.* **1990**, *25*, 149.
- 20) Kohl, N. W.; Emini, E. A.; Schleif, W. A.; Davies, L. J.; Heimback, J. C.; Dixon, R. A. F.; Scolnick, E. M.; Sigal, E. S. *Proc. Natl. Acad. Sci.* **1988**, *85*, 4686.
- 21) Navia, M. A.; Fitzgerald, P. M. D.; McKeever, B. M.; Leu, C. T.; Heimbach, J. C.; Herber, W. K.; Sigal, I. S.; Darke, P. L. *Nature (London)* **1989**, *337*, 615.
- 22) Sham, H. L.; Wideburg, N. E.; Spanton, S. G.; Kohlbrenner, W. E.; Betebenner, D. A.; Kempf, D. J.; Norbeck, D. W.; Plattner, J. J.; Erickson, J. W. *J. Chem. Soc. Chem. Comm.* **1991**, 110.
- 23) Sham, H. L.; Betebenner, D. A.; Wideburg, N. E.; Saldivar, A. C.; Kohlbrenner, W. E.; Craig-Kennard, A.; Vasavanonda, S.; Kempf, D. J.; Clement, J. J.; Erickson, J. E.; Plattner, J. J.; Norbeck, D. W. *FEBS Lett.* **1993**, *329*, 144.
- 24) Sham, H. L.; Betebenner, D. A.; Wideburg, N. E.; Kempf, D. J.; Plattner, J. J.; Norbeck, D. W. *J. Fluorine Chem.* **1995**, *73*, 221-224.
- 25) Schirlin, D.; Dorssleer, V. V.; Tarnus, C.; Taylor, D. L.; Tyms, A. S.; Baltzer, S.; Weber, F.; Remy, J. M.; Brennan, T.; Farr, R.; Janowick, D. *Bioorg. Med. Chem. Lett.* **1994**, *4*, 241.
- 26) Podlogar, B. L.; Farr, R. A.; Friedrich, D.; Tarnus, C.; Huber, E. W.; Cregge, R. J.; Schirlin, D. *J. Med. Chem.* **1994**, *37*, 3684.

## Chapter 15

# Inhibition of Ornithine Aminotransferase: A New Target for Therapeutic Intervention

J. B. Ducep<sup>1</sup>, K. Jund<sup>1</sup>, B. Lesur<sup>1</sup>, S. Sarhan<sup>1</sup>, M. Schleimer<sup>1</sup>,  
P. R. Zimmermann<sup>1</sup>, and N. Seiler<sup>2</sup>

<sup>1</sup>Strasbourg Center, Marion Merrell Dow Research Institute,  
16 rue d'Ankara, 67080 Strasbourg Cedex, France

<sup>2</sup>Groupe de Recherche en Thérapeutique Anticancéreuse, Unité  
de Recherche Associé au Centre National de la Recherche Scientifique  
1529, Institut de Recherche Contre le Cancer, Faculté de Médecine,  
Université de Rennes, 2 avenue du Pr. Léon Bernard,  
F-35043 Rennes Cedex, France

5-Fluoromethylornithine (5-FMorn) is an irreversible inhibitor of ornithine aminotransferase (OAT). Among the four enantiomers, only one enantiomer had inhibitory activity. (*S,S*)-5FMorn **2a** was synthesized and found to be the active enantiomer. OAT inhibition was shown to enhance other ornithine metabolic pathways, such as the urea cycle and polyamine formation. Thus, **2a** improved ammonia detoxification through enhancement of urea formation. Therefore it can be expected that **2a** will be of therapeutic value in diseases characterized by elevated concentrations of ammonia in blood and cerebrospinal fluid. Increased polyamine formation may support tissue and nerve regeneration after trauma.

Ornithine (2,5-diaminopentanoic acid; Orn) and the most abundant inhibitory neurotransmitter amino acid, 4-aminobutyric acid (GABA), have certain features in common. Their major catabolic pathways are initiated by the transfer of the  $\omega$ -amino groups to 2-oxoglutarate. These reactions are catalyzed by similar pyridoxal phosphate-dependent enzymes. Both amino acids are present in virtually all tissues of the vertebrate organism, though at different concentrations: in accordance with its neurotransmitter function GABA concentrations are highest in brain (1), whereas highest Orn concentrations are found in liver (2,3), in agreement with its role in urea formation.

Due to its well established physiological role all aspects of GABA metabolism have been extensively studied (4), and several inhibitors of 4-aminobutyrate:2-oxoglutarate aminotransferase (GABA-T) were synthesized. One of the inactivators of GABA-T became an antiepileptic drug (5). In contrast, our knowledge of the physiological and pharmacological aspects of Orn is incomplete. Only with the availability of the racemic mixture of 5-fluoromethylornithine (MDL 72912, (*R/S*)-

0097-6156/96/0639-0196\$15.00/0

© 1996 American Chemical Society



5FMOrn) (6), it became possible to study consequences of the selective inactivation of ornithine:2-oxoglutarate aminotransferase (OAT) *in vivo*. It became apparent (7) that only one out of the four enantiomers, namely (*S,S*)-6-fluoro-2,5-diaminohexanoic acid, was an inactivator of OAT. Therefore, the synthesis of this compound became of major interest.

## 2. Biochemical Implications

**2.1. Ornithine Metabolism.** In liver ornithine is at the crossing of three major metabolic pathways (Fig. 1):

a). Orn reacts with carbamoyl phosphate to form citrulline. This reaction, catalyzed by ornithine:carbamoyltransferase (OCT), is the first step of the urea cycle. The final product of the reaction sequence is arginine, which is hydrolyzed by arginase to form Orn and urea. The role of the urea cycle is the elimination of ammonia from the organism, the most important endogenous CNS toxicant. Citrulline formation occurs nearly exclusively in the liver. In most other organs OCT activity is low or absent. However, most tissues contain arginase. In muscle Orn is formed by transfer of the amidino group of arginine to glycine (Fig. 1).

b). Orn is decarboxylated by ornithine decarboxylase (ODC) to form putrescine (1,4-butanediamine). This reaction is the initial, highly regulated step of polyamine formation (8,9). The transformation of putrescine to spermidine, and the formation of spermine from spermidine is catalyzed by specific synthases.

The polyamines are constituents of all cells. They are required to ensure basic functions, such as growth, proliferation and differentiation.

In agreement with their ubiquitous occurrence the decarboxylation of Orn is a general reaction, it plays, however, quantitatively a minor role, compared to the other reactions of Orn.

c) Orn reacts with 2-oxoglutarate to form glutamic acid and glutamic acid semialdehyde. OAT, the enzyme which catalyzes this reaction, is a mitochondrial matrix enzyme. It is presumably present in most vertebrate tissues. Glutamic acid semialdehyde is mainly transformed to glutamic acid by glutamic acid semialdehyde dehydrogenase, but it is also a precursor of proline, which may be formed via  $\Delta^1$ -pyrroline 5-carboxylic acid (Fig. 1). There are not only metabolic, but also regulatory interrelationships between Orn and GABA (10), even though most of the glutamate used in the brain to form GABA is formed by hydrolysis of glutamine, not by the pathway shown in Fig. 1.

It is evident from the above statements that the transamination of Orn and its role as precursor of putrescine are general, whereas its function within the urea cycle is nearly exclusive for liver. The relative rates of the three reactions of Orn change with physiologic and also under pathologic conditions. To mention only one example: In the case of malignant liver tumors, the activities of both OCT and OAT are reduced, whereas ODC activity is enhanced (11). Increased activities of ODC and enhanced formation of putrescine are usually signalling the increase of cell proliferation rates of both normal (embryonal development) and tumor cells (12).

**2.2. Ornithine: 2-Oxoacid Aminotransferase (OAT).** The analysis of the gene structure suggests one expressed gene and several pseudogenes (13,14), but there are observations in favor of the existence of more than one form of OAT. The enzyme has been purified e.g. by Peraino et al. (15) from several sources (mol. wt. 43 - 45 kDa). Its physical properties have been extensively studied. For example, a preliminary x-ray diffraction study of human recombinant OAT has been reported (16), the amino acid sequence, including that of the active site of the enzyme is known (17,18), and the quaternary structure of the enzyme from pig kidney has been studied by high-resolution electron microscopy (19). The activity of the liver OAT is affected by multiple factors among which hormones and diet are most important.

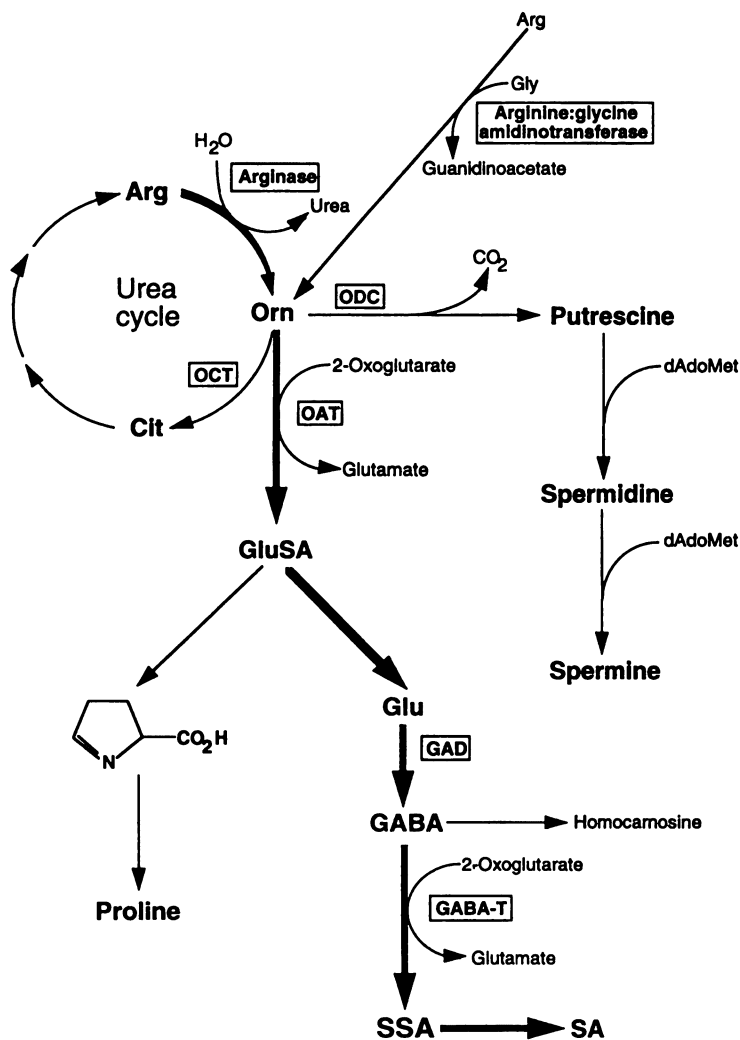


Fig. 1. Major reactions involved in ornithine metabolism

*Enzymes:* arginase; arginine:glycine amidinotransferase; ornithine:2-oxoacid aminotransferase (OAT), ornithine:carbamoyltransferase (OCT); ornithine decarboxylase (ODC).

*Abbreviations:* Arg arginine, Cit citrulline, Gly glycine, Glu glutamic acid, GluSA glutamic acid semialdehyde, GAD glutamic acid decarboxylase, GABA 4-aminobutyric acid, GABA-T 4-aminobutyric acid:2-oxoacid aminotransferase, dAdoMet decarboxylated S-adenosylmethionine.

**2.3. Inhibitors of OAT.** It has been mentioned that OAT is a pyridoxal phosphate-dependent enzyme (15). The key step in the transamination sequence is the abstraction of the pro-S hydrogen atom at C5 (20). These properties suggested the search for inhibitors of OAT.

**2.3.1. Pyridoxal Phosphate Scavengers.** Non-specific inhibition of OAT by carbonyl reagents was predictable. For example 0.2 mM amino-oxyacetic acid inhibits almost completely OAT from rat liver mitochondria (21). This compound is known to inhibit also GABA-T, and many other transaminases and glutamate decarboxylase (22,23). *l*-Canaline [(*S*)-2-amino-amino-oxybutyric acid], a close structural analog of Orn, is a rather potent and selective inhibitor of OAT (24). Scavenging of pyridoxal phosphate as the mechanism of inactivation has been established (25,26). Inactivation is not restricted to the natural *S* enantiomer, however, the *R* enantiomer reacts considerably slower with the enzyme (7). Although rather selective *in vitro*, *l*-canaline is not well suited for *in vivo* studies. It appears to be rapidly metabolized. Consequently high doses are required, and the effects are relatively short lasting, as has been shown for the racemate (7,10).

**2.3.2. Enzyme-activated Irreversible Inhibitors.** Enzyme-activated irreversible inhibitors (mechanism based inactivators) are relatively unreactive molecules which require a considerable structural similarity to the natural substrate, in order to allow competition for binding within the active site of the enzyme, and activation by the catalytic reaction (27,28). The close relationship between GABA-T and OAT is documented by the fact that most enzyme-activated irreversible inhibitors of GABA-T [(*S/R*)-4-amino-5-hexynoic acid; (*S*)-4-amino-5,6-heptadienoic acid; 5-amino-1,3-cyclohexadienyl carboxylic acid (gabaculin)] are potent inactivators of OAT, both *in vitro* and *in vivo* (29-31).

Mono or difluorinated methyl analogs of 3-aminopropionic acid, GABA and homoGABA were also found to be irreversible inhibitors of both GABA-T and/or OAT. (Table 1).

Based on this knowledge, (*R/S*)-5FMOrn was conceived as a potential inactivator of OAT. Indeed, (*R/S*)-5FMOrn exhibits concentration- and time-dependent inactivation of OAT *in vitro*. The inactivation rate is reduced in the presence of Orn, indicating competition for binding at the active site of the enzyme. No significant inhibitory effect is exerted on OCT, but (*R/S*)-5-FMOrn is decarboxylated by ODC at a rate approximately 100-times slower than Orn. The compound did not inactivate GABA-T, and even long-term administration of the compound did not show any evidence for the accumulation of GABA in brain (3). In mice it caused a dose- and time-dependent decrease of OAT activity, virtually in all tissues. A dose of 25 mg/kg given intraperitoneally produced maximal (85 - 95%) inactivation between 1 and 24 h. The extent of OAT inhibition depended on the tissue; a fraction of OAT activity present in most tissues was refractory to inactivation by (*R/S*)-5FMOrn, but was inhibited competitively (33). During the time of maximal inhibition of OAT, Orn concentrations increased dramatically in all organs, including the brain. However, even chronic administration of the compound to mice at daily intraperitoneal doses of 10 - 20 mg/kg, or by oral administration (with the drinking fluid) at an average daily dose of 40 mg/kg did not produce any toxicology, or gross behavioral changes (3). Specific attention was paid to the possibility of the development of gyrate atrophy, since it was believed (34) that elevated Orn concentration in the eye is a major pathogenetic factor in gyrate atrophy of the choroid and retina.

### 3. Consequences and Therapeutic Rationale of OAT Inhibition

(*R/S*)-5FMOrn is the first compound that allows one to produce long lasting elevations of tissue Orn concentrations without producing toxic effects. Therefore, potential therapeutic applications of OAT inhibition were envisaged. Since Orn accumulates rapidly in virtually all organs of the vertebrate organism one has to

assume that transamination is indeed the major general catabolic pathway of Orn, and that Orn cannot be eliminated at an appropriate rate by urinary excretion. A consequence of the elevation of Orn concentrations during long-term blockade of OAT is its channeling into the remaining pathways (Fig. 1). The enhanced formation of putrescine, and of citrulline could be expected, unless the enzymes responsible for the key reactions were saturated under physiological conditions.

**3.1. Enhancement of Polyamine Metabolism.** Administration of (*R/S*)-5FMOrn elevates only moderately putrescine concentrations in tissues, and has no significant effect on the concentrations of spermidine and spermine. However, as was established for mouse brain, the turnover of spermidine is increased by 100% (35). The increase of polyamine concentrations is avoided due to the close regulation of their intracellular concentration (8,9), but as the experiments demonstrated, an enhanced flux of the putrescine moiety along the polyamine metabolic pathway was obvious.

Major efforts of the last 15 years were devoted to establish methods for the inhibition of polyamine formation, in order to prevent neoplastic growth (36). Potential targets for the opposite, namely the enhancement of polyamine biosynthesis, are therapeutically required growth processes, specifically the regeneration of injured tissues. It is known that administration of the 2-oxoglutarate salt of Orn has, among others, beneficial effects in surgical and other trauma (37,38), and in burn injury (39). Most probably the enhancement of polyamine formation contributes to the favorable effect of this treatment (40,41). After injury of their axons, neurons appear to shift their metabolic activity into a reparative mode, aimed at survival and regeneration. Alternatively they undergo degeneration and die. Treatment with polyamines is known to enhance functional regeneration of peripheral nerves after axotomy (42-45) and favors the survival of neurons after axonal injury or ischemia (46,47).

These few examples may be sufficient to indicate potential applications for the inhibition of OAT in an area of great therapeutic importance. Up to now very little work has been done concerning effects of (*R/S*)-5FMOrn on models of tissue regeneration. This may change with the general availability of the active enantiomer of 5FMOrn.

**3.2. Detoxification of Ammonia by Enhancement of Urea Formation.** Inactivation of OAT by (*R/S*)-5FMOrn is not only evident from the enhanced citrulline and urea formation and the suppression of the ammonia-induced pathologic excretion of orotic acid (48,49), but also from the impressive protection of treated animals from lethal intoxication with ammonium salts. Pretreatment with 0.042 mmol/kg of the drug before administration of 13 mmol/kg ammonium acetate is sufficient to protect 90% of the animals from death for more than 10 h (50). By comparison, 20 mmol/kg of arginine or Orn are needed to achieve a short lasting (<2h) protection against the same dose of an ammonium salt. The protective effect can even be potentiated if the treatment with (*R/S*)-5FMOrn is combined with the administration of *l*-carnitine or *l*-acetylcarnitine (51). The mechanism, by which carnitine antagonizes ammonia intoxication has not been clarified. The protection by (*R/S*)-5FMOrn is clearly due the prevention of the accumulation of lethal concentrations of ammonia in the brain. Treatment with (*R/S*)-5FMOrn was, however, ineffective, if blood-flow through the liver was bypassed by a portacaval shunt (52).

Sparse fur mice have in analogy to the human hereditary OCT deficiency (53) a defective OCT, and have, therefore, chronically elevated ammonia levels in plasma and tissues, and they excrete enormous amounts of orotic acid. Treatment with (*R/S*)-5FMOrn nearly completely restored normal blood ammonia levels and orotic acid excretion (54) in these mice.

In a model of hepatic encephalopathy (injection of thioacetamide) repeated administration of (*R/S*)-5FMOrn prevented the development of lethal pathology, and ameliorated many symptoms of the disease (49,55).

There are a considerable number of disease states, which are characterized by elevated blood and cerebrospinal fluid ammonia concentrations, frequently paired

with orotic aciduria. Examples are summarized in Table 2. Ammonia-induced excretion of orotic acid indicates a conditional deficiency of Orn (56). Based on the experience with animal models it is quite conceivable that inhibition of OAT by a selective inhibitor would in many of these illnesses improve the ammonia-induced symptoms. Efficacy of OAT inhibition is especially expected in those disease states with a less severely impaired liver function. Alzheimer's Disease is presumably a target of especial importance (85,86).

#### 4. (*S,S*)-5-Fluoromethylornithine (2*S*,5*S*-6-fluoro-2,5-diaminohexanoic acid).

Based on the following considerations (*S,S*)-5FMOrn **2a** was presumed to be the active enantiomer of 6-fluoro-2,5-diaminohexanoic acid:

- Only one of the four enantiomers of (*R/S*)-5FMOrn reacted with OAT (7).
- (2*S*)-Orn, not (2*R*)-Orn is a substrate of OAT.
- The key reaction of Orn transamination is the abstractions of the pro*S* hydrogen of the  $\omega$ -carbon atom (20).

Proof for this assumption was expected from the synthesis of (*S,S*)-5FMOrn.

**4.1. Synthesis of (*S,S*)-5FMOrn.** Racemic 5-fluoromethylornithine is a mixture of enantiomers (*RR*, *SS* and *RS*, *SR*). Our strategy for the synthesis of the *SS*-diastereomer was to convert diaminoadipic acid **1** into 2*S*, 5*S*-5-fluoromethylornithine via a diastereomeric separation and an enantiomeric resolution.

The diastereomeric resolution of diaminoadipic acid can be performed through the dilactams **4a,b**: only the *RR*, *SS* diastereoisomers are able to give 2,5-diazabicyclo [2, 2, 2] octane-3, 6- dione (**4a,b**) (87) while the meso isomer gives only six membered ring monolactams which upon epimerization may produce the dilactams **4a,b** (Scheme 1).

Treatment of the dilactams **4a,b** with methanolic hydrochloric acid (0.27M) opened one of the lactam rings to give 3-amino-6-carbomethoxy-2-piperidinones hydrochloride (**5a,b**) (Scheme 2) which were, after neutralization with silver carbonate and acylation with phenylacetic acid (dicyclohexylcarbodiimide in methylene chloride) gave the 6-carbomethoxy-3-phenylacetamido-2-piperidinones (**6a,b**) (90 % from **4a,b**). The methyl esters were reduced to alcohols **7a,b** using lithium borohydride with a catalytic amount of lithium triethylborohydride (88). About 10 % epimerization occurred during reduction. Recrystallization from methanol afforded alcohols **7a,b** (75 %, 99 % de) (89). These alcohols were fluorinated with one equivalent of DAST in methylene chloride to yield **8a,b** (66 %, 99 %de) (89).

Treatment of lactams **8a,b** with benzylpenicillinase (90) hydrolysed one enantiomer faster (Scheme 3). Separation of the amino lactam **9a** from the unchanged one **8b** followed by complete hydrolysis of each fraction gave the active enantiomer **2a** along with its epimer **2b**.

The selectivity of phenylacetamide functionality hydrolysis of the ester and alcohol lactams **6a,b**, **7a,b** respectively by benzylpenicillinase was the same in each case: the *SS* enantiomer was cleaved faster than the *RR* enantiomer by benzyl penicillinase.

In order to obtain an ee > 90 % we had to stop rapidly the enzymatic hydrolysis. The low yield of free amine was of no preparative value.

To overcome this difficulty we decided to run twice the enzymatic hydrolysis using the fluoromethyl derivatives **8a,b** (Scheme 4). The first hydrolysis was run until total hydrolysis of one enantiomer (89). This was reconverted to the phenylacetamide and then again treated with benzylpenicillinase. The *SS* enantiomer was obtained with excellent enantiomeric purity (ee = 95%) (89). Reprotection of the free amine **9a** by phenylacetamidation facilitated purification of the *S,S* enantiomer and a 20 % chemical yield was obtained for the resolution. Complete hydrolysis of **8a** afforded 2*S*,5*S*-5-fluoromethyl ornithine (**2a**).

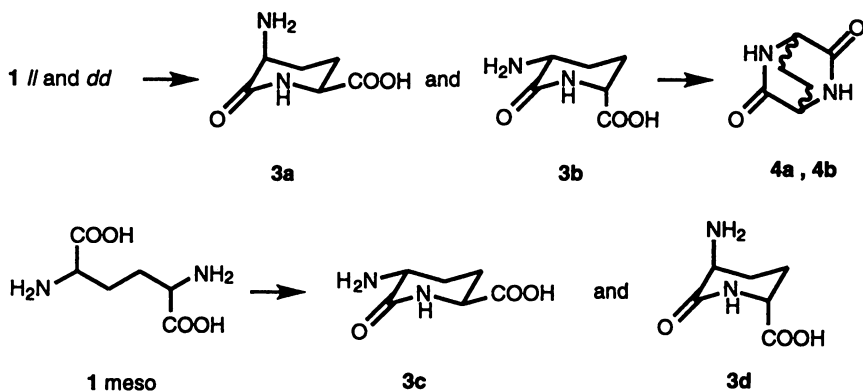
Table 1. Inactivation of GABA-T and OAT by mono- and difluorinated methyl analogs of GABA and its homologs

ENTRY	GABA T	OAT
$\begin{array}{c} \text{FH}_2\text{C} \\   \\ \text{CH} \\   \\ \text{NH}_2 \\   \\ \text{CH}_2 \\   \\ \text{COOH} \end{array}$	$t_{1/2}$ =8min at 1mM	20% inhibition at 30min, 1mM
$\begin{array}{c} \text{FH}_2\text{C} \\   \\ \text{CH} \\   \\ \text{NH}_2 \\   \\ \text{CH}_2 \\   \\ \text{CH}_2 \\   \\ \text{COOH} \end{array}$	$t_{1/2}$ =10min at 1mM	$t_{1/2}$ =23min at 1mM
$\begin{array}{c} \text{FH}_2\text{C} \\   \\ \text{CH} \\   \\ \text{NH}_2 \\   \\ \text{CH} \\   \\ \text{CH}=\text{CH} \\   \\ \text{COOH} \end{array}$	$t_{1/2}$ =4min at 1mM	$t_{1/2}$ =8min at 2mM
$\begin{array}{c} \text{F}_2\text{HC} \\   \\ \text{CH} \\   \\ \text{NH}_2 \\   \\ \text{CH}_2 \\   \\ \text{CH}_2 \\   \\ \text{CH}_2 \\   \\ \text{COOH} \end{array}$	N.A. at 10mM	30% inhibition at 45min, 1mM
$\begin{array}{c} \text{FH}_2\text{C} \\   \\ \text{CH} \\   \\ \text{NH}_2 \\   \\ \text{CH}_2 \\   \\ \text{CH}_2 \\   \\ \text{CH}_2 \\   \\ \text{COOH} \end{array}$	$t_{1/2}$ =1min at 10mM	$t_{1/2}$ =24min at 1mM

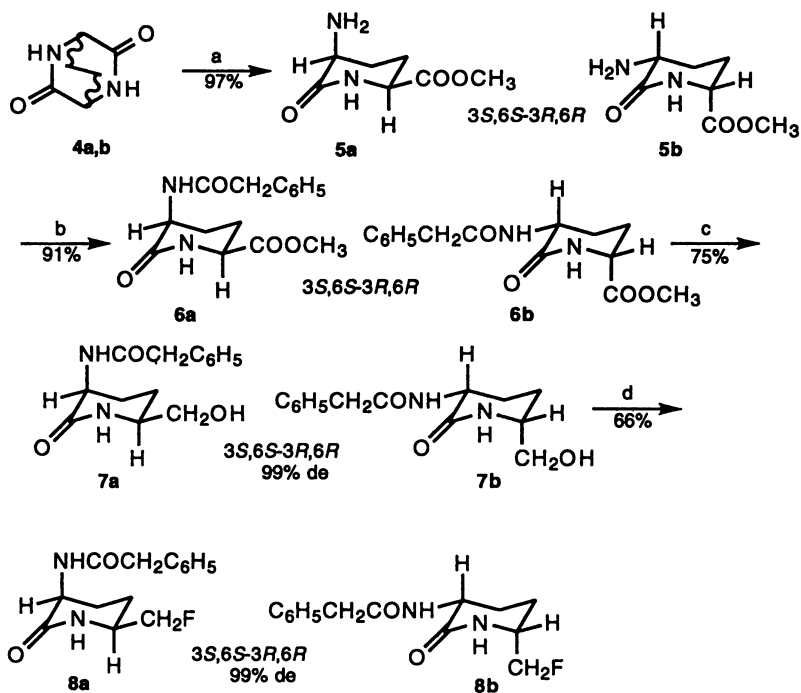
Table 2. Human illnesses and therapeutic interventions which are associated with elevated blood or cerebrospinal fluid ammonia concentrations\*.

Hepatic encephalopathy	(57,58)	Reye's syndrome	(71,72)
Fulminant hepatic failure	(59)	Systemic carnitine deficiency	(73)
Alzheimer's Disease	(60-62)	Hyperornithinemia, hyperammonemia, homocitrullinemia syndrome	(74)
Urinary tract (bladder) infections	(63,64)	Nonketotic hyperglycinemia	(75)
Congestive heart failure	(65)	Progressive neuronal degeneration of childhood (Alper's syndrome)	(76)
Pulmonary emphysema	(66)	Uretersigmoidostomy	(78-80)
Shock	(67)	Complications of hemodialysis	(81)
IgD multiple melanomas	(68)	Valproate therapy	(82-84)
Hereditary deficiencies of urea cycle enzymes	(69,70)		

\* References in parentheses.

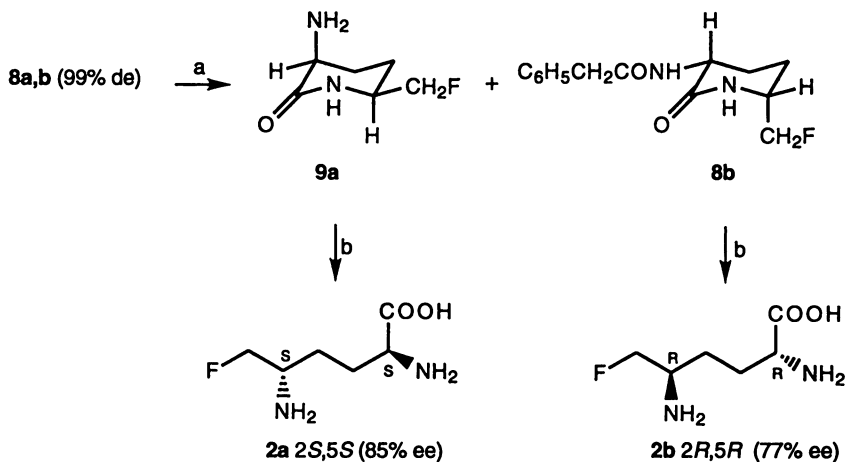


Scheme 1



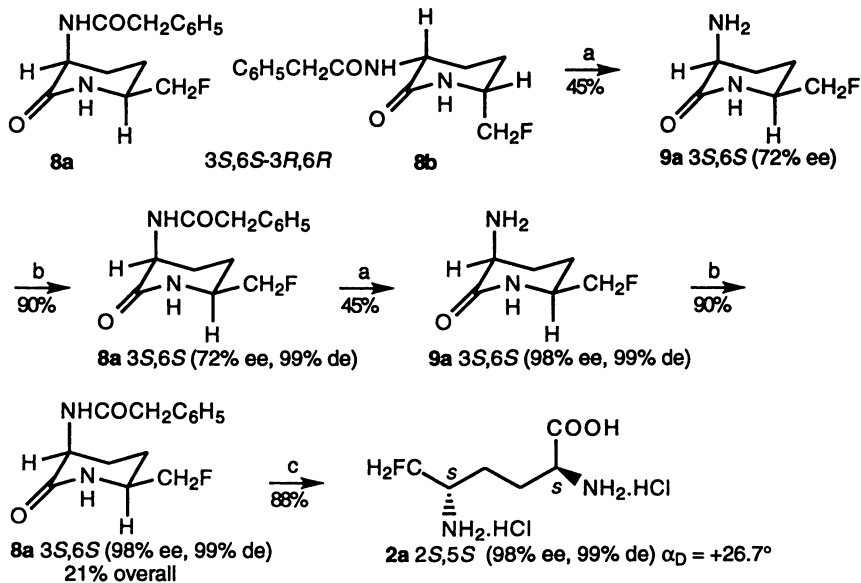
a) HCl/CH<sub>3</sub>OH (0.27M), overnight; Ag<sub>2</sub>CO<sub>3</sub> (1.1eq); b) C<sub>6</sub>H<sub>5</sub>CH<sub>2</sub>COOH (1eq, DCC (1eq), pyridine (1.2eq), DMAP (cat.), CH<sub>2</sub>Cl<sub>2</sub>, RT, 48h; c) LiBH<sub>4</sub> (1eq), LiEt<sub>3</sub>BH (0.1eq), THF, reflux overnight; d) DAST (1eq), CH<sub>2</sub>Cl<sub>2</sub>, RT overnight.

Scheme 2



a) Benzylpenicillinase; b) Hydrolysis.

Scheme 3



a) Benzylpenicillinase, phosphate buffer (pH=7), RT, 10 min; b) C<sub>6</sub>H<sub>5</sub>CH<sub>2</sub>COOH (1eq), DCC (1eq), pyridine (1.2eq), DMAP (cat.), CH<sub>2</sub>Cl<sub>2</sub>, 48 h; c) HCl 6N, reflux, 4h.

Scheme 4



The pure lactam ester **6a**, the precursor of 2*S*,5*S*-5-FMOrn was obtained by preparative HPLC (89). Its complete hydrolysis gave diaminoadipic acid **1** with an  $\alpha_D$  of + 38.6° which correlated with *SS* or *ll* enantiomer of diaminoadipic acid (lit  $\alpha_D$  = + 26.5°) (91).

**4.2. Kinetics of OAT Inactivation.** Partially purified OAT from rat liver (20) was inactivated in parallel experiments by (*R/S*)-5FMOrn and (*S,S*)-5FMOrn **2a**, using the conditions described earlier (7). Fig. 2. shows the time- and concentration dependent decrease of OAT activity during incubation at 37°C. The evaluation of the data according to Kitz and Wilson (92) showed with  $14 \pm 2$  min for the racemic mixture a slightly higher  $t_{1/2}$  than for the active enantiomer ( $11 \pm 1$  min). The  $K_i$  for the active enantiomer ( $2.4 \pm 0.3 \mu\text{M}$ ) was lower by a factor of 4.6, than the value found for the racemate ( $11 \pm 2 \mu\text{M}$ ). These data are a clear indication for the fact that only one of the four enantiomers of (*R/S*)-5FMOrn, **2a**, contributed to the inactivation of OAT, whereas the three remaining stereoisomers had, if any, only a negligible influence on the reaction. They are neither inactivators, nor obviously effective competitors for the active site of the enzyme. These observations are also indicators for the absolute stereoselectivity of the transamination reaction by OAT.

**4.3. Effects of (2*S*,5*S*)-6-Fluoro-2,5-diaminohexanoic acid on OAT and Orn Concentrations.** Using **2a**, the key experiments reported previously for (*R/S*)-5FMOrn (**6**) were repeated, and gave the expected results. After the intraperitoneal administration of a single 10 mg/kg dose of (*S,S*)-5FMOrn to mice OAT was rapidly inactivated in all tissues up to about 90% of the control values (Fig. 3). The previously observed OAT activity refractory to inactivation by the racemate (**33**) was observed again. With time enzyme activity recovered at different rates in different organs, with  $t_{1/2}$  of 3 - 5 days. The mechanism underlying recovery of active OAT (reactivation or induction) has not yet been clarified.

As is exemplified for brain (Fig. 3), maximal Orn concentrations were observed in all tissues between 16 and 24 h after drug administration. The relatively rapid decline of Orn concentrations at a time when only a small fraction of OAT activity had recovered is due to the fact that OAT is not a rate limiting enzyme. It is normally present in most tissues in large excess. Even a fraction of the physiologic activity (<35% in brain) is sufficient to prevent an increase of Orn concentrations above normal level.

The dose-effect relationships are shown for 16 h after drug administration in Fig. 4 for mouse brain, kidney and liver. An intraperitoneal dose of 5 - 10 mg/kg of (*S,S*)-5FMOrn was sufficient to produce near maximal OAT inactivation in all tissues. In spite of this fact Orn concentrations increased with a further increase of the dose, most probably due to the fact that the mentioned 5-FMOrn-refractory OAT activity is competitively inhibited by the drug (33). The extent of Orn increase is very much dependent on the tissue. In mouse brain, with a normal level of  $17 \pm 4$  nmol/g, 20 mg/kg (*S,S*)-5FMOrn produced a 50-fold increase; in liver, with a basal level of 700 nmol/g the increase was only about 10-fold. However, the absolute concentrations of Orn in liver are higher by about an order of magnitude than in most other tissues.

**4.4. Protection against Acute Intoxication with a Lethal Dose of Ammonium Acetate.** As in previous experiments with the racemate (**50**) groups of 10 mice received single intraperitoneal doses of **2a** and 16 h later an intraperitoneal dose of 13 mmol/kg of ammonium acetate. In controls, the ammonium acetate produced the typical syndrome: hyperventilation followed by clonic seizures, loss of righting reflex, coma, and tonic hind limb extension frequently followed by death. Pretreatment with the OAT inactivator prevented tonic seizures (and death) in a dose-dependent manner at very low doses (Table 3). (*R/S*)-5FMOrn is not an anticonvulsant in a series of standard animal seizure models (50).

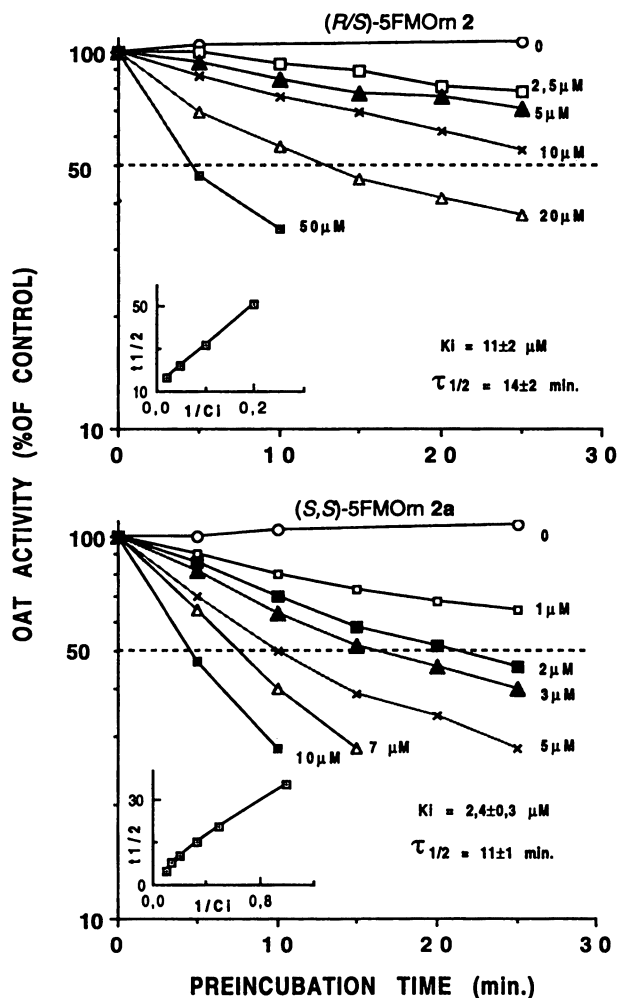


Fig. 2. Time and concentration-dependent inactivation of ornithine aminotransferase by (*R/S*)-5-fluoromethylornithine (**2**) (upper panel) and (*S,S*)-5-fluoromethylornithine (**2a**) (lower panel). Insets: Kitz-Wilson plots.

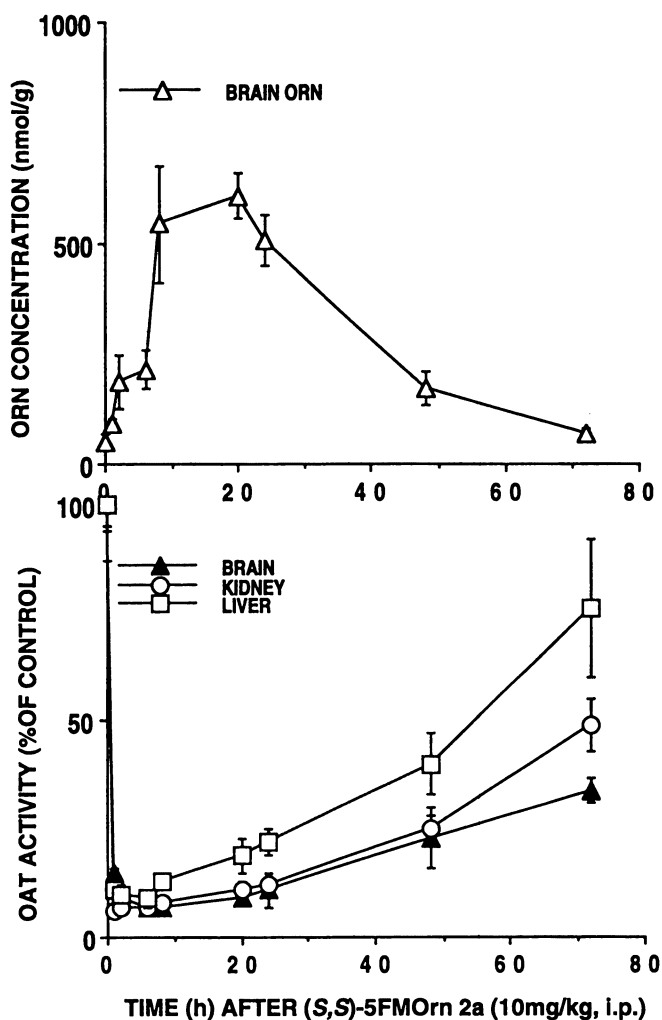


Fig. 3. Time course of ornithine aminotransferase activity in liver, kidney and brain of mice after the intraperitoneal administration of 10 mg/kg of (*S,S*)-5-fluoromethylornithine (**2a**) to mice (upper panel). Time course of ornithine aminotransferase activity and of ornithine concentration in mouse brain after intraperitoneal administration of 10 mg/kg of **2a** (lower panel). (Mean values of four animals; the vertical bars indicate  $\pm$  S.D.)

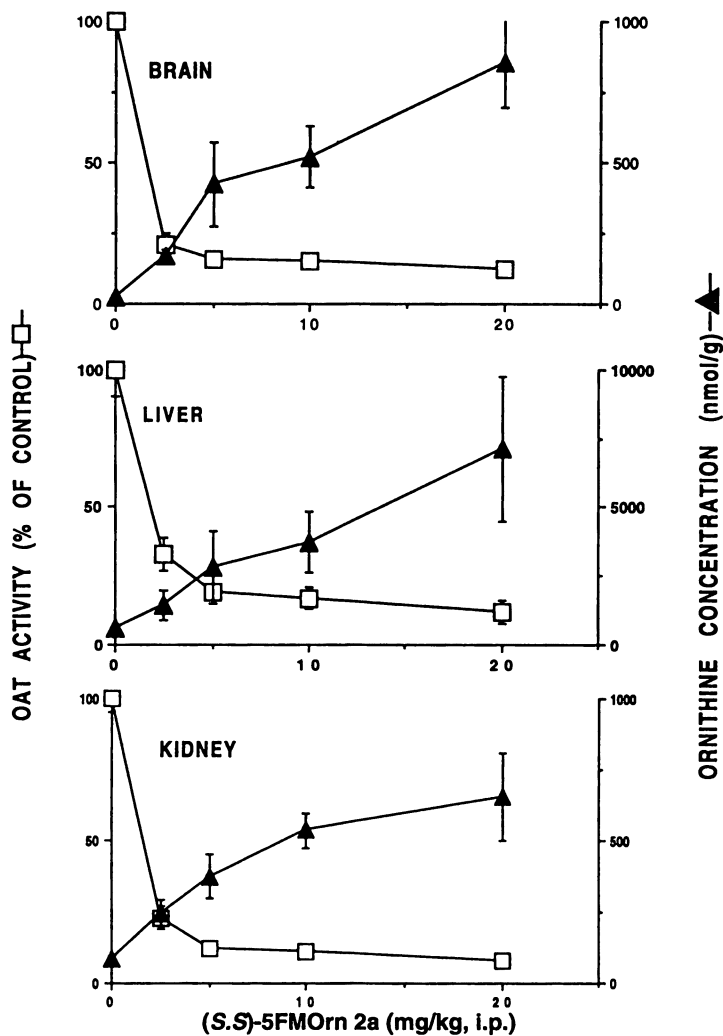


Fig. 4. Dose-related effect of (*S,S*)-5-fluoromethylornithine (**2a**) on ornithine aminotransferase activity and ornithine concentrations in brain, liver and kidney of mice, 16 h after the intraperitoneal administration of the drug. (Mean values of four animals; the vertical bars indicate  $\pm$  S.D.).

Table 3. Effect of (*S,S*)-5-FMorn **2a** on acute intoxication with ammonium acetate

Dose of <b>2a</b> mmol/kg	Percent of animals		
	with loss of righting reflex	with tonic seizures	surviving
0	100	60	70
0.00105	60*	40	80
0.0021	30*	20*	90
0.0042	20*	0*	100*
0.0105	0*	0*	100*

The asterisk indicates a significant ( $p < 0.005$ ) difference between treated and control groups (non parametric statistics).

Each treatment group consisted of 10 mice; 13 mmol/kg ammonium acetate was given intraperitoneally 16 h after the intraperitoneal administration of **2a**.

## 5. Conclusions

The biochemical properties of (*S,S*)-5FMOrn clearly demonstrate that it is the active enantiomer of 6-fluoro-2,5-diaminohexanoic acid. Although long-term administrations of the active enantiomers have not been carried out, it is beyond any doubt that it will exhibit the same low level of toxicity as the racemate. Therefore, the exploration of therapeutic applications for this new compound with a new biochemical profile is an obvious must.

## Literature cited

1. Perry, T.L. In *Handbook of Neurochemistry* (Lajtha, A. Ed.) 2nd. ed. Plenum, New York, 1982, vol. 1; pp 151-188.
2. Meister, A. *Biochemistry of the Amino Acids*, 2nd. ed. , Academic, New York, 1965, pp 108-113.
3. Daune-Anglard, G.; Bonaventure, N.; Seiler, N. *Pharmacol. & Toxicol.* 1993, 73, 29.
4. Seiler, N.; Lajtha, A. In *Neurotrophic Activity of GABA During Development*. (Redburn, D.A.; Schousboe, A. Eds.), Alan Liss Inc. New York, 1987, pp 1-56.
5. Grant, S.M.; Heel, R.C. *Drugs* 1991, 41, 889.
6. Daune, G.; Gerhart, F.; Seiler, N. *Biochem. J.* 1988, 253, 481.
7. Bolkenius, F.N.; Knoedgen, B.; Seiler, N. *Biochem. J.* 1990, 268, 409.
8. Pegg, A.E. *Biochem. J.* 1986, 234, 249.
9. Seiler, N.; Heby, O. *Acta Biochim. Biophys. Hung.* 1988, 23, 1.
10. Seiler, N.; Daune-Anglard, G. *Metabolic Brain Dis.* 1993, 8, 151.
11. Williams-Ashman, H.G.; Coppoc, G.L.; Schenone, A.; Weber, G. In *Polyamines in Normal and Neoplastic Growth* (Russell, D.H. Ed.) Raven, New York, 1973, pp 181-197.
12. Jänne, J.; Pösö, H.; Raina, A. *Biochim. Biophys. Acta* 1978, 473, 241.
13. Shull, J.D.; Pennington, K.L.; George, S.M.; Kilibarda, K.A. *Gene* 1991, 104, 203.
14. Shull, J.D.; Pennington, K.L.; Pitot, H.C.; Boryca, V.S.; Schulte, B.L. *Biochim. Biophys. Acta* 1992, 1132, 214.
15. Peraino, C.; Bunville, L.G.; Tahmisian, T.N. *J. Biol. Chem.* 1969, 244, 2241.
16. Shen, B.W.; Ramesh, V.; Mueller, R.; Hohenester, E.; Hennig, M.; Jansonius, J.N. *J. Mol. Biol.* 1994, 243, 128.
17. Mueckler, M.M.; Pitot, H.C. *J. Biol. Chem.* 1985, 260, 12993.
18. Simmaco, M.; John, R.A.; Barra, D.; Bossa, F. *FEBS Lett.* 1986, 199, 39.
19. Luensdorf, H.; Hecht, H.-J.; Tsai, H. *Eur. J. Biochem.* 1994, 225, 205.
20. Williams, J.A.; Bridge, G.; Fowler, L.J.; John, R.A. *Biochem. J.* 1982, 201, 221.
21. Murphy, B.J.; Brosnan, M.E. *Biochem. J.* 1976, 157, 33.
22. Baxter, C.F. In *Handbook of Neurochemistry* (Lajtha, A. Ed.) 1st ed. , Plenum, New York, 1970, Vol. 3; pp 289-353.
23. Rognstad, R.; Clark, D.G. *Arch. Biochem. Biophys.* 1974, 161, 638.
24. Rosenthal, G.A. *Life Sci.* 1978, 23, 93.
25. Sanada, Y.; Shiotani, T.; Okuno, E.; Katunuma, N. *Eur. J. Biochem.* 1976, 69, 507.
26. Kito, K.; Sanada, Y.; Katunuma, N. *J. Biochem. (Tokyo)* 1978, 83, 201.
27. Abeles, R.H. In *Enzyme-Activated Irreversible Inhibitors* (Seiler, N., Jung, M.J. and Koch-Weser, J. Eds.) Elsevier/North Holland, Amsterdam, 1978, pp 1-12.
28. Rando, R.R. In *Enzyme-Activated Irreversible Inhibitors*. (Seiler, N.; Jung, M.J.; Koch-Weser, J. Eds.) Elsevier: North Holland, Amsterdam, 1978, pp.13-26.
29. Jung, M.J.; Seiler, N. *J. Biol. Chem.* 1978, 253, 7431.
30. Jung, M.J.; Heydt, J. G.; Casara, P. *Biochem. Pharmacol.* 1984, 33, 3717.
31. Daune, G.; Seiler, N. *Neurochem. Res.* 1988, 13, 69.

32. Bey, P.; Jung, M.J.; Gerhart, F.; Schirlin, D.; Van Dorsselaer, V.; Casara, P. *J. Neurochem.* **1981**, *37*, 1341.
33. Daune, G.; Seiler, N. *Neurochem. Int.* **1988**, *13*, 383.
34. Kaiser-Kupfer, M.I.; De Monasterio, F.M.; Valle, D.L.; Walser, M.; Brusilow, S. *Science* **1980**, *210*, 1128.
35. Seiler, N.; Daune, G.; Bolkenius, F.N.; Knoedgen, B. *Int. J. Biochem.* **1989**, *21*, 425.
36. McCann, P.P.; Pegg, A.E.; Sjoerdsma, A. (Eds.) *Inhibition of Polyamine Metabolism*. Academic, Orlando, **1987**.
37. Wernerman, J. *Clin. Nutr.* **1993**, *12*, 58.
38. Jeevanandam, M. *Clin. Nutr.* **1993**, *12*, 61.
39. Donati, L.; Signorini, M.; Grappolini, S. *Clin. Nutr.* **1993**, *12*, 70.
40. Cynober, L. *Clin. Nutr.* **1993**, *12*, 54.
41. Jeevanandam, M.; Ali, M.R. *J. Clin. Nutr. Gastroenterol.* **1991**, *6*, 23.
42. Sebillé, A.; Bondoux-Jahan, M. *Exp. Neurol.* **1980**, *70*, 507.
43. Dornay, M.; Gilad, V.H.; Shiler, I.; Gilad, G.M. *Exp. Neurol.* **1986**, *92*, 665.
44. Kauppi, T. *Brain Res.* **1992**, *575*, 299.
45. Wong, B.J.; Mattox, S.E. *Exp. Neurol.* **1991**, *111*, 263.
46. Gilad, G.M.; Gilad, V.H. *Devl. Brain Res.* **1988**, *38*, 175.
47. Gilad, G.M.; Gilad, V.H. *Exp. Neurol.* **1991**, *111*, 349.
48. Seiler, N.; Grauffel, C.; Daune, G.; Gerhart, F. *Life Sci.* **1989**, *45*, 1009.
49. Sarhan, S.; Knoedgen, B.; Grauffel, C.; Seiler, N. *Neurochem. Res.* **1993**, *18*, 539.
50. Seiler, N.; Sarhan, S.; Knoedgen, B.; Hornsperger, J.M.; Sablone, M. *Pharmacol. & Toxicol.* **1993**, *72*, 116.
51. Sarhan, S.; Knoedgen, B.; Seiler, N. *Metab. Brain Dis.* **1994**, *9*, 67.
52. Therrien, G.; Sarhan, S.; Knoedgen, B.; Butterworth, R.F. *Metab. Brain Dis.* **1994**, *9*, 211.
53. Briand, P.; Francois, B.; Rabier, D.; Cathelineau, L. *Biochim. Biophys. Acta* **1982**, *704*, 100.
54. Seiler, N.; Grauffel, C.; Daune-Anglard, G.; Sarhan, S.; Knoedgen, B. *J. Inher. Metab. Dis.* **1994**, *17*, 691.
55. Seiler, N.; Sarhan, S.; Knoedgen, B. *Pharmacol. & Toxicol.* **1992**, *70*, 373.
56. Zieve, L. *J. Am. Coll. Nutr.* **1986**, *5*, 167.
57. Plum, F. *Exp. Biol. Med.* **1971**, *4*, 34.
58. Butterworth, R.F. *Dig. Dis. Sci.* **1992**, *37*, 321.
59. Capocaccio, L.; Angelico, M. *Dig. Dis. Sci.* **1991**, *36*, 775.
60. Fisman, M.; Gordon, B.; Felcki, V.; Helmes, E.; Appel, J.; Rabhern, K. *Am. J. Psychiatry* **1985**, *142*, 71.
61. Branconnier, R.J.; Dessain, E.C.; McNiff, M.E.; Cole, J.O. *Am. J. Psychiatry* **1986**, *143*, 1313.
62. Hoyer, S.; Nitsch, R.; Oesterreich, K. *Neurosci. Lett.* **1990**, *117*, 358.
63. Samtoy, B.; DeBeukelaer, M.M. *Pediatrics* **1980**, *65*, 294.
64. Drayna, C.J.; Titcomb, C.B.; Varma, R.R.; Soergel, K.M. *N. Eng. J. Med.* **1981**, *304*, 766.
65. Valero, A.; Alroy, G.; Eisenkraft, B.; Itskovitch, J. *Thorax*, **1974**, *29*, 703.
66. Dutton, R.J.; Nicholas, W.; Fischer, C.J.; Renzetti, A.D. *N. Eng. J. Med.* **1959**, *261*, 1369.
67. Nelson, R.M.; Seligson, D. *Surgery*, **1953**, *34*, 1.
68. Caminal, L.; Castellanos, E.; Mateos, V.; Astudillo, A.; Moreno, C.; Dieguez, M.A. *J. Intron. Med.* **1993**, *233*, 277.
69. Brusilow, S.W. *J. Clin. Invest.* **1984**, *74*, 2144.
70. Bachmann, C.; Colombo, J.P. *Eur. J. Pediatr.* **1980**, *134*, 109.
71. Huttenlocher, R.P.; Schwartz, A.D.; Klatskin, G. *Pediatrics* **1969**, *43*, 443.
72. Shannon, D.C.; DeLong, R.; Bercu, B.; Glick, T.; Therrin, J.T.; Moylan, F.M.B.; Todres, I.D. *Pediatrics*, **1975**, *56*, 999.

73. Chapoy, P.R.; Angelini, C.; Brown, W.J.; Stiff, J.E.; Shung, A.L. Cederbaum, S.D. *N. Eng. J. Med.* **1980**, *303*, 1389.
74. Gordon, B.A.; Gatiel, D.P.; Haust, D. *Clin. Invest. Med.* **1987**, *10*, 329.
75. Schiffmann, R. *Isr. J. Med. Sci.* **1992**, *28*, 91.
76. Wilson, D.C.; McGibben, D.; Hicks, E.M.; Allen, I.V. *Eur. J. Pediatr.* **1993**, *152*, 260.
77. Goldberg, R.N.; Cabal, L.A.; Sinatra, F.R.; Plajstec, C.E.; Hodgman, J.E. *Pediatrics* **1979**, *64*, 336.
78. Mortensen, E.; Lyng, G.; Juhl, E. *Lancet* **1972**, *1*, 1024.
79. Edwards, R.H. *Arch. Neurol.* **1984**, *41*, 1211.
80. Van Laethem, J.L.; Gay, F.; Franck, N.; van Gossum, A. *Dig. Dis. Sci.* **1992**, *37*, 1754.
81. Canzanello, V.J.; Rasmussen, R.T.; McGoldrick, M.D. *Ann. Intern. Med.* **1983**, *99*, 190.
82. Batshaw, M.L.; Brusilow, S.W. *Ann. Neurol.* **1982**, *11*, 319.
83. Zaret, B.S.; Beckner, R.R.; Marini, A.M.; Wagle, W.; Passarelli, C. *J. Am. Coll. Nutr.* **1986**, *5*, 167.
84. Binek, J.; Hany, A.; Heer, M. *Med. Wochenschr.* **1991**, *121*, 228.
85. Seiler, N. *Neurochem. Res.* **1993**, *18*, 235.
86. Hoyer, S. *Adv. Exp. Med. Biol.* **1994**, *368*, 197.
87. Sturm, P.A.; Henry, D.W.; Thompson, P.E.; Zeigler, J.B.; McCall, J.W. *J. Med. Chem.* **1974**, *17*, 481.
88. Brown, H.C.; Narasimhan, S. *J. Org. Chem.* **1982**, *47*, 1604.
89. HPLC separations a) Phenylacetamide; column ID Chiralpack AD (5  $\mu\text{m}$ ) from Diacel, mobil phase ethanol/heptane 60/40 (v/v) or methanol/ethanol/heptane 45/25/30 (v/v/v).  
b) Free aminoderivatives: the separation was performed after o-phtaladehyde-derivatization using Merck LiChrocart RP18, mobil phase 57/43 (v/v) mixture of 0.2M sodium acetate buffer (pH 4.52) and methanol.
90. Margolin, A.L. *Tetrahedron Lett.* **1993**, *34*, 1239.
91. Toi, K.; Izumi, Y. *Nippon Kagaku Zanki* **1960**, *81*, 652.
92. Kitz, R.; Wilson, B. *J. Biol. Chem.* **1962**, *237*, 3245.



## Chapter 16

# Fluorinated Vitamin D<sub>3</sub> Analog with In Vivo Anticancer Activity

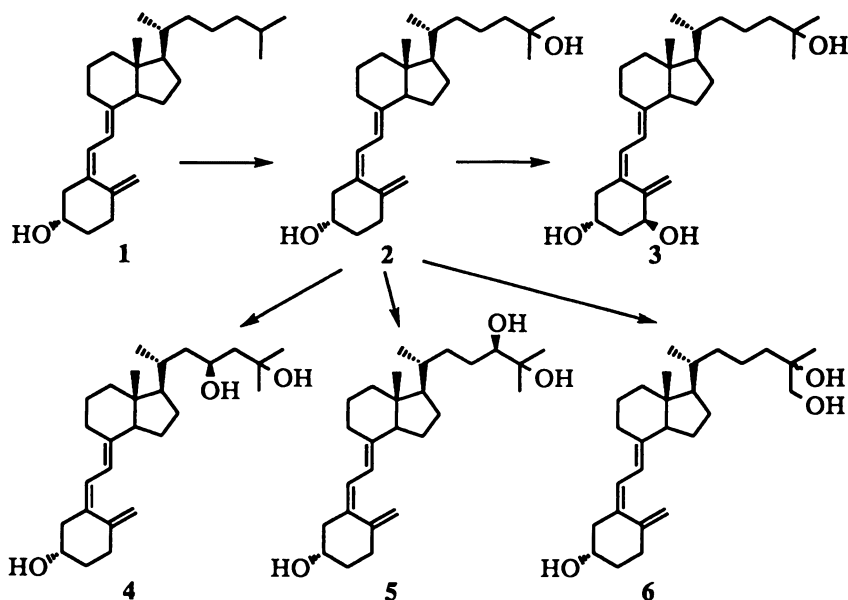
Katsuhiko Iseki and Yoshiro Kobayashi

MEC Laboratory, Daikin Industries, Ltd., Tsukuba, Ibaraki 305, Japan

To synthesize vitamin D<sub>3</sub> analogs with *in vivo* anticancer activity but not calcemic activity, eight different fluorinated analogs were synthesized and structure-activity relationships were determined. Modifications such as 26,27-fluorination, side chain homologation and introduction of a hydroxyl group were carried out. The fluorinated vitamin D<sub>3</sub> analog, (22*S*)-26,26,26,27,27,27-hexafluoro-24-homo-1 $\alpha$ ,22,25-trihydroxyvitamin D<sub>3</sub>, was found to inhibit the growth of human colon cancer cells (HT-29) in culture to an extent ten times that of the active metabolite of vitamin D<sub>3</sub>, 1 $\alpha$ ,25-dihydroxyvitamin D<sub>3</sub>. The growth of human colon cancer (HT-29) implanted beneath the renal capsule of SCID (severe combined immunodeficiency) mice was suppressed by 63% by the fluorinated analog (3  $\mu$ g/kg body weight *i.p.* every other day, 5 times) with no increase in serum calcium.

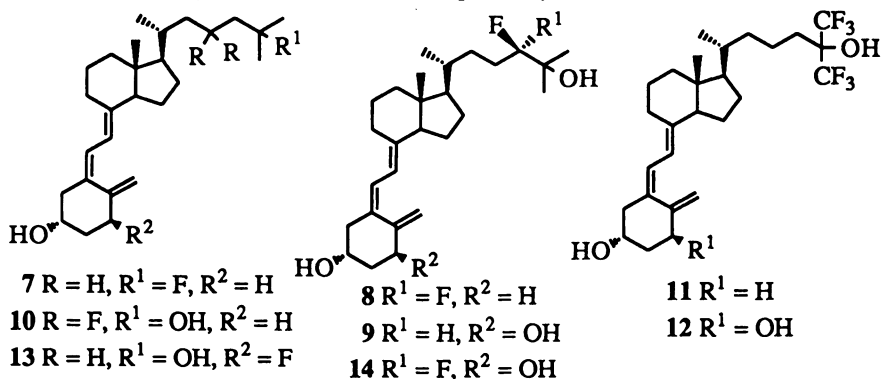
The synthesis of fluorinated vitamin D<sub>3</sub> analogs was initially prompted by extensive investigation of vitamin D<sub>3</sub> metabolism (1-3). Vitamin D<sub>3</sub> (1) in the skin or absorbed from the small intestine is transported to the liver to be hydroxylated at carbon 25 to yield 25-hydroxyvitamin D<sub>3</sub> (2). This compound is the major circulating metabolite of vitamin D<sub>3</sub> and undergoes further hydroxylation in the kidney, depending on physiological conditions. Low serum calcium stimulates hydroxylation at carbon 1 to produce 1 $\alpha$ ,25-dihydroxyvitamin D<sub>3</sub> (1 $\alpha$ ,25-(OH)<sub>2</sub>D<sub>3</sub>, 3). When circulating calcium is high, 25-hydroxyvitamin D<sub>3</sub> (2) is hydroxylated at carbon 23, carbon 24 or carbon 26 to form 23*S*,25-dihydroxyvitamin D<sub>3</sub> (4), 24*R*,25-dihydroxyvitamin D<sub>3</sub> (5), or 25,26-dihydroxyvitamin D<sub>3</sub> (6), respectively. 1 $\alpha$ ,25-(OH)<sub>2</sub>D<sub>3</sub>, (3), the most biologically active form of vitamin D<sub>3</sub>, is essential to the regulation of calcium metabolism in animals and is also of use for treating bone diseases such as osteoporosis. This active metabolite undergoes degradation by oxidation of the side chain, such as hydroxylation at carbon 26.

0097-6156/96/0639-0214\$15.00/0  
© 1996 American Chemical Society



**Scheme 1. Functional Metabolites of Vitamin D<sub>3</sub>.**

As a potential inhibitor of 25-hydroxylase which converts vitamin D<sub>3</sub> to 25-hydroxyvitamin D<sub>3</sub> (2), a vitamin D<sub>3</sub> analog blocked at this position with a fluorine atom, 25-fluorovitamin D<sub>3</sub> (7), has been synthesized (4-5). For assessment of the physiological significance of metabolic 24-hydroxylation, 24,24-difluoro-25-hydroxyvitamin D<sub>3</sub> (8) (6-7) and 24*R*-fluoro-1 $\alpha$ ,25-dihydroxyvitamin (9) (8) were synthesized. For 23-hydroxylation, 23,23-difluoro-25-hydroxyvitamin D<sub>3</sub> (10) was synthesized (9). 26,26,26,27,27,27-Hexafluoro-25-hydroxyvitamin D<sub>3</sub> (11) (10), 26,26,26,27,27,27-hexafluoro-1 $\alpha$ ,25-dihydroxyvitamin D<sub>3</sub> (26,27-F<sub>6</sub>-1 $\alpha$ ,25-(OH)<sub>2</sub>D<sub>3</sub>, 12) (11) and 1 $\alpha$ -fluoro-25-hydroxyvitamin D<sub>3</sub> (13) (12) were prepared to examine the 26- and 1 $\alpha$ -hydroxylation of vitamin D<sub>3</sub>, respectively.



**Scheme 2. Fluorinated Vitamin D<sub>3</sub> Analogs.**

Many fluorinated vitamin D<sub>3</sub> analogs have been found quite useful for determining the significance of hydroxylation in vitamin D metabolism, as well as proving augmented biological activity in certain cases of importance. 24,24-Difluoro-1 $\alpha$ ,25-dihydroxyvitamin D<sub>3</sub> (14) (13) and 26,27-F<sub>6</sub>-1 $\alpha$ ,25-(OH)<sub>2</sub>D<sub>3</sub> (12) (14) have been shown 5-10 times more potent than 1 $\alpha$ ,25-(OH)<sub>2</sub>D<sub>3</sub> (3) in *in vivo* vitamin D responsive systems such as increasing intestinal calcium transport and bone calcium mobilization in vitamin D-deficient rats. Of great importance is the fact that the action of these fluoro analogs persists for longer times than that of 1 $\alpha$ ,25-(OH)<sub>2</sub>D<sub>3</sub> (3). 26,27-F<sub>6</sub>-1 $\alpha$ ,25-(OH)<sub>2</sub>D<sub>3</sub> (12) is presently being studied for application to the treatment of bone diseases such as osteoporosis.

In 1981, Suda *et al.* discovered new functions of 1 $\alpha$ ,25-(OH)<sub>2</sub>D<sub>3</sub> (3), such as inhibition of cell growth and the induction of cell differentiation in human leukemia cells (15-16). This active metabolite induces the differentiation of human colon cancer cells (17). In an *in vivo* study, 1 $\alpha$ ,25-(OH)<sub>2</sub>D<sub>3</sub> (3) was found to inhibit the growth of human colon cancer xenografts in mice (18). The risk of colon cancer has been shown inversely correlated with the dietary intake of vitamin D<sub>3</sub> (19). 1 $\alpha$ ,25-(OH)<sub>2</sub>D<sub>3</sub> (3) would thus appear useful for the prevention and treatment of human cancer including colon cancer. The high calcemic activity of this drug, however, would limit such potential application. Problems may be encountered at hypercalcemia at concentrations required for inhibiting cell growth and the inducement of cell differentiation. Thus, many analogs of 1 $\alpha$ ,25-(OH)<sub>2</sub>D<sub>3</sub> (3) with *in vitro* anticancer activity but not calcemic activity have been synthesized as clinically useful anticancer agents (20-21). However, few low calcemic analogs with *in vitro* anticancer activity have *in vivo* anticancer effect (22-24), possibly owing to their rapid clearance *in vivo*.

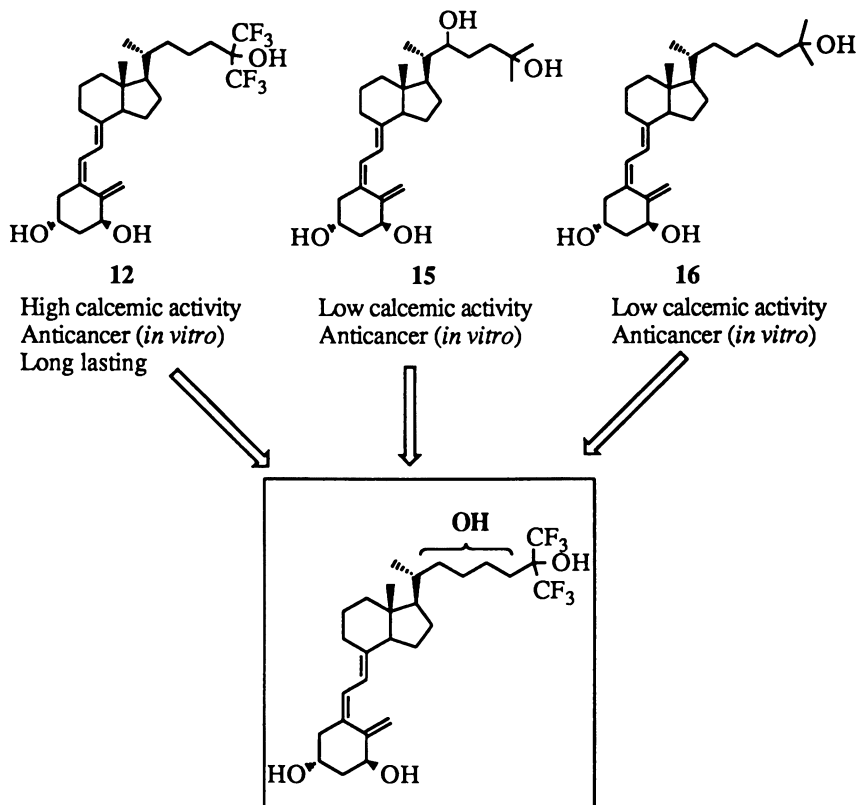
To obtain therapeutic agents for colon cancer, eight fluorinated analogs of 1 $\alpha$ ,25-(OH)<sub>2</sub>D<sub>3</sub> (3) were synthesized in this study and their structure-activity relationships were determined based on calcemic activity in rats and antiproliferative effect on HT-29 human colon cancer cells in culture. The analog DD-003, (22S)-26,26,26,27,27,27-hexafluoro-24-homo-1 $\alpha$ ,22,25-trihydroxyvitamin D<sub>3</sub> (25), expresses high anticancer activity toward colon cancer cells in culture with no hypercalcemia in rats. *In vivo* activity of DD-003 toward human colon cancer was determined. The growth of HT-29 colon cancer implanted beneath the renal capsule of SCID (severe combined immunodeficiency) mice was effectively suppressed by DD-003 (26).

### Design of Fluorinated Vitamin D<sub>3</sub> Analogs

The design was such as would permit the separation of activities in tumor prevention and calcium regulation and provide *in vivo* anticancer activity. 26,27-Hexafluoro analog 12 is about 100 and 10 times more potent than 1 $\alpha$ ,25-(OH)<sub>2</sub>D<sub>3</sub> (3) for inhibiting the growth of human cancer cells in culture and elevating serum calcium, respectively. The action of the fluoro analog 12 persists longer than that of 1 $\alpha$ ,25-(OH)<sub>2</sub>D<sub>3</sub> (3) for augmenting serum phosphorus following oral administration (14).

1 $\alpha$ ,22,25-Trihydroxyvitamin D<sub>3</sub> (15) (27-28) and 24-homo-1 $\alpha$ ,25-dihydroxyvitamin D<sub>3</sub> (16) (29-30) induce the differentiation of human leukemia cells (HL-60) but express no calcemic activity. Homologation of the side chain and introduction of a hydroxyl group into this chain lessens calcium-regulating capacity.

The introduction of a hydroxyl group into the side chain and homologation of this side chain of 26,27-F<sub>6</sub>-1 $\alpha$ ,25-(OH)<sub>2</sub>D<sub>3</sub> (**12**) were the objectives of the present research.

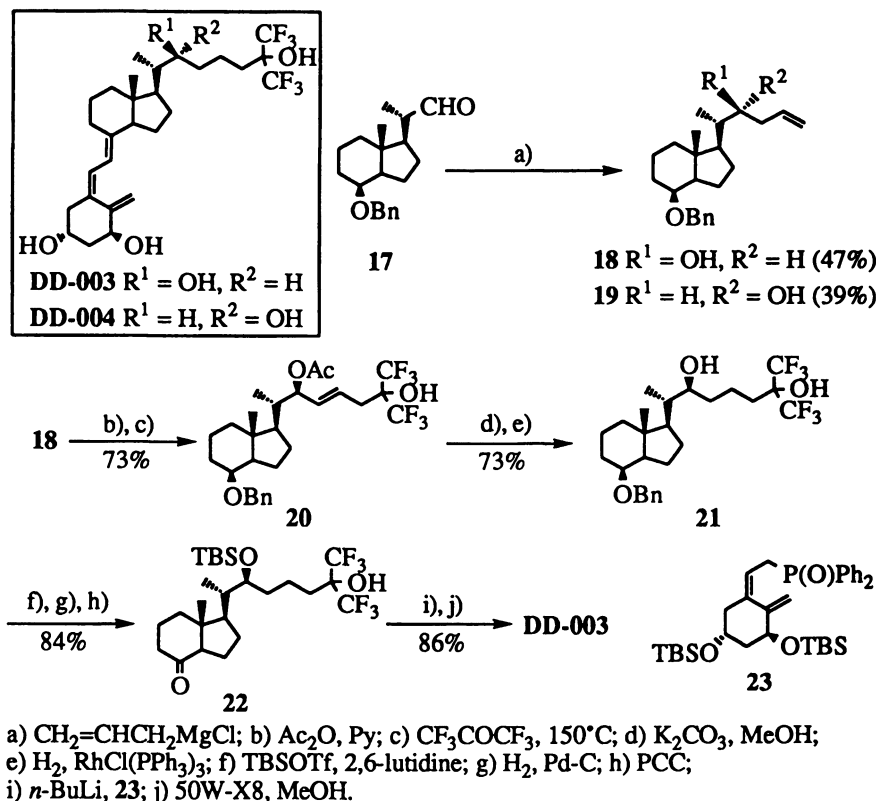


**Scheme 3. Design of Fluorinated Vitamin D<sub>3</sub> Analogs.**

### Synthesis of Fluorinated Vitamin D<sub>3</sub> Analogs

**26,26,26,27,27,27-Hexafluoro-24-homo-1 $\alpha$ ,22,25-trihydroxyvitamin D<sub>3</sub>.** 22-Hydroxylated analogs (DD-003 and DD-004) were synthesized using the ene reaction of hexafluoroacetone for side chain construction (**25**). The results of retrosynthetic analysis indicated that aldehyde **17**, readily available from vitamin D<sub>2</sub> via the oxidation procedure of Toh and Okamura (*31*), should be used as starting material. This aldehyde was reacted with allylmagnesium chloride in ether-THF at 0°C to give alcohol **18** (47%) along with isomer **19** (39%). Alcohol **18** was acetylated and the acetate thus obtained was treated with hexafluoroacetone in a sealed tube at 150°C for 35 h to afford allyl acetate **20** in 73% yield in two steps. The deacetylation of **20**, followed by hydrogenation of the resulting alcohol in the presence of Wilkinson's catalyst gave alcohol **21**. The silylation of **21**, hydrogenolysis and PCC oxidation furnished ketone **22** in 84% overall yield. According to the general approach of Lythgoe *et al.* (*32-33*), the Horner-Wittig reaction of ketone **22** with the phosphinoyl

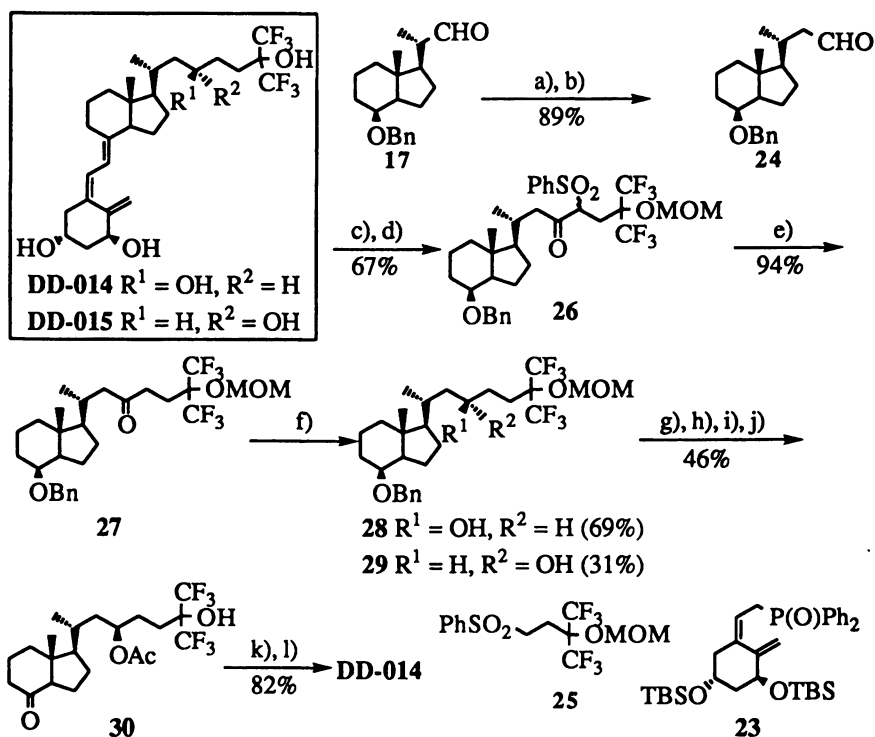
carbanion derived from **23** and *n*-BuLi afforded the bis(TBS) ether which was desilylated with cation exchange resin (50W-X4) in MeOH to give **DD-003** in 86% yield. In the same manner, **DD-004** was prepared from allyl alcohol **19**.



**Scheme 4. Synthesis of 26,26,26,27,27,27-Hexafluoro-24-homo-1 $\alpha$ ,22,25-trihydroxyvitamin D<sub>3</sub>.**

**26,26,26,27,27,27-Hexafluoro-24-homo-1 $\alpha$ ,23,25-trihydroxyvitamin D<sub>3</sub>.** 23-Hydroxylated analogs (**DD-014** and **DD-015**) were synthesized using the coupling reaction of aldehyde **24** with sulfone **25** to construct the side chain (Iseki, K; Takahashi, M.; Kobayashi, Y., Daikin Industries Ltd., unpublished data.). The Wittig reaction of aldehyde **17** with (methoxymethyl)triphenylphosphonium chloride, followed by treatment of the enol ether thus obtained with mercuric acetate gave aldehyde **24** in 89% yield. Reaction of **24** with the carbanion derived from sulfone **25** and Swern oxidation furnished sulfonyl ketone **26** in 67% overall yield. The desulfonylation of **26** with samarium iodide afforded ketone **27** in 94% yield. Reduction of **27** with sodium borohydride gave alcohol **28** (69%) along with isomer **29** (31%). The demethoxymethylation of **28**, acetylation, hydrogenolysis and PCC oxidation provided ketone **30** in 46% overall yield. Ketone **30** was converted to **DD-014** by the Wittig reaction with the phosphinoyl carbanion derived from **23** and

deprotection with cation exchange resin (50W-X4) in MeOH in 82% yield. In the same manner, DD-015 was prepared from alcohol 29.

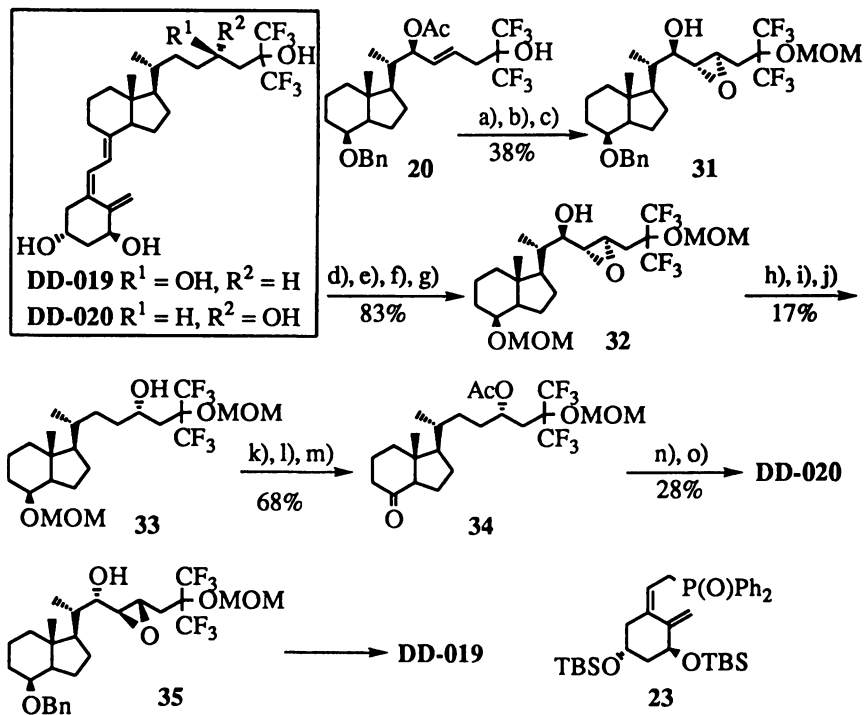


- a) (MeOCH<sub>2</sub>)<sub>3</sub>P<sup>+</sup>Cl<sup>-</sup>, *t*-BuOK; b) Hg(OAc)<sub>2</sub>; c) 25, *n*-BuLi; d) Swern oxidation; e) SmI<sub>2</sub>; f) NaBH<sub>4</sub>; g) conc. HCl-dioxane, 65°C; h) Ac<sub>2</sub>O, Py; i) H<sub>2</sub>, Pd-C; j) PCC; k) *n*-BuLi, 23; l) 50W-X8, MeOH.

**Scheme 5. Synthesis of 26,26,26,27,27,27-Hexafluoro-24-homo-1 $\alpha$ ,23,25-trihydroxyvitamin D<sub>3</sub>.**

**26,26,26,27,27,27-Hexafluoro-24-homo-1 $\alpha$ ,24,25-trihydroxyvitamin D<sub>3</sub>.** 24-Hydroxylated analogs (DD-019 and DD-020) were synthesized using the regio- and stereoselective opening of epoxides to introduce the hydroxyl group into the side chain (Iseki, K; Oishi, S.; Kobayashi, Y., Daikin Industries Ltd., unpublished data.). Allyl acetate 20, prepared from 17, was converted to epoxy alcohol 31 by methoxymethylation, deacetylation and epoxidation in 38% overall yield. The acetylation of 31, hydrogenolysis, methoxymethylation and deacetylation gave epoxy alcohol 32 in 83% yield in four steps. The mesylation of 32 and reduction with dissolving sodium followed by hydrogenation of the resulting allyl alcohol in the presence of platinum oxide furnished alcohol 33 in 17% overall yield. The acetylation of 33, demethoxymethylation and PCC oxidation gave ketone 34 in 68% yield in three steps. Ketone 34 was converted to DD-020 by the Wittig reaction with the phosphinoyl carbanion derived from 23 and deprotection with cation exchange resin

(50W-X4) in MeOH in 20% yield. In the same manner, DD-019 was prepared from the 22R isomer of 20.

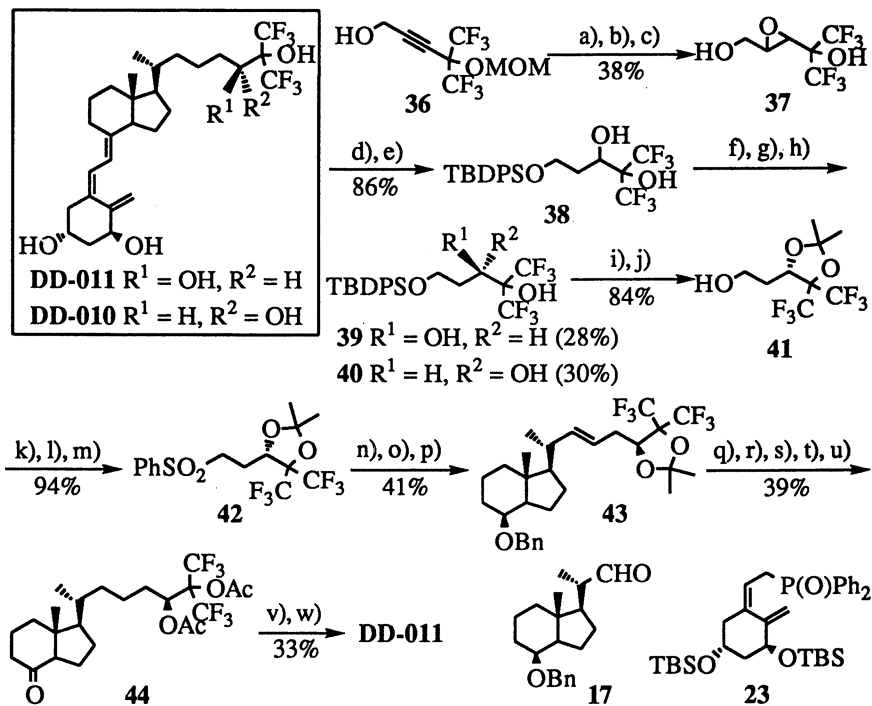


a) MOMCl, *i*-Pr<sub>2</sub>NEt; b) K<sub>2</sub>CO<sub>3</sub>; c) MCPBA, Na<sub>2</sub>HPO<sub>4</sub>; d) Ac<sub>2</sub>O, Et<sub>3</sub>N, DMAP; e) H<sub>2</sub>, Pd-C; f) MOMCl, *i*-Pr<sub>2</sub>NEt; g) K<sub>2</sub>CO<sub>3</sub>, MeOH; h) MsCl, Py; i) Na, NH<sub>3</sub>; j) H<sub>2</sub>, PtO<sub>2</sub>; k) Ac<sub>2</sub>O, Et<sub>3</sub>N, DMAP; l) conc. HCl-dioxane, 60°C; m) PCC; n) *n*-BuLi, 23; o) 50W-X8, MeOH.

**Scheme 6. Synthesis of 26,26,26,27,27,27-Hexafluoro-24-homo-1 $\alpha$ ,24,25-trihydroxyvitamin D<sub>3</sub>.**

**26,26,26,27,27,27-Hexafluoro-24-homo-1 $\alpha$ ,24',25-trihydroxyvitamin D<sub>3</sub>** (Iseki, K; Nagai, T.; Kobayashi, Y., Daikin Industries Ltd., unpublished data.) Alcohol 36 (34), easily prepared from propargyl alcohol and hexafluoroacetone, was reduced with lithium aluminum hydride followed by demethoxymethylation of the (*E*)-alcohol thus obtained to give the corresponding diol which was converted to epoxide 37 using *t*-butyl hydroperoxide and vanadyl acetylacetonate. The reduction of 37 and *t*-butyldiphenylsilylation furnished silyl ether 38 in 86% yield in two steps. The diesterification of 38, separation of the resulting diastereomers, treatment with lithium aluminum hydride and silylation with *t*-butyldiphenylsilyl chloride gave (*R*)-alcohol 39 (28%) along with (*S*)-alcohol 40 (30%). The acetonization of 40 and removal of the silyl group afforded alcohol 41 in 84% yield in two steps. The mesylation of 41 and treatment with potassium thiophenoxide, followed by oxidation of the resulting thioether with *m*-chloroperbenzoic acid provided sulfone 42 in 94% yield in three steps. The coupling reaction of 42 with aldehyde 17, acetylation and reduction with

sodium amalgam gave **43** in 41% overall yield. The hydrogenation of **43** catalyzed with platinum oxide, deketalization, acetylation, hydrogenolysis and PCC oxidation furnished ketone **44** in 39% yield in five steps. The Wittig reaction of **44** with the phosphinoyl carbanion derived from **23** and deprotection with cation exchange resin (50W-X4) in MeOH gave **DD-011** in 33% yield. In the same manner, **DD-010** was obtained from alcohol **39**.



a)  $\text{LiAlH}_4$ ; b) conc.  $\text{HCl-MeOH}$ ; c)  $t\text{-BuOOH}, \text{VO}(\text{acac})_2$ ; d)  $\text{LiAlH}_4$ ; e)  $\text{TBDPSCl}, \text{imidazole}$ ; f) i) (-)-camphanic chloride, ii) resolution; g)  $\text{LiAlH}_4$ ; h)  $\text{TBDPSCl}, \text{imidazole}$ ; i)  $\text{Me}_2\text{C}(\text{OMe})_2, \text{TsOH}$ ; j)  $\text{TBAF}$ ; k)  $\text{MsCl}, \text{Et}_3\text{N}$ ; l)  $\text{PhSH}, \text{KOH}$ ; m)  $\text{MCPBA}$ ; n)  $n\text{-BuLi}$ , then **17**; o)  $\text{Ac}_2\text{O}$ ; p)  $\text{Na-Hg}$ ; q)  $\text{H}_2, \text{PtO}_2$ ; r) conc.  $\text{HCl-MeOH}$ ; s)  $\text{Ac}_2\text{O}, \text{DMAP}, \text{Py}$ ; t)  $\text{H}_2, \text{Pd-C}$ ; u)  $\text{PCC}$ ; v)  $n\text{-BuLi}$ , **23**; w)  $50\text{W-X8}, \text{MeOH}$ .

**Scheme 7.** Synthesis of 26,26,26,27,27,27-Hexafluoro-24-homo- $1\alpha,24',25$ -trihydroxyvitamin  $\text{D}_3$ .

### *In Vitro* Biological Activity of Fluorinated Vitamin $\text{D}_3$ Analogs

**Growth Inhibition of Human Colon Cancer Cells (HT-29) in Culture.** *In vitro* assessment for inhibition activity by the fluorinated vitamin  $\text{D}_3$  analogs toward the growth of human cancer cells, HT-29, was carried out by measuring mitochondrial dehydrogenase of viable cells with MTT (26). Activity values relative to  $1\alpha,25\text{-(OH)}_2\text{D}_3$  (**3**) are shown in Table I. Based on half-maximum concentrations, the potency of the 22(*S*)-hydroxylated analog (**DD-003**) in inhibiting HT-29 cell growth was shown to be 10 times that of  $1\alpha,25\text{-(OH)}_2\text{D}_3$  (**3**). **DD-003** was 10 times less



effective than 26,27-F<sub>6</sub>-1 $\alpha$ ,25-(OH)<sub>2</sub>D<sub>3</sub> (12). The configuration of the 22-hydroxyl group was essential for growth inhibition activity. The 22(*S*)-isomer (DD-003) was 100 times more active than the 22(*R*) isomer (DD-004) and the 23(*R*)-isomer (DD-014), 10 times more than 1 $\alpha$ ,25-(OH)<sub>2</sub>D<sub>3</sub> (3). The effect of configuration of hydroxyl group on growth inhibition was much less in the case of 23-isomers (DD-014 vs. DD-015), and that of 24'(*S*)-isomer (DD-011) was basically the same as that of the 24'(*R*)-isomer (DD-010). To induce the differentiation of human leukemia cells, HL-60, DD-003 was found 6 times more potent than 1 $\alpha$ ,25-(OH)<sub>2</sub>D<sub>3</sub> (3).

**Table I. Inhibition of Colon Cancer Cell Proliferation (HT-29)  
-Activity Relative to 1 $\alpha$ ,25-Dihydroxyvitamin D<sub>3</sub>-**

1	10	0.2
100	1	10
10	8	10
0.1		

All values >1 indicate the analog more potent than 1 $\alpha$ ,25-(OH)<sub>2</sub>D<sub>3</sub> (3)

**In Vitro Binding Assays.** The fluorinated vitamin D<sub>3</sub> analogs were examined for binding activity to vitamin D<sub>3</sub> receptor (VDR) and vitamin D binding protein (DBP). Table II shows relative activities toward 1 $\alpha$ ,25-(OH)<sub>2</sub>D<sub>3</sub> (3). The 22(*S*)-hydroxylated analog (DD-003) was 100 times less effective than 1 $\alpha$ ,25-(OH)<sub>2</sub>D<sub>3</sub> (3) for binding to the chick embryonic intestinal 1 $\alpha$ ,25-(OH)<sub>2</sub>D<sub>3</sub> receptor (VDR). The configuration of the 22-hydroxyl group was essential for VDR binding activity. The 22(*S*)-isomer (DD-003) was 125 times more active than the 22(*R*) isomer (DD-004) and the 23(*R*)-isomer (DD-014), 17 times more potent than DD-003. The effect of the configuration of hydroxyl group on binding to VDR was much less for the 23-isomers (DD-014 vs. DD-015), and that of 24'(*S*)-isomer (DD-011) was basically the same as that of the 24'(*R*)-isomer (DD-010).

As for the binding affinity toward vitamin D binding protein (DBP) from vitamin D deficient rats, the 22(*S*)-hydroxylated analog (DD-003) was 250 times less effective than 1 $\alpha$ ,25-(OH)<sub>2</sub>D<sub>3</sub> (3). All fluorinated analogs except 26,27-F<sub>6</sub>-1 $\alpha$ ,25-(OH)<sub>2</sub>D<sub>3</sub> (12) were much less active than 1 $\alpha$ ,25-(OH)<sub>2</sub>D<sub>3</sub> (3).

Binding affinity toward VDR and DBP showed no correlation with inhibitory activity toward human cancer cell growth, HT-29.

**Table II. *In Vitro* Binding Activity**  
**-Activity Relative to 1 $\alpha$ ,25-Dihydroxyvitamin D<sub>3</sub>-**

Compound	1 $\alpha$ ,25-(OH) <sub>2</sub> D <sub>3</sub> Receptor	Vitamin D Binding Protein
1 $\alpha$ ,25-(OH) <sub>2</sub> D <sub>3</sub> (3)	1	1
26,27-F <sub>6</sub> -1 $\alpha$ ,25-(OH) <sub>2</sub> D <sub>3</sub> (12)	0.5	0.25
DD-003	0.01	0.004
DD-004	0.00008	0.003
DD-014	0.17	0.02
DD-015	0.06	0.003
DD-011	0.5	0.005
DD-010	0.5	0.006

All values >1 indicate the analog more potent than 1 $\alpha$ ,25-(OH)<sub>2</sub>D<sub>3</sub>.

#### ***In Vivo* Calcemic Activity of Fluorinated Vitamin D<sub>3</sub> Analogs**

Male Wistar rats (3 weeks old) were kept on a low calcium and vitamin D-deficient diet. When serum calcium decreased to less than 6 mg/dl, each compound was injected on five consecutive days intraperitoneally (7.2 nmol/kg/day). Rat serum was collected from the tail vein to measure serum calcium colorimetrically at 575 nm using *o*-cresolphthalein.

As shown in Figure 1, 1 $\alpha$ ,25-(OH)<sub>2</sub>D<sub>3</sub> (3) considerably increased serum calcium while the 22(*S*)-hydroxylated analog (DD-003) had much less effect. The 22(*R*)-isomer (DD-004) was less potent than the 22(*S*)-isomer (DD-003).

Hydroxylation at carbon 22 or carbon 23 greatly reduced calcemic activity compared to 1 $\alpha$ ,25-(OH)<sub>2</sub>D<sub>3</sub> (3). The extent of serum calcium increase by 24'-hydroxylated isomers (DD-010 and DD-011) was virtually the same as that by 1 $\alpha$ ,25-(OH)<sub>2</sub>D<sub>3</sub> (3). The calcemic activity of fluorinated vitamin D<sub>3</sub> analogs showed close correlation with VDR binding affinity but not with DBP binding affinity.

#### **Inhibition of HT-29 Human Colon Cancer Growth beneath the Renal Capsule of SCID (Severe Combined Immunodeficiency) Mice by DD-003**

***In Vivo* Growth Inhibition of HT-29 Tumor Cells.** Fibrin clots of colon cancer cells (HT-29) were implanted beneath the renal capsule of 5 week-old SCID mice. At 7 days following implantation, the mice were administered 3  $\mu$ g/kg body weight DD-003 or the vehicle i.p. every other day 5 times. Eleven days after the initial administration, tumor growth and serum calcium were determined. In both groups, mice appeared healthy and essentially the same in final body weight. Tumors in DD-003-treated mice were smaller, invading to a lesser extent surrounding tissue. Central necrosis was greater compared to the control. DD-003 greatly suppressed HT-29 tumor growth. As shown in Table III, serum calcium of the mice treated with DD-003 was basically the same as that of the control mice and malignant growth of colon cancer cells was inhibited by 63%.

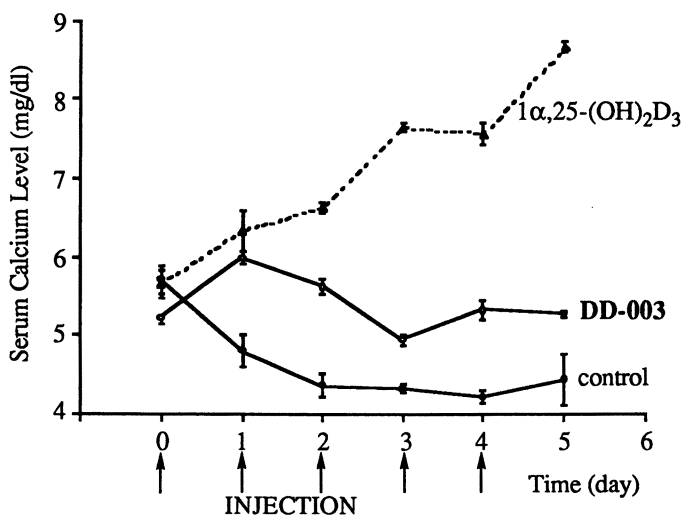


Figure 1. Effects of Vitamin D<sub>3</sub> Analogs on Serum Calcium.

Table III. Inhibition of Human Colon Cancer Growth in SCID Mice by DD-003

	Initial Tumor diameter (mm)	Increase in Tumor diameter (mm)	Serum Calcium (mg/dl)
Control	1.61 ± 0.15	2.29 ± 0.39	7.9 ± 0.6
DD-003	1.40 ± 0.38	0.85 ± 0.26*	8.4 ± 0.7

\*Significantly different from the control;  $P < 0.001$ . Reproduced with permission from reference 26.

**Time- and Dose-dependent Growth Inhibition of HT-29 Tumor Cells.** As shown in Figure 2, at 2 days following implantation of colon cancer cells (HT-29), the mice were given 1  $\mu$ g/kg body weight of DD-003 or the vehicle i.p. three times a week for a specified period of time. Tumors in the control mice grew greatly, reaching a plateau in 19 days. Inhibition of cell growth was not significant after 1 week of DD-003 treatment but became progressively significant with prolonged time. The tumors remained small throughout the experimental period.

Since 3 weeks of treatment were sufficient to detect drug effect on tumor growth, as shown in Figure 2, dose-dependent studies were conducted in which various amounts of DD-003 were injected i.p. three times a week for three weeks. As shown in Table IV, DD-003 considerably inhibited the growth of colon cancer cells dose-dependently. Body weight and serum calcium of the mice treated with DD-003 at all concentrations were essentially the same as for the control mice.

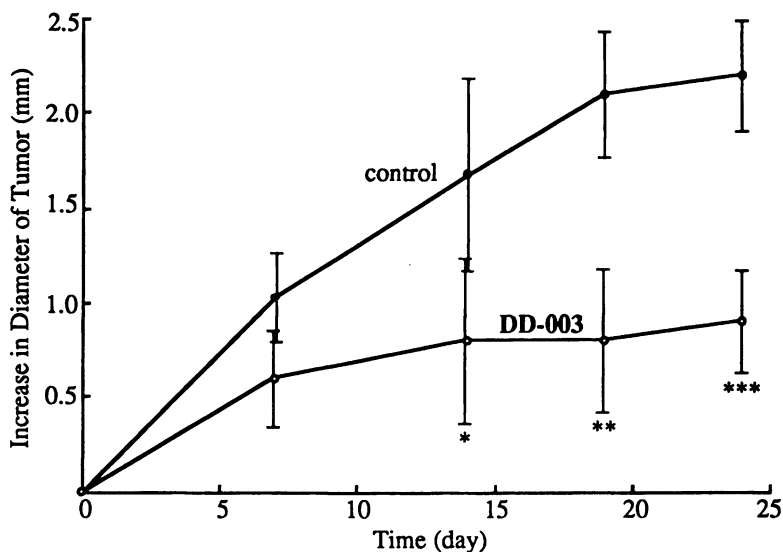


**Figure 2. Time-dependent Growth Inhibition of HT-29 in SCID Mice by DD-003: \***,  $P < 0.05$ ; **\*\***,  $P < 0.005$ ; **\*\*\***,  $P < 0.001$ . Reproduced with permission reference 26.

**Table IV. Dose-dependent Inhibition of HT-29 Growth in SCID Mice by DD-003**

	Increase in Tumor diameter (mm)	Increase in Tumor volume (mm <sup>3</sup> )	Serum Calcium (mg/dl)
Control	2.20 ± 0.40	20.3 ± 2.8	8.2 ± 1.6
<b>DD-003 (μg/kg body weight)</b>			
0.1	1.60 ± 0.50*	12.4 ± 4.5**	7.7 ± 0.8
1.0	0.99 ± 0.50**	8.2 ± 3.2***	9.0 ± 1.2
10	0.79 ± 0.26***	6.9 ± 2.3***	8.9 ± 0.9

Significantly different from the control; \*,  $P < 0.05$ ; \*\*,  $P < 0.005$ ; \*\*\*,  $P < 0.001$ . Reproduced with permission from reference 26.

## Conclusion

The most effective molecular modification for separating calcemic activity from anticancer activity was found to be 26,27-hexafluorination, 24-homologation and 22-hydroxylation in combination. 22(*S*)-26,26,26,27,27,27-Hexafluoro-24-homo-

1 $\alpha$ ,22,25-trihydroxyvitamin D<sub>3</sub> (DD-003) exerted the strongest anticancer effect on colon cancer cells in culture with no indication of hypercalcemia *in vivo*. The growth of implanted human colon cancer (HT-29) was suppressed by DD-003 with no increase in serum calcium. This fluorinated analog should thus prove clinically applicable to the postsurgical chemotherapy of colon cancer.

### Acknowledgement

The research in this report was conducted as a joint project with Professor Nobuo Ikekawa of Iwaki Meisei University, Professor Yokō Tanaka of Veterans Affairs Medical Center & Albany Medical College and Dr. Makoto Kawai of Aichi Medical University. The significant contributions of these collaborators are gratefully acknowledged.

### Literature Cited

1. Kobayashi, Y.; Taguchi, T. In *Biomedical Aspects of Fluorine Chemistry*; Filler, R.; Kobayashi, Y., Eds.; Kodansha Ltd.: Tokyo, 1982.
2. Kobayashi, Y.; Taguchi, T. *J. Syn. Org. Chem. Jap.* **1985**, *43*, 1073.
3. Ikekawa, N. *Med. Chem. Rev.* **1987**, *7*, 333.
4. Onisko, B. L.; Schnoes, H. K.; DeLuca, H. F. *Tetrahedron Lett.* **1977**, 1107.
5. Yang, S. S.; Dorn, C. P.; Jones, H. *Tetrahedron Lett.* **1977**, 2315.
6. Yamada, S.; Yamada, A.; Ohmori, M.; Takayama, H. *Tetrahedron Lett.* **1979**, 1859.
7. Kobayashi, Y.; Taguchi, T.; Terada, T.; Oshida, J.; Morisaki, M.; Ikekawa, N. *Tetrahedron Lett.* **1979**, 2023.
8. Partridge, J. J.; Shiuey, S.-J.; Uskokovic, M. R. *US Appl.* 297,446 (1981).
9. Taguchi, T.; Mitsuhashi, S.; Yamanouchi, A.; Kobayashi, Y.; Sai, M.; Ikekawa, N. *Tetrahedron Lett.* **1984**, *25*, 4933.
10. Kobayashi, Y.; Taguchi, T.; Kanuma, N.; Ikekawa, N.; Oshida, J. *J. Chem. Soc., Chem. Commun.* **1980**, 459.
11. Kobayashi, Y.; Taguchi, T.; Mitsuhashi, S.; Eguchi, T.; Oshima, E.; Ikekawa, N. *Chem. Pharm. Bull.* **1982**, *30*, 4297.
12. Oshima, E.; Sai, H.; Takatsuto, S.; Ikekawa, N.; Kobayashi, Y.; Yanaka, Y.; DeLuca, H. F. *Chem. Pharm. Bull.* **1984**, *32*, 3525.
13. Okamoto, S.; Tanaka, Y.; DeLuca, H. F.; Ikekawa, N.; Kobayashi, Y. *Am. J. Physiol.* **1982**, *244*, E159.
14. Tanaka, Y.; DeLuca, H. F.; Kobayashi, Y.; Ikekawa, N. *Arch. Biochem. Biophys.* **1984**, *229*, 348.
15. Miyaura, C.; Abe, E.; Kuribayashi, T.; Tanaka, H.; Konno, H.; Nishii, Y.; Suda, T. *Biochem. Biophys. Res. Commun.* **1981**, *102*, 937.
16. Abe, E.; Miyaura, C.; Sakagami, H.; Takeda, M.; Konno, K.; Yamazaki, T.; Yoshiki, S.; Suda, T. *Proc. Natl. Acad. Sci., U.S.A.* **1981**, *78*, 4990.
17. Tanaka, Y.; Bush, K. K.; Klauck, T. M.; Higgins, P. J. *Biochem. Pharmacol.* **1989**, *38*, 3859.
18. Eisman, J. A.; Barkla, D. H.; Tutton, J. M. *Cancer Res.* **1987**, *47*, 21.
19. Garland, C. F.; Shekelle, R. B.; Barrett-Connor, E.; Crioui, M. H.; Rosssof, A. H.; Paul, O. *Lancet* **1985**, *1*, 307.
20. Ikekawa, N.; *Bioorg. Med. Chem. Lett.* **1993**, *3*, 1789.
21. Norman, A. W.; Zhou, J. Y.; Henry, H. L.; Uskokovic, M. R.; Koeffler, H. P. *Cancer Res.* **1990**, *50*, 6857.
22. Abe, J.; Nakano, T.; Nishii, Y.; Matsumoto, T.; Ogata, E.; Ikeda, K. *Endocrinology* **1991**, *129*, 832.

23. Colson, K. W.; MacKay, A. G.; James, S. Y.; Binderup, L.; Chander, S.; Coombes, R. C. *Biochem. Pharmacol.* **1992**, *44*, 2273.
24. Wali, R. K.; Bissonnette, M.; Khare, S.; Hart, J.; Sitrin, M. D.; Brasitus, T.A. *Cancer Res.* **1995**, *55*, 3050.
25. Iseki, K.; Nagai, T.; Kobayashi, Y. *Chem. Pharm. Bull.* **1992**, *40*, 1346.
26. Tanaka, Y.; Wu, A.-Y. S.; Ikekawa, N.; Iseki, K.; Kawai, M.; Kobayashi, Y. *Cancer Res.* **1994**, *54*, 5148.
27. Hirano, Y.; Ikekawa, N.; Tanaka, Y.; DeLuca, H. F. *Chem. Pharm. Bull.* **1981**, *29*, 2254.
28. Eguchi, T.; Yoshida, M.; Ikekawa, N. *Bioorg. Chem.* **1989**, *17*, 294.
29. Ostrem, V. K.; Tanaka, Y.; Prahl, J.; DeLuca, H. F.; Ikekawa, N. *Proc. Natl. Acad. Sci., U.S.A.* **1987**, *84*, 2610.
30. Ostrem, V. K.; Lau, W. F.; Lee, S. H.; Perlman, K.; Prahl, J.; Schnoes, H. K.; DeLuca, H. F.; Ikekawa, N. *J. Biol. Chem.* **1987**, *262*, 14164.
31. Toh, H. T.; Okamura, W. H. *J. Org. Chem.* **1983**, *48*, 1414.
32. Lythgoe, B.; Moran, T. A.; Nambudiry, M. E. N.; Ruston, S. *J. Chem. Soc., Perkin Trans. 1* **1976**, 2386.
33. Lythgoe, B.; Moran, T. A.; Nambudiry, M. E. N.; Tideswell, J.; Wright, P. W. *J. Chem. Soc., Perkin Trans. 1* **1978**, 590.
34. Ohira, U.; Taguchi, T.; Iseki, K.; Kobayashi, Y. *Chem. Pharm. Bull.* **1992**, *40*, 1647.

## Chapter 17

# Syntheses, Biological Activity, and Conformational Analysis of Fluorine-Containing Taxoids

Iwao Ojima<sup>1</sup>, Scott D. Kuduk<sup>1</sup>, John C. Slater<sup>1</sup>, Rayomand H. Gimi<sup>1</sup>,  
Chung Ming Sun<sup>1</sup>, Subrata Chakravarty<sup>1</sup>, Michele Ourevitch<sup>2</sup>,  
Ahmed Abouabdellah<sup>2</sup>, Danièle Bonnet-Delpon<sup>2</sup>, Jean-Pierre Bégué<sup>2</sup>,  
Jean M. Veith<sup>3</sup>, Paula Pera<sup>3</sup>, and Ralph J. Bernacki<sup>3</sup>

<sup>1</sup>Department of Chemistry, State University of New York at Stony Brook,  
Stony Brook, NY 11794-3400

<sup>2</sup>Faculté de Pharmacie, BIOCIS—Centre National de la Recherche  
Scientifique, Université Paris-Sud, 5 rue Jean-Baptiste Clément,  
92296 Châtenay-Malabry, France

<sup>3</sup>Department of Experimental Therapeutics, Grace Cancer Drug Center,  
Roswell Park Cancer Institute, Buffalo, NY 14263

A series of fluorine-containing analogs of paclitaxel and docetaxel are synthesized by coupling (3*R*,4*S*)-1-acyl- $\beta$ -lactams of high enantiomeric purity with properly protected baccatin III, 10-deacetyl-baccatin III, and 14 $\beta$ -hydroxy-10-deacetyl-baccatin III as the key step. 3'-Trifluoromethyl-10-acetyl analog of docetaxel is synthesized through highly efficient kinetic resolution of racemic 1-(*t*-Boc)-4-CF<sub>3</sub>- $\beta$ -lactam in the coupling reaction with 7-*TES*-baccatin III. The 3'-(4-F-C<sub>6</sub>H<sub>4</sub>), 3'-(4-F-C<sub>6</sub>H<sub>4</sub>)-10-Ac, and 3'-CF<sub>3</sub>-10-Ac analogs of docetaxel exhibit better cytotoxicity than paclitaxel, and the 3'-CF<sub>3</sub>-10-Ac analog possesses more than one order of magnitude higher potency than paclitaxel and docetaxel against a drug-resistant human breast cancer cell line. This analog can be regarded as an excellent lead for the second generation taxoid anticancer agents. Difluoro-paclitaxel, bearing fluorine labels at the 3'-(4-F-C<sub>6</sub>H<sub>4</sub>CONH) and 3'-(4-F-C<sub>6</sub>H<sub>4</sub>) moieties, is proved to be very useful for the conformational analysis of paclitaxel in solution using <sup>19</sup>F NMR. A combination of <sup>19</sup>F and <sup>1</sup>H variable temperature NMR measurements of the <sup>19</sup>F chemical shifts and J<sub>H2'-H3'</sub> values as well as molecular modeling including restrained molecular dynamics has identified three key conformers including the one that has never been predicted by the previous molecular modeling and NMR studies. This conformation might be the molecular structure first recognized by the  $\beta$ -tubulin binding site on microtubules.

Taxol® (paclitaxel) (1,3), a naturally occurring taxane, and Taxotere® (docetaxel) (1,4), a semisynthetic taxoid, are exciting and unique agents for cancer chemotherapy. Paclitaxel and docetaxel block cell mitosis by inhibiting the depolymerization of microtubules, showing strong antitumor activity against different cancers that have not been effectively treated by existing anticancer drugs. Paclitaxel has been extensively used for the treatment of advanced ovarian cancer (FDA approval in 1992) as well as metastatic breast cancer (FDA approval in 1994) (1). Docetaxel is in the final stage of clinical trials for breast and lung cancers worldwide and will be on the market shortly (1,5).

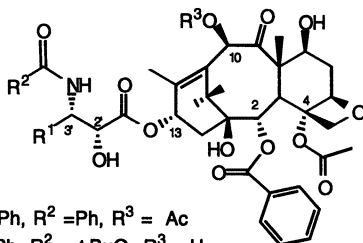
0097-6156/96/0639-0228\$15.00/0

© 1996 American Chemical Society

These taxane antitumor agents are, however, not exceptional from their numerous undesirable side effects, and have limitations in their efficacy against certain tumor types (6). Accordingly, it is apparent that the development of new generation taxoid anticancer drugs, that have less undesirable side effects and high efficacy against various tumor types, is very important. As a part of our ongoing structure-activity relationship (SAR) study on new taxoid antitumor agents (7-12), we incorporated fluorine(s) into paclitaxel (13-17) and taxoids to investigate the effects of fluorine on cytotoxicity. We were also interested in the possible blocking of known metabolic pathways by the site specific introduction of fluorine(s) and the use of fluoro-taxoids as probes for the conformational analysis of paclitaxel and taxoid antitumor agents.(24)

It has been proposed that both paclitaxel and docetaxel take a "hydrophobic cluster" conformation in aqueous media (18,19). Thus, the introduction of a 4-fluorophenyl or a trifluoromethyl at the C-3' position instead of the phenyl may enhance the formation of hydrophobic cluster with the benzoate at C-2 (Ph moiety) and the acetate at C-4 (Me moiety). It has been shown that, in the metabolism of paclitaxel, the primary sites of hydroxylation by the cytochrome P450 family of enzymes are (a) the *para* position of 3'-phenyl, (b) the *meta* position of 2-benzoate, (c) 6-methylene, and (d) 19-methyl (20,21): The predominant metabolic pathway is the hydroxylation of 3'-phenyl at the *para* position by the cytochrome 3A family (20). The biomedical studies of fluorine containing amino acids and peptides (22,23) have shown that the replacement of C-H bond with C-F bond can substantially slow down the enzymatic oxidation (22). Thus, it is reasonable to assume that the introduction of a fluorine to the *para* position of 3'-phenyl would slow down the enzymatic hydroxylation.(24) The use of fluorine-labeled paclitaxel and docetaxel as probes enables us to perform conformational analyses of paclitaxel and docetaxel based on variable temperature  $^{19}\text{F}$  NMR as well as  $^{19}\text{F}$ - $^1\text{H}$  hetero-nOe's.

Fluorine-containing taxoids 1-7 shown below were synthesized (24-29) by means of the  $\beta$ -Lactam Synthron Method (30-34), their cytotoxicities against human cancer cell lines examined, and the conformational analyses of 2 and 4 performed.



**Paclitaxel:**  $\text{R}^1 = \text{Ph}$ ,  $\text{R}^2 = \text{Ph}$ ,  $\text{R}^3 = \text{Ac}$

**Docetaxel:**  $\text{R}^1 = \text{Ph}$ ,  $\text{R}^2 = t\text{-BuO}$ ,  $\text{R}^3 = \text{H}$

**1:**  $\text{R}^1 = 4\text{-F-C}_6\text{H}_4$ ,  $\text{R}^2 = \text{Ph}$ ,  $\text{R}^3 = \text{Ac}$

**2:**  $\text{R}^1 = 4\text{-F-C}_6\text{H}_4$ ,  $\text{R}^2 = 4\text{-F-C}_6\text{H}_4$ ,  $\text{R}^3 = \text{Ac}$

**3:**  $\text{R}^1 = 4\text{-F-C}_6\text{H}_4$ ,  $\text{R}^2 = t\text{-BuO}$ ,  $\text{R}^3 = \text{H}$

**4:**  $\text{R}^1 = 4\text{-F-C}_6\text{H}_4$ ,  $\text{R}^2 = t\text{-BuO}$ ,  $\text{R}^3 = \text{Ac}$

**5:**  $\text{R}^1 = \text{CF}_3\text{CH}_2\text{CH}_2$ ,  $\text{R}^2 = t\text{-BuO}$ ,  $\text{R}^3 = \text{H}$

**6:**  $\text{R}^1 = \text{CF}_3\text{CH}_2\text{CH}_2$ ,  $\text{R}^2 = t\text{-BuO}$ ,  $\text{R}^3 = \text{Ac}$

**7:**  $\text{R}^1 = \text{CF}_3$ ,  $\text{R}^2 = t\text{-BuO}$ ,  $\text{R}^3 = \text{Ac}$

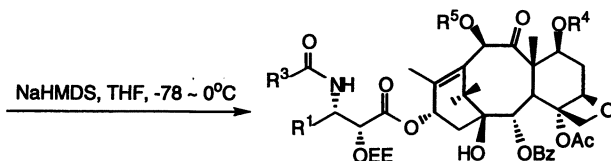
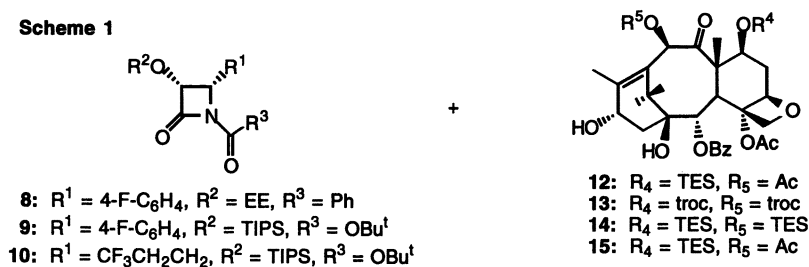
(Modified from Ref. 24)

### Syntheses of Fluorine-Containing Taxoids (24)

The syntheses of 3'-dephenyl-3'-(4-fluorophenyl)paclitaxel (1) (25), 3'-dephenyl-3'-(4-fluorophenyl)docetaxel (3) (27), 3'-dephenyl-3'-(4-fluorophenyl)-10-acetyldocetaxel (4), 3'-dephenyl-3'-(3,3,3-trifluoropropyl)docetaxel (5) and 3'-dephenyl-3'-(3,3,3-trifluoropropyl)-10-acetyldocetaxel (6) were carried out through the coupling of 1-acyl- $\beta$ -lactams (8-10) and baccatin III with proper protecting groups at C-7 and/or C-10 (12-15) by means of the protocol developed in our laboratories (11,35-37) (Scheme 1) (24).

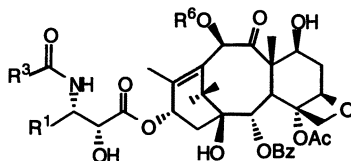


## Scheme 1



- 16:  $R^1 = 4\text{-F-C}_6\text{H}_4$ ,  $R^2 = \text{Ph}$ ,  $R^3 = \text{Ac}$ ,  $R^4 = \text{TES}$ ,  $R^5 = \text{Ac}$   
 17:  $R^1 = 4\text{-F-C}_6\text{H}_4$ ,  $R^2 = t\text{-BuO}$ ,  $R^3 = \text{H}$ ,  $R^4 = \text{TES}$ ,  $R^5 = \text{TES}$   
 18:  $R^1 = 4\text{-F-C}_6\text{H}_4$ ,  $R^2 = t\text{-BuO}$ ,  $R^3 = \text{Ac}$ ,  $R^4 = \text{TES}$ ,  $R^5 = \text{Ac}$   
 19:  $R^1 = \text{CF}_3\text{CH}_2\text{CH}_2$ ,  $R^2 = t\text{-BuO}$ ,  $R^3 = \text{H}$ ,  $R^4 = \text{troc}$ ,  $R^5 = \text{troc}$   
 20:  $R^1 = \text{CF}_3\text{CH}_2\text{CH}_2$ ,  $R^2 = t\text{-BuO}$ ,  $R^3 = \text{Ac}$ ,  $R^4 = \text{TES}$ ,  $R^5 = \text{Ac}$

- (a) 0.5 N HCl, EtOH (for 16)  
 (b) HF-pyridine (for 17, 18, 20)  
 (c) HF-Pyr, then Zn, 0.5 N HCl, THF (for 19)

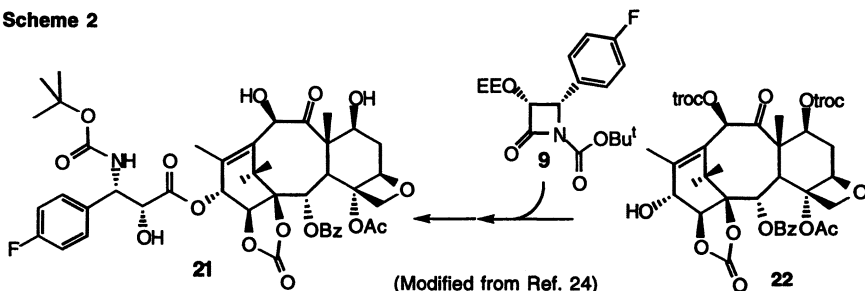


- 1:  $R^1 = 4\text{-F-C}_6\text{H}_4$ ,  $R^2 = \text{Ph}$ ,  $R^6 = \text{Ac}$   
 3:  $R^1 = 4\text{-F-C}_6\text{H}_4$ ,  $R^2 = t\text{-BuO}$ ,  $R^6 = \text{H}$   
 4:  $R^1 = 4\text{-F-C}_6\text{H}_4$ ,  $R^2 = t\text{-BuO}$ ,  $R^6 = \text{Ac}$   
 5:  $R^1 = \text{CF}_3\text{CH}_2\text{CH}_2$ ,  $R^2 = t\text{-BuO}$ ,  $R^6 = \text{H}$   
 6:  $R^1 = \text{CF}_3\text{CH}_2\text{CH}_2$ ,  $R^2 = t\text{-BuO}$ ,  $R^6 = \text{Ac}$

(Modified from Ref. 24)

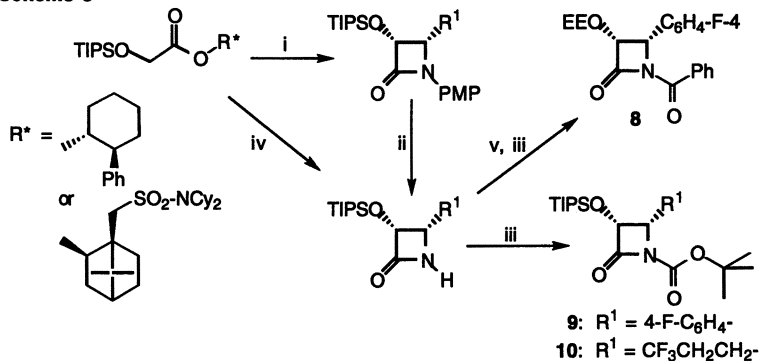
In the same manner, 3'-dephenyl-3'-(4-fluorophenyl)-14-OH-docetaxel-1,14-carbonate (**21**) was synthesized through the coupling of 14β-Hydroxy-10-deacetyl-baccatin-1,14-carbonate (**22**) (39) with 1-*t*-Boc-β-lactam **9** (Scheme 2) (24).

## Scheme 2



The enantiomerically pure fluorine-containing (3*R*,4*S*)-1-acyl- $\beta$ -lactams **8-10** were synthesized through chiral ester enolate – imine cyclocondensation (35-38) (Scheme 3) (24).

Scheme 3



i. (a) LDA, THF, (b)  $R^1\text{CH=N-PMP}$ ; ii. (a) CAN,  $\text{CH}_3\text{CN-H}_2\text{O}$ ;

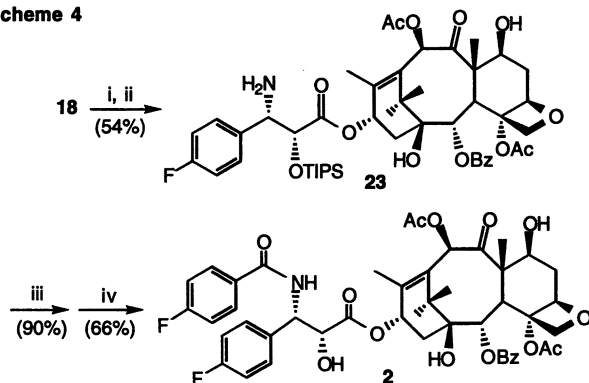
iii.  $\text{PhCOCl}$  or  $t\text{-Boc}_2\text{O}$ , DMAP, TEA; iv. (a) LDA, THF, (b)  $R^1\text{CH=N-TMS}$

v. (a) TBAF, THF, (b) EVE, TSA, THF

(Modified from Ref. 24)

3'-*N*-Debenzoyl-3'-*N*-(4-fluorobenzoyl)-3'-dephenyl-3'-(4-fluorophenyl)paclitaxel (**2**) was synthesized via Schotten-Baumann acylation of 3'-*N*-debenzoyl-3'-(4-fluorophenyl)paclitaxel (**23**) prepared from 2',7-protected fluoro-docetaxel **18** (Scheme 4) (24).

Scheme 4



i.  $\text{HCOOH}$ , MeOH,  $0 \rightarrow 25^\circ\text{C}$ , 1 h; ii.  $\text{Na}_2\text{CO}_3$ ;

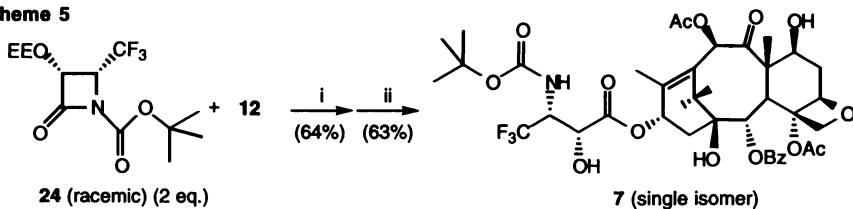
iii.  $4\text{-F-C}_6\text{H}_4\text{COCl}$ , TEA,  $0^\circ\text{C} \rightarrow \text{RT}$ ,  $\text{CH}_2\text{Cl}_2$ , 1.5 h;

iv. HF-py., pyridine,  $\text{CH}_3\text{CN}$ ,  $0 \rightarrow 25^\circ\text{C}$ , overnight.

(Modified from Ref. 24)

3'-Dephenyl-3'-trifluoromethyl-10-acetyldocetaxel (**7**) was obtained as a single stereoisomer through the coupling of 7-TES-baccatin (**12**) with racemic 1-*t*-Boc-3-EEO-4-trifluoromethyl-azetidin-2-one (**24**) where a highly selective kinetic resolution took place (33,40), i.e., only (3*R*,4*S*)-isomer of **24** reacted with baccatin **12** (Scheme 5).

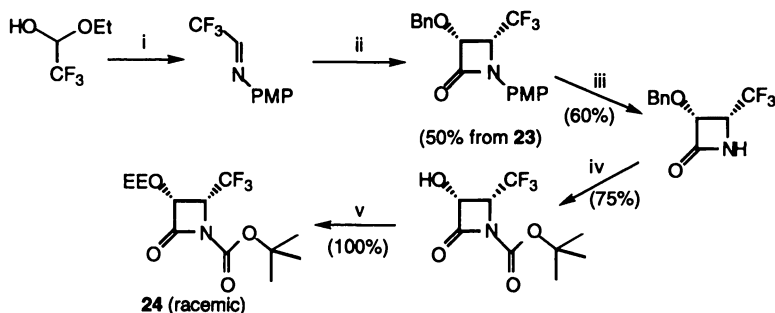
Scheme 5



i. LiHMDS, THF, -40 ~ 0 °C, 1.25 h; ii. 0.5 N HCl, 0 °C, 30 h.

Racemic 4-CF<sub>3</sub>-β-lactam **24** was prepared via ketene-imine [2 + 2] cycloaddition followed by *N*-acylation as shown in Scheme 6.

Scheme 6



i. *p*-anisidine, TSA, benzene, reflux; ii. BnOCH<sub>2</sub>COCl, TEA, CH<sub>2</sub>Cl<sub>2</sub>, 40 °C; iii. CAN, CH<sub>3</sub>CN-H<sub>2</sub>O, 0 °C; iv. (a) *t*-Boc<sub>2</sub>O, DMAP, TEA, CH<sub>2</sub>Cl<sub>2</sub>, (b) H<sub>2</sub>, Pd/C, EtOAc; v. TAS, EVE, THF, 0 °C.

### Biological Activity of Fluorine-Containing Taxoids

All fluorine containing taxoids thus synthesized were evaluated for their activity against different human cancer cell lines. Results are summarized in Table 1. Activities of paclitaxel and docetaxel in the same assay are also listed for comparison.

3'-Dephenyl-3'-(4-fluorophenyl)docetaxel (**3**) (**27**) and 3'-dephenyl-3'-(4-fluorophenyl)-10-acetyldocetaxel (**4**) possess strong activities against human ovarian (A121), non-small cell lung (A549), colon (HT-29), and breast cancer (MCF7) cells, which are substantially better than paclitaxel except for HT-29 and a drug-resistant breast cancer cell line (MCF7-R), and also better than docetaxel against A549 and MCF7. The 3'-monofluorophenyl analog of paclitaxel **1** shows a comparable activity to that of paclitaxel except for MCF7-R, but the difluoro-analog of paclitaxel **2** shows reduced activity. The 1,14-carbonate analog of monofluoro-docetaxel **21** shows only slightly weaker activity than that of paclitaxel. 3'-Dephenyl-3'-(3,3,3-trifluoropropyl)docetaxel (**5**) shows reduced activity, but its 10-acetyl analog **6** recovers activity. It is noteworthy that 3'-dephenyl-3'-trifluoromethyl-10-acetyldocetaxel (**7**) exhibits excellent cytotoxicity in all cell lines, surpassing that of both paclitaxel and docetaxel. Particularly interesting is the very strong activity (>10 times better than paclitaxel and docetaxel) against the drug-resistant breast cancer cells (MCF7-R). The marked difference in cytotoxicity observed for 3'-(3,3,3-trifluoropropyl) analogs, **5** and **6**, and 3'-trifluoromethyl analog **7** strongly indicates the importance of the size of the alkyl substituent at this position on activity. *These results clearly demonstrate that 3'-phenyl or 3'-aryl group is not a requisite for high activity, and the activity can be*

substantially improved by introducing proper size alkyl groups such as trifluoromethyl and other alkyl and alkenyl groups (7,42). 3'-Dephenyl-3'-trifluoromethyl-10-acetyl-docetaxel (7) can be regarded as an excellent lead for the second generation taxoids.

**Table 1. Cytotoxicities (IC<sub>50</sub> nM)<sup>a</sup> of Fluorine Containing Taxoids**

F-Taxoid	A121	A549	HT-29	MCF7	MCF7R
Paclitaxel	6.3	3.6	3.6	1.7	300
Docetaxel	1.2	1.0	1.2	1.0	235
<b>1</b>	6.3	4.2	14.5	5.1	>1000
<b>2</b>	76	35	51	45	>1000
<b>3</b>	1.3	<b>0.49</b>	3.9	<b>0.48</b>	477
<b>4</b>	1.2	<b>0.47</b>	3.5	<b>0.42</b>	315
<b>5</b>	78	36	44	36	>1000
<b>6</b>	10	14	7.1	9.3	219
<b>7</b>	<b>0.37</b>	<b>0.25</b>	<b>0.40</b>	<b>0.25</b>	<b>17</b>
<b>21</b>	11.3	2.4	5.2	3.6	721

<sup>a</sup> The concentration of compound which inhibit 50% (IC<sub>50</sub>, nM) of the growth of human tumor cell line, A121 (ovarian carcinoma), A549 (non-small cell lung carcinoma), HT-29 (colon carcinoma), MCF7 (mammary carcinoma), and MCF7-R (mammary carcinoma cells 180 fold resistant to adriamycin) after 72 h drug exposure according to the method developed by Skehan et al. (41) The data represent the mean values of at least three separate experiments.

Since 3'-(4-fluorophenyl) analog of paclitaxel **1** did not show particularly strong activity *in vitro*, *in vivo* assay against human cancer xenografts has not been carried out yet. Thus, we do not have proof for the blocking of the metabolic pathway, i.e., P-450 oxidation (*vide supra*), by introducing a fluorine at the *para* position of the 3'-phenyl of paclitaxel. Nevertheless, it is still an interesting possibility. Introduction of 3'-trifluoromethyl to paclitaxel should completely block the oxidation by P-450 at the C-3' position. This possibility will be investigated in due course.

### Conformational Analysis of Paclitaxel and Docetaxel Using Fluorine as a Probe

One approach toward the design of highly potent taxoids is to understand the conformation(s) of paclitaxel and docetaxel in solution that may be relevant to the bioactive conformation at the  $\beta$ -tubulin binding site on microtubules (43-46).

Three dimensional structures of paclitaxel and docetaxel pharmacophore have been studied by NMR in conjunction with molecular modeling (18,47-54) as well as X-ray crystallographic analyses (55,56). These studies identified two conformations, structures **A** and **B**, for paclitaxel (Figure 1) with some very minor variations between different studies (57,58).

The structure **A** is based on the X-ray crystal structure of docetaxel (55), replacing the 3'-(*t*-Boc)NH moiety with 3'-PhCONH group followed by minimization in molecular modeling (SYBYL 6.04). The *N*-benzoylphenylisoserine moiety at the C-13 position of the structure **A** has a gauche conformation with the H2'-C2'-C3'-H3' torsion angle of ca. 60° and there appears to be a hydrophobic clustering among the 3'-PhCONH (Ph), 2-benzoate (Ph), and 4-acetoxy (CH<sub>3</sub>) moieties. This conformation has been commonly observed in aprotic solvents such as CHCl<sub>3</sub> and CH<sub>2</sub>Cl<sub>2</sub> (57,58), and

proposed to be the likely bioactive conformation based on the unproved assumption that the paclitaxel binding site on microtubules is hydrophobic (59).

The structure **B** was first recognized by Williams et al. based on the conformational analysis of the *N*-benzoylphenylisoserine moiety and molecular modeling (48). Then, Vander Velde et al. verified it on the basis of 2D NMR experiments (NOESY and ROESY) on paclitaxel and docetaxel in DMSO-water and proposed it as the "hydrophobic collapse" conformation (18). The *N*-benzoylphenylisoserine moiety at C-13 of the structure **B** takes another gauche conformation in which the H2'-C2'-C3'-H3' torsion angle is ca. 180°, and there is a clear hydrophobic clustering among the 3'-Ph, 2-benzoate (Ph), and 4-acetoxy (CH<sub>3</sub>) moieties. The Kansas group ascribed this marked conformational change in aqueous media to the "hydrophobic collapse" phenomenon (60) rather than intramolecular hydrogen bonding, and implied that this conformation might be the one first recognized by the tubulin binding site (18,19,58). Recently, this conformation was indeed found in the X-ray crystal structure of paclitaxel obtained by slow evaporation of a dioxane/H<sub>2</sub>O/xylene solution, in which the H2'-C2'-C3'-H3' torsion angle is 176° (56).

The conformational analyses of docetaxel have led to essentially the same two structures **A** and **B** with replacement of the 3'-PhCONH moiety by 3'-(*t*-Boc)NH group (49, 57).

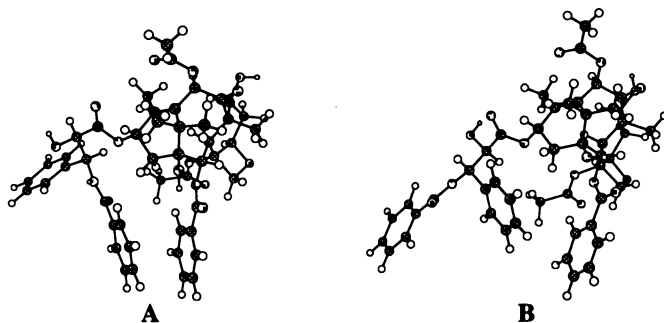


Figure 1. Two conformations of paclitaxel.

The NMR studies on the solution structures of paclitaxel and docetaxel mentioned above assigned the structure **A** or **B** to be highly populated in each solvent system, assuming gauche conformations in the phenylisoserine moiety at C-13. However, no systematic study on the dynamics of these two and other possible conformations had been performed when we became interested in identifying possible bioactive conformation(s) of paclitaxel and taxoid antitumor agents. The observation of *n*Oe's does not necessarily mean that there is only one fixed structure. Also, the observed  $J_{H2'-H3'}$  coupling constant (7.3-7.8 Hz) in DMSO-D<sub>2</sub>O appeared to be too small for the pure *trans* geometry, i.e., the H2'-C2'-C3'-H3' torsion angle is ca. 180°. It is natural to think that different conformations are in equilibrium in solution and it is highly likely that the paclitaxel molecule is dynamic and an averaged structure in the NMR time scale is observed. Accordingly, we decided to look at the dependence of <sup>19</sup>F chemical shift(s) of the difluoro-paclitaxel **2** and the monofluoro-docetaxel **3**. The use of <sup>19</sup>F NMR for variable temperature (VT) NMR study of a molecule of this complexity is apparently advantageous over the use of <sup>1</sup>H NMR because of the wide dispersion of the <sup>19</sup>F chemical shifts that allows fast dynamic processes to be frozen out. Also, the sensitivity of <sup>19</sup>F NMR is much higher than that of <sup>13</sup>C NMR although <sup>13</sup>C NMR offers wide dispersion.

We carried out the VT experiments on the fluoro analogs **2** and **3** in CD<sub>2</sub>Cl<sub>2</sub>, CD<sub>3</sub>OD, and DMSO(*d*<sub>6</sub>)-D<sub>2</sub>O (3:1). The dependence of <sup>19</sup>F chemical shifts of **2** in

these three solvents is summarized in Figure 2 (376.3 MHz), and the VT  $^{19}\text{F}$  NMR spectra of **2** in  $\text{CD}_3\text{OD}$  (235.2 MHz) is shown in Figure 3 as an example.

As Figures 2 and 3 clearly show, the  $^{19}\text{F}$  signal ( $\text{F}_\text{B}$ ) of the 3'-(4-F- $\text{C}_6\text{H}_4$ ) moiety that appears in a higher field than that ( $\text{F}_\text{A}$ ) of the 4-F- $\text{C}_6\text{H}_4$ -CONH moiety decoalesces at ca.  $-60^\circ\text{C}$  (235.2 MHz) (Figure 3) or at ca.  $-70^\circ\text{C}$  (376.3 MHz) (Figure 2) in  $\text{CD}_3\text{OD}$ . Then, this  $^{19}\text{F}$  signal becomes two distinct signals  $\text{F}_{\text{B-1}}$  (lower field) and  $\text{F}_{\text{B-2}}$

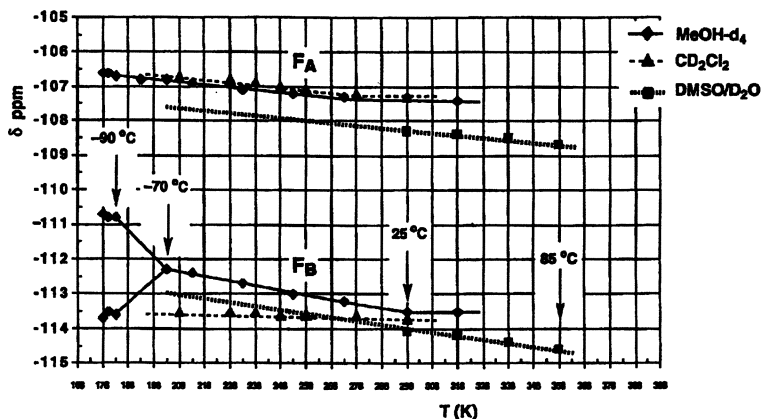


**Figure 2.** Dependence of  $^{19}\text{F}$  chemical shifts of difluoro-paclitaxel **2** on temperature in different solvents (376.3 MHz).

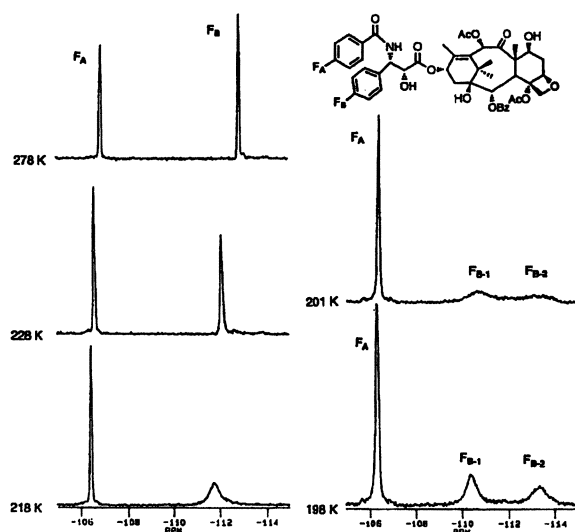


**Figure 3.** Variable temperature  $^{19}\text{F}$  NMR spectra of difluoro-paclitaxel **2** in  $\text{CD}_3\text{OD}$  (235.2 MHz).

(higher field) with the relative ratio of 3:2. The estimated activation free energy is 39 KJ/mol (9.4 Kcal/mol). The VT  $^{19}\text{F}$  NMR spectra of **3** shows essentially the same phenomenon in  $\text{CD}_3\text{OD}$  [ $E_A = 37.5$  KJ/mol (9.0 Kcal/mol)] for the 3'-(4-F-C $_6$ H $_4$ ) moiety.

This observation unambiguously indicates that two conformers are in equilibrium in a wide temperature range (25 ~ -95 °C). In sharp contrast with the  $F_B$  signal, the  $F_A$  signal does not show any significant change except for a small solvent-dependent systematic shift, and no decoalescence is observed. This can be ascribed to either the fast movement of the 4-F-C $_6$ H $_4$ -CONH moiety even at -90 °C or this moiety being completely fixed even at ambient temperature. However, the latter possibility is highly unlikely and the restrained molecular dynamics (RMD) study (*vide infra*) has confirmed the high flexibility of the 4-F-C $_6$ H $_4$ -CONH moiety. These observations for the  $F_A$  and  $F_B$  signals strongly suggest the occurrence of hydrophobic clustering including the 3'-(4-F-C $_6$ H $_4$ ) moiety and as a result the 4-F-C $_6$ H $_4$ -CONH moiety is placed outside of the hydrophobic cluster.

On the contrary, the chemical shift of the  $F_B$  signal is virtually unchanged in  $\text{CD}_2\text{Cl}_2$ . The  $F_A$  signal in  $\text{CD}_2\text{Cl}_2$  shows a small solvent-dependent systematic shift in almost the same manner as that in  $\text{CD}_3\text{OD}$ . No decoalescence is observed even at -100 °C. This strongly suggests that there is only one conformer in  $\text{CD}_2\text{Cl}_2$ , which appears to be consistent with the previous NMR studies mentioned above.

In  $\text{DMSO}(d_6)$ - $\text{D}_2\text{O}$ , the temperature dependence is examined in the range of 25 ~ 85 °C because of the freezing of this solvent system below 0 °C in our experiments (61). The temperature dependence of the  $F_A$  and  $F_B$  signals follows the same trend as that in  $\text{CD}_3\text{OD}$ . This implies that the equilibrium between different conformers exists in  $\text{DMSO}(d_6)$ - $\text{D}_2\text{O}$  as well.

In order to identify the structures of the two conformers observed in  $\text{CD}_3\text{OD}$  and also to confirm the existence of equilibrium between different conformers in  $\text{DMSO}(d_6)$ - $\text{D}_2\text{O}$ , we looked at the temperature dependence of  $J_{H_2'-H_3'}$  in the same set of solvents. Results are shown in Figure 4.

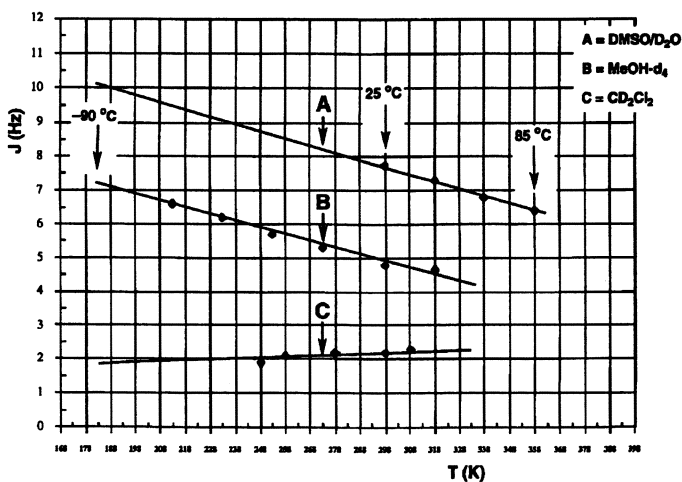


**Figure 4.** Dependence of the  $J_{H_2'-H_3'}$  of difluoro-paclitaxel **2** on temperature in different solvents (400 MHz).

As Figure 4 shows, the  $J_{H_2'-H_3'}$  is clearly dependent on temperature in  $CD_3OD$  and  $DMSO(d_6)-D_2O$ , increasing its value at lower temperatures, whereas the  $J_{H_2'-H_3'}$  in  $CD_2Cl_2$  (ca. 2 Hz) is much less dependent on temperature, slightly increasing at higher temperatures. These observations are consistent with those for the temperature dependence of the  $^{19}F$  chemical shifts for  $F_B$  (Figure 2) discussed above. Since the  $J_{H_2'-H_3'}$  values directly reflect the torsion angle of these two protons, it is possible for us to deduce the conformations of the *N*-benzoylphenylisoserine moiety at C-13.

The  $J_{H_2'-H_3'}$  value of 2.0 Hz observed in  $CD_2Cl_2$  at  $-15^\circ C$  corresponds to the torsion angle of  $54^\circ$  based on the MM2 calculation (Macromodel 4.0) of the *N*-benzoylphenylisoserine moiety (Conformer A). This torsion angle ( $54^\circ$ ) is in good agreement with the one in the X-ray crystal structure of docetaxel ( $56.6^\circ$ ) (55).

In  $CD_3OD$ , the  $J_{H_2'-H_3'}$  is extrapolated to be 7.2 Hz at  $-90^\circ C$  at which temperature decoalescence takes place (see Figure 2), and this J value should be the average of the J values of the two conformers (3:2 ratio) corresponding to the  $F_{B-1}$  and the  $F_{B-2}$  signals (Figure 3). As the slopes A ( $DMSO(d_6)-D_2O$ ) and B ( $CD_3OD$ ) ( $25 \sim -90^\circ C$  range) (Figure 4) are virtually parallel, it is very reasonable to assume that the same two conformers exist in different ratios in these solvent systems. In  $DMSO(d_6)-D_2O$ , the  $J_{H_2'-H_3'}$  value of 7.8 Hz at  $25^\circ C$  is in good agreement with the reported value by the Kansas group for paclitaxel (18). However, as the slope A (Figure 4) strongly suggests, this J value should be the average of the two conformers. The extrapolated J value at  $-90^\circ C$  is 10.1 Hz, which corresponds to the  $H_2'-C_2'-C_3'-H_3'$  torsion angle of  $178^\circ$  based on the MM2 calculation (Conformer B). Therefore, this conformer should be exactly the one observed in the X-ray crystal structure of paclitaxel (56), and corresponds to the  $F_{B-2}$  conformer (higher field signal) since the hydrophobic clustering of the 3'-(4-F- $C_6H_4$ ), 2-benzoate (Ph), and 4-acetyl ( $CH_3$ ) moieties is highly likely to cause substantial shielding effect. The  $J_{H_2'-H_3'}$  value of the  $F_{B-1}$  conformer is calculated to be 5.2 Hz in a straightforward manner from the J value (10.1 Hz) of the  $F_{B-2}$  conformer, the ratio of the  $F_{B-1}$  and  $F_{B-2}$  conformers (3:2), and the estimated average J value (7.2 Hz) in  $CD_3OD$  at  $-90^\circ C$ . The J value of 5.2 Hz corresponds to the  $H_2'-C_2'-C_3'-H_3'$  torsion angle of  $124^\circ$  based on the MM2 calculation, i.e., this is a nearly eclipsed conformation (Conformer C). The Newman projections ( $C_2'-C_3'$ ) of the three conformers of the *N*-phenylisoserine moiety are shown in Figure 5.

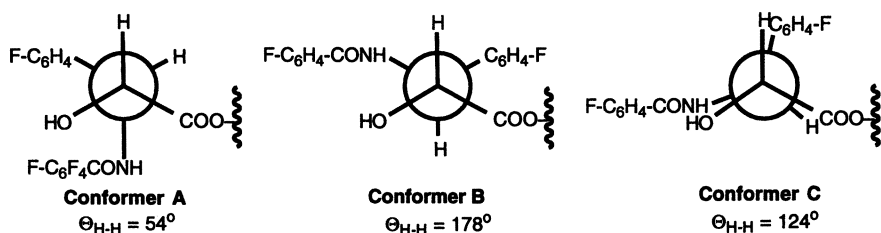


**Figure 5.** Newman projections of the three conformers of difluoro-paclitaxel 2.

The whole structures of the Conformers A and B (SYBYL 6.04) are virtually the same as the structures A and B (Figure 1) except for the two fluorine atoms. The Chem 3D representation of the Conformer C (SYBYL 6.04) is shown in Figure 6. Although this semi-eclipsed conformation at the  $C_2'-C_3'$  bond is obviously unfavorable based on the molecular modeling study of the simple *N*-phenylisoserine methyl ester (48), the Conformer C has four H-bondings among the 2'-OH, 3'-NHCO, and 1'-CO, and is apparently a favorable conformation as a whole molecule in protic media. Accordingly, the "fluorine probe" approach has succeeded in finding a new important



conformer that has never been predicted by the previous molecular modeling studies (57). Strong supporting evidence for this rather uncommon conformation can be found in the solution structure of a water-soluble paclitaxel analog, paclitaxel-7-MPA (MPA = *N*-methylpyridinium acetate), in D<sub>2</sub>O reported by Nicolaou and co-workers (62), i.e., the H2'-C2'-C3'-H3' torsion angle of the *N*-phenylisoserine moiety is 127°, that is only a few degrees different from the value for the Conformer C (Figure 6). Both structures in Figure 6 clearly show the hydrophobic clustering of the 3'-Ph (or 4-F-C<sub>6</sub>H<sub>4</sub>), 2-benzoate (Ph), and 4-acetoxy (CH<sub>3</sub>) groups although the distance between the 3'-Ph (or 4-F-C<sub>6</sub>H<sub>4</sub>) and the 2-benzoate (Ph) groups is larger than that of the Conformer B.

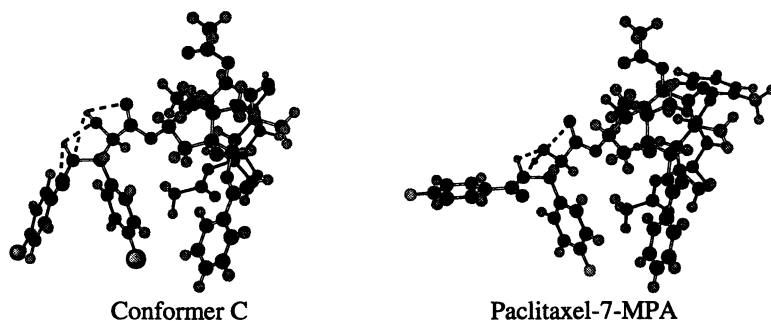


**Figure 6.** Conformer C (63) and the proposed structure of a water-soluble paclitaxel analog in D<sub>2</sub>O (62)

The major difference between the Conformer C and the proposed solution structure of paclitaxel-7-MPA is the position of the benzoylamino moieties, i.e., these two are rotamers at the C3'-N and N-CO bonds. The structure of paclitaxel-7-MPA as shown in Figure 6 has three hydrogen bondings while the Conformer C has four hydrogen bondings as mentioned above including the one between the N(H) and 4-F-C<sub>6</sub>H<sub>4</sub>-C(O) groups as the fourth interaction.

It is interesting to note that the Conformer C appears to have another hydrophobic clustering between the two aromatic groups of the 4-F-C<sub>6</sub>H<sub>4</sub>CONH and 3'-(4-F-C<sub>6</sub>H<sub>4</sub>) moieties. However, it is more reasonable to think that the fixation of the movement of the 4-F-C<sub>6</sub>H<sub>4</sub>CONH (or PhCONH) moiety only takes place in the solid state or the frozen state, and this moiety should have high flexibility in solution at ambient temperature.

Accordingly, we carried out the restrained molecular dynamics (RMD) of the Conformer C and the overlay of twenty representative structures is depicted in Figure 7. As Figure 7 shows, the 4-F-C<sub>6</sub>H<sub>4</sub>CONH moiety is indeed flexible. *The most remarkable finding in this RMD study is the fact that the molecule is quite rigid (except for the 3'-acylamino moiety) once the torsion angle of the H2'-C2'-C3'-H3' is fixed through self-organization by hydrogen bondings and/or hydrophobic clustering.* This newly identified conformation might be the molecular structure that is first recognized by the  $\beta$ -tubulin binding site since the contribution of this conformation at around ambient temperature is substantial in protic solvents (see Figure 4).

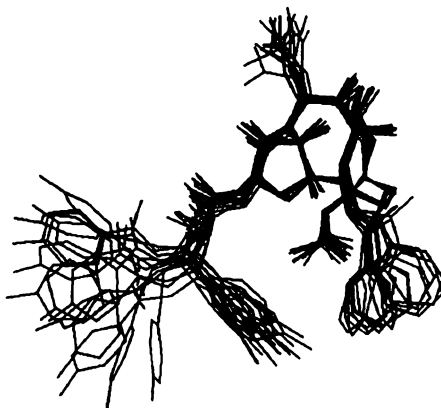


**Figure 7.** RMD of the Conformer C (63) of difluoro-paclitaxel 2.

In order to confirm that the Conformers A, B, and C thus identified are consistent with the 2D NMR studies of paclitaxel and docetaxel reported from other laboratories (57), we carried out the  $^1\text{H}$ - $^1\text{H}$  NOESY measurements of difluoro-paclitaxel 2 and monofluoro-docetaxel 3 in  $\text{CDCl}_3$  and  $\text{DMSO}(d_6)$ - $\text{D}_2\text{O}$ . As expected, clear nOe's were indeed observed between the 3'-(4-F- $\text{C}_6\text{H}_4$ ) and 2-benzoate (Ph) protons in  $\text{DMSO}(d_6)$ - $\text{D}_2\text{O}$ . The  $^{19}\text{F}$ - $^1\text{H}$  heteronuclear nOe measurements have also been carried out for 2 and 3 in  $\text{CD}_3\text{OD}$  and  $\text{DMSO}(d_6)$ - $\text{D}_2\text{O}$ . Although the  $^{19}\text{F}$ - $^1\text{H}$  nOe's were smaller than their  $^1\text{H}$ - $^1\text{H}$  counterparts, crosspeaks were clearly observed between the fluorine of 3'-(4-F- $\text{C}_6\text{H}_4$ ) and the phenyl protons of 2-benzoate as shown in Figure 8 (only the results for 2 are shown for brevity).

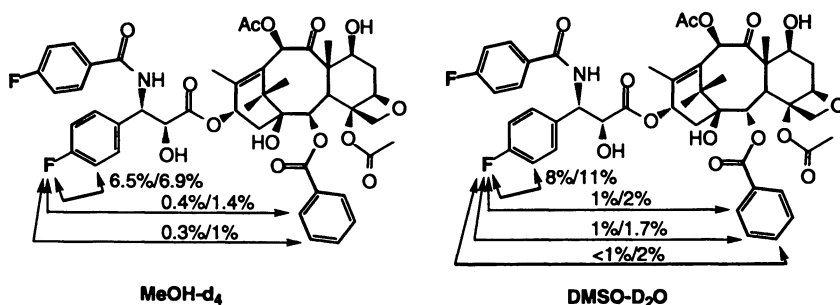


**Figure 8.** Representative  $^1\text{H}$ - $^{19}\text{F}$  heteronuclear nOe's for difluoro-paclitaxel 2 in  $\text{CD}_3\text{OD}$  and  $\text{DMSO}(d_6)$ - $\text{D}_2\text{O}$  at 25 °C.

The presence of these nOe's is consistent with the hydrophobic clustering conformations, i.e., Conformers B and C. However, it should be noted that these nOe's are very likely to be for an averaged structure of the Conformers B and C. No  $^1\text{H}$ - $^1\text{H}$  and  $^{19}\text{F}$ - $^1\text{H}$  nOe's between 3'-(4-F- $\text{C}_6\text{H}_4$ ) and 2-benzoate moieties were observed in  $\text{CD}_2\text{Cl}_2$  or  $\text{CDCl}_3$  for both compounds. Despite the apparent clustering of the two aryl

groups of 4-C<sub>6</sub>H<sub>4</sub>CONH (or PhCONH for paclitaxel) and 2-benzoate of the energy minimized Conformer A (or the structure A for paclitaxel), no nOe's have been observed between the two groups in this study as well as previous ones. These results strongly suggest the great flexibility of this conformation in solution, which is indeed confirmed by our RMD study of the Conformer A (63).

The NMR and molecular modeling studies discussed above unambiguously indicate that the *N*-phenylisoserine moiety at C-13 is strongly self-organized in each solvent examined. In CD<sub>2</sub>Cl<sub>2</sub> (or CDCl<sub>3</sub>), it is obvious that intramolecular hydrogen bondings are responsible for the strong self-organization, which is virtually not affected by temperature. On the contrary, various intermolecular interactions, e.g., solvation including hydrogen bondings between the solvent molecules and paclitaxel (or its analogs) and aggregation should play a significant role at lower temperatures in protic solvents. The fact that the Conformer B (or structure B) is predominant at lower temperature suggests that this conformation is susceptible to those intermolecular interactions. Along the same line, the fact that the contribution of the Conformer C becomes predominant at higher temperatures indicates that this conformation holds strong intramolecular hydrogen bondings and/or hydrophobic clustering in protic solvents.

The "fluorine probe" approach has been proved to be very useful for the conformational analysis of paclitaxel and its analogs in connection with possible bioactive conformations. Further studies along this line are actively underway. A future challenge will be to use a paclitaxel analog with triple fluorine-label at all three phenyl groups and determine the distances between these three fluorines, probably by solid state NMR, when the fluorine probe binds to the  $\beta$ -tubulin of microtubules.

**Acknowledgments.** This research was supported by grants from the National Institutes of Health (GM417980 to I.O., and CA13038 to R.J.B.), Rhône-Poulenc Rorer (to I.O.), and the Centre National de la Recherche Scientifique (to J.P.B. and D.B.D.). A generous support from Indena, SpA (to I.O.) is also gratefully acknowledged. The authors would like to thank Dr. Ezio Bombardelli, Indena, SpA for providing them with 14 $\beta$ -OH-DAB. Two of the authors (S.D.K. and J.C.S.) would like to thank the U.S. Department of Education for GAANN fellowships.

## Literature Cited

1. *Taxane Anticancer Agents: Basic Science and Current Status*; Georg, G. I.; Chen, T. T.; Ojima, I.; Vyas, D. M., Ed.; American Chemical Society: Washington D.C., 1995.
2. Suffness, M. In *Annual Reports in Medicinal Chemistry*; J. A. Bristol, Ed.; Academic Press: San Diego, 1993; Vol. 28; Chapter 32, pp 305-314.
3. Suffness, M. *Taxol: Science and Applications*; CRC Press: New York, 1995.
4. Guénard, D.; Guéritte-Vogelein, F.; Potier, P., *Acc. Chem. Res.* **1993**, *26*, 160-167.
5. Ravdin, P. M. In *Stony Brook Symposium on Taxol and Taxotère*; Stony Brook, NY, May 14-15, 1993; pp Abstracts p. 18.
6. Verweij, J.; Clavel, M.; Chevalier, B., *Ann. Oncol.* **1994**, *5*, 495-505.
7. Ojima, I.; Duclos, O.; Kuduk, S. D.; Sun, C.-M.; Slater, J. C.; Lavelle, F.; Veith, J. M.; Bernacki, R. J., *BioMed. Chem. Lett.* **1994**, *4*, 2631.
8. Ojima, I.; Park, Y. H.; Sun, C.-M.; Fenoglio, I.; Appendino, G.; Pera, P.; Bernacki, R. J., *J. Med. Chem.* **1994**, *37*, 1408.
9. Ojima, I.; Fenoglio, I.; Park, Y. H.; Pera, P.; Bernacki, R. J., *BioMed. Chem. Lett.* **1994**, *4*, 1571-1576.

10. Ojima, I.; Fenoglio, I.; Park, Y. H.; Sun, C.-M.; Appendino, G.; Pera, P.; Bernacki, R. J., *J. Org. Chem.* **1994**, *59*, 515-517.
11. Ojima, I.; Duclos, O.; Zucco, M.; Bissery, M.-C.; Combeau, C.; Vrignaud, P.; Riou, J. F.; Lavelle, F., *J. Med. Chem.* **1994**, *37*, 2602-2608.
12. Ojima, I.; Park, Y. H.; Fenoglio, I.; Duclos, O.; Sun, C.-M.; Kuduk, S. D.; Zucco, M.; Appendino, G.; Pera, P.; Veith, J. M.; Bernacki, R. J.; Bissery, M.-C.; Combeau, C.; Vrignaud, P.; Riou, J. F.; Lavelle, F. In *Taxane Anticancer Agents: Basic Science and Current Status*; G. I. Georg; T. T. Chen; I. Ojima and D. M. Vyas, Ed.; ACS Symp. Series 583; American Chemical Society: Washington, D. C., 1995; pp 262-275.
13. Georg, G. I., 3'-N-(4-Azido-2,3,5,6-tetrafluorobenzoyl)paclitaxel and 7-(4-Azido-2,3,5,6-tetrafluorobenzoyl)paclitaxel have been synthesized as potential photoaffinity labels. See Ref. 14.
14. Georg, G. I.; Harriman, G. C. B.; Park, H.; Himes, R. H., *BioMed. Chem. Lett.* **1994**, *4*, 487-490.
15. Chen, S.-H., For the incorporation of fluorine to the baccatin moiety, see Refs. 16 and 17.
16. Chen, S. H.; Kant, J.; Mamber, S. W.; Roth, G. P.; Wei, J.; Marshall, D.; Vyas, D.; Farina, V., *BioMed. Chem. Lett.* **1994**, *4*, 2223-2228.
17. Chen, S. H.; Farina, V. In *Taxane Anticancer Agents: Basic Science and Current Status*; G. I. Georg; T. T. Chen; I. Ojima and D. M. Vyas, Ed.; ACS Symp. Series 583; American Chemical Society: Washington D.C., 1995; pp 247-261.
18. Vander Velde, D. G.; Georg, G. I.; Grunewald, G. L.; Gunn, C. W.; Mitscher, L. A., *J. Am. Chem. Soc.* **1993**, *115*, 11650-11651.
19. Georg, G. I.; Harriman, G. C. B.; Vander Velde, D. G.; Boge, T. C.; Cheruvallath, Z. S.; Datta, A.; Hepperle, M.; Park, H.; Himes, R. H.; Jayasinghe, L. In *Taxane Anticancer Agents: Basic Science and Current Status*; G. I. Georg; T. T. Chen; I. Ojima and D. M. Vyas, Ed.; ACS Symp. Series 583; American Chemical Society: Washington D.C., 1995; pp 217-232.
20. Vuilhorgne, M.; Gaillard, C.; Sanderlink, G. J.; Royer, I.; Monsarrat, B.; Dubois, J.; Wright, M. In *Taxane Anticancer Agents: Basic Science and Current Status*; G. I. Georg; T. T. Chen; I. Ojima and D. M. Vyas, Ed.; ACS Symp. Series 583; American Chemical Society: Washington D. C., 1995; pp 98-110.
21. Monsarrat, B.; Mariel, E.; Cros, S.; Garès, M.; Guénard, D.; Guéritte-Voegelein, F.; Wright, M., *Drug Metab. Dispos.* **1990**, *18*, 895.
22. *Organofluorine Compounds in Medicinal Chemistry and Biomedical Applications*; Filler, R.; Kobayashi, Y.; Yagupolskii, L. M., Ed.; Elsevier: Amsterdam, 1993; Vol. 48.
23. Kukhar, V. P.; Soloshonok, V. A. *Fluorine-containing Amino Acids: Synthesis and Properties*; John Wiley & Sons: Chichester, 1995.
24. Ojima, I.; Kuduk, S. D.; Slater, J. C.; Gimi, R. H.; Sun, C. M., *Tetrahedron* **1996**, *52*, 209-224.
25. Compound **1** was independently synthesized by Georg et al. (see Ref. 26) and assayed against B16 melanoma cell line:  $ED_{50}/ED_{50(\text{paclitaxel})} = 1.2$ .
26. Georg, G. I.; Cheruvallath, Z. S.; Harriman, G. C. B.; Hepperle, M.; Park, H.; Himes, R. H., *BioMed. Chem. Lett.* **1994**, *4*, 2331.
27. Compound **3** was also independently synthesized by Commerçon et al. (see Refs. 28 and 29) and assayed against P388 leukemia cell line ( $IC_{50}/IC_{50(\text{docetaxel})} = 0.75$ ) and B16 melanoma *in vivo* ( $ED_{50}/ED_{50(\text{docetaxel})} = 1.49$ ; %T/C = 6; log cell kill 3.2) (see Ref. 28).
28. Commerçon, A.; Bourzat, J. D.; Didier, E.; Lavelle, F. In *Taxane Anticancer Agents: Basic Science and Current Status*; G. I. Georg; T. T. Chan; I. Ojima and D. M. Vyas, Ed.; American Chemical Society: Washington, D. C., 1995; pp 233-246.

29. Commerçon, A.; Bezar, D.; Bernard, F.; Bourzat, J. D., *Tetrahedron Lett.* **1992**, 33, 5185-5188.
30. Ojima, I. In *Advances in Asymmetric Synthesis*; A. Hassner, Ed.; JAI Press: Greenwich, 1995; Vol. 1; pp 95-146.
31. Ojima, I. In *The Organic Chemistry of  $\beta$ -Lactam Antibiotics*; G. I. Georg, Ed.; VCH Publishers: New York, 1992; pp 197-255.
32. Ojima, I., *Acc. Chem. Res.* **1995**, 28, 383-389.
33. Holton, R. A.; Biediger, R. J.; Boatman, P. D. In *Taxol@: Science and Applications*; M. Suffness, Ed.; CRC Press: New York, 1995; pp 97-121.
34. Georg, G. I.; Cheruvallath, Z. S.; Himes, R. H.; Mejillano, M. R.; Burke, C. T., *J. Med. Chem.* **1992**, 35, 4230-4237.
35. Ojima, I.; Habus, I.; Zhao, M.; Zucco, M.; Park, Y. H.; Sun, C. M.; Brigaud, T., *Tetrahedron* **1992**, 48, 6985-7012.
36. Ojima, I.; Sun, C. M.; Zucco, M.; Park, Y. H.; Duclos, O.; Kuduk, S. D., *Tetrahedron Lett.* **1993**, 34, 4149-4152.
37. Ojima, I.; Zucco, M.; Duclos, O.; Kuduk, S. D.; Sun, C. M.; Park, Y. H., *BioMed. Chem. Lett.* **1993**, 3, 2479-2482.
38. Ojima, I.; Habus, I.; Zhao, M.; Georg, G. I.; Jayasinghe, R., *J. Org. Chem.* **1991**, 56, 1681-1684.
39. Appendino, G.; Gariboldi, P.; Gabetta, B.; Pace, R.; Bombardelli, E.; Viterbo, D., *J. Chem. Soc., Perkins Trans 1* **1992**, 2925-2929.
40. Holton, R. A.; Biediger, R. J., *U.S. Patent* **1993**, 5,243,045.
41. Skehan, P.; Streng, R.; Scudierok, D.; Monks, A.; McMahon, J.; Vistica, D.; Warren, J. T.; Bokesch, H.; Kenney, S.; Boyd, M. R., *J. Nat. Cancer Inst.* **1990**, 82, 1107-1112.
42. Ali, S. M.; Hoemann, M. Z.; Aube, J.; Mitscher, L. A.; Georg, G. I.; McCall, R.; Jayasinghe, L. R., *J. Med. Chem.* **1995**, 38, 3821-3828.
43. Rao, S.; Horwitz, S. B.; Ringel, I., *J. Natl. Cancer Inst.* **1992**, 84, 785-788.
44. Rao, S.; Krauss, N. E.; Heerding, J. M.; Swindell, C. S.; Ringel, I.; Orr, G. A.; Horwitz, S. B., *J. Biol. Chem.* **1994**, 269, 3132-3134.
45. Dasgupta, D.; Park, H.; Harriman, G. C. B.; Georg, G. I.; Himes, R. H., *J. Med. Chem.* **1994**, 37, 2976-2980.
46. Ojima, I.; Duclos, O.; Dormán, G.; Simonot, B.; Prestwich, G. D.; Rao, S.; Lerro, K. A.; Horwitz, S. B., *J. Med. Chem.* **1995**, 38, 3891-3894.
47. Williams, H. J.; Scott, A. I.; Dieden, R. A.; Swindell, C. S.; Chirlian, L. E.; Franci, M. M.; Heerding, J. M.; Krauss, N. E., *Can. J. Chem.* **1994**, 252-260.
48. Williams, H. J.; Scott, A. I.; Dieden, R. A.; Swindell, C. S.; Chirlian, L. E.; Franci, M. M.; Heerding, J. M.; Krauss, N. E., *Tetrahedron* **1993**, 49, 6545-6560.
49. Dubois, J.; Guénard, D.; Guéritte-Voegelein, F.; Guedira, N.; Potier, P.; Gillet, B.; Beloeil, J.-C., *Tetrahedron* **1993**, 49, 6533-6544.
50. Boge, T. C.; Himes, R. H.; Vander Velde, D. G.; Georg, G. I., *J. Med. Chem.* **1994**, 37, 3337-3343.
51. Chmurny, G. N.; Hilton, B. D.; Brobst, S.; Look, S. A.; Witherup, K. M.; Beutler, J. A., *J. Nat. Prod.* **1992**, 54, 416-423.
52. Hilton, B. D.; Chmurny, G. N.; Muschik, G. M., *J. Nat. Prod.* **1992**, 55, 1157-1161.
53. Baker, J. K., *Spectroscopy Lett.* **1992**, 25, 31-48.
54. Falzone, C. J.; Benesi, A. J.; Lecomte, J. T., *Tetrahedron Lett.* **1992**, 33, 1169-1172.
55. Guéritte-Voegelein, F.; Mangatal, L.; Guénard, D.; Potier, P.; Guilhem, J.; Cesario, M.; Pascard, C., *Acta Crystallogr.* **1990**, C46, 781-784.
56. Mastropaolo, D.; Camerman, A.; Luo, Y.; Brayer, G. D.; Camerman, N., *Proc. Natl. Acad. Sci. USA* **1995**, 92, 6920-6924.
57. Georg, G. I., For a comprehensive review on the conformational studies on paclitaxel and docetaxel, see Ref. 58.

58. Georg, G. I.; Boge, T. C.; Cheruvallath, Z. S.; Clowers, J. S.; Harriman, G. C. B.; Hepperle, M.; Park, H. In *Taxol<sup>®</sup>: Science and Applications*; M. Suffness, Ed.; CRC Press: New York, 1995; pp 317-375.
59. Cachau, R. E.; Gussio, R.; Beutler, J. A.; Chmurny, G. N.; Hilton, B. D.; Muschik, G. M.; Erickson, J. W., *Int. J. Supercomput. Appl.* **1994**, *8*, 24-34.
60. Wiley, R. A.; Rich, D. H., *Med. Res. Rev.* **1993**, *3*, 327-384.
61. Vander Velde et al. claimed that NMR study in DMSO-D<sub>2</sub>O (3:1) could be performed at -20 °C (see Ref. 18), but we did not have any luck in keeping the solution from freezing below 0 °C although we were able to obtain clean NMR spectra in glassy state at -20 °C.
62. Paloma, L. G.; Guy, R. K.; Wrasidlo, W.; Nicolaou, K. C., *Chem. Biol.* **1994**, *2*, 107-112.
63. Ojima, I.; Kuduk, S. D.; Chakravarty, S.; Ourevitch, M., Unpublished results.

## Chapter 18

# Design of a Fluoro-olefin Cytidine Nucleoside as a Bioprecursor of a Mechanism-Based Inhibitor of Ribonucleotide Reductase

James R. McCarthy<sup>1,3</sup>, Prasad S. Sunkara<sup>1,3</sup>, Donald P. Matthews<sup>1,4</sup>, Alan J. Bitonti<sup>1</sup>, Esa T. Jarvi<sup>1</sup>, Jeffrey S. Sabol<sup>1</sup>, Robert J. Resvick<sup>1</sup>, Edward W. Huber<sup>1</sup>, Wilfred A. van der Donk<sup>2</sup>, Guixue Yu<sup>2</sup>, and JoAnne Stubbe<sup>2</sup>

<sup>1</sup>Hoechst Marion Roussel, Inc., 2110 East Galbraith Road, Cincinnati, OH 45215

<sup>2</sup>Departments of Chemistry and Biology, Massachusetts Institute of Technology, Cambridge, MA 02139

MDL 101,731 (**3**) is a fluoro olefin cytidine nucleoside designed as a bioprecursor of a mechanism-based inhibitor of ribonucleotide diphosphate reductase (RDPR) targeted for the treatment of tumors. The rationale for the use of a fluoro olefin in the design of **3** are discussed. A new stereospecific method to fluoro olefins was developed as a key step in the synthesis of MDL 101,731. Studies showing inactivation of both the R1 and R2 subunits of RDPR from *E. coli* by the diphosphate of MDL 101,731 are presented, and a proposed mechanism for the process is discussed. In addition, the antitumor profile of the drug is outlined. MDL 101,731 has recently entered clinical trials for the treatment of solid tumors in the US and Japan.

Ribonucleotide diphosphate reductases (RDPRs) catalyze the rate determining step in DNA biosynthesis, i.e. the conversion of nucleotides (NDPs) into the corresponding deoxynucleotides (dNDPs)(1-3). The *E. coli* RDPR is composed of two homodimeric subunits R1 and R2, and serves as the prototype of the mammalian enzyme. R1 contains the active site for the reduction of both purine and pyrimidine substrates, additional binding sites for nucleoside triphosphates that allosterically control both the reactivity and the selectivity of the enzyme (1), and five cysteines that are required for catalysis (4). R2 contains the essential tyrosyl radical-diferric cluster cofactor (5) which is thought to generate a thiyl radical in the active site on the R1 subunit by a series of coupled electron and proton transfers (2).

<sup>3</sup>Current address: Department of Medicinal Chemistry, Neurocrine Biosciences, Inc., 3050 Science Park Road, San Diego, CA 92121-1102

<sup>4</sup>Current address: Lilly Research Laboratories, Eli Lilly and Company, Indianapolis, IN 46285

0097-6156/96/0639-0246\$15.00/0  
© 1996 American Chemical Society

The central role of RDPRs in metabolism have made them attractive targets for the design of inhibitors with potential use as anti-tumor or anti-viral agents. In this chapter we describe the synthesis of a novel nucleoside analog, MDL 101,731 (3), designed as a bioprecursor of a mechanism-based inhibitor of RDPR. *In vivo* studies with MDL 101,731 indicate potent antiproliferative activity against a wide variety of tumor cell lines, and *in vitro* studies with the corresponding nucleoside diphosphate show this compound to be a potent inactivator of RDPR from *E. coli*.

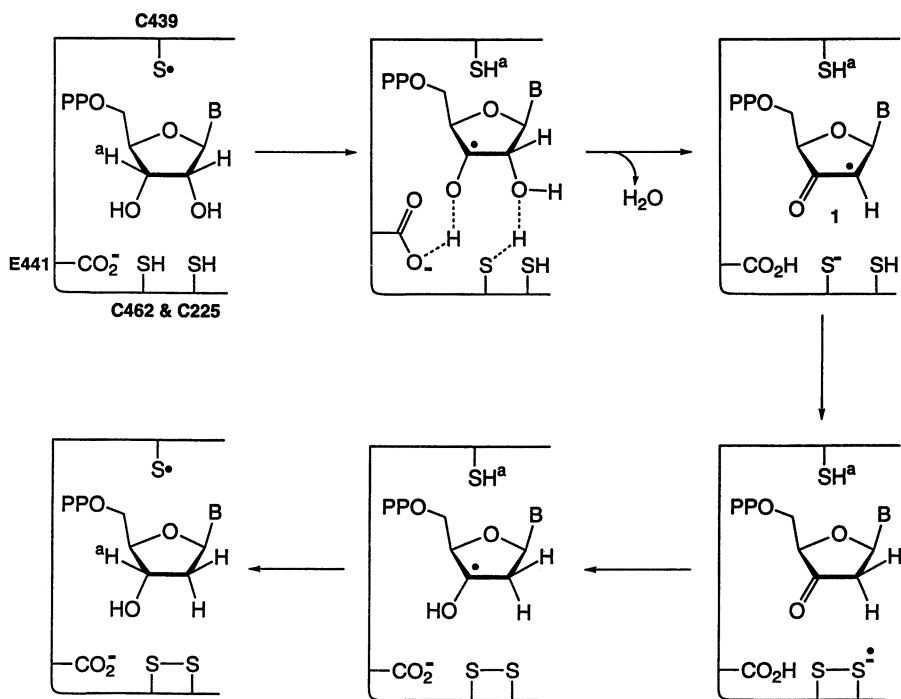
### Mechanisms of Nucleotide Reduction and RDPR Inhibition

A detailed understanding of the mechanism of nucleotide reduction by RDPRs is essential for the successful design of selective and potent inhibitors. Over the past decade extensive biochemical (2), molecular biological (4,6) and crystallographic studies (7,8) have provided strong support for a model for nucleotide reduction first proposed by Stubbe and coworkers in 1990 (Scheme 1) (2). Catalysis is initiated by hydrogen atom abstraction from the 3' position of the substrate by the thiyl radical on Cys439 of R1 generated from the tyrosyl radical on the R2 subunit (9). After elimination of the 2'-hydroxyl group as water, reduction of the intermediate  $\alpha$ -keto radical 1 occurs by oxidation of cysteines 225 and 462 to the corresponding disulfide. Reabstraction of the originally removed hydrogen atom from Cys439 by the 3'-deoxynucleotide radical then produces the product and regenerates the thiyl radical on Cys439. As described subsequently, this proposed model for nucleotide reduction and the results obtained in previous studies with RDPR inactivators served as the basis for the design of MDL 101,731 as a potential bioprecursor for a mechanism based inhibitor of RDPR.

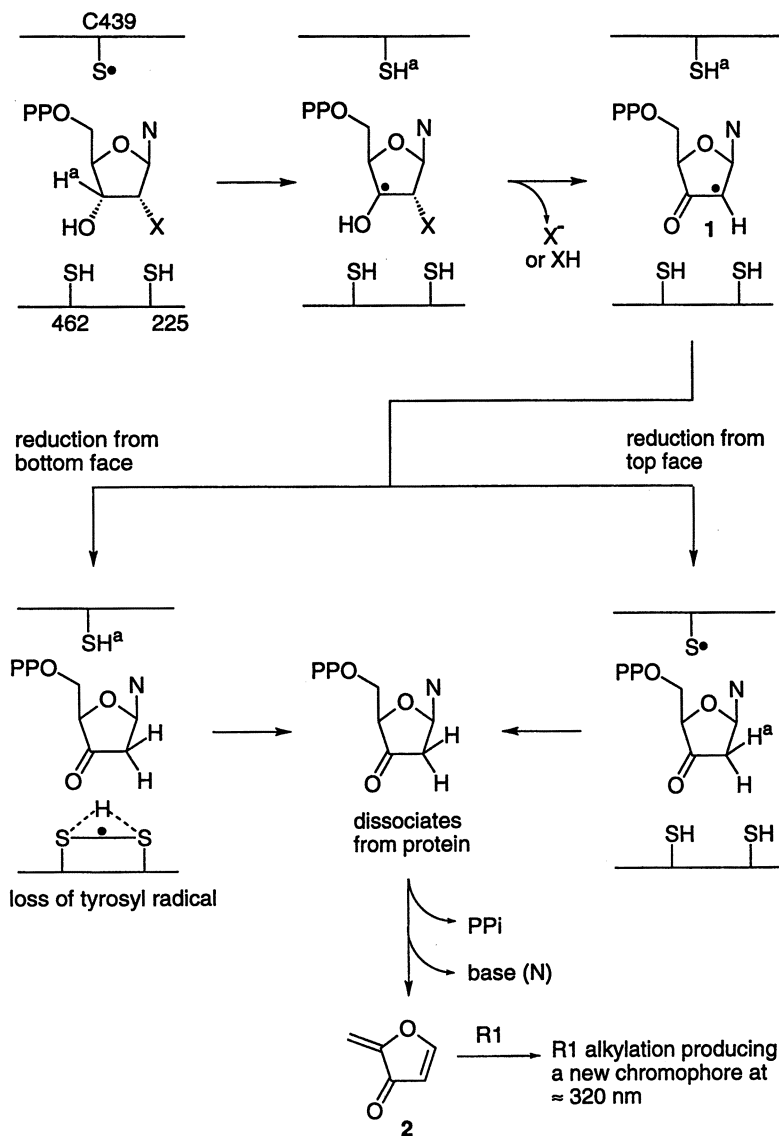
Several strategies for RDPR inactivation have been previously reported (10,11). Hydroxyurea abolishes enzyme activity by reduction of the essential tyrosyl radical on the R2 subunit (12). This compound has shown clinical utility in the treatment of leukemia and malignant melanoma, but suffers from the disadvantage that relatively high concentrations are required. Thiosemicarbazones such as 2-pyridinecarboxaldehyde thiosemicarbazone comprise another class of inhibitors targeting the tyrosyl radical (13,14). A different approach has been reported for the inhibition of RDPR from herpes simplex virus, focusing on the disruption of subunit interaction. Two groups independently showed that a nonapeptide corresponding to the C-terminal residues of the R2 subunit serves as a potent inhibitor of the viral reductase by competing with R2 for binding to the R1 subunit (15-17).

A third class of inactivators involve nucleotide analogs as mechanism based inhibitors. The first such compounds, 2'-chloro-2'-deoxycytidine 5'-diphosphate (ClCDP) and 2'-azido-2'-deoxycytidine 5'-diphosphate (N<sub>3</sub>CDP), were reported in 1976 by Thelander and Eckstein and their coworkers (18). Subsequent studies have revealed the details of the mechanism by which these compounds (and their uridine analogs) inactivate RDPR from *E. coli* (2). For both compounds, chemistry is initiated by homolytic cleavage of the 3' carbon-hydrogen bond by the thiyl radical at Cys439 (Scheme 2). The substituent at the 2'-position is then eliminated as X<sup>-</sup> or XH generating the same putative  $\alpha$ -keto radical 1 as during normal turn-over. In the case of these inhibitors, however, this intermediate is not converted into product,





Scheme 1. Proposed mechanism for nucleotide reduction by RDPRs. (Adapted from reference 11).



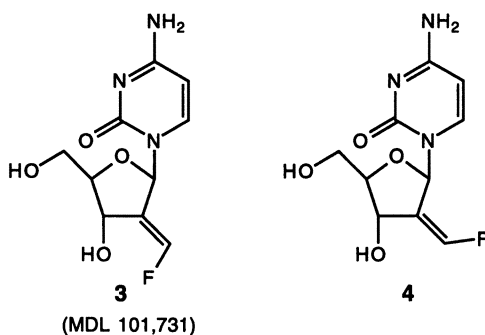
Scheme 2. Mechanism of inhibition of a RDPR by a nucleotide analog. (Adapted from reference 11).

presumably because of a distorted geometry of the active site (19) or a subtle change in protonation state of the thiols in the active site (compare Schemes 1 and 2). Instead this radical is reduced by hydrogen abstraction from one of the cysteines in the active site. When this abstraction occurs from the  $\alpha$ -face (bottom) of the ribose involving either Cys225 or Cys462, the protein loses the ability to regenerate the tyrosyl radical causing inactivation (Scheme 2). Alternatively, the intermediate  $\alpha$ -keto radical can be reduced by Cys439, regenerating the thiyl radical and thus the tyrosyl radical. The 3'-keto-2'-deoxynucleotide intermediate formed can then dissociate from the active site and decompose in solution by elimination of free nucleic acid base N (Scheme 2) and pyrophosphate. This produces the highly electrophilic furanone species **2** which is trapped by nucleophilic residues on the R1 subunit inactivating it and giving rise to a distinctive new chromophore at 320 nm. While the former pathway is the predominant mode of inactivation with N<sub>3</sub>UDP (19-22) and the latter of inhibition by CIUDP (23-25), with most mechanism-based inhibitors studied to date, inactivation occurs by partitioning between these two pathways.

Recently, 2',2'-difluoro-2'-deoxycytidine (gemcitabine) was reported to be a bioprecursor to a mechanism-based inhibitor of RDPR (26). At present, the mechanism of its action is not well understood. This compound is currently undergoing registration review of Phase III clinical trials for treatment of non-small cell lung and pancreatic cancer (27).

### Design of a Novel Inhibitor of RDPR

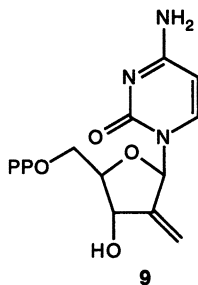
(*E*)- and (*Z*)-2'-Fluoromethylene-2'-deoxycytidine (**3** and **4**, respectively) were designed as bioprecursors of mechanism-based inhibitors of RDPR based on the



proposed mechanisms of substrate reduction and enzyme inactivation by substrate analogs (Schemes 1 and 2) (28). A cytosine based nucleoside analog was selected because it has been shown that deoxycytidine kinase exhibits broad substrate specificity for the conversion of cytosine analogs to their corresponding 5'-monophosphates (29). The fluoride moiety of the molecule was incorporated as a potential leaving group, anticipating that conversion of these compounds by RDPR would also be initiated by 3'-hydrogen atom abstraction. Two possible modes of

inactivation were envisioned (Scheme 3). The fluoroallyl radical produced in the first step would be expected to abstract a hydrogen atom from one of the cysteines in the active site. The enol produced could then generate the reactive species **7** or **8** by elimination of fluoride or cytosine, respectively. Unlike the case of CIUDP in which the electrophile **2** is generated relatively slowly in solution, the  $\alpha,\beta$ -unsaturated compounds **7** and **8** would be formed inside the active site of the enzyme, and would be expected to efficiently and stoichiometrically react with an active site residue leading to rapid enzyme inhibition.

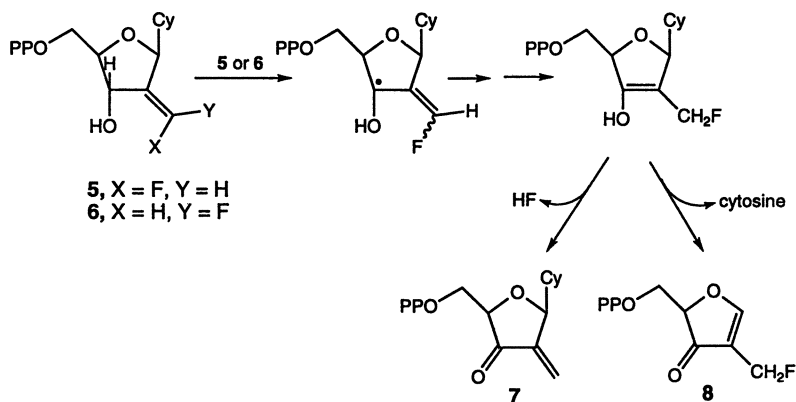
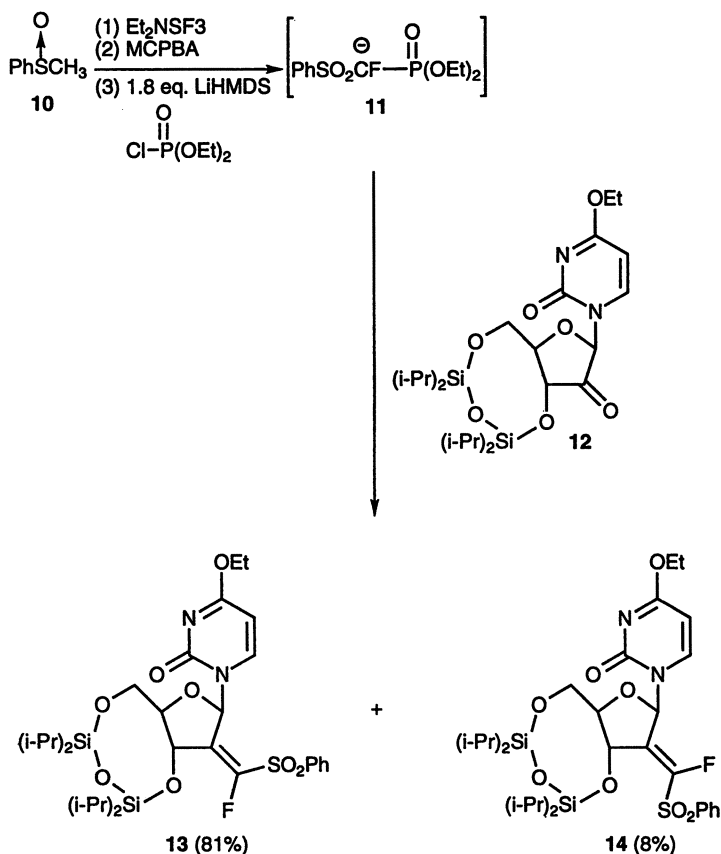
A major issue that was addressed before the decision to proceed with the synthesis of the **3** and **4** was the spatial constraints for a 2'-fluoro olefin functional group on a potential nucleotide substrate (mechanism-based inhibitor) in the active site of the enzyme. Molecular models indicated that the 2'-fluoromethylene group would be accepted by RDPR since 2'-chloro-2'-deoxycytidine 5'-diphosphate is a mechanism-based inhibitor of the enzyme (2). Furthermore, the subsequent disclosure that 2'-methylene-2'-deoxycytidine 5'-diphosphate (**9**) is a mechanism-based inhibitor of RDPR (albeit much less potent) (26) is consistent with our observations made with molecular models.



## Synthesis

The 2'-ketonucleoside **12** (Scheme 4) was chosen as the precursor of the desired fluoro olefin since it provided a convergent route and its synthesis had previously been reported (30). The pivotal step in the synthesis of **3** involves the introduction of the fluoro olefin using the fluoro-Pummerer reaction (31, 32) via the carbanion of diethyl 1-fluoro-1-(phenylsulfonyl)methanephosphonate (**11**) (Scheme 4). This compound was generated starting with methyl phenyl sulfoxide (**10**) and diethylaminosulfur trifluoride (DAST), and oxidation of the intermediate fluoromethyl phenyl sulfide to the sulfone (33, 34). Treatment of the sulfone with one equivalent of diethyl chlorophosphate and 1.8 equivalents of lithium hexamethyldisilazane afforded the carbanion **11**, which was then condensed in situ with 2'-ketonucleoside **12** to provide a 10 to 1 ratio of the (*Z*) and (*E*) isomers of the fluorovinyl sulfones **13** and **14**, respectively.

The step in the proposed reaction sequence that we assumed would proceed smoothly was the reductive removal of the vinyl sulfone with amalgamated aluminum (34, 35). However, this reaction gave multicomponent mixtures as determined by

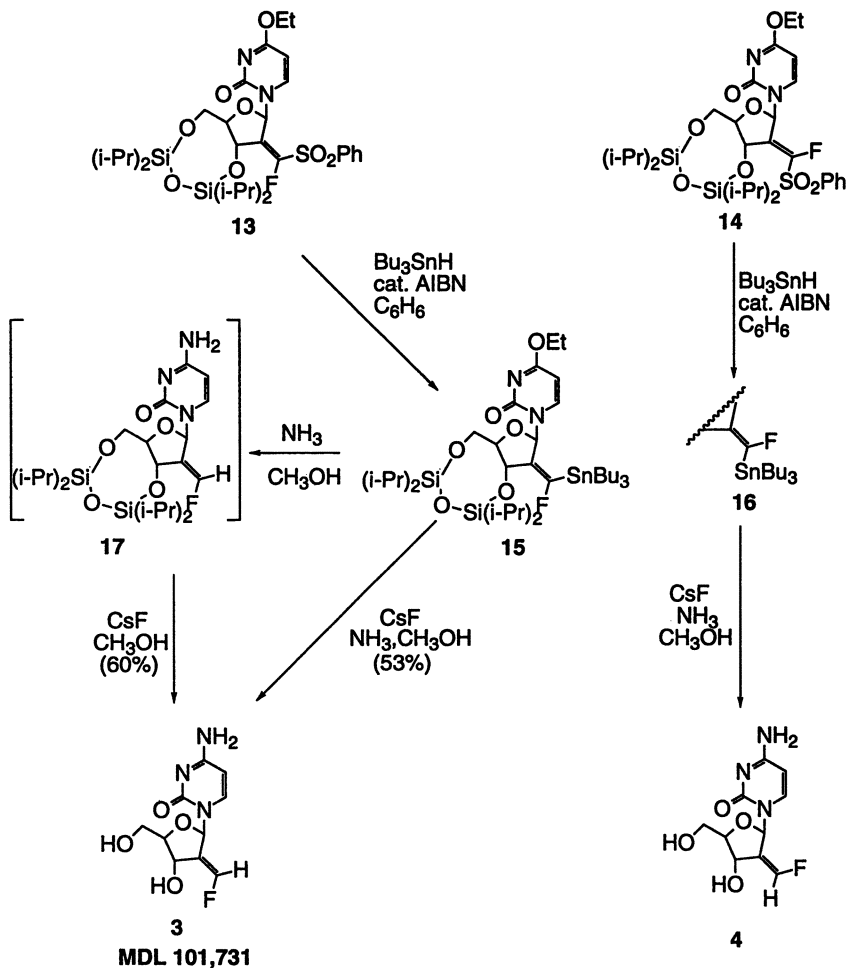
Scheme 3. Proposed mechanism for inactivation of RDPR by **5** and **6**.Scheme 4. Synthesis of **13** and **14**.

thin layer chromatography. This unexpected result required us to develop a new method for stereospecific conversion of sulfones to the corresponding fluoro olefins.

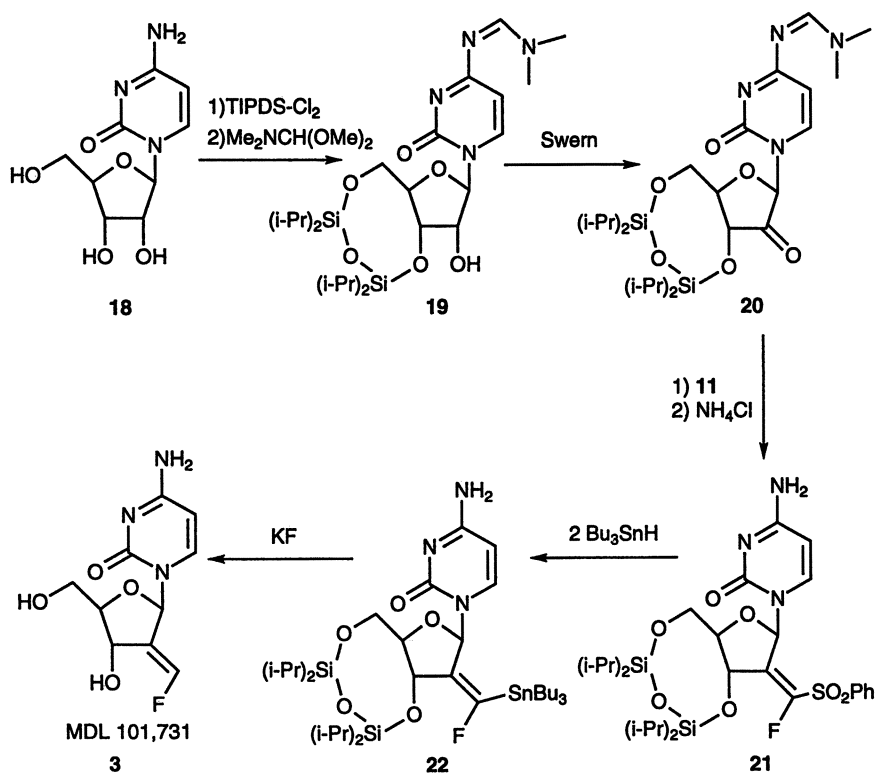
The reaction sequence for this new route to fluoro olefins is outlined in Scheme 5. Fluorovinyl sulfone **13** was transformed to (fluorovinyl)stannane **15** by treatment with two equivalents of tributyltin hydride (Scheme 5). In addition, sulfone **14** formed stannane **16** exclusively. Watanabe and coworkers were the first to observe the conversion of vinyl sulfones to mixtures of (*E*)- and (*Z*)-vinylstannanes on treatment with two equivalents of tributyltin hydride (*36*). An electron-transfer mechanism consistent with the formation of mixtures of (*E*)- and (*Z*)-vinylstannanes was proposed. However, 2,2-disubstituted vinyl sulfones were not studied by this group, and 2-monosubstituted fluorovinyl sulfones formed mixtures of (*E*)- and (*Z*)-(fluorovinyl)stannanes. On the basis of these observations, we proposed a radical addition-elimination mechanism in which elimination is faster than free rotation resulting in exclusive *cis*-elimination when rotation is restricted. The mechanism is consistent with the retention of configuration of (fluorovinyl)stannanes derived from less constrained 2,2-disubstituted acyclic (*E*)- and (*Z*)-fluorovinyl sulfones (*28*) and is the first report of a stereospecific radical reaction of this kind involving tributyltin hydride.

(*E*)- and (*Z*)-2'-Deoxy-2'-(fluoromethylene)cytidines (**3** and **4**) were obtained as pure geometric isomers by treating **15** and **16**, respectively, with cesium fluoride and methanolic ammonia. Alternately, **15** was treated with methanolic ammonia to provide **17**, which upon treatment with cesium fluoride, yielded **3**. The stereospecific destannylation reaction is also catalyzed by refluxing methanolic sodium methoxide or potassium fluoride. The latter two routes are usually the methods of choice for the destannylation reaction. It should be noted that the geminal fluorine increases the susceptibility of the carbon-tin bond to cleavage. Treatment of the vinylstannane obtained from benzophenone with MeOH/NaOMe for 16 h at reflux resulted in no reaction whereas the fluorinated vinylstannane provided 1,1-diphenyl-2-fluoroethylene in 91% yield (*28*).

An improved synthesis of the (*E*) fluoro olefin **3** was developed and allowed the compound to proceed ahead as a clinical candidate targeted for the treatment of solid tumors. The new synthesis is outlined in Scheme 6. The key aspects of the new synthesis are as follows. The 3'- and 5'-hydroxyl groups of cytidine (**18**) were protected with the 1,1,3,3-tetraisopropyl disiloxane group (TIPDS), and the N-4 amino group was protected as the *N,N*-dimethylamidine by the addition of dimethylformamide dimethyl acetal to the reaction mixture. The bis-protected nucleoside **19** was isolated in high yield as a crystalline solid. The ketone **20**, obtained from the Swern oxidation of **19** was isolated by nonaqueous workup in over 90% yield as white crystals. This ketone was converted to the fluoro olefin **3** (MDL 101,731) by a slight modification of the original synthesis, i.e. potassium fluoride was used to remove both the vinylstannane and the TIPDS protecting group. The fluoro olefin **3** was obtained in an overall yield of 28% in five steps from cytidine (*37*).



Scheme 5. Original synthesis of 3 and 4. (Adapted from reference 28).



Scheme 6. Improved synthesis of 3. (Adapted from reference 37).



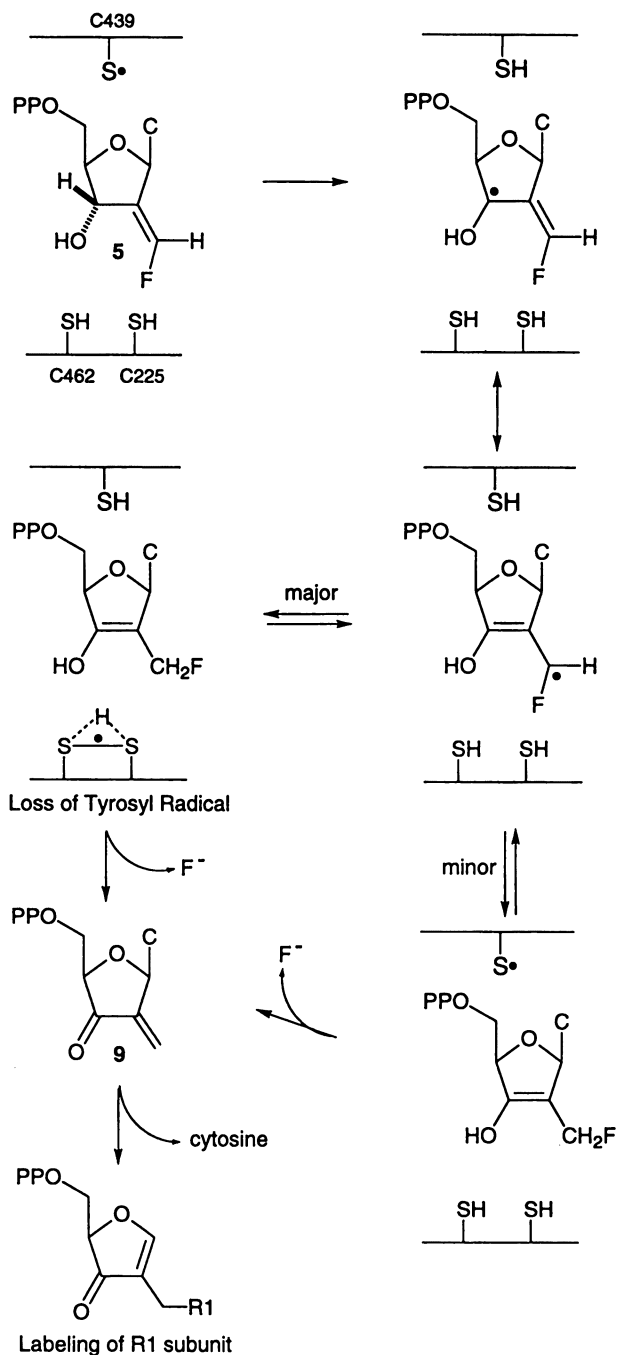
### Enzyme Inhibition and Biological Activity

The diphosphates of MDL 101,731 (**5**) and the geometric isomer (**6**) were potent mechanism-based inhibitors of RDPR (see below). However, MDL 101,731 was substantially more active as an antiproliferative agent against HeLa cells ( $IC_{50} = 58$  nM) than the geometric isomer **4** ( $IC_{50} = 3870$  nM) (*28*). Based on the potent antiproliferative activity of MDL 101,731 and the inhibition of RDPR by the diphosphate, additional enzyme inhibition studies and antitumor studies were performed on the diphosphate of **5**. These studies are summarized below.

**Inhibition of RDPR.** *In vitro* studies with purified RDPR from *E. coli* established that both geometric isomers of the diphosphate of MDL 101,731 are potent mechanism-based inhibitors of this protein. About two equivalents of these compounds were sufficient to abolish all enzymatic activity in a time dependent manner (*38*). The kinetics of inactivation with both inhibitors and under a variety of conditions were multiphasic due to inactivation of both the R1 and R2 subunits, and thus have prevented determination of accurate kinetic parameters. Studies with [ $5\text{-}^3\text{H}$ ]-**5** and [ $6\text{'-}^{14}\text{C}$ ]-**5** (i.e.  $^{14}\text{C}$  label on the fluoromethylene group) revealed that R1 inactivation was due to stoichiometric covalent labeling, and that this label is attached to R1 via the sugar moiety of the inhibitor. The inactivation of R2 resulted from rapid loss of the essential tyrosyl radical. The inactivation process was accompanied by release of 1.4 equivalents of fluoride and 0.5 equivalents of cytosine. A possible mechanism to account for these experimental observations is shown in Scheme 7. Preliminary studies have indicated that these inhibitors are also potent *in vitro* inactivators of mammalian RDPR from mouse.

It is interesting to note that these fluoromethylene nucleotide analogs are more potent inactivators of *E. coli* RDPR than the corresponding non-fluorinated inhibitor 2'-methylene-2'-deoxycytidine 5'-diphosphate (**9**) (*26*). Inhibition studies with this compound showed that about 33 equiv. were necessary to completely inactivate the enzyme (*26*). Furthermore, the inactivation characteristics were much different from those of **5**. No tyrosyl radical loss was observed with **9**, indicating that inactivation with this nucleotide analog results from inhibition of the R1 subunit (*39*).

**Antiproliferative activity of MDL 101,731.** MDL 101,731 showed potent inhibitory activity against the growth of a number of rodent and human tumor cell lines in culture. The  $IC_{50}$  values against various ascites and solid tumor cells ranged from 10-272 nM (Table I). The compound was equipotent against mouse (P388 leukemia,  $IC_{50} = 10\text{-}12$  nM) and human (epidermoid carcinoma,  $IC_{50} = 58\text{-}67$  nM) multidrug resistant and sensitive cell lines. Furthermore, the compound has potent cytotoxic activity against HeLa cells as evidenced by 100% cell kill based on the survival of treated cells in a colony forming assay after 48 h treatment with 195 nM concentration of MDL 101,731 (*40*).



Scheme 7. Proposed mechanism for RDPR inhibition by 5.

**Table I. Antiproliferative Activity Of MDL 101,731 Against Rodent And Human Tumor Cell Lines<sup>a</sup>**

Species	Tumor Cell Line	IC <sub>50</sub> (nM)
Mouse	L1210 Leukemia	26.5
	P388 Leukemia	10.5
	P388 Leukemia (multidrug resistant)	12.0
	B16 melanoma	272
Human	Cervical carcinoma (HeLa)	58.0
	Epidermoid carcinoma( KB)	58.0
	Multi drug resistant epidermoid carcinoma (KBV1)	67.0
	Breast cancer(MCF-7)	17
	Breast cancer (MDA-MB-231)	26
	Breast cancer (MDA-MB-468)	15
	Breast cancer (MDA-MB-435)	15

<sup>a</sup>IC<sub>50</sub> = 50 % inhibitory concentration. This data was abstracted from reference (40).

**Antitumor activity of MDL 101,731 against mouse leukemias.** A dose dependent increase in survival time (% T/C) of L1210 leukemia bearing animals was observed after treatment with MDL 101,731 by intraperitoneal (i.p) or oral route of administration (Table II). A maximum % T/C value of 300 with 20% cures was observed when the leukemia bearing animals were treated with the compound at 10 mg/kg, i.p, once daily from day 1-9. Oral administration of the compound at 10 mg/kg at similar schedule resulted in a % T/C value of 226-251. The optimal dose and schedule was found to be i.p administration of the compound twice daily from day 1-14 resulting in 60-80% cures and an increase in survival time of 400% in the rest of the animals.

The compound also showed significant activity in multidrug resistant P388 leukemia which is resistant to adriamycin and vinblastine, two widely used anticancer drugs (Table II). At a dose of 10 mg/kg of MDL 101,731 an increase in survival time of 200% was observed when administered once daily by i.p, iv and oral routes of administration from day 1-9 after tumor inoculation. The most effective dose and schedule that resulted in cures of 38% and % T/C of 282 was twice daily i.p administration of the compound from day 1-14. These data are significant due to the fact that this tumor is resistant to widely used antitumor drugs.

**Table II. Antitumor Activity of MDL 101,731 Against Mouse Leukemias<sup>a</sup>**

Tumor	Route	Schedule	Dose (mg/kg)	Cures	% T/C
L1210 leukemia	i.p	once daily, day 1-9	5.0		271
	i.p	once daily, day 1-9	10.0	2/10	280 - 314
	i.p	once daily, day 1-9	15.0	1/5	290
	Oral	once daily, day 1-9	5.0		211
	Oral	once daily, day 1-9	10.0		226-251
	Oral	once daily, day 1-9	15.0		271
	i.p	b.i.d, day 1-14	2.0	4/5	443
	i.p	b.i.d, day 1-14	3.0	8/14	408
	Multidrug-resistant P388	i.p	once daily, day 1-9	5.0	
i.p		once daily, day 1-9	10.0	2/10	207
i.v		once daily, day 1-9	10.0		194
Oral		once daily, day 1-9	10.0		200
Oral		once daily, day 1-9	15.0		219
i.p		b.i.d, day 1-9	3.0	1/5	287
i.p		b.i.d, day 1-14	3.0	6/16	282

<sup>a</sup>This data was abstracted from reference (40). Leukemic cells (100,000) / mouse were inoculated i.p on day 0. The compound was dissolved in sterile distilled water and administered as indicated. The survival of the animals was recorded and % T/C was calculated.

$$\% \text{ T/C} = 100 \times \frac{\text{Average days of survival in treated}}{\text{Average days of survival in untreated control}}$$

#### Antitumor activity of MDL 101,731 against rodent and human solid tumors.

The compound showed a dose dependent inhibition of tumor growth ranging from 71-97 % at doses 2.5 -10 mg/kg by i.p administration from day 1-15 day (Table III). MDL 101731 showed dramatic activity against Lewis lung carcinoma as evidenced by 90% of the animals being tumor free and, in the other 10%, a 99% inhibition of tumor growth. Furthermore, at all the doses tested, a total inhibition of metastasis was observed (40).

The compound was also evaluated against drug resistant human epidermoid carcinoma(KBVI) and ovarian carcinoma(HTB-161) in athymic nude mice. At a dose of 10 mg/kg of the compound, administered i.p once daily from day 1-12 resulted in 77-88% inhibition of tumor growth. Tumor regression was also observed by

**Table III. Antitumor Activity Of MDL 101,731 Against Rodent And Human Solid Tumors<sup>a</sup>**

Species	Tumor	Route	Schedule	Dose (mg/kg)	% Inhibition
Mouse	B16 melanoma	i.p.	Once daily, day 1-15	2.5	71
		i.p.	Once daily, day 1-15	5.0	91
		i.p.	Once daily, day 1-15	10.0	97
		Oral	Once daily, day 1-15	30.0	45
	Lewis Lung Carcinoma(3LL)	i.p.	Once daily, day 1-14	10.0	84-100 (5/10 cures)
		i.p.	Once daily, day 1-14	15.0	100 (9/10 cures)
		i.v.	Once daily, day 1-14	10.0	95 (4/5 Cures)
		Oral	Once daily, day 1-14	30.0	88
Human	Ovarian Carcinoma (HTB-161)	i.p.	Once daily, day 1-15	5.0	67
		i.p.	Once daily, day 1-15	10.0	93 (tumor regression)
	Multidrug resistant epidermoid carcinoma (KBV1)	i.p.	Once daily, day 1-15	5.0	62-75
		i.p.	Once daily, day 1-15	10.0	77-88 (tumor regression)

<sup>a</sup>This data was abstracted from reference (40).

following the tumor volume measurements (40). Treatment of established ovarian carcinoma tumor at a dose 5 and 10 mg/kg, once daily from day 1-23 resulted in 67% inhibition at the lower dose and caused tumor regression at the higher dose of 10 mg/kg (40).

**Antitumor activity of MDL 101,731 against human breast tumor xenografts.** Human breast tumor xenografts implanted subcutaneously in nude mice were very sensitive to MDL 101,731 when drug was administered i.p five days/week for 5-6 weeks (Table IV). The estrogen dependent MCF-7 tumor responded with complete regressions in several mice treated with 5.0 mg/kg; lower doses were ineffective. Regressions were observed after approximately three weeks of treatment. MDA-MB-231 tumors were exquisitely sensitive to the effects of MDL 101,731. Complete regression of all tumors was obtained with 1.0, 2.0, and 5.0 mg/kg MDL 101,731. A dose of 0.5 mg/kg MDL 101,731 caused approximately 50% reduction in growth and complete tumoristasis in some mice, but lower doses were without effect. A second estrogen independent tumor, MDA-MB-468, was found to be somewhat less sensitive than MDA-MB-231. While approximately 50% inhibition of growth was obtained using 2.0 and 5.0 mg/kg MDL 101,731, 10 mg/kg gave only 50% tumor regression. No complete regressions were observed. Toxicity on nude mice was generally mild with doses and regimens utilized except for some mice with 10 mg/kg which exhibited some loss of body weight (41).

## Conclusion

MDL 101,731 (3) was designed and synthesized as a bioprecursor of a mechanism-based inhibitor of RDPR. The fluoro olefin incorporated into the 2'-position was the key functional group in the design of the inhibitor. A stereospecific method to terminal fluoro olefins was developed for the synthesis of MDL 101,731. About two equivalents of the diphosphate of MDL 101,731 (5) was sufficient to completely inactivate *E. coli* RDPR in a time dependent manner. RDPR inactivation is due to inhibition of both the R1 and R2 subunits with the release of about 1.4 equivalents of fluoride. MDL 101,731 is a potent antitumor agent against a number of solid tumors including B16 melanoma, Lewis lung carcinoma in mice, human ovarian, epidermoid carcinoma and breast tumor xenografts in athymic nude mice. MDL 101,731 is currently undergoing clinical trials in the US and Japan for the treatment of solid tumors.

## Acknowledgments

We thank Dr. Philippe Bey for his support and interest in this project, Dr. Shujaath Mehdi for early discussions on the enzymology and Dr. Rich Donaldson for his enthusiastic work and collaboration on the process and scale up of MDL 101,731. In addition, we thank Tracey Hill for typing the manuscript.

**Table IV. Antitumor Activity of MDL 101,731 Against Human Breast Tumor Xenografts<sup>a</sup>**

<b>Tumor</b>	<b>Type</b>	<b>Schedule</b>	<b>Dose (mg/kg)</b>	<b>Summary of Effects</b>
MCF-7	Estrogen dependent	daily, 6 weeks	1.0	no growth inhibition
		daily, 6 weeks	2.0	no growth inhibition
		daily, 6 weeks	5.0	significant regression, some complete
MDA-MB-231	Estrogen independent	daily, 5 weeks	0.1	no growth inhibition
		daily, 5 weeks	0.2	no growth inhibition
		daily, 5 weeks	0.5	>50% growth inhibition
		daily, 5 weeks	1.0	complete regression
		daily, 5 weeks	2.0	complete regression
MDA-MB-468	Estrogen independent	daily, 5 weeks	5.0	complete regression
		daily, 6 weeks	2.0	~ 50% growth inhibition
		daily, 6 weeks	5.0	~ 50% growth inhibition
		daily, 6 weeks	10.0	~ 50% growth regression

<sup>a</sup>Tumor pieces were transplanted into nude mice and allowed to grow to approximately 100 mm<sup>3</sup> before drug treatments began. MDL 101,731 was administered intraperitoneally, 5 days/week. This data was abstracted from reference (41).

**Literature Cited**

1. Eriksson, S.; Sjöberg, B. M. in *Allosteric Enzymes*; Hervé, G. Ed.; CRC, Boca Raton, Florida, 1989; pp 189-215.
2. Stubbe, J. *Adv. Enzymol. Relat. Areas Mol. Biol.* **1990**, *63*, 349.
3. Reichard, P. *Science* **1993**, *260*, 1773.
4. Mao, S. S.; Holler, T. P.; Yu, G. X.; Bollinger, J. M.; Booker, S.; Johnston, M. I.; Stubbe, J. *Biochemistry* **1992**, *31*, 9733. General paper with the model of the 5 cysteine residues involved in catalysis
5. Sjöberg, B.-M.; Reichard, P.; Gräslund, A.; Ehrenberg, A. *J. Biol. Chem.* **1977**, *252*, 536.
6. Åberg, A.; Hahne, S.; Karlsson, M.; Larsson, Å.; Ormö, M.; Åhgren, A.; Sjöberg, B. M. *J. Biol. Chem.* **1989**, *264*, 2249.
7. Nordlund, P.; Eklund, H. *J. Mol. Biol.* **1993**, *232*,
8. Uhlin, U.; Eklund, H. *Nature* **1994**, *370*, 533-539.
9. Mao, S. S.; Yu, G. X.; Chalfoun, D.; Stubbe, J. *Biochemistry* **1992**, *31*, 9752-9759. Evidence suggesting that C439 may be the R1 protein radical responsible for initiating catalysis
10. Cory, J. G.; Cory, A. H. Ed., In *Inhibitors of Ribonucleotide Diphosphate Reductase Activity*, Pergamon Press: New York, 1989.
11. Stubbe, J.; van der Donk, W. A. *Chem. & Biol.* **1995**, *2*, 793-801.
12. Moore, E. C.; Hurlbert, R. B. in *Inhibitors of Ribonucleotide Diphosphate Reductase Activity*; Cory, J. G. Cory, A. H. Eds.; Pergamon Press, New York, 1989; pp 165-202.
13. Moore, E. C.; Sartorelli, A. C. in *Inhibitors of Ribonucleoside Diphosphate Reductase Activity*; J.G., C. Cory, A. H. Ed.; Pergamon Press, New York, 1989; pp 203.
14. Blumenkopf, T. A.; Harrington, J. A.; Koble, C. S.; Bankston, D. D.; Morrison Jr., R. W.; Bigham, E. C.; Styles, V. L.; Spector, T. *J. Med. Chem.* **1992**, *35*, 2306.
15. Dutia, B. M.; Frame, M. C.; Subak-Sharpe, J. H.; Clark, W. N.; Marsden, H. S. *Nature* **1986**, *321*, 439.
16. Cohen, E. A.; Gaudreau, P.; Brazeau, P.; Langelier, Y. *Nature* **1986**, *321*, 441.
17. Liuzzi, M.; Déziel, R.; Moss, N.; Beaulieu, P.; Bonneau, A.; Bousquet, C.; Chafouleas, J. G.; Garneau, M.; Jaramillo, J.; Krogsrud, R. L.; Lagacé, L.; McCollum, R. L.; Nawoot, S.; Guindan, Y. *Nature* **1994**, *372*, 695.
18. Thelander, L.; Larsson, B.; Hobbs, J.; Eckstein, F. *J. Biol. Chem.* **1976**, *251*, 1398.
19. van der Donk, W. A.; Stubbe, J.; Gerfen, G. J.; Bellew, B. F.; Griffin, R. G. *J. Am. Chem. Soc.* **1995**, *117*, 8908-8916.
20. Sjöberg, B.-M.; Gräslund, A.; Eckstein, F. *J. Biol. Chem.* **1983**, *258*, 8060.
21. Ator, M.; Salowe, S. P.; Stubbe, J.; Emptage, M. H.; Robins, M. J. *J. Am. Chem. Soc.* **1984**, *106*, 1886.
22. Salowe, S. P.; Ator, M.; Stubbe, J. *Biochemistry* **1987**, *26*, 3408.



23. Stubbe, J.; Kozarich, J. W. *J. Am. Chem. Soc.* **1980**, *102*, 2505.
24. Harris, G.; Ator, M.; Stubbe, J. *Biochemistry* **1984**, *23*, 5214.
25. Ator, M. A.; Stubbe, J. *Biochemistry* **1985**, *24*, 7214.
26. Baker, C. H.; Banzon, J.; Bollinger, J. M., Jr; Stubbe, J.; Samano, V.; Robins, M. J.; Lippert, B.; Jarvi, E.; Resvick, R. *J. Med. Chem.* **1991**, *34*, 1879-1884.
27. Hertel, L.W.; Krsin, J.S.; Grossman, C.S.; Duor, A.F.; Stornovlo, A.M.V.; Plunkett, W.; Gandhi, V.; Huang, P. accompanying chapter.
28. McCarthy, J. R.; Matthews, D. P.; Stemerick, D. M.; Huber, E. W.; Bey, P.; Lippert, B. J.; Snyder, R. D.; Sunkara, P. S. *J. Am. Chem. Soc.* **1991**, *113*, 7439.
29. Eriksson, S.; Kierdaszuk, B.; Munch-Petersen, B.; Oberg, B.; Johansson, N. G. *Biochem. Biophys. Res. Commun.* **1991**, *176*, 586.
30. Matsuda, A.; Itoh, H.; Takenuki, K.; Susaki, T.; Ueda, T. *Chem. Pharm. Bull.* **1988**, *36*, 945.
31. McCarthy, J.R.; Peet, N.P.; LeTourneau, M.E.; Inbasekaran, M. *J. Am. Chem. Soc.*, **1985**, *107*, 735.
32. Robins, M.J.; Wnuk, S.F. *Tetrahedron Lett.*, **1988**, *29*, 5729.
33. McCarthy, J.R.; Matthews, D.P.; Paolini, J.P. *Org. Synth.*, **1993**, *72*, 209.
34. Inbasekaran, M.; Peet, N.P.; McCarthy, J.R.; LeTourneau, M.E. *J. Chem. Soc. Chem. Commun.*, **1985**, 678.
35. McCarthy, J.R.; Matthews, D.P.; Edwards, M.L.; Stemerick, D.M.; Jarvi, E.T. *Tetrahedron Lett.*, **1990**, *31*, 5449.
36. Watanabe, Y.; Ueno, Y.; Araki, T.; Endo, T.; Okawara, M. *Tetrahedron Lett.*, **1986**, *27*, 215.
37. Matthews, D.P.; Persichetti, R.A.; Sabol, J.S.; Stewart, N.T.; McCarthy, J.R.; *Nucleosides and Nucleotides*, **1993**, *12*, 115.
38. van der Donk, W. A.; Yu, G.; Silva, D. J.; Stubbe, J.; McCarthy, J. R.; Jarvi, E. T.; Matthews, D. P.; Resvick, R. J.; Wagner, E. *Biochemistry*, submitted.
39. Yu, G.; Stubbe, J. unpublished results.
40. McCarthy, J.R.; Sunkara, P.S. In *Chemical and Structural Approaches to Rational Drug Design*; Weiner, D.B.; Williams, W.B., Eds; CRC Press, Boca Raton, Florida, **1995**; pp 3-34.
41. Bitonti, A. J.; Dumont, J. A.; Bush, T. L.; Cashman, E. A.; Cross-Doersen, D. E.; Wright, P. S.; Matthews, D. P.; McCarthy, J. R.; Kaplan, D. A. *Cancer Res.*, **1994**, *54*, 1485.

## Chapter 19

# Synthesis and Biological Activity of 2',2'-Difluorodeoxycytidine (Gemcitabine)

L. W. Hertel<sup>1</sup>, J. S. Kroin<sup>1</sup>, C. S. Grossman<sup>1</sup>, Gerald B. Grindey<sup>1</sup>,  
A. F. Dorr<sup>1</sup>, A. M. V. Stornio<sup>1</sup>, W. Plunkett<sup>2</sup>, V. Gandhi<sup>2</sup>,  
and P. Huang<sup>2</sup>

<sup>1</sup>Lilly Research Laboratories, Eli Lilly and Company,  
Indianapolis, IN 46285

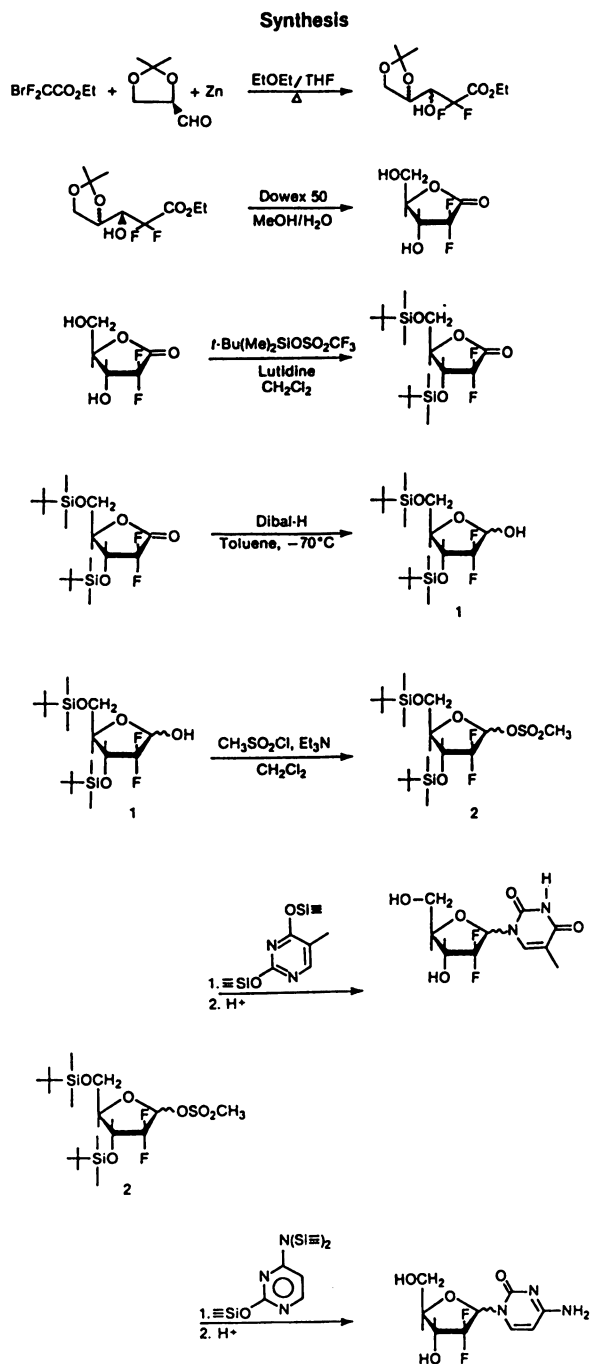
<sup>2</sup>Department of Medical Oncology, M. D. Anderson Cancer Center,  
University of Texas, Houston, TX 77030

GEMZAR<sup>®</sup> (gemcitabine-HCl) is a difluorinated analog of deoxy cytidine. It was initially synthesized as a novel anti-viral compound with broad spectrum *in vitro* activity against both RNA and DNA viruses. However, the compound proved to have a narrow therapeutic index when it was administered daily during the *in vivo* evaluation of antiviral activity. Using a staggered schedule of administration, GEMZAR is found to be a potent antitumor agent in murine and human xenograft solid tumor models. Studies have shown that gemcitabine diphosphate is a ribonucleotide reductase inhibitor, whereas the triphosphate is a potent and unique terminator of DNA synthesis. In phase I studies a variety of dose schedules were investigated. Based on phase I studies including pharmacokinetic data, phase II studies were initiated. Activity was observed in a variety of solid tumors. The results are specially encouraging for non-small cell lung and pancreatic cancer. GEMZAR is currently undergoing registration review of the Phase III clinical trials for treatment of non-small cell lung and pancreatic cancer.

It is generally understood that among other structural variations in a carbohydrate or a nucleoside, modifications to the 2' carbon of the sugar, and C-5 of the pyrimidine base can dramatically alter the pharmacological profile of certain nucleosides. The potent antiviral activity of FIAU, FMAU, Acyclovir, and BVDU in tissue culture against herpes viruses illustrates the point.(1-2)

In light of these discoveries, a program was initiated to synthesize fluorinated D-ribose and fluorinated nucleosides with hopes of finding some unique biological activity. Our approach is illustrated by a simple and stereocontrolled synthesis of 2-deoxy-2,2-difluoro-D-ribose. This was followed with the synthesis of a series of 1-(2-deoxy-2,2-difluororibofuranosyl)pyrimidines as part of a program in the design and synthesis of nucleosides of potential value as anticancer and /or antiviral agents. (3) (Scheme 1).

0097-6156/96/0639-0265\$15.00/0  
© 1996 American Chemical Society



Scheme 1.

## Synthesis.

(R)-2,3-O-Isopropylidenglyceraldehyde was prepared from D-mannitol by the modification of the method of Baer and Fischer.(4) Ethyl bromodifluoroacetate was prepared by the procedure described by Morel and Dawans, (5) or, more conveniently, it may be purchased. The coupling, using standard Reformatskii conditions, i.e., activated Zn in ether/THF, afforded a 3:1 mixture of diastereomers. These products were separated by HPLC (silica gel, methylene chloride with 0.5% methanol), giving the major isomer in 65% yield.

The major and minor products from the reaction of the zinc enolate with the alpha-alkoxy aldehyde was predicted using Felkin's model for asymmetric induction (6); i.e., the addition of a nucleophile to a carbonyl compound (bearing an alpha-asymmetric center) is anti to the large group (the one having the lowest energy sigma\* C-2-X orbital). The major isomer, was subjected to hydrolytic removal of the isopropylidene group, with closure to the lactone (94%). The lactone was silylated with tert-butyldimethylsilyl triflate in lutidine to give the bis(tertbutyldimethylsilyl) derivative in 92% yield. Reduction of this product with DIBAH gave the disilyl lactol 1 (79%) ([ $\alpha$ ]D +25.1°). The optical rotation of the synthetic material was identical with that of the product reported by Kozikowski,(7) which he obtained by silylating authentic 2-deoxy-D-ribose. Removal of the silyl groups with HBr in methylene chloride yielded 2-deoxy-2,2-difluoro-D-ribose in 79% yield.

Reaction of disilyl derivative with methanesulfonyl chloride under standard conditions yielded the mesylate derivative 2 in 90% yield. Condensation of the mesylate with trimethylsilylated cytosine, dichloroethane, and trimethylsilyl triflate at reflux for 15h afforded blocked nucleoside, which was deprotected by hydrolytic removal of protecting groups to give 2'-deoxy-2',2'-difluorocytidine (dFdC, GEMZAR). The uridine nucleoside analogues were obtained by the same procedure, i.e., condensation of 2 with the corresponding trimethylsilylated uracils.

The procedure, involving condensation in dichloroethane in the presence of trimethylsilyl triflate, gave a 40% yield of the  $\alpha$ -anomer and a 10% yield of the  $\beta$ -anomer after HPLC separation (C18/water). The assignment of anomeric configuration was made by NMR spectra. Confirmatory structural assignment was obtained from an X-ray crystal structure analysis of the anomers. Recently, a synthesis has been published that utilized the same synthetic scheme but selected benzoyl over tert-butyldimethylsilyl as the protecting group for hydroxyl groups. With this modification, a crucial selective crystallization is now possible. This modification also yields a 1 : 1 anomeric mixture of the final nucleosides. This 1 : 1 anomeric mixture is a vast improvement over the 4 : 1 mixture when tert-butyldimethyl silyl was used as the protecting group. (8)

## Biological activity.

**Antiviral activity.** *In Vitro* antiviral testing was done on the pyrimidine nucleosides. As Table 1 indicates, the compounds most effective in suppressing HSV-1 [Mayo] in BSC-1 cells were 4A [GEMZAR, dFdC], 4F [5-fluoro-dFdC] in

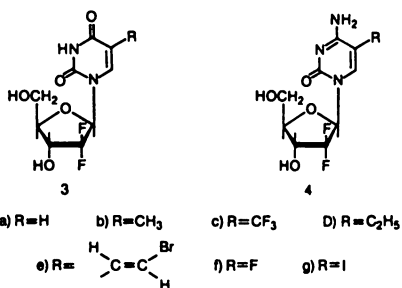


**Table 1. Antiherpes Activity<sup>a</sup> and Cytotoxicity<sup>b</sup> of Some 2',2'-Difluoro-5-substituted Nucleosides**

Compound	IC <sub>50</sub> μg/ml			Cytotoxicity (CCRF-CEM)
	HSV-1 (Mayo)	HSV-2 (RAPP)	HSV-1 TK <sup>-</sup> (B2006)	
3a	9.3	10.2	>12.5	5.4
3b	0.8, (0.32 HeLa)	1.4, (0.6 HeLa)	>100	180
3c	>25	>25		>200
3d	2.5	4.74		18.6
3e	0.13	1.43		175
3f	>25	16		>20
4a	0.06	<0.04	0.06	0.001
4b	>100			0.3
4f	1.5	3.7	6.0	0.2
4g	11.0			
FMAU	0.09	0.23		
FIAC	0.06	0.07 HeLa		
Acyclo- guanosine	0.54	0.13		13.7
BVdU	0.02	0.77		42

a. Tested in a plaque reduction assay using green monkey kidney cells (BSC-1), unless otherwise indicated

b. 72 hour cytotoxicity assay in human leukemia (CCRF-CEM) cells.

the cytidine series, and 3B [dFT], 3E [dFBVDU] and 3D [5-ethyl-dFdU] in the uridine series with IC<sub>50</sub>'s ranging from 0.06 ug/ml for dFdC to 0.13 ug/ml for dFBVDU and 0.8 ug/ml for dFT. The cytidine series exhibited a more potent and broader spectrum of activity than the difluorouridines. In fact, in tissue culture, 4A and 4F were active against vaccinia, pseudorabies, pseudorabies TK<sup>-</sup>, as well as the RNA viruses, polio, Friend leukemia and influenza. Compounds in the cytidine series were also the most cytotoxic with 4A able to inhibit the growth of CCRF-CEM cells in culture by 50% at 0.001 μg/ml. Substitution at the C-5 position in the cytidine series invariably reduced both antiviral activity and cytotoxicity. The 5-fluoro derivative 4F, was about 25 times less potent than 4A against HSV-1 and over 100 times less potent against HSV-2. Substitution at C-5 with iodo, 4G, reduced HSV-1 activity 200 fold, and placing a methyl group at C-5 made the compound 4B essentially inactive. The IC<sub>50</sub>'s in the CEM assay for these three substituted difluorocytidines were in the 0.2 to 0.3 ug/ml range, i.e., 200 to 300 times less cytotoxic than 4A. The uridine nucleosides were more selective for HSV-1 and HSV-2 and much less cytotoxic. The HSV-1 data for 3B [dFT] and 3E [dFBVDU] were comparable to acycloguanosine at 0.8 and 0.13 ug/ml respectively, with CEM values of about 180 ug/ml these compounds were essentially nontoxic in this screen. 3A, 3B and 3D had activity against HSV-2 about equal to their HSV-1 activity. In the uridine series only the 5-trifluoromethyl substituted 3C was inactive in the herpes screen.

Enzyme studies have shown that neither 3A [dFdU] nor 3B [dFT] are effectively cleaved by either *E. Coli* uridine phosphorylase or thymidine phosphorylase in the presence of phosphate. These reactions were incubated with 50 units of each enzyme for 18 hours at 37°C. In addition both compounds were effectively phosphorylated by VZV thymidine kinase at rates 1.0 to 1.3 times as fast as thymidine. (Koszalka and Averett, Burroughs Wellcome Co., Unpublished data).

GEMZAR (4A) was very active in the cell culture antiviral screen, inhibiting both RNA and DNA viruses without exhibiting toxicity in preformed monolayers. GEMZAR also inhibited thymidine kinase negative HSV-1 mutants resistant to FMAU and Acycloguanosine. The compound was tested in a variety of animal models for an antiviral effect. Although the compound inhibited virus multiplication in acute virus infections in animals, we were unsuccessful in separating toxicity from virus activity. The compound proved to have a narrow therapeutic index when it was administered daily. However we obtained very high activity in Friend leukemia virus infections in mice that could be separated from toxicity by altering the dose schedule. Both spleen enlargement and polyerythroblastosis could be inhibited by 90% under conditions that allowed normal weight gain. A dose schedule calling for treatment every fifth day was used. Activity was observed by both the oral and IP routes.(9)

**Anticancer activity.** Ara-C and GEMZAR each differ from the parent nucleoside deoxycytidine by a modification at the 2' position of the sugar moiety. While ara-C is known as the most effective drug in the treatment of adult acute leukemia (10), solid tumors have not been responsive to this drug. Because of the similarities of

the two nucleoside structures, comparative *in vivo* antitumor testing was done. (Table 2).

The initial *in vivo* evaluation of GEMZAR was conducted with L1210 leukemia. While the activity can be observed on a daily schedule of GEMZAR administration with this tumor model, a less chronic schedule of administration is more effective. Excellent antitumor activity was observed when the compound was administered on days 1, 4, 7 and 10. On this treatment schedule, GEMZAR was substantially more active than ara-C administered on a daily schedule of administration. While 80/mg/day is the maximum tolerated dose of ara-C in this experiment, the maximum tolerated dose of GEMZAR on this staggered schedule of administration is above 125 mg/kg.

While no significant differences in antitumor activity were observed between GEMZAR and ara-C in two leukemia models, dramatic differences in activity were observed with murine solid tumor models. GEMZAR produced complete inhibition of tumor growth in the X-5563 plasma cell myeloma from 5 up to 40mg/kg/day. No toxicity or weight loss occurred in the mice treated with the dose of 40 mg/kg/day. Substantial activity was also observed at 1.25 and 2.5 mg/kg/day as well. Since the maximum dose of GEMZAR on this intermittent schedule is in excess of 125 mg/kg/day, therapeutic activity can be observed over a 2-log range of GEMZAR concentrations. In marked contrast, ara-C, administered on its optimum schedule of daily administration, is completely inactive in this tumor model.

Much higher doses of GEMZAR (160 mg/kg/day, every third day for 4 doses) were required before significant antitumor activity (93% inhibition) was observed against B-16 melanoma. No toxic deaths were observed with GEMZAR in this experiment. As expected, less than 50% inhibition of tumor growth was observed with ara-C at the maximum tolerated dose of 80 mg/kg/day. Excellent antitumor activity was also observed for GEMZAR against CA-755 adenocarcinoma, M5 ovarian carcinoma and 6C3HED lymphosarcoma. No toxic deaths or weight losses were observed in the mice treated with GEMZAR.

We have shown that GEMZAR has good to excellent *in vivo* antitumor activity against a spectrum of mouse leukemias and solid tumor models.<sup>(11)</sup> In keeping with its clinical activity, ara-C was also active against the mouse leukemias, but was inactive against the mouse solid tumors. To increase our understanding of the antitumor activity of GEMZAR, we have studied its activity against a diverse panel of human tumor xenograft models. The initial results compare the antitumor activity of ara-C and GEMZAR against xenograft models of human breast, colon and lung carcinomas.

At maximally tolerated doses, GEMZAR had good to excellent antitumor activity against the human carcinomas used in this study. (Table 2) The colon carcinoma models were very responsive to the antitumor activity of GEMZAR. After one course of therapy, GEMZAR inhibited the growth of the CX-1, HC-1, GC3 and VRC5 colon carcinomas by 92, 96, 98, and 99 percent, respectively. Since the VRC5 colon carcinoma model was very responsive to GEMZAR, it was used to study the effect of one course of GEMZAR treatment on the number of tumor-free mice and the regrowth of residual tumor. In this study GEMZAR was given at 40, 80, and 160 mg/kg every 3 days for approximately 2 weeks. When measured one day after the last dose, GEMZAR inhibited tumor growth by 95%,

or greater. In the groups dosed with either 40 or 80 mg/kg, there were no tumor-free mice, but the residual tumor did not begin to regrow until about 2 weeks after the last dose. In the group treated with 160 mg/kg, 3 out of 8 mice were tumor-free, and the residual tumor in remaining mice (not cured) did not begin to regrow until 3 weeks after the last dose. Thus GEMZAR has excellent antitumor activity against human colon carcinoma xenografts and this activity was manifested for several weeks after the end of treatment.

GEMZAR also had good antitumor activity against the MX-1 breast and LX-1 non-small cell lung carcinoma models (table 2). After one course of therapy, it inhibited the growth of MX-1 tumor by 92% and the growth of the LX-1 tumors by 79%. These carcinoma xenograft models have been shown to be very nonresponsive to a large number of conventional anticancer drugs.

### Mechanism of Action

**Preclinical Profile of GEMZAR.** GEMZAR is a new anticancer drug with novel metabolic properties and mechanisms of action. As a nucleoside analog, GEMZAR is a pro-drug that must be metabolized in the cell to its active nucleotide forms. Once it is transported into the cell, GEMZAR is a good substrate for phosphorylation by deoxycytidine kinase, the rate-limiting enzyme for active metabolite formation. (12) It has been demonstrated that both gemcitabine diphosphate and gemcitabine triphosphate inhibit processes required for DNA synthesis. Furthermore, the unique actions that gemcitabine metabolites exert on cellular regulatory processes serve to enhance the overall inhibitory activities on cell growth. This interaction is termed "self-potential", and is evidenced in very few other anticancer drugs.

The sites of action of gemcitabine nucleotides and the pathways of metabolic self-potential are illustrated in Fig. 1. dFdCDP is an inhibitory alternative substrate for ribonucleotide reductase (pathway 1), the enzyme that produces deoxynucleotides required for DNA synthesis and repair. (13-14) The subsequent decrease in cellular deoxynucleotides, particularly dCTP, is particularly important because dFdCTP competes directly with dCTP for incorporation into DNA by DNA polymerases (pathway 2). Thus, the decrease in the cellular concentration of dCTP is an important self-potentiating mechanism that would result in more gemcitabine nucleotide incorporation into DNA. Incorporation of dFdCTP into DNA is most likely the major mechanism of which GEMZAR causes cell death; this is strongly correlated with loss of cell viability. (15) Molecular studies have shown that after gemcitabine nucleotide is incorporated on the end of the elongating DNA strand, one more deoxynucleotide is incorporated, and that thereafter, the DNA polymerases are unable to proceed. This action apparently locks the drug into DNA, because other studies have demonstrated that proof-reading enzymes are unable to remove gemcitabine nucleotide from this position. This is different from the case of ara-C, which is incorporated at a terminal position and is removed relatively readily by exonucleases. Presumably, the presence of gemcitabine nucleotide in this penultimate position distorts the growing DNA chain such that it is no longer an efficient substrate for DNA polymerases. (15) We have coined the term "masked chain termination" to describe this phenomena.



**Table 2. Comparative Antitumor Activity of Gemzar and Ara-C<sup>a</sup>**

	Gemzar	Ara-C
<b>Murine Leukemias</b>		
L-1210	++	++
P-388	+	++
<b>Murine Solid Tumor Models</b>		
X-5563 myeloma	+++	-
CA755 adenocarcinoma	+++	-
M5 ovarian carcinoma	+++	+++
6C3HED lymphosarcoma	+++	NT
B-16 melanoma	++	-
P1534J leukemia	++	NT
<b>Human Tumor Xenograft Models</b>		
LX-1 lung carcinoma	+	-
CX-1 colon carcinoma	+++	-
MX-1 mammary carcinoma	++	-
HC1 colon carcinoma	+++	NT
GC3 colon carcinoma	+++	NT
VRC5 colon carcinoma	+++	NT
<b>Solid Tumors (s.c.)</b>		
+++ 95-100% inhibition	+++	Leukemias (i.p.) >200% ILS
++ 80-95% inhibition	++	100-200% ILS
+ 60-80% inhibition	+	50-100% ILS
- <60% inhibition	-	< 50% ILS
NT Not tested	NT	Not tested

<sup>a</sup>Gemzar was dosed on days 1, 4, 7 and 10, while Ara-C was dosed daily x 10.

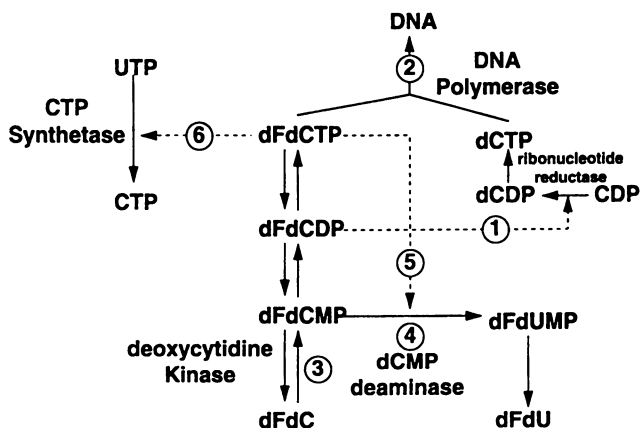


Figure 1. Mechanisms of Action of Gemzar.

The activity of deoxycytidine kinase is inhibited by dCTP (reaction 3); when the cellular dCTP level is lowered, the rate of gemcitabine phosphorylation is increased. This results in more dFdCTP accumulation in the cell as a substrate for incorporation into DNA, as well as higher levels of dFdCDP to maintain inhibition of reductase. In contrast, dCTP is a required co-factor for the activity of dCMP deaminase (reaction 4), the rate-limiting enzyme for elimination of gemcitabine nucleotides from the cell. When the cellular dCTP levels declines after inhibition of ribonucleotide reductase by dFdCTP, dCMP deaminase activity also decreases. This action, which results in a lower rate of gemcitabine nucleotide removal from the cell, probably contributes to the retention of the active nucleotides in tumor cells. Furthermore, dFdCTP is itself capable of inhibiting dCMP deaminase (reaction 5), indicating an additional mechanism which contributes to the prolonged retention of gemcitabine nucleotides.<sup>(16)</sup> Prolonged retention of gemcitabine triphosphate has been observed in human leukemia cells during clinical trials.<sup>(17)</sup> Finally, at high cellular concentrations, dFdCTP inhibits CTP synthetase (reaction 6), blocking the synthesis of CTP and by mass action, that of dCTP as well.<sup>(18)</sup>

In summary, an extraordinary array of self-potentiating mechanisms increase the concentrations and prolong the retention of the active nucleotides of GEMZAR in tumor cells. Inhibition of ribonucleotide reductase by gemcitabine diphosphate lowers dCTP levels and facilitates incorporation of the drug into DNA. The cytotoxic action of GEMZAR is related to the incorporation of the gemcitabine triphosphate into DNA, and the consequent inhibition of further DNA synthesis. This mechanism, which is sustained because cells are generally unable to remove the drug from DNA, is probably effective at inhibiting both DNA replication and repair. Thus, it is likely that GEMZAR will synergize with drugs that damage DNA and also with radiation. Surveillance mechanisms that allow cells to perceive the inability to re-establish DNA synthesis and unreparable DNA damage, subsequently activate a signaling pathway that results in cell death by apoptosis.

### Clinical trials

**Non-Small Cell Lung Cancer.** Lung carcinoma is now the leading cause of death from malignant disease in the United States of America, both in males and females, and this situation will not be substantially changed in the next decade. Approximately 80% of lung carcinomas are of the non-small cell subtype (NSCLC).

Many cytotoxic agents have been tested in NSCLC but only a few drugs are reported to yield an objective response rate greater than 15% including navelbine, ifosfamide, vindesine, vinblastine, cisplatin and mitomycin. Generally speaking, all these drugs have toxic effects and, therefore, it is necessary to seek new drugs which combine efficacy with moderate toxicity.

GEMZAR has demonstrated high activity against a range of human tumor xenografts including lung tumors. This preclinical activity was confirmed in phase I clinical studies and based on these data, Phase II studies were started. The phase I studies had indicated that administration of GEMZAR once a week for 3 weeks followed by a week of rest, gave the most favorable therapeutic index.<sup>(19-22)</sup> In patients who had already received chemotherapy, the maximum tolerated dose was

approximately 800 mg/m<sup>2</sup>/week. However, in the phase II studies the dose of 800 mg/m<sup>2</sup> was found to be very conservative and starting doses were increased to 1000 and 1250 mg/m<sup>2</sup>.(23)

Three initial studies were conducted in the United States of America, Europe, and South Africa, respectively, followed by a fourth, "International", study.(23-26) The aim of these four trials was to define the efficacy of GEMZAR alone, given once a week for 3 weeks followed by a rest week, in chemo-naive patients with NSCLC. Restricted inclusion criteria were approximately identical in these four studies, so that the population enrolled could be compared from one study to another. Efficacy is determined by an objective, measurable decrease in tumor mass (a regression). A partial response is a 50% reduction in measurable lesions by their perpendiculars without appearance of any new lesions. A complete response is the disappearance of all evidence of tumor. Response rate is the sum of partial and complete responses.

In terms of efficacy, the American study recorded a response rate of only 3% compared to 22.5% in the European, and 20% in the South African study. In an attempt to reconcile these results, a large International phase II trial was initiated. This study enrolled 161 patients from whom 151 were eligible for response. An objective response of 21.8% with 30 partial responses and 3 complete responses confirmed the activity of GEMZAR in this disease.

In all of these studies, the toxicity was generally low. Mild myelosuppression occurred with anemia grade 3 and 4 in less than 7.2% and 0.6% of the patients, respectively; neutropenia grade 3 and 4 in less than 26% and 6% of patients, respectively; thrombocytopenia grade 3 and 4 was rare. Modest hepatotoxicity was seen, manifest as transient, asymptomatic, rapidly reversible elevation of liver enzymes. Other toxicities which were not dose limiting included skin rash, mild fever on the day of treatment proteinuria, lethargy, and peripheral edema. Long-term toxicity data are available for several patients who received GEMZAR for a prolonged period, some even longer than 1 year. There has been no evidence of significant cumulative toxicity in any of these patients.

**GEMZAR and Cisplatin in NSCLC.** GEMZAR has reproducibly achieved a 20% objective response rate in NSCLC as a single agent. Cisplatin is one of the most common components of combination chemotherapy regimens in NSCLC and cisplatin and GEMZAR have been shown to be synergistic in some preclinical models.(27) Based on their single-agent activities and on the promising preclinical data, clinical trial combining GEMZAR and cisplatin in NSCLC was initiated. (28-31)

GEMZAR was dosed at 1000mg/m<sup>2</sup> over 30 minutes on day 1, 8, 15 every 28 days in each study. Cisplatin was dosed at 100mg/m<sup>2</sup> on day 1 or day 15 or at 30 mg/m<sup>2</sup> on day 1, 8, and 15.

Response rate with this combination regimen in six multinational studies ranged from a low of 38.5% to a high of 48.1%. The average response rate from 193 evaluable patients was 43%. The treatment was well tolerated at all dose levels with no life threatening toxicity. These results are encouraging and suggest that the combination has significantly greater activity than either agent used alone. This

may support the preclinical data which demonstrated synergistic tumor cell killing between the two compounds. The combination is particularly interesting for patients with NSCLC because of its favorable toxicity profile.

**Pancreatic cancer.** Pancreas cancer is the fifth most common cause of cancer-related mortality in the United States, following lung, colorectal, breast, and prostate cancers. It is the fourth leading cause of death from cancer in men and the fifth leading cause of death from cancer in women. It was estimated that 27,000 cases of pancreatic cancer would be diagnosed in the United States in 1994, and that 25,000 deaths would be expected to occur as a result of this disease. Unfortunately, over the past 40 years, there have been few significant advances in either the diagnosis or treatment of this disease. Only a minority of patients present with localized disease amenable to potentially curative surgical resection. Most patients with advanced disease have significant symptoms; abdominal and back pain, weakness, marked weight loss, and declining performance status. Patients with advanced disease face a bleak prognosis. Median survival is 3 to 6 months, and 90% of patients die within 1 year of diagnosis.

Many cytotoxic chemotherapeutic agents have been evaluated in patients with advanced pancreatic cancer. Reported response rates vary widely. Early reports of favorable results with any single agent or combination chemotherapy have not been reproduced in other studies. No regime has been shown to clearly improve survival. There is no standard treatment for patients with non-resectable, pancreatic cancer. No single agent or combination chemotherapy program has demonstrated a survival advantage over 5-FU alone. Many oncologists consider 5-FU as standard chemotherapy for the treatment of advanced pancreatic cancer, therefore, 5-FU is an appropriate control arm for a randomized trial testing a new treatment for patients with advanced pancreatic cancer.

Following the phase II clinical observation that patients with pancreas cancer experienced improvement in disease-related symptoms when treated with GEMZAR, a quantitative definition of clinical benefit (CB) was developed as a primary measure of efficacy for clinical trials. Clinical benefit response was defined as a  $\geq 50\%$  reduction in pain, a  $\geq 50\%$  reduction in daily analgesic consumption, or a  $\geq 20$  point improvement in Karnofsky performance score that was sustained for  $\geq 4$  weeks without worsening of any other component. Each parameter is measured at baseline and regularly throughout the study. Following a lead-in period to characterize and stabilize pain, 126 chemo-naïve patients with confirmed advanced or metastatic adenocarcinoma of the pancreas (measurable or evaluable) were randomized to GEMZAR, 1000 mg/m<sup>2</sup> over 30 mins weekly x 7 followed by a week of rest, and then weekly x 3 every 4 weeks thereafter, or to 5-FU 600 mg/m<sup>2</sup> over 30 mins once weekly.<sup>(32)</sup> Patients on both treatment arms were balanced in terms of gender, age and disease stage. CB response was the primary endpoint and 23.8% of the GEMZAR pts were CB responders versus only 4.8% of the 5-FU pts ( $p=0.0022$ ). The median survival in months for GEMZAR pts was 5.65 and for 5-FU was 4.41 ( $p=0.0025$ ), with 24% of GEMZAR pts and 6% of the 5-FU pts alive at 9 months. WHO  $\geq$  grade 3 neutropenia was seen in 23% of GEMZAR pts and 5% of 5-FU pts and  $\geq$  grade 3

nonhematological toxicity (N & V, diarrhea) was seen in 15% of the GEMZAR pts and 10% of 5-FU pts. This randomized study confirms the positive effect of GEMZAR on clinical benefit, and shows a survival benefit for GEMZAR as the initial treatment of patients with pancreatic cancer.

We designed and conducted a prospective, single arm, multicenter Phase II trial with clinical benefit as the primary endpoint. GEMZAR 1000 mg/m<sup>2</sup> was administered as a 30 min. infusion q wk x 7 followed by a 1 wk rest x 1 and q wk x 3 followed by a 1 wk rest thereafter. Sixty-three pts (32M, 31F) with adenocarcinoma of the pancreas that had progressed despite one prior 5-FU-based therapy were enrolled. (33) Median age: 62 (range: 33-77). Median KPS: 70 (range: 50-90), median baseline pain intensity: 29 on a 100 point scale (range 3-68), median baseline analgesic requirement: 60mg morphine-equivalents/day (range: 0-1159). Therapy was very well tolerated with only 1 pts (2%) experiencing Grade 4 nausea, vomiting, neutropenia, bleeding, or anemia. Grade 3 toxicities included neutropenia-15 pts (25%), anemia-6pts (10%), thrombocytopenia-3pts (5%), nausea/vomiting-4 pts (6%), diarrhea-1 pts (2%), and fever-1 pts (2%). Under our stringent criteria, 17 of 63 pts (27%) attained a clinical benefit response (95% CI: 16-38%). This study demonstrates that objective criteria can be used to evaluate the clinical impact of new therapies for pancreas cancer, a highly symptomatic disease that is difficult to assess by traditional tumor response parameters. Our findings suggest that GEMZAR has substantial activity as a palliative agent in patients with 5-FU-refractory pancreas cancer.

## Literature Cited

1. Elion, G. B.; Furman, P. A.; Fyfe, J. A. *Proc. Nat'l. Acad. Sci. USA*, **1977**, vol. 74, pp.5716-5720.
2. Lopez, C.; Watanabe, K. A.; Fox, J. J. *J. Antimicrob. Agents Chemother.*, **1980**, vol. 17, pp. 803-806.
3. Hertel, L. W.; Kroin, J. S.; Misner, J. W.; Tustin, J. M. *J. Org. Chem.* **1988**, vol. 53, pp. 2406-2409.
4. Hertel, L. W.; Grossman, C. S.; Kroin, J. S. *Syn. Comm.*,**1991**, vol. 21 (2), pp. 151-154.
5. Morel, D.; Dawans, F. *Tetrahedron*, **1977**, vol. 33, pp.1445-1447.
6. Cherest, M.; Felkin, H.; Pruden, N. *Tetrahedron Lett.*, **1968**, pp. 2199-2204.
7. Kozikowski, A. P.; Ghosh, A. K. *J. A. Chem. Soc.*, **1982**, vol. 104, pp. 5788-5789.
8. Chou, T. S. ; Heath, P. C.; Patterson, L. E.; Poteet, L. M.; Lakin, R. E.; Hunt, A. H. *Synthesis*, **1992**, pp. 565-570.
9. Delong, D. C.; Hertel, L. W.; Tang, J.; Kroin, J. S.; Nelson, J. D.; Terry, J.; Lavender, J. F. *Am. Soc. of Microbiologists*, **March 24-28, 1986**, Washington, D. C.

10. Keating, M. J.; McCredie, K. B.; Bodey, G. P.; Smith, T. L.; Gehan, E.; Freireich, E. J. *JAMA*, **1982**, vol. 248, pp. 2481-2486.
11. Hertel, L. W.; Goder, G. B.; Kroin, J. S.; Rinzel, S. M.; Poore, G. A.; Todd, G. C.; Grindey, G. B. *Cancer Reseach*, **1990**, vol. 50, pp. 4417-4422.
12. Heinemann, V.; Hertel, L. W.; Grindey, G. B.; Plunkett, W. *Cancer Research*, **1988**, vol. 48, pp. 4024-4031.
13. Heinemann, V.; Xu, Y-Z.; Chubb, S.; Sen, A.; Hertel, L. W.; Grindey, G. B.; Plunkett, W. *Molecular Pharmacology*, **1990**, vol. 38, pp. 567-572.
14. Baker, C. H.; Banzon, J.; Bollinger, J. M.; Stubbe, J.; Samano, V.; Robins, M. J.; Lippert, B.; Jarvi, E.; Resvick, R. *J. Med. Chem.* **1991**, vol. 34, pp. 1879-1884.
15. Huang, P.; Plunkett, W. *Cancer Res.*, **1991**, vol. 51, pp.6110-6117.
16. Heinemann, V.; Xu, Y-Z.; Chubb, S.; Sen, A.; Hertel, L. W.; Grindey, G. B.; Plunkett, W. *Cancer Res.* **1992**, vol. 52, pp. 533-536.
17. Grunewald, R.; Kantarjian, H. Du, M.; Faucher, K.; Tarassoff, P.; Plunkett, W. *J. Clin. Oncol.*, **1992**, vol. 10, pp. 406-413.
18. Heinemann, V.; Schulz, L.; Issels, R. D.; Plunkett, W. *Sem.inars in Oncology*, **1995**, vol. 22, no.4, suppl. 11, pp. 11-18.
19. O'Rourke, T. J.; Brown, T. D.; Havlin, K.; et.al., *Eur. J. Cancer*, **1994**, vol. 30, pp. 417-418.
20. Poplin, E.; Corbett, T.; Flaherty, L.; et. al., *Invest. New Drugs*, **1992**, vol. 10, pp. 165-170.
21. Vermorken, J.; Guastall, J. P.; Hatty, S. R.; et. al., *Eur. J. Cancer*, Submitted
22. Abbruzzese, J. L.; Grunewald, R.; Weeks, E. A.; et. al., *J. Clin. Oncol.*, **1991**, vol. 9, pp. 491-498.
23. Kaye, S. B. *J. C.in. Oncol.*, **1994**, vol. 12, pp. 1527-1531.
24. Anders, H.; Lund, G.; Bachj, F.; Thatcher, N.; Walling, J.; Hansen, H. H.; *J. Clin Oncol.*, **1994**, vol. 12, pp. 1821-1826.
25. Abratt, R. P.; Bezwoda, W. R.; Falkson, G.; Goedhals, S. L.; Hacking, D. Rugg, T. *J. Clin. Oncol.*, **1994**, vol. 12, pp. 1535-1540.
26. Le Chevalier, T.; Gottfried, M.; Gatzemeir, M.; et. al. *Eur. J. Cancer*, **1993**, vol. 29A(suppl. 6), pp. s160.
27. Braakhuis, G. J. M.; Ruiz van Haperen, V. W. T.; Bergman, A. M.; et. al. *Ann. Oncol.*, **1994**, vol. 5 (Suppl. 5), pp. 82-86.
28. Steward, W. P.; Dunlop, D. J.; Cameron, C.; Talbot, D. C.; Kleisbauer, J-P.; Thomas, P. Guerin, J. C.; Perol, M.; Sanson, C.;

- Dabo;uis, G.; Lacoix, H. *Proc. ASCO, March 1995, vol. 14, abstr. 1064*, pp. 351.
29. Crino, L.; Scagliotti, G.; Marangolo, M.; Figoli, G.; Clarici, M. DeMarinis, F.; Salvati, G. Cruciani, G.; Dogliotti, L.; Cocconi, G.; Paccagnella, A.; Adamo, G.; Incoronato, P.; Scarcell, L.; Mosconi, A. M.; Tonato, M. *Proc. ASCO, March 1995, vol. 14, abstr. 1066*, pp. 352.
30. Sandler, A. B.; Ansari, R.; McClean, J.; Fisher, W.; Dorr, A.; Einhorn, L. H. *Proc. ASCO, March 1995, vol. 14, abstr. 1089*, pp. 357.
31. Abratt, R. P.; Bezwoda, W. R.; Goedhals, L.; Hacking, D. J. *Proc. ASCO, March 1995, vol. 14, abstr. 1159*, pp. 375.
32. Moore, M.; Andersen, J.; Burris, H.; Tarassoff, P.; Green, M.; Casper, E.; Portenoy, R.; Modiano, M.; Cripps, C.; Nelson, R.; Storniolo, A.; Von Hoff, D. *Proc. ASCO, March 1995, vol. 14, abstr. 473*, pp. 199.
33. Rothenberg, M. L.; Burris III, H. A.; Andersen, J. S.; Moore, M.; Green, M. R.; Portenoy, R. K.; Casper, E. S.; Tarassoff, P. G.; Storniolo, A. M.; Von Hoff, D. D. *Proc. ASCO, March 1995, vol. 14, abstr. 470*, pp. 198.

## Chapter 20

# Fluorinated Sugars as Probes of Glycosidase Mechanisms

Mark Namchuk, Curtis Braun, John D. McCarter, and  
Stephen G. Withers<sup>1</sup>

Departments of Chemistry and Biochemistry, University of British  
Columbia, Vancouver, British Columbia V6T 1Z1, Canada

Fluorinated sugars have proved to be valuable mechanistic probes of glycosidases in several ways. This is illustrated for *Agrobacterium*  $\beta$ -glucosidase, a retaining glycosidase which hydrolyses glycosidic bonds with net retention of anomeric configuration via a double displacement mechanism involving a glycosyl-enzyme intermediate. Both ground state and transition state interactions with the individual hydroxyl groups have been probed by use of a series of deoxy- and deoxyfluoro-glycosides revealing the importance of interactions at the 2-position. Two new approaches to the trapping of the glycosyl-enzyme intermediate are now described. Incorporation of two fluorines at C-2 slows both the glycosylation and deglycosylation steps enormously, and allows the incorporation of an exceptionally good leaving group at the anomeric centre without undue lability. Thus the 2,4,6-trinitrophenyl  $\alpha$ -D-2-deoxy-2,2-difluoro *arabino* and *malto* glycosides are time-dependent inactivators of yeast  $\alpha$ -glucosidase and human pancreatic  $\alpha$ -amylase, respectively. Alternatively, installation of a single fluorine at C-5 along with a fluoride leaving group at the anomeric centre provides a novel class of mechanism-based inactivators of both  $\alpha$ - and  $\beta$ -glycosidases, and has allowed identification of the active site nucleophile in yeast  $\alpha$ -glucosidase.

Glycosidases are enzymes which catalyse the hydrolysis of glycosidic linkages. These enzymes fall into two major mechanistic categories: those which hydrolyse the glycosidic bond with net inversion of configuration (inverting enzymes) and those which do so with net retention of anomeric configuration (retaining enzymes) (1, 2). Mechanisms for these two enzyme classes were proposed by Koshland (3). Although the two mechanisms are distinctly

<sup>1</sup>Corresponding author



different, they do have a number of features in common, as illustrated in Scheme 1. Inverting glycosidases are believed to function by a single step mechanism in which a water molecule effects a direct displacement at the anomeric centre *via* a general-acid/base catalysed process.

Retaining glycosidases function through a double displacement mechanism in which a glycosyl enzyme intermediate is formed and hydrolyzed by sequential attack of an enzymic nucleophile and water. Again the reaction is facilitated by acid/base catalysis, but in this case it is probable that the same carboxyl group plays both roles. Transition states for these chemical steps in both classes of enzymes have considerable oxocarbenium ion character.

**Non-covalent interactions and catalysis** Not shown on the above representations, but of considerable importance, are the non-covalent interactions between the enzyme and the substrate which provide the initial recognition, but which are optimised only at the transition state (4). The increased strength of interactions at the transition state necessarily results in its stabilization, therefore in catalysis. In order to investigate the importance of interactions at each individual hydroxyl group to such transition state stabilisation, a detailed study of the rates of enzyme-catalysed hydrolysis of a series of deoxy- and deoxyfluoro- glycosides by the *Agrobacterium faecalis*  $\beta$ -glucosidase (Abg) has been performed. Such an approach relies upon the fact that the *only* truly sterically conservative substitutions for the hydroxyl groups are those for hydrogen (deoxy sugars) and for fluorine (deoxyfluoro sugars). Further, while the original hydroxyl group is capable of accomodating three hydrogen bonds (two as acceptor, one as donor), the hydrogen of the deoxy sugar provides no significant hydrogen bonding interaction while the fluorine of a deoxyfluoro sugar is limited in its hydrogen bonding capabilities, at best functioning as a weak acceptor. Therefore changes in *binding* of substrates upon substitution of a single hydroxyl group will provide estimates of ground state interactions at that position {from  $\Delta\Delta G^{\circ} = -RT \log(K_1/K_2)$ }, while changes in *turnover rate* will provide estimates of transition state interactions {from  $\Delta\Delta G^{\ddagger} = -RT \log(k_{cat1}/K_m / k_{cat2}/K_m)$  (5, 6). Effects on the two steps (glycosylation and deglycosylation) can be assessed individually through pre-steady state kinetic measurements by stopped-flow analysis. Indeed the choice of a 2,4-dinitrophenyl leaving group was made on this basis since not only is it highly chromogenic, but also since the use of this excellent leaving group should maximise the chance that the second step, deglycosylation, will be rate limiting, therefore allowing measurement of both steps independently.

Michaelis-Menten parameters for the hydrolysis of such a series of substituted 2,4-dinitrophenyl glycosides by Abg are shown in Table I, and pre-steady state kinetic parameters, derived from stopped-flow measurements, in Table II (7). In all cases, except for those substrates with no equatorial C-4 substituent,  $k_{cat}$  values are lowered upon substitution.  $K_m$  values are also generally lowered, but this is a consequence of the deglycosylation step being rate-limiting, thus  $K_m$  values are lowered as a result of accumulation of the glycosyl-enzyme intermediate. The  $K_d$  values shown in Table II provide more useful insights into effects on ground state interactions. Deglycosylation is rate-limiting for all substrates except those with no equatorial substituent at C-4 (Gal, 4DGLu and 4FGal), as was shown by the absence of a "burst" in the stopped-flow experiment, and as is reflected in the generally higher  $K_m$  values for these substrates. This observation, along with the fact that these three substrates also have the highest  $k_{cat}$  values of all those studied indicates that the deglycosylation

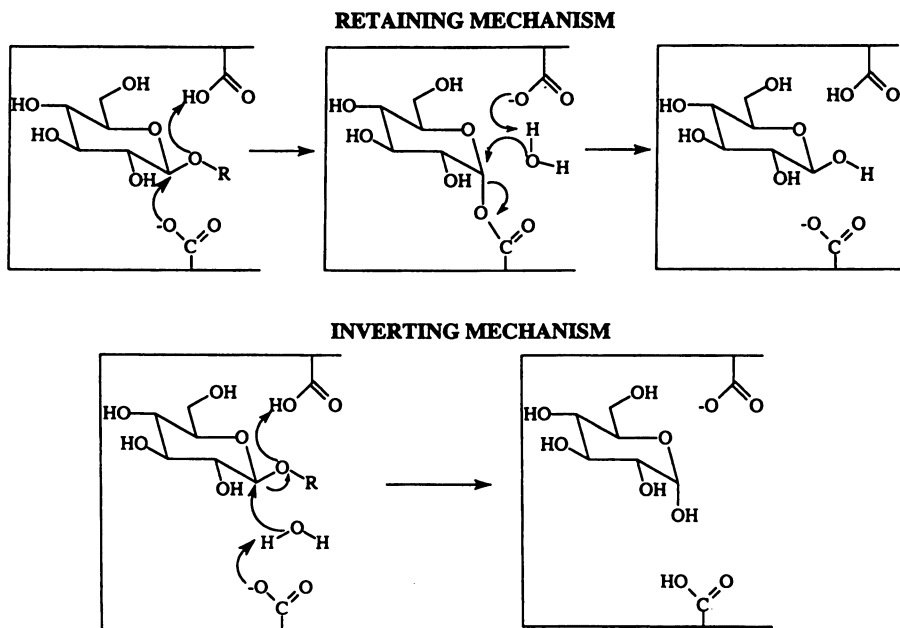
**Scheme 1**

Table I.  
Steady State Kinetic Parameters for Hydrolysis of DNPglycosides by Abg at 37°C

Substrate	$K_m$ (mM)	$k_{cat}$ ( $\text{sec}^{-1}$ )	$k_{cat}/K_m$ ( $\text{mM}^{-1}\text{sec}^{-1}$ )
DNPglucoside	0.0218 (0.0012)	130 (3)	5960
DNP6Dglucoside	0.0227 (0.004)	44.8 (0.25)	1974
DNP4Dglucoside	0.170 (0.01)	380 (11)	2260
DNP3Dglucoside	0.029 (0.003)	9.9 (0.42)	342
DNP6Fglucoside	0.0020 (0.0001)	8.68 (0.15)	4340
DNP4Fglucoside	0.020 (0.0016)	9.62 (0.27)	481
DNP3Fglucoside	0.0020 (0.0004)	1.12 (0.05)	560
DNP2F glucoside <sup>a</sup>		$\sim 2.0 \times 10^{-7}$	
DNPgalactoside	0.840 (0.10)	175 (8)	208
DNP4Fgalactoside	0.500 (0.034)	137 (4)	271
DNPalloside	0.0068 (0.0002)	0.100 (0.007)	14.7
DNPmannoside	0.106 (0.014)	0.126 (0.007)	1.19

<sup>a</sup> Data obtained from Reference 10.

step is accelerated by the removal of the equatorial substituent, while the glycosylation step (from  $k_{cat}/K_m$ ) is slowed.

Effects of substitution of individual hydroxyl groups on each step are best summarised in Table III where changes in free energy of binding and activation free energy are provided. These data are consistent with the transition states for both steps having substantial oxocarbenium ion character since not only are rates slowed more for the fluorosugars than for the deoxysugars, as would be expected on the basis of inductive effects, but also the largest effects are observed at C-2, with an enormous  $52 \text{ kJ mol}^{-1}$  increase in activation free energy for the deglycosylation step with the 2-fluoro substituent. However, the rate decreases are not due to inductive effects alone, as the deoxy substrates are also slowed, and on the basis of inductive effects alone, these should have been FASTER substrates than the parent. These rate decreases are most likely due to the absence of transition state binding interactions, thus the  $\Delta\Delta G^{0\ddagger}$  values for the deoxy sugars shown in Table III represent a *minimum* estimate of the contributions of hydrogen bonding interactions to transition state stabilisation at that position. It is clear from this data that, at least for the deglycosylation step, the strongest interactions are at the 2-position contributing at *least*  $22 \text{ kJ mol}^{-1}$  on the basis of the deoxy sugar data, and probably much more since positive inductive effects will be maximised at C2. Interactions at the 3- and 6- positions are significantly less important, while those at the 4-position appear to actually be inhibitory to this step!

As has been shown previously (8-10), this very large inductive and binding effect at C2 can be put to good use in trapping of the 2-deoxy-2-fluoroglycosyl-enzyme intermediate. Incorporation of a very good leaving group such as 2,4-dinitrophenolate into a 2-deoxyfluoro glycoside allows this intermediate to be formed, but to turn over only very slowly. This provides a highly effective class of mechanism-based inactivators of retaining  $\beta$ -glycosidases, which have been used to identify the active site nucleophilic residues in a number of these enzymes (see (11) for a recent review).

**Trapping the intermediate on  $\alpha$ -glycosidases: 2,2-difluoro glycosides** By contrast with the  $\beta$ -glycosidases, the corresponding 2-deoxy-2-fluoro  $\alpha$ -glycosides have proved largely ineffective as mechanism-based inactivators of  $\alpha$ -glycosidases, functioning rather as slow substrates with no accumulation of the glycosyl-enzyme intermediate (11). This indicates that the deglycosylation step is not sufficiently slowed by the presence of a single fluorine substituent, suggesting that this second step has less oxocarbenium ion character than is the case for  $\beta$ -glycosidases. One approach to slow this step further would involve the addition of a second fluorine at C-2, thereby further destabilising the oxocarbenium ion-like transition state. Since this will also slow the glycosylation step, an even better leaving group such as 2,4,6-trinitrophenolate (picrate) is required at the anomeric centre to speed up the glycosylation step and allow the accumulation of the intermediate. The increased stability of the 2,2-difluoro glycosides should allow such compounds to be synthesized without being unduly labile.

Synthesis of 2,4,6-trinitrophenyl 2-deoxy-2,2-difluoro- $\alpha$ -D-glucopyranoside (TNPDFG) was achieved as follows. Treatment of 3,4,6-tri-O-acetyl 2-deoxy-2-fluoro  $\alpha$ -D-glucopyranosyl bromide with triethylamine in acetonitrile resulted in elimination of HBr and generation of 3,4,6-tri-O-acetyl-2-fluoro- D-glucal. Treatment of this with acetyl hypofluorite produced a mixture

Table II.  
Pre-Steady State Kinetic Parameters for Reaction of DNPglycosides with Abg at 5 °C

Substrate <sup>a</sup>	$K_d$ (mM)	$k_2$ (sec <sup>-1</sup> )	$k_2/K_d$ (mM <sup>-1</sup> sec <sup>-1</sup> )
DNPglucoside	0.65 (0.022)	1300 (21)	2000
DNP6Dglucoside	2.7 (0.34)	530 (35)	195
DNP3Dglucoside	0.43 (0.04)	33 (1.3)	77
DNP6Fglucoside	5.6 (2.0)	1800 (500)	320
DNP4F glucoside	2.7 (0.58)	90(14)	34
DNP3F glucoside	0.31 (0.04)	81 (5)	266
DNP2F glucoside	0.34 (0.05)	0.355 (0.02)	1.06
DNPgalactoside <sup>b</sup>	2.74 (0.37)	22.1 (1.7)	8.1
DNPmannoside	2.65 (0.37)	1.04 (0.10)	0.392

a) Neither DNP4Fgalactoside nor DNP4Dglucoside show a pre-steady state 'burst', therefore, no pre-steady state kinetic data were obtained.

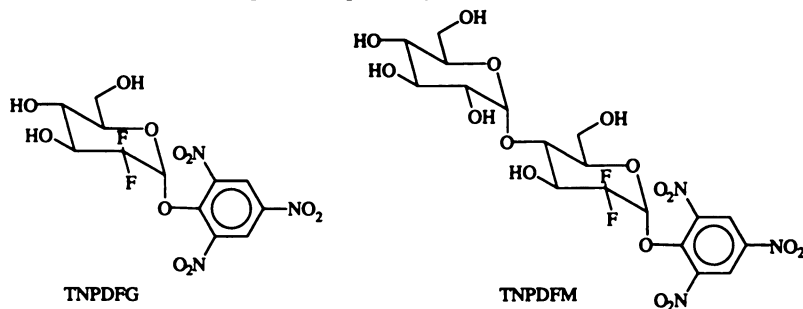
b)  $K_d$  and  $k_2$  were estimated from  $K_m$  and  $k_{cat}$  determined at 5 °C.

Table III  
Free Energy Changes at each Step Resulting from Hydroxyl Substitution on DNP glycosides

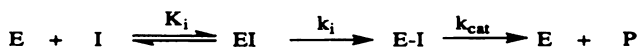
Substitution	$\Delta\Delta G^0$ , $K_d$ (kJ.mol <sup>-1</sup> )	$\Delta\Delta G^{0\ddagger}$ , $k_2$ (kJ.mol <sup>-1</sup> )	$\Delta\Delta G^{0\ddagger}$ , $k_3$ (kJ.mol <sup>-1</sup> )	$\Delta\Delta G^{0\ddagger}$ , $k_{cat}/K_m$ (kJ.mol <sup>-1</sup> )
6-deoxy	3.3	2.1	2.7	2.9
4-deoxy	-	-	-	2.5
3-deoxy	-1.0	8.5	6.6	7.4
2-deoxy	-	-	~22 <sup>a</sup>	-
6-fluoro	5.0	-0.8	7.0	0.8
4-fluoro	3.3	6.2	6.7	6.5
3-fluoro	-1.7	6.4	12	6.1
2-fluoro	-1.5	19	52	15

<sup>a</sup> Value derived from a comparison of  $k_{cat}$  for this substrate with  $k_{cat}$  for PNPglucoside

of the two 1,3,4,6-tetra-O-acetyl 2-deoxy-2,2-difluoro-D-glucopyranoses which was subjected to selective anomeric O-deprotection by treatment with hydrazine acetate. Subsequent reaction of this hemi-acetal with fluoro-2,4,6-trinitrobenzene plus a hindered base in  $\text{CH}_2\text{Cl}_2$  for an extended time period resulted in the generation of the  $\alpha$ -anomer of the protected trinitrophenyl glycoside. Deprotection to yield the desired derivative was achieved by use of methanolic HCl. An equivalent approach was used for the synthesis of the maltose derivative 2,4,6-trinitrophenyl 2-deoxy-2,2-difluoro- $\alpha$ -D-maltopyranoside (TNPDFM), starting with maltal hexa-O-acetate. Both compounds provided the expected elemental and spectroscopic analyses (12).



Incubation of both yeast  $\alpha$ -glucosidase with TNPDFG and human pancreatic  $\alpha$ -amylase ( $\alpha$ -amylase) with TNPDFM resulted in time-dependent inactivation, as shown for  $\alpha$ -amylase in Figure 1a (12). Inactivation followed pseudo-first order kinetic behaviour for at least two half-lives, allowing estimation of pseudo-first order rate constants for inactivation at each concentration of inactivator. These data were then analysed according to the kinetic scheme below:



A reciprocal replot of the *pseudo*-first order rate constants ( $k_{obs}$ ) at each inhibitor concentration, taken from slopes of the lines in Figure 1a, *versus* inhibitor concentration is shown in Figure 1b, the slope of this plot yielding a value of  $k_i/K_i = 0.0073 \text{ min}^{-1}\text{mM}^{-1}$  for human pancreatic  $\alpha$ -amylase. Individual values of  $k_i$  and  $K_i$  could not be reliably determined because the solubility of the inhibitor (maximum concentration achieved = 11 mM) precluded measurements at concentrations anywhere near the probable  $K_i$  value. In the presence of the known competitive inhibitor acarbose the inactivation rate was decreased from  $0.044 \text{ min}^{-1}$  to  $0.008 \text{ min}^{-1}$  (Figure 1c) indicating that inactivation is a consequence of modification of the active site.

The reaction of  $\alpha$ -amylase with the inactivator was also studied by monitoring the release of trinitrophenolate at 400 nm, yielding the biphasic time course shown in Figure 2. The first, fast phase corresponds to the release of TNP upon inactivation of the enzyme; the second, slower phase to the breakdown of the substrate, as demonstrated in a control experiment with no enzyme. Back extrapolation of the essentially linear steady state phase and of the initial burst phase to time zero revealed that  $26 \mu\text{M}$  TNP was released in the initial burst phase, corresponding well to the concentration of  $\alpha$ -amylase in the

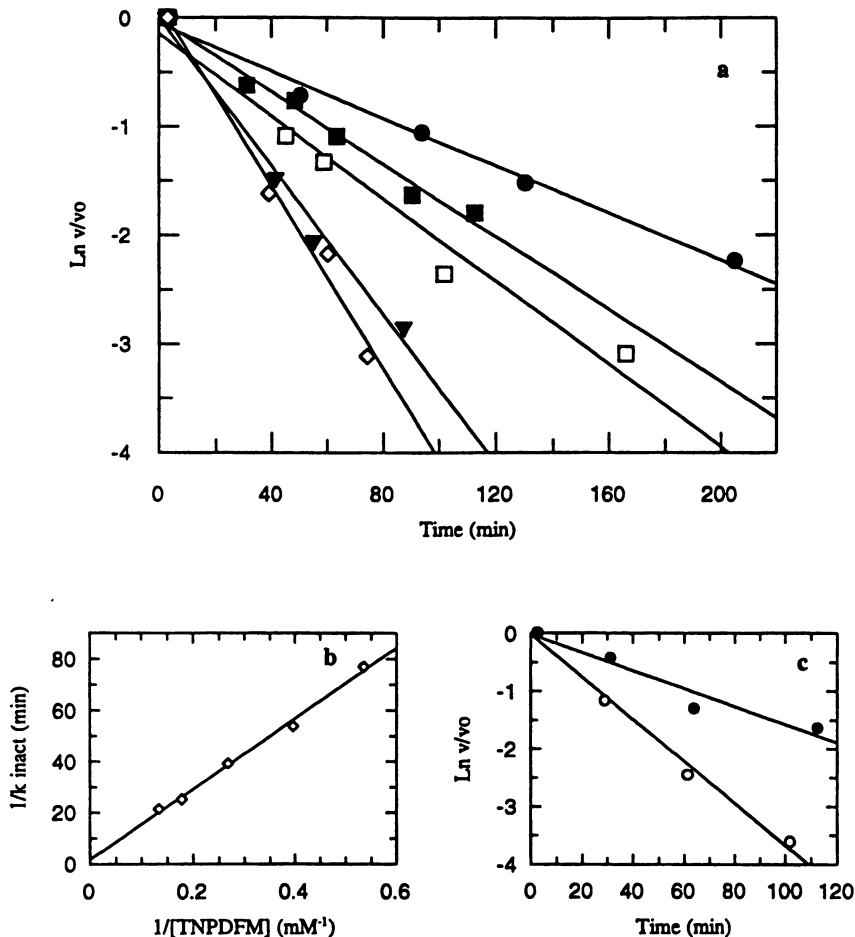


**Figure 1:** Inactivation of human pancreatic  $\alpha$ -amylase by TNPDFM. (a) Semilogarithmic plot of residual activity vs time at the indicated inactivator concentrations ( $\diamond$ ) 7.5 mM; ( $\blacktriangledown$ ) 5.6 mM; ( $\square$ ) 3.7 mM; ( $\blacksquare$ ) 2.5 mM; ( $\bullet$ ) 1.9 mM. (b) Replot of first-order rate constants from (a). (c) Inactivation with 5.6 mM TNPDFM in the ( $\circ$ ) absence and ( $\bullet$ ) presence of 65  $\mu\text{M}$  acarbose (Reproduced with permission from Reference 12).

cell (23  $\mu\text{M}$ ) and indicating a stoichiometry of one TNP released per enzyme molecule. Similar data were acquired with yeast  $\alpha$ -glucosidase inactivated by TNPDFG, a value of  $k_i/K_i = 0.25 \text{ min}^{-1} \text{ mM}^{-1}$  being obtained. In this case again, a competitive inhibitor, 1-deoxynojirimycin (45  $\mu\text{M}$ ,  $K_i = 12.6 \mu\text{M}$ ), was shown to protect the enzyme against inactivation, reducing the rate of inactivation in the presence of 1.6 mM TNPDFG from 0.13  $\text{min}^{-1}$  to 0.073  $\text{min}^{-1}$ . No reactivation ( $k_{\text{cat}} = 0$ ) of either inactivated enzyme was seen when a sample of the inactivated enzyme was dialysed to remove excess inactivator, then incubated for up to 30 days and aliquots removed for assay. These new inactivators therefore appear to work by forming stable 2-deoxy-2,2-difluoro glycosyl-enzyme intermediates at the active sites of their respective enzymes. In addition to providing a new class of mechanism-based inactivators of glycosidases, indeed the first such class for  $\alpha$ -glycosidases to function *via* the trapping of an intermediate, these inactivators provide strong evidence for the commonality of mechanisms of retaining  $\alpha$ - and  $\beta$ -glycosidases.

**Trapping the intermediate on  $\alpha$ - and  $\beta$ -glycosidases: 5-fluoro glycosyl fluorides.** While the previously described 2,2-difluoro sugar strategy was being developed, an alternative strategy was explored which had the potential for generating inactivators not only of  $\alpha$ -glycosidases but also of N-acetyl hexosaminidases. These latter enzymes are not susceptible to the 2-fluoro strategy as a consequence of their crucial 2-substituent. This alternative approach involved placing the electronegative fluorine not at the 2-position, but at the electronically similar 5-position. Such 5-fluoro glycosides with good leaving groups might be expected to inactivate retaining glycosidases by formation of a stabilized 5-fluoro glycosyl-enzyme intermediate through a trapping mechanism analogous to that of the 2-deoxy-2-fluoro glycosides. A sterically conservative fluorine substituent at C5 of a glycosyl oxocarbenium ion exerts electronic effects similar to or greater than those of a C2 fluorine, both atoms being adjacent to centres of developing positive charge. However, crucial transition state binding interactions between the enzyme and the usual C2 substituent which are disrupted in the case of the 2-deoxy-2-fluoro sugars are still possible for the 5-fluoro glycosides (13).

Synthesis of the 5-fluoroglycosyl fluorides hinged upon the known radical photobromination reaction at C5 of per-O-acetylated  $\beta$ - and  $\alpha$ -glucosyl fluorides (14-16). Thus bromination of the per-O-acetylated  $\beta$ - and  $\alpha$ -glucosyl fluorides with N-bromosuccinimide yielded the protected 5-bromoglycosyl fluorides. Fluorination of the protected 5-bromo- $\beta$  glucosyl fluoride ( $\text{AgBF}_4$ , toluene) afforded the protected 5-fluoro- $\beta$ -D-glucosyl fluoride, but unfortunately only in low yield. 5-Fluoro  $\alpha$ -glucosyl fluoride (2) was synthesized by treatment of the protected 5-bromo  $\alpha$ -glucosyl fluoride with fluoride ( $\text{AgF}$ ,  $\text{CH}_3\text{CN}$ ), followed by  $\text{HF/pyridine}$ . Deacetylation ( $\text{NH}_3$ ,  $\text{CH}_3\text{OH}$ ) and chromatography (27:2:1 EtOAc/ $\text{CH}_3\text{OH}/\text{H}_2\text{O}$ ) on silica gel yielded the desired 5-fluoroglycosyl fluorides which were characterised by NMR, and elemental analysis.

5-Fluoro- $\beta$ -D-glucosyl fluoride (5F $\beta$ GluF, 1) inactivated Abg according to essentially pseudo-first order kinetics, though inactivation, particularly at lower inactivator concentrations, did not proceed to completion (Figure 3) (13). This is consistent with the kinetic model shown in the previous section in which turnover ( $k_{\text{cat}}$ ) of the glycosyl-enzyme is significantly slower than its formation ( $k_i$ ) at high, but not low, inactivator concentrations. A re-plot of the rate

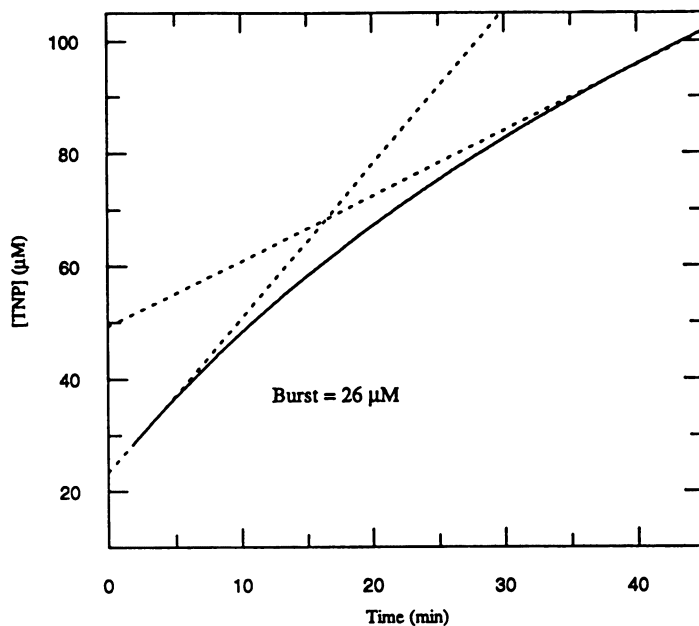


Figure 2: Release of TNP from the reaction mixture containing 0.49 mM TNPDM and 0.023 mM  $\alpha$ -amylase (Reproduced with permission from Reference 12).

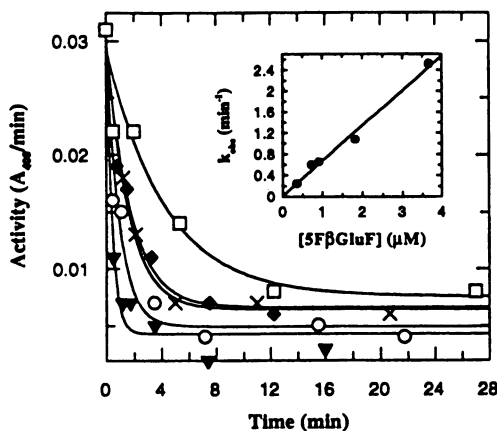
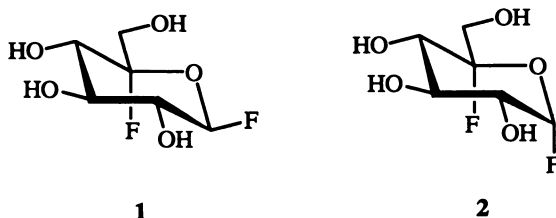


Figure 3: Inactivation of *Agrobacterium*  $\beta$ -glucosidase by 5F $\beta$ GluF. Enzyme was incubated with the following concentrations of 5F $\beta$ GluF and aliquots assayed with p-nitrophenyl  $\beta$ -D-fucoside at the indicated times: 3.68  $\mu$ M ( $\blacktriangledown$ ), 1.84  $\mu$ M ( $\circ$ ), 0.921  $\mu$ M ( $\times$ ), 0.736  $\mu$ M ( $\blacklozenge$ ), 0.368  $\mu$ M ( $\square$ ). Inset: replot of rate constants from Figure 1 (Reproduced with permission from Reference 13).





constants from the initial exponential phase was linear at concentrations up to  $3.7 \mu\text{M}$  (Figure 3, Inset), beyond which inactivation became too rapid to accurately measure. Thus saturation of the binding site is not observed within this range. Nonetheless, a second order rate constant of  $k_i/K_i = 660 \text{ min}^{-1}\text{mM}^{-1}$  was obtained from the slope of this plot. The competitive inhibitor castanospermine ( $K_i = 3 \mu\text{M}$ ) protected the enzyme against inactivation, a concentration of  $4.7 \mu\text{M}$  reducing the pseudo-first order rate constant of inactivation by  $1.84 \mu\text{M}$   $5\text{F}\beta\text{GluF}$  from  $1.07$  to  $0.18 \text{ min}^{-1}$ .

The covalent nature of the inactivation reaction was shown by ultrafiltration of the sample to remove excess inactivator, when assay revealed that the enzyme was still inactive. However, upon incubation in buffer at  $37^\circ\text{C}$ , a first-order recovery of enzyme activity was observed ( $k_{\text{cat}} = 0.082 \text{ min}^{-1}$ , corresponding to  $t_{1/2} = 8.5 \text{ min}$ ). This indicates that a covalent, but catalytically competent intermediate has been formed, and that it is capable of normal turnover, but at a greatly reduced rate. This finding is supported by electrospray mass spectral analysis of the  $5\text{F}\beta\text{Glu}$ -inactivated  $\beta$ -glucosidase which showed that the mass of the protein increased from  $51,216 \pm 6 \text{ Da}$  to  $51,397 \pm 6 \text{ Da}$  upon inactivation. This increase of  $181 \pm 12 \text{ Da}$  is that expected for the covalent attachment of *one* 5-fluoro glucosyl moiety ( $181 \text{ Da}$ ). A further measure of the effectiveness of this inhibitor is provided by the steady state  $K_i'$  value of  $0.3 \mu\text{M}$  determined, one of the best inhibitors yet found for this enzyme.

Similar accumulation of an intermediate occurred with yeast  $\alpha$ -glucosidase using the  $\alpha$  analogue, but this was reflected slightly differently in the kinetic behaviour observed. Incubation of yeast  $\alpha$ -glucosidase with 5-fluoro- $\alpha$ -D-glucosyl fluoride ( $5\text{F}\alpha\text{GluF}$ , 2) resulted in very rapid inhibition, even when assayed at the shortest possible time intervals. Indeed no time-dependence could be observed, the inactivation event being complete within the time of mixing. However, complete inhibition was not observed since turnover of the intermediate ( $k_{\text{cat}}$ ) was also rapid, allowing the establishment of a significant steady-state rate. The consequence of this was that  $5\text{F}\alpha\text{GluF}$  functions as a slow substrate, but one for which formation of the intermediate is much faster than its turnover. This was explored by following the turnover with a fluoride ion electrode. Incubation of  $5\text{F}\alpha\text{GluF}$  with  $\alpha$ -glucosidase was shown to result in slow release of two ( $2.0 \pm 0.3$ ) equivalents of fluoride. The time course of fluoride release was linear over virtually the entire course of the hydrolysis reaction, even at micromolar concentrations of  $5\text{F}\alpha\text{GluF}$ . The absence of any significant observable curvature in this plot as the concentration dropped indicates that the substrate has a *very* low  $K_m (= K_i')$  value: the slope of the plot yielded a  $k_{\text{cat}}$  value of  $6.6 \text{ min}^{-1}$ . This very tight binding, due to the significant accumulation of an intermediate, precluded direct determination of the  $K_m$  value due to the insensitivity of the fluoride electrode at the low concentrations

required. However, a steady-state  $K_i'$  of 1.4  $\mu\text{M}$  was determined, one of the lowest such values yet seen with yeast  $\alpha$ -glucosidase.

Similar inactivation was observed with 5-fluoro- $\beta$ -L-idosyl fluoride (5F $\beta$ IdoF), the C-5 epimer of 5F $\alpha$ GluF, though in this case the inactivation process was slower ( $K_i = 1.8 \text{ mM}$  and  $k_i = 1.4 \text{ min}^{-1}$ ) (17). However, the reactivation reaction was also much slower ( $t_{1/2} = 330 \text{ min}$ ), allowing formation of a relatively stable intermediate.

### Identification of the active site nucleophile in yeast $\alpha$ -glucosidase.

The fact that the 5-fluoroglycosyl enzyme accumulates at the active site of the yeast  $\alpha$ -glucosidase afforded the opportunity to identify the active site nucleophile of this enzyme which belongs to a large and important "super-family" of sequence-related  $\alpha$ -glycosidases and  $\alpha$ -glycosyl transferases. The approach followed involved digesting a reaction mixture of enzyme plus inhibitor with the acid protease pepsin, thereby obtaining a mixture of peptides, one of which contained the glycosylated amino acid of interest. This peptide was located and then sequenced by use of tandem mass spectrometry (18-20), as follows.

Peptic digestion of the 5F $\beta$ Ido-labeled yeast  $\alpha$ -glucosidase resulted in a mixture of peptides which was separated by HPLC using the mass spectrometer as a detector yielding the total ion chromatogram (TIC) shown in Figure 4A (17). The labeled peptides were identified in a second run using tandem mass spectrometry in neutral loss mode, in which the ions are subjected to limited fragmentation by an inert gas in a collision cell. Under these conditions the ester bond between the inhibitor and the peptide undergoes homolytic cleavage resulting in loss of a neutral sugar, thus the peptide of interest decreases in mass by an exactly known amount. The two quadrupoles are therefore scanned in a linked mode so that only those ions differing by the mass of the label could be detected.

Scanning in neutral loss mode for the mass loss  $m/z$  181 from a singly-charged peptide revealed two peaks (Figure 4B) in the 5F $\beta$ Ido-labeled digest that were absent in an unlabeled, control digest (Figure 4C). The strong peak at 18.9 min was due to a singly-charged labeled peptide measured at  $925 \pm 1$  (Figure 4D), corresponding to a singly-charged unlabeled peptide of mass  $745 \pm 1$  (i.e.,  $925 - 181 + 1$ ). The less intense peak at 20.5 min was due to a singly-charged labeled peptide measured at  $1073 \pm 1$  (Figure 4E), corresponding to a singly-charged unlabeled peptide of mass  $893 \pm 1$ . Inspection of the protein sequence revealed six possible candidate singly-charged peptides of mass  $745 \pm 1$ , and only twelve of mass  $893 \pm 1$ . However, only two individual glutamic or aspartic acids, residues which are known to act as catalytic nucleophiles in glycosidases, were present in candidate peptides of *both* masses. These residues were Asp-214 in peptides RIDTAGL (residues 212-218) and FRIDTAGL (211-218), and Glu-390 in peptides GQEIGQI (388-394) and VYQGQEI (385-392). Further, of these, only Asp-214, is highly conserved among this family of proteins as would be expected of a catalytically essential residue (21, 22), and the following data show that the peaks observed at  $m/z$  925 and 1073 indeed correspond to labeled peptides with the sequences RIDTAGL and FRIDTAGL.

The first technique applied to the definitive identification of these candidate peptides involves tandem mass spectrometry to fragment the selected ions by collision-induced dissociation (CID) and detect the fragments so generated. Daughter ion scans of the 5F $\beta$ Ido-derived peak at  $m/z$  925 at increased collision gas energy resulted in loss of the label giving rise to the peak at  $m/z$  745 along with a series of other fragments (Figure 5). The peak at  $m/z$

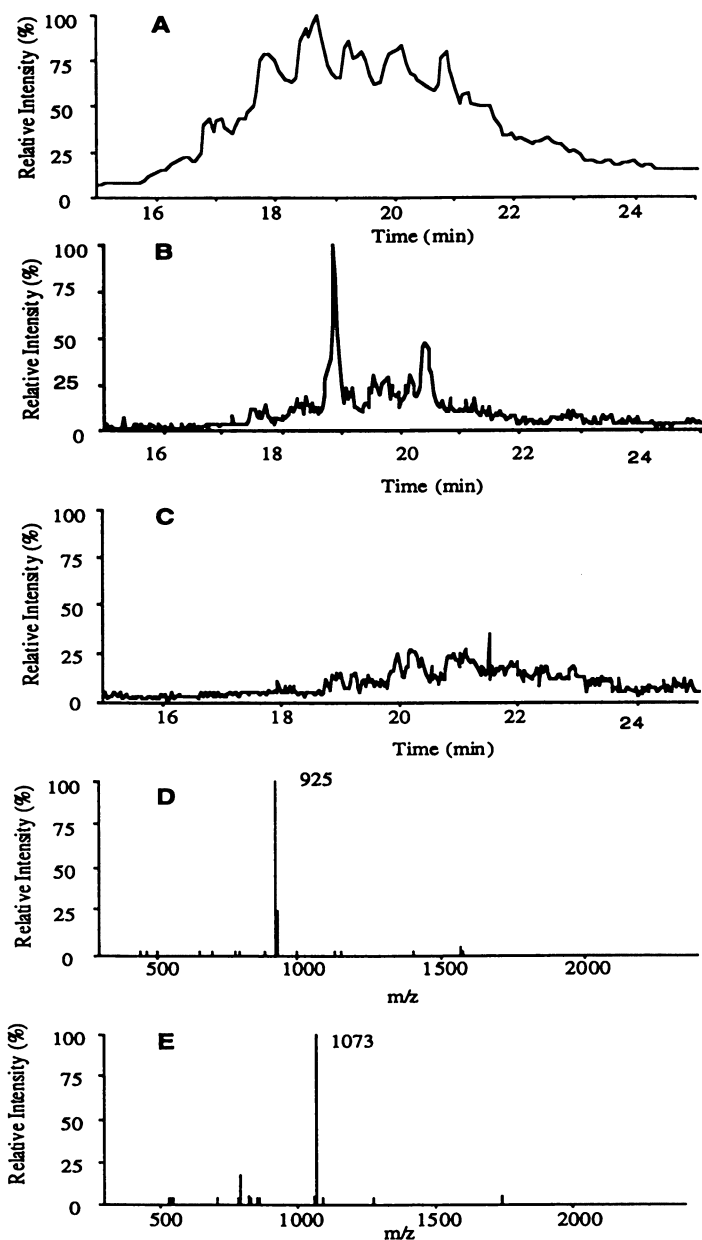


Figure 4. ESMS experiments on  $\alpha$ -glucosidase proteolytic digests. (A) Labeled with 5F $\beta$ I do, TIC in normal MS mode, (B) labeled with 5F $\beta$ I do, TIC in neutral loss mode, and (C) unlabeled, in neutral loss mode. (D) Mass spectrum of peptide at 18.9 min in panel B (E) Mass spectrum of peptide at 20.5 min in panel B (Reproduced with permission from Reference 17).

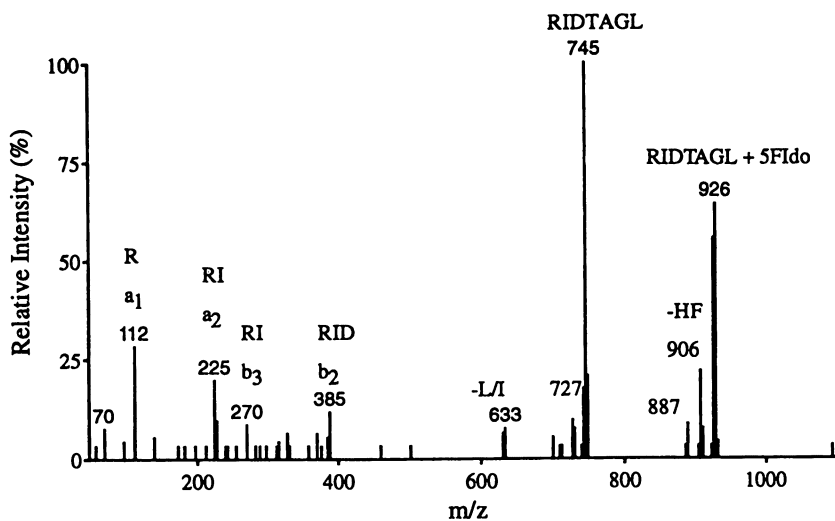


Figure 5. Tandem MS/MS daughter ion spectrum of the 5F $\beta$ Ido-labeled active site peptide ( $m/z$  925 in the singly-charged state).

906 is consistent with the elimination of HF (-20) from the 5-fluoro glycosyl-labeled peptide. Ions at  $m/z$  887 and 727 are consistent with elimination of water (-18) from threonine-containing peptides at  $m/z$  906 and 745. The peak at  $m/z$  633 is likely due to side chain loss from leucine and isoleucine. Further peptide bond fragmentation was also observed, with ions at  $m/z$  385 ( $b_2$ ) and 270 ( $b_3$ ) corresponding to arginylisoleucyl-aspartyl and arginylisoleucyl species resulting from losses of TAGL and DTAGL fragments, respectively, from the C-terminus of the parent peptide. Typical of arginine-containing peptides,  $a_n$  ions were observed, both arginylisoleucyl and arginyl species at  $m/z$  225 ( $a_2$ ) and 112 ( $a_1$ ) having also lost ammonia (-17). These data indicate that the labeled peak at  $m/z$  925 has the sequence RIDTAGL.

Further confirmation of the sequence was obtained by high resolution liquid secondary ion mass spectrometry (LSIMS) of the 5F $\beta$ Ido-derived peptides. The accurate masses, determined by LSIMS, of the peaks at  $m/z$  925 and 745 (putatively the labeled and unlabeled RIDTAGL peptides in the singly-charged state) were 925.46193 and 745.41832, respectively. Of the possible candidates, *only* the 5-fluoro glycosyl-labeled RIDTAGL species (calculated mass 925.46423,  $\Delta m = 2.48$  ppm) is consistent with this mass, and *only one* possible peptide has a mass within 5 ppm of the measured 745.41832 mass of the unlabeled peptide: RIDTAGL, with a calculated mass of 745.42082 ( $\Delta m = 3.36$  ppm). These results therefore confirm that Asp 214 is the catalytic nucleophile in yeast  $\alpha$ -glucosidase.

The aspartic acid equivalent to Asp-214 is absolutely conserved in all members of Family 13 glycosyl hydrolases (Figure 3), and it has been suggested previously that this residue could be the catalytic nucleophile in this family (22, 23). Consistent with the assignment of a catalytic nucleophilic role to Asp-214, mutagenesis of the equivalent residue (Asp-176) in the *Bacillus subtilis*  $\alpha$ -amylase of Family 13 to asparagine results in the expected drastic reduction in activity, from 8500 Units in the wild-type to  $< 0.069$  Units in the mutant with starch as substrate, a  $> 10^5$ -fold reduction in wild-type activity (24).

### Conclusions

Deoxyfluoro sugars have therefore proved to be extremely valuable probes of the mechanisms of glycosidases. They have provided useful insights into the role of hydrogen bonding interactions in stabilisation of enzyme-substrate interactions, both in the ground state and at the all-important transition state. They have also, largely as a consequence of the electronegativity of the fluorine substituent, allowed the trapping of the glycosyl-enzyme intermediate in catalysis when positioned adjacent to centres of positive charge development at the transition state. In this way several new classes of mechanism-based inactivators of both  $\alpha$ - and  $\beta$ -glycosidases have been developed and used to identify the key active site nucleophiles in these enzymes.

### Acknowledgments

We thank the Natural Sciences and Engineering Research Council of Canada, the Medical Research Council of Canada and the Protein Engineering Network of Centres of Excellence of Canada for financial support. We also thank Dr. Ruedi Aebersold for access to electrospray mass spectrometry facilities.

**Literature cited**

1. McCarter, J., D. and Withers, S. G. *Current Opinion in Structural Biology*. **1994**, *4*, 885-892.
2. Sinnott, M. L. *Chem. Rev.* **1990**, *90*, 1171-1202.
3. Koshland, D. E. *Biol. Rev.* **1953**, *28*, 416-436.
4. Jencks, W. P. *Adv. Enzymol.* **1975**, *43*, 219-410.
5. Street, I. P., Armstrong, C. R. and Withers, S. G. *Biochemistry* **1986**, *25*, 6021-6027.
6. Street, I. P., Rupitz, K and Withers, S. G. *Biochemistry* **1989**, *28*, 1581-1587.
7. Namchuk, M. and Withers, S. G. *Biochemistry* **1996**, *34*, 16194-16202.
8. Withers, S. G., Street, I. P., Bird, P. and Dolphin, D. H. *J. Am. Chem. Soc.* **1987**, *109*, 7530-7531.
9. Withers, S. G. and Street, I. P. *J. Amer. Chem. Soc.* **1988**, *110*, 8551-8553.
10. Street, I. P., Kempton, J. B. and Withers, S. G. *Biochemistry* **1992**, *31*, 9970-9978.
11. Withers, S. G. and Aebersold, R. *Protein Science* **1995**, *4*, 361-372.
12. Braun, C., Brayer, G. D. and Withers, S. G. *J. Biol. Chem.* **1995**, *270*, 26778-26781.
13. McCarter, J. D. and Withers, S. G. *J. Amer. Chem. Soc.* **1995**, *118*, 241-242.
14. Praly, J. P. and Descotes, G. *Tetr. Lett.* **1987**, *28*, 1405-1408.
15. Somsák, L. and Ferrier, R. J. *Adv. Carb. Chem. Biochem.* **1991**, *49*, 37-92.
16. Ferrier, R. J. and Tyler, P. J. *C. S. Perkin I* **1980**, 1528-1534.
17. McCarter, J. D. and Withers, S. G. *J. Biol. Chem.* **1996**, *271*, 6889-6894.
18. Busch, K. L. and Cooks R. G. *In* John Wiley & Sons: New York, **1983**.
19. Hess, D., Covey, T. C., Winz, R., Brownsey, R. and Aebersold, R. *Prot. Sci.* **1993**, *2*, 1342-1351.
20. Miao, S., McCarter, J. D., Grace, M., Grabowski, G., Aebersold, R., and Withers, S. G. *J. Biol. Chem.* **1994**, *269*, 10975-10978.
21. Svensson, B. *Plant Mol. Biol.* **1994**, *25*, 141-157.
22. Svensson, B. and Sogaard, M. *J. Biotechnol.* **1993**, *29*, 1-37.
23. Mooser, G. *In* *The Enzymes*; Academic Press Inc.: 1992; pp 187-233.
24. Takase, K., Matsumoto, T., Mizuno, H. and Yamane, K. *Biochim. Biophys. Acta* **1992**, *1120*, 281-288.

## Chapter 21

# **<sup>19</sup>F-Labeled Amino Acids as Structural and Dynamic Probes in Membrane-Associated Proteins**

Zhen-Yu Sun, E. Ann Pratt, and Chien Ho<sup>1</sup>

Department of Biological Sciences, Carnegie Mellon University,  
Pittsburgh, PA 15213

<sup>19</sup>F-NMR spectroscopy, combined with genetic engineering techniques, provides an excellent means to study membrane-associated proteins labeled with <sup>19</sup>F-labeled amino acids. Site-specific mutagenesis can be used to replace individual amino acids for NMR resonance assignments, and to insert additional <sup>19</sup>F-labeled amino acids for probing the local environment and global conformational changes of proteins. Specific information, such as solvent exposure, local mobility, proximity to lipophilic probes in the membrane-binding region, conformational change induced by substrate binding, as well as internuclear distance measured by solid-state NMR experiments, can be obtained.

Membrane proteins make up as much as 50% of the cell membrane by weight, and carry out many important biological functions. Because membrane proteins contain hydrophobic transmembrane domains or membrane-binding regions, they tend to aggregate, thus making it difficult to grow protein crystals for X-ray crystallography studies. The molecular size of membrane proteins and their complexes is often larger than 25,000, which restricts the use of conventional nuclear magnetic resonance (NMR) spectroscopy for solution structure determination. As a consequence, membrane proteins have been less studied than soluble cytoplasmic proteins. Our laboratory has obtained very fruitful results using a combination of <sup>19</sup>F-labeled amino acids, <sup>19</sup>F-NMR spectroscopy, and genetic engineering techniques to study a number of membrane-associated proteins.

### **Examples of Membrane-Associated Proteins Studied and Advantages of <sup>19</sup>F-NMR**

We have chosen two model systems for study: the periplasmic binding proteins, including the histidine-binding protein J (J protein) of *Salmonella typhimurium* and the glutamine-binding protein (GlnBP) of *Escherichia coli*; and the membrane-associated respiratory protein D-lactate dehydrogenase (D-LDH) from *E. coli*.

Periplasmic binding proteins bind specific substrates, such as sugar and amino acids, and interact with corresponding membrane-bound transport proteins to

<sup>1</sup>Corresponding author

facilitate the transport of such substrates across the cytoplasmic membrane (1). The genes for both J protein and GlnBP have been cloned and sequenced (2,3). Each protein has a molecular weight of about 25,000, and binds the amino acid L-histidine or L-glutamine respectively with very high affinities. D-LDH is a membrane-associated primary respiratory enzyme that catalyzes the oxidation of D-lactate to pyruvate, and subsequently transfers two electrons and two protons to the electron-transfer chain (4,5). The gene for D-LDH has also been cloned and sequenced (6-8). D-LDH has a molecular weight of 65,000, and contains a cofactor, flavin adenine dinucleotide (FAD). The enzyme activity of D-LDH is enhanced in the presence of a variety of detergents and lipids, and detergent is required during the isolation and purification of the protein (9,10).

<sup>19</sup>F-Labeled amino acids, such as fluorotryptophan, fluorophenylalanine and fluorotyrosine, can be biosynthetically incorporated into the proteins of interest to be studied by <sup>19</sup>F-NMR spectroscopy. <sup>19</sup>F-NMR spectroscopy has many unique advantages (11,12). The <sup>19</sup>F nuclear spin (spin 1/2) has very high NMR sensitivity, about 83% of that of <sup>1</sup>H. <sup>19</sup>F also has a natural abundance of 100% with very low background signals in <sup>19</sup>F-NMR spectra. The <sup>19</sup>F-NMR resonances have a large range of chemical shift values, making it easier to detect small changes in the chemical environment surrounding the <sup>19</sup>F labels. In typical situations, there are usually very few <sup>19</sup>F-labeled amino acid residues in the <sup>19</sup>F-labeled proteins being studied; hence, the <sup>19</sup>F-NMR spectra are much simpler and better resolved compared with the <sup>1</sup>H-NMR spectra. The <sup>19</sup>F chemical shifts in the <sup>19</sup>F-NMR spectra are expressed relative to trifluoroacetic acid (TFA), and the <sup>1</sup>H chemical shifts are expressed relative to tetramethylsilane (TMS).

### **Incorporation of <sup>19</sup>F-Labeled Amino Acids and Site-Specific Mutagenesis**

<sup>19</sup>F-Labeled amino acids may be incorporated by using auxotrophic strains of bacteria in which to express the proteins. The fluorine substitution of a single aromatic proton of Trp, Phe or Tyr generally does not cause significant perturbation to the protein structure (11,12). This is evident by testing the function of the fluorine-labeled proteins and comparing to the unlabeled ones. The L-glutamine transport activity of 6F-Trp-labeled GlnBP (two Trp residues) (13), the L-histidine binding property of 5F-Trp-labeled J protein (one Trp residue) (14), and the enzymatic activities of 4F-, 5F-, and 6F-Trp-labeled wild-type D-LDH (five Trp residues) (15,16), are essentially the same as the unlabeled proteins. The incorporation efficiencies of F-Trp labeling range from 64 to 80% in our studies. D-LDH has also been labeled with *m*-, *p*-, and *o*-F-Phe (26 Phe residues), and *m*-F-Tyr (23 Tyr residues) (17). These F-Phe- and F-Tyr-labeled proteins have similar enzyme kinetic parameters compared with the unlabeled D-LDH, although the incorporation efficiencies, about 15%, are much lower.

In many cases involving F-Trp labeling, multiple <sup>19</sup>F resonance peaks are observed when the <sup>19</sup>F-labeled proteins contain more than one Trp residue. The assignments of these peaks can be accomplished by replacing the Trp residues one at a time with other amino acids using site-specific mutagenesis. For example, GlnBP contains Trp residues at the amino acid positions 32 and 220. To assign the <sup>19</sup>F resonances, two mutants, GlnBP(W32Y) and GlnBP(W220Y), were generated by substituting Tyr for Trp (13). The <sup>19</sup>F resonance peaks corresponding to W32 and W220 are readily identified when comparing the <sup>19</sup>F-NMR spectra of the 6F-Trp-labeled wild-type and mutant proteins (Figure 1). For the larger size protein D-LDH, all five Trp resonances in the 4F-, 5F-, and 6F-Trp-labeled D-LDH have been assigned to individual Trp residues by substituting Phe or Tyr for Trp (16).



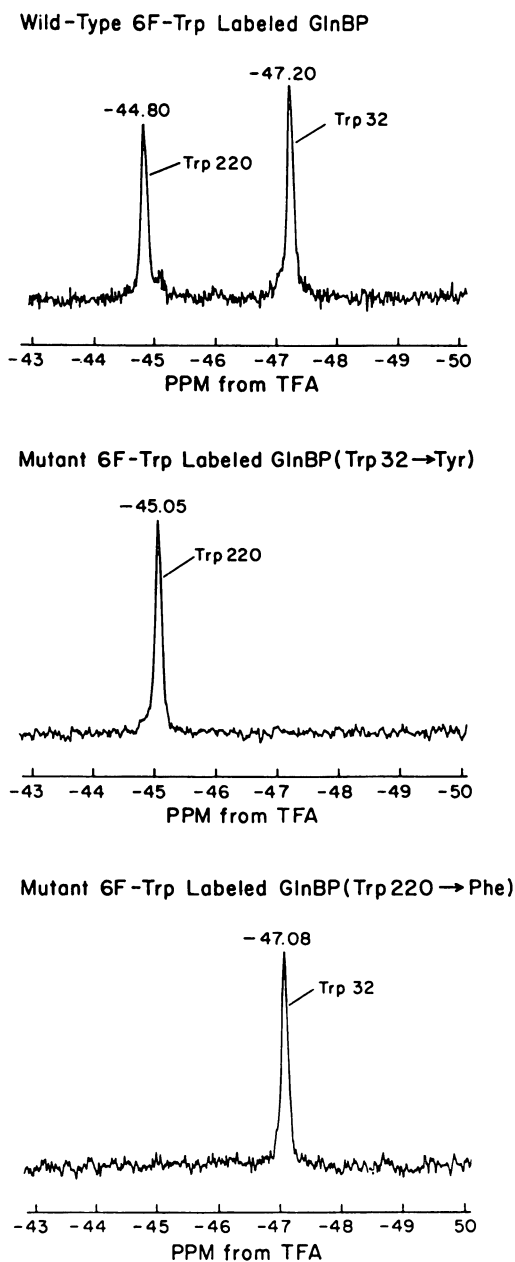


Figure 1. The 282.4 MHz  $^{19}\text{F}$ -NMR spectra of 2 mM wild-type and mutant 6F-Trp-labeled GlnBPs in 100 mM potassium phosphate (pH 7.2) in  $\text{D}_2\text{O}$  and at  $29^\circ\text{C}$ . (Reproduced with permission from ref. 13. Copyright 1989 Academic Press.)

Site-specific mutagenesis not only is very important in the assignments of <sup>19</sup>F resonances, but can also be used to introduce additional <sup>19</sup>F probes. Amino acid residues at desired locations in the protein may be replaced by F-Trp to be used as probes in addition to the native Trps, provided the protein structure is not perturbed in any significant manner. In this way, the local environment at the substitution sites throughout the entire protein polypeptide can be studied. Trp substitution for aromatic amino acid residues Phe and Tyr is less perturbing to the protein folding due to their similarity to Trp in both bulk volume and hydrophobicity (18,19). More than thirty Trp substitution mutants of D-LDH have been generated to investigate its structure-function relationship (16,17,20). The properly folded mutant D-LDHs have enzyme kinetic parameters similar to the wild-type protein, although some of them appear to be temperature-sensitive folding mutants (21).

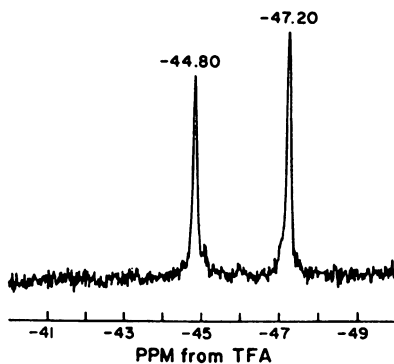
### **<sup>19</sup>F-Labeled Amino Acids Can Indicate Global Structural Change**

The chemical shift value of a <sup>19</sup>F resonance can be used to monitor the global conformational change of a protein. Protein conformational changes are often associated with the binding of the substrate or ligands to the protein. For example, the <sup>19</sup>F-NMR spectrum of the 5F-Trp-labeled J protein in the presence of excess L-histidine shows that the 5F-Trp resonance is shifted 0.6 ppm downfield when compared with the ligand-free protein, indicating a ligand-induced protein conformational change (14,22). The <sup>19</sup>F-NMR spectra of 6F-Trp-labeled GlnBP show that the binding of non-saturating amounts of L-glutamine results in the appearance of two new resonances, one -0.3 ppm upfield from the W220 resonance, the other 0.17 ppm downfield from the W32 resonance (Figure 2) (13). When excess L-glutamine is added, the original resonances disappear completely, leaving only the two new resonances in the NMR spectrum. These results indicate a conformational change of GlnBP induced by the binding of L-glutamine, and suggest that the exchange of GlnBP between the ligand-free and bound forms is slow on the NMR time scale.

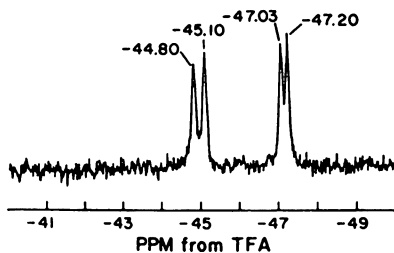
The <sup>19</sup>F-NMR spectrum of 5F-Trp-labeled wild-type D-LDH in the presence of the substrate, D-lactate, shows that the W469 resonance at -47.1 ppm is broadened and shifted downfield to -46.7 ppm (Figure 3) (16). This spectral change results from a chemical exchange process between two different conformational states. In the <sup>19</sup>F-NMR spectrum of the 5F-Trp-labeled mutant D-LDH(Y228W), the resonance from the native W469 residue appears at an even further downfield position at -46.3 ppm (17). The new resonance of W469 at -46.3 ppm and the original resonance at -47.1 ppm correspond to the two conformational states involved in the exchange process, since both are broadened and shifted to the same resonance position when D-lactate is added. In addition, small but similar broadening and shifting effects have also been observed for the 5F-Trp resonances from the native W407 and W384 residues of D-LDH. Thus, the chemical exchange effect of D-LDH upon binding of D-lactate appears to correspond to a global conformational change occurring on the NMR time scale.

<sup>19</sup>F-NMR spectroscopy has been used to study the lipid-protein interaction of 5F-Trp-labeled D-LDH (16). The <sup>19</sup>F-NMR spectra of 5F-Trp-labeled wild-type D-LDH in the presence of various lipids and detergents do not show any major protein conformational changes caused by specific protein-lipid interactions. The linewidths of the 5F-Trp resonances, however, are narrowed in the presence of lipids and detergents as a result of decreased protein aggregation. Figure 4 shows the effect of lysolecithin concentration on the <sup>19</sup>F resonance linewidths in the NMR spectra of the 5F-Trp-labeled wild-type D-LDH (16). The linewidths of the <sup>19</sup>F resonances become narrower with increasing amounts of lysolecithin. The D-LDH

## A. 1 mM 6F-Trp Labeled GlnBP



## B. 1 mM 6F-Trp Labeled GlnBP + 0.5 mM L-Gln



## C. 1 mM 6F-Trp Labeled GlnBP + 3 mM L-Gln

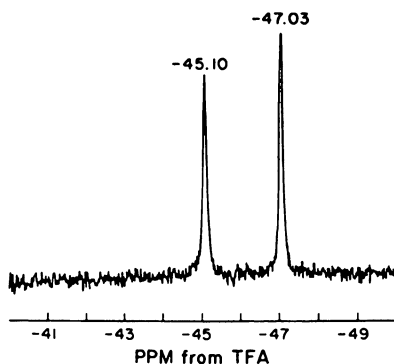


Figure 2. Effects of L-glutamine on the 282.4 MHz  $^{19}\text{F}$ -NMR spectrum of 6F-Trp-labeled GlnBP in 100 mM potassium phosphate (pH 7.2) in  $\text{D}_2\text{O}$  and at  $29^\circ\text{C}$ : (A) 1 mM 6F-Trp-labeled GlnBP; (B) 1 mM 6F-Trp-labeled GlnBP, 0.5 mM L-glutamine; and (C) 1 mM 6F-Trp-labeled GlnBP, 3 mM L-glutamine. (Reproduced with permission from ref. 13. Copyright 1989 Academic Press.)

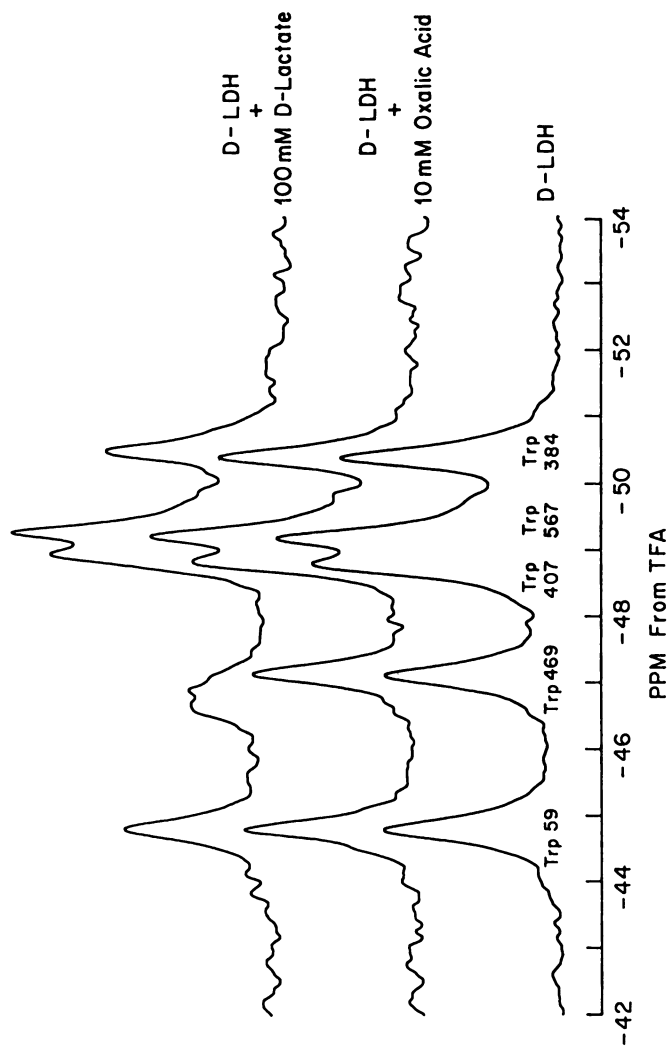


Figure 3. Effects of D-lactate and oxalate on the <sup>19</sup>F NMR spectrum of 5F-Trp-labeled D-LDH. The concentration of D-LDH was 1 mM. The  $K_i$  for oxalate is in the micromolar range; thus, all of the D-LDH will contain a bound oxalate. A large excess of D-lactate was used in order to ensure that the FAD cofactor remained reduced throughout the NMR experiment. (Reproduced with permission from ref. 16. Copyright 1987 American Chemical Society.)

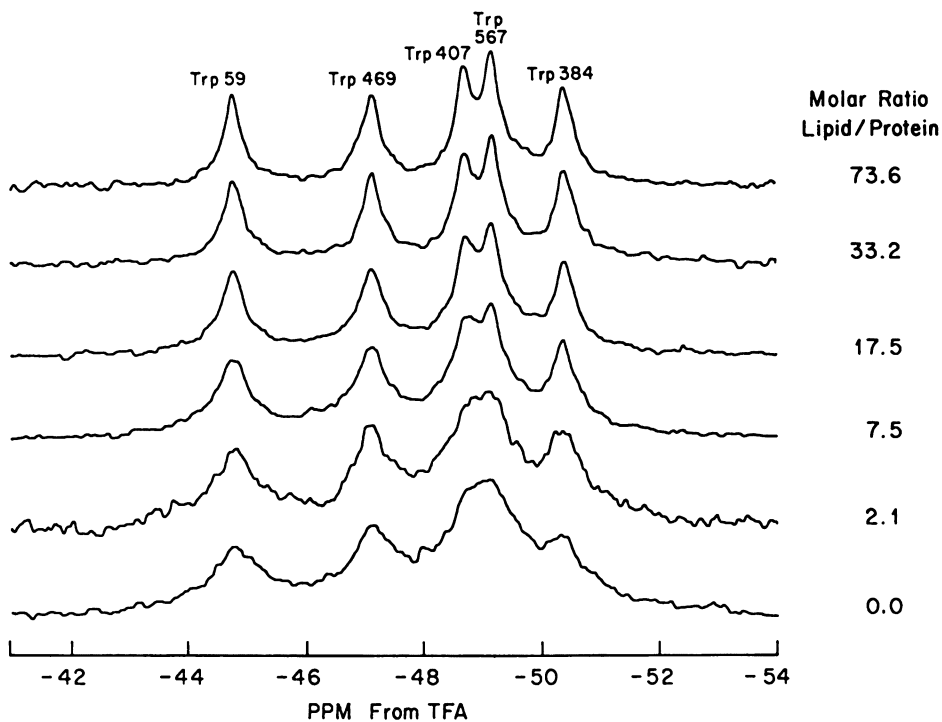


Figure 4. Effects of lysolecithin on the 282.4 MHz  $^{19}\text{F}$ -NMR spectrum of 1 mM 5F-Trp labeled D-LDH. (Reproduced with permission from ref. 16. Copyright 1987 American Chemical Society.)

molecules appear to dissociate from the protein aggregates and form protein-micelle complexes with lysolecithin molecules. From the result of this titration experiment, it was concluded that the lipid-binding region of D-LDH is small and each protein molecule would bind a maximum of 40-60 lysolecithin molecules (16).

### **<sup>19</sup>F-Labeled Amino Acids As Probes for Local Environment**

The <sup>19</sup>F resonances from <sup>19</sup>F-labeled amino acids are very sensitive to the local environment. For example, the resonance frequency of <sup>19</sup>F from 5F-tryptophan in solution is shifted 0.23 ppm downfield in H<sub>2</sub>O compared to in D<sub>2</sub>O. Similar solvent-induced isotopic shift (SIIS) effects are observed for <sup>19</sup>F labels in the protein that are exposed to the solvent (16,23). By comparing the <sup>19</sup>F-NMR spectra of F-Trp-labeled proteins in H<sub>2</sub>O and D<sub>2</sub>O, the extent of aqueous exposure for the Trp residues at various locations can be determined. The SIIS experimental results for the 6F-Trp-labeled GlnBP show that the W220 residue is sensitive to the solvent composition and is partially exposed to the solvent, while W32 is buried in the protein (Figure 5) (13). Similarly, the SIIS experimental results for 5F-Trp-labeled wild-type and Trp substitution mutant D-LDHs suggest that the amino-terminal region of D-LDH is more tightly folded, while the carboxyl-terminal region is more accessible to the solvent (20).

Cistola and Hall have used <sup>1</sup>H-<sup>19</sup>F heteronuclear NOE spectroscopy (HOESY) to probe internal water molecules in the binding pocket of the intestinal fatty-acid binding protein by using fluorinated fatty acids (24). We have carried out <sup>1</sup>H-<sup>19</sup>F HOESY experiments using a similar pulse sequence (with a 4.0-second relaxation delay time) to detect bound water in 5F-Trp-labeled D-LDH. The 2D <sup>1</sup>H-<sup>19</sup>F HOESY spectrum of 5F-Trp-labeled wild-type D-LDH in H<sub>2</sub>O in the presence of lysolecithin shows five correlation peaks between water and the <sup>19</sup>F resonances from the five Trp residues [Figure 6A(1) and (2)]. These correlation peaks indicate the presence of bound water molecules near the native Trp residues. The 2D HOESY spectrum of the 5F-Trp-labeled mutant D-LDH(F340W) in H<sub>2</sub>O in the presence of lysolecithin shows also the presence of the five native Trp peaks; but a correlation peak between water and the <sup>19</sup>F resonance from the F340W residue is absent [Figure 6B(1) and (2)]. This result suggests that the correlation peaks between water and the five native Trp residues are not due to a non-selective <sup>1</sup>H spin-diffusion effect during the 200-msec mixing time in our experiments. The HOESY spectrum of the mutant D-LDH(F340W) shows an additional correlation peak between the F340W residue and a CH<sub>2</sub> <sup>1</sup>H resonance at 1.3 ppm, possibly from the fatty acid chain of the lysolecithin molecules [Figure 6B(1)]. This result is consistent with the previous findings that the F340W residue is in the hydrophobic lipid-binding region, and is not exposed to the solvent (17,25).

The NMR relaxation rates obtained from <sup>19</sup>F resonances of the <sup>19</sup>F-labeled amino acid residues can be used to interpret the local mobility inside the protein. The NMR relaxation times and NOEs of 5F-Trp-labeled J protein have been studied extensively (14). The <sup>19</sup>F chemical shift anisotropy plays no significant role in spin-lattice relaxation, but contributes considerably to the linewidth at higher magnetic fields. The measured <sup>19</sup>F longitudinal relaxation time T<sub>1</sub> from the 5F-Trp resonance of the ligand-bound form of J protein is 0.35 sec and the true linewidth (inversely related to the transverse relaxation time T<sub>2</sub>) is 14 Hz at 27°C, all in agreement with theoretical predictions based on the assumption of Trp residue immobility. Interestingly, the linewidth of the 5F-Trp resonance of the ligand-free form of J protein is much larger compared to that of the ligand-bound form, indicating a slow fluctuation of protein conformations occurring in the ligand-free J protein. The result of the broad-band <sup>1</sup>H-<sup>19</sup>F NOE experiment shows that the <sup>19</sup>F-NMR signal

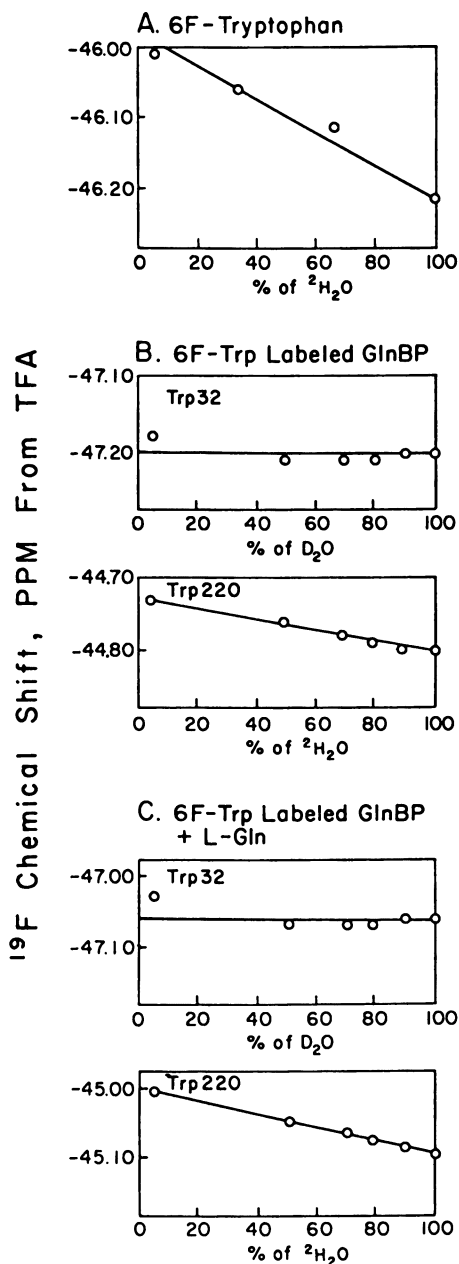


Figure 5. Effects of  $\text{D}_2\text{O}$  content on the  $^{19}\text{F}$  chemical shift of 100 mM 6F-Trp and 6 mM 6F-Trp-labeled GlnBP in 100 mM potassium phosphate (pH 7.2) and at  $29^\circ\text{C}$ : (A) 6F-tryptophan; (B) 6F-Trp-labeled GlnBP; and (C) 6F-Trp-labeled GlnBP, 20 mM L-glutamine. (Reproduced with permission from ref. 13. Copyright 1989 Academic Press.)

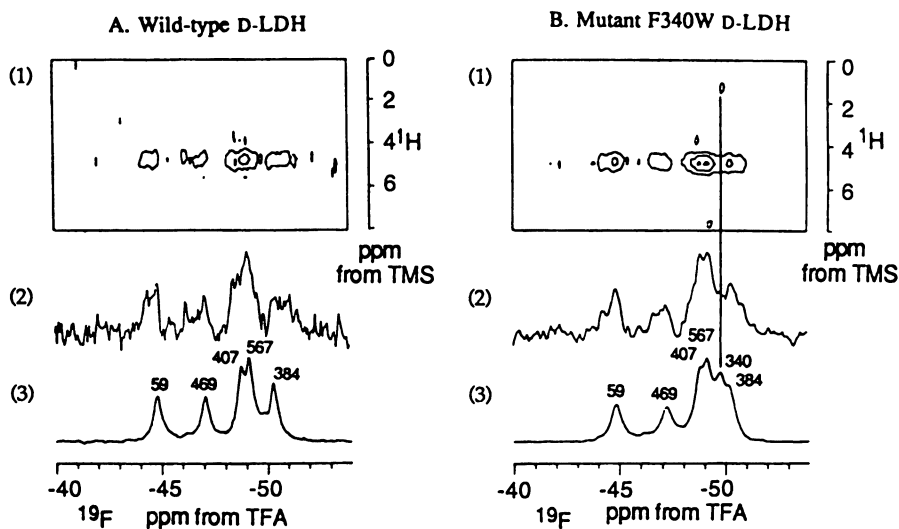


Figure 6. 2D <sup>1</sup>H-<sup>19</sup>F-HOESY spectrum (1), 1D slice at 4.6 ppm (<sup>1</sup>H) of water resonance (2), and 1D <sup>19</sup>F-NMR spectrum (3) of (A) 5F-Trp-labeled wild-type D-LDH, and (B) mutant D-LDH (F340W) in the presence of lysolecithin at 37°C. Notice in [B(1) and (2)], the correlation peak between F340W and water is missing; but there is a correlation peak between F340W and a CH<sub>2</sub> resonance possibly from lysolecithin [B(1)].



disappears completely (i.e., NOE = -1) after irradiation of the protons. This maximum NOE value is consistent with the conclusion that the Trp residue of J protein is virtually immobile. In the case of D-LDH, the NOEs of 4F- and 5F-Trp-labeled wild-type D-LDH have been measured (25). The results show that most of the NOEs from the F-Trps are not -1, indicating that local motions are occurring at these native Trp residues. Analysis of the NOEs and other dynamic data further suggest that these 5F-Trp residues may possess different modes of internal motion (25).

### **<sup>19</sup>F-Labeled Amino Acids in Combination with Nitroxide Spin Label**

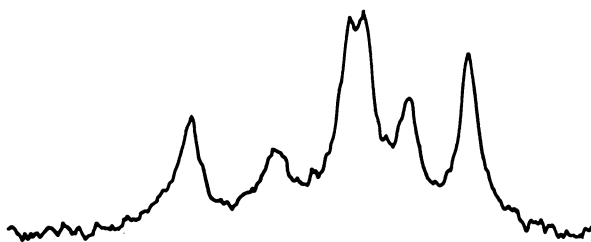
Nitroxide spin label contains one unpaired electron, which can broaden the NMR resonance of any nucleus within a radius of 15 Å (26). The combination of the use of nitroxide spin label and <sup>19</sup>F-labeled proteins can provide detailed structural information that is otherwise unavailable, such as in the case of studying the membrane-binding domain of D-LDH (17,20). As shown in Figure 7 (27), the <sup>19</sup>F-NMR spectrum of the 5F-Trp-labeled mutant D-LDH(F361W) in sonicated unilamellar vesicles (SUVs) shows a resonance peak corresponding to the F361W residue in addition to the five native Trp resonances (Figure 7A). When 8-doxyl palmitate is incorporated into the SUVs, the resonance from F361W disappears completely (Figure 7B). Moreover, the F361W resonance reappears upon reduction of the nitroxide spin label by the presence of the enzyme substrate, D-lactate (Figure 7C). These results clearly demonstrate that the F361W residue, but none of the native Trp residues, is in close proximity to the nitroxide-labeled fatty acids. Experiments using SUVs consisting in part of nitroxide-labeled lipids yield the same results, suggesting that the F361W residue is indeed in the membrane-binding region of D-LDH. The <sup>19</sup>F-NMR results of the effect of nitroxide spin-labeled fatty acids on many of the Trp-substitution mutant D-LDHs have led to the proposal of a three-domain model for D-LDH, which includes a membrane-binding domain between the catalytic and the cofactor-binding domains(20).

As an alternative approach to finding the extent of the lipid-binding region of membrane proteins by Trp substitution using individual Trp probes, one can also label a large number of hydrophobic residues at once. The size of the membrane-binding region can then be gauged by the number of the <sup>19</sup>F-labeled amino acids affected by the nitroxide-labeled lipophilic probe. <sup>19</sup>F-Labeled amino acids *m*-, *p*-, and *o*-F-Phe and *m*-F-Tyr have been incorporated separately to help map the membrane-binding region of D-LDH (17). By comparing the integrated area of the <sup>19</sup>F resonance peaks in the presence and absence of a nitroxide spin-labeled fatty acid, it was found that 9-10 Phe residues (out of 26 Phes) (Figure 8), and 3-4 Tyr residues (out of 23 Tyrs) are located in the lipid phase. These results, combined with the <sup>19</sup>F-NMR experimental results using the Trp-substitution mutants, suggest that the membrane-binding domain of D-LDH is between amino acid residues Y228 and F369, but is not continuous within this region (17).

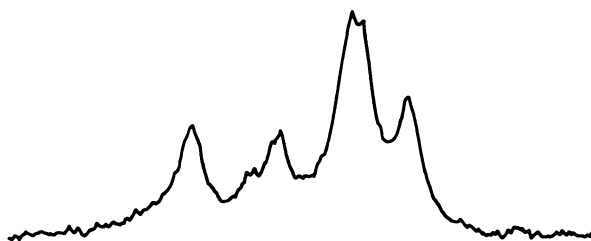
### **<sup>19</sup>F-Labeled Amino Acids Used in Internuclear Distance Measurements**

The nuclear dipolar coupling constant is proportional to the product of the gyromagnetic ratios of the two coupled nuclear spins, and inversely proportional to the internuclear distance to the third power. The gyromagnetic ratio  $\gamma_F$  of <sup>19</sup>F is 83% of that of <sup>1</sup>H, thus making <sup>19</sup>F a very sensitive probe to measure nuclear dipolar interactions. Solid-state NMR spectroscopy, combined with <sup>19</sup>F and isotopic labeling, is very useful in studying large membrane-associated proteins because of the ease of sample preparation as compared with conventional solution NMR and

C. D-LDH (Phe361→Trp) + 28 mM 8-Doxyl Palmitic Acid + 100 mM D-Lactate



B. D-LDH (Phe361→Trp) + 28 mM 8-Doxyl Palmitic Acid



A. D-LDH (Phe361→Trp)

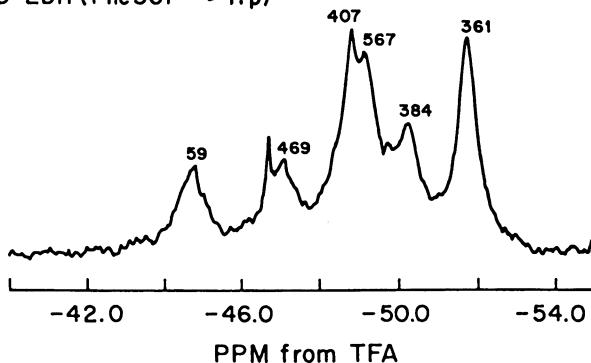


Figure 7. Effects of spin-labeled fatty acid and substrate on the 282.4-MHz <sup>19</sup>F-NMR spectrum of the F361W mutant D-LDH at 42°C in (A) SUVs, (B) SUVs containing 28 mM 8-doxyl palmitic acid, and (C) SUVs containing 28 mM 8-doxyl palmitic acid with 100 mM D-lactate added. The sharp peak at -46.7 ppm is due to contaminating F<sup>-</sup> ion from the glassware used for sonication during the preparation of the samples. (Reproduced with permission from ref. 27. Copyright 1991 American Chemical Society.)

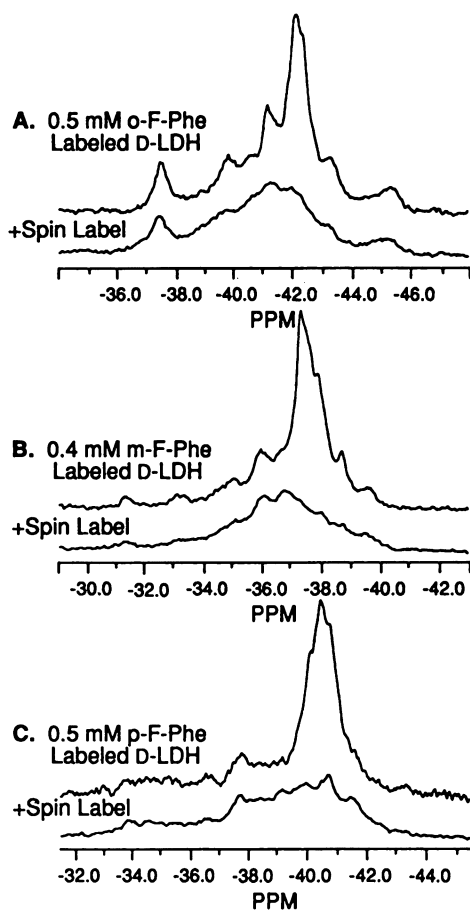


Figure 8. The 282.4 MHz  $^{19}\text{F}$ -NMR spectra of F-Phe-labeled wild-type D-LDHs in 10 mM phosphate buffer, 0.2 mM EDTA, pH 7.2, with 100 mM lysolecithin, in the absence (top) or presence (bottom) of 28 mM 8-doxyl palmitic acid: (A) 0.5 mM *o*-F-Phe-labeled D-LDH; (B) 0.4 mM *m*-F-Phe-labeled D-LDH; and (C) 0.5 mM *p*-F-Phe-labeled D-LDH. (Reproduced with permission from ref. 17. Copyright 1993 Cambridge University Press.)

X-ray crystallography studies. In solid-state NMR experiments, chemical shift anisotropy and nuclear dipolar couplings that cause severe line-broadening effects can be averaged out by using the magic angle spinning technique. The nuclear dipolar interaction can be reintroduced by applying rotor-synchronized dephasing pulses in rotational echo double resonance (REDOR) experiments (28). The resulting nuclear dipolar coupling causes dephasing of the selected NMR signal according to the dipolar coupling constant. Thus, the internuclear distance between <sup>19</sup>F and other nuclear spins, such as <sup>13</sup>C and <sup>15</sup>N, can be determined by measuring their nuclear dipolar coupling constants.

<sup>19</sup>F-REDOR NMR spectroscopy has been used to obtain detailed structural information at the ligand-binding site of GlnBP (29). The <sup>19</sup>F-labeled amino acid *m*-F-Tyr was incorporated into <sup>15</sup>N-uniformly-labeled GlnBP. <sup>15</sup>N-Observed, <sup>19</sup>F-dephased REDOR experiments were performed under the assumption that only one Tyr is involved in the binding of the substrate L-glutamine, and no ring-flipping of this Tyr residue occurs. The results of the REDOR experiments indicate an internuclear distance of 8.6 Å between a <sup>19</sup>F label and the <sup>15</sup>N<sub>δ</sub> of the His156 residue, and a distance of 8.1 Å between the <sup>19</sup>F and the <sup>15</sup>N<sub>ε</sub> of the His156 residue in the substrate-binding site. From the refined molecular model of GlnBP, these distances could be associated with the <sup>19</sup>F labels on either Tyr143 or Tyr185 of GlnBP (29). In cases when the resonances from uniform labeling are not resolved, specific double labeling is required to insert a second nuclear probe in addition to the <sup>19</sup>F-labeled amino acids. Combined with molecular dynamics calculations, this method of distance measurement using <sup>19</sup>F-labeled amino acids provides a new analytical method for selecting acceptable protein structure models.

## Summary

In summary, we have found that <sup>19</sup>F-NMR spectroscopy, in combination with genetic engineering, provides an excellent means to investigate the structure-function relationship in membrane-associated proteins of large molecular weight. By incorporating <sup>19</sup>F-labeled amino acids into the proteins of interest, detailed structural information can be determined by various <sup>19</sup>F-NMR techniques. Site-specific mutagenesis has been used both to replace specific amino acids to achieve resonance assignment, and to insert additional amino acids to probe any desired location in the protein. <sup>19</sup>F-Labeled amino acids can be used as probes to monitor global conformational changes of proteins, e.g., that induced by substrate binding, as well as to obtain information about the local environment, e.g., exposure to the solvent and mobility at the labeling site. Incorporation of 5F-Trp, combined with Trp-substitution mutants and the use of nitroxide lipophilic probes, has made it possible to produce a low-resolution map of the membrane-binding region of D-LDH. Through new techniques such as solid-state <sup>19</sup>F REDOR NMR, <sup>19</sup>F-labeled amino acids will have more applications in the structural determination of membrane-associated proteins.

## Acknowledgments

Our research on membrane-associated proteins has been supported by a research grant from the National Institutes of Health (GM-26874).

## Literature Cited

- (1) Furlong, C. E. In *Escherichia coli and Salmonella typhimurium: Cellular and Molecular Biology*; Neidhardt, F. C., Ingraham, J. L.; Low, K. B.;

- Magasanik, B; Schaechter M; Umbarger, H E., Eds.; American Society for Microbiology: Washington D.C., 1987, Vol. 1; 768-796.
- (2) Nohno, T.; Saito, T.; Hong, J.-S. *Mol. Gen. Genet.* **1986**, *205*, 260.
  - (3) Higgins, C. F.; Haag, P. D.; Nikaido, K.; Ardeshir, F.; Garcia, G.; Ames, G. F.-L. *Nature* **1982**, *298*, 723.
  - (4) Futai, M. *Biochemistry* **1973**, *12*, 2468.
  - (5) Kohn, L. D.; Kaback, H. R. *J. Biol. Chem.* **1973**, *248*, 7012.
  - (6) Young, I. G.; Jaworowski, A.; Poulis, M. *Biochemistry* **1982**, *21*, 2092.
  - (7) Campbell, H. D.; Rogers, B. L.; Young, I. G. *Eur. J. Biochem.*, **1984**, *144*, 367.
  - (8) Rule, G. S.; Pratt, E. A.; Chin, C. C. Q.; Wold, F.; Ho, C. *J. Bacteriol.* **1985**, *161*, 1059.
  - (9) Tanaka, Y.; Anraku, Y.; Futai, M. *J. Biochem.* **1976**, *80*, 821.
  - (10) Pratt, E. A.; Fung, L. W.-M.; Flowers, J. A.; Ho, C. *Biochemistry* **1979**, *18*, 312.
  - (11) Gerig, J. T. *Prog. NMR Spectrosc.* **1994**, *26*, 293.
  - (12) Ho, C.; Dowd, S. R.; Post, J. F. M. *Curr. Topic Bioenergetics* **1985**, *14*, 53.
  - (13) Shen, Q.; Simplaceanu, V.; Cottam, P. F.; Wu, J.-L.; Hong, J.-S.; Ho, C. *J. Mol. Biol.* **1989**, *210*, 859.
  - (14) Post, J. F. M.; Cottam, P. F.; Simplaceanu, V.; Ho, C. *J. Mol. Biol.* **1984**, *179*, 729.
  - (15) Pratt, E. A.; Jones, J. A.; Cottam, P. F.; Dowd, S. R.; Ho, C. *Biochim. Biophys. Acta* **1983**, *729*, 167.
  - (16) Rule, G. S.; Pratt, E. A.; Simplaceanu, V.; Ho, C. *Biochemistry* **1987**, *26*, 549.
  - (17) Sun, Z.-Y.; Truong, H.-T. N.; Pratt, E. A.; Sutherland, D. C.; Kulig, C. E.; Homer, R. J.; Groetsch, S. M.; Hsue, P. Y.; Ho, C. *Prot. Sci.* **1993**, *2*, 1983.
  - (18) Chothia, C. *Nature* **1975**, *254*, 304.
  - (19) Matsumura, M.; Becktel, W. J.; Matthews, B. W. *Nature* **1988**, *334*, 406.
  - (20) Peersen, O. B.; Pratt, E. A.; Truong, H.-T. N.; Ho, C.; Rule, G. S. *Biochemistry* **1990**, *29*, 3256.
  - (21) Truong, H.-T. N.; Pratt, E. A.; Rule, G. S.; Hsue, P. Y. N.; Ho, C. *Biochemistry* **1991**, *30*, 10722.
  - (22) Robertson, D. E.; Kroon, P. A.; Ho, C. *Biochemistry* **1977**, *16*, 1443.
  - (23) Hagen, D. S.; Weiner, J. H.; Sykes, B. *Biochemistry* **1979**, *18*, 2007.
  - (24) Cistola, D. P.; Hall, K. B. *J. Biomol. NMR* **1995**, *5*, 415.
  - (25) Ho, C.; Pratt, E. A.; Rule, G. S. *Biochim. Biophys. Acta* **1989**, *988*, 173.
  - (26) Arseniev, A. S.; Utkin, Yu. N.; Pashkov, V. S.; Tsetlin, V. I.; Ivanov, V. T.; Bystrov, V. F.; Ovchinnikov, Yu. A. *FEBS Lett.* **1981**, *136*, 269.
  - (27) Truong, H.-T. N.; Pratt, E. A.; Ho, C. *Biochemistry* **1991**, *30*, 3893.
  - (28) Gullion, T.; Schaefer, J. *J. Magn. Reson.* **1989**, *81*, 196.
  - (29) Hing, A. W.; Tjandra, N.; Cottam, P. F.; Schaefer, J.; Ho, C. *Biochemistry* **1994**, *33*, 8651.

## Chapter 22

# Fluorinated Amino Acids in Nerve Systems

**Kenneth L. Kirk and Jun-Ying Nie**

**Laboratory of Bioorganic Chemistry, National Institute of Diabetes  
and Digestive and Kidney Diseases, National Institutes of Health,  
Building 8A, Room B1A-02, Bethesda, MD 20892**

Fluorinated analogues of amino acid precursors of amine neurotransmitters have had many applications related to biochemistry and neuropharmacology. We have studied the effects of ring-fluorination on the biological properties of a series of aromatic (tyrosine, dihydroxyphenylalanine, dihydroxyphenylserine) and heteroaromatic amino acids (histidine) that function as precursors of amine neurotransmitters. In addition, we have synthesized fluorinated neurotransmitter amines (tyramine, dopamine, norepinephrine, epinephrine, serotonin, histamine) and have examined the effects of fluorine on such properties as receptor interactions and interaction with metabolic enzymes. Studies with monofluorinated analogues have now been extended to di- and trifluoro-substituted analogues.

Certain amino acids function directly as neurotransmitters, while other amino acids play important roles in neurotransmission by serving as bioprecursors of amine neurotransmitters (*I*). In both situations, modulation of biological actions of the amino acid, by changes in bio-concentration, by structural modification, or by other means, can have important effects on functioning of nerve systems. For example, administration of L-dihydroxyphenylalanine (L-DOPA) to Parkinsonian patients can alleviate symptoms of this disease owing to the resulting increase in concentration of L-DOPA-derived dopamine. In another example, drugs that cross the blood-brain barrier and inhibit the activity of  $\gamma$ -aminobutyric acid (GABA) transaminase, the enzyme responsible for inactivating GABA, an inhibitory amino acid neurotransmitter, are effective anticonvulsants.

As with other classes of compounds, fluorinated analogues of amino acids have had many useful applications in drug development. With respect to agents designed to

This chapter not subject to U.S. copyright  
Published 1996 American Chemical Society

effect neuronal function, notable examples would include the use of  $\alpha$ -fluoromethyl- and  $\alpha,\alpha$ -difluoromethylene amino acids that function as inhibitors of amino acid decarboxylases, enzymes that convert amino acids to amines, including amine neurotransmitters (2).

For several years, we have been studying the biochemistry and pharmacology of ring-fluorinated analogues of aromatic amino acids and of the amine neurotransmitters that correspond to the products of enzymatic decarboxylation of these amino acids (3). In many cases, the presence of fluorine has marked effects on biological properties. In addition, biological consequences of ring-fluorination also is often dependent on the site of fluorination, with different regioisomers having strikingly different behavior. Results of this research will be reviewed in this report (2). Synthetic methodologies will be discussed briefly, especially in cases wherein new procedures have supplanted original synthetic methods.

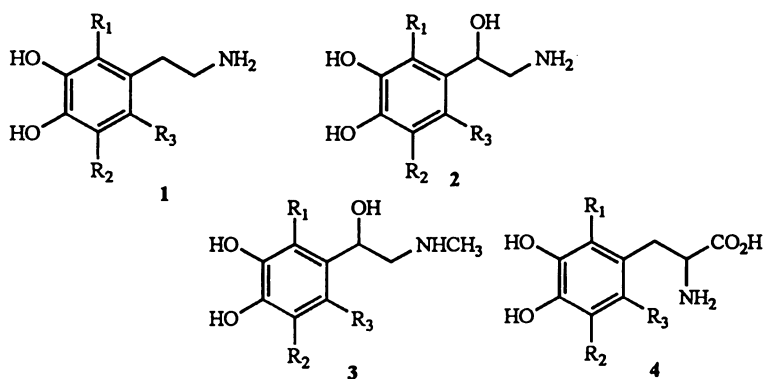
### Amino acids and Nerve Function

A brief review of the functions of amino acids in nerve systems is provided to place this work in perspective. More thorough discussions can be found in recent reviews (1).

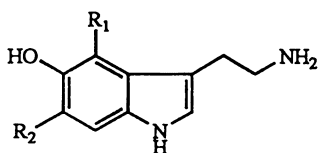
**Amino Acids as Neurotransmitters.** Several amino acids are now recognized as important neurotransmitters in the central nervous system. These are classified neuropharmacologically as excitatory or inhibitory, depending whether their initial action is to depolarize or to hyperpolarize neurons. Excitatory amino acids include glutamic acid, aspartic acid, cysteic acid, and homocysteic acid. Inhibitory amino acids are  $\gamma$ -aminobutyric acid (GABA), glycine, taurine, and  $\beta$ -alanine (all  $\omega$ -amino acids) (1).

**Amino Acids as Precursors of Amine Neurotransmitters.** The naturally occurring catecholamines, dopamine (DA) (1a), norepinephrine (NE) (2a), and epinephrine (EPI) (3a), play key roles in neurotransmission, metabolism, and in the control of various physiological processes. For example, norepinephrine is the primary neurotransmitter in the sympathetic nervous system and also functions as a neurotransmitter in the central nervous system (CNS). Epinephrine, elaborated by the adrenal gland, has potent effects on the heart, vascular and other smooth muscles, and also functions as a neurotransmitter in the CNS. Dopamine is an important neurotransmitter in the CNS, and has important peripheral effects in such organs as the kidney and heart. The catecholamines are synthesized from tyrosine in the brain, chromaffin cells, sympathetic nerves, and sympathetic ganglia. In the initial and rate-limiting step, tyrosine hydroxylase-catalyzed hydroxylation of tyrosine produces dihydroxyphenylalanine (DOPA, 4a). DOPA-decarboxylase-mediated decarboxylation of DOPA forms the neurotransmitter dopamine. In the presence of dopamine- $\beta$ -hydroxylase, norepinephrine is formed from dopamine. Phenethanolamine-*N*-methyl-transferase converts norepinephrine to epinephrine.

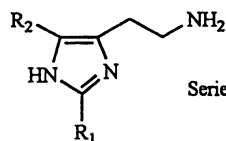
Tryptophan hydroxylase-catalyzed hydroxylation of tryptophan, followed by enzymatic decarboxylation produces 5-hydroxytryptamine (serotonin, 5-HT) (5a). In the CNS, 5-HT is closely associated with neuropsychopharmacology, having functions related to pain perception, sleep, and behavior, both normal and abnormal. 5-HT is found in



- Series a)  $R_1 = R_2 = R_3 = H$       e)  $R_1 = R_2 = F, R_3 = H$   
 b)  $R_1 = F, R_2 = R_3 = F$       f)  $R_1 = R_3 = F, R_2 = H$   
 c)  $R_2 = F, R_1 = R_3 = H$       g)  $R_2 = R_3 = F, R_1 = H$   
 d)  $R_3 = F, R_1 = R_2 = H$       h)  $R_1 = R_2 = R_3 = F$



5



6

- Series a)  $R_1 = R_2 = H$   
 b)  $R_1 = F, R_2 = H$   
 c)  $R_2 = F, R_1 = H$



many cell types, with a broad range of responses related to cardiovascular, respiratory, and gastrointestinal systems.

The action of histidine decarboxylase on histidine produces histamine (6a). Histamine is found in most mammalian tissues and elicits such responses as muscle contraction, muscle relaxation, and gastric acid secretion. Histamine is also found in the CNS.

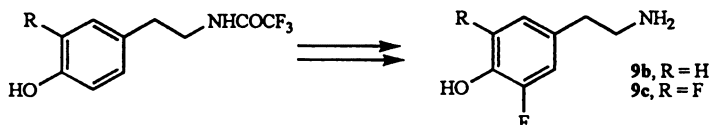
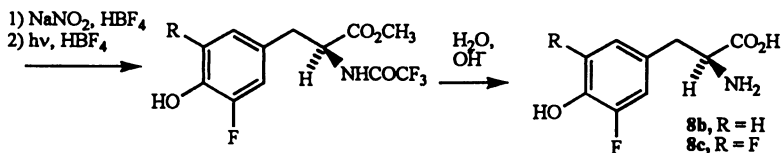
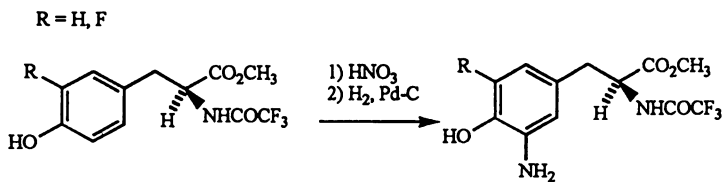
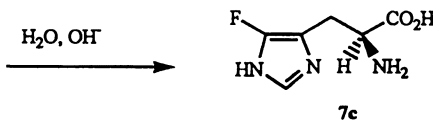
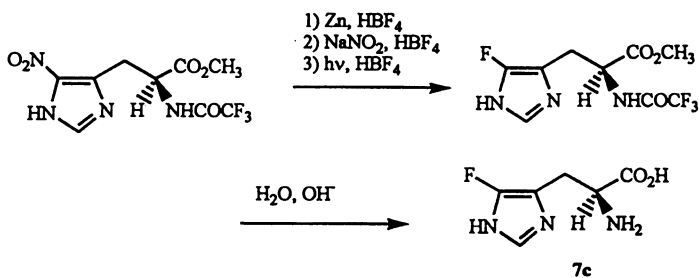
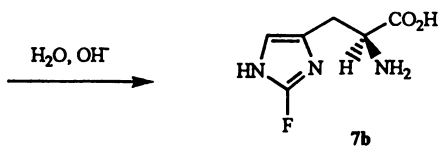
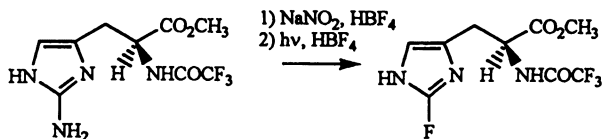
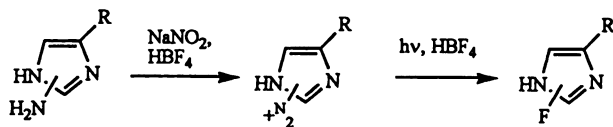
In addition to its function as an excitatory neurotransmitter, glutamate also is decarboxylated by glutamate decarboxylase to give  $\gamma$ -aminobutyric acid, an inhibitory neurotransmitter.

### **Synthesis of Ring-fluorinated Analogues of Aromatic and Heteroaromatic Amine Neurotransmitters and of Amino Acid Precursors of Amine Neurotransmitters**

**Fluorohistidines and Fluorohistamines.** When we initiated our studies over 25 years ago, we were impressed by the absence of any reports of ring-fluorinated imidazoles, in view of the importance of the imidazole ring in biology. Many of the functional and structural roles of bioimidazoles are related to the basic imidazole ring, and it seemed quite likely that introduction of fluorine could have dramatic effects on biological properties. Unfortunately, repeated attempts to prepare ring-fluorinated imidazoles using the usual fluorination procedures, such as thermal decomposition of imidazole diazonium fluoroborates, met with complete failure. This made the absence of previous reports of fluoroimidazoles more understandable. Ultimately, we discovered that, unlike thermal decomposition of imidazole diazonium fluoroborates, a procedure that usually led to intractable tars, photochemical decomposition of a series of imidazole diazonium fluoroborates cleanly produced the corresponding fluorinated derivatives (equation 1) (4). An especially attractive feature of this reaction was the fact that isolation of the intermediate diazonium salt, formed in situ by addition of aqueous sodium nitrite to a solution of the amine in fluoroboric acid, was not necessary (5). Application of this procedure to the synthesis of 2-fluoro- and 4-fluorohistidine (7b,c) is shown in equation 1 (4-6). Because of instability of most 4-aminoimidazoles, a new synthesis of these intermediates also was developed. Addition of Zn dust to a solution of the corresponding nitroimidazole in fluoroboric acid produced the amino imidazole, which then could be diazotized and irradiated in situ (equation 2) (7). Fluorohistamines were prepared analogously.

The biochemistry and pharmacology of ring-fluorinated imidazoles proved to be an exceptionally fruitful area of study. 2-Fluorohistidine had a particularly broad range of biological properties, including antibacterial, antiviral, and antimalarial activity, and served as a substrate for mammalian and bacterial protein synthesis. It did not, however, function as a substrate for histidine decarboxylase. 4-Fluorohistidine was a substrate for bacterial, but not mammalian, histidine decarboxylase. 2-Fluorohistamine had weak agonist activity at histamine receptors (8).

**Fluorotyrosines and Fluorotyramines.** The photochemical Schiemann reaction was a key step in the preparation of 3-fluoro-L-tyrosine (8b) from N-trifluoroacetyl-L-tyrosine



methyl ester. The sequence included nitration, reduction, diazotization, photolysis and deblocking. The same sequence of reactions, beginning with the intermediate *N*-trifluoroacetyl-3-fluoro-*L*-tyrosine methyl ester produced 3,5-difluoro-*L*-tyrosine (**8c**) (equation 3). Likewise, 3-fluorotyramine (**9b**) was prepared from *N*-trifluoroacetyl tyramine using this route. Repeating the scheme with the intermediate *N*-trifluoroacetyl-3-fluorotyramine gave 3,5-difluorotyramine (**9c**) (equation 4). Also produced in this sequence was *N*-trifluoroacetyl-5-fluorodopamine, presumably a product of competing water attack on the photochemically produced carbonium ion (9).

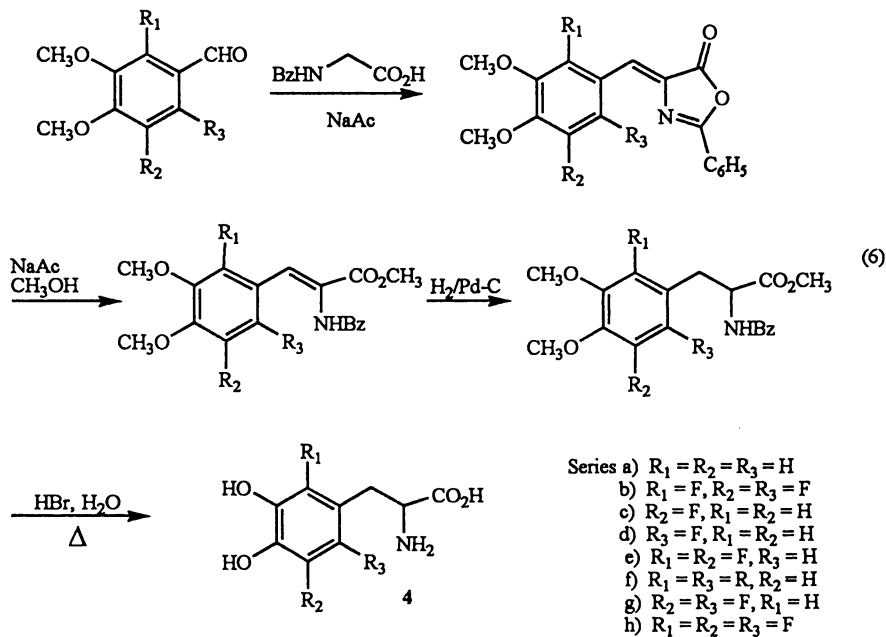
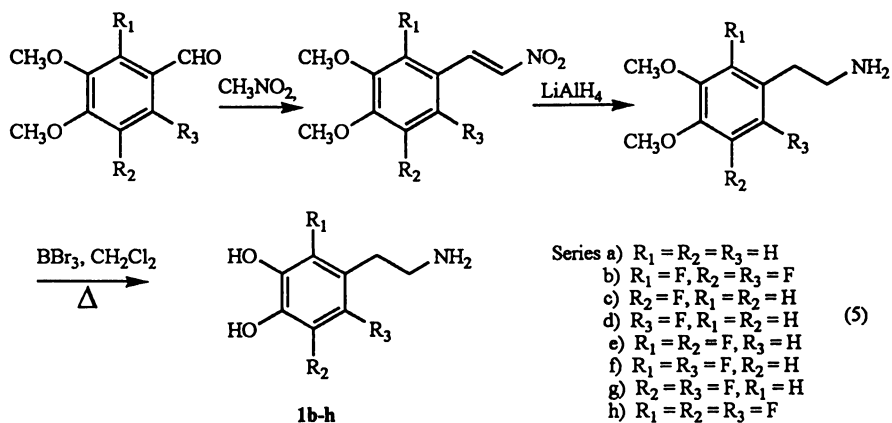
3-Fluoro-*L*-tyrosine and 2-fluoro-*L*-tyrosine (prepared subsequently by tyrosine phenol lyase catalyzed condensation of serine with 2-fluoro- and 3-fluorophenol, respectively) are oxygenated by mushroom tyrosinase, giving 5-fluoro-DOPA and 6-fluoro-DOPA, respectively (10).

**Synthesis of Fluoro-DOPA's and Fluorodopamines.** The biochemistry and pharmacology of fluorodopamines and fluoro-DOPAs have received much attention, in part because of the potential of using these analogues in PET imaging (11). As part of our work in this area, we synthesized the three monofluoro analogues of dopamine (**1b-d**) (12) and of DOPA (**4b-d**) (13,14). 6-Fluorodopamine was initially prepared from *N*-trifluoroacetyl-2-(4,5-dimethoxy-2-nitrophenyl)-ethylamine by reduction of the nitro group to the amine and carrying out the photochemical Schiemann reaction, as described above for the syntheses of 3-fluorotyramine and 3-fluoro-*L*-tyrosine (12). In later work, more convenient routes to fluorodopamines were developed based on side chain elaboration of fluoroveratraldehydes (J.-Y. Nie and K. L. Kirk, unpublished results) (equation 5) or the corresponding benzyl chlorides (15). Likewise, fluoroveratraldehydes were used as the starting point for the syntheses of ring-fluorinated DOPAs (equation 6).

2-Fluoro-, 5-fluoro-, and 6-fluoroveratraldehyde have been key intermediates for the synthesis of fluoro-DOPAs, fluorodopamines, fluoronorepinephrines, other catecholamines and amino acids, and their metabolites. In our early work, the photochemical Schiemann reaction was used to prepare these compounds from the corresponding amines (12,16). Ladd and Winstock subsequently devised a route to 2-fluoroveratraldehyde from 3-fluoroanisole (15). We later developed a convenient synthesis of 4-fluoroveratrole from 4-aminoveratrole using a variation of the thermal Schiemann reaction. Electrophilic formylation ( $\text{CH}_3\text{OCHCl}_2$ ;  $\text{TiCl}_4$ ) of 4-fluoroveratrole gave an excellent yield of 6-fluoroveratraldehyde, providing a procedure for large-scale synthesis (14). The original photochemical procedure remains our route to 5-fluoroveratraldehyde. New routes to fluorinated veratraldehydes based on electrophilic fluorination are discussed below.

**Fluorinated Norepinephrines and Fluorinated Epinephrines.** The syntheses of the fluorinated analogues of norepinephrine from precursor fluorobenzaldehydes are shown in equation 7 (15).

**Fluorinated 5-Hydroxytryptamines (Fluoroserotonins).** 6-Fluoro- and 4,6-difluoroserotonin were prepared from 3-fluoro-4-methoxy- and 3,5-difluoro-4-



methoxyaniline, respectively, by the Abramovitch adaption of the Fischer indole synthesis (17).

### Summary of the Biochemical Properties of Fluorinated Amine Neurotransmitters.

Neurotransmitter levels in a neuron are controlled by such factors as biosynthesis, feedback inhibition of biosynthesis, storage, release, re-uptake into the neuron, and metabolic deactivation. Interaction of the neurotransmitter with pre- and/or post-synaptic receptors ultimately initiates the biochemical events associated with the firing of the neuron. We have investigated the effects of ring fluorination of aromatic amine neurotransmitters with respect to interactions with metabolic enzymes (monoamine oxidases A and B; catechol *O*-methyl transferase), transport and re-uptake mechanisms, and, especially, interactions with aminergic receptors.

**Fluorinated Analogues as Substrates for Monoamine Oxidases.** Although reuptake of released neurotransmitters into the neuron is the principal mechanism for rapid curtailment of neuronal stimulation, two important catabolic routes are also available for regulation of amine levels. Monoamine oxidase (MAO) is a flavin-linked mitochondrial enzyme that catalyzes the oxidation of monoamines to carbonyl compounds. Recognition of mood-elevating effects of MAO inhibitors has led to their use for the treatment of depressive illness.

Two forms of MAO, designated MAO A and MAO B, occur in human and rat brain. MAO A prefers more polar substrates such as NE and 5HT, both of which are essentially pure MAO A substrates. MAO B preferentially deaminates the more lipophilic substrates such as benzylamine. DA and tyramine are effectively deaminated by both MAO A and MAO B. The influence of fluorine substitution on MAO substrate selectivity appears to reflect increased lipophilicity of fluorinated amines. For example, both 3-fluorotyramine ( $K_m = 18 \mu\text{M}$ ) and 3,5-difluorotyramine ( $K_m = 25 \mu\text{M}$ ) are better substrates for MAO B than is tyramine ( $K_m = 170 \mu\text{M}$ ). Likewise, as opposed to 5HT ( $K_m \approx 1000 \mu\text{M}$ ), 4,6-difluoro-5HT is an excellent substrate for MAO B ( $K_m = 50 \mu\text{M}$ ) (19). These studies are being extended to polyfluorinated analogues of catecholamines that have recently become available (see below).

**Fluorinated Catecholamines as Substrates for Catechol-*O*-methyl Transferase.** Catechol-*O*-methyl transferase (COMT) catalyzes the transfer of a methyl group from *S*-adenosyl methionine (AdoMet) to one of the hydroxyl groups of a catechol, providing an important mechanism for deactivation of biologically active catechols such as catecholamines, catecholamino acids, and steroidal catechols. Fluorinated catecholamines and amino acids have been used effectively to study mechanistic details of this process.

Methylation of NE, EPI, and DOPA with COMT gives predominantly *meta*-methylation, despite comparable acidities of the 3- and 4-OH group, suggesting that side-chain orientation and other factors control regiochemistry. On the other hand, investigations of the regioselectivity of methylation of fluoro-DOPAs and FNEs indicate that the more acidic hydroxyl group is methylated preferentially. Thus, the rank order of preference for *para*-methylation (5-FNE > NE > 6-FNE > 2-FNE) seen at pH 7 is even more pronounced at pH 9 (19). For each compound, the percentage of *para*-methylation

increases with increasing pH, indicating that phenol ionization favors *para*-methylation. This relative increase of *para*-methylation appears to follow a titration curve corresponding to the ionization of a group with  $pK_a$  values of 8.6, 7.7, 7.9, and 8.4 for NE, 2-, 5-, and 6-FNE, respectively. These  $pK_a$  values are the same as, or similar to the  $pK_a$  values of a phenolic group of these substrates (20). As with NE, the acidities of the 3- and 4-OH groups of 2,5-diFNE (2e) are comparable. Likewise, *meta*-methylation of 2,5-diFNE is favored at all pH values examined. However, the percent of *para*-methylation again increases with increasing pH, in this case the increase following a titration curve of a group with a  $pK_a$  of 7.2 (the  $pK_a$  of 2,5-diFNE) (21).

Information on the methylation of fluorinated catecholamines and fluoro-DOPAs is important with respect to development of  $^{18}\text{F}$ -labelled catecholamines and amino acids as PET-scanning agents. Results of examination of F-DOPAs are given below.

**Effects of Fluorination on Receptor Binding.** Our interest in ring-fluorinated catecholamines was spurred in part by the expectation that the presence of fluorine could produce significant alterations in the electronic distribution of the electron-rich catechol ring. This, in turn, should influence the receptor-catecholamine interactions. Initial results with dopamine revealed that, in general, fluorine substitution led to no profound alterations on dopaminergic or adrenergic activities. For example, 2-, and 5-FDA were essentially equipotent at DA renal vascular receptor, while 6-FDA was about four times less potent (21). With respect to CNS receptors, DA and the three monofluorinated DAs had comparable affinities at the  $D_2$  and  $D_3$  DA receptors, and all had comparable affinities at  $\alpha$ - and  $\beta$ -adrenergic receptors (22). We are currently reevaluating these results with additional dopamine and adrenergic receptor subtypes, and with additional, di- and trifluorinated dopamine analogues (See below).

In contrast to our results with DA, we have found that fluorine substitution has a marked effect on the interaction of NE, EPI, and other phenethanolamine adrenergic agonists. For example, fluorine present in the 2-position of NE reduces the binding affinity to the  $\alpha$ -adrenergic receptor making 2-FNE a selective  $\beta$ -adrenergic agonist, whereas fluorine in the 6-position reduces binding affinity to the  $\beta$ -adrenergic receptor, making 6-FNE a selective  $\alpha$ -adrenergic agonist. These receptor selectivities were observed for fluorinated analogues of EPI, isoproterenol, phenylephrine and other adrenergic agonists. We have exploited these results in a number of pharmacological studies, and have investigated the mechanism(s) by which fluorine substitution affects adrenergic selectivity (2).

### **The Development of [ $^{18}\text{F}$ ]-labelled 6-FDOPA, 6-FDA, and 6-FNE as a PET-scanning Agents.**

Ring-fluorinated analogues of DOPA received early attention because of interest in the development of [ $^{18}\text{F}$ ]-labelled DOPA as a PET-scanning agent for the quantitation of regional brain dopaminergic activity. Research from several groups demonstrated that [ $^{18}\text{F}$ ]-6-fluoro-DOPA ([ $^{18}\text{F}$ ]-6-FDOPA) is an effective PET-scanning agent that can be used, for example, as a diagnostic tool in Parkinson's disease. Injected [ $^{18}\text{F}$ ]-6-FDOPA crosses the blood-brain barrier, is decarboxylated, and the resulting [ $^{18}\text{F}$ ]-6-FDA is taken up and stored in central dopaminergic neurons. Quantitation of stored [ $^{18}\text{F}$ ]-6-FDA by

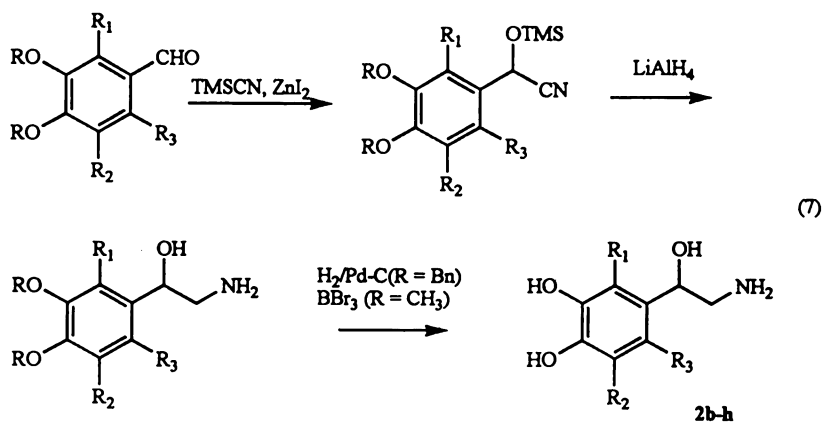
PET has been used to study central dopaminergic activity, in both normal and abnormal subjects (23,24). In related work,  $^{18}\text{F}$ -labelled 6-FDA (25, 26) and (*R*) and (*S*)-6-FNE (27) have been prepared and used to quantitate *in vivo* peripheral adrenergic activity.

**Metabolites of 6-FDOPA.** Successful application of [ $^{18}\text{F}$ ]-6-FDOPA as a PET-scanning agent requires precise knowledge of the identities of positron-emitting species in the experimental subject as a function of time following injection. This, in turn, requires knowledge of the metabolism and biodistribution of the administered agent. Our results from biochemical and pharmacological studies of fluorinated amines, discussed briefly above, have helped validate the use of [ $^{18}\text{F}$ ]-6-FDOPA for PET studies. These studies also reveal that fluorine in the 6-position of catecholamines can alter significantly such pharmacological behavior as receptor affinity, and interaction with COMT. The processing of DOPA and dopamine by MAO, COMT, and other metabolic enzymes produces an array of metabolites. In addition to 6-fluoro analogues of DOPA, DA, NE, and EPI described above, we also have prepared other metabolites of 6-FDOPA, including the 6-fluoro derivatives of 3-*O*-methyl-DOPA, 3-*O*-methylnorepinephrine, dihydroxyphenylacetic acid, homovanillic acid, 4-hydroxy-3-methoxyphenylglycol, and 4-hydroxy-3-methoxymandellic acid (28). These analogues have been used extensively by several groups to study the metabolism of administered 6-FDOPA in research related to PET studies.

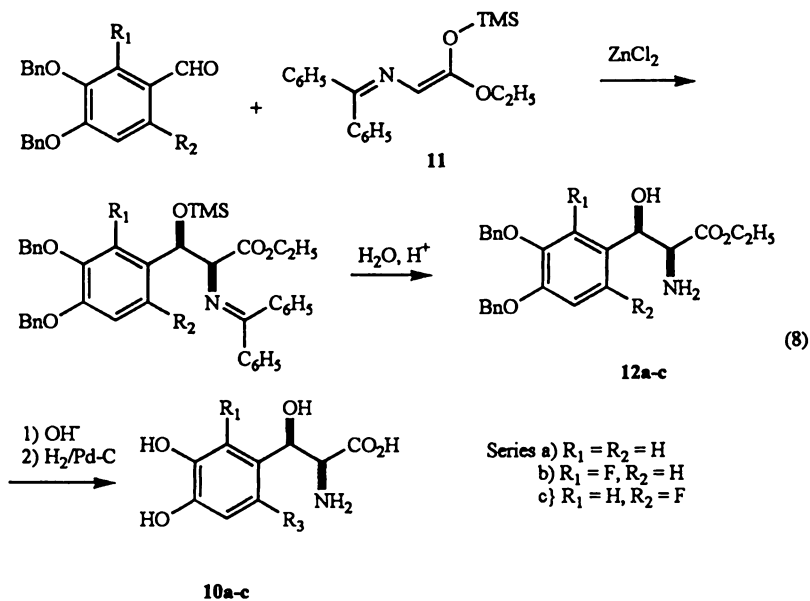
**Effects of Fluorination on COMT-Catalyzed Methylation of DOPA.** The methylation of DOPA to produce 3-methoxytyrosine is the principal mechanism by which DOPA is cleared from the circulation. The presence of fluorine on the aromatic ring effects not only the regioselectivity of methylation, but also the rate of methylation of DOPA by COMT. Of particular significance for PET-scanning applications is the fact that, while the rate of methylation of 2- and 5-FDOPA by COMT is some three to four times that of DOPA, the rate of methylation of 6-FDOPA is nearly 10 times slower. The differences in methylation rates reflect the relative affinities of the substrates for COMT (13,29).

**Fluorinated Analogues of 2-(3,4-dihydroxyphenyl)-serine (DOPS) as Prodrugs for FNE.**

Recently, attention has been given to the pharmacological properties and therapeutic potential of *L-threo*-(3,4-dihydroxyphenyl)serine (*threo*-DOPS) (10a), enzymatic decarboxylation of which produces NE directly, bypassing dopamine DA as an intermediate. There is evidence that administered *threo*-DOPS crosses the blood-brain barrier and is decarboxylated to produce NE in the central nervous system, particularly in conditions of catecholamine deficiencies (30). For example, Tohgi and coworkers found a dose-dependent increase in cerebrospinal fluid NE concentrations in advanced Parkinsonian patients, accompanied by relief of "freezing phenomenon" symptoms in three of six patients (31). *threo*-DOPS administration also has produced an improvement of certain memory functions in patients with Korsakoff's disease (amnesia induced by chronic alcoholism) (32). Orthostatic hypotension in Shy-Drager syndrome (33) and familial amyloid neuropathy (34) have responded to *threo*-DOPS treatment. These and other pharmacological properties of *L-threo*-DOPS assure interest in the biological



- Series a)  $R_1 = R_2 = R_3 = H$     e)  $R_1 = R_2 = F, R_3 = H$   
 b)  $R_1 = F, R_2 = R_3 = F$     f)  $R_1 = R_3 = F, R_2 = H$   
 c)  $R_2 = F, R_1 = R_3 = H$     g)  $R_2 = R_3 = F, R_1 = H$   
 d)  $R_3 = F, R_1 = R_2 = H$     h)  $R_1 = R_2 = R_3 = F$





properties of this NE precursor. If 2- and 6-fluoro-*threo*-DOPS serve as precursors for biosynthesis of the corresponding fluorinated FNEs, this would provide a pro-drug strategy to deliver the selective  $\alpha$ - and  $\beta$ -adrenergic agonists, 2-FNE and 6-FNE, to the central nervous system for a variety of potential uses. In addition to pharmacological and therapeutic potential, fluorinated analogues of *threo*-DOPS labelled with  $^{18}\text{F}$  may have potential as PET-scanning agents for central adrenergic activity.

Based on these considerations, we recently have completed a diastereoselective synthesis of 2- and 6-fluoro-*threo*-DOPS (**10b,c**) (equation 8) (35). Based on a recent report of Kellogg and coworkers (36),  $\text{ZnCl}_2$ -catalyzed aldol condensations between trimethylsilyl ketene acetal derived from the benzophenone imine of glycine ethyl ester **11** and benzyl-protected 2- and 6-fluoropro-catechualdehyde gave, following mild acid treatment, the 2- and 6-fluoro-substituted 3-(3,4-dibenzyloxyphenyl)-2-amino-3-hydroxyphenylalanine ethyl ester (**12b,c**), (*threo/erythro* = 6-7 to 1 as determined by NMR). After isolation of the major isomer, saponification of the ester followed by hydrogenolysis ( $\text{H}_2/\text{Pd-C}$ ) gave 2- and 6-fluoro-*threo*-DOPS (**10b,c**). Stereochemical analysis was confirmed by the demonstration that the same sequence with dibenzyloxy-benzaldehyde produced *threo*-DOPS, identical to authentic commercial material (Aldrich). A similar sequence using acid-labile catechol protecting groups unexpectedly gave mainly *threo*-products (35).

### Polyfluorinated Analogues of Catecholamines and Amino Acids.

The many applications of ring-monofluorinated catecholamino acids and amines made di- and tri-fluorinated analogues obvious synthetic targets. For example, the effects of fluorine substituted on the 2- or 6-position of NE and other phenethanolamine adrenergic agonists made examination of the adrenergic properties of 2,6-difluoronorepinephrine and epinephrine (2,6-DiFNE, 2,6-DiFEPI) a matter of priority in our investigation of the mechanism of fluorine-induced adrenergic selectivities.

**2,5-Difluoro- and 2,6-Difluoronorepinephrine.** These analogues were prepared by side-chain elaboration of precursor ring-difluorinated benzaldehydes by the usual procedure shown in equation 6 (37). Similar to 2-FNE, 2,5-DiFNE was found to bind selectively to  $\beta$ -adrenergic receptors. In contrast, 2,6-DiFNE had only weak affinity at both  $\alpha$ - and  $\beta$ -adrenergic receptors. Thus, the negative effects of fluorine substitution on binding appear to be cumulative. (37).

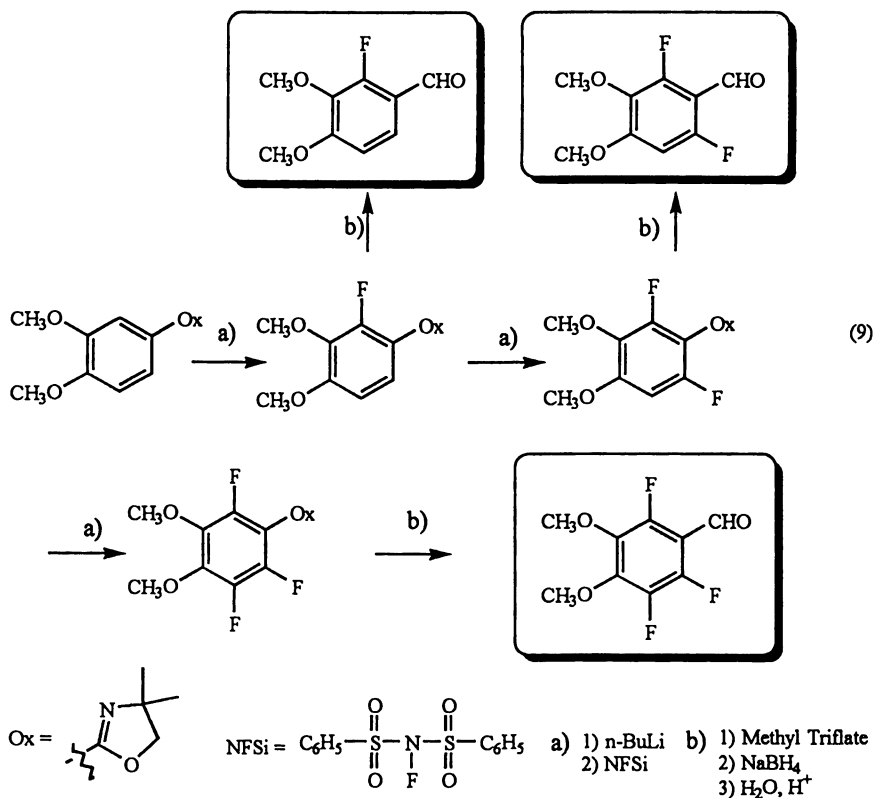
**Preparation of Fluoro- and Polyfluoroveratraldehydes by Electrophilic Fluorination.** A particular challenge in the preparation of the difluorinated analogues described above was the preparation of 2,6-difluoroveratraldehyde. Although synthesis of this key intermediate from 2,4-difluorophenol was achieved in seven steps with an overall yield of 14%, complications with scale-up made difficult accumulation of material sufficient for our needs. Although we earlier had explored electrophilic fluorination of mono-fluoro substrates, or anions derived therefrom, as an alternative strategy for the preparation of difluorinated intermediates, we had met with no success. We were encouraged to reinvestigate this strategy, based on the recent report of Snieckus and coworkers on the facile fluorination of aryllithium intermediates using *N*-

fluorobenzenesulfonimide (NFSi) or *N*-fluoro-*O*-benzenedisulfonimide (38). We applied this sequence (*n*-butyllithium, NFSi) to oxazolines derived from veratric acid and its fluorinated analogues and, through reductive hydrolysis of the derived products, have achieved facile preparations of 2,6-difluoroveratraldehyde as well as of the previously unreported 2,5,6-trifluoroveratraldehyde (equation 9). Fluorination yields were moderate to good. (39).

A direct route to the previously unreported 5,6-difluoroveratraldehyde was achieved by lithiation of 4-fluoroveratrol followed by reaction with NFSi, followed by formylation with dichloromethyl methyl ether catalyzed by titanium tetrachloride (equation 10).

**Preparation of Di- and Trifluorinated Analogues of DOPA.** The chemistry described in the previous section has made the three isomeric difluoroveratraldehydes, as well as 2,5,6-trifluoroveratraldehyde, readily available. The corresponding DOPAs have been prepared by the sequence used to prepare the mono-fluoro analogues (equation 6) (40) (Nie, J.-Y.; Kirk, K L. Unpublished results). In this series, we were particularly interested in 2,6-DiFDOPA for at least two reasons. As discussed above, we had found that the presence of fluorine on the aromatic ring of dopamine (DA) (1a) had little effect on binding of this amine to either dopaminergic or noradrenergic receptors. The fact that 2,6-DiF-NE was found to be relatively inactive at both the  $\alpha$ - and  $\beta$ -adrenergic receptors suggested an approach to a prodrug directed selectively to dopaminergic systems. Thus, the action of aromatic amino acid decarboxylase on 2,6-DiFDOPA (4f) should produce 2,6-diflurodopamine (2,6-DiFDA) (1f) *in vivo*. If disubstitution with fluorine has little effect on interaction of 2,6-DiFDA with dopaminergic receptors, this amine should retain substantial dopaminergic agonist properties. However, *in vivo*  $\beta$ -hydroxylation of 2,6-DiFDA to give 2,6-DiFNE (2f) would not produce significant adrenergic responses, owing to the relative inactivity of 2f at noradrenergic receptors. An additional factor prompted our efforts to synthesize 2,6-DiFDOPA (4f). Several laboratories have prepared [ $^{18}\text{F}$ ]-6-FDOPA by electrophilic fluorination of DOPA. We have provided to several research groups authentic samples of 6-F-DOPA, as well as the isomeric 2-F- and 5-F-DOPA, for chromatographic analyses of product mixtures produced by these electrophilic fluorinations (R. Finn, private communication; K. Hatona, private communication). There have been indications that a difluorination product [presumably 2,6-DiF-DOPA (4f)] is produced by electrophilic fluorination of DOPA. The availability of an authentic sample of 4f thus provides another internal standard for analyses of products obtained during this radiochemical fluorination procedure.

**Preparation of Di- and Trifluorinated Analogues of Dopamine.** Condensation of the fluorinated veratraldehydes with nitromethane followed by LAH reduction and  $\text{BBr}_3$  demethylation gave the di- and trifluorinated DAs (equation 5). We have measured the affinities of these analogues at  $\text{D}_1$ ,  $\text{D}_2$ ,  $\text{D}$  and  $\text{D}$ -dopamine receptors and have reexamined the affinities of 2F-, 5F-, and 6F-DA at the same receptors. From these results, it becomes apparent that polyfluorination appears to be detrimental to binding.



In particular, the presence of fluorine in the 6-position results in decreased binding at all three receptor types. This decrease in binding affinity becomes more pronounced when additional ring positions are fluorinated (Nie, J.-Y.; Shi, D.; Daly, J. W.; Kirk, K. L. unpublished data).

### Summary

Fluorinated analogues of amino acids involved in neurotransmission, and of amine neurotransmitters, have proven to be valuable tools, with important applications in pharmacology, biochemistry, and medicine. Whereas many effects of fluorine substitution on biological activity can be explained readily by steric and electronic factors, other results, such as fluorine-induced adrenergic selectivities remain to be fully rationalized. With advances in organofluorine chemistry making additional analogues more readily available, we plan to extend our studies to include more thorough examination of di- and polyfluorinated analogues of catecholamines and amino acids. Research also will continue directed toward a better understanding of the mechanisms by which fluorine substituents alter biological responses. We also plan to direct research toward the development of additional  $^{18}\text{F}$ -labeled PET-scanning agents.

### Literature Cited

1. Cooper, J. R.; Bloom, R.; Roth, R. H. *The Biochemical Basis of Neuroparmacology*; Oxford University Press, New York, NY, 1991; pp 133-189, 220-380.
2. Kirk, K. L.; *Biochemistry of Halogenated Compounds*; Plenum Press, New York, NY, 1991; pp 278-295.
3. Kirk, K. L. In *Selective Fluorination in Organic and Bioorganic Chemistry*, Welch, J. T., Ed., ACS Symposium Series 456; American Chemical Society, Washington, D.C., 1991, pp 136-155.
4. Kirk, K. L.; Cohen, L. A. *J. Am. Chem. Soc.* **1971**, *93*, 3060-3061.
5. Kirk, K. L.; Cohen, L. A. *J. Am. Chem. Soc.* **1973**, *95*, 4619-4624.
6. Kirk, K. L.; Cohen, L. A. *J. Am. Chem. Soc.* **1973**, *95*, 8389-8392.
7. Kirk, K. L.; Cohen, L. A. *J. Org. Chem.* **1973**, *38*, 3647-3648.
8. Kirk, K. L.; Cohen, L. A. In *Biochemistry of the Carbon-Fluorine Bond*, Filler, R. ed, ACS Symposium Series 28; American Chemical Society, Washington, D.C., 1976, pp 23-36.
9. Kirk, K. L. *J. Org. Chem.* **1980**, *45*, 2015-2016.
10. Phillips, R. S; Fletcher, J. G., Von Tersh, R. L.; Kirk, K. L. *Arch. Biochem. Biophys.*, **1990**, *276*, 65-69.
11. Fowler, J. S. in *Organo Fluorine Compounds in Medicinal Chemistry and Biomedical Applications*, Filler, R.; Kobayashi, Y.; Yagupolskii, L. M., Eds., Elsevier Science Publishers B.V., 1993, pp 309-338.
12. Kirk, K. L. *J. Org. Chem.* **1976**, *41*, 2373-2376.
13. Creveling, C. R.; Kirk, K. L. *Biochem. Biophys. Res. Commun.* **1985**, *136*, 1123-1131.

14. Furlano, D. C.; Kirk, K. L. *J. Org. Chem.*, **1986**, *51*, 4073-4075.
15. Ladd, D. C.; Weinstock, J. *J. Org. Chem.*, **1981**, *46*, 203-206.
16. Kirk, K. L.; Cantacuzene, D.; Nimitkitpaisan, Y.; McCulloh, D.; Padgett, W. L.; Daly, J. W. *J. Med. Chem.* **1979**, *22*, 1493-1497.
17. Kirk, K. L. *J. Heterocyc. Chem.*, **1976**, *13*, 1253-1256.
18. Kirk, K. L.; Cantacuzene, D.; Creveling, C. R. in *Biomedical Aspects of Fluorine Chemistry*, Filler, R.; Kobayashi, Y., Eds., Kodansha, Tokyo, 1982, pp 75-91.
19. Creveling, C. R.; McNeal, E. T.; Cantacuzene, D.; Kirk, K. L. *J. Med. Chem.*, **1981**, *24*, 1395-1399.
20. Thakker, D. R.; Boehlert, C.; Kirk, K. L.; Antkowiak, R.; Creveling, C. R. *J. Biol. Chem.*, 1986, *261*, 178-184.
21. Goldberg, L. I.; Kohli, J. D.; Cantacuzene, D.; Kirk, K. L.; Creveling, C. R. *J. Pharmacol. Exp. Ther.* **1980**, *213*, 509-513.
22. Nimit, Y.; Cantacuzen, D.; Kirk, K. L.; Creveling, C. R.; Daly, J. W. *Life Sciences*, **1980**, *27*, 1577-1585.
23. Garnett, E. S.; Firnau, G.; Nahmias, C. *Nature*, **1983**, *305*, 137-138.
24. Playford, E. D.; Brooks, D. J. *Cerebrovas. Brain Metab. Revs.* **1992**, *4*, 144-171.
25. Nie, J.-Y.; Kirk, K. L. *J. Fluorine Chem.* **1992**, *55*, 259-269.
26. Firnau, G.; Snood, S.; Pantel, R.; Garnett, S. *Mol. Pharmacol.* **1981**, *19*, 130-133.
27. Goldstein, D. S.; Chang, P. C.; Eisenhofer, G.; Miletich, R.; Finn, R.; Bacher, J.; Kirk, K. L.; Bacharach, S.; Kopin, I. J. *Circulation* **1990**, *81*, 1606-1621.
28. Ding, Y.S.; Fowler, J. S.; Gatley, S. J.; Dewey, S. L.; Wolf, A. P.; Schlyer, D. J. *J. Med. Chem.* **1991**, *34*, 863-864.
29. Ding, Y.-S.; Fowler, J. S.; Gatley, S. J.; Dewey, S. L.; Wolf, A. P. *J. Med. Chem.* **1991**, *34*, 767-771.
30. Kondo, T. *Adv. Neurology*, **1993**, *60*, 660-665.
31. Tohgi, H.; Abe, T.; Takahshi, S.; Takahshi, J.; Ueno M.; Nozaki, Y. *Neuroscience Letters*, **1990**, *116*, 194-197.
32. Langlais, P. J.; Mair, R. G.; Whalen, P. J.; McCourt, W.; McEntee, W. J. *Psychopharmacology*, **1988**, *95*, 250-254.
33. Sakoda, T.; Suzuki, S.; Higa, S.; Ueji, M.; Kishimoto, S.; Matsumoto, M.; Yoneda, S. *Eur. Neurol.*, **1985**, *24*, 330-334.
34. Suzuki, T.; Higa, S.; Sakoda, S.; Hayashi, A.; Yamamura, Y.; Takaba, Y.; Nakajima, A. *Neurology (NY)*, **1981**, *31*, 1323-1326.
35. Chen, B.-H.; Nie, J.-Y.; Singh, M.; Pike, V. W.; Kirk, K. L. *J. Fluor. Chem.* **1995**, *75*, 93-101.
36. van der Werf, A. W.; Kellogg, R. M.; van Bolhuis, F.; *J. Chem. Soc. Chem Commun.* **1991**, 682-683.
37. Chen, G. T.; Gusovsky, F.; Creveling, C. R.; Chen, B.-H.; Daly, J. W.; Kirk, K. L. *J. Med. Chem.*, **1993**, *36*, 3947-3955.
38. Snieckus, V.; Beaulieu, F.; Mohri, F.; Han, W.; Murphy, C. K.; Davis, F. A. *Tetrahedron Lett.*, **1994**, *35*, 3465-3468.
39. Nie, J.-Y.; Kirk, K. L. *J. Fluorine Chem.*, **1995**, *74*, 297-301.
40. Nie, J.-Y.; Kirk, K. L. *J. Fluorine Chem.*, **1995**, *74*, 303-306.

## Chapter 23

# **$^{18}\text{F}$ -Labeled Tracers for Positron Emission Tomography Studies in the Neurosciences**

**Yu-Shin Ding and Joanna S. Fowler**

**Department of Chemistry, Brookhaven National Laboratory,  
Upton, NY 11973**

Fluorine-18 is a positron emitting isotope of fluorine. It has the longest half-life (110 minute) and the lowest positron energy (0.635 Mev) of the four common positron emitters for positron emission tomography (PET). PET, in conjunction with appropriate radiotracers labeled with fluorine-18, has been used to assess functional activity, biochemical transformations and drug pharmacokinetics and pharmacodynamics in the human and animal body. The PET method, F-18 labeling of organic molecules, and some of the applications of F-18 labeled compounds in the neurosciences (brain and heart) are described.

Positron Emission Tomography (PET) is an imaging method which uses short-lived positron emitting isotopes to track labeled compounds in the living human and animal body (see Table I for the commonly used positron emitters). In a PET study, a radiotracer labeled with a short-lived positron emitting isotope is administered either by intravenous injection or inhalation and the spatial and temporal distribution of the radioactivity are quantitatively measured using a positron emission tomograph. The short half-life of the PET isotopes and their decay to non-radioactive products combine to make this an imaging method exquisitely suited to the study of biochemical processes and drug action in the living human body. In addition, the positron emitters have very high specific activities (radioactivity/unit of chemical mass) and thus PET studies can be carried out at true tracer doses which avoid perturbing the process being measured.

PET derives its flexibility and scientific versatility from the chemical characteristics and short half-life of positron emitters which allow their incorporation into structurally diverse organic compounds for monitoring biochemical transformations. It has become a powerful tool for basic investigations in the neurosciences and has also been expanded to clinical practice where it provides unique information relative to the management of cancer, epilepsy and cardiovascular disease.<sup>1</sup>

Once a priority structure for synthesis has been chosen, the choice of the label must be considered. The turnover rates of the physiological process of interest is generally a factor that influences the choice of the nuclide. With carbon-11 labeled tracers two or three studies can be carried out on the same subject on the same day. Fluorine-18 labeled biomolecules are useful for studying slower biological processes and permit a more flexible experimental design. This chapter will focus on fluorine-18, the positron emitter with the

0097-6156/96/0639-0328\$15.00/0

© 1996 American Chemical Society

longest half-life, the lowest positron energy and probably, the most challenging chemistry. The incorporation of F-18 into organic compounds presents many challenges, including: the need to synthesize and purify the compound within a 2-3 hour time frame; the limited number of labeled precursor molecules; the need to work on a microscale; and the need to produce radiotracers which are chemically and radiochemically pure, sterile and pyrogen-free, and suitable for intravenous injection.

The PET method and F-18 labeling of organic molecules will be described followed by highlights of the applications of F-18 labeled compounds in the neurosciences (brain and heart) and neuropharmacology. For a comprehensive survey of the literature of fluorine-18 and PET, the reader is also referred to other literature on the subject.<sup>2, 3, 4, 5</sup>

Table I. Physical properties of the short-lived positron emitters

Isotope	Half-life (min)	Specific Activity (Ci/mmol)*	Maximum Energy (MeV)	Range (mm) in H <sub>2</sub> O**	Decay Product
fluorine-18	110	1.71 x 10 <sup>6</sup>	0.635	2.4	oxygen-18
carbon-11	20.4	9.22 x 10 <sup>6</sup>	0.96	4.1	boron-11
oxygen-15	2.1	9.08 x 10 <sup>7</sup>	1.72	8.2	nitrogen-15
nitrogen-13	9.96	1.89 x 10 <sup>7</sup>	1.19	5.4	carbon-13

\* Theoretical maximum; in reality the measured specific activities of <sup>11</sup>C, <sup>18</sup>F, <sup>13</sup>N and <sup>15</sup>O are ca. 10-10,000 times lower because of unavoidable dilution with the stable element.

\*\* maximum linear range

### PET Imaging

Positron decay is the physical process which is at the heart of PET. A positron is a particle which carries a positive charge and has essentially the same mass as an electron. When it is emitted as a result of the radioactive decay of an unstable radionuclide such as fluorine-18, it travels a short distance from the nucleus, typically about 2-8 mm maximum range. It loses its kinetic energy during this flight and then annihilates with an electron. This results in the creation of two photons of equal energy, i.e. 511 keV, which travel in opposite directions very close to 180° apart. It is the distance between the decaying nucleus and the point of annihilation and the fact that the annihilation photons are not emitted at exactly 180° apart that ultimately limits the spatial resolution possible in PET. Since fluorine-18 has the lowest positron energy of the four common short-lived positron emitters (Table I), the average range of the positron before annihilation is shorter compared to the other isotopes. This could affect image resolution with tomographs of very high resolution.<sup>6</sup>

The positron emission tomograph typically consists of a cylindrical array of scintillation crystals, commonly bismuth germinate or sodium iodide, which are designed to register a decay event only when 2 photons enter crystals on opposite sides at essentially the same time, i.e. so called coincidence detection.<sup>7</sup> These events are registered and then processed by an algorithm which allows an

image to be reconstructed by computer. The range of resolution of modern PET instruments is from 2.5 to 5 mm. PET instruments have been designed with small apertures to image the brain and also with larger apertures to image the heart and other organs and tumors. Though PET is most commonly used to study the brain and the heart, whole body PET can be used to image any part of the human body. In fact the use of whole body PET to detect metastatic cancer is a rapidly growing application.<sup>8</sup>

### Labeling Organic Compounds with Fluorine-18

**General Considerations.** The physical properties of the fluorine atom and the characteristics of the carbon-fluorine bond (high bond strength and similar van der Waals radius to hydrogen) also are major factors in the utility of fluorine-18 as a label for radiotracers.<sup>9, 10</sup> The 110 minute half life is sufficient for relatively complex synthetic manipulations and purifications and the resulting radiotracer or its labeled metabolites can be monitored *in vivo* for several hours. Although fluorine in chemical combination with carbon rarely occurs in nature, the development of synthetic approaches for its incorporation into organic molecules by substitution for hydrogen, hydroxyl or some other functional group often leads to organic compounds with biological properties which resemble the parent structures. The ability to substitute fluorine-18 for hydrogen while maintaining the desired biological behavior of the parent compound is well illustrated by 2-deoxy-2-[<sup>18</sup>F]fluoro-D-glucose ([<sup>18</sup>F]FDG, a PET tracer for 2-deoxy-D-glucose<sup>11</sup>) and 6-[<sup>18</sup>F]fluoro-L-DOPA (a PET tracer for LDOPA<sup>12</sup>), two major radiotracers in PET research in the neurosciences today (Figure 1).

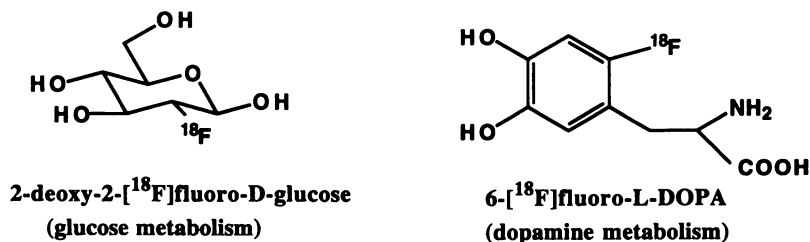


Figure 1. Structures of [<sup>18</sup>F]FDG and 6-[<sup>18</sup>F]fluoro-L-DOPA

**Fluorine-18 Production.** The short-lived positron emitters are generally produced by bombarding appropriate stable isotopes (referred to as the "target") with charged particles such as protons, deuterons, helium-3 and helium-4 traveling at high kinetic energies. Fluorine-18 production and targetry have been described in a number of publications.<sup>5, 13</sup> The most commonly used nuclear reactions to produce fluorine-18, the <sup>18</sup>O(p,n)<sup>18</sup>F and the <sup>20</sup>Ne(d,α)<sup>18</sup>F reactions, are presented in Table II. The <sup>18</sup>O(p,n)<sup>18</sup>F reaction which yields fluorine-18 as fluoride ion is preferred in terms of yield and precursor specific activity.<sup>14</sup> The most common target is oxygen-18 enriched water.<sup>15, 16</sup> Targetry using oxygen-18 enriched carbon dioxide and oxygen gas have also been developed. The enriched carbon dioxide target produces F-18 in the chemical form of [<sup>18</sup>F]fluoride ion and was developed because of the ease of recovery of enriched carbon dioxide relative to enriched water.<sup>17</sup> The oxygen-



<sup>18</sup>F gas target was developed to produce labeled elemental fluorine taking advantage of the higher F-<sup>18</sup> yields from the <sup>18</sup>O(p,n)<sup>18</sup>F reaction relative to the <sup>20</sup>Ne(d,α)<sup>18</sup>F reaction.<sup>18</sup> The <sup>20</sup>Ne(d,α)<sup>18</sup>F nuclear reaction is most commonly carried out using neon containing 0.1% F<sub>2</sub> to yield <sup>18</sup>F elemental fluorine<sup>19</sup> which can be either used directly in synthesis or converted to other electrophilic fluorination reagents such as acetyl hypofluorite.<sup>20, 21</sup>

The nucleophilic and electrophilic fluorination reagents (H[<sup>18</sup>F] and [<sup>18</sup>F]F<sub>2</sub> and precursors derived from them) have been described.<sup>3, 4, 5</sup> In general, for equal amounts of radioactivity, the chemical mass associated with an [<sup>18</sup>F]F<sub>2</sub> derived radiotracer (carrier-added) far exceeds that of an [<sup>18</sup>F]fluoride ion derived radiotracer (no-carrier-added). Though this has been a limitation in the application of electrophilic fluorination reagents in the synthesis of F-<sup>18</sup> labeled compounds for tracer studies where saturation, physiological and toxicological effects play important role, there has been a recent breakthrough in achieving high specific activity F-<sup>18</sup> labeled acetyl hypofluorite using F-<sup>18</sup> fluoride from an enriched water target. In this elegant study, <sup>18</sup>F-labeled fluoromethane ([<sup>18</sup>F]CH<sub>3</sub>F) was first prepared and subjected to an electrical discharge in the presence of unlabeled elemental fluorine (280 nmol) to yield [<sup>18</sup>F]F<sub>2</sub> which was converted to [<sup>18</sup>F]acetyl hypofluorite in a specific activity of 0.35-0.6 Ci/μmol at the end of bombardment.<sup>22</sup> This method has been used in the radiosynthesis of 2β-carbomethoxy-3β-(4-[<sup>18</sup>F]fluorophenyl)tropane ([<sup>18</sup>F]CFT or WIN 35428), a cocaine analogue, for PET studies.

Table II. Fluorine-<sup>18</sup> production methods

NUCLEAR REACTION	TARGET MATERIAL	CHEMICAL FORM PRODUCED	SPECIFIC ACTIVITY	Reference
<sup>18</sup> O(p,n) <sup>18</sup> F	H <sub>2</sub> <sup>18</sup> O	[ <sup>18</sup> F]fluoride ion	ca. 2000 Ci/mmol	15, 16, 23
		[ <sup>18</sup> F]acetyl hypofluorite	350-600 Ci/mmol	22
	C <sup>18</sup> O <sub>2</sub>	[ <sup>18</sup> F]fluoride ion	ca. 2000 Ci/mmol	17
	<sup>18</sup> O <sub>2</sub>	[ <sup>18</sup> F]fluorine or [ <sup>18</sup> F]acetyl hypofluorite	<15 Ci/mmol	18
<sup>20</sup> Ne(d,α) <sup>18</sup> F	Ne + F <sub>2</sub>	[ <sup>18</sup> F]fluorine	<15 Ci/mmol	5, 19

**Rapid Synthesis with Fluorine-<sup>18</sup>.** <sup>18</sup>F-labeled aryl fluorides, aliphatic fluorides, acyl and aroyl fluorides have been synthesized using both nucleophilic and electrophilic sources of <sup>18</sup>F as labeled precursors (H[<sup>18</sup>F] and [<sup>18</sup>F]F<sub>2</sub> and precursors derived from them<sup>3, 4, 5</sup>). To date, the ability to produce *high specific activity* F-<sup>18</sup> labeled compounds still remains one of the most challenging areas in F-<sup>18</sup> synthesis. This section describes a few examples in the recent development of routes to obtain high specific activity F-<sup>18</sup> labeled aromatic compounds.

### High Specific Activity F-18 Labeled Aromatic Compounds.

Over the past 25 years, many different methods have been reported for introducing  $^{18}\text{F}$  into aromatic compounds.<sup>5</sup> However, to date, only the nucleophilic aromatic substitution<sup>24</sup> satisfies the need for an efficient synthesis of aryl fluorides, especially in the case of complex molecules. The mechanism and conditions necessary for successful substitution have been the subject of a series of papers<sup>24, 25, 26</sup> and many F-18 labeled aromatic compounds have been synthesized using this general method.<sup>5</sup>

The minimal structural requirements for the nucleophilic aromatic substitution reaction are the presence of an electron withdrawing, activating substituent such as RCO, CN,  $\text{NO}_2$  etc., as well as a leaving group, such as  $\text{NO}_2$  or  $^+\text{NMe}_3$ . However, there are numerous important radiotracers such as neurotransmitters and false neurotransmitters<sup>27, 28</sup> with electron donating substituents on the ring which can make the substitution reaction proceed in low yield or be ineffective. While these can be prepared using elemental fluorine or other electrophilic fluorination reagents, the resulting low specific activity products are a limitation with chemical compounds which are physiologically active at low administered doses. For example, F-18 labeled 6-fluorodopamine and 6-fluorometaraminol prepared from electrophilic fluorination reagents produce hemodynamic effects when administered *in vivo*.<sup>27, 28</sup>

In order to extend the utility of the nucleophilic aromatic substitution reaction to molecules containing electron donating substituents, an investigation of structure-activity relationships was carried out.<sup>29</sup>  $^{13}\text{C}$ -NMR was used to probe the electron density at the ring carbon atoms of a series of aromatic nitroaldehydes with different hydroxyl protecting groups. A good correlation between the radiochemical yields for fluorine-18 substitution and the  $^{13}\text{C}$ -NMR chemical shifts of the reaction center (where the nitro group is attached) has been demonstrated for structurally similar compounds<sup>29, 30</sup>. There is a large difference in radiochemical yield between 6-nitropiperone and 6-nitroveratraldehyde. Perhaps due to the ring strain, the electron donating effect becomes less effective in 6-nitropiperone as determined by the  $^{13}\text{C}$  chemical shift. Application of this methodology has resulted in the first synthesis of no-carrier-added 6- $^{18}\text{F}$ fluorodopamine (Figure 2), (+) and (-)-6- $^{18}\text{F}$ fluoronorepinephrine and 6- $^{18}\text{F}$ fluoro-L-DOPA<sup>29, 31, 32</sup> where the methylenedioxy moiety was used as a masked catechol which was readily removed at the end of the synthesis.

More recent developments in the synthesis of high specific activity aromatic and heteroaromatic compounds have been reported, including the reaction of F-18 fluoride with arylodonium salts to prepare NCA aryl fluorides<sup>33</sup> and a study on reactivity and positional selectivity of F-18 fluoride on several substituted pyridines and diazines.<sup>34</sup>

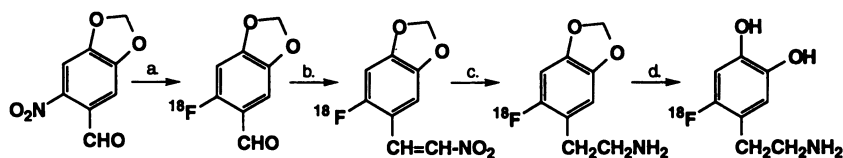


Figure 2. Synthesis of No-Carrier-Added 6- $^{18}\text{F}$ Fluorodopamine. a.  $\text{K}^{18}\text{F}$ ; b.  $\text{CH}_3\text{NO}_2$ ; c.  $\text{LiAlH}_4$ ; d. HI

## Applications of PET Radiotracers in the Neurosciences

Once a labeling method has been established, the *in vivo* specificity of a labeled compound for a specific molecular target is determined. This is usually accomplished by studies in small animals or by *in vivo* PET studies to assess pharmacological specificity, stereoselectivity and/or kinetic isotope effects where appropriate. The extraction of quantitative physiological information usually requires the application of a kinetic model.<sup>35,36,37</sup>

PET, in conjunction with appropriate radiotracers, has been used to assess the functional and neurochemical parameters in the normal and diseased human brain and heart. As a result, information which could only be previously investigated in animals or in the postmortem human is accessible in human subjects. This has enabled initial investigations of the relation between the neurochemical changes in the human body and its functional and clinical consequences. Specific examples of radiotracer applications in the neurosciences (brain and heart) are given in the following sections.

**Brain Glucose Metabolism.** The major radiotracer for brain studies has been 2-deoxy-2-<sup>[18F]</sup>fluoro-D-glucose (<sup>[18F]</sup>FDG) which was developed nearly 20 years ago and was the first radiotracer to be widely employed in PET research. <sup>[18F]</sup>FDG measures regional brain glucose metabolism<sup>38</sup> in all brain regions simultaneously. Regional brain glucose metabolism reflects activity in nerve terminals and synaptic elements within it.<sup>37</sup> The <sup>[18F]</sup>FDG method is based on the metabolic trapping of <sup>[18F]</sup>FDG-6-phosphate, the product of hexokinase catalyzed phosphorylation of <sup>[18F]</sup>FDG. Since glucose derivatives missing the hydroxyl group on C-2 do not undergo further steps in glycolysis, the radioactivity in tissue after the injection consists only of free <sup>[18F]</sup>FDG and <sup>[18F]</sup>FDG-6-phosphate (which remains intracellularly trapped for the time course of the measurement), allowing the measurement of glucose metabolism via a kinetic model. <sup>[18F]</sup>FDG has become a major tool in studies of neurological and psychiatric disease<sup>39</sup> as well as assessing myocardial viability and tumor metabolism.<sup>1</sup> It has also been used to measure the effects of drugs and substances of abuse, cognitive processing and somatosensory stimulation on brain glucose metabolism. Although the <sup>[18F]</sup>FDG method does not provide direct information on the particular neurochemical mechanism(s) involved in a disease or in drug mechanisms, the involvement of particular brain regions has been a valuable tool in understanding diseases and drug mechanisms.<sup>39</sup>

**Neurotransmitter Activity (Brain).** A number of neurological and psychiatric disorders have been linked with abnormalities in neurotransmitter properties. The neurotransmitter systems commonly under investigation with PET include the dopamine, serotonin, opiate, benzodiazepine and cholinergic systems and F-18 labeled radiotracers which selectively bind to different synaptic elements (eg transporters, vesicles, receptors) and those which are sensitive to changes in neurotransmitter concentration have been developed.

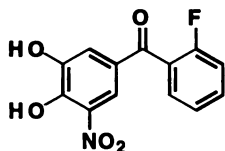
**The Dopamine System.** By far, the greatest effort in PET research has been directed toward the study of the brain dopamine system. This has been stimulated by the importance of dopamine in Parkinson's disease, schizophrenia and substance abuse and its vulnerability in normal aging. (for a review see<sup>40</sup>, in press) Aspects of the dopaminergic synapse which have been studied are dopamine metabolism, the dopamine transporter, the dopamine D<sub>1</sub> and D<sub>2</sub> receptors,<sup>41</sup> vesicular storage and changes in synaptic dopamine.<sup>40</sup>

Since dopamine does not cross the blood-brain barrier, the investigation of brain dopamine metabolism with PET has required a fluorine-18 labeled derivative of DOPA, 6-[ $^{18}\text{F}$ ]fluoro-L-DOPA. 6-[ $^{18}\text{F}$ ]Fluoro-L-DOPA has been widely used for studies of dopamine synthesis and metabolism and has been applied in clinical research in Parkinson's disease.<sup>42, 43</sup> 6-[ $^{18}\text{F}$ ]Fluoro-DOPA crosses the blood-brain barrier and is converted to 6-[ $^{18}\text{F}$ ]fluorodopamine via L-aromatic amino acid decarboxylase (AADC). It is also extensively metabolized by both monoamine oxidase (MAO) and catechol-*O*-methyltransferase (COMT) in the periphery producing labeled metabolites, especially 3-*O*-methyl-6-[ $^{18}\text{F}$ ]fluoro-DOPA, which contribute to striatal F-18 radioactivity as visualized by PET. Consequently, other tracers with a simpler metabolic profile have been developed. These include [ $^{18}\text{F}$ ]fluoro-*m*-tyrosine<sup>44, 45</sup> and  $\beta$ -fluoromethylene-6-[ $^{18}\text{F}$ ]fluoro-*m*-tyrosine.<sup>46</sup> These tracers are substrates for AADC but not for COMT.

The most widely used dopamine  $\text{D}_2$  receptor PET ligands are the  $^{11}\text{C}$  and  $^{18}\text{F}$ -labeled butyrophenones such as spiroperidol and its derivatives and the benzamides such as raclopride.<sup>41, 47, 48, 49, 50, 51</sup>

Several radioligands have been developed to measure the dopamine transporter system for studies of addiction, normal aging and neurodegeneration,<sup>40</sup> and reference therein. Many of these have been labeled with carbon-11 and include [ $^{11}\text{C}$ ]nomifensine, [ $^{11}\text{C}$ ]cocaine and [ $^{11}\text{C}$ ]d-threo-methylphenidate and [ $^{11}\text{C}$ ]WIN 35428, a cocaine analog. F-18 labeled tracers for this system include [ $^{18}\text{F}$ ]GBR 13119 and [ $^{11}\text{C}$ ] and [ $^{18}\text{F}$ ]WIN 35428<sup>22</sup> and  $^{18}\text{F}$ -labeled cocaine analogs<sup>52, 53</sup>. These radioligands differ with respect to their affinities and their specificity for the dopamine transporter as well as their kinetics and the choice of the optimal radiotracer must be made in the context of its intended application.

MAO (EC 1.4.3.4) and COMT (EC 2.1.1.6) are the two major enzymes which metabolize the catecholamines, such as dopamine. Radiotracers for studying MAO have been developed though most are labeled with carbon-11.<sup>54, 55</sup> An exception is  $^{18}\text{F}$ -labeled derivative of L-deprenyl which has undergone initial studies<sup>56</sup> and an F-18 labeled derivative of Ro19 6327 which has recently been reported.<sup>57</sup> The development of tracers for measuring COMT in the brain has also been undertaken, stimulated by reports of highly selective COMT inhibitor drugs having central activity. One of these is Ro41-0960, a fluorine containing nitrocatechol with a high affinity for COMT.<sup>58</sup> It was recently labeled with fluorine-18 using the nucleophilic aromatic substitution reaction. PET studies in baboons revealed that its brain uptake is negligible but that it may be useful for measuring COMT activity in peripheral organs.<sup>59</sup> The unexpected observation of negligible brain uptake reveals the power of PET to examine the uptake of drugs in a living brain. This information is difficult to obtain in animals and impossible to obtain in humans by other methods.



Ro 41-0960 (COMT inhibitor)

**The Serotonin system.** The brain serotonin (5-HT) system is associated with a number of neurological abnormalities and psychiatric disorders and it is also an important molecular target for anti-depressant drugs.<sup>60</sup> Ligands

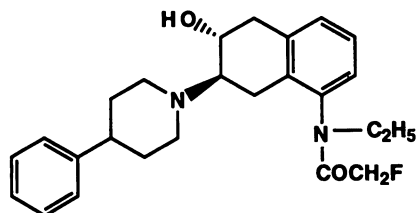
to study serotonin 5-HT<sub>2</sub> receptors, such as [<sup>18</sup>F]sepiroperone,<sup>61</sup> [<sup>18</sup>F]ritanserin,<sup>62</sup> [<sup>18</sup>F]altanserin,<sup>63</sup> 3-N-(2"-[<sup>18</sup>F])fluoroethylspiperone,<sup>64</sup> and [<sup>18</sup>F]fluoroethylketanserin,<sup>65</sup> have been prepared using the nucleophilic aromatic substitution reaction. Recently, a highly potent and selective 5HT<sub>2</sub> receptor antagonist SR 46349B has been labeled with <sup>11</sup>C and <sup>18</sup>F to study the interactions between neurotransmitter systems.<sup>66,67</sup> Derivatives of N-phenethylpiperidine have also been labeled and are under evaluation.<sup>68, 69, 70, 71</sup>

The mechanism of action of some antidepressant drugs is believed to involve adaptive changes in central serotonin 5-HT<sub>1A</sub> receptors. Therefore, the development of radiotracers for serotonin 5-HT<sub>1A</sub> receptors has received considerable attention. Although much effort has been focused on <sup>11</sup>C (e.g., a selective antagonist [<sup>11</sup>C]WAY 100635<sup>72,73</sup>), the development of <sup>18</sup>F derivatives are also underway.<sup>74</sup>

The development of serotonin transporter imaging agents has also been of great interest in order to study the role of this regulatory site in a variety of psychiatric, psychomotor and addictive disorders.<sup>75</sup> Citalopram,<sup>76</sup> paroxetine,<sup>77</sup> fluoxetine,<sup>78</sup> and nitroquipazine,<sup>79</sup> potent serotonin transporter ligands, have been radiolabeled with carbon-11 or fluorine-18 for evaluation as radiotracers for imaging and quantifying serotonin transporter sites in the brain using PET. Recently, a potent serotonin transporter inhibitor, trans-1,2,3,5,6,10β-hexahydro-[4-(methylthio)phenyl]pyrrolo[2,1-α]isoquinoline (McN-5652Z), has been labeled with C-11<sup>80</sup> and a fluoroethylthio analogue of this pyrroloisoquinoline derivative has been also labeled with F-18 for evaluation as a potential PET serotonin transporter ligand.<sup>81,82</sup>

**The Cholinergic System.** The characterization of the cholinergic system *in vivo* is of interest because of its role in memory and its involvement in Alzheimer's disease. Radiotracer development in this area has focussed on Alzheimer's disease with a view to presymptomatic detection of degenerative processes and for monitoring drug therapy. Two major structural classes of compounds, the benzovesamicols and trozamicols, have been developed and radiolabeled to map the cholinergic neurons<sup>83,84,85,86</sup> based on the rationale that these high affinity ligands can selectively bind to vesicular receptors which are uniquely situated on the cholinergic synaptic vesicles.<sup>87</sup> One of these is [<sup>18</sup>F](-)-4-N-ethyl-fluoroacetamidobenzovesamicol.<sup>88</sup>

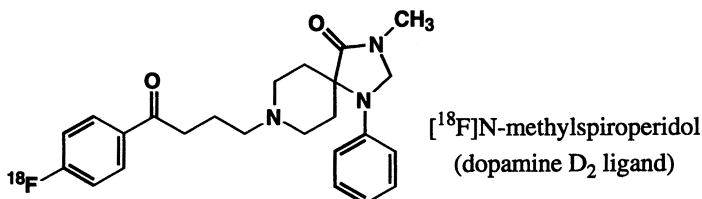
Radiotracers for postsynaptic cholinergic receptors have also been developed. For example, F-18 labeled fluoroalkyl derivatives of quinuclidinyl benzilate are under investigation as subtype selective muscarinic ligands.<sup>89</sup> 2- and 4-[<sup>18</sup>F]Fluorodexetimide also have been developed to study muscarinic-cholinergic receptors.<sup>90,91</sup> Recently, fluorine-18 labeled analogue of epibatidine has been developed for evaluation as a radiotracer for nicotinic-cholinergic receptors.<sup>92</sup>



[<sup>18</sup>F](-)-4-N-ethyl-fluoroacetamidobenzovesamicol  
(cholinergic vesicular receptor ligand)

**The Opioid System.** The opioid system has been implicated in a number of neurological and psychiatric conditions including pain, addiction and seizure disorders. F-18 labeled opiate receptor ligands, such as 6 $\beta$ -fluorocyclofentanyl,<sup>93</sup> fluoroalkyl derivatives of diprenorphine and buprenorphine<sup>93, 94, 95, 96</sup> and derivatives of fentanyl,<sup>97</sup> have been developed for evaluation as PET radiotracers.

**Neurotransmitter Interactions.** Though many radiotracers have been developed to selectively probe discrete neurotransmitter systems *in vivo* with PET, it is well known that different neurotransmitters also interact with one another. Recently, studies have also been designed to probe neurotransmitter interactions with PET; for example, to evaluate the ability of acetylcholine,<sup>98, 99, 100</sup> GABA,<sup>101</sup> serotonin,<sup>102</sup> and opiate systems<sup>103</sup> to modulate striatal dopamine release using dopamine D<sub>2</sub> ligand [<sup>18</sup>F]N-methylspiroperidol or [<sup>11</sup>C]raclopride. In human, the interactions between dopamine and acetylcholine have been investigated in healthy normal subjects.<sup>104</sup> Striatal dopamine D<sub>2</sub> receptors and acetylcholine interactions have also been studied in primates using [<sup>18</sup>F](-)-4-N-ethyl-fluoroacetamidobenzovesamicol as a radioligand marking cholinergic activity.<sup>88</sup>



**Neurotransmitter Activity (Heart).** (-)-Norepinephrine is the major neurotransmitter of the sympathetic nervous system. It is synthesized and stored within the cardiac sympathetic neuron and released in response to nerve impulses. The major mechanism for terminating the action of released (-)-norepinephrine is reuptake via the norepinephrine transporter (uptake 1) and storage within the cardiac neuron. Dysfunction in this system may underlie a number of cardiac diseases and may also play a role in the cardiotoxicity of psychostimulant drugs such as cocaine.

Radiotracers have been developed to study cardiac sympathetic activity *in vivo*. These include false neurotransmitters labeled with carbon-11 ([<sup>11</sup>C]hydroxyephedrine<sup>105</sup>) and with fluorine-18 ([<sup>18</sup>F]metaraminol<sup>106</sup>) as well as the simple fluorine substituted derivatives of norepinephrine, (-)- and (+)-6-[<sup>18</sup>F]fluoronorepinephrine ((-) and (+)-6-[<sup>18</sup>F]FNE<sup>107</sup>) along with 6-[<sup>18</sup>F]fluorodopamine (6-[<sup>18</sup>F]FDA,<sup>27, 108</sup> which is converted to (-)-6-[<sup>18</sup>F]FNE *in vivo*<sup>109</sup>).

Mechanistic studies employing the deuterium isotope effect have been carried out to understand the behavior of 6-[<sup>18</sup>F]FDA *in vivo*, in particular its uptake and rapid clearance from the heart which differs from (-)-6-[<sup>18</sup>F]FNE which has a very slow clearance rate. In the metabolism of the parent compound, dopamine, MAO catalyzes the cleavage of the C-H bond alpha to the amino group<sup>110</sup> and DBH (dopamine  $\beta$ -hydroxylase) cleaves the benzylic C-H bond leading to the formation of (-)-norepinephrine<sup>111, 112</sup>. In order to selectively probe the contribution of these two metabolic enzymes to the kinetics of 6-[<sup>18</sup>F]fluorodopamine *in vivo* (Figure 3), doubly labeled (fluorine-18 and

deuterium) isotopomers of 6-[<sup>18</sup>F]fluorodopamine were synthesized and used in PET studies<sup>113, 114</sup> The kinetics of the parent radiotracer and the deuterium substituted derivatives were compared using PET in baboons. The clearance rate of F-18 from the heart was reduced by deuterium substitution in the  $\alpha$  position to the amino group but not the  $\beta$ -position indicating that MAO catalyzed oxidation is responsible for the rapid clearance of F-18 from the heart after the injection of 6-[<sup>18</sup>F]FDA (Figure 4). This study demonstrates that deuterium substitution is an effective mechanistic tool allowing the identification of the specific chemical transformation contributing to a PET image *in vivo* without tissue sampling and without pharmacological intervention.

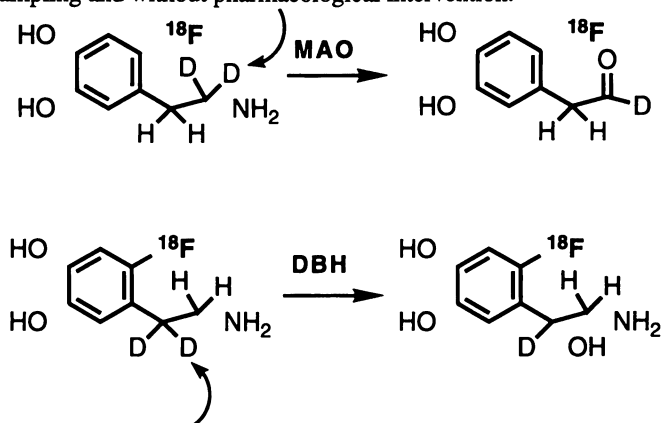


Figure 3. Specifically deuterated 6-[<sup>18</sup>F]FDA derivatives for probing MAO and DBH. (Reproduced with permission from reference 114. Copyright 1995 Raven Press.)

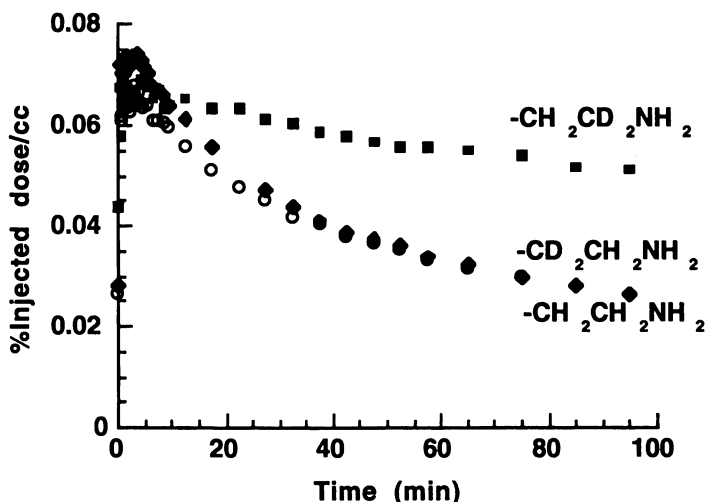


Figure 4. Uptake and clearance of <sup>18</sup>F after injection of 6-[<sup>18</sup>F]FDA (open circles) and 6-[<sup>18</sup>F]FDA- $\alpha,\alpha$ -D<sub>2</sub> (squares), and 6-[<sup>18</sup>F]FDA- $\beta,\beta$ -D<sub>2</sub> (diamonds) in baboon heart. (Reproduced with permission from reference 114. Copyright 1995 Raven Press.)

## PET and F-18 Tracers in Neuropharmacology

PET has become an important scientific tool for examining the behavioral, therapeutic and toxic properties of drugs and substances of abuse<sup>115</sup> PET provides a new perspective on drug research because it can assess both pharmacokinetic and pharmacodynamic aspects of drug action directly in the human body both in normal controls and in patients. The ability to assess the behavior of a drug at its site of action directly in human subjects is important because the behavior of a drug may vary across animal species and even between different categories of human subjects where it can be affected by age, gender, disease, drug status and other factors. PET also enables the assessment of drug behavior in diseases where there are no animal models. This information places PET in a unique position to characterize drug binding sites and to understand the molecular mechanisms underlying drug action.

The pharmacokinetics of a drug can be monitored with F-18, providing that the drug is a fluorine containing compound and is amenable to labeling with fluorine-18. There are a number of examples of fluorine-containing drugs which have been labeled with fluorine-18 including the antipsychotic drugs haloperidol<sup>116</sup> and BMY 14802<sup>117</sup> Fluorine-containing anesthetics have also been labeled with F-18 and their distribution and kinetics studied in the human brain.<sup>118</sup> These studies are most often undertaken to determine the amount of drug which reaches its target organ as well as to better understand drug mechanisms.

While drug pharmacokinetics can be measured using the labeled drug, the effects of the drug on the body (pharmacodynamics) can be measured using radiotracers. For example, PET studies of the effects of chronic cocaine use on the human brain with both [<sup>18</sup>F]FDG (which measures brain glucose metabolism) and [<sup>18</sup>F]N-methylspiroperidol (which measures dopamine D<sub>2</sub> receptor availability), have revealed that cocaine abusers have decreased dopamine D<sub>2</sub> receptor availability and that there is a significant correlation between decreased dopamine D<sub>2</sub> receptor availability and metabolism in frontal areas.<sup>40</sup> This has led to the suggestion that dopamine dysregulation may be responsible for the loss of control and compulsive drug taking behavior seen in the cocaine abuser. Another study using (-)-6-[<sup>18</sup>F]fluoronorepinephrine to assess the functional activity of the norepinephrine transporter in the heart revealed that an acute dose of cocaine disables the uptake of norepinephrine into the sympathetic neuron (uptake 1 mechanism).<sup>119</sup> This mechanism may play a role in the cardiotoxicity of cocaine.

PET has also been used to examine the pharmacokinetics and pharmacodynamics of the widely used antipsychotic drug, haloperidol.<sup>116, 120, 121, 122</sup> In these studies, [<sup>18</sup>F]haloperidol was used to assess the distribution and kinetics of the drug in the brain and [<sup>18</sup>F]N-methylspiroperidol was used to assess the time course of occupancy of dopamine D<sub>2</sub> receptors by haloperidol<sup>121</sup> and the relationship between plasma drug levels and receptor occupancy.<sup>123</sup> These studies showed that increasing the dose of haloperidol does not result in increased receptor occupancy, consequently, promoting the use of lower doses of antipsychotic medication in the treatment of patients with psychotic disorders.

In another study, an F-18 labeled derivative of captopril, an angiotensin converting enzyme (ACE) inhibitor used to treat hypertension, was used to examine the behavior of a series of ACE drugs.<sup>124</sup>



## Summary and Outlook

Though the major focus of this chapter was on fluorine-18 labeled radiotracers, there is a strong synergism between the radiotracer development with fluorine-18 and radiotracer development with carbon-11. Thus a well-balanced perspective of the field requires the consideration of progress with each of these isotopes. Within this context, it is important to emphasize the essential and pivotal role that organic synthesis has played in the progression of the PET field over the past twenty years from one in which only a handful of institutions possessed the instrumentation and staff to carry out research to the present-day situation where there are more than 200 PET centers worldwide. During this period PET has become an important scientific tool in the neurosciences, cardiology and oncology.

It is important to point out that PET is by no means a mature field. The fact that a hundreds of different F-18 labeled compounds have been developed but only a few possess the necessary selectivity and sensitivity *in vivo* to track a specific biochemical process illustrates this and underscores a major difficulty in radiotracer development, namely the selection of priority structures for synthesis and the complexities of the interactions between chemical compounds and living systems.

New developments in rapid organic synthesis are needed in order to investigate new molecular targets and to improve the quantitative nature of PET experiments. Though PET is a challenging and expensive technology, it is exquisitely suited to human studies, particularly to studies of the functional and neurochemical organization of the normal human brain and other organs and to delineating mechanisms underlying neurological and psychiatric disorders. It also provides uniquely useful clinical information relative to the management of brain tumors, epilepsy and heart disease. Its use in drug research and development holds promise in understanding drug action, in facilitating drug discovery and in the introduction of new drugs into the practice of medicine. A new challenge is also present with the advent of functional magnetic resonance imaging (fMRI) and new strategies are being developed for synergistic imaging in which the data from both image modalities is fused to generate an image that has the spatial resolution of MRI with the biochemical information from PET.

## Acknowledgment

This research was carried out at Brookhaven National Laboratory under contract DE-AC02-76CH00016 with the U.S. Department of Energy and supported by its Office of Health and Environmental Research.

## References

- (1) *J. Nucl. Med.* **1991**, *32*, Entire Issue.
- (2) Phelps, M. E.; Mazziotta, J. C.; Schelbert, H. *Positron, Emission Tomography and Autoradiography: Principles and Applications for the Brain and Heart*; Raven Press: New York, 1986.
- (3) Fowler, J. S.; Wolf, A. P. *The synthesis of carbon-11, fluorine-18, and nitrogen-13 labeled radiotracers for biomedical applications.*; Technical Information Center, U.S. Department of Energy: Washington, DC, 1982.
- (4) Fowler, J. S.; Wolf, A. P. in *Positron emitter-labeled compounds: priorities and problems.*; Phelps, M. E.; Mazziotta, J. C. Schelbert, H. R.; Raven Press, New York, 1986; pp 391-450.

- (5) Kilbourn, M. R. *Fluorine-18 labeling of radiopharmaceuticals*; National Academy Press: Washington, DC, 1990.
- (6) Phelps, M. E.; Hoffman, E. J.; Mullani, N. A., et al. *J. Nucl. Med.* **1975**, *16*, 649-652.
- (7) Hoffman, E. J.; Phelps, M. E. in *Positron emission tomography: principles and quantitation*; Phelps, M. E.; Mazziotta, J. C. Schelbert, H. R.; Raven Press, New York, 1986; pp 237-286.
- (8) Hawkins, R. A.; Hoh, C.; Glasby, J., et al. *Sem. Nucl. Med.* **1992**, *22*, 268-284.
- (9) Pauling, L. in *The Nature of the Chemical Bond*; Cornell Univ. Press, Ithaca, New York, 1960; pp 82.
- (10) Goldman, P. *Science* **1969**, *164*, 1123-1130.
- (11) Fowler, J. S.; Wolf, A. P. *Int. J. Appl. Radiat. Isot.* **1986**, *37*, 663-668.
- (12) Firnau, G.; Garnett, E. S.; Chirakal, R., et al. *Int. J. Appl. Radiat. Isot.* **1986**, *37*, 669-675.
- (13) Guillaume, M.; Luxen, A.; Nebeling, B.; Argentini, M.; Clark, J. C.; Pike, V. W. *Appl. Radiat. Isot.* **1991**, *42*, 749-762.
- (14) Ruth, T. J.; Wolf, A. P. *Radiochim. Acta* **1979**, *26*, 21-24.
- (15) Wieland, B. W.; Wolf, A. P. *J. Nucl. Med.* **1983**, *24*, 122.
- (16) Kilbourn, M. R.; Hood, J. T.; Welch, M. J. *Appl. Radiat. Isotopes* **1984**, *35*, 599-602.
- (17) Firouzbakht, M. L.; Schlyer, D. J.; Gatley, S. J., et al. *Int. J. Appl. Radiat. Isot.* **1993**, *44*, 1081-1084.
- (18) Nickles, R. J.; Daube, M. E.; Ruth, T. J. *Int. J. Appl. Radiat. Isot.* **1984**, *35*, 117-122.
- (19) Casella, V.; Ido, T.; Wolf, A. P., et al. *J. Nucl. Med.* **1980**, *21*, 750-757.
- (20) Shiue, C.-Y.; Salvadori, P. A.; Wolf, A. P. *J. Nucl. Med.* **1982**, *23*, 899.
- (21) Adam, M. J. *J. Chem. Soc. Chem. Comm.* **1982**, 730.
- (22) Bergman, J.; Haaparanta, M.; Solin, O. *Eleventh International Symposium on Radiopharmaceutical Chemistry*, Vancouver, **1995**, 46-48.
- (23) Shefer, R. E.; Klinkowstein, R. E.; Hughey, B. J., et al. *J. Nucl. Med.* **1991**, *32*, 1096p.
- (24) Attina, M.; Cacace, F.; Wolf, A. P. *J. Chem. Soc., Chem. Commun.* **1983**, 109.
- (25) Cacace, F.; Speranza, M.; Wolf, A. P., et al. *J. Label. Compds. Radiopharm.* **1981**, *18*, 1721.
- (26) Angelini, G.; Speranza, M.; Wolf, A. P., et al. *J. Fluorine Chem.* **1985**, *27*, 177.
- (27) Goldstein, D. S.; Chang, P. C.; Eisenhofer, G., et al. *Circulation* **1990**, *81*, 1606-1621.
- (28) Mislankar, S. G.; Gildersleeve, D. L.; Wieland, D. M., et al. *J. Med. Chem.* **1988**, *31*, 362.
- (29) Ding, Y. S.; Shiue, C. Y.; Fowler, J. S., et al. *J. Fluorine Chem* **1990**, *48*, 189-206.
- (30) Rengan, R.; Chakraborty, P. K.; Kilbourn, M. R. *J. Label. Compds. Radiopharm.* **1993**, *33*, 563-572.
- (31) Ding, Y.-S.; Fowler, J. S.; Gatley, S. J., et al. *J. Med. Chem.* **1991**, *34*, 767-771.
- (32) Ding, Y. S.; Fowler, J. S.; Gatley, S. J., et al. *J. Med. Chem.* **1991**, *34*, 861-863.
- (33) Pike, V. W.; Aigbirhio, F. I. *J. Chem. Soc. Chem. Commun.* **1995**, 2215.
- (34) Angelini, G.; Margonelli, A.; Sparapani, C., et al. *J. Label. Compds. Radiopharm.* **1994**, *35*, 562.

- (35) Logan, J.; Fowler, J. S.; Volkow, N. D., et al. *J. Cereb. Blood Flow Metab* **1990**, *10*, 740-747.
- (36) Patlak, C. S.; Blasberg, R. G.; Fenstermacher, J. D. *J. Cereb. Blood Flow Metab* **1983**, *3*, 1-7.
- (37) Sokoloff, L.; Reivich, M.; Kennedy, C., et al. *J. Neurochem.* **1977**, *28*, 897-916.
- (38) Reivich, M.; Kuhl, D.; Wolf, A. P., et al. *Circ. Res.* **1979**, *44*, 127-137.
- (39) Volkow, N. D.; Fowler, J. S. *Sem. Nucl. Med.* **1992**, *22*, 254-267.
- (40) Volkow, N. D.; Fowler, J. S.; Gatley, J., et al. *J. Nucl. Med.* **1995**, in press.
- (41) Halldin, C. *Med. Chem. Res.* **1995**, *5*, 127-149.
- (42) Garnett, E. S.; Firnau, G.; Nahmias, C. *Nature* **1983**, *305*, 137.
- (43) Playford, E. D.; Brooks, D. J. *Cerebrovas. Brain Metab. Rev.* **1992**, *4*, 144-171.
- (44) DeJesus, O. T.; Sunderland, J. J.; Chen, C.-A., et al. *J. Nucl. Med.* **1989**, *30*, 930.
- (45) Melega, W. P.; Perlmutter, M. M.; Luxen, A., et al. *J. Neurochem.* **1989**, *53*, 311.
- (46) DeJesus, O. T.; Holden, J. E.; Endres, C. *Brain Res.* **1992**, *597*, 151-154.
- (47) Arnett, C. D.; Fowler, J. S.; Wolf, A. P., et al. *Life Sciences* **1985**, *36*, 1359-1366.
- (48) Arnett, C. D.; Shiue, C.-Y.; Wolf, A. P., et al. *J. Neurochem.* **1985**, *44*, 835-844.
- (49) Coenen, H. H.; Laufer, P.; Stocklin, G., et al. *Life Sci.* **1987**, *40*, 81.
- (50) Moerlein, S. M.; Perlmutter, J. S.; Welch, M. J. *Nucl. Med. Biol.* **1995**, *22*, 809-815.
- (51) Mach, R. H.; Ehrenkauf, R. L. E.; Nader, M. A., et al. *11th International Symposium on Radiopharmaceutical Chemistry*, Vancouver, **1995**, 21.
- (52) Goodman, M. M.; Keil, R.; Shi, B., et al. *J. Nucl. Med.* **1995**, *36*, 38p.
- (53) Neumeyer, J. L.; Wang, S.; Gao, Y., et al. *J. Med. Chem.* **1994**, *37*, 1558-1561.
- (54) Fowler, J. S. in *Positron emitter labeled enzyme inhibitors*; Nunn, A. D.; Marcel Dekker, Inc., New York, 1992; pp 267-296.
- (55) Ding, Y.-S.; Rehder, K.; Vassallo, M., et al. *J. Nucl. Med.* **1994**, *35*, 7p.
- (56) Plenevaux, A.; Fowler, J. S.; Dewey, S. L., et al. *Int. J. Radiat. Appl. Instrum. Part A.* **1990**, *42*, 121-127.
- (57) Ametamey, S. M.; Haeberli, M.; Beer, H.-F., et al. *11th International Symposium on Radiopharmaceutical Chemistry*, Vancouver, **1995**, 71.
- (58) Mannisto, P. T.; Kaakkola, S. *Pharmacol. Toxicol.* **1990**, *66*, 317-323.
- (59) Ding, Y.-S.; Gatley, S. J.; Fowler, J. S., et al. *J. Life Sciences (in press)* **1995**,
- (60) Jacobs, B. L.; Azmitia, E. C. *Pharmacol. Rev.* **1992**, *72*, 165-215.
- (61) Blin, J.; Pappata, S.; Kiyosawa, M., et al. *Eur. J. Pharmacol.* **1988**, *147*, 73-82.
- (62) Crouzel, C.; Venet, M.; Sanz, G., et al. *J. Label. Compds. Radiopharm.* **1988**, *25*, 827.
- (63) Lemaire, C.; Cantineau, R.; Guillaume, G., et al. *J. Nucl. Med.* **1991**, *32*, 2266-2272.
- (64) Jovkar, S.; Wienhard, K.; Coenen, H. H. *Eur. J. Nucl. Med.* **1991**, *18*, 158.
- (65) Moerlein, S. M.; Perlmutter, J. S. *Neurosci. Lett.* **1991**, *123*, 23.
- (66) Tan, P.; Dewey, S. L.; Gatley, S. J., et al. *J. Nucl. Med.* **1994**, *35*, 67p.
- (67) Tan, P.; Fowler, J. S.; Ding, Y.-S., et al. *J. Nucl. Med.* **1995**, *36*, 149p.
- (68) Hwang, D.-R.; Banks, W. R.; Adkins, J., et al. *J. Nucl. Med.* **1994**, *35*, 252p.
- (69) Hwang, D.-R.; Hwang, Y.-C.; Mantil, J. C. *J. Nucl. Med.* **1995**, *36*, 58p.

- (70) Hwang, D.-R.; Hwang, Y.-C.; Mantil, J. C. *J. Nucl. Med.* **1995**, *36*, 149p.
- (71) Hwang, D.-R.; Hwang, Y. C.; Mathis, C. A., et al. *11th International Symposium on Radiopharmaceutical Chemistry*, Vancouver, **1995**, 299.
- (72) Mathis, C. A.; Simpson, N. R.; Mahmood, K., et al. *Life Sci.* **1994**, *55*, 403.
- (73) Pike, V. W.; McCarron, J. A.; Hume, S. P., et al. *Med. Chem. Res.* **1995**, *5*, 208.
- (74) Mathis, C. A.; Mahmood, K.; Simpson, N. R., et al. *11th International Symposium on Radiopharmaceutical Chemistry*, Vancouver, **1995**, 292.
- (75) Murphy, D. L.; Mueller, E. A.; Garric, N. A., et al. *J. Clin. Psychiatr.* **1986**, *47*, (suppl)9-15.
- (76) Hume, S. P.; Pascali, C.; Pike, V. W. *Nucl. Med. Biol.* **1991**, *18*, 339-351.
- (77) Suehiro, M.; Wilson, A. A.; Scheffel, U., et al. *J. Nucl. Med. Biol.* **1991**, *18*, 791-796.
- (78) Kilbourn, M. R.; Haka, M. S.; Mulholland, G. K., et al. *J. Label. Compds. Radiopharm.* **1989**, *26*, 412-414.
- (79) Mathis, C.; Longford, C. P. D.; Simpson, N., et al. *J. Nucl. Med.* **1993**, *34*, 7p-8p.
- (80) Suehiro, M.; Scheffel, U.; Dannals, R. F., et al. *J. Nucl. Med.* **1993**, *34*, 120-127.
- (81) Suehiro, M.; Greenberg, J. H.; Shiue, C.-Y., et al. *J. Nucl. Med.* **1995**, *36*, 151p.
- (82) Shi, B.; Faraj, B.; Goodman, M. M. *11th International Symposium on Radio-pharmaceutical Chemistry*, Vancouver, **1995**, 311.
- (83) Rogers, G. A.; Kornreich, W. D.; Hand, K., et al. *Mol. Pharmacol.* **1993**, *44*, 633-641.
- (84) Mulholland, G. K.; Jung, Y.-W.; Sherman, P. S. *J. Label. Compds. Radiopharm.* **1993**, *32*, 487.
- (85) Efange, S. M. N.; Mach, R. H.; Khare, A. B., et al. *Appl. Radiat. Isot.* **1994**, *45*, 465-472.
- (86) Staley, J. K.; Mash, D. C.; Parsons, S. M., et al. *11th International Symposium on Radiopharmaceutical Chemistry*, Vancouver, **1995**, 370.
- (87) Parsons, S. M.; Prior, C.; Marshall, I. G. *Intl. Review Neurobiol.* **1993**, *35*, 279-390.
- (88) Ingvær, M.; Stone-Elander, S.; Roger, G., et al. *NeuroReport* **1993**, *4*, 1311-1314.
- (89) Kiesewetter, D. O.; Lang, L.; Lee, J. T., et al. *210th American Chemical Society National Meeting*, Chicago, **1995**, Div. of Nucl. Chem. and Tech., Abst. 072.
- (90) Hwang, D.-R.; Dence, C. S.; Mckinnon, Z. A. *Nucl. Med. Biol.* **1991**, *18*, 247.
- (91) Wilson, A. A.; Scheffel, U. A.; Dannals, R. F. *Life Sci.* **1991**, *48*, 1385.
- (92) Patt, J. T.; Westera, G.; Buck, A., et al. *11th International Symposium on Radiopharmaceutical Chemistry*, Vancouver, **1995**, 355.
- (93) Kawai, R.; Carson, R. E.; Dunn, B., et al. *J. Cereb. Blood Flow Metab.* **1991**, *11*, 529.
- (94) Bai, L.-Q.; Teng, R. R.; Shiue, C.-Y. *Nucl. Med. Biol.* **1990**, *17*, 217.
- (95) Chesis, P. L.; Hwang, D.-R.; Welch, M. J. *J. Med. Chem.* **1990**, *33*, 1482.
- (96) Chesis, P. L.; Griffeth, L. K.; Mathias, C. J., et al. *J. Nucl. Med.* **1990**, *31*, 192.
- (97) Hwang, D.-R.; Feliu, A. L.; Wolf, A. P. *J. Label. Compds. Radiopharm.* **1986**, *23*, 277.
- (98) Dewey, S. L.; Wolf, A. P.; Fowler, J. S., et al. *XVI C.I.N.P. Congress*, **1988**, 162.

- (99) Dewey, S. L.; Brodie, J. D.; Fowler, J. S., et al. *Synapse* **1990**, *6*, 321-327.
- (100) Dewey, S. L.; Brodie, J. D.; MacGregor, R. R., et al. *J. Nucl. Med.* **1990**, *31*, 780p.
- (101) Dewey, S. L.; Smith, G. W.; Logan, J., et al. *J. Neurosci.* **1992**, *12*, 3773-3780.
- (102) Dewey, S. L.; Smith, G. S.; Logan, J., et al. *Society for Neuroscience Abstracts* **1992**, *18*, 385.7.
- (103) Smith, G. S.; Dewey, S. L.; Logan, J. *Society for Neuroscience Abstracts* **1993**, *19*, 128.9.
- (104) Dewey, S. L.; Smith, G. S.; Logan, J., et al. *Proc. Natl. Acad. Sci.* **1993**, *90*, 11816-11820.
- (105) Schwaiger, M.; Kalf, V.; Rosenspire, K., et al. *Circulation* **1990**, *82*, 457-464.
- (106) Wieland, D. M.; Rosenspire, K. C.; Hutchins, G., et al. *J. Med. Chem.* **1990**, *33*, 956-964.
- (107) Ding, Y. S.; Fowler, J. S.; Gatley, S. J., et al. *J Med Chem* **1991**, *34*, 767-771.
- (108) Ding, Y. S.; Fowler, J. S.; Gatley, S. J., et al. *J Med Chem* **1991**, *34*, 861-863.
- (109) Ding, Y. S.; Fowler, J. S.; Dewey, S. L., et al. *J. Nucl. Med.* **1993**, *34*, 619-629.
- (110) Yu, P. H.; Barclay, S.; Davis, B., et al. *Biochemical. Pharm.* **1981**, *30*, 3089-3094.
- (111) Ahn, N. G.; Klinman, J. P. *J. Biological Chemistry* **1989**, *264*, 12259-12265.
- (112) Kato, T.; Nagatsu, T.; Hashimoto, Y., et al. in *Isotope effects in the hydroxylation of dopamine by dopamine-beta-hydroxylase (DBH)*; Usdin, E.; Kopin, I. J. Barchas, J.; Pergamon:Elmsford, New York, 1979; pp 144-146.
- (113) Ding, Y.-S.; Fowler, J. S.; Wolf, A. P. *J. Label. Compds. Radiopharm.* **1993**, *33*, 645-654.
- (114) Ding, Y. S.; Fowler, J. S.; Gatley, S. J., et al. *J. Neurochem.* **1995**, *65*, 682-690.
- (115) Burns, H. D.; Gibson, R. E.; Dannals, R. F., et al. *Nuclear Imaging in Drug Discovery, Development, and Approval*; Birkhauser Boston, Inc.: Boston, 1993.
- (116) Schyler, D. J.; Volkow, N. D.; Fowler, J. S. *Synapse* **1992**, *11*, 10-19.
- (117) Ding, Y.-S.; Fowler, J. S.; Dewey, S. L., et al. *J. Nucl. Med.* **1993**, *34*, 246.
- (118) Satter, M. R.; Nickles, R. J. *J. Label. Compds. Radiopharm.* **1991**, *30*, 58.
- (119) Fowler, J. S.; Ding, Y.-S.; Volkow, N. D., et al. *Synapse* **1994**, *16*, 312-317.
- (120) Farde, L.; Wiesel, F.-A.; Halldin, C., et al. *Arch. Gen. Psychiat.* **1988**, *45*, 71-76.
- (121) Smith, M.; Wolf, A. P.; Brodie, J. D., et al. *Biol. Psych.* **1988**, *23*, 653 .
- (122) Wolkin, A.; Barouche, F.; Wolf, A. P., et al. *Am. J. Psych.* **1989**, *146*, 905-908.
- (123) Wolkin, A.; Brodie, J. D.; Barouche, F., et al. *Arch. Gen. Psych.* **1989**, *46*, 482-483.
- (124) Hwang, D.-R.; Eckelman, C. J.; Mathias, C. J. *J. Nucl. Med.* **1991**, *32*, 1730.

## Author Index

- Abouabdellah, Ahmed, 228  
Asai, Tomoyuki, 83  
Bégué, Jean-Pierre, 59,228  
Bergmann, K., 129  
Bernacki, Ralph J., 228  
Bitonti, Alan J., 246  
Bonnet-Delpon, Danièle, 59,228  
Boros, L. G., 129  
Braun, Curtis, 279  
Burger, Klaus, 42  
Chakravarty, Subrata, 228  
Cieplak, Piotr, 143  
Coward, James K., 118  
DeCorte, B., 129  
Ding, Yu-Shin, 328  
Dorr, A. F., 265  
Ducep, J. B., 196  
Farr, R., 169  
Filler, Robert, 1  
Fowler, Joanna S., 328  
Gandhi, V., 265  
Gimi, R., 129  
Gimi, Rayomand H., 228  
Grindey, Gerald B., 265  
Grossman, C. S., 265  
Hertel, L. W., 265  
Ho, Chien, 296  
Huang, P., 265  
Huber, Edward W., 246  
Iseki, Katsuhiko, 214  
Jakubke, Hans-Dieter, 42  
Jarvi, Esa T., 246  
Jund, K., 196  
Kirk, Kenneth L., 1,312  
Kitazume, Tomoya, 105  
Kobayashi, Yoshiro, 214  
Kokschi, Beate, 42  
Kollman, Peter A., 143  
Kroin, J. S., 265  
Kuduk, Scott D., 228  
Lesur, B., 196  
Lin, J., 129  
Matsumura, Yasushi, 83  
Matthews, Donald P., 246  
McCarter, John D., 279  
McCarthy, James R., 246  
McGuire, John J., 118  
Mizutani, Kenji, 105  
Morikawa, Tsutomu, 73  
Morizawa, Yoshitomi, 83  
Nakano, Takashi, 83  
Namchuk, Mark, 279  
Newton, M. G., 95  
Nie, Jun-Ying, 312  
Ojima, Iwao, 228  
Ourevitch, Michele, 228  
Pera, Paula, 228  
Phillips, R. S., 95  
Plunkett, W., 265  
Podlogar, B., 169  
Poulter, C. Dale, 158  
Pratt, E. Ann, 296  
Radomski, Jan P., 143  
Resvick, Robert J., 246  
Rondeau, J. M., 169  
Sabol, Jeffrey S., 246  
Sarhan, S., 196  
Schirlin, D., 169  
Schleimer, M., 196  
Secundo, F., 95  
Seiler, N., 196  
Sewald, Norbert, 42  
Sham, Hing L., 184  
Shibuya, Akira, 73  
Slater, John C., 228  
Soloshonok, V. A., 26  
Storniolo, A. M. V., 265  
Stubbe, JoAnne, 246  
Sun, Chung Ming, 228  
Sun, Zhen-Yu, 296  
Sunkara, Prasad S., 246  
Taguchi, Takeo, 73

- Tardif, C., 169  
 Tarnus, C., 169  
 Tsukamoto, Takashi, 118  
 van der Donk, Wilfred A., 246  
 Van Dorselaer, V., 169  
 Veith, Jean M., 228  
 VonTersch, R. L., 95  
 Welch, J. T., 129  
 Withers, Stephen G., 279  
 Yamazaki, Takashi, 105  
 Yu, Guixue, 246  
 Zimmermann, P. R., 196

## Affiliation Index

- Abbott Laboratories, 184  
 Asahi Glass Company, Ltd., 83  
 Brookhaven National  
 Laboratory, 328  
 Carnegie Mellon University, 296  
 CNR (Italy), 95  
 Daikin Industries, Ltd., 214  
 Eli Lilly and Company, 265  
 Hoechst Marion Roussel, Inc., 246  
 Illinois Institute of Technology, 1  
 Marion Merrell Dow Research  
 Institute, 169,196  
 Massachusetts Institute of  
 Technology, 246  
 National Institutes of Health, 1,312  
 R. W. Johnson Pharmaceutical  
 Research Institute, 169  
 Roswell Park Cancer Institute,  
 118,228  
 State University of New York  
 at Albany, 129  
 State University of New York  
 at Stony Brook, 228  
 Tokyo College of Pharmacy, 73  
 Tokyo Institute of Technology, 105  
 Ukrainian Academy of Sciences, 26  
 U.S. Naval Academy, 95  
 Université de Rennes, 196  
 Université Paris-Sud, 59,228  
 University of British Columbia, 279  
 University of California—  
 San Francisco, 143  
 University of Georgia, 95  
 University of Leipzig, 42  
 University of Michigan, 118  
 University of Texas, 265  
 University of Utah, 158  
 University of Warsaw, 143

## Subject Index

### A

- Accepting glutamate, definition, 118  
 Acyl donors, amino acids in peptide  
 synthesis, 44–46  
 S-Adenosylhomocysteine hydrolase,  
 inhibition, 8–10f  
 Ala-Ψ[(Z)-CF=C]-Pro isostere, 129–140  
 Aldol reactions  
 second-order asymmetric transformations  
 of products, 32  
 synthesis of enantiopure fluorinated  
 amino acids, 26–39  
 D-Amicetose, synthesis, 108–110  
 Amide isosteric replacements, 129–130  
 Amino acid(s)  
 fluorinated, *See* Fluorinated amino acids  
 functions, 312  
 polyfluorinated analogues, 323–326  
 probes in membrane-associated proteins,  
<sup>19</sup>F-labeled, *See* <sup>19</sup>F-labeled amino acids  
 as probes in membrane-associated  
 proteins  
 trifluoromethyl substituted, *See* α-Tri-  
 fluoromethyl-substituted amino acids  
 in peptides

- Amino acid precursors of amine neurotransmitters, synthesis, 315–319
- $\beta$ -Amino alcohols, 59
- 4-Aminobutyric acid, 196
- Ammonia detoxification, enhancement of urea formation, 200–202t
- Angiotensin-converting enzyme inhibitors, control of high blood pressure, 184
- Anorectic agents, use of fluorinated analogues, 17,19f
- Antibacterials, use of fluorinated analogues, 15,16f
- Antibiotics
- antibacterials, 15,16f
  - antifungal agents, 17,18f
  - antimalarial drugs, 15,18f
  - use of fluorinated analogues, 15–18f
- Anticancer activity, 2',2'-difluorodeoxycytidine, 269–272t
- Anticancer agents, use of fluorinated analogues, 12–14f
- Antidepressants, use of fluorinated analogues, 17,19f
- Antidiabetics, use of fluorinated analogues, 20,21f
- Antifungal agents, use of fluorinated analogues, 17,18f
- Anti-hepatitis B virus agents, 12,15
- Antimalarial drugs, use of fluorinated analogues, 15,18f
- Antiviral activity, 2',2'-difluorodeoxycytidine, 267–269
- Antiviral agents, use of fluorinated analogues, 12,14–15,16f
- Arteflene, use as antimalarial drug, 15,18f
- Artemether, use as antimalarial drug, 15,18f
- Aspartyl protease, inhibition by fluorine-containing peptide mimetics, 184–194
- Asymmetric aldol reactions, synthesis of enantiopure fluorinated amino acids, 26–39
- Asymmetric synthesis of functionalized fluorinated cyclopropanes
- difluorocarbene addition to chiral olefin, 75–77
  - regio- and stereoselective synthesis of functionalized difluorocyclopropane using bromodifluorocrotonate, 77–80
- Asymmetric synthesis of functionalized fluorinated cyclopropanes—*Continued*
- Simmons–Smith reaction of fluoroallyl alcohol derivative, 73–75
- ## B
- Belokon aldol reaction, enantiopure fluorinated amino acid synthesis, 29–34
- Bicalutamide, use as anticancer agents, 12
- Biological activity
- 2',2'-difluorodeoxycytidine, 267–272
  - fluorinated vitamin D<sub>3</sub> analogues, 221–223
  - fluorine-containing taxoids, 232–233
- Biomedical chemistry of fluorine-containing compounds
- CF and CF<sub>2</sub> as O replacements, 11,13f
  - fluorinated analogues, 9,11–20
  - fluorine-containing enzyme inhibitors, 2–10
  - hydrolytic stability of fluorinated analogues
    - 2'-deoxy-2-fluoronucleotides, 9,13f
    - fluorinated prostacyclins and thromboxane, 9,10f
- BMY 14802, tracer for positron emission tomography in neurosciences, 338
- Brain glucose, metabolism, 333
- Breast tumor xenografts, antitumor activity of fluoroolefin cytidine nucleotide, 261,262t
- ## C
- C-terminal position of peptides, incorporation of  $\alpha$ -trifluoromethyl-substituted amino acids, 42–56
- Calcemic activity, fluorinated vitamin D<sub>3</sub> analogues, 223,224f
- Captopril, tracer for positron emission tomography in neurosciences, 338
- Carotenoids, function, 158
- Catecholamines, polyfluorinated analogues, 323–326
- Catechol-O-methyl transferase, fluorinated catecholamines as substrates, 319–320
- Central nervous system agents, 17,19f



- Cerebrocrase, use as cognition enhancer, 17,19f
- CF and CF<sub>2</sub>, O replacements in fluorine-containing compounds, 11,13f
- Chiral 6-deoxy-6,6,6-trifluoro sugar synthesis, 106–114
- Chiral glycine Ni(II) complex, 29–30
- Chiral olefin, difluorocarbene addition, 75–77
- Cholinergic system, neurotransmitter activity, 335
- Ciprofloxacin, 15,16f
- Cisplatin, activity against non-small-cell lung cancer, 273–275
- Cognition enhancers, use of fluorinated analogues, 17,19f
- Colon cancer, inhibition by fluorinated vitamin D<sub>3</sub> analogues, 223–225
- Conformational analysis, use of fluorine as probe, 233–240
- Cyclopropane(s), functionalized fluorinated, asymmetric synthesis, 73–80
- Cyclopropane subunit, biological effects, 73
- D**
- DD–003, use as anticancer agent, 12,14f
- 1-(2-Deoxy-2,2-difluoro-D-ribofuranosyl)-pyrimidines, reasons for synthesis, 265
- 2-Deoxy-2,2-difluoro-D-ribose, 265
- Deoxyfluoro sugars, probes of glycosidase mechanisms, 279
- 2-Deoxy-2-fluoroglucose, tracer for positron emission tomography in neurosciences, 333,338
- 2'-Deoxy-2'-fluoroguanosine, use as anticancer agent, 15,16f
- 2'-Deoxy-2-fluoronucleotides, hydrolytic stability, 9,13f
- 6-Deoxy-6,6,6-trifluoro sugar synthesis via intramolecular 1,2-*O,O*-silyl migration, 106–114
- Dexfenfluramine, use as anorectic agent, 17,19f
- (–)-2',3'-Dideoxy-5-fluoro-3'-thiacytidine, use as anticancer agent, 12,14f
- 2',2'-Difluorodeoxycytidine anticancer activity, 269–271,272t
- biological activity, antiviral activity, 267–269
- mechanism of action, 271–276
- ribonucleotide diphosphate reductase inhibition, 250
- synthesis, 267
- 2,2-Difluoroglycosides, trapping the intermediate on  $\alpha$ -glycosidases, 282,284–287f
- 3,4-(Difluoromethano)glutamic acid, synthesis, 73–80
- Difluoromethylene 1,3-diketone, inhibition of HIV–1 protease, 179–190
- Difluoromethylene ketone retroamide, inhibition of HIV–1 protease, 177,179
- 2',2'-Difluoromethylene-2'-deoxycytidine, ribonucleotide diphosphate reductase inhibition, 250
- Difluoroprostacyclin derivatives, 89,91f,92
- Difluorostatones
- alternate binding mode, 176–178f
- HIV–1 protease inhibition, 169–182
- Dihydrofolate reductase, 118
- Dihydrofolic acid, 118
- Dimethylallyl analogues, synthesis of fluorinated allylic isoprenoid substrates, 160–161
- Docetaxel, 228–240
- Dopamine
- neurotransmitter activity, 333–334
- role as precursors of amino neurotransmitters, 313,314f
- E**
- Elastases, inhibition, 3,4f,6f
- Enantiopure fluorinated amino acid
- synthesis by asymmetric aldol reactions
- Belokon aldol reaction
- chiral glycine Ni(II) complex
- characteristics and reactivity, 29–30
- (2*S*,3*S*)- $\beta$ -(fluoroalkyl)- $\beta$ -alkylserine
- synthesis, 35–36
- syn*-(2*S*)- $\beta$ -(fluoroalkyl)serine
- synthesis, 34

- Enantiopure fluorinated amino acid synthesis by asymmetric aldol reactions—*Continued*
- Belokon aldol reaction—*Continued*
- syn-(2*R*)- $\beta$ -(fluorophenyl)serine synthesis, 33–34
- kinetic and thermodynamic control of stereoselectivity, 31–32
- kinetic control of stereoselectivity, 30–31
- second-order asymmetric transformations of products in aldol reactions, 32
- thermodynamic control product stereochemistry, 32–33
- biomedical interest in fluorine-containing analogues of  $\alpha$ -amino- $\beta$ -hydroxycarboxylic acids, 27–29
- experimental description, 26–27
- Hayashi aldol reactions, 36–39*f*
- Enzymatic optical resolution, chiral 6-deoxy-6,6,6-trifluoro sugar synthesis, 105–114
- Enzyme inhibitors
- use of fluorine, 2–10
- molecular design, 143–154
- See also* Human immunodeficiency virus 1 (HIV-1) protease
- EP receptors, function, 83,85
- Epinephrine, role as precursors of amino neurotransmitters, 313,314*f*
- Eukaryotic prenylated proteins, 158
- F**
- <sup>18</sup>F-labeled tracers for positron emission tomography in neurosciences
- applications
- neuropharmacology, 338
- neurotransmitter activity, 330,333–337
- experimental description, 328–329
- labeling organic compounds with fluorine-18, 330–332
- positron emission tomography imaging, 329–330
- <sup>19</sup>F-labeled amino acids as probes in membrane-associated proteins
- advantages of <sup>19</sup>F-NMR spectroscopy, 297
- combination with nitroxide spin-label, 306–308*f*
- <sup>19</sup>F-labeled amino acids as probes in membrane-associated proteins—*Continued*
- examples of membrane-associated proteins studied, 296–297
- incorporation of <sup>19</sup>F-labeled amino acids, 297–298
- indication of global structural change, 299–303
- probes for local environment, 303–306
- site-specific mutagenesis, 299
- use in internuclear distance measurements, 306,309
- <sup>19</sup>F-NMR spectroscopy, <sup>19</sup>F-labeled amino acids as probes in membrane-associated proteins, 296–309
- Farnesyl analogues, synthesis of fluorinated allylic isoprenoid substrates, 162–163
- Fenfluramine, use as anorectic agent, 17
- Fluconazole, use as antifungal agent, 17,18*f*
- Fluorinated allylic isoprenoid substrates, synthesis, 160–163
- Fluorinated amine neurotransmitter biochemical properties, 319–320
- Fluorinated amino acids
- applications in drug development, 312–313
- analogues of folic acid and methotrexate biochemistry and pharmacology, 123–127
- chemistry of synthesis, 119–122
- experimental description, 119
- reaction, 119
- enantiopure, synthesis by asymmetric aldol reactions, 26–39
- nerve systems
- biochemical properties, 319–320
- development as positron emission tomography scanning agents, 320–321
- neurotransmitters, 313
- polyfluorinated analogues of catecholamines and amino acids, 323–326
- precursors of amine neurotransmitters, 313–315
- prodrugs for fluoronorepinephrine, 321–323
- synthesis, 315–319
- Fluorinated amino alcohols, 68–69

- Fluorinated analogues  
mechanistic probes  
peptidoglycan biosynthesis, 11,13f  
terpene biosynthesis, 9,11  
medicinal applications  
antibiotics, 15–17,18f  
anticancer agents, 12,13–14f  
antidiabetics, 20,21f  
antiviral agents, 12,14–15,16f  
central nervous system agents, 17,19f  
development, 11–12  
examples of new drugs and new applications, 20  
fluorinated liposomal membranes, 20  
hypolipidemic drugs, 17,19f
- Fluorinated carbohydrates, use as building blocks, 105–106
- Fluorinated cyclopropanes, 73–80
- Fluorinated epinephrines, 317,322f
- Fluorinated 5-hydroxytryptamines, 317,319
- Fluorinated liposomal membranes, medicinal applications, 20
- Fluorinated norepinephrines, 317,322f
- Fluorinated nucleosides, 265
- Fluorinated prostacyclins, hydrolytic stability, 9,10f
- Fluorinated D-ribose, 265
- Fluorinated substrate analogues, prenyl transfer reaction, 158–167
- Fluorinated sugars as probes of glycosidase mechanisms  
identification of active site nucleophile in  $\alpha$ -glucosidase, 289–292  
noncovalent interactions and catalysis, 280–283f  
trapping the intermediate on glycosidases, 282,284–289
- Fluorinated tyrosine  
 $\beta,\beta$ -difluorotyrosine synthesis, 102–103  
experimental description, 96–97  
mechanism of enzyme, 100–101  
reactivity, 99–102  
synthesis, 98–99  
2,3,5-trifluorotyrosine as mechanistic probe in tyrosine protein kinase substrate, 103  
2,3,6-trifluoro-L-tyrosine hydrochloride hydrate structure, 98
- Fluorinated vitamin D<sub>3</sub> analogues  
applications, 216  
design, 216–217  
experimental description, 216  
in vitro biological activity, 221–223  
in vivo calcemic activity, 223,224f  
inhibition of HT–29 human colon cancer growth, 223–225  
structures, 215  
synthesis, 217–221
- Fluorine  
applications, 1  
use as deceptor, 2,4f  
use as probe for conformational analysis, 233–240
- Fluorine-containing analogues  
 $\alpha$ -amino- $\beta$ -hydroxycarboxylic acids, 27–29  
biomedical chemistry, 1–21  
development, 26
- Fluorine-containing enzyme inhibitors  
S-adenosylhomocysteine hydrolase inhibitors, 8–10f  
fluorine as deceptor, 2,4f  
irreversible inhibitors of pyridoxal phosphate dependent enzyme, 8,10f  
protease inhibitors, 3–8,10f
- Fluorine-containing peptide mimetics  
aspartyl protease inhibitors  
HIV–1 protease inhibitors, 192–194  
renin inhibitors, 185–192  
molecular design, 143–154
- Fluorine-containing taxoids, 229–233
- Fluoroalkyl alcohols, enzyme inhibitory properties, 61–62
- Fluoroalkyl- $\beta$ -amino alcohols, 59–60  
(2*S*,3*S*)- $\beta$ -(Fluoroalkyl)- $\beta$ -alkylserine, 35–36
- Fluoroalkyl ketones, enzyme inhibitory properties, 61–62  
*syn*-(2*S*)-(Fluoroalkyl)serine, 34
- Fluorodopamine  
synthesis, 317,318f  
tracer for positron emission tomography in neurosciences, 332,336–337
- Fluorohistamines, synthesis, 315,316f
- Fluorohistidines, synthesis, 315,316f
- Fluoro-3-hydroxy-L-tyrosine  
synthesis, 317,318f

- Fluoro-3-hydroxy-L-tyrosine—*Continued*  
 tracer for positron emission tomography  
 in neurosciences, 332
- Fluoroketones, 184–194
- Fluoromethano amino acids, asymmetric  
 synthesis of functionalized  
 fluorinated cyclopropanes, 73–80
- 2-Fluoro-2,3-methano-4-aminobutanoic  
 acid, synthesis, 73–80
- Fluoronorepinephrine, tracer for positron  
 emission tomography in neurosciences,  
 332,338
- Fluoroolefin cytidine nucleotide design  
 antiproliferative activity,  
 246–247,256,258*t*  
 antitumor activity, 258–262*t*  
 design, 250–252  
 nucleotide reduction mechanism, 247–248  
 ribonucleotide diphosphate  
 reductase inhibition mechanism,  
 247,249–250,256–257  
 synthesis, 251–255
- Fluoroolefin isosteres as peptide mimetics  
 dipeptidyl peptidase IV  
 Ala-Ψ[(Z)-CF=C]-Pro isostere  
 synthesis, 136–139  
 inhibition, 136,139–140  
 examples, 131  
 Gly-Ψ[CF=C]-Pro synthesis via Peterson  
 fluorolefination, 132–136  
 prolylamides, 131–132
- Fluoroorganic synthesis, 26  
*syn*-(2*R*)-(Fluorophenyl)serine, 33–34
- Fluoroprostacyclins  
 difluoroprostacyclin derivatives, 89,91*f*,92  
 experimental description, 85  
 monofluoroprostacyclin derivatives,  
 85–91*t*
- Fluoroserotonins, 317,319
- Fluorosteroids, vitamin D<sub>3</sub> analogues,  
 214–226
- Fluorotyramines, 315,317,318*f*
- Fluorotyrosines, 315,317,318*f*
- Fluoxetine, use as anorectic agent, 17
- Fluoxetine hydrochloride, use as  
 antidepressant, 17
- Flutrimazole, use as antifungal agent,  
 17,18*f*
- Fluvastatin sodium, use as hypolipidemic  
 drug, 17,19*f*
- Folic acid, fluorinated amino acid  
 containing analogues, 118–127
- Folylpoly-γ-glutamate synthetase, 118–119
- Free energy derivatives, JG-365 inhibitor,  
 151–154
- Free energy perturbation, JG-365  
 inhibitor, 146–151
- Functionalized difluorocyclopropane,  
 regio- and stereoselective synthesis,  
 77–80
- Functionalized fluorinated cyclopropanes,  
 asymmetric synthesis, 73–80
- ## G
- Gemcitabine, *See*  
 2',2'-Difluorodeoxycytidine
- GEMZAR, *See*  
 2',2'-Difluorodeoxycytidine
- Geranyl analogues, synthesis of  
 fluorinated allylic isoprenoid  
 substrates, 162–163
- γ-Glutamyl hydrolase, 118–119
- Gly-Ψ[CF=F]-Pro, 129–140
- Glycosidases, 279–292
- Gold(I)-catalyzed asymmetric aldol  
 reaction, enantiopure fluorinated amino  
 acid synthesis, 36
- Gonadotropin-releasing hormone,  
 α-trifluoromethyl-substituted amino  
 acid incorporation into peptides, 54–55
- ## H
- Haloperidol, tracer for positron emission  
 tomography in neurosciences, 338
- Hayashi aldol reactions, enantiopure  
 fluorinated amino acid synthesis, 36–38
- Hexafluorohomotrihydroxyvitamin D<sub>3</sub>,  
 synthesis, 217–221
- Histamine, role as precursor of amine  
 neurotransmitter, 314*f*,315

- Homochiral trifluoromethyl- $\beta$ -amino alcohols, synthesis, 65–66
- HT–29 human colon cancer, inhibition by fluorinated vitamin D<sub>3</sub> analogues, 223–225
- Human immunodeficiency virus 1 (HIV–1) protease  
catalytic mechanism, 169–172  
inhibition  
by difluorostatones, 176–182  
by difluoroalcohols, 192–193  
by difluoroketones, 192–193  
overview, 5  
molecular design of peptide mimetics, 143–154
- Hydrolytic stability,  $\alpha$ -trifluoromethyl-substituted amino acids in peptides, 49
- 5-Hydroxytryptamine, role as precursors of amino neurotransmitters, 313–315
- 25-Hydroxyvitamin D<sub>3</sub>, hydroxylation, 214
- Hypolipidemic drugs, use of fluorinated analogues, 17,19f
- I
- Incoming glutamate, definition, 118
- Inhibition  
aspartyl protease, 184–194  
HIV–1 protease by difluorostatones, 169–182  
ornithine aminotransferase, 196–210
- Inhibitors, renin, *See* Renin inhibitors
- Internuclear distance measurements, <sup>19</sup>F-labeled amino acids as probes, 306,309
- IP receptor, function, 83,85
- Isoprenoid compounds, 158–161
- J
- JG–365 inhibitor  
advantages of peptide mimetic for modification, 144–146  
experimental description, 143  
free energy derivatives, 151–154f  
free energy perturbation, 146–151  
structure, 144,145f
- L
- Leukemias, antitumor activity of fluoroolefin cytidine nucleotide, 258–259
- Levofloxacin, use as antibacterial, 15,16f
- M
- Macrocyclic analogues, structure-assisted design, 176,178f
- Masked chain termination, 271
- MDL 101,731  
antiproliferative activity, 246–247,256,258t  
antitumor activity, 258–262t  
design, 250–252  
nucleotide reduction mechanism, 247–248  
ribonucleotide diphosphate reductase inhibition mechanism, 247,249–250,256–257  
synthesis, 251–255  
use as anticancer agent, 12,13f
- Membrane-associated proteins, <sup>19</sup>F-labeled amino acids as probes, 296–309
- Methotrexate  
dihydrofolate reductase inhibition, 118  
fluorinated amino acid containing analogues, 118–127
- 5-Methyl-2'-deoxycytidine transferase, inhibition, 2,4f
- Methyl isocanoacetate, aldol reactions, 36–39f
- Molecular design of fluorine-containing peptide mimetics  
advantages of peptide mimetic for modification, 144–146  
experimental description, 143  
free energy derivatives, 151–154f  
free energy perturbation, 146–151
- Monoamine oxidases, fluorinated analogues as substrates, 319
- Monofluoroprostacyclin derivatives, 85–91t
- N
- N-terminal position of peptides, incorporation of  $\alpha$ -trifluoromethyl-substituted amino acids, 42–56

- Neurotransmitter activity, use of fluorine-18-labeled tracers for positron emission tomography, 328–339
- Nitroxide spin-label, use with <sup>19</sup>F-labeled amino acids as probes in membrane-associated proteins, 296–309
- Non-small-cell lung cancer, role of 2',2'-difluorodeoxycytidine, 273–275
- Norepinephrine  
role as precursors of amino neurotransmitters, 313,314f  
tracer for positron emission tomography in neurosciences, 336–337
- Nucleophiles, amino acids in dipeptide synthesis, 46–49
- Nucleosides, structure vs. pharmacology, 265
- Nucleotide, reduction mechanism, 247–248
- O**
- Opioid system, neurotransmitter activity, 336
- Ornithine, occurrence and metabolism, 196–198
- Ornithine aminotransferase inhibition characterization, 197
- enzyme-activated irreversible inhibitors, 199,202t
- (*S*)-5-(fluoromethyl)ornithine, 201,203–209t
- potential therapeutic applications, 200–202t
- P**
- Paclitaxel  
applications, 228  
biological activity, 232–233  
conformational analysis using fluorine as probe, 233–240  
limitations, 228–229  
syntheses, 229–232
- Pancreatic cancer, role of 2',2'-difluorodeoxycytidine, 273–275
- Paroxetine, use as antidepressant, 17,19f
- Peptide(s)  
modification of backbone structure, 129  
 $\alpha$ -trifluoromethyl-substituted amino acid synthesis and incorporation, 42–56
- Peptide drugs, 42
- Peptide mimetics  
advantages as choice of inhibitor modification, 144–146  
fluorine containing  
molecular design, 143–154  
use as aspartyl protease inhibitors, 184–194  
use of fluoroolefin isosteres, 129–140
- Peptidoglycan biosynthesis, fluorinated analogues as mechanistic probes, 11,13f
- Peptidylfluoro ketones, protease inhibition, 8,10f
- Polyamine metabolism, enhancement, 200
- Polyfluorinated analogues, catecholamines and amino acids, 323–326
- Poly- $\gamma$ -glutamate conjugates, 118
- Positron emission tomography, 328–330
- Positron emission tomography scanning agents, development of fluorinated amino acids in nerve systems, 320–321
- Prenyl transfer reaction with fluorinated substrate analogues  
catalysis, 159,161  
enzyme-catalyzed reactions farnesyl diphosphate synthase, 165–166  
fluorine substitution effect, 159–160  
nucleophilic substitutions, 159,161  
protein farnesyltransferase, 165–167  
synthesis of fluorinated allylic isoprenoid substrates, 160–163
- Prodrugs, fluorinated amino acids in nerve systems, 321–323
- Propylamides, 131–132
- Prostacyclin, 83,84f
- Prostanoid receptors, sequences and functions, 83,85
- Protease, inhibition, 2–4f

Proteins, membrane associated,  $^{19}\text{F}$ -labeled amino acids as probes, 296–309  
Proteolytic stability,  $\alpha$ -trifluoromethyl-substituted amino acids in peptides, 49–53  
Pyridoxal phosphate dependent enzyme, inhibition, 8,10f

## R

Regioselective synthesis, functionalized difluorocyclopropane using bromodifluorocrotonate, 77–80  
Renin, inhibition, 3,5–7f  
Renin–angiotensin system, function, 184  
Renin inhibitors  
difluoroketone containing dipeptide isostere, 187–188  
difluoroketone with sulfone moiety at C terminus, 190–191  
 $\alpha,\alpha$ -difluoro- $\beta$ -aminodeoxystatine-containing compounds, 191–192  
difluorostatone-containing compounds, 187–186  
difluorostatine-containing compounds, 185–186  
fluoroketones, 184  
fluoroketones with retroamide-type bond, 186–187  
fluorodipeptide mimic, 187  
perfluoroalkyl ketone containing compounds, 189–190  
reaction, 185  
tetrafluoroketone-containing compounds, 191  
trifluoromethyl alcohol and ketone containing compounds, 188–189  
D-Rhodinose, synthesis, 108–110  
Ribonucleotide diphosphate reductase, 246–262  
Ring-fluorinated analogues of aromatic and heteroaromatic amine neurotransmitters, synthesis, 315–319  
RU58668, use as anticancer agent, 12,14f

## S

Serotonin system, neurotransmitter activity, 334–335  
1,2-*O*-Silyl migration, chiral 6-deoxy-6,6,6-trifluoro sugar synthesis, 105–114  
Simmons–Smith reaction, fluoroalkyl alcohol derivative, 73–80  
Solid tumors, antitumor activity of fluoroolefin cytidine nucleotide, 259–261  
Sparfloxacin, use as antibacterial, 15,16f  
Statine strategy, *See* Renin  
Stereochemistry, thermodynamic control, 32–33  
Stereoselective synthesis, functionalized difluorocyclopropane using bromodifluorocrotonate, 77–80  
Stereoselectivity, 30–32  
Sterols, function, 158  
Substance P modification,  $\alpha$ -trifluoromethyl-substituted amino acids in peptides, 55–56  
Sugars, fluorinated, *See* Fluorinated sugars as probes of glycosidase mechanisms  
Synthesis  
chiral 6-deoxy-6,6,6-trifluoro sugars via intramolecular 1,2-*O*-silyl migration, 105–114  
enantiopure fluorinated amino acids by asymmetric aldol reactions, 26–39  
fluorinated amino acid(s), 68–69,315–319  
fluorinated amino acid containing analogues of folic acid and methotrexate, 118–127  
fluorinated tyrosine, 95–103  
fluorinated vitamin D<sub>3</sub> analogues, 217–221  
fluorine-containing taxoids, 229–232  
fluoroolefin cytidine nucleoside, 251–255  
fluoroprostacyclins, 83–92  
homochiral trifluoromethyl  $\beta$ -amino alcohols, 65–66

## Synthesis—Continued

- $\alpha$ -trifluoromethyl-substituted amino acids in peptides, 42–56  
*syn*-3-(trifluoromethyl)isoserine, 68–69
- T**
- Tacrine, use as cognition enhancer, 17,19f  
Taxoids, fluorine-containing, synthesis, biological activity, and conformational analysis, 228–240  
Taxol, *See* Paclitaxel  
Taxotere, *See* Docetaxel  
Terpene biosynthesis, fluorinated analogues as mechanistic probes, 9,11  
Thromboxane, hydrolytic stability, 9,10f  
Thymidylate synthase, inhibition, 2  
Thyrotropin releasing hormone,  $\alpha$ -trifluoromethyl-substituted amino acid incorporation into peptides, 53  
Tolrestat, use as antidiabetic, 20,21f  
Tosufloxacin, use as antibacterial, 15,16f  
TP receptor, function, 83,85  
Tracers for positron emission tomography in neurosciences, *See* Fluorine-18-labeled tracers for positron emission tomography in neurosciences  
Trifluorinated triols, stereoselective synthesis, 111–112  
Trifluoro- $\beta$ -peptidyl alcohols inhibition of serine proteases, 66–68 synthesis, 60–61  
Trifluoromethyl- $\beta$ -amino alcohols, 60–65  
Trifluoromethyl-containing compounds, synthesis problems, 105  
 $\alpha$ -Trifluoromethyl-substituted amino acids in peptides acyl donors in peptide synthesis, 44–46 advantages, 42–43 amino acid incorporation into peptides, 53–56 hydrolytic stability, 49 nucleophiles in dipeptide synthesis, 46–49 proteolytic stability, 49–53 synthesis, 43–44  
*syn*-3-(Trifluoromethyl)isoserine, 68–69  
6,6,6-Trifluoro-L-oliiose, 112–113  
2,3,5-Trifluoro-L-tyrosine, 95–103  
Tyrosine, synthesis using tyrosine phenol-lyase, 95–103  
Tyrosine phenol-lyase, role in fluorinated tyrosine synthesis, 95–103
- U**
- Ubiquinones, function, 158
- V**
- Vitamin D<sub>3</sub>, functional metabolites, 214–215
- W**
- WIN-63843, use as anticancer agent, 15,16f
- Z**
- Zifrosilone, use as cognition enhancer, 17,19f  
Zopolrestat, use as antidiabetic, 20,21f